Design and evaluation of **nucleic acid**-based medicinal products to **address corneal inflammation** by gene therapy

Itziar Gómez Aguado

Vitoria-Gasteiz 2022

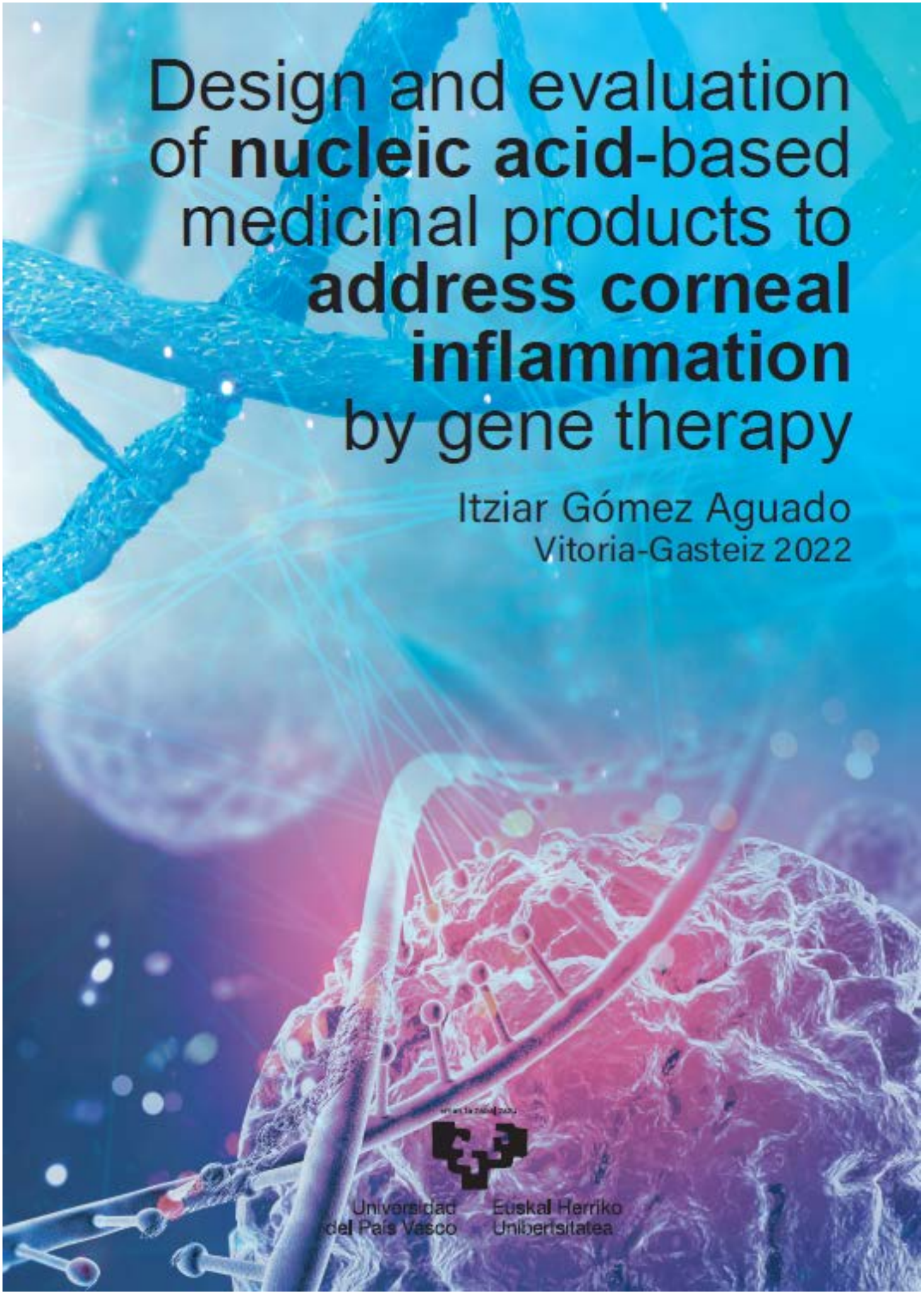

Universidad del País Vasco
Euskal Herriko Unibertsitatea

Design and evaluation of nucleic-acid based medicinal products to address corneal inflammation by gene therapy

---

Azido nukleikoak administratzeko sendagaien diseinua eta ebaluazioa, gene-terapiaren bitartez kornearen hantura tratatzeko

Itziar Gómez Aguado

Grupo Farmacocinética, Nanotecnología y Terapia génica (PharmaNanoGene)

Laboratorio de Farmacia y Tecnología Farmacéutica

Universidad del País Vasco/Euskal Herriko Unibertsitatea

Facultad de Farmacia

Vitoria-Gasteiz 2022

AGRADECIMIENTOS

Mucha gente ha pasado conmigo estos años de tesis. Me gustaría agradecer a cada uno de ellos el apoyo y el cariño que me han dado durante todo este tiempo.

En primer lugar, me gustaría comenzar agradeciendo a Ana, Marian, Alicia y Arantxa por dejarme ser partícipe de todo este mundo y por haber confiado en mí. Ana, gracias por enviarme ese correo y apostar por mí. Marian, gracias por los ánimos y el apoyo recibido durante toda la tesis. Gracias a las cuatro por haberme hecho sentir valorada y capaz de llevar este trabajo adelante. Thank you very much Luigi for giving me the opportunity to work with you, even if it was virtually. You have helped me a lot.

En segundo lugar, quiero agradecer a mi familia. A mis padres, porque sin vuestro apoyo esto no hubiera sido posible. Gracias por preocuparos por mí, por vuestra ayuda y por vuestra generosidad. Sois mi ejemplo a seguir. Gracias a vosotros he aprendido que todo lo que se quiere se puede llegar a conseguir. A mi hermano, por estar siempre que lo he necesitado. Gracias a mi abuela Pili por estar pendiente de mí. A mi abuelo Benito, allá donde estés sé que estarías muy orgulloso de mí.

A mis compañeros de laboratorio, mis PNGs, que habéis sido como mi segunda familia. Mónica, gracias por todos los momentos vividos, las conversaciones, las eternas llamadas de teléfono, consejos, risas y lágrimas… y lo que nos quedan por vivir. Qué suerte habernos encontrado en el camino. Julen, más que un compañero, un amigo. Hemos sido un equipo. Gracias por ser el hombro en el que desahogarme y en el que apoyarme en los momentos más difíciles y también los más bonitos. Ana, un descubrimiento. Gracias por estar ahí y escucharme. Gracias a todas las personas que han pasado por el laboratorio durante estos años, Josune, Pietro y Chiara, porque he aprendido mucho de vosotros.

También quiero agradecer a la familia de doctorandos. Por ser consuelo y sobre todo alegría. Gracias por esas comidas de los jueves, esos pintxopotes y esas sidrerías. Enrique, Ainara, Patri, Eva, Víctor, Julián y Amaia, sin vosotros, esto no hubiera sido lo mismo.

A mis aguilareños, por ser desconexión y aire puro. Porque cuando nos juntamos no hay quién nos pare. Esti, Elena y María, gracias por ser apoyo en lo bueno, pero sobre todo en lo malo. Leyre, porque después de tantos años, todo sigue igual y no hayan cambiado las cosas. A Anne y a Esti, con vosotras empezó esta etapa en Vitoria, gracias por vuestra vitalidad.

Por último, no me quiero olvidar de lo mejor que me ha dado este doctorado, conocerte a ti Víctor. Gracias por estar pendiente de mí, preocuparte y ser mi gran apoyo. Gracias por ayudarme a sacar lo mejor de mí en cada momento y hacer ver que todo tiene solución. Muchas gracias sol.

¡Muchas gracias a todos! Eskerrik asko guztioi! Thank you very much!

La felicidad no se define, «se experimenta». Para conocerla hay que haberla sentido y, una vez se ha sentido, las palabras se quedan cortas para explicarla. […] La felicidad consiste en tener una vida lograda, donde intentamos sacar el mejor partido a nuestros valores y a nuestras aptitudes. La felicidad es hacer una pequeña obra de arte con la vida, esforzándonos cada día por sacar nuestra mejor versión. […] La felicidad verdadera no está en el tener, sino en el ser. […] La felicidad no es lo que nos pasa, sino cómo interpretamos lo que nos pasa. Tu realidad depende de cómo decides percibirla. […] Nuestra forma de ser es la base de la verdadera felicidad. […] La felicidad es la capacidad de vivir instalado de manera sana en el presente, habiendo superado las heridas del pasado y mirando con ilusión el futuro.

Cómo hacer que te pasen cosas buenas

Marian Rojas Estapé

Acknowledgements to the financial support

Itziar Gómez Aguado thanks the University of the Basque Country (UPV/EHU) for her research grant (PIF17/067). This research was funded by the UPV/EHU (GIU17/032 and GIU20/048).

Acknowledgements to the technical assistance

Itziar Gómez Aguado and authors of experimental work wish to thank the technical and human support provided by SGIker of "Analytical and High-Resolution Microscopy in Biomedicine" (UPV/EHU/ERDF, EU).

Acknowledgements to the editorials

Authors would like to acknowledge the editorial MDPI for granting the license to reuse the published publications in this thesis.

GLOSSARY

7-AAD: 7-amino-actinomycin D

AAV: adeno-associated viruses

AdV: adenovirus

AIDS: acquired immune deficiency syndrome

ARPE-19: Human Retinal Pigmented Epithelial cells

ASO: antisense oligonucleotides

ATP: adenosine triphosphate

AuNPs: gold nanoparticles

CAR T cell: chimeric antigen receptor T cell

CCK-8: cell counting kit-8

CCR5: C-C motif chemokine receptor type 5

CMV: cytomegalovirus

CNV: corneal neovascularization

COVID-19: coronavirus disease 2019

CRISPR/Cas9: clustered regularly interspaced short palindromic repeats (CRISPR)-associated nuclease Cas9 (Cas9)

CRISPR: clustered regularly interspaced short palindromic repeats

DAPI: 4',6-diamidine-2'-phenylindole dihydrochloride

DC: dendritic cells

DLS: dynamic light scattering

DMEM/F-12: Dulbecco´s Modified Eagle´s Medium/Nutrient Mixture F-12

DNA: deoxyribonucleic acid

DNase I: Deoxyribonuclease I

DODAP: 1,2-dioleoyl-3-dimethylammonium propane

DODMA: 1,2-dioleyloxy-N,N-dimethyl-3-aminopropane

DOPE: dioleoylphosphatidylethanolamine

DOTAP: 1,2-dioleoyloxy-3-(trimethylammonium)propane)

DOTMA: N-[1-(2,3-dioleyloxy)propyl]-N,N,N-trimethylammonium chloride

DSB: double strand break

DSPC: 1,2-distearoyl-sn-glycero-3-phosphocholine

DX: dextran

ECM: extracellular matrix

ELISA: enzyme-linked immunosorbent assay

EMA: European Medicinal Agency

EMEM: Eagle's Minimum Essential Medium

FBS: fetal bovine serum

FDA: Food and Drug Administration

FGF: fibroblast growth factor

GABP: GA binding protein

GFP: green fluorescent protein

gp100: glycoprotein 100

HA: hyaluronic acid

HCE-2: Human Corneal Epithelium cells

HDR: homologous-dependent repair

HEK-293: Human Embryonic Kidney cells

HII: hexagonal phase II

HIV: human immunodeficiency virus

HLA-G: human leukocyte antigen-G

HSK: herpes simplex virus-induced stromal keratitis

HSV-1: herpes simplex virus type 1

HUVEC: Human Umbilical Vein Endothelial Cells

HVJ: hemagglutinating virus of Japan

IFN-γ: interferon-gamma

IL: interleukin

IVT mRNA: *in vitro* transcribed mRNA

LDP: laser doppler velocimetry

LNP: lipid nanoparticle

LSGS: Low Serum Growth Supplement

LV: lentivirus

MC3: Dlin-MC3-DMA

MHC: major histocompatibility complex

MMP: matrix metalloproteinase

MNPs: magnetic nanoparticles

MPS: mucopolysaccharidosis

mRNA: messenger RNA

NHEJ: non-homologous end joining

OTC: ornithine transcarbamylase

P: protamine sulfate salt

pbs: first binding site

PBS: phosphate buffered saline

PCSK9: pro-protein convertase subtilisin/kexin 9

PDGF: platelet-derived growth factor

PDI: polydispersity index

pDNA: plasmid DNA

PEG: polyethylene glycol

PEI: polyethyleneimine

PFA: paraformaldehyde

POPE: 1-palmitoyl-2-oleoylsn- glycero-3-phosphoethanolamine

PPARγ: peroxisome proliferator-activated receptor gamma

p-shRNA: plasmid codifying shRNA

p-shRNA-MMP-9: short-hairpin interference RNA against MMP-9

p-shRNA-MMP-9-GFP: short-hairpin interference RNA against MMP-9 and GFP

PVA: polyvinyl alcohol

RFU: relative fluorescent units

RLB: reported lysis buffer

RNA: ribonucleic acid

RNAi: interference RNA

RV: retrovirus

SARS-CoV-2: severe acute respiratory syndrome coronavirus-2

SDS: sodium dodecyl sulphate

sgRNA: single RNA guide

shRNA: short hairpin RNAs

shRNAscr: p-shRNA-scramble

siRNA: short interference RNA

SLNs: Solid Lipid Nanoparticles

$SLN_{C:}$ coacervation SLNs

SLN_{EE}: evaporation/emulsification

SLN_{HM}: hot-melt emulsification SLNs

sVEGFR2: cell surface membrane-bound VEGF receptor 2

TAA: tumor-associated antigens

TALEN: transcription activator-like effector nucleases

TEM: Transmission Electron Microscopy

TGF-β: transforming growth factor beta

TNF: tumor necrosis factor

TTR: transthyretin

VEGF: vascular endothelial growth factor

VEGFR1: cell surface membrane-bound VEGF receptor 1

ZFNs: zinc finger nucleases

Table of contents

ENGLISH VERSION

SECTION 1: INTRODUCTION

1. STATE OF THE ART

1.1. Gene therapy medicinal products

According to the European Medicines Agency (EMA), a gene therapy medicinal product generally consists of a vector or delivery formulation/system containing a genetic construct engineered to express a specific transgene ('therapeutic sequence') for the regulation, repair, replacement, addition or deletion of a genetic sequence [1]. Nevertheless, scientifically a broader view is usually accepted, and the concept of gene therapy includes the therapeutic application of products containing any nucleic acid.

Gene therapy has been clinically implemented primarily through two different approaches: *ex vivo* or *in vivo* (Figure 1). In *ex vivo* therapy, cells are harvested from the patient or a donor, *in vitro* modified with the therapeutic nucleic acid and finally, re-infused into the patient. *In vivo* gene therapy is applied by direct administration of the vector containing the nucleic acid into the patient [2].

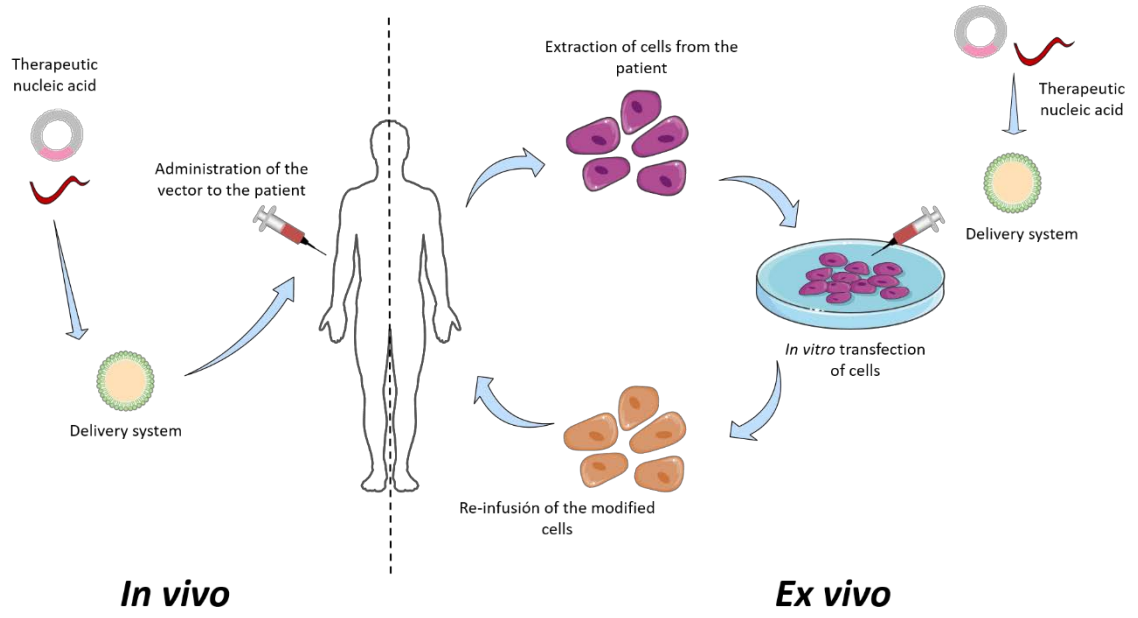

Figure 1. Representative scheme of in vivo and ex vivo approaches to gene therapy.

Depending on the final objective, gene therapy can be applied to gene augmentation, gene silencing, or gene editing (Figure 2) [3]. So that, diverse nucleic acids are used to address the development of these new medicinal products. DNA and messenger RNA (mRNA) induce protein expression, whereas small interfering RNA (siRNA), microRNA, oligonucleotides or aptamers provides posttranslational gene silencing [4]. Molecular scissor and gene editing approaches such as zinc finger nucleases (ZFNs), transcription activator-like effector nucleases (TALEN), and

clustered regularly interspaced short palindromic repeats (CRISPR)-associated nuclease Cas9 (CRISPR/Cas9) are also being developed.

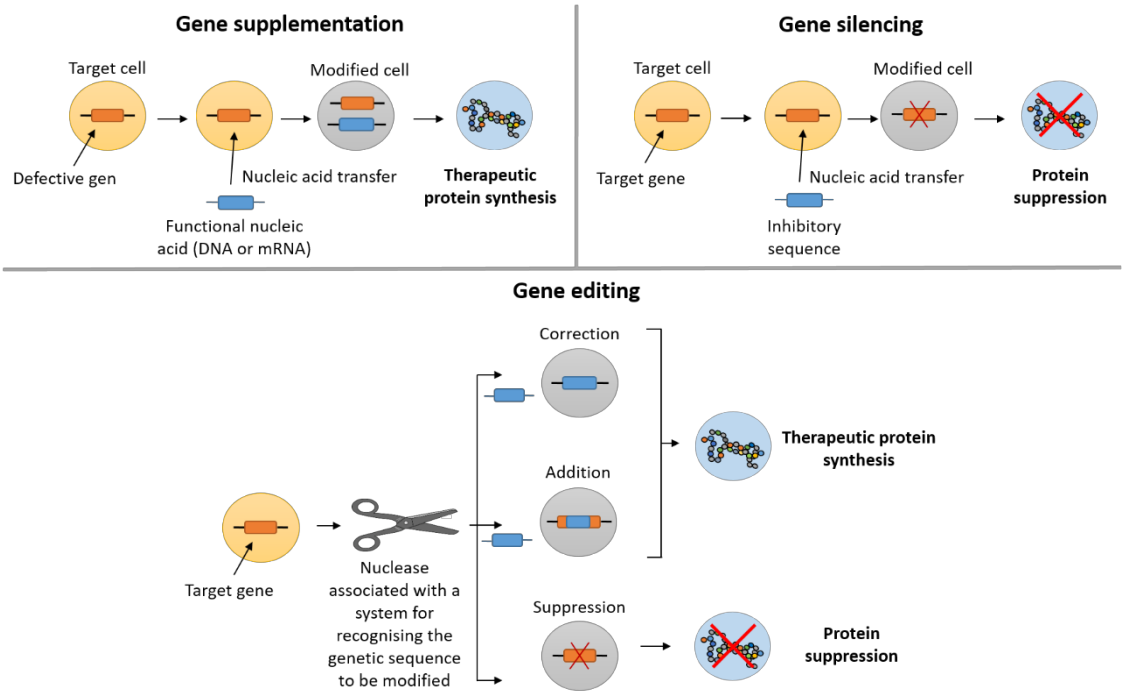

Figure 2. Representative scheme of the different strategies of gene therapy depending on the final objective.

Gene supplementation consists of the delivery of functional copies of a nucleic acid (DNA or mRNA) to express a therapeutic protein. Classically, protein supplementation has been addressed through the administration of plasmid DNA (pDNA), and in recent times, mRNA therapeutics have gained much attention due to specific characteristics that make it a promising alternative to pDNA. Firstly, mRNA does not need the machinery of the nucleus to be functional, as DNA therapies do [5–8]. Therefore, once mRNA reaches the cytoplasm, it starts translating the protein that encodes, being effective in both, mitotic and non-mitotic cells [9–11]. Secondly, mRNA has a better safety profile because unlike DNA, it does not integrate into the host genome, thereby reducing the risk of carcinogenesis and mutagenesis, [5–8,11]. In addition, it works without encoding additional genes [9]. Thirdly, the synthesis of the encoded protein is fast and its expression is temporary [6,9]. Onset of expression is usually detected within 1 hour after transfection with a peak in expression 5–7 hours later [12]. Finally, the production of *in vitro* transcribed mRNA (IVT mRNA) is easier than the manufacturing of DNA, and it can be standardized maintaining its reproducibility [7].

Indeed, mRNA therapy has gained much attention after its application in the vaccination against the severe acute respiratory syndrome coronavirus-2 (SARS-CoV-2) [13–15]. It should be noted

that during the coronavirus disease 2019 (COVID-19) pandemic, the first vaccines approved for distribution and use against SARS-CoV-2 by the EMA and the United States Food and Drug Administration (FDA) were based on mRNA encapsulated in lipid nanoparticles [16,17]. These mRNA vaccines have been well-tolerated and have demonstrated approximately 95% efficacy against COVID-19, with few adverse events [18,19].

Nevertheless, the use of IVT mRNA for clinical purposes has been mostly limited by its physical instability, its immunogenic capacity, and the difficulty in passing through the cellular membrane, due to the anionic nature of mRNA molecules [8,20,21]. The knowledge of mRNA structure has boosted modifications designed to improve stability and translation efficacy, and to reduce immunogenicity; however, optimized IVT mRNA still has to overcome several extracellular and intracellular barriers.

The formulation of nucleic acids in suitable nanosystems or vectors is frequently a requirement for surpassing these extracellular and intracellular barriers. As observed in Figure 3, nucleic acid-nanosystems need to beat several barriers before reaching their intracellular target: extracellular environment, cell membrane, intracellular trafficking, escape from endocytic vesicles and, in the case of DNA also the nuclear envelope [7,22].

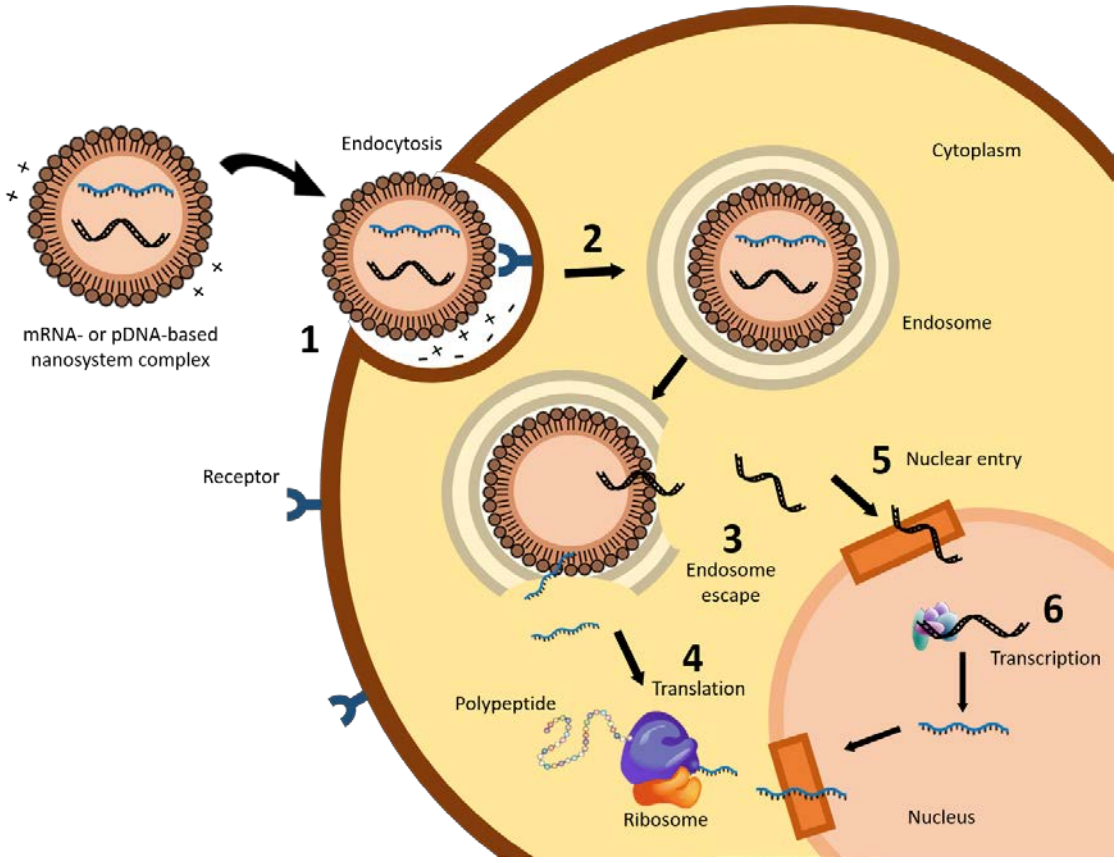

Figure 3. Intracellular barriers for nucleic acid delivery systems: (1) interaction between delivery system and cell membrane, (2) endocytosis, (3) endosomal escape and release of the genetic material to the

cytoplasm, (4) translation of mRNA, (5) nuclear entry of pDNA, and (6) transcription process of the pDNA to obtain mRNA and release to cytoplasm to start translation process. Adapted from: I Gómez-Aguado, J. Rodríguez-Castejón, M. Vicente-Pascual, et al. Nanomedicines to Deliver mRNA: State of the Art and Future Perspectives. Nanomaterials 2020, 10, 364; https://doi.org/10.3390/nano10020364.

The first step for an efficient internalization of nucleic acid is the interaction between the delivery system and the cell membrane. The attachment to the cell surface may occur through electrostatic interactions between the system and the membrane surface, which is favored for those presenting a cationic nature [23]. Cell binding can also be improved by incorporating ligands into the vectors, which are able to interact with specific cell surface receptors [24,25].

The main mechanism of cell entry is endocytosis. It comprises a variety of complex processes that determine the intracellular disposition of the genetic material. The vectors are included into endosomes by the invagination of the cell membrane. Endosomes mature and fuse with lysosomes, where the acidic environment and the presence of hydrolytic enzymes can degrade the vector and the nucleic acid. Therefore, the endosomal escape before degradation is considered a bottleneck for a successful nucleic acid delivery, and, as in the case of the cellular internalization, the delivery system plays a crucial role. The foremost proposed mechanisms of endosomal escape include endosome disruption, active transport, or fusion of the delivery system with the endosomal membrane [26]. However, Patel et al. have recently identified that late endosome/lysosome formation is essential for functional delivery of exogenously presented mRNA [27].

1.1.1. Nucleic acid delivery systems

A key challenge for the clinical application of nucleic acid-based medicinal products entails the availability of delivery systems specifically adapted to their features and purpose. A vehicle for the protection of genetic material in addition to protecting it and providing specificity to reach the target cell, must afford an adequate intracellular disposition of the nucleic acid that enables the translation process, and all of this, while preventing the activation of the immune response [28,29].

Currently, around 70% of the clinical trials with nucleic acids use recombinant viruses as delivery systems, such as retroviruses (RV), lentiviruses (LV), adenoviruses (AdV) and adeno-associated viruses (AAVs), among others [30]. Viral systems are genetically modified viruses that prevent their replication in the host cell; they present high capacity of transfection, but also oncogenic and immunogenic potential. Moreover, viral vectors present a limitation regarding the size of the nucleic acid they can transport [31]. Despite the major advances achieved in DNA delivery with viral vectors, they do not play an important role for mRNA delivery [7,32–35]. Non-viral

systems are safer, their production is simpler, more economical and reproducible than viral vectors. Moreover, the size of nucleic acid to be packed is not usually an obstacle. However, their efficacy of transfection is still a limitation, and although it has been improved by different strategies, the efforts are still ongoing [32,34,36].

Therapeutic application of nucleic acids without the help of a delivery system presents important drawbacks [37]. Naked nucleic acids have been mainly applied *ex vivo* by using physical methods, including electroporation, microinjection and gene gun; these methods are able to disrupt the cell membrane and facilitate the entry of genetic material into the cell [38]. Electroporation consists of generating pores in a cell membrane through electric pulses. This technique has shown efficient mRNA transfection for the introduction of tumor antigens into dendritic cells (DCs) [39]; even in some studies mRNA electroporation has been more efficient compared to that of DNA, with faster and more homogeneous protein expression *in vivo* [40]. Microinjection, the direct injection of a nucleic acid into the target cell by using microneedles [41,42], and gene gun, in which naked genetic material is pneumatically shot into the target cell, have also been used [43–46]. Intravenously administered naked nucleic acids are rapidly degraded by nucleases and the innate immune system can be activated. In contrast, local injections, such as subcutaneous, intramuscular or intranodal, have been useful for naked mRNA delivery. Especially for the activation of the immune system, and when a small amount of protein is required, as happens in vaccination [47].

Chemical nanocarriers are nowadays at the forefront of pharmaceutical research for mRNA delivery; in contrast to DNA-based gene therapy, in which viral vectors are preferred. Thanks to the advances made in material sciences, nanotechnology, and nucleic acid chemistry, an extensive work is currently ongoing to develop new systems [39]. Chemical nanocarriers are formed by synthetic or natural biocompatible components that form complexes with the mRNA, and vary in composition, size, shape, and physicochemical characteristics. In addition to the function of protecting the nucleic acid from degradation and denaturation, they all should facilitate the transfection process, by being minimally toxic and immunologically responses [48]. Moreover, these delivery systems could be also useful to programme the release profile of the active substance, improve the pharmacokinetic profile, reduce the toxicity in healthy organs/tissues and increase the blood circulation time [28,49]. As it can be seen in Figure 4, nanocarriers for nucleic acid delivery evolve into various forms, including lipidic, polymeric and polypeptide systems, dendrimers, gold nanoparticles, and hybrid systems. The design of specific delivery systems adapted to the nucleic acid features are necessary to protect the genetic material allowing a suitable intracellular disposition to favor the transduction process.

Considering the increased knowledge and current availability of tools to design novel nanomaterials, it is expected that new formulation strategies can further improve pharmacological profiles, and thus, expand mRNA utility.

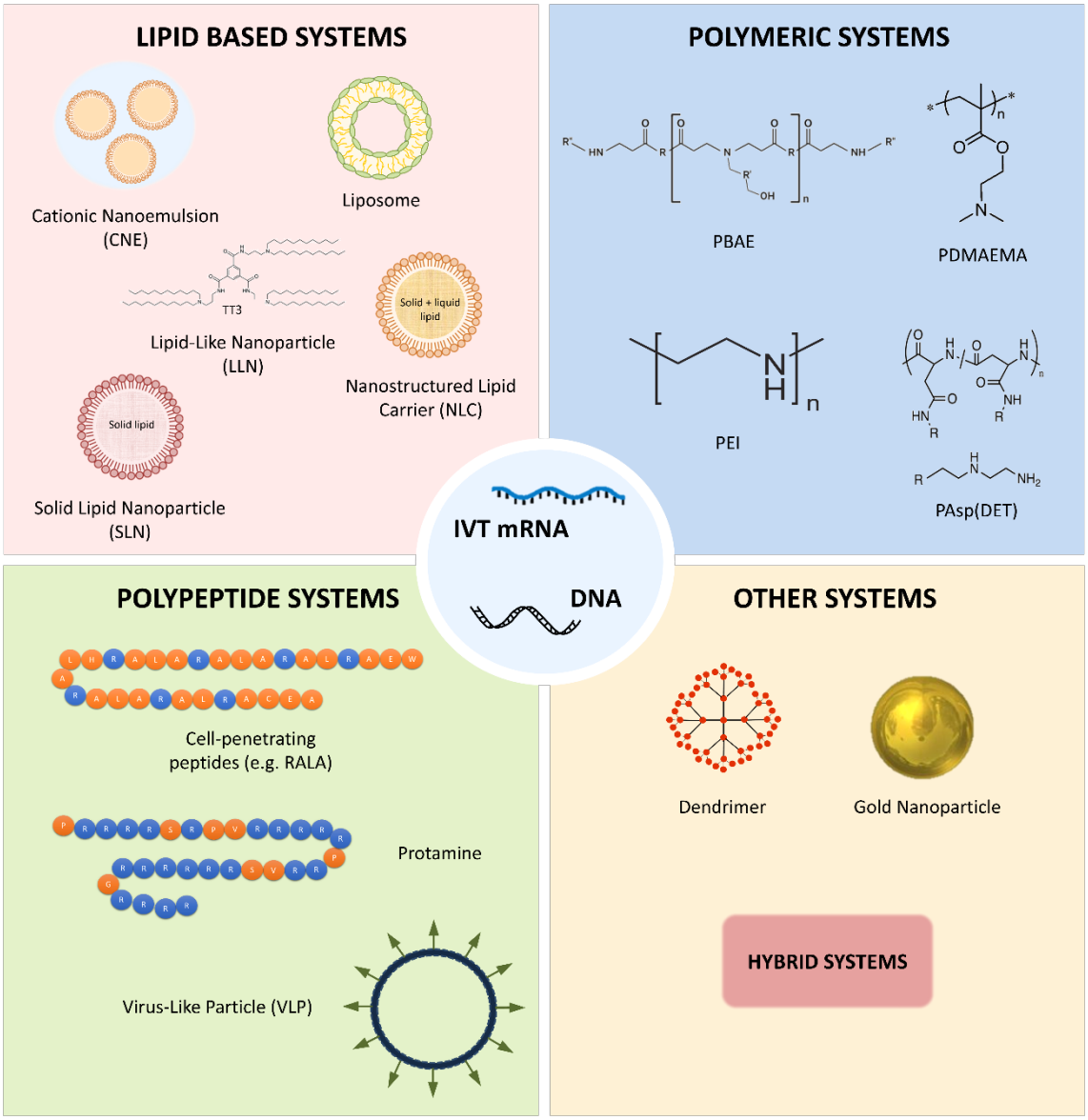

Figure 4. Representative scheme of chemical nanocarriers for the nucleic acid delivery. PBAE: poly(β-amino ester); PDMAEMA: poly(2-dimethylaminoethyl methacrylate); PEI: polyethyleneimine; PAsp(DET) 1,2-diaminoethane poly(aspartamide). Adapted from: I Gómez-Aguado, J. Rodríguez-Castejón, M. Vicente-Pascual, et al. Nanomedicines to Deliver mRNA: State of the Art and Future Perspectives. Nanomaterials 2020, 10, 364; https://doi.org/10.3390/nano10020364.

Among them, lipid-based vectors are the most widely used non-viral carriers for nucleic acids. The main components of lipidic systems are cationic lipids, which are able to interact with nucleic acids by electrostatic interactions, leading to the formation of a complex called lipoplex [35].

DOTMA (N-[1-(2,3-dioleyloxy)propyl]-N,N,N-trimethylammonium) is one of the most studied cationic lipids for nucleic acid delivery, and it was the first synthetic cationic lipid utilized to complex IVT mRNA [50]. DOTAP (1,2-dioleoyloxy-3-(trimethylammonium)propane) is another traditional synthetic lipid derived from DOTMA, which is more economical to synthesize and presents greater efficacy [35]. DOTAP has been frequently combined with the zwitterionic lipid DOPE (1,2-dioleoyl-sn-glycero-3-phosphoethanolamine), to prepare colloidal systems able to bind the nucleic acids. This mixture facilitates the endosomal escape under acidic pH conditions, thanks to the capacity of DOPE to modify the lipoplex from a bilayer model to hexagonal phase II (HII) structures, known to induce supramolecular arrangements which result in the fusion of lipid bilayers [7,51]. The use of DOTAP alone or in combination with the helper lipid DOPE has been applied to DNA and mRNA delivery [52–55].

More recently, ionizable lipids with lower toxicity, but preserving the transfection capacity, such as 1,2-dioleoyl-3-dimethylammonium-propane (DODAP) or 1,2-dioleyloxy-3-dimethylamino-propane (DODMA), have been developed as an alternative to conventional cationic lipids [5]. While cationic lipids present alkylated quaternary ammonium groups and retain their cationic nature regardless of their pH, ionizable lipids acquire positive charges, due to the protonation of free amines as pH decreases [20]. These new lipids are neutral at physiological pH but positively charged inside the endosome, when pH values are below its pKa.

The electrostatic interactions between naturally occurring anionic lipids in endosomal membranes and the ionizable cationic lipids have been proposed as the underlying mechanism of nucleic acid release [46]. These interactions are able to promote membrane lytic nonbilayer structures, such as the HII, culminating in the intracellular nucleic acid delivery [56].

Nowadays, nanocarriers containing ionizable cationic lipids are among the leading delivery system candidates with promising applications for siRNA and mRNA delivery [35]. Figure 5 shows chemical structure of the the most frequently used cationic and ionizable lipids to formulate nucleic acid delivery systems.

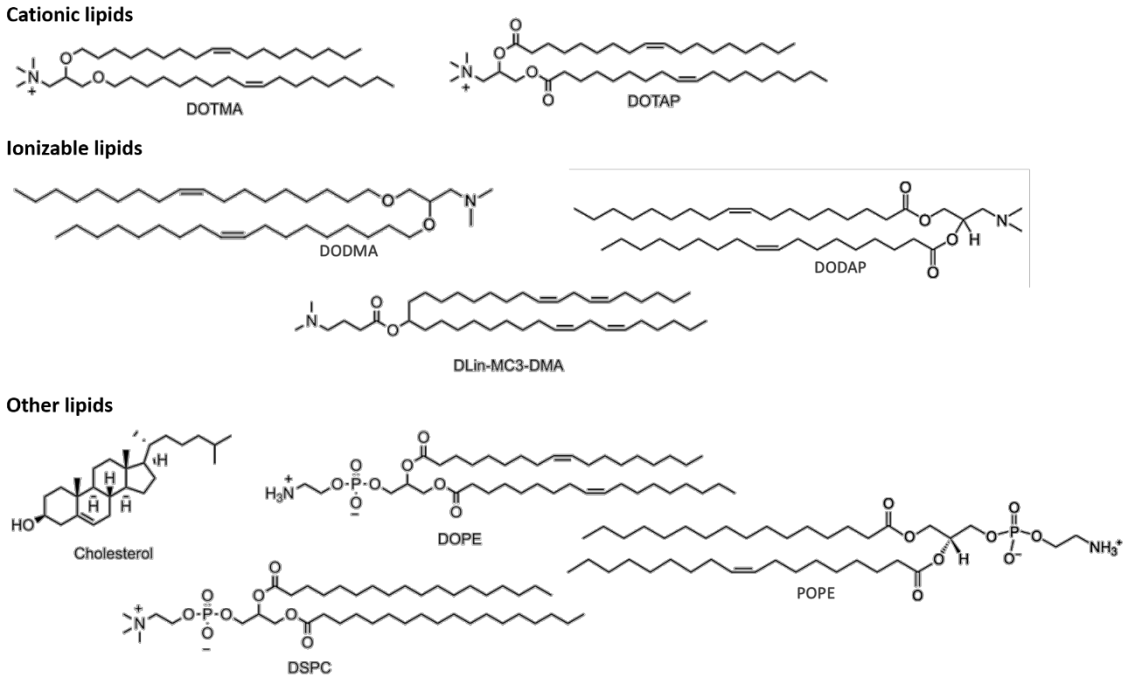

Figure 5. Chemical structure of the cationic and ionizable lipids most frequently used to formulate nucleic acid delivery systems. DOTMA: N-[1-(2,3-dioleyloxy)propyl]-N,N,N-trimethylammonium chloride; DOTAP: 1,2-dioleoyloxy-3-(trimethylammonium)propane); DODMA: 1,2-dioleyloxy-N,N-dimethyl-3-aminopropane; DODAP: 1,2-dioleoyl-3-dimethylammoniumpropane; DOPE: dioleoylphosphatidylethanolamine; DSPC: 1,2-distearoyl-sn-glycero-3-phosphocholine; POPE: 1-palmitoyl-2-oleoylsn- glycero-3-phosphoethanolamine.

Cationic lipids are usually formulated to prepare lipid nanoparticles (LNPs). LNPs include liposomes and other lipid-based nanoparticles, and they are regarded as one of the most studied non-viral vectors in clinical research. Currently, several LNP platforms are at the forefront of clinical trials, and they are clinically validated delivery systems for RNA therapy. In the beginning, LNPs were considerably promising for the delivery of siRNA, being their utility as mRNA delivery agents more recent [57]. In this sense, Patisiran (ONPATTRO™), a siRNA formulated in LNPs targeted to inhibit hepatic transthyretin protein, received the FDA approval in 2018, leading to significant progress in the field [58]. This product contains a novel ionizable lipid, Dlin-MC3-DMA (MC3) [59], and after Patisiran approval, MC3 has also been used as a vehicle for transferring mRNA [60]. The previous experience in siRNA formulation is benefiting the development of mRNA nanosystems, although the different structure of mRNA may interfere the packing capacity of nanoparticles [57].

Liposomes were introduced as carriers for the delivery of nucleic acids over two decades ago and to date, they still represent the most widely studied vectors for gene delivery. Liposome based formulations are amphiphilic spherical vesicles formed by one or more lipid bilayers enveloping an aqueous core with a size ranging from 20 nm to a few microns. They generally

contain a cationic lipid combined with: (a) a helper lipid that supports the bilayer structure and facilitates the endocytosis; (b) cholesterol to stabilize the lipid bilayer of the LNP; and (c) a polyethylene glycol (PEG)-lipid. PEG lends the nanoparticle a hydrating layer to improve colloidal stability, reduces protein adsorption and non-specific uptake, and prevents reticuloendothelial clearance [20,48]. Additionally, helper lipids, such as DSPC (1,2-distearoyl-sn-glycero-3-phosphocholine), DOPE and POPE (1-palmitoyl-2-oleoyl-sn-glycero-3-phosphoethanolamine) are frequently used in these systems [61].

The *in vivo* delivery of mRNA by using this kind of lipid-based system was already evaluated in 1994 [62], proving a comparable efficacy to liposome-DNA complexes in accomplishing *in situ* tumor transfection. That study also showed that mRNA might be considered as an alternative to pDNA for genetic immunopotentiation applications. More recently, LNPs containing an ionizable cationic lipid, phosphatidylcholine, cholesterol and PEG-lipid were used to encapsulate IVT mRNA encoding the pre-membrane and envelope glycoproteins of a strain from Zika virus [63]. A single intradermal low-dose immunization elicited potent and durable neutralizing antibody responses and protective immunity in mice and non-human primates. A self-amplifying mRNA (SAM) vaccine platform is another example of a synthetic mRNA delivered by LNPs. SAM vaccine encoding an influenza H1HA antigen from N1H1 virus, and formulated with 1,2-dilinoleyloxy-3-dimethylaminopropane, 1,2-diastearoyl-sn-glycero-3-phosphocholine, cholesterol and PEG-DMG 2000, has demonstrated to be immunogenic in mice at low doses, and to elicit antibody responses that were comparable to the licensed vaccine [64]. The use of mRNA-liposomes in cancer therapy has increased dramatically, since the first study in 1999. Zhou et al. [65] used the hemagglutinating virus of Japan (HVJ)-based liposomes for the synthesized mRNA encoding the human melanoma-associated antigen glycoprotein 100 (gp100). Direct injection into the mouse spleen induced gp100 antibody expression and cellular immune responses against B16 melanoma cells. Recently, the first-in-human, open label phase I study in ovarian cancer patients has been approved. Patients will be vaccinated intravenously prior, and during (neo)-adjuvant chemotherapy with a liposome formulated mRNA vaccine (W_ova1 vaccine) which includes three ovarian cancer- tumor-associated antigens (TAAs) RNAs (ClinicalTrials.gov Identifier: NCT04163094).

LNP has also been applied for CRISPR/Cas9 delivery. Finn et al. [66] developed an LNP-based formulation including a biodegradable and ionizable lipid termed LP01, Spy Cas9 mRNA, and a single RNA guide (sgRNA). A single systemic administration to mice of the LNP-based CRISPR/Cas9, produced significant editing of the mouse transthyretin (*Ttr*) gene in the liver resulting in >97% reduction of TTR serum protein levels that persisted for at least 12 months.

Solid lipid nanoparticles (SLNs) are regarded as one of the most effective lipid-based colloidal systems in gene therapy [67]. SLNs were developed, principally, with a view to address the efficacy and safety limitations that liposomes present [68]. SLNs are spherical nanometric particles formed by an aqueous dispersion stabilized by surfactants surrounding a solid lipid core matrix, which are usually made of well-tolerated physiological lipids [69–72]. SLNs present good stability and can be sterilized and lyophilized. Moreover, SLNs can be easily functionalized for targeting by incorporating specific ligands taking into account the features of the genetic material and the target cell [73–75]. SLNs have demonstrated to be efficient as nucleic acid delivery systems *in vitro* and *in vivo* mainly for pDNA delivery in lysosomal storage disorders [76,77], various types of cancer [32] and ocular diseases [75,78–80].

1.2. New strategies based on gene therapy for the treatment of corneal inflammation

The eye is a highly specialized organ, in which each individual structure works together to capture and process visual information. It is generally divided into two compartments, the anterior and posterior segments [81]. The cornea is a transparent tissue localized in the anterior segment of the eye, which contributes to eyesight by focusing a visual image through light refraction. The cornea is comprised of three layers and two membranes: the external stratified epithelium and the medial stromal layer are separated by the transparent Bowman's membrane, and the Descemet's basement membrane separates the stroma and the inner endothelium (Figure 6). A tear film coats the convex anterior surface of the cornea, whereas the concave posterior surface is in direct contact with the aqueous humor. Both the cornea and the sclera constitute the whole external coat of the eye.

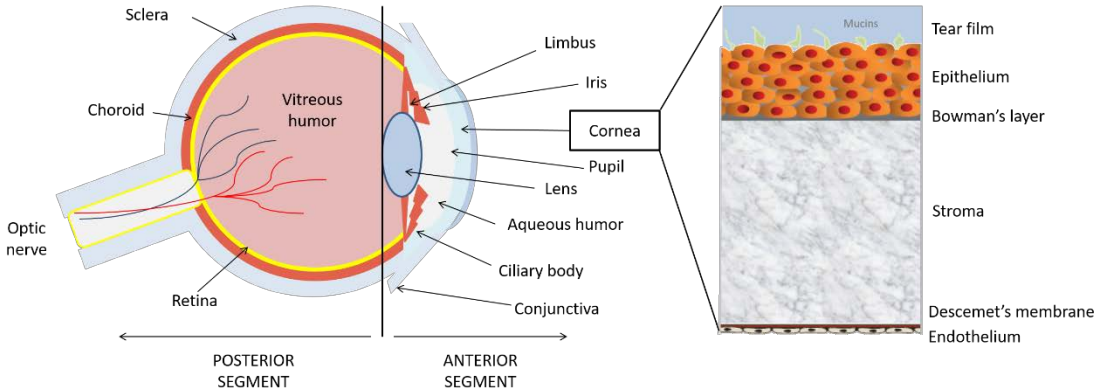

Figure 6. Schematic representation of the human eyeball and corneal layer structure.

The eye is considered the perfect target for gene therapy due to its physiological features: it is easy to access and examine, it has a well-defined anatomy and it is relatively immune privileged.

Moreover, from an experimental point of view, in the same subject, one eye can be used as a control, whereas the other eye can be used as the experimental target [82–84]. Additionally, the anatomic location of corneal epithelium allows the non-invasive direct topical instillation of the nucleic acid delivery systems. Finally, the cornea permits visual, non-invasive and rapid examination by conventional ophthalmological procedures without patient risk [85].

It was 1994 when the first study about corneal gene therapy was reported [86]. In this study, the potential application of gene therapy correcting acquired inflammatory diseases of the cornea was noted after successful transduction of corneal tissues using replication-deficient adenoviruses. Most studies use viral vectors for transfecting the cornea, in particular RVs, LVs, AdVs, and AAVs. However, the induction of immune response and inflammation, even considering the immune-privilege of the cornea, limits the application of viral-based vectors in inflammatory diseases [78]. In addition, the administration of viral vectors has mainly been carried out by invasive methods, including intrastromal, intralimbal, intracameral, or after removing the corneal epithelium [67,87,88]. In contrast, non-viral gene therapy has demonstrated to be a promising alternative for corneal gene therapy even after topical administration [89–92]. Among others, magnetic nanoparticles [93], hyaluronan/chitosan nanoparticles [89], hybrid nanoparticles based on gelatin and chondroitin sulphate [94], polyethylenimine [95], gold nanoparticles [91], polyethylenimine-conjugated gold nanoparticles [96], and SLNs [90] have been tested as non-viral vectors for corneal gene therapy. SLNs have demonstrated to be effective for ocular topical drug administration [97].

Topical ocular administration shows several advantages: it is non-invasive, drug absorption into the systemic circulation is minimized, first pass metabolism is prevented, and formulations are easy to administer. However, the main issue of conventional ocular drug delivery systems relies on the poor retention onto the ocular surface due to corneal clearance; as a consequence, the amount of drug that is able to get through the cornea and access the ocular structures is small. Therefore, an effective ocular drug delivery system should increase corneal retention time and enhance drug permeation through the cornea [98]. SLNs possess suitable characteristics for improving corneal permeation and retention after topical drug administration, such as nanometer size-range, lipophilic properties, and usually positive surface charge. [99,100].

Several factors can damage the cornea and provoke corneal inflammation or keratitis, such as infections, dry eye, eyelid disorders, physical and chemical damage, and a wide variety of underlying diseases [78]. Infections are the principal cause of corneal inflammation, specifically, those provoked by herpes simplex virus type I (HSV-1), with an incidence of about 1.5 million,

including 40,000 new cases of related blindness each year [101]. In developing countries, the infection of HSV-1 is the leading cause of keratitis-associated infectious blindness [102].

Although some of the keratitis cases result of unknown factors, the main risk factors involve any rupture or disruption of the superficial layer of the cornea. Moreover, the risk of keratitis increases as contact lens wear increases, as well as, by alterations of immune system due to diseases, including immune deficiency syndrome (AIDS), or the use of medicinal drugs, such as, corticosteroids or chemotherapy [103,104].

Regardless of the keratitis origin, common symptoms include pain in the eye, blurred vision, photophobia, tearing and redness of the eyes. In addition, chronic inflammation of the cornea induces visual disturbance, and often results in tissue destruction that leads to corneal ulceration, scarring and, even, perforation, causing visual impairment and blindness [105].

1.2.1. Inflammation process

The inflammation process involves a complex and active wound healing process, in which a wild variety of molecules participate modulating the response to inflammatory stimuli. These molecules are extracellular matrix (ECM) proteins, cytokines and growth factors, among others. Three different phases that can be temporally overlapped occur in the inflammation process: inflammatory phase, proliferative phase and tissue remodeling and/or maturation phase. In the beginning, the recruitment of neutrophils and macrophages in the wound area is triggered in response to chemokines. In the next phase, ECM deposition occurs, which comprises the migration and proliferation of cells into the matrix of the scaffold, including the formation of new blood vessels, the proliferation of fibroblast and ECM production. The disruption of corneal integrity provokes the differentiation of normal corneal quiescent keratocytes into fibroblasts and/or myofibroblasts [106]. Finally, there is a degradation of matrix stroma by the proteolytic enzymes, in addition to vascular regression, the remodeling of the granulation tissue and the new formation of ECM components [107,108].

A group of enzymes that present a key role in all phases of the inflammatory process are matrix metalloproteinases (MMPs) [109–113]. They are involved in ECM remodeling, epithelial barrier function and corneal epithelial cell migration to the underlying stroma [110,114–118].

The cells of the immune system produce and secrete pro-inflammatory or anti-inflammatory cytokines and proteins that control the inflammation process and preserve the physiological condition of the cell [119,120]. Around twenty five cytokines have been detected in healthy subject tears that maintain the ocular surface in physiological conditions [119]. Within these cytokines we can find: interferon-gamma (IFN-γ), transforming growth factor beta (TGF-β)

interleukins (IL), and chemokines (small cytokines) participating in cellular and humoral immune responses [121]. The proinflammatory cytokines include IL-13, IL-6, IL-1b and tumor necrosis factor (TNF)-α. These molecules participate in the corneal inflammation by increasing angiogenic factors, such as vascular endothelial growth factor (VEGF) and MMP-9 [116,120,122–125]. In the anti-inflammatory cytokines group, IL-10 excels in the inhibition of the production of monokines including IL-1, IL-6, IL-8 and TNF-α [126–130].

1.2.2. Inflammation and corneal neovascularization

Angiogenesis is a vital process in the reproduction and development of tissues, as well as for wound healing. However, in corneal development and physiology it is more important the production of higher levels of angiostatic factors than angiogenic factors in order to maintain an avascular stroma. A wide range of pathological challenges to the cornea can alter its intrinsic balance and promote angiogenesis and corneal neovascularization (CNV) in any layer of the cornea. The inflammatory process can induce an imbalance between angiogenic and anti-angiogenic factors leading to vascularization of the cornea, that is CNV [131]. Although neovascularization is part of the repair process of extensive damage to the eye surface [132], it can compromise visual acuity because the cornea loses its avascularity feature.

Current treatment options for CNV include the topical application of nonsteroidal or corticosteroidal anti-inflammatory agents, immunosuppressive drugs or surgical interventions, such as photodynamic therapy cauterization and-irradiations [133]. However, the limited efficacy and adverse effects restrict the current treatment therapies [134] and makes necessary the finding of new therapeutic strategies.

1.2.3. Application of gene therapy to corneal inflammation

The main strategies of gene therapy to treat corneal inflammation are directed to either inflammatory mediators or neovascularization. [135,136]. Gene supplementation with pDNA and gene silencing strategies, including short hairpin RNA (shRNA), have been studied.

1.2.3.1. Gene therapy targeted to corneal neovascularization

The treatment of CNV based on gene therapy can be tackled with two different approaches: gene supplementation to express an anti-angiogenic factor, and/or gene suppression to inhibit the synthesis of a pro-angiogenic factor [112]. A current review reports a broad and complete overview of therapeutic target genes and potential vectors to treat CNV [134]. Table 1 summarizes the main anti-angiogenic and pro-angiogenic factors involved in CNV.

Table 1. The main anti-angiogenic and pro-angiogenic factors involved in CNV.

Anti-angiogenic factors	Pro-angiogenic factors
Vasohibin-1 [137]	Vascular endothelial growth factor (VEGF) [138,139]
Endostatin [140–142]	Cell surface membrane-bound VEGF receptor 1 (VEGFR1, also known as sflt-1) [138]
Angiostatin [143,144]	Cell surface membrane-bound VEGF receptor 2 (sVEGFR2) [145]
Peroxisome proliferator-activated receptor gamma (PPARγ) [146]	Fibroblast growth factor (FGF) [147]
Decorin [148]	Angiogenin [105,149]
Brain-specific angiogenesis inhibitor [150]	Prostaglandins [151]

Among pro-angiogenic factors, MMPs and in particular MMP-9 is one of the primary extracellular matrix remodeling enzymes that participate in pathological conditions of the cornea, including CNV [123]. MMPs are enzymes that are capable of cleaving numerous extracellular matrix proteins, which facilitates the migration of corneal epithelial cells to the underlying stroma and the formation of corneal neovascularization [116–118,152]. In fact, the increased production and activity of MMPs are related to a more migratory and invasive cell phenotype [153,154]. Indeed, the suppression of MMP-9 synthesis in the ocular surface contributed to the improvement in the corneal barrier function in a model of dry eye mice [155]. The suppression of the pro-angiogenic factor MMP-9 could be also a strategy for the treatment of CNV-associated inflammation.

Gene suppression strategy can be carried out by interference RNA (RNAi) technology [156]. Among RNAi molecules, shRNA, also known as expressed RNAi activator, is a plasmid-coded RNA. In contrast to other forms of RNAi [87,157], shRNA is continuously produced in the host cell and, therefore, it induces a more lasting gene silencing effect.

1.2.3.2. Gene therapy targeted to inflammatory mediators

A large number of studies have evaluated the capacity of gene therapy to express specified anti-inflammatory mediators as a treatment strategy for corneal diseases in which inflammation was involved, such as herpetic keratitis infections, since the virus induces an immunoinflammatory corneal response. It should be noted that around 10% of injured corneas due to HSV-1 ends up in corneal transplantation [158]. Although new strategies in relation with to HSV-1 genome are under study, the majority of strategies against HSV keratitis (HSK) based on gene therapy are targeted to the inflammation process [157].

In the recurrent HSK pathogenesis, the immunorregulatory cytokine IL-10 has an essential role [159]. A study has reported that the development of necrotizing stromal keratitis was hindered, and that severity of corneal disease was inhibited when intracorneal injection of recombinant IL-10 was administered after HSV infection [160]. However, the short half-life and poor eye bioavailability after topical instillation makes necessary repeated administrations to induce the therapeutic effect [161]. Alternatively, a continuous production of IL-10 *de novo* would be achieved by the genetic supplementation strategy. In fact, in a previous study, a potent expression of IL-10 was produced in murine corneas by electroporation [162].

Viral vectors have also been employed to transfer IL-10 *in vitro* and *ex vivo* to ovine and human corneas, with adenoviral vectors inducing higher efficiency than lentiviruses [163]. More recently, human leukocyte antigen-G (HLA-G), an immunomodulatory and anti- inflammatory molecule, was formulated in an AAV vector and tested in rabbits. After a single intrastromal injection, the vector demonstrated the prevention of CNV, the inhibition of trauma-induced T-lymphocyte infiltration (some of which were CD8+), and significant reduction of myofibroblasts formation [164].

Non-viral SLN-based vectors containing pDNA encoding IL-10 gene were also studied *in vitro* and *ex vivo* in rabbit cornea explants, which proved the capacity to transfect multiple corneal layers, regarding the vector composition [79]. Moreover, another study has demonstrated that gene augmentation strategy induced IL-10 production into the cornea of wild type and IL-10 knockout mice treated with SLNs containing pDNA IL-10 [80]. mRNA could be an alternative option to tackle corneal inflammation, thanks to its high efficacy, safety profile, and versatility for fast protein production.

2. METHODOLOGY

In this section, the main methods used throughout the thesis are briefly explained. Any specific methodology is accurately explained in their respective Appendixes.

2.1. Preparation of SLNs and vectors

Three different techniques were used with the aim of studying the influence of the preparation method on the characteristics of the SLNs: solvent evaporation/emulsification, hot-melt emulsification, and coacervation.

Evaporation/emulsification SLNs (SLN_{EE}) were made up as previously reported by our research group [165]. The oil phase containing Precirol® ATO 5 dissolved in dichloromethane was added to an aqueous phase of Tween 80 and the cationic lipid DOTAP, or to a mixture of DOTAP and ionizable lipids (DODAP or DOBAQ), and sonicated for 30 sec at 50 W. SLNs were obtained after dichloromethane evaporation.

Hot-melt emulsification technique (SLN_{HM}), however, avoids the use of organic solvents. In this case, the aqueous solution of cationic lipid DOTAP and Tween 80 was mixed with the melted solid lipid Precirol® ATO 5 and sonicated for 30 min at 50 W. SLNs were obtained by cooling the obtained nanoemulsion on ice for 30 min.

Finally, coacervation method (SLN_C) leads to the formation of SLNs composed of the lipid matrix behenic acid coated by the suspending agent polyvinyl alcohol (PVA) 9000 and the cationizing agent DEAE-dextran, as previously reported [80]. Briefly, sodium behenate and PVA 9000 were dissolved in water under hot agitation, and when the solution reached 80 °C and became translucent, NaOH was added. Then, when the solution turned completely transparent DEAE-dextran was added drop by drop, turning the mixture turbid. Later, HCl was rapidly added and when the suspension turned white, it was cooled under stirring in a water bath. The final product was re-melted by heating it again and cooling it by agitation in a water bath.

Table 2 summarizes the composition and preparation method of the SLNs evaluated along this doctoral thesis.

Table 2. Composition of the SLNs used along this doctoral thesis.

Type of SLN	Cationic lipid (%)			Sodium behenate (%) (w/v)	PVA 9000 (%) (w/v)	DEAE-dextran (%) (w/v)	Tween 80 (%)
	DOTAP	DODAP	DOBAQ				
$SLN1_{EE}$	0.4						0.1
$SLN2_{EE}$	0.2	0.2					0.1
$SLN3_{EE}$			0.4				0.1
$SLN4_{EE}$	0.2		0.2				0.1
$SLN1_{HM}$	0.4						0.1
SLN_C				2.1	1.05	0.33	

$SLN1_{EE}$: solid lipid nanoparticle prepared by emulsification-evaporation method containing DOTAP cationic lipid. $SLN2_{EE}$: solid lipid nanoparticle prepared by emulsification-evaporation method containing a mixture of DOTAP cationic lipid and DODAP ionizable lipid; $SLN3_{EE}$: solid lipid nanoparticle prepared by emulsification-evaporation method containing DOBAQ ionizable lipid; $SLN4_{EE}$: solid lipid nanoparticle prepared by emulsification-evaporation method containing a mixture of DOTAP cationic lipid and DOBAQ ionizable lipid; $SLN1_{HM}$: solid lipid nanoparticle prepared by hot-melt emulsification method containing DOTAP calitioc lipid; SLN_C: solid lipid nanoparticle prepared by coacervation method; PVA: polyvinyl alcohol.

The final vectors consist of SLNs, a nucleic acid, and protamine (P), and optionally, a polysaccharide and gold nanoparticles (AuNPs). After mixing all the components, electrostatic interactions allowed the formation of the final vectors. First, a complex was prepared by mixing and aqueous solution of the nucleic acid (pDNA, mRNA or plasmid shRNA (p-shRNA)) with an aqueous solution of P, and when the polysaccharide was necessary, an aqueous solution of dextran (DX) or hyaluronic acid (HA) was added. Finally, the suspension of SLNs was added to these complexes.

For pDNA studies, plasmid pcDNA3-EGFP encoding green fluorescent protein (GFP) and plasmid pUNO1-hIL10 encoding human IL-10 were used. For mRNA studies, CleanCap™ EGFP mRNA (5moU) encoding GFP and mRNA encoding human IL-10 were employed. Finally, for p-shRNA studies, plasmid encoding a short-hairpin interference RNA against MMP-9 (p-shRNA-MMP-9) and the plasmid encoding both a short-hairpin interference RNA against MMP-9 and GFP (p-shRNA-MMP-9-GFP) were used.

The composition of the formulations used along this doctoral thesis have been summarized in Table 3.

Table 3. . Composition of the different vectors used along this doctoral thesis.

Appendix	Name of the vector	Nucleic acid			Ligands				Cationic agent			
		pDNA	mRNA	p-shRNA	P	DX	HA	AuNPs	DOTAP	DODAP	DOBAQ	DEAE-dextran
II	pDNA-DX-SLN1$_{EE}$	X			X	X			X			
II	pDNA-DX-SLN2$_{EE}$	X			X	X			X	X		
II	pDNA-DX-SLN4$_{EE}$	X			X	X			X		X	
II	pDNA-HA-SLN1$_{EE}$	X			X		X		X			
II	pDNA-HA-SLN2$_{EE}$	X			X		X		X	X		
II and IV	mRNA-DX-SLN1$_{EE}$		X		X	X			X			
II	mRNA-DX-SLN2$_{EE}$		X		X	X			X	X		
II and IV	mRNA-HA-SLN1$_{EE}$		X		X		X		X			
II	mRNA-HA-SLN2$_{EE}$		X		X		X		X	X		
II	mRNA-P-SLN1$_{EE}$		X		X				X			
II	mRNA-P0.5-SLN2$_{EE}$		X		X				X	X		
II	mRNA-P1-SLN2$_{EE}$		X		X				X	X		
III	DX:P:p-shRNA-MMP-9:SLN1$_{EE}$			X	X	X			X			
IV	mRNA-DX-SLN1$_{HM}$		X		X	X			X			
IV	mRNA-HA-SLN1$_{HM}$		X		X		X		X			
IV	mRNA-SLN$_{C}$		X		X							X
IV	mRNA-HA-SLN$_{C}$		X		X		X					X
IV	pDNA-DX-SLN1$_{HM}$	X			X	X			X			
IV	pDNA-HA-SLN1$_{HM}$	X			X		X		X			
VI	pDNA-DX-SLN1$_{EE}$ _Au	X			X	X		X	X			

VI	pDNA-HA-SLN1$_{EE}$ _Au	X	X	X	X	X
VI	mRNA-DX-SLN1$_{EE}$ _Au	X	X	X	X	X
VI	mRNA-HA-SLN1$_{EE}$ _Au	X	X	X	X	X

P: protamine; DX: dextran; HA: hyaluronic acid; Au: gold; AuNPs: golden nanoparticles; SLN1$_{EE}$: solid lipid nanoparticle prepared by emulsification-evaporation method containing DOTAP cationic lipid; SLN2$_{EE}$: solid lipid nanoparticle prepared by emulsification-evaporation method containing a mixture of DOTAP cationic lipid and DODAP ionizable lipid; SLN4$_{EE}$: solid lipid nanoparticle prepared by emulsification-evaporation method containing a mixture of DOTAP cationic lipid and DOBAQ ionizable lipid; SLN1$_{HM}$: solid lipid nanoparticle prepared by hot-melt emulsification method containing DOTAP calitioc lipid; SLN$_{C}$: solid lipid nanoparticle prepared by coacervation method; PVA: polyvinyl alcohol.

2.2. Physicochemical characterization of SLNs and vectors

2.2.1. Size, PDI and ζ-potential

After the appropriate dilution in Milli-Q™ water, SLNs and vectors were characterized in terms of size, polydispersity index (PDI) and superficial charge by ZetaSizer Nano ZS (Malvern Panalytical, Malvern, UK). Size and PDI were measured by Dynamic Light Scattering (DLS) and ζ-potential was determined by Laser Doppler Velocimetry (LDP). Three replicate analyses were performed for each formulation. Data are expressed as mean ± standard deviation.

2.2.2. Transmission Electron Microscopy (TEM) images

The surface characteristics of SLN-based vectors were examined by Transmission Electron Microscopy (TEM) (Philips EM208S TEM), using electron microscopy negative staining. To this end, 10 µL of the vectors were adsorbed for 60 sec onto glow discharged carbon coated grids. Then, the remaining liquid was removed, via blotting on filter paper, and the staining was carried out with 2% uranyl acetate for 60 sec. For acquisition of digital images, an Olympus SIS purple digital camera was used.Technical and human support for TEM was provided by the Advanced Research Facilities (SGIker) of Analytical and High Resolution Microscopy in Biomedicine at the University of the Basque Country UPV/EHU (Leioa, Basque Country, Spain).

2.2.3. Agarose gel electrophoresis assay

The binding, protection and release capacity of the nucleic acids from the vectors were evaluated. The studies of pDNA-based vectors were performed in 0.7% agarose gel electrophoresis labeled with Gel Red™. The gels were run for 30 min at 120 V and immediately they were analyzed with the Uvitec Uvidoc D-55-LCD-20 M Auto transilluminator. For binding study, pDNA was diluted in Milli-Q™ water to a final concentration of 0.03 µg pDNA/µL in each well. Protection was evaluated by the addition of 1 U DNase I/2.5 µg pDNA and incubation at 37 °C for 30 min in a heater. Then, a final concentration of 1% sodium dodecyl sulphate (SDS) solution was added. The release study was performed by the addition of the same SDS solution. Two controls for the integrity of the pDNA were included in the gels: 1 kb pDNA ladder from NIPPON Genetics Europe (Dueren, Germany) and untreated pcDNA3-EGFP plasmid.

The studies of mRNA-based vectors were performed in 1.2% agarose gel electrophoresis for 60 min at 75 V containing Gel Red™. The bands were analyzed with Uvitec Uvidoc D-55-LCD-20 M Auto transilluminator. For binding study, mRNA was diluted in Milli-Q™ water to a final concentration of 0.12 µg mRNA/µL in each well. Protection was evaluated by the addition of 6 U RNase I/µg mRNA and incubation at 37 °C for 40 min in a heater. Then, a final concentration of 1% SDS solution was added. The release study was performed by the addition of the same

SDS solution. Two controls for the integrity of the mRNA were included in the assay: RiboRuler High Range RNA Ladder and untreated CleanCapTM EGFP mRNA (5moU).

2.3. Cell culture studies

In vitro studies were carried out in four cell lines:

- Human Retinal Pigmented Epithelial (ARPE-19) cells. ARPE-19 cells were maintained in culture in Dulbecco's Modified Eagle Medium:Nutrient Mixture F-12 (DMEM / F-12) with 10% fetal bovine serum and 1% penicillin and streptomycin antibiotic.
- Human Embryonic Kidney (HEK-293) cells. HEK-293 cells were kept in culture in Eagle's Minimum Essential Medium (EMEM) with 10% fetal bovine serum and 1% penicillin and streptomycin antibiotic.
- Human Corneal Epithelium (HCE-2) cell line. HCE-2 cell line was maintained in DMEM/F-12 GlutaMAX medium supplemented with 15% (v/v) heat-inactivated fetal bovine serum (FBS), insulin (4 mg/mL), EGF (10 ng/mL), and penicillin–streptomycin (1%).
- Human Umbilical Vein Endothelial Cells (HUVEC). HUVEC were maintained in Human large vessel endothelial cell basal medium (Medium 200) and Low Serum Growth Supplement (LSGS).

All cell cultures were incubated at 37 °C in a 5% CO_2 air atmosphere, and the culture medium was changed every 2 or 3 days and subcultured every 7 days.

2.3.1. Gene silencing efficacy

2.3.1.1. Percentage of transfected cells and GFP production

To evaluate the rate of cells transfected, the vectors were prepared with the p-shRNA-MMP-9-GFP plasmid, which silences the MMP-9 and encodes the reporter gene GFP. Cells were transfected with the vectors and four hours after the addition of the vectors, the media was replaced and the cell culture was allowed to grow up to 72 h at 37 °C and 5% CO_2 before quantification. The percentage of transfected cells was measured using a CytoFLEX flow cytometer. Cells were rinsed with phosphate buffered saline (PBS) (three times), separate from plates, and resuspended in PBS. Finally, samples were evaluated by flow cytometry at 525 nm collecting 1×10^4 events per sample. The amount of intracellular GFP, in terms of relative fluorescence units (RFU)/mg total protein, was quantified by fluorometry. To do that, the culture media were substituted with 300 mL of 1× reported lysis buffer (RLB) and frozen. The cells were then scraped and centrifuged at 4 °C and 12,000 *× g* for 2 min. The GFP fluorescence in the supernatant was measured by using a Glomax™ Multi-Detection System (Promega Biotech

Iberica, Madrid, Spain). The fluorescence was corrected by the amount of protein, quantified by a Micro BCA™ Protein Assay kit (Thermo Scientific, Madrid, Spain).

2.3.1.2. Silencing of MMP-9

HCE-2 cells were transfected with the nanocarriers bearing the p-shRNA-MMP-9 plasmid in order to know the capacity of the nanocarriers to downregulate the MMP-9. A p-shRNA-scramble (shRNAscr) plasmid and a naked p-shRNA-MMP-9 plasmid were used as negative controls. The silencing activity was evaluated at 72 h by measuring the MMP-9 secreted to the culture medium, and by detecting the MMP-9 at an intracellular level. The amount of MMP-9 secreted by the cells was measured in the culture medium by an Enzyme-linked Immunosorbent Assay (ELISA) kit (R&D Systems, Minneapolis, MN, USA).

The presence of MMP-9 in HCE-2 was evaluated by immunocytochemistry. For this purpose, untreated and transfected cells were seeded in 24-well plates with cover glasses in the bottom that were previously treated with the attachment factor protein. After adequate washing in PBS, the cells were blocked and permeabilized with PB buffer, 0.3% Triton X-100, 10% donkey serum for 30 min. A goat monoclonal anti-MMP-9 antibody in PBS buffer (2.5% donkey serum, 0.1% triton X-100) was then added and maintained for 1 h. After 3 more washes with PBS, the cells were dyed with the secondary antibody Alexa Fluor 568-conjugated donkey anti-goat IgG for 1 h in the dark. Finally, the nuclei were dyed with the mounting media DAPI Fluoromount-G®. The specificity of the staining was controlled by incubating cells without the primary antibody. The images were obtained with an inverted fluorescence microscope (Nikon TMS, Izasa Scientific, Madrid, Spain) at 40× magnification. Intracellular MMP-9 was also evaluated in HCE-2 cells previously stimulated with 10 ng of TNF-α, a proinflammatory mediator, for 6 h.

2.3.1.3. Cell migration assay

The effect of the formulations on the migration of HCE-2 cells was studied using a wound healing assay. For this purpose, HCE-2 cells were grown to confluence in 24-well plates coated with attachment factor containing gelatin (substrate of MMP-9) and a linear wound was created with a pipette tip. Afterward, cultures were rinsed twice with PBS to remove detached cells and 1 mL of fresh serum-free medium was added. Untreated cells, cells treated with the vector, and cells stimulated with 10 ng of TNF-α were allowed to migrate at 37 °C under 5% CO_2. After 4 h, the medium was changed by a 1 mL complete medium. The wound width was measured at 7 different points at 7, 24, and 48 h. The relative distance filled was calculated with the formula: $m = (1 - nt/r) \times 100\%$, where m is the migration, nt is the width of the scratch at time t, and r is the initial width of the scratch [166]. Blank nanoparticles were also assayed.

2.3.1.4. HUVEC tube formation assay

The HUVEC cell line was employed to evaluate if MMP-9 downregulation is able to inhibit capillary tube formation. HUVEC cells were seeded onto Geltrex® LDEV-Free Reduced Growth Factor Basement Membrane Matrix in 96-well plates and the culture medium was replaced with conditioned culture medium from HCE-2 cells untreated or treated with DX:P:p-shRNA-MMP-9:SLN1$_{EE}$ vector, TNF-α, or TNF-α plus DX:P:p-shRNA-MMP-9:SLN1$_{EE}$ vector. The plates were incubated at 37 °C, and tube formation was evaluated after 15 h of incubation under an optic inverted microscope. Morphometric measurements in captured images were obtained using the ImageJ software (National Institutes of Health, Bethesda, MA, USA) [167].

2.3.2. Gene augmentation efficacy

2.3.2.1. GFP transfection efficacy

The percentage of transfected cells and intensity of fluorescence, as well as cell viability, were measured using a CytoFLEX flow cytometer (Beckman Coulter) 48 h and 72 h after the addition of mRNA- and pDNA-based vectors, respectively. For this purpose, cells were washed with PBS and detached by incubation with Trypsin/EDTA from the plates. After cell suspension centrifugation, the supernatant was removed, and the pellet of cells was resuspended in PBS. For each sample, 10,000 events were collected. Transfection efficacy was measured at 525 nm (FITC), and cell viability was determined at 610 nm (ECD), after the addition of 7-amino-actinomycin D (7-AAD) viability dye to the samples. The percentage of transfected cells and the intensity of fluorescence was calculated counting the positive fluorescent GFP cells over the total cells. Moreover, the effect of temperature on cell transfection was studied by the incubation of cells at 4 °C before and after the addition of the vectors.

2.3.2.2. IL-10 transfection efficacy

The secreted and intracellular IL-10 was measured by the ELISA kit 48 h and 72 h after the addition of mRNA- and pDNA-based vectors encoding human IL-10, respectively. For the secreted IL-10, the medium of each well was removed and centrifuged. For the intracellular IL-10, the cells were washed with PBS twice, and then 400 µL of reporter lysis buffer 1× was added. Finally, the plate was frozen to complete the lysis of cell culture. After thawing, each well was detached by a scrapper and the lysate was centrifuged. A total of 100 µL of each sample was added to a 96-well plate that was covered with the corresponding capture antibody; then the assay was performed according to the manufacturer's instructions.

2.3.3. Cell viability

For gene silencing studies, viability of HCE-2 cells treated with nanocarriers was measured with the CCK-8 assay following the manufacturer's protocol. In short, the cells were seeded in a 96-well plate at a density of 1×10^3 cells/well and incubated overnight at 37 °C in a CO_2 incubator followed by transfection with the different vectors. CCK-8 reactive solution was added to each well, incubated at 37 °C for 4 h. Finally, the absorbance was measured in a microplate reader at 450 nm.

For gene augmentation studies, cell viability was measured using a CytoFLEX flow cytometer (Beckman Coulter) 48 h and 72 h after the addition of mRNA- and pDNA-based vectors, respectively. For this purpose, cells were washed with PBS and detached by incubation with Trypsin/EDTA from the plates. After cell suspension centrifugation, the supernatant was removed and the pellet of cells was resuspended in PBS. For each sample, 10,000 events were collected. Cell viability was determined at 610 nm (ECD), after the addition of 7-AAD viability dye to the samples. Moreover, the effect of temperature on cell transfection was studied by the incubation of cells at 4 °C before and after the addition of the vectors.

2.3.4. Cellular uptake

The internalization of the vectors was studied by the addition of vectors containing SLNs labeled with the fluorescent Nile Red dye (λ = 590 nm) to the cells, as reported before [79]. Two hours after the addition of the vectors, the culture medium was removed, washed with PBS and detached by incubation with Trypsin/EDTA from the plates. The entrance of the vectors was analyzed by using a CytoFLEX flow cytometer (Beckman Coulter) at 610 nm (ECD). For each sample, 10,000 events were collected. Moreover, the effect of temperature on cell transfection was studied by the incubation of cells at 4 °C before and after the addition of the vectors.

2.3.5. Intracellular disposition of the vectors

Cells were seeded in Millicell EZ slides (Millipore) and incubated at 37 °C and 5% CO_2 for 24 h. Then, vectors labeled with CleanCap™ Cyanine 5 EGFP mRNA (5moU) or pcDNA3-EGFP plasmid labeled with Label IT® Cy®5 as nucleic acid were added. After 4 h, the slides were washed with PBS, fixed with paraformaldehyde (PFA) 4% and covered with the mounting fluid DAPI-fluoromount-G™ to label the nuclei. Then, a Leica DM IL LED Fluo inverted microscope (Leica Microsystems CMS GmbH, Wetzlar, Germany) was used to analyze the slides.

2.4. *In vivo* studies

Five-week-old male BALB/c OlaHsd mice, with a weight ranging between 20 and 25 g (Envigo), were employed for the *in vivo* studies. The use of the mice (license M20/2018/142) was

approved by The Animal Experimentation Ethics Committee of the University of the Basque Country UPV/EHU following the Spanish and European Union (EU) laws. All the procedures were followed in accordance. The animals were accommodated under controlled temperature, humidity, and 12 h day-night cycles, with food and water *ad libitum* access.

The mice were anesthetized with 1–2% isoflurane (IsoFlo, Abbott, Madrid, Spain) in air, at a flow rate of 0.5–1 L/min with the aim of preventing distress during experimental manipulation.

The mice were humanely euthanatized by cervical dislocation, and then their eyes were removed. After the enucleation, the eyes were washed in a physiological saline solution, fixed with 4% PFA during 30 min and washed with PBS for 5 min. Then, the eyes were immersed in 30% sucrose in PBS at 4 °C until the eyes precipitated. Then, half of the volume was removed and substituted with Tissue-Tek® O.C.T.™ and shaken at room temperature for 2 h. Finally, the eyeballs were stored in 100% Tissue-Tek® O.C.T.™ to freeze at 80 °C for future studies.

2.4.1. Administration of the vectors

The formulations described in Table 4, as well as naked mRNA encoding GFP or human IL-10, were viscosized with 1% PVA (85,000–124,000 M_w). Two doses per day for 3 days were administered to the mice by eye drop instillation. For each dose, three instillations of 2.5 µL at 3 min intervals were carried out, administering a final dose of 4.5 µg of nucleic acid per day.

Table 4. Evaluated formulations for topical administration as eye drops for in vivo study.

Formulations	GFP evaluation	IL-10 evaluation
Naked GFP mRNA	X	
Naked IL-10 mRNA		X
mRNA-DX-SLN1$_{EE}$	X	X
mRNA-HA-SLN1$_{EE}$	X	X
mRNA-DX-SLN1$_{HM}$	X	X
mRNA-HA-SLN1$_{HM}$	X	X
mRNA-SLN$_C$	X	X
mRNA-HA-SLN$_C$	X	
pDNA-DX-SLN1$_{HM}$	X	
pDNA-HA-SLN1$_{HM}$	X	
mRNA-DX-SLN1$_{EE}$_Au	X	
mRNA-HA-SLN1$_{EE}$_Au	X	

DX: dextran; HA: hyaluronic acid; Au: gold; GFP: green fluorescent protein; IL-10: interleukin 10; SLN1$_{EE}$: solid lipid nanoparticle prepared by emulsification-evaporation method containing DOTAP cationic lipid; SLN1$_{HM}$: solid lipid nanoparticle prepared by hot-melt emulsification method containing DOTAP calitioc lipid; SLN$_C$: solid lipid nanoparticle prepared by coacervation method.

2.4.2. Evaluation of gene expression

Gene expression was evaluated by measuring:

- The presence of the GFP produced, which is located at intracellular level.
- The IL-10 secreted.

Both assays were evaluated qualitatively by immunofluorescence. Eyes were histologically analyzed by sections of 14 µm on a cryostat (Cryocut 3000, Leica, Bensheim, Germany). Sections were washed with PB buffer. The samples were blocked and permeabilized employing a solution of 20% PB, 0.3% Triton X-100, 10% goat serum, and water q.s. 100%. Then, the respective primary antibody, anti-GFP or anti-IL-10, was added and incubated for 24 h at 4 °C. Secondary antibody goat anti-rabbit IgG Alexa Fluor 488 was added after washing for 30 min protected from light. Finally, after washing and drying the samples, they were mounted with DAPI-Fluoromount-G™. Tissue sections were examined by a Zeiss LSM800 confocal microscope (ZEISS microscopy, Oberkochen, Germany). The overlapping of fluorescence emission spectra was avoided by sequential acquisition. Six sections for each cornea were analyzed as representations of the entire tissue. Technical and human support for confocal microscope was provided by the Advanced Research Facilities (SGIker) of Analytical and High Resolution Microscopy in Biomedicine at the University of the Basque Country UPV/EHU (Leioa, Basque Country, Spain).

2.5. Data analysis

Experimental data analysis was analyzed by IBM SPSS Statistics 26 (IBM) computer software. Saphiro–Wilk test and Levene test were employed for the evaluation of homogeneity and variance, and normal distribution of samples, respectively. Student's t-test was used to compare means from two independent groups and ANOVA for multiple comparisons, followed by Bonferroni or T3 Dunnet post-hoc, depending on the results of the Levene test of homogeneity of variances. p values < 0.05 were considered as statistically significant.

3. HYPOTHESIS AND OBJECTIVES

3.1. Hypothesis

Gene therapy is a novel approach to treat, cure or ultimately prevent diseases by modifying the expression of genes. To date, innovative therapeutic strategies appropriate to delivery nucleic acids with the aim of regulating gene expression have been developed. One of these strategies is gene supplementation, which consists of the overexpression of a gene by delivering functional copies of a nucleic acid (DNA or mRNA) to express a therapeutic protein. Classically, gene supplementation has been addressed through the administration of pDNA. However, mRNA therapeutics have gained much attention in recent times due to specific characteristics that make it a promising alternative to pDNA. Firstly, from a delivery point of view, mRNA does not need the machinery of the nucleus to be functional, as DNA therapies do. Therefore, once mRNA reaches the cytoplasm, translation of the encoding protein begins, being effective in both, mitotic and non-mitotic cells. Secondly, from a safety point of view, mRNA does not integrate into the host genome; hence, the risk of carcinogenesis and mutagenesis usually associated with DNA disappears. In addition, mRNA works without encoding additional genes (i.e., those related to antibiotic resistance). Thirdly, the synthesis of the encoded protein is fast, and its expression is temporary. Finally, the production of IVT mRNA is easier than the manufacturing of DNA, and it can be standardized, maintaining its reproducibility. However, IVT mRNA also shows some limitations, including the immunogenicity, the instability in biological fluids and the difficulty to overcome several extracellular and intracellular barriers. In order to overcome these drawbacks, delivery systems specifically adapted to the type of nucleic acid, the route of administration and target cell are necessary.

LNPs are regarded as one of the most advanced systems for nucleic acid delivery. In this sense, the global pandemic from COVID-19 has boosted the approval of the first mRNA vaccines based on LNP. SLNs are a kind of LNPs consisting in an aqueous dispersion of a layer of surfactants surrounding a solid lipid core. They can be easily produced at large scale, can be autoclaved, sterilized or freeze-dried, and are stable in biological fluids and during storage. The ability of the SLNs to protect the nucleic acids from degradation, to facilitate cell internalization and endosomal escape, to release them in the cytoplasm, and to promote the entrance to the nucleus, has been widely demonstrated. Another advantage of this delivery system is the possibility to functionalize its surface incorporating ligands to target the genetic material to specific cells, as well as to modulate the intracellular trafficking and the nucleic acid release, increasing their efficacy and safety. SLNs have shown promising results as nucleic acid delivery systems, especially in the field of ocular diseases. They possess a nanometre sized-range,

lipophilic properties, and usually positive surface charges. These features make them suitable for eye topical drug administration, and for improving corneal permeation and retention.

Gene therapy has been proposed as an effective alternative for the treatment of ocular diseases and, specifically, for corneal application, thanks, in part, to the advantages of the cornea in terms of transparency, well-defined anatomy, accessibility, non-invasive examination, easy administration and its immune privileged condition. Several factors can injure the cornea (i.e. infections, dry eye, disorders of the eyelids, physical and chemical damage) resulting in corneal inflammation or keratitis. Chronic inflammation of the cornea induces visual disturbance, and often results in tissue destruction that leads to corneal ulceration, scarring and, even, perforation, causing visual impairment and blindness. Furthermore, CNV can occur during the inflammatory process as a result of an imbalance between pro-angiogenic and anti-angiogenic factors. Neovascularization can damage the ocular surface during the repairing process. Current treatments of corneal inflammation mainly consist of the use of corticosteroids, but its use is limited due to the adverse effects and the short duration effect. Therefore, new therapeutic strategies are needed to address corneal inflammation. In this sense, the topical administration of the anti-inflammatory IL-10 has been suggested as an efficient treatment, although its low ocular bioavailability and short half-life limit the therapeutic use of this cytokine. Hence, a gene supplementation strategy by nucleic acid delivery to express IL-10 *de novo* in corneal cells could be a promising strategy to obtain anti-inflammatory responses in the cornea. Moreover, CNV-associated inflammation can be addressed by gene silencing targeted to the pro-angiogenic factor MMP-9, one of the primary extracellular matrix remodeling enzymes that participate in pathological conditions of the cornea.

3.2. Objectives

The main objective of this thesis is the development and evaluation of nucleic acid delivery systems based on SLNs containing pDNA or mRNA for the treatment of corneal inflammation by topical instillation. To achieve this aim, the following steps were carried out:

1. Revision of the state of art of the strategies employed to enhance the functionality and efficacy of IVT mRNA, including the optimization of its stability and translational efficiency, as well as the regulation of its immunostimulatory properties (Appendix I). Moreover, an overview of technological approaches and nanosystems developed for a successful IVT mRNA delivery, as well as a description of the potential applications of mRNA therapies were performed (Appendix V).

2. Design, optimization, physicochemical characterization, long-term stability and *in vitro* transfection of different types of SLNs-based nucleic acid delivery formulations. (Appendix II).

3. Design, optimization, physicochemical characterization and *in vitro* evaluation in HCE-2 cells of the capacity of the SLN-based formulations to address corneal inflammation by MMP-9 gene silencing (Appendix III) and IL-10 gene supplementation (Appendix IV).

4. *In vivo* evaluation of the SLN-based formulations containing pDNA or mRNA after topical instillation on the ocular surface of mice. The transfection efficacy of the formulations, the ability to produce IL-10 and the distribution of this therapeutic cytokine in corneal tissues were evaluated (Appendix IV).

5. Design, optimization, physicochemical characterization, *in vitro* studies and *in vivo* evaluation of the transfection capacity after ocular topical administration to mice of new golden lipid nanoparticles (Appendix VI).

4. RESULTS AND DISCUSSION

The development of safe and effective nucleic acid delivery systems remains a challenge, with lipid-based systems as one of the most promising non-viral vectors. Among them, SLNs are regarded as one of the most versatile and effective for gene therapy. In this doctoral thesis, DNA and mRNA delivery systems based on SLNs were optimized and evaluated to address corneal inflammation. On the one hand, cationic and ionizable lipids were combined to formulate the SLNs; on the other hand, SLNs were prepared by different techniques. Finally, cationic and nano-sized nucleic acid-based medicinal products were obtained by combining SLNs with different ligands, including peptides, polysaccharides and gold nanoparticles (AuNPs).

The formulations were prepared by combining the following components: SLNs, a nucleic acid (pDNA, mRNA or p-shRNA), the cationic peptide P, and a polysaccharide -DX or HA. Eventually, a new nanovector for nucleic acid delivery was developed by the incorporation of AuNPs to the formulation. The electrostatic interactions between the different components play a major role in the vector formation, conditioning the final structure. To prepare nanovectors, the nucleic acid was first condensed with P, which contributes to bind and protect the genetic material at intra and extracellular level [168,169]. Secondly, in some of them, a polysaccharide, DX or HA, was added. Both polysaccharides possess suitable properties to improve nucleic acid delivery and show low cytotoxicity, can be chemically modified and have stealth properties. DX is a biocompatible polyanion that hinders interactions with other biological components, such as serum proteins. HA also present mucoadhesive properties and targeting moieties [74,75,170]. Finally, the complex formed with the nucleic acid, P and the polysaccharide was added to the SLNs. The incorporation of SLNs results necessary for transfection, since the treatment of cells with complexes prepared with the nucleic acid, P, and DX or HA, resulted in a percentage of transfected cells lower than 0.8%.

The results obtained in the different stages of this work are summarized and discussed in the following sections.

4.1. Cationic and ionizable lipids: *in vitro* characterization of SLNs-based nucleic acid delivery formulations and long-term stability

In the first part of the doctoral thesis, SLNs were prepared by emulsification/evaporation method (SLN_{EE}). The influence of different combinations of cationic lipid and ionizable lipids on the physicochemical characteristics of SLNs and their transfection efficiency was evaluated.

The traditional cationic lipid 1,2-dioleoyl-3-trimethylammonium-propane (DOTAP) is one of the most used for mRNA and DNA delivery. This lipid is completely protonated at pH 7.4, so it has been postulated that, for successful transfection, high energy is required for the separation of nucleic acid from the lipoplex. Thus, to improve its efficacy in nucleic acid delivery, DOTAP can be combined with helper lipids [171]. The use of ionizable lipids, such DODAP and N-(4-carboxybenzyl)-N,N-dimethyl-2,3-bis(oleoyloxy)propan-1-aminium (DOBAQ), is a more recent strategy; these lipids are neutral at physiological pH but become protonated in the acidic environment of the endosome. The electrostatic interactions between the lipids of the endosomal membranes and the ionizable cationic lipids promote membrane lytic non-bilayer structures such as the hexagonal phase (HII), facilitating the endosomal scape and the intracellular nucleic acid delivery [46,54].

Table 5 shows the mean diameter, PDI and ζ-potential of SLNs prepared with different cationic and ionizable lipids. The particle size of SLNs ranged from 185.1 nm to 423.5 nm, PDI was below 0.4 except for $SLN3_{EE}$, and zeta potential ranged from -28.0 mV to +59.5 mV.

Table 5. Physical characterization of solid lipid nanoparticles (SLNs) prepared with different cationic and ionizable lipids

Type of SLN	Cationic Lipid (%)			Size (nm)	PDI	ζ-Potential (mV)
	DOTAP	DODAP	DOBAQ			
$SLN1_{EE}$	X			185.1 ± 3.5	0.30 ± 0.03	+59.5 ± 1.9
$SLN2_{EE}$	X	X		208.8 ± 0.4	0.27 ± 0.01	+50.2 ± 1.1
$SLN3_{EE}$			X	423.5 ± 51.7	0.57 ± 0.05	-28.0 ± 0.8
$SLN4_{EE}$	X		X	211.3 ± 3.5	0.36 ± 0.01	+42.4 ± 1.2

$SLN1_{EE}$: solid lipid nanoparticle prepared by emulsification-evaporation method containing DOTAP cationic lipid. $SLN2_{EE}$: solid lipid nanoparticle prepared by emulsification-evaporation method containing a mixture of DOTAP cationic lipid and DODAP ionizable lipid; $SLN3_{EE}$: solid lipid nanoparticle prepared by emulsification-evaporation method containing DOBAQ ionizable lipid; $SLN4_{EE}$: solid lipid nanoparticle prepared by emulsification-evaporation method containing a mixture of DOTAP cationic lipid and DOBAQ ionizable lipid. PDI: polydispersity index. Data are expressed as mean ± standard deviation; *n*=3.

As it is observed in Table 5, $SLN3_{EE}$, prepared only with the ionizable lipid DOBAQ presented a particle size higher than 400 nm, PDI higher than 0.5 and negative surface charge of -28 mV. Considering these results, $SLN3_{EE}$ was discarded for preparing vectors.

Once the SLNs were characterized, the final vectors were prepared with mRNA or DNA encoding GFP. Table 6 shows the size and zeta potential of the SLN-based vectors. pDNA formulations presented a particle size and a PDI similar to the plain SLNs but lower ζ-potential. mRNA

formulations showed higher particle size and PDI values, and lower superficial charge than those prepared with pDNA.

Table 6. Physical characterization of SLN_{EE}-based vectors containing pDNA or mRNA.

Nucleic acid	Vectors	Size (nm)	PDI	ζ-Potential (mV)
pcDNA3-EGFP plasmid	pDNA-DX-$SLN1_{EE}$	176.4 ± 0.4	0.27 ± 0.01	+45.4 ± 2.7
	pDNA-DX-$SLN2_{EE}$	165.8 ± 1.7	0.27 ± 0.01	+42.2 ± 0.9
	pDNA-DX-$SLN4_{EE}$	211.9 ± 14.6	0.40 ± 0.07	+32.6 ± 0.9
	pDNA-HA-$SLN1_{EE}$	201.2 ± 1.3	0.17 ± 0.01	+29.8 ± 1.1
	pDNA-HA-$SLN2_{EE}$	194.2 ± 0.8	0.20 ± 0.00	+35.6 ± 1.9
CleanCap™ EGFP mRNA (5moU)	mRNA-DX-$SLN1_{EE}$	246.8 ± 1.3	0.39 ± 0.02	+37.2 ± 1.0
	mRNA-DX-$SLN2_{EE}$	210.1 ± 0.8	0.26 ± 0.01	+36.5 ± 0.3
	mRNA-HA-$SLN1_{EE}$	202.4 ± 2.2	0.35 ± 0.00	+27.5 ± 0.6
	mRNA-HA-$SLN2_{EE}$	349.2 ± 9.9	0.39 ± 0.02	+18.5 ± 0.9
	mRNA-P0.25-$SLN1_{EE}$	251.6 ± 6.5	0.35 ± 0.01	+28.8 ± 0.7
	mRNA-P0.5-$SLN2_{EE}$	233.7 ± 2.8	0.24 ± 0.00	+25.4 ± 0.6
	mRNA-P1-$SLN2_{EE}$	261.7 ± 4.0	0.29 ± 0.02	+23.1 ± 1.3

P: protamine; DX: dextran; HA: hyaluronic acid; $SLN1_{EE}$: solid lipid nanoparticle prepared by emulsification-evaporation method containing DOTAP cationic lipid. $SLN2_{EE}$: solid lipid nanoparticle prepared by emulsification-evaporation method containing a mixture of DOTAP cationic lipid and DODAP ionizable lipid; $SLN4_{EE}$: solid lipid nanoparticle prepared by emulsification-evaporation method containing a mixture of DOTAP cationic lipid and DOBAQ ionizable lipid. PDI: polydispersity index. Data are expressed as mean ± standard deviation; *n*=3.

A successful transfection depends upon the balance between the protection provided by the nanosystem to the nucleic acid against degradation, and its capacity to unpack and release it inside the cell. The study by electrophoresis on agarose gels of the binding, protection and release capacity of the nucleic acids in the vectors showed that formulations prepared with the mixture of DOTAP and DOBAQ ($SLN4_{EE}$) had a low capacity to protect the pDNA; consequently, $SLN4_{EE}$–based vectors were excluded for following experiments. The incorporation of DODAP to the SLNs ($SLN2_{EE}$) resulted in a lower capacity to protect the mRNA than to protect pDNA, which indicates that the mRNA is more exposed to external agents, such as RNases. The difference in the capacity of the vectors to protect the nucleic acid may be related to the unique structure of mRNA, which is a single-stranded molecule that folds into complex secondary and tertiary structures, and takes forms that differ from the double stranded pDNA [37].

After physicochemical studies, transfection efficacy and cell uptake of pDNA- and mRNA-based vectors were evaluated in two cell models, ARPE-19 and HEK-293 cells. These cell lines have been previously selected to study the behavior of SLN-based vectors as pDNA delivery systems,

because of their different features in terms of cell division rate (which is lower in ARPE-19 cells) and of the main endocytic processes [172]. All formulations were able to transfect both cell lines, regardless of the type of SLN, although the transfection efficacy varied depending on the cell line, on the type of nucleic acid and, on the composition of the vectors.

The effect of temperature on cell transfection and cell uptake was also studied. All the components that form the vector determine the interaction with the target cells, and, therefore, the internalization process, the intracellular behavior of the genetic material and the transfection capacity [74,90]. It is well known that the degree of cellular uptake and endosomal escape of the vectors condition transfection efficiency [173]. The major entry mechanism of SLN-based vectors is the endocytosis. The two main endocytic processes are reported to be pinocytosis and phagocytosis. The former is mainly associated to nanoparticle uptake, and different pathways are involved (micropinocytosis, clathrin-mediated, caveolin dependent or independent) [174]. The predominant entry pathway depends on the target cells and on the composition and physicochemical characteristics of the non-viral vectors [32]. The endocytosis is an energy-dependent and temperature-dependent process, and it is inhibited at 4 °C because cells consume less (adenosine triphosphate) ATP and block the active transport at this temperature [175,176].

In ARPE-19 cells at 37 °C, pDNA-based vectors (Figure 7A) induced a lower percentage of transfected cells than those containing mRNA (Figure 7C), but pDNA-transfected cells provided the highest fluorescence intensities (Figure 7B and Figure 7D); namely, pDNA transfection is more effective for protein production in this cell line. In HEK-293 cells (Figure 8), pDNA-based vectors induced lower transfection efficacy than mRNA-vectors in terms of transfected cells and protein production. Among pDNA vectors, the highest transfection efficacy was observed with HA-containing vectors in both cell lines, and in ARPE-19 cells especially with the vector containing pDNA, HA and $SLN1_{EE}$. Regarding mRNA formulations, the inclusion of a polysaccharide did not have a great impact on the *in vitro* transfection efficacy.

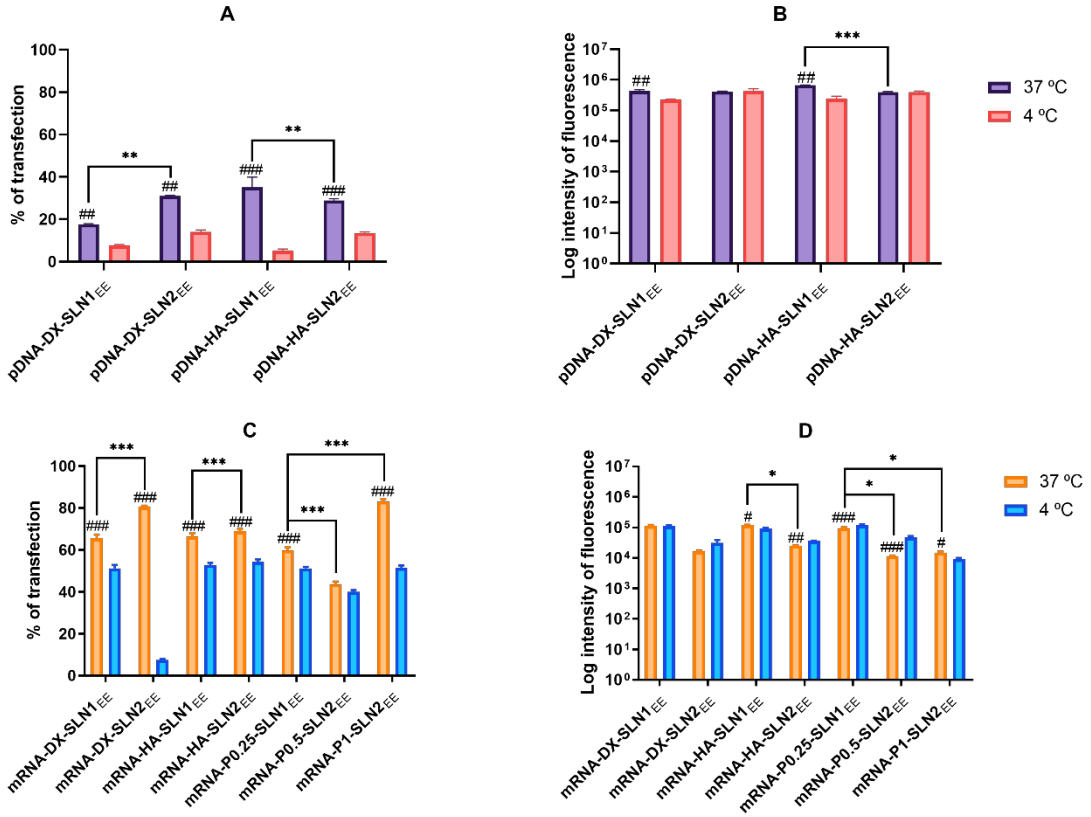

*Figure 7. Percentage of transfected cells and intensity of fluorescence of ARPE-19 cells after incubation with SLN1$_{EE}$- and SLN2$_{EE}$-based vectors at 37 °C and 4 °C. Percentage of transfection values correspond to the positive fluorescent GFP cells over the total cells. Log of intensity of fluorescence indicates the average intensity of fluorescence per labeled cell. A: Percentage of transfected ARPE-19 cells 72 h after treatment with pDNA vectors. B: Intensity of fluorescence of transfected ARPE-19 cells 72 h after treatment with pDNA vectors. C: Percentage of transfected ARPE-19 cells 48 h after treatment with mRNA vectors. D: Intensity of fluorescence of transfected ARPE-19 cells 48 h after treatment with mRNA vectors. Data are expressed as mean ± standard deviation; n = 3. # p < 0.05 with respect to the same vector at 4 °C. ## p < 0.01 with respect to the same vector at 4 °C. ### p < 0.001 with respect to the same vector at 4 °C. * p < 0.05 with respect to the other formulation. ** p < 0.01 with respect to the other formulation. *** p < 0.001 with respect to the other formulation. P: protamine; DX: dextran; HA: hyaluronic acid; SLN1$_{EE}$: solid lipid nanoparticle prepared by emulsification-evaporation method containing DOTAP cationic lipid; SLN2$_{EE}$: solid lipid nanoparticle prepared by emulsification-evaporation method containing a mixture of DOTAP cationic lipid and DODAP ionizable lipid.*

Overall, cellular uptake of all vectors, pDNA and mRNA, was over 90% at 37 °C. Therefore, the lower percentage of transfected cells with pDNA vectors is due to intracellular barriers; the bottleneck for a successful pDNA transfection seems to be the nuclear entry, despite our systems contains P, which favors the transcription process and the entry of the pDNA into the nucleus thanks to their nuclear localization signals [168].

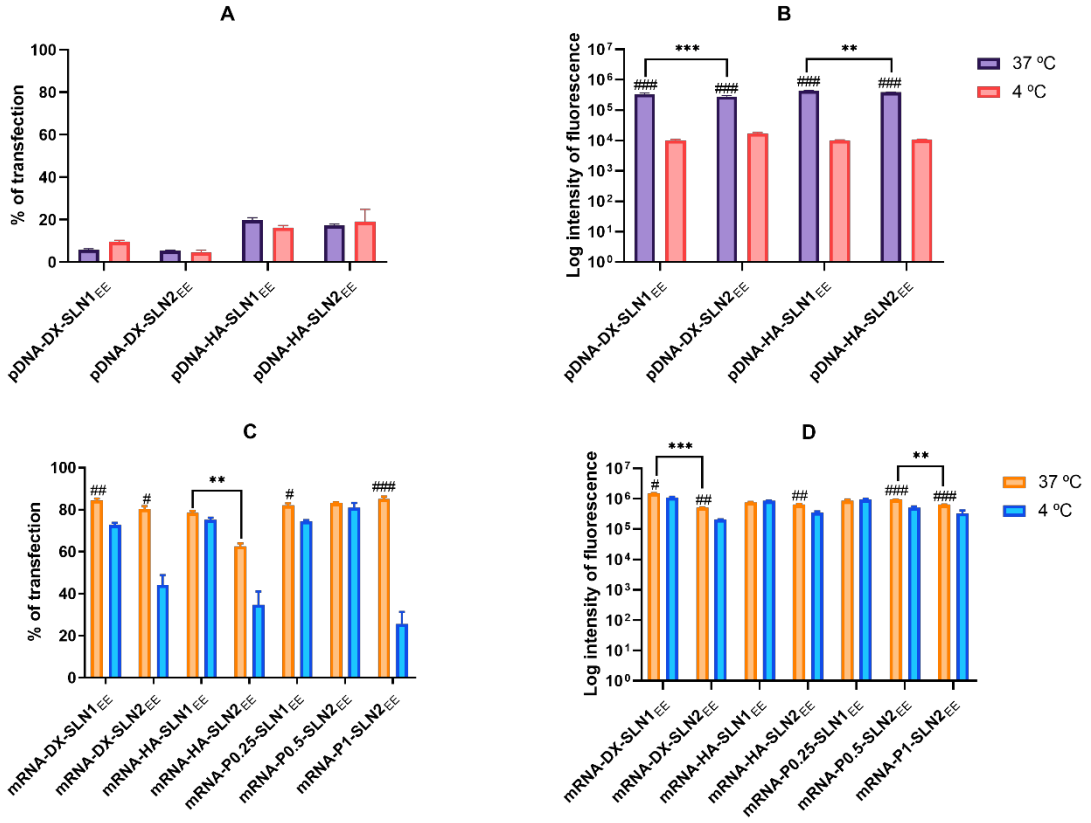

*Figure 8. Percentage of transfected cells and intensity of fluorescence of HEK-293 cells after incubation with SLN1$_{EE}$ - and SLN2$_{EE}$ -based vectors at 37 °C and 4 °C. Percentage of transfection values correspond to the positive fluorescent GFP cells over the total cells. Log of intensity of fluorescence indicates the average intensity of fluorescence per labeled cell. A: Percentage of transfected HEK-293 cells 72 h after treatment with pDNA vectors. B: Intensity of fluorescence of transfected HEK-293 cells 72 h after treatment with pDNA vectors. C: Percentage of transfected HEK-293 cells 48 h after treatment with mRNA vectors. D: Intensity of fluorescence of transfected HEK-293 cells 48 h after treatment with mRNA vectors. Data are expressed as mean ± standard deviation; n = 3. # p < 0.05 with respect to the same vector at 4 °C. ## p < 0.01 with respect to the same vector at 4 °C. ### p < 0.001 with respect to the same vector at 4 °C. ** p < 0.01 with respect to the other formulation. *** p < 0.001 with respect to the other formulation. P: protamine; DX: dextran; HA: hyaluronic acid; SLN1$_{EE}$: solid lipid nanoparticle prepared by emulsification-evaporation method containing DOTAP cationic lipid; SLN2$_{EE}$: solid lipid nanoparticle prepared by emulsification-evaporation method containing a mixture of DOTAP cationic lipid and DODAP ionizable lipid.*

In order to evaluate the energy dependence of the entry mechanisms, transfection and uptake studies were carried out at 4 °C. In ARPE-19 cells the percentage of transfected cells decreased significantly for almost all formulations, and mainly for pDNA formulations (Figure 7). The lower cellular uptake of pDNA-SLN1$_{EE}$ formulations at 4 °C explains the decrease of the transfection efficacy of these formulations. On the contrary, the percentage of entry of pDNA-SLN2$_{EE}$ and mRNA vectors was hardly affected at 4 °C, which reveals the presence of energy-independent entry mechanisms. It has to be taken also in mind that due to the nature of biological systems, several dynamic processes might take place in parallel, which might turn in compete with one

another [177]. The higher protein production observed at 4 °C, despite the lower number of transfected cells, indicates that in ARPE-19 cells energy-independent mechanisms are more effective to induce protein production, principally in the case of the vectors containing DODAP, which may be related to the effect of this lipid on the intracellular nucleic acid release.

In HEK-293 cells, cell uptake decreased drastically at 4 °C. This cell line presents a high caveolae-dependent endocytic activity, and the blocking of the active transport has a very relevant influence on the uptake. In the case of pDNA vectors, the fluorescence intensity of transfection decreased also notably at 4 °C but the percentage of transfected cells did not suffer changes (Figure 8). In the case of mRNA vectors, both the percentage of transfection and the intensity of fluorescence decreased at low temperature, but mRNA-SLN1$_{EE}$ vectors were less affected than the SLN2$_{EE}$ formulations. Taking in mind all these results, we can conclude that in HEK-293, cell energy-dependent entry mechanisms are the most effective for protein production, regardless of the kind of the SLN used for preparing the pDNA vectors, and mainly for SLN2$_{EE}$ formulations in the case of mRNA. Endosomal escape is recognized as the rate limiting step for mRNA delivery [178] and ionizable lipids, such as DODAP, could facilitate this process. Nevertheless, recently, Patel et al. have reported that late endosome/lysosome formation is essential for the functional delivery of exogenously presented mRNA [27]. The balance between endosomal escaping capability and stability of translocated nucleic acids in cytoplasm is essential for an effective transfection. It is essential that the early steps of the development of nucleic acid-based medicinal products include mechanistic studies in the target cell for an in depth understanding of the intracellular nucleic acid nanomedicines behavior. This knowledge will allow a properly design of the formulations specifically adapted to the nucleic acid features, clinical application and therapeutic purpose.

In the present work, the composition of the formulations had a greater influence on the intracellular disposition of mRNA than that of pDNA. As it can be seen in Figure 9, mRNA formulated in SLN1$_{EE}$ appeared dispersed in the cytoplasm, especially in HEK-293 cells, which may be indicative of a higher exposure to degradation. This could be the reason why mRNA was more effective in ARPE-19 than in HEK-293 cells. In the case of mRNA-SLN2$_{EE}$ vectors, the nucleic acid was hardly detected both in ARPE-19 and HEK-293 cells, which correlates with the lower protection degree of the mRNA observed on the agarose gel. Therefore, the differences in the intracellular disposition were related to the entry mechanism and the intracellular trafficking of the vectors, which are cell line dependent processes, but also to the presence of the ionizable lipid and the capacity of the vectors to bind, condense and protect the nucleic acid.

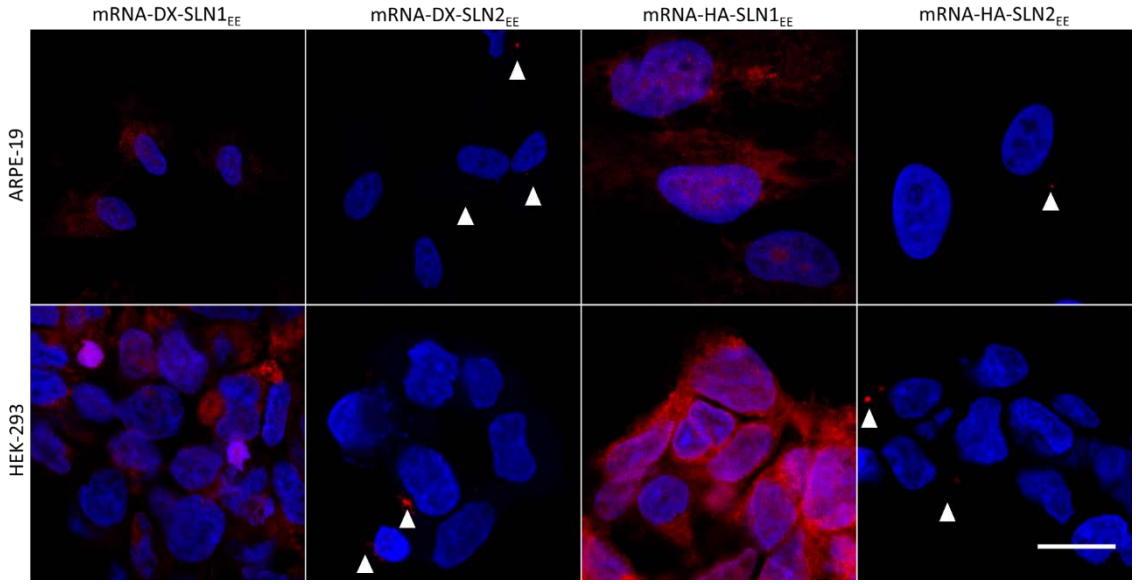

Figure 9. Fluorescence microscopy images 4 h after the addition of $SLN1_{EE}$- and $SLN2_{EE}$-based on mRNA vectors in ARPE-19 and HEK-293 cells. Vectors are formulated with CleanCap™ Cyanine 5 EGFP mRNA (5moU) P, DX or HA. Nuclei were labeled with DAPI (blue). Magnification 60×.Scale bar: 15 µm. White triangles indicate the condensed mRNA. DX: dextran; HA: hyaluronic acid; $SLN1_{EE}$: solid lipid nanoparticle prepared by emulsification-evaporation method containing DOTAP cationic lipid; $SLN2_{EE}$: solid lipid nanoparticle prepared by emulsification-evaporation method containing a mixture of DOTAP cationic lipid and DODAP ionizable lipid.

Efficacy and stability of the delivery systems should be guaranteed during storage over time. In fact, thermal stability of nucleic acid-based medicinal products is a major issue, since storage conditions involve a logistical problem for stockpiling and distribution, particularly in countries that lack infrastructure to maintain the cold chain [179]. In this doctoral thesis, physicochemical characteristics and transfection efficacy in ARPE-19 cells of nanovectors have been studied along 7 months of storage at 4 °C.

pDNA formulations showed physicochemical changes from the second month, but transfection efficacy was maintained for 7 months *in vitro*. On the contrary, mRNA vectors were more stable in terms of physicochemical features, but transfection decreased drastically from the first month with the vectors containing $SLN2_{EE}$. The lower number of positive charges of the lipid DODAP is related to its lower capacity to condense the genetic material, which could be the reason of the worse stability of $SLN2_{EE}$-based vectors, especially for mRNA. The vectors prepared with mRNA and $SLN1_{EE}$ showed a percentage of transfection higher than 80% during the 7 months of the study, except for the formulation prepared without polysaccharide. Therefore, in the $SLN1_{EE}$-formulations for mRNA delivery, the inclusion of a polysaccharide confers stability, apart from the previously mentioned beneficial properties, such as stealth capacity and ability to modulate the mechanism of entry to the target cell [74,75,172].

The formulation of SLNs with an ionizable lipid modified the capacity to condense and protect the nucleic acid. Despite the ionizable lipids facilitate the endosomal escape, its inclusion in the nanovectors did not always result in an improvement of the transfection efficacy. Considering both the efficacy and the long-term stability, the medicinal products prepared only with the cationic lipid DOTAP seems to be the most promising formulations for pDNA and mRNA delivery, and they were selected for the following studies.

4.2. *In vitro* evaluation in HCE-2 cells of the capacity of the SLN-based formulations to address corneal inflammation

4.2.1. Gene silencing of MMP-9

As previously mentioned, the vascularization of the cornea, also known as CNV, can occur as a result of an imbalance between angiogenic and anti-angiogenic factors during the inflammatory process [131]. Neovascularization can damage the ocular surface during the repairing process and affect visual acuity, as cornea loses its particular avascularity [132]. Among the different strategies used in the treatment of CNV-associated inflammation, gene silencing has been shown to be useful for targeting proangiogenic factors [180]. One of these pro-angiogenic factors is MMP-9, one of the primary extracellular matrix remodeling enzymes that participate in pathological conditions of the cornea, including CNV [123].

In this second part of the doctoral thesis, vectors formulated with $SLN1_{EE}$, P, DX and p-shRNA-MM9 were developed. shRNA, also called expressed RNAi activators, are plasmid-coded RNA that must be transcribed in the nucleus to finally produce siRNA and down-regulate the expression of a target gene. Vectors with different proportion of P and DX were prepared. Nanovectors bearing p-shRNA-MMP-9 showed suitable features for transfection: particle size in the range of nanometers, ranging from 182 nm to 216 nm, cationic superficial charge, ranging from +36.1 mV to +45.7 mv, and the ability to bind, release, and protect the p-shRNA-MMP-9 against nucleases. Nanovectors were able to transfect HCE-2 cells, with the vector prepared at the DX:P:p-shRNA-MMP9:$SLN1_{EE}$ ratio 2:1:1:5 (w:w:w:w) being the most efficacious in terms of percentage of cells transfected (5.6 %) and the amount of protein expressed as well. This vector was able to induce a decrease of approximately 30% for MMP-9 synthesized by the HCE-2 cells. The effect of the vector was related to extensive internalization and to the ability of the plasmid to be released in the cytoplasm close to the nuclear membrane.

Once the efficacy in silencing MMP-9 in HCE-2 cells was demonstrated, SLN-based vector was evaluated in TNF-α stimulated cells. TNF-α is a pro-inflammatory mediator that plays an important role in a variety of corneal diseases [181]. It disrupts the barrier function of HCE cells

and contributes to ocular inflammation [182,183]. TNF-α is reportedly elevated in corneas from individuals suffering keratitis [183], and this cytokine has been shown to stimulate MMP-9 activity in HCE cells [123]. We confirmed the increase in MMP-9 levels after the stimulation of the HCE-2 cells with TNF-α and the ability of the SLN-based vector to reduce the production of the MMP-9 in TNF-α-induced cells. These results indicate the suitability of TNF-α induced HCE-2 cells as an *in vitro* model to evaluate new formulations based on the MMP-9 downregulation for CNV.

MMPs are enzymes that are capable of cleaving numerous extracellular matrix proteins, which facilitates the migration of corneal epithelial cells to the underlying stroma [67,116–118,152]. Actually, the increased production and activity of MMPs are related to a more migratory and invasive cell phenotype [153,154]; conversely, the reduction of MMP-9 in HCE cells inhibits cell migration [184]. The effect of DX:P:p-shRNA-MMP9:SLN1$_{EE}$ on HCE-2 cell migration was evaluated in a wound healing *in vitro* assay (Figure 10). The results show that the vector was able to decrease the migration of HCE-2 cells. This effect can be related to the inhibition of MMP-9 production. MMP-9 degrades type IV collagen and gelatin substrates [185], which, in turn, favors HCE migration. A decrease in MMP-9 levels will result in a lower capacity to degrade the gelatin, used in this study as extracellular matrix protein, and a reduced migration of corneal epithelial cells.

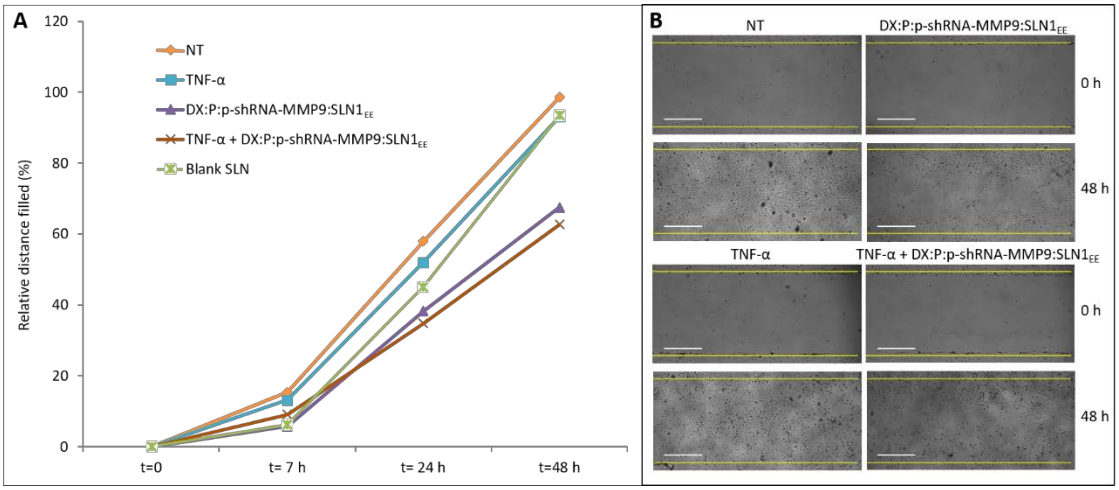

*Figure 10. The effect of DX:P:p-shRNA-MMP9:SLN1$_{EE}$ on HCE-2 cell migration. A: The evolution of the distance between cells of the edge of the wound; the mean data of reduction of the wound width from the 4 replicates (measures) in each condition. B Phase contrast representative images (4×). NT: non-treated cells. TNF-α: tumor necrosis factor alpha. P: protamine; DX: dextran; SLN1$_{EE}$: solid lipid nanoparticle prepared by emulsification-evaporation method containing DOTAP cationic lipid. Statistics at 48 h. * p < 0.05 respect to NT. ** p < 0.05 respect to cells treated with TNF-α. Scale bar: 60 µm.*

MMP-9 has also been revealed to play an important role in angiogenesis and, specifically, in angiogenesis associated with herpetic keratitis [125]. Corneal avascularity relies on the balance

between pro-angiogenic and anti-angiogenic factors [186]. In response to a stimulus such as an injury, the corneal epithelial cells release angiogenic growth factors that bind to receptors on the vascular endothelial cells of pericorneal vessels [134], and although CNV occurs in the corneal stroma, it is regulated by corneal epithelium-expressed factors. DX:P:p-shRNA-MMP9:SLN1$_{EE}$ vector was able to partially suppress the tube formation in an *in vitro* HUVEC tube formation assay (Figure 11). Morphometric measurements revealed that total master segment length, the number of meshes, total segments length, and total length decreased when the HUVEC were supplemented with the conditioned culture medium from HCE-2 cells treated with the vector. The magnitude of the inhibition of the tube formation was in the same order as the reduction of the secreted MMP-9 levels by the HCE-2 cells. The effect of our vector was observed also for TNF-α-stimulated cells.

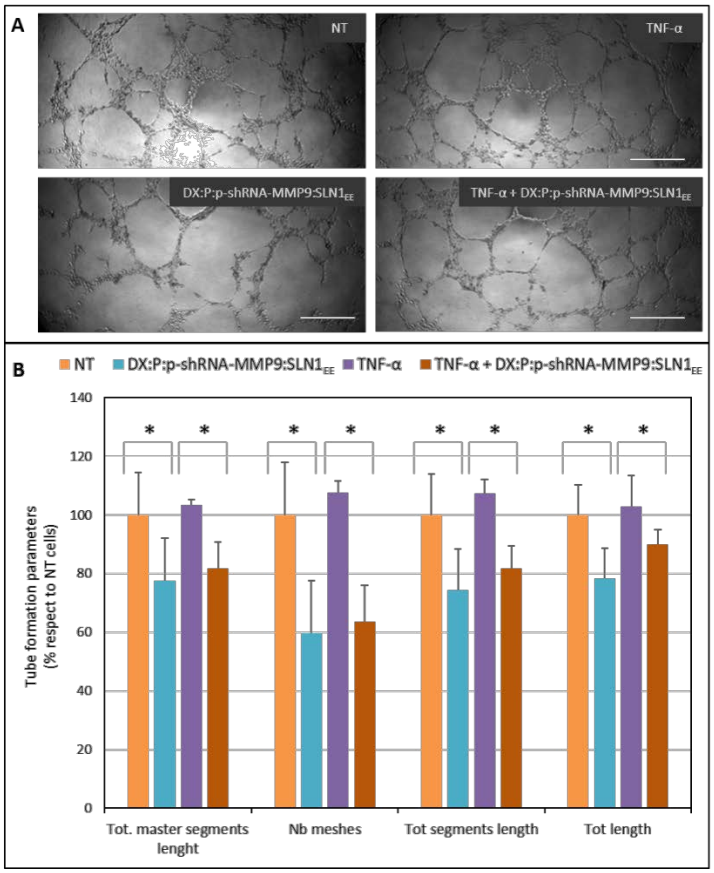

*Figure 11. (A) The representative images obtained in the tube formation assay in human umbilical vein endothelial cells (HUVECs) and (B) the quantification of tube formation. NT: non-treated cells. TNF-α: tumor necrosis factor alpha. P: protamine; DX: dextran; SLN1$_{EE}$: solid lipid nanoparticle prepared by emulsification-evaporation method containing DOTAP cationic lipid. Data were normalized relative to the values of NT cells. * $p < 0.05$. Scale bar: 60 µm.*

4.2.2. Gene augmentation of IL-10

Other strategy to treat corneal inflammation is the induction of *de novo* synthesis of anti-inflammatory mediators, such as IL-10, in corneal cells by protein supplementation with nucleic

acids. In this case, gene supplementation strategy with nanovectors bearing mRNA and pDNA as nucleic acids was evaluated. Three different SLNs, made up by three different methods, were prepared with the aim of evaluating corneal transfection. SLN_{EE} were compared with those prepared by hot-melt emulsification (SLN_{HM}) or by coacervation (SLN_C). In particular, SLN_{EE} and SLN_{HM}, were made up with the cationic lipid DOTAP, whereas SLN_C was made up with different chemical components. Table 7 shows the mean diameter, PDI and ζ-potential of the SLNs. The preparation method of SLNs influenced physicochemical features of the SLNs, in terms of particle size and surface charge. The solvent-free coacervation method led to the highest particle size (307.8 nm) and the lowest ζ-potential (+ 21.1 mV). Particle size ranged from 93.3 nm in the case of hot emulsification procedure, which avoids the use of organic solvent, but involves high operating temperature, to 198.7 nm in the case of evaporation/solvent method.

Table 7. Physical characterization of solid lipid nanoparticles (SLNs) made up by different methods.

Type of SLN	Cationic agent		Size (nm)	PDI	ζ-Potential mV)
	DOTAP	DEAE-dextran			
$SLN1_{EE}$	X		198.7 ± 2.0	0.26 ± 0.01	+57.8 ± 1.7
$SLN1_{HM}$	X		93.3 ± 0.4	0.28 ± 0.01	+68.5 ± 0.7
SLN_C		X	307.8 ± 3.5	0.17 ± 0.01	+21.1 ± 0.8

$SLN1_{EE}$: solid lipid nanoparticle prepared by emulsification-evaporation method containing DOTAP cationic lipid; $SLN1_{HM}$: solid lipid nanoparticle prepared by hot-melt emulsification method containing DOTAP calitioc lipid; SLN_C: solid lipid nanoparticle prepared by coacervation method. PDI: polydispersity indez. Data are expressed as mean ± standard deviation; *n*=3.

After characterization of SLNs, the final vectors were prepared with mRNA or DNA encoding GFP or IL-10. GFP is an intracellular protein, used to evaluate the transfection efficacy in terms of number of transfected cells an intensity of fluorescence in the transfected cells. On the other hand, IL-10 is the therapeutic protein, which is secreted from cells, and it is used to evaluate the transfection efficacy in terms of IL-10 production.The complex formed with the nucleic acid, P and the polysaccharide was added to the SLNs to obtain the final medicinal products.

For corneal transfection, small sized particles, between 10 and 1,000 nm, reduce eye irritability after topical administration. Moreover, they show mucoadhesive properties, which help to prolong the residence time and, consequently, to increase the drug bioavailability in the ocular tissues [98,187]. The vectors prepared in this section for ocular administration showed a mean size lower than 300 nm, and a positive superficial charge, which facilitates cellular uptake [99] and prolongs retention time at the corneal epithelium, thanks to the electrostatic interactions with the negatively charged ocular surface [188].

SLN_C-vectors presented a weak protection capacity of the nucleic acid against external agents, and a low release ability of both mRNA and pDNA. In the case of mRNA-$SLN1_{EE}$ and mRNA-$SLN1_{HM}$ vectors, differences in the condensation degree were observed. Nevertheless, both formulations protected and released the mRNA effectively. As occurred in the first experimental part of this doctoral thesis, mRNA seems to be more sensitive to the formulation-related factors than pDNA.

The influence of temperature (37 °C *vs* 4 °C) on transfection efficacy) was studied in the HCE-2 cells. Cellular uptake remained stable at both temperatures, which indicates that not only energy-dependent but also energy-independent entry mechanisms are undertaken. Conversely, the percentage of GFP transfected cells (Figure 12) decreased significantly at 4 °C, whereas the intensity of fluorescence, indicative of the amount of protein produced by transfected cells, remained almost stable. Therefore, at cold temperature the few transfected cells are able to produce a high amount of protein. These results show that the transfection of HCE-2 cells is favored by energy-dependent mechanisms, although the production of protein seems to be more efficient when the vectors are taken up by energy-independent mechanisms. The transfection capacity of mRNA- and pDNA-based vectors was similar in terms of transfected cells and intensity of fluorescence. These results indicate that the bottleneck for a successful transfection in corneal epithelial cells is previous to the nuclear entry; consequently, the intra-cytoplasmic behavior of the nanovectors seems to be the limiting step for the transfection.

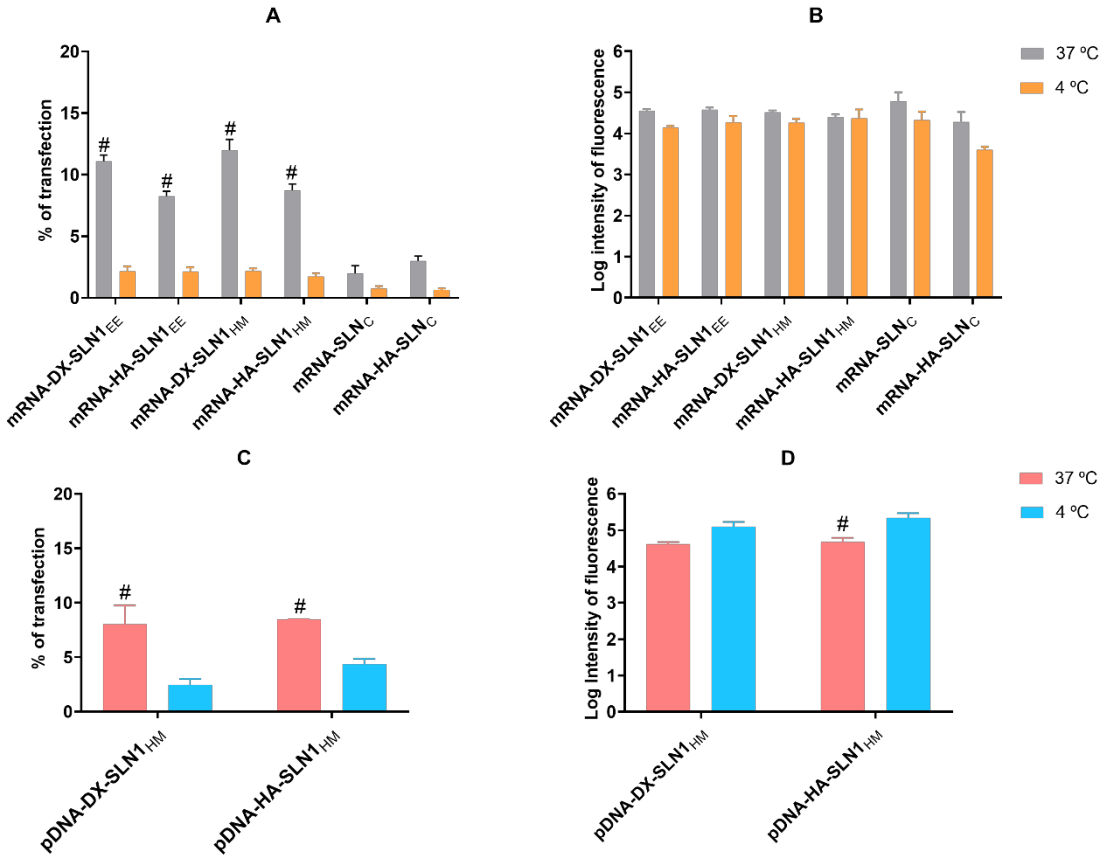

Figure 12. Flow cytometry analysis of GFP transfection efficacy and intensity of fluorescence of HCE-2 cells after the incubation with $SLN1_{EE}$, $SLN1_{HM}$ and SLN_C vectors at 37 °C and 4 °C. Percentage of transfection values correspond to the positive fluorescent GFP cells over the total cells. Log of intensity of fluorescence indicates the average intensity of fluorescence per labeled cell. A: Percentage of transfected HCE-2 cells at 37 °C and 4 °C 48 h after administration of mRNA-based vectors. B: Log of intensity of fluorescence of transfected HCE-2 cells 48 h after administration of mRNA-based vectors. C: Percentage of transfected HCE-2 cells at 37 °C and 4 °C 72 h after administration of pDNA-based vectors. D: Log of intensity of fluorescence of transfected HCE-2 cells 72 h after administration of pDNA-based vectors. Data are expressed as mean ± standard deviation; n = 3. # $p < 0.05$ with respect to the same vector at 4 °C. DX: dextran; HA: hyaluronic acid; $SLN1_{EE}$: solid lipid nanoparticle prepared by emulsification-evaporation method containing DOTAP cationic lipid; $SLN1_{HM}$: solid lipid nanoparticle prepared by hot-melt emulsification method containing DOTAP calitioc lipid; SLN_C: solid lipid nanoparticle prepared by coacervation method.

Transfection studies with the nanovectors bearing pDNA or mRNA encoding the anti-inflammatory cytokine IL-10 were also carried out in HCE-2 cells (Figure 13). IL-10 was measured in the culture media and at intracellular level. The most efficient mRNA vectors in terms of IL-10 production were those containing $SLN1_{EE}$. For $SLN1_{EE}$ and $SLN1_{HM}$ those vectors containing DX were more effective than those containing HA. mRNA-vectors formulated with SLN_C hardly produced IL-10. Levels of IL-10 secreted by cells treated with the vectors prepared with $SLN1_{HM}$ and either mRNA or pDNA were similar. It is expected that levels over 0.8 ng/mL of IL-10 would exert the anti-inflammatory effect [189]. In this case, the IL-10 levels obtained with mRNA-

$SLN1_{EE}$ were higher than this value; in particular, the most effective formulation, mRNA-DX-$SLN1_{EE}$, showed IL-10 levels almost 3 folds higher.

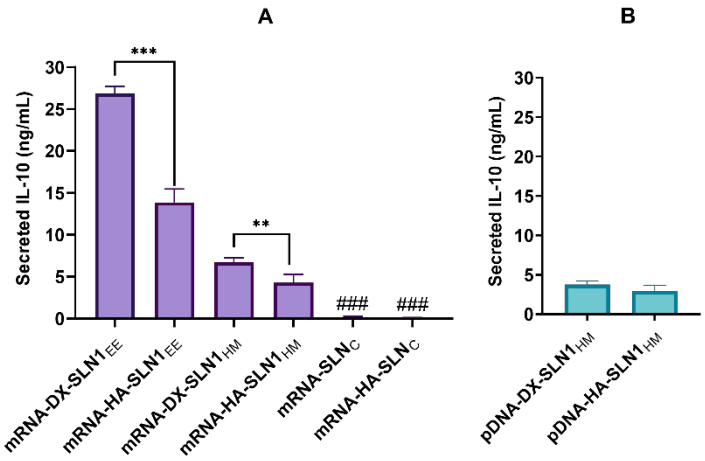

*Figure 13. Levels of secreted IL-10 by HCE-2 cells after the administration of SLN-based vectors bearing IL-10 mRNA and pUNO1-hIL10 plasmid. (A) Concentration of secreted IL-10 48 h after the administration of mRNA-based vectors. (B) Concentration of secreted IL-10 72 h after the administration of pDNA-based vectors. ### p < 0.001 with respect to the mRNA-$SLN1_{EE}$ and mRNA-SLN_C formulations. ** p < 0.01 with respect to the other formulation. *** p < 0.001 with respect to the other formulation. DX: dextran; HA: hyaluronic acid; $SLN1_{EE}$: solid lipid nanoparticle prepared by emulsification-evaporation method containing DOTAP cationic lipid; $SLN1_{HM}$: solid lipid nanoparticle prepared by hot-melt emulsification method containing DOTAP calitioc lipid; SLN_C: solid lipid nanoparticle prepared by coacervation method.*

After evaluating *in vitro* the different treatment strategies for corneal inflammation, and taking into account the high levels of IL-10 obtained with some of the formulations, the strategy based on gene augmentation of IL-10 was selected for *in vivo* evaluation.

4.3. *In vivo* evaluation of the SLN-based formulations containing pDNA or mRNA after topical instillation on the ocular surface of mice

The formulation of nanodelivery systems plays a crucial role in the development of medicinal products based on gene therapy, and specifically, in ocular gene therapy. An optimal ophthalmic drug formulation should comply to an adequate bioavailability, an increased permeability, an improved stability against degradation, a prolonged retention on the eye surface, and an augmented interaction with the cornea and targeted delivery [190]. Indeed, due to the pseudoplastic properties of the tear fluid, the inclusion of thickening agents could be advantageous in order to increase the corneal retention time and ocular bioavailability [191].

For the *in vivo* studies, the thickening agent PVA was added to the vectors. The non-ionic and synthetic biodegradable hydrophilic polymer PVA [192] is approved by the FDA for use in ophthalmic formulations [193]. PVA has been widely used because of its mucomimetic properties, high water retention capacity, oxygen permeability and low toxicity [194]. These

properties confer to the nanosystems the ability to increase the residence time, and consequently improve the ocular bioavailability, reducing the drainage from lachrymal fluid. Moreover, ophthalmic formulations should have the pH of the lacrimal fluid, or a pH within the range of the ocular comfort range, in order to ensure the good tolerance [195,196]. The ocular pH ranges from 6.6 to 7.8; it is reported that a pH value of an ocular preparation outside 5.0-8.5 causes extra lachrymation and decreases the ocular residence time [197]. Our formulations showed pH values within the ocular tolerance range, from 7.1 to 7.5.

In vivo studies in mice were first carried out to evaluate the formulations containing mRNA or pDNA for GFP expression, after the instillation on the mice ocular surface. Since GFP, once produced, remains at intracellular level, it allowed us to identify the corneal layers where transfection occurs. In the case of pDNA formulations, only SLN_{HM} vectors were studied, as pDNA-$SLN1_{EE}$ an pDNA-SLN_C were evaluated in previous studies [80].

In the present study, GFP was detected in 100% of the sections analyzed. As it is observed in Figure 14, all formulations were able to transfect and produce GFP in the corneal epithelium. GFP produced by naked mRNA was difficult to observe, whereas the intensity of fluorescence of GFP was higher when mRNA was formulated in the vectors. Thus, the SLNs resulted necessary to obtain a high transfection efficiency.

SLN-based formulations were able to transfect only the epithelial cells but not the inner layers of the cornea, regardless of their different particle size. In fact, GFP produced by mRNA-DX-$SLN1_{EE}$ and mRNA-DX-$SLN1_{HM}$ was localized continuously along the epithelium surface. In the case of mRNA-HA-$SLN1_{EE}$, mRNA-HA-$SLN1_{HM}$, and mRNA-SLN_C, uninterrupted segments of GFP were observed. In contrast, GFP in the corneas transfected with mRNA-HA-$SLN1_C$ was localized discontinuously. Regarding transfection of the corneas with the nanocarriers prepared with pDNA, GFP was detected in a wider area with pDNA-HA-$SLN1_{HM}$ than with pDNA-DX- $SLN1_{HM}$.

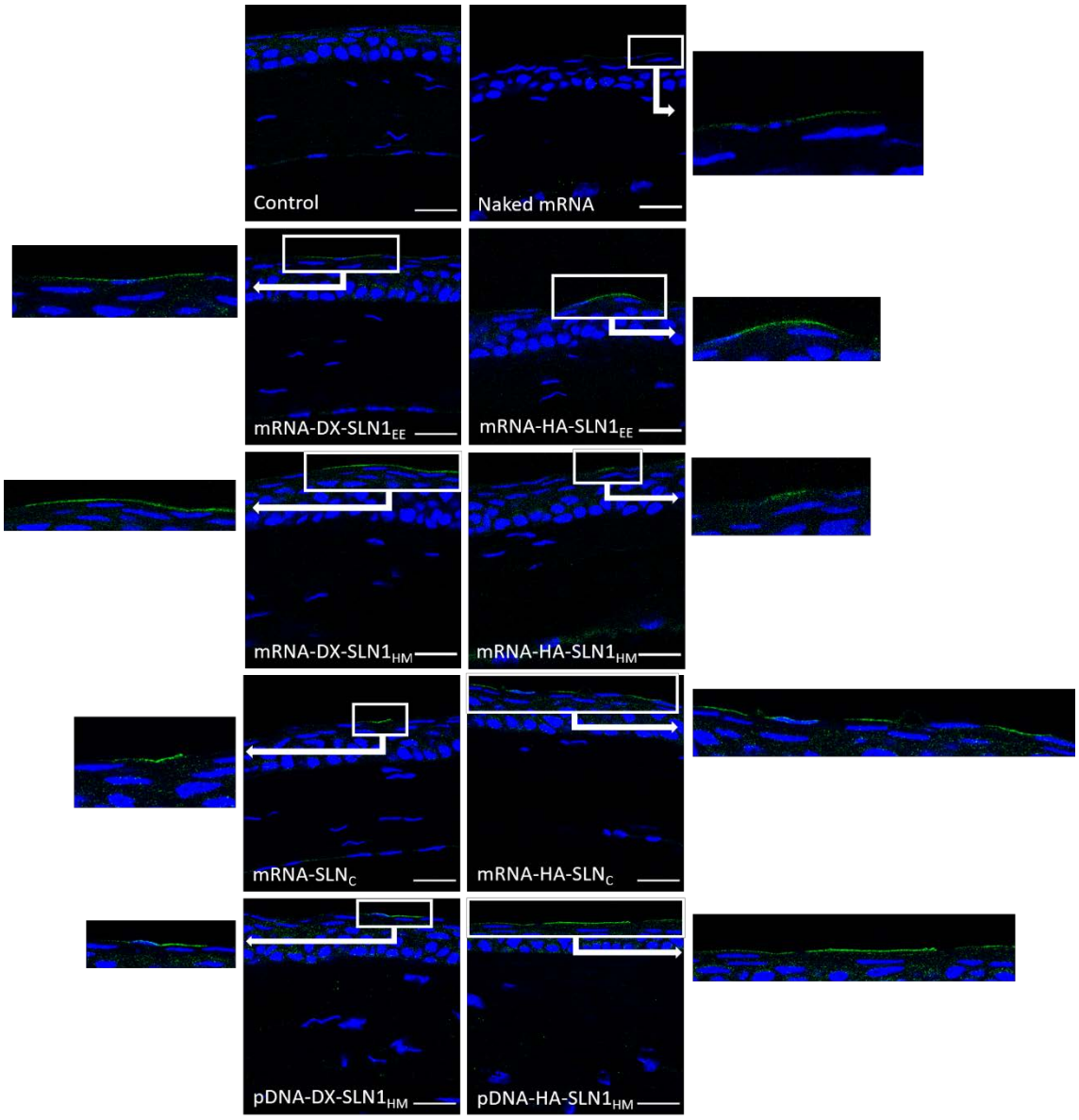

Figure 14. In vivo corneal transfection in mice 48 h after the administration of mRNA- and pDNA-vectors encoding GFP with the viscosifier PVA (63×). Blue: nuclei stained with DAPI. Green: GFP detected by immunofluorescence with the secondary antibody labeled with Alexa Fluor 488. Scale bar: 20 µm. DX: dextran; HA: hyaluronic acid; $SLN1_{EE}$: solid lipid nanoparticle prepared by emulsification-evaporation method containing DOTAP cationic lipid; $SLN1_{HM}$: solid lipid nanoparticle prepared by hot-melt emulsification method containing DOTAP calitioc lipid; SLN_C: solid lipid nanoparticle prepared by coacervation method.

Since the cornea is a complex structure, nucleic acid-delivery systems are engineered to induce the therapeutic protein expression, specifically in the stratified and renewable epithelial layer, where a high number of cells can be transfected. Another alternative could be the transfection of the innermost layer of the cornea, the endothelial layer, associated to a difficult accessibility. Indeed, this layer contains a low number of cells that do not undergo division and gene expression could be maintained for longer times. To this aim, DNA could be most advantageous, since it provides a more persistent transgene production than mRNA. However, mRNA possesses

several advantages, including high efficacy, safety profile, and versatility for fast protein production, which could make it a better option for corneal inflammation management. Moreover, taking into account that the corneal epithelium only needs 7 to 14 days to achieve a complete renewal [198] a short term expression of the protein can be enough for efficacy.

In the next step, we evaluated the capacity of mRNA-formulations to induce the production of the anti-inflammatory cytokine IL-10 *in vivo*. The nucleic acids medicinal products designed were formulated as eye drop and administered topically to mice. In view of the fact that IL-10 is a secreted protein, it may be produced in the epithelial corneal cells and diffuse through the cornea to reach deeper layers. Moreover, for corneal inflammation management, a quick expression of IL-10 would help to deal with the progression of the disease. In this context, we administered the formulations with PVA during 3 days, and 24 h after the last administration the presence of IL-10 in the cornea was assessed.

IL-10 was observed continuously along the corneal epithelium in all analyzed sections. The intensity of the fluorescence signal was higher when the corneas were treated with the nanovectors than in the case of the naked mRNA. When mice were treated with mRNA-DX-$SLN1_{EE}$ vector, the best performing formulation in *in vitro* experiments in HCE-2 cells (Figure 13), the interleukin was even observed in the deeper layers of the epithelium (Figure 15). mRNA-HA-SLN_C vector also showed a high capacity to produce IL-10, despite the low efficacy observed *in vitro*.

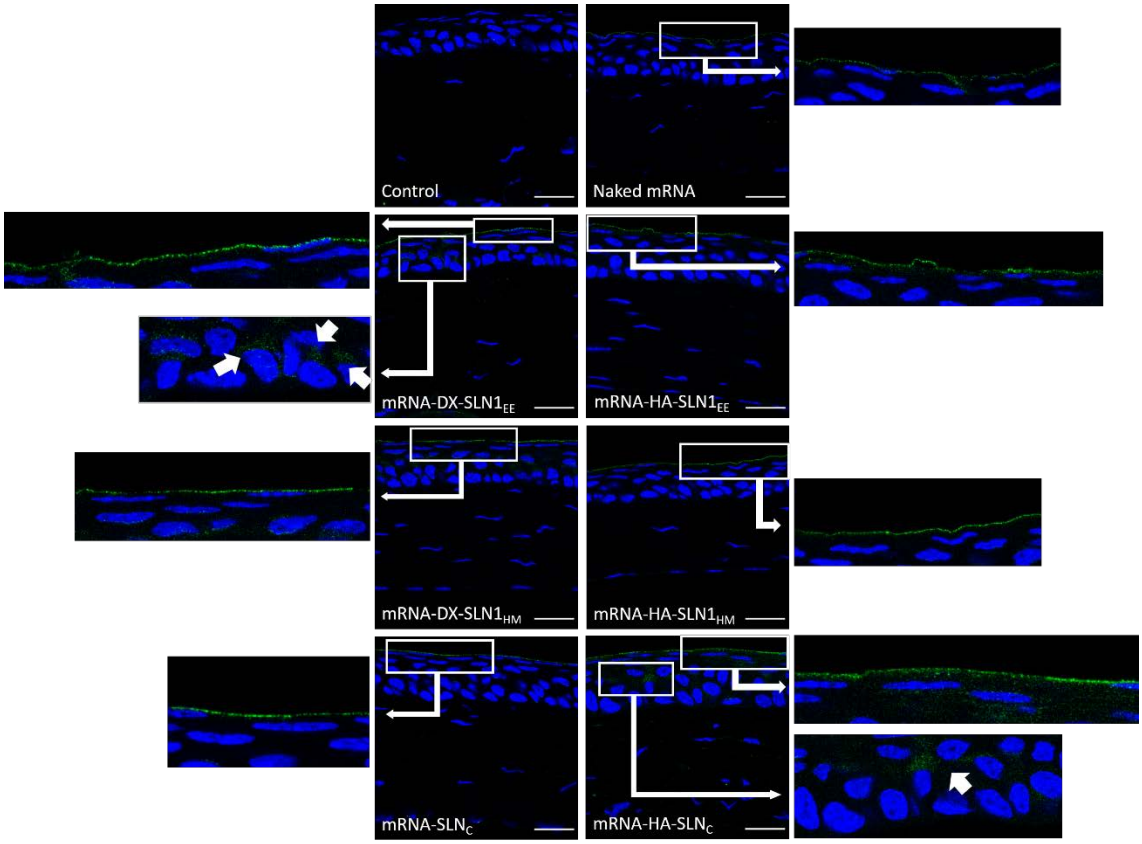

Figure 15. In vivo corneal transfection in mice 24 h after the administration of mRNA-vectors encoding human IL-10 with the viscosifier PVA (63×). Blue: nuclei stained with DAPI. Green: IL-10 detected by immunofluorescence with the secondary antibody labeled with Alexa Fluor 488. Scale bar: 20 µm. DX: dextran; HA: hyaluronic acid; $SLN1_{EE}$: solid lipid nanoparticle prepared by emulsification-evaporation method containing DOTAP cationic lipid; $SLN1_{HM}$: solid lipid nanoparticle prepared by hot-melt emulsification method containing DOTAP calitioc lipid; SLN_C: solid lipid nanoparticle prepared by coacervation method.

The lack of correlation between *in vitro* and *in vivo* studies [199–202] also observed in this study highlights the necessity to perform the latter ones at the earliest phases of the pharmaceutical development process, in order to perform an adequate selection and optimization of candidate formulations.

In order to improve the transfection efficacy and versatility of the nanovectors, in the last part of the doctoral thesis, it was carried out the design of new formulations composed by SLNs, P, polysaccharides and AuNPs, as pDNA or mRNA delivery systems.

4.4. *In vitro* and *in vivo* evaluation of lipid-based nanovectors containing inorganic nanoparticles for nucleic acid delivery

Among inorganic particles, noble metals and in particular AuNPs, are characterized by unique chemical, physical and, optical properties, which makes them attractive for biomedical applications, in particular in drug and gene delivery and photothermal treatment in cancer [203–

205]. AuNPs are bio-inert and biocompatible, and they have reported low cytotoxicity and good stability against oxidation and degradation *in vivo*, and are easy to functionalize with a wide range of ligands, which influence in their size and properties [206]. Moreover, AuNPs have demonstrated to possess intrinsic therapeutic properties, such as anti-angiogenic [207][208] and anti-inflammatory [209] effects. Additionally, these inorganic nanoparticles have the capacity to condense the genetic material at high packing densities, providing efficient delivery, decreasing the risk of enzymatic degradation [210][211]. These properties make AuNPs an interesting component to be included in non-viral vectors for mRNA and DNA delivery against CNV associated to inflammation [204].

The golden lipid nanoparticles containing pDNA or mRNA encoding GFP, P, a polysaccharide (DX or HA), $SLN1_{EE}$ and AuNPs were firstly optimized, *in vitro* studied and then, *in vivo* evaluated after topical administration to eye mice.

Table 8 shows the size, PDI and superficial charge of representative vectors containing AuNPs.

Table 8. Physical characterization of the golden lipid nanoparticles.

Name of the vector	Size (nm)	PDI	ζ-Potential (mV)
mRNA-DX- $SLN1_{EE}$_Au	184.33 ± 2.22	0.29 ± 0.02	+39.78 ± 1.54
mRNA-HA- $SLN1_{EE}$_Au	212.80 ± 5.46	0.32 ± 0.04	+28.23 ± 0.61
pDNA-DX- $SLN1_{EE}$_Au	151.33 ± 1.70	0.28 ± 0.03	+43.75 ± 1.74
pDNA-HA- $SLN1_{EE}$_Au	208.97 ± 3.62	0.34 ± 0.01	+29.35 ± 0.39

DX: dextran; HA: hyaluronic acid; Au: gold; $SLN1_{EE}$: solid lipid nanoparticle prepared by emulsification-evaporation method containing DOTAP cationic lipid. Data are expressed as mean ± standard deviation; *n*=3.

Physicochemical features showed that the incorporation of AuNPs in SLNs were capable of reducing the size and PDI, especially in mRNA nanovectors. Despite a further component was added, the golden lipid nanoparticles showed a PDI below 0.35. The smaller the PDI is, the higher the homogeneity in the size of the particles of the sample, demonstrating a monodisperse sample population, which is considered acceptable for drug and gene delivery [212]. Figure 16 shows representative TEM photographs of mRNA- and pDNA-golden lipid nanoparticles.

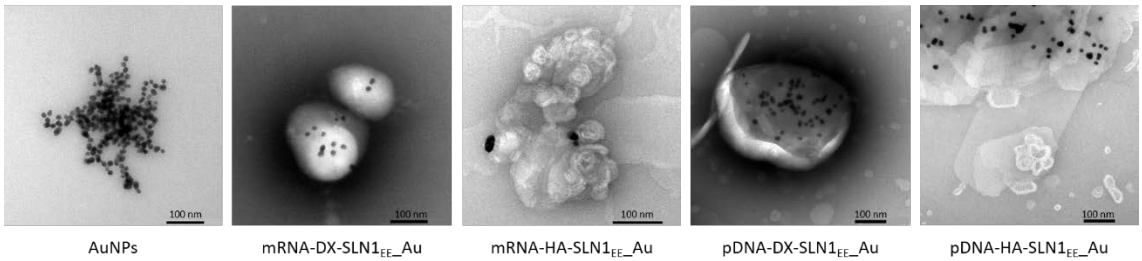

Figure 16. Images of mRNA- and pDNA-golden lipid nanoparticles acquired by TEM. DX: dextran; HA: hyaluronic acid; Au: gold; SLN1EE: solid lipid nanoparticle prepared by emulsification-evaporation method containing DOTAP cationic lipid.

The capacity of the golden lipid nanoparticles to bind, protect and release the mRNA (Figure 17A) and the pDNA (Figure 17B) was also evaluated by agarose gel electrophoresis assay.

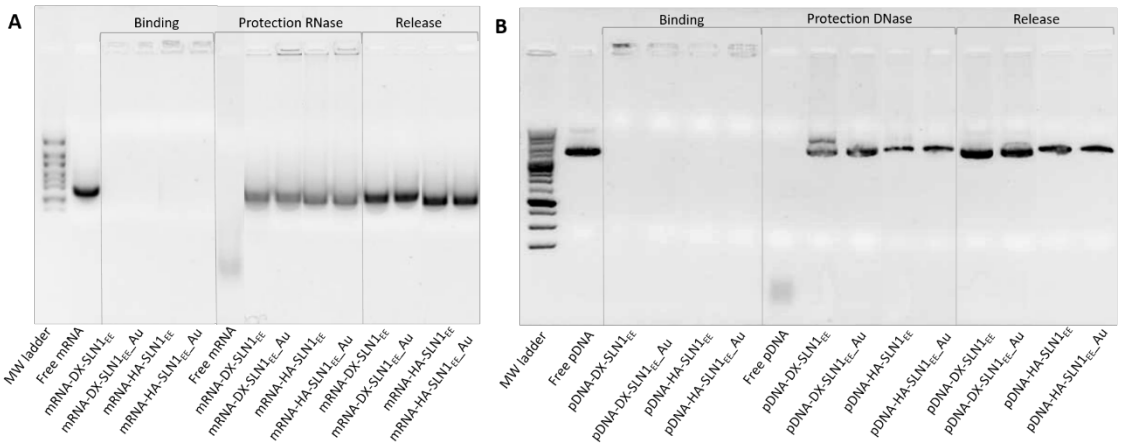

Figure 17. Binding, protection and release capacity of golden lipid nanoparticles. A: mRNA-golden lipid nanoparticles. B: pDNA-golden lipid nanoparticles. DX: dextran; HA: hyaluronic acid; Au: gold; SLN1EE: solid lipid nanoparticle prepared by emulsification-evaporation method containing DOTAP cationic lipid.

Regarding the binding capacity, in both gels the absence of bands on the corresponding lanes and the presence of mRNA and pDNA on the loading wells indicate that the nucleic acid was unable to migrate through the gel, and, therefore, it was completely bound to the vector. The golden lipid nanoparticles were able to protect mRNA and pDNA when treated with RNase I and DNase I, respectively, while free mRNA and free pDNA were totally degraded. However, the disappearance of one of the two bands of pDNA-DX-SLN1$_{EE}$ when AuNPs were incorporated in the formulation indicates than the conformation of the nucleic acid had changed. It could be related to the capacity of AuNPs to condense and increase the packaging of the nucleic acids, and therefore, protecting the nucleic acid from degradation, which provides stability to the systems at intracellular level. After the treatment with SDS, mRNA and pDNA were able to migrate from the loading wells, which demonstrates its ability to be released from the golden lipid nanoparticles.

Transfection efficacy studies of the golden lipid nanoparticles were carried out in different cell lines: ARPE-19 cells (Figure 18A), HEK-293 cells (Figure 18B) and HCE-2 cells. Overall, the percentage of transfected cells and the intensity of fluorescence, indicative of protein production, were higher with the golden lipid nanoparticles. Regarding mRNA, in ARPE-19 cells, the addition of AuNPs lead to the increment of the percentage of transfected cells from 58% to 86%. In HEK-293 cells, the increment was even greater with mRNA-DX-SLN1$_{EE}$ vector. In fact, the transfection increased from 4% to 48%. In the case of mRNA-HA-SLN1$_{EE}$ vector, although the percentage of transfected cells was maintained with the incorporation of AuNPs, an increment in the intensity of fluorescence was produced. The transfection efficacy of mRNA-golden lipid nanoparticles in HCE-2 cells was similar than that obtained in vectors without AuNPs. In fact, the percentage of transfected cells of mRNA formulations ranged from 12% without AuNPs to 18% with AuNPs. However, an increment in the intensity of fluorescence was shown. Cell viability was approximately 98% for all formulations.

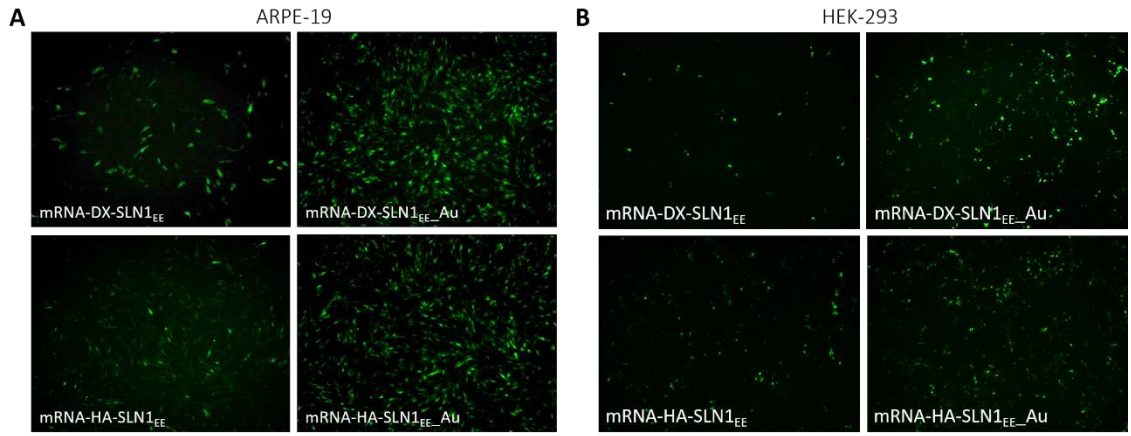

Figure 18. Transfection efficacy of mRNA-golden lipid nanoparticles in (A) ARPE-19 cells and (B) HEK-293 cells. DX: dextran; HA: hyaluronic acid; Au: gold; SLN1$_{EE}$: solid lipid nanoparticle prepared by emulsification-evaporation method containing DOTAP cationic lipid.

Finally, the golden lipid nanoparticles bearing mRNA encoding GFP were administered to mice by topical instillation into the eye, as an *in vivo* proof of concept to evaluate their possible application in ocular diseases. The results depicted in the Figure 19 show that all nanovectors evaluated were able to produce GFP in the corneal tissue. Moreover, the intensity of fluorescence in the epithelial and endothelial layers were more intense with the nanovectors containing AuNPs than without the inorganic particles, especially with mRNA-HA-SLN1$_{EE}$_Au formulation. These transfection results together with the intrinsic therapeutic features of anti-angiogenic [207,208] and anti-inflammatory [209] effects that AuNPs possess make gold lipid

nanoparticles a potential medicinal product for corneal inflammation, although additional studies are necessary.

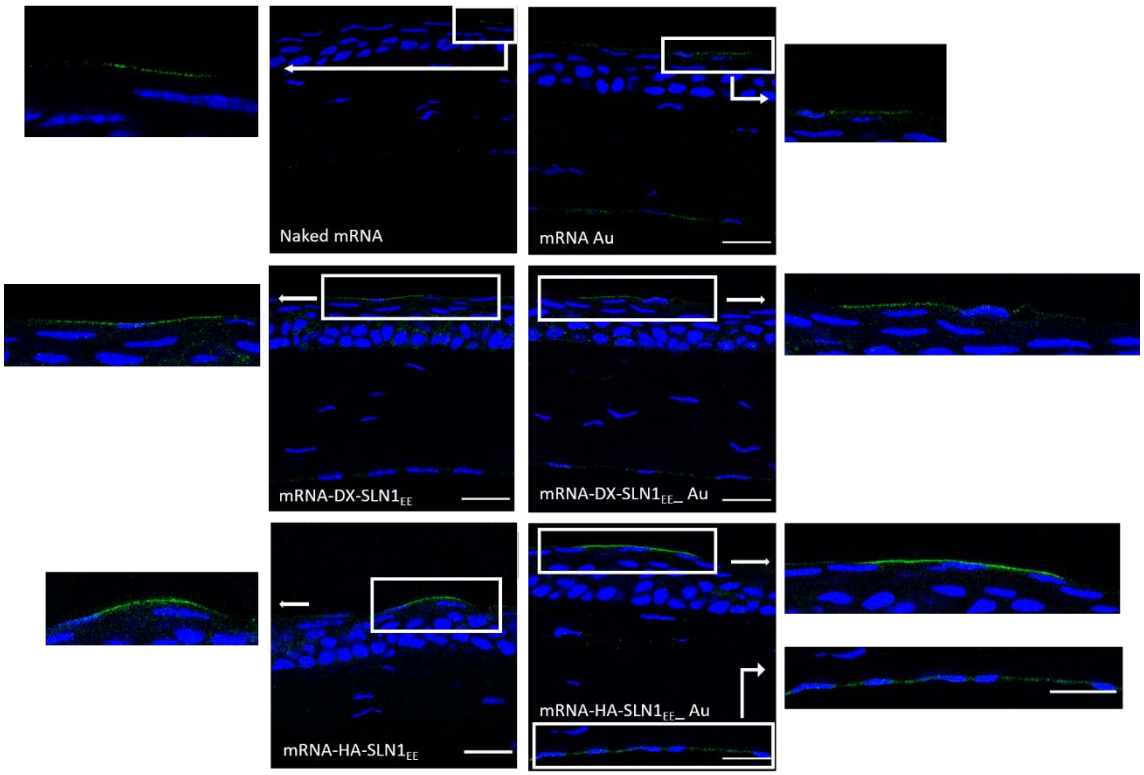

Figure 19. In vivo corneal transfection in mice 48 h after the administration of mRNA- and pDNA-golden lipid nanoparticles encoding GFP (63×). Blue: nuclei stained with DAPI. Green: GFP detected by immunofluorescence with the secondary antibody labeled with Alexa Fluor 488. DX: dextran; HA: hyaluronic acid; Au: gold; $SLN1_{EE}$: solid lipid nanoparticle prepared by emulsification-evaporation method containing DOTAP cationic lipid.

In summary, in this doctoral thesis, DNA and mRNA delivery systems based on SLNs have been designed to address corneal inflammation by gene therapy. First, the composition of SLNs, the preparation technique and the incorporation of different ligands were optimized to obtain cationic and nucleic acid-based nanosized medicinal products with high *in vitro* efficacy and long-term stability. The shRNA-medicinal products developed against the proangiogenic factor MMP-9 showed *in vitro* the potential of RNAi technology for the treatment of inflammation-associated CNV by gene silencing. The present dissertation also demonstrates that topical administration of mRNA- and pDNA-based medicinal products formulated as eye drops to mice induced the synthesis of the anti-inflammatory cytokine IL10 in the cornea, underlining the possible contribution of non-viral gene supplementation therapy to the future clinical approach of corneal inflammation. Finally, the combination of AuNPs with SLNs-based nanovectors show a great advantage in terms of the physical properties and *in vivo* transfection efficacy, highlighting the potential of innovative golden lipid nanoparticles as nucleic acid delivery systems. The

novelty of these results has led to the filling of a patent application entitled “Golden lipid nanoparticles for gene therapy” (International publication number WO 2021/130215 A1).

5. REFERENCES

1. European Medicines Agency. Guideline on the quality, non-clinical and clinical aspects of gene therapy medicinal products. *Eur. Med. Agency Guidel.* 2015, *44*, 1–41.

2. Thorne, B.; Takeya, R.; Vitelli, F.; Swanson, X. Gene Therapy. In *New Bioprocessing Strategies: Development and Manufacturing of Recombinant Antibodies and Proteins*; Kiss, B., Gottschalk, U., Pohlscheidt, M., Eds.; Springer International Publishing: Cham, 2018; pp. 351–399 ISBN 978-3-319-97110-0.

3. Anguela, X.M.; High, K.A. Entering the Modern Era of Gene Therapy. *Annu. Rev. Med.* 2019, *70*, 273–288, doi:10.1146/annurev-med-012017-043332.

4. del Pozo-Rodríguez, A.; Rodríguez-Gascón, A.; Rodríguez-Castejón, J.; Vicente-Pascual, M.; Gómez-Aguado, I.; Battaglia, L.S.; Solinís, M.Á. Gene Therapy. In *Current Applications of Pharmaceutical Biotechnology*; Silva, A.C., Moreira, J.N., Lobo, J.M.S., Almeida, H., Eds.; Springer International Publishing: Cham, 2020; pp. 321–368 ISBN 978-3-030-40464-2.

5. Hajj, K.A.; Whitehead, K.A. Tools for translation: Non-viral materials for therapeutic mRNA delivery. *Nat. Rev. Mater.* 2017, *2*, 1–17, doi:10.1038/natrevmats.2017.56.

6. Sahin, U.; Karikó, K.; Türeci, Ö. MRNA-based therapeutics-developing a new class of drugs. *Nat. Rev. Drug Discov.* 2014, *13*, 759–780, doi:10.1038/nrd4278.

7. Meng, Z.; O'Keeffe-Ahern, J.; Lyu, J.; Pierucci, L.; Zhou, D.; Wang, W. A new developing class of gene delivery: Messenger RNA-based therapeutics. *Biomater. Sci.* 2017, *5*, 2381–2392, doi:10.1039/c7bm00712d.

8. Zarghampoor, F.; Azarpira, N.; Khatami, S.R.; Behzad-Behbahani, A.; Foroughmand, A.M. Improved translation efficiency of therapeutic mRNA. *Gene* 2019, *707*, 231–238, doi:10.1016/j.gene.2019.05.008.

9. Zhong, Z.; Mc Cafferty, S.; Combes, F.; Huysmans, H.; De Temmerman, J.; Gitsels, A.; Vanrompay, D.; Portela Catani, J.; Sanders, N.N. mRNA therapeutics deliver a hopeful message. *Nano Today* 2018, *23*, 16–39, doi:10.1016/j.nantod.2018.10.005.

10. Schlake, T.; Thess, A.; Thran, M.; Jordan, I. mRNA as novel technology for passive immunotherapy. *Cell. Mol. Life Sci.* 2019, *76*, 301–328, doi:10.1007/s00018-018-2935-4.

11. Patel, S.; Athirasala, A.; Menezes, P.P.; Ashwanikumar, N.; Zou, T.; Sahay, G.; Bertassoni, L.E. Messenger RNA Delivery for Tissue Engineering and Regenerative Medicine Applications. *Tissue Eng. - Part A* 2019, *25*, 91–112, doi:10.1089/ten.tea.2017.0444.

12. Hecker, J.G. Non-Viral, Lipid-Mediated DNA and mRNA Gene Therapy of the Central Nervous System (CNS): Chemical-Based Transfection. In *Gene Therapy for Neurological Disorders: Methods and Protocols*; Manfredsson, F.P., Ed.; Springer New York: New York, NY, 2016; pp. 307–324 ISBN 978-1-4939-3271-9.

13. May, M. After COVID-19 successes, researchers push to develop mRNA vaccines for other diseases. *Nat. Med.* 2021, *27*, 930–932, doi:10.1038/s41591-021-01393-8.

14. Igyártó, B.Z.; Jacobsen, S.; Ndeupen, S. Future considerations for the mRNA-lipid nanoparticle vaccine platform. *Curr. Opin. Virol.* 2021, *48*, 65–72, doi:10.1016/J.COVIRO.2021.03.008.

15. Chakraborty, C.; Sharma, A.R.; Bhattacharya, M.; Lee, S.-S. From COVID-19 to Cancer

mRNA Vaccines: Moving From Bench to Clinic in the Vaccine Landscape. *Front. Immunol.* 2021, *12*, 1–17, doi:10.3389/fimmu.2021.679344.

16. U.S. Department of Health and Human Services. Food and Drug Administration. COVID-19 Vaccines. Available online: https://www.fda.gov/emergency-preparedness-and-response/coronavirus-disease-2019-covid-19/covid-19-vaccines (accessed on 28 December 2021).

17. European Medicines Agency. Science Medicines Health. COVID-19 vaccines. Available online: https://www.ema.europa.eu/en/human-regulatory/overview/public-health-threats/coronavirus-disease-covid-19/treatments-vaccines/covid-19-vaccines (accessed on 28 Decem.

18. Gediz Erturk, A.; Sahin, A.; Ay, E.B.; Pelit, E.; Bagdatli, E.; Kulu, I.; Gul, M.; Mesci, S.; Eryilmaz, S.; Yildirim, T.; et al. molecules A Multidisciplinary Approach to Coronavirus Disease (COVID-19). 2021, doi:10.3390/molecules26123526.

19. Bajaj, V.; Gadi, N.; Spihlman, A.P.; Wu, S.C.; Choi, C.H.; Moulton, V.R. Aging, Immunity, and COVID-19: How Age Influences the Host Immune Response to Coronavirus Infections? *Front. Physiol.* 2021, *11*, doi:10.3389/fphys.2020.571416.

20. Vallazza, B.; Petri, S.; Poleganov, M.A.; Eberle, F.; Kuhn, A.N.; Sahin, U. Recombinant messenger RNA technology and its application in cancer immunotherapy, transcript replacement therapies, pluripotent stem cell induction, and beyond. *Wiley Interdiscip. Rev. RNA* 2015, *6*, 471–499, doi:10.1002/wrna.1288.

21. Kowalski, P.S.; Rudra, A.; Miao, L.; Anderson, D.G. Delivering the Messenger: Advances in Technologies for Therapeutic mRNA Delivery. *Mol. Ther.* 2019, *27*, 710–728, doi:10.1016/j.ymthe.2019.02.012.

22. Xiong, Q.; Lee, G.Y.; Ding, J.; Li, W.; Shi, J. Biomedical applications of mRNA nanomedicine. *Nano Res.* 2018, *11*, 5281–5309, doi:10.1007/s12274-018-2146-1.

23. del Pozo-Rodríguez, A.; Delgado, D.; Solinís, M.A.; Gascón, A.R.; Pedraz, J.L. Solid lipid nanoparticles for retinal gene therapy: Transfection and intracellular trafficking in RPE cells. *Int. J. Pharm.* 2008, *360*, 177–183, doi:10.1016/j.ijpharm.2008.04.023.

24. Gan, L.; Wang, J.; Zhao, Y.; Chen, D.; Zhu, C.; Liu, J.; Gan, Y. Hyaluronan-modified core-shell liponanoparticles targeting CD44-positive retinal pigment epithelium cells via intravitreal injection. *Biomaterials* 2013, *34*, 5978–5987, doi:10.1016/j.biomaterials.2013.04.035.

25. Apaolaza, P.S.; del Pozo-Rodríguez, A.; Solinís, M.A.; Rodríguez, J.M.; Friedrich, U.; Torrecilla, J.; Weber, B.H.F.; Rodríguez-Gascón, A. Structural recovery of the retina in a retinoschisin-deficient mouse after gene replacement therapy by solid lipid nanoparticles. *Biomaterials* 2016, *90*, 40–49, doi:https://doi.org/10.1016/j.biomaterials.2016.03.004.

26. Stewart, M.P.; Sharei, A.; Ding, X.; Sahay, G.; Langer, R.; Jensen, K.F. In vitro and ex vivo strategies for intracellular delivery. *Nature* 2016, *538*, 183–192, doi:10.1038/nature19764.

27. Patel, S.; Ashwanikumar, N.; Robinson, E.; Duross, A.; Sun, C.; Murphy-Benenato, K.E.; Mihai, C.; Almarsson, Ö.; Sahay, G. Boosting Intracellular Delivery of Lipid Nanoparticle-Encapsulated mRNA. *Nano Lett.* 2017, *17*, 5711–5718, doi:10.1021/acs.nanolett.7b02664.

28. Ulkoski, D.; Bak, A.; Wilson, J.T.; Krishnamurthy, V.R. Recent advances in polymeric materials for the delivery of RNA therapeutics. *Expert Opin. Drug Deliv.* 2019, *16*, 1149–1167, doi:10.1080/17425247.2019.1663822.

29. Rodríguez-Gascón, A.; del Pozo-Rodríguez, A.; Solinís, M.Á. Development of nucleic acid vaccines: Use of self-amplifying RNA in lipid nanoparticles. *Int. J. Nanomedicine* 2014, *9*, 1833–1843, doi:10.2147/IJN.S39810.

30. Gene Therapy Clinical Trials Worldwide. Provided by Journal of Gene Medicine, John Wileys and Sons LTD. 2021. Available online: https://a873679.fmphost.com/fmi/webd/GTCT (accessed on 18 Sept 2021).

31. Carvalho, M.; Sepodes, B.; Martins, A.P. Regulatory and Scientific Advancements in Gene Therapy: State-of-the-Art of Clinical Applications and of the Supporting European Regulatory Framework. *Front. Med.* 2017, *4*, 182, doi:10.3389/fmed.2017.00182.

32. del Pozo-Rodríguez, A.; Solinís, M.Á.; Rodríguez-Gascón, A. Applications of lipid nanoparticles in gene therapy. *Eur. J. Pharm. Biopharm.* 2016, *109*, 184–193, doi:10.1016/j.ejpb.2016.10.016.

33. Wang, Y.; Rajala, A.; Rajala, R.V.S. Lipid Nanoparticles for Ocular Gene Delivery. *J. Funct. Biomater.* 2015, *6*.

34. Yin, H.; Kanasty, R.L.; Eltoukhy, A.A.; Vegas, A.J.; Dorkin, J.R.; Anderson, D.G. Non-viral vectors for gene-based therapy. *Nat. Rev. Genet.* 2014, *15*, 541–555, doi:10.1038/nrg3763.

35. Guan, S.; Rosenecker, J. Nanotechnologies in delivery of mRNA therapeutics using nonviral vector-based delivery systems. *Gene Ther.* 2017, *24*, 133–143, doi:10.1038/gt.2017.5.

36. Rodríguez-Gascón, A.; del Pozo-Rodríguez, A.; Isla, A.; Solinís, M.A. Vaginal gene therapy. *Adv. Drug Deliv. Rev.* 2015, *92*, 71–83, doi:10.1016/j.addr.2015.07.002.

37. Lorenz, C.; Fotin-Mleczek, M.; Roth, G.; Becker, C.; Dam, T.C.; Verdurmen, W.P.R.; Brock, R.; Probst, J.; Schlake, T. Protein expression from exogenous mRNA: Uptake by receptor-mediated endocytosis and trafficking via the lysosomal pathway. *RNA Biol.* 2011, *8*, doi:10.4161/rna.8.4.15394.

38. Gascón, A.R.; del Pozo-Rodríguez, A.; Solinís, M.A. Non-Viral Delivery Systems in Gene Therapy. In *Gene Therapy*; Molina, F.M., Ed.; IntechOpen: Rijeka, 2013.

39. Van Tendeloo, V.F.I.; Ponsaerts, P.; Lardon, F.; Nijs, G.; Lenjou, M.; Van Broeckhoven, C.; Van Bockstaele, D.R.; Berneman, Z.N. Highly efficient gene delivery by mRNA electroporation in human hematopoietic cells: Superiority to lipofection and passive pulsing of mRNA and to electroporation of plasmid cDNA for tumor antigen loading of dendritic cells. *Blood* 2001, *98*, 49–56, doi:10.1182/blood.V98.1.49.

40. Bugeon, S.; De Chevigny, A.; Boutin, C.; Coré, N.; Wild, S.; Bosio, A.; Cremer, H.; Beclin, C. Direct and efficient transfection of mouse neural stem cells and mature neurons by in vivo mRNA electroporation. *Dev.* 2017, *144*, 3968–3977, doi:10.1242/dev.151381.

41. Golombek, S.; Pilz, M.; Steinle, H.; Kochba, E.; Levin, Y.; Lunter, D.; Schlensak, C.; Wendel, H.P.; Avci-Adali, M. Intradermal Delivery of Synthetic mRNA Using Hollow Microneedles for Efficient and Rapid Production of Exogenous Proteins in Skin. *Mol. Ther. - Nucleic Acids* 2018, *11*, 382–392, doi:https://doi.org/10.1016/j.omtn.2018.03.005.

42. Moody, S.A. Microinjection of mRNAs and oligonucleotides. *Cold Spring Harb. Protoc.* 2018, *2018*, 923–932, doi:10.1101/pdb.prot097261.

43. Ainger, K.; Avossa, D.; Morgan, F.; Hill, S.J.; Barry, C.; Barbarese, E.; Carson, J.H. Transport and localization of exogenous myelin basic protein mRNA microinjected into oligodendrocytes. *J. Cell Biol.* 1993, *123*, 431–441, doi:10.1083/jcb.123.2.431.

44. Belyantseva, I.A. Helios® Gene Gun-Mediated Transfection of the Inner Ear Sensory Epithelium: Recent Updates. In *Auditory and Vestibular Research: Methods and Protocols*; Sokolowski, B., Ed.; Springer New York: New York, NY, 2016; pp. 3–26 ISBN 978-1-4939-3615-1.

45. Vassilev, V.B.; Gil, L.H.V.G.; Donis, R.O. Microparticle-mediated RNA immunization against bovine viral diarrhea virus. *Vaccine* 2001, *19*, 2012–2019, doi:10.1016/S0264-410X(00)00438-2.

46. Ramezanpour, M.; Schmidt, M.L.; Bodnariuc, I.; Kulkarni, J.A.; Leung, S.S.W.; Cullis, P.R.; Thewalt, J.L.; Tieleman, D.P. Ionizable amino lipid interactions with POPC: implications for lipid nanoparticle function. *Nanoscale* 2019, *11*, 14141–14146, doi:10.1039/C9NR02297J.

47. Islam, M.A.; Xu, Y.; Tao, W.; Ubellacker, J.M.; Lim, M.; Aum, D.; Lee, G.Y.; Zhou, K.; Zope, H.; Yu, M.; et al. Restoration of tumour-growth suppression in vivo via systemic nanoparticle-mediated delivery of PTEN mRNA. *Nat. Biomed. Eng.* 2018, *2*, 850–864, doi:10.1038/s41551-018-0284-0.

48. Kauffman, K.J.; Webber, M.J.; Anderson, D.G. Materials for non-viral intracellular delivery of messenger RNA therapeutics. *J. Control. Release* 2016, *240*, 227–234, doi:10.1016/j.jconrel.2015.12.032.

49. Phua, K.K.L.; Leong, K.W.; Nair, S.K. Transfection efficiency and transgene expression kinetics of mRNA delivered in naked and nanoparticle format. *J. Control. Release* 2013, *166*, 227–233, doi:https://doi.org/10.1016/j.jconrel.2012.12.029.

50. Malone, R.W.; Felgner, P.L.; Verma, I.M. Cationic liposome-mediated RNA transfection [cationic lipid vesicies/N-[1-(2,3-dioleyloxy)propyl]-NNN-timethylammonium chloride (DOTMA)/translationj. *Proc. Natl. Acad. Sci. USA* 1989, *86*, 6077–6081.

51. Koltover, I.; Salditt, T.; Rädler, J.O.; Safinya, C.R. An inverted hexagonal phase of cationic liposome-DNA complexes related to DNA release and delivery. *Science (80-.).* 1998, *281*, 78–81, doi:10.1126/science.281.5373.78.

52. Ruponen, M.; Honkakoski, P.; Rönkkö, S.; Pelkonen, J.; Tammi, M.; Urtti, A. Extracellular and intracellular barriers in non-viral gene delivery. *J. Control. Release* 2003, *93*, 213–217, doi:https://doi.org/10.1016/j.jconrel.2003.08.004.

53. Koynova, R.; Wang, L.; Tarahovsky, Y.; MacDonald, R.C. Lipid Phase Control of DNA Delivery. *Bioconjug. Chem.* 2005, *16*, 1335–1339, doi:10.1021/bc050226x.

54. Sayour, E.J.; De Leon, G.; Pham, C.; Grippin, A.; Kemeny, H.; Chua, J.; Huang, J.; Sampson, J.H.; Perez, L.S.; Flores, C.; et al. Systemic activation of antigen-presenting cells via RNA-Loaded nanoparticles. *Oncoimmunology* 2017, *6*, 1–14, doi:10.1080/2162402X.2016.1256527.

55. Kranz, L.M.; Diken, M.; Haas, H.; Kreiter, S.; Loquai, C.; Reuter, K.C.; Meng, M.; Fritz, D.; Vascotto, F.; Hefesha, H.; et al. Systemic RNA delivery to dendritic cells exploits antiviral defence for cancer immunotherapy. *Nature* 2016, *534*, 396–401,

doi:10.1038/nature18300.

56. Kulkarni, J.A.; Cullis, P.R.; Van Der Meel, R. Lipid Nanoparticles Enabling Gene Therapies: From Concepts to Clinical Utility. *Nucleic Acid Ther.* 2018, *28*, 146–157, doi:10.1089/nat.2018.0721.

57. Kauffman, K.J.; Dorkin, J.R.; Yang, J.H.; Heartlein, M.W.; DeRosa, F.; Mir, F.F.; Fenton, O.S.; Anderson, D.G. Optimization of Lipid Nanoparticle Formulations for mRNA Delivery in Vivo with Fractional Factorial and Definitive Screening Designs. *Nano Lett.* 2015, *15*, 7300–7306, doi:10.1021/acs.nanolett.5b02497.

58. Adams, D.; Gonzalez-Duarte, A.; O'Riordan, W.D.; Yang, C.C.; Ueda, M.; Kristen, A. V.; Tournev, I.; Schmidt, H.H.; Coelho, T.; Berk, J.L.; et al. Patisiran, an RNAi therapeutic, for hereditary transthyretin amyloidosis. *N. Engl. J. Med.* 2018, *379*, 11–21, doi:10.1056/NEJMoa1716153.

59. Zhang, X.; Goel, V.; Robbie, G.J. Pharmacokinetics of Patisiran, the First Approved RNA Interference Therapy in Patients With Hereditary Transthyretin-Mediated Amyloidosis. *J. Clin. Pharmacol.* 2019, doi:10.1002/jcph.1553.

60. Sedic, M.; Senn, J.J.; Lynn, A.; Laska, M.; Smith, M.; Platz, S.J.; Bolen, J.; Hoge, S.; Bulychev, A.; Jacquinet, E.; et al. Safety Evaluation of Lipid Nanoparticle–Formulated Modified mRNA in the Sprague-Dawley Rat and Cynomolgus Monkey. *Vet. Pathol.* 2018, *55*, 341–354, doi:10.1177/0300985817738095.

61. Li, B.; Zhang, X.; Dong, Y. Nanoscale platforms for messenger RNA delivery. *Wiley Interdiscip. Rev. Nanomedicine Nanobiotechnology* 2019, *11*, 1–14, doi:10.1002/wnan.1530.

62. Lu, D.; Benjamin, R.; Kim, M.; Conry, R.M.; Curiel, D.T. Optimization of methods to achieve mRNA-mediated transfection of tumor cells in vitro and in vivo employing cationic liposome vectors. *Cancer Gene Ther.* 1994, *1*, 245–252.

63. Pardi, N.; Hogan, M.J.; Pelc, R.S.; Muramatsu, H.; Andersen, H.; DeMaso, C.R.; Dowd, K.A.; Sutherland, L.L.; Scearce, R.M.; Parks, R.; et al. Zika virus protection by a single low-dose nucleoside-modified mRNA vaccination. *Nature* 2017, *543*, 248–251, doi:10.1038/nature21428.

64. Hekele, A.; Bertholet, S.; Archer, J.; Gibson, D.G.; Palladino, G.; Brito, L.A.; Otten, G.R.; Brazzoli, M.; Buccato, S.; Bonci, A.; et al. Rapidly produced SAM(®) vaccine against H7N9 influenza is immunogenic in mice. *Emerg. Microbes Infect.* 2013, *2*, e52, doi:10.1038/emi.2013.54.

65. Zhou, W.Z.; Hoon, D.S.B.; Huang, S.K.S.; Fujii, S.; Hashimoto, K.; Morishita, R.; Kaneda, Y. RNA melanoma vaccine: Induction of antitumor immunity by human glycoprotein 100 mRNA immunization. *Hum. Gene Ther.* 1999, *10*, 2719–2724, doi:10.1089/10430349950016762.

66. Finn, J.D.; Smith, A.R.; Patel, M.C.; Shaw, L.; Youniss, M.R.; van Heteren, J.; Dirstine, T.; Ciullo, C.; Lescarbeau, R.; Seitzer, J.; et al. A Single Administration of CRISPR/Cas9 Lipid Nanoparticles Achieves Robust and Persistent In Vivo Genome Editing. *Cell Rep.* 2018, *22*, 2227–2235, doi:10.1016/j.celrep.2018.02.014.

67. Solinís, M.Á.; del Pozo-Rodríguez, A.; Apaolaza, P.S.; Rodríguez-Gascón, A. Treatment of ocular disorders by gene therapy. *Eur. J. Pharm. Biopharm.* 2015, *95*, 331–342, doi:https://doi.org/10.1016/j.ejpb.2014.12.022.

68. Müller, R.H.; Radtke, M.; Wissing, S.A. Solid lipid nanoparticles (SLN) and nanostructured lipid carriers (NLC) in cosmetic and dermatological preparations. *Adv. Drug Deliv. Rev.* 2002, *54*, 131–155, doi:10.1016/S0169-409X(02)00118-7.

69. Yadav, N.; Khatak, S.; Singh Sara, U.V. Solid lipid nanoparticles- A review. *Int. J. Appl. Pharm.* 2013, *5*, 8–18, doi:10.9790/3013-26103444.

70. Ramamoorth, M.; Narvekar, A. Non viral vectors in gene therapy - An overview. *J. Clin. Diagnostic Res.* 2015, *9*, GE01–GE06, doi:10.7860/JCDR/2015/10443.5394.

71. Trucillo, P.; Campardelli, R. Production of solid lipid nanoparticles with a supercritical fluid assisted process. *J. Supercrit. Fluids* 2019, *143*, 16–23, doi:10.1016/j.supflu.2018.08.001.

72. Chattopadhyay, P.; Shekunov, B.Y.; Yim, D.; Cipolla, D.; Boyd, B.; Farr, S. Production of solid lipid nanoparticle suspensions using supercritical fluid extraction of emulsions (SFEE) for pulmonary delivery using the AERx system. *Adv. Drug Deliv. Rev.* 2007, *59*, 444–453, doi:10.1016/j.addr.2007.04.010.

73. Delgado, D.; del Pozo-Rodríguez, A.; Angeles Solinís, M.; Bartkowiak, A.; Rodríguez-Gascón, A. New gene delivery system based on oligochitosan and solid lipid nanoparticles: 'In vitro' and 'in vivo' evaluation. *Eur. J. Pharm. Sci.* 2013, *50*, 484–491, doi:https://doi.org/10.1016/j.ejps.2013.08.013.

74. Apaolaza, P.S.; Delgado, D.; Pozo-Rodríguez, A. Del; Gascón, A.R.; Solinís, M.Á. A novel gene therapy vector based on hyaluronic acid and solid lipid nanoparticles for ocular diseases. *Int. J. Pharm.* 2014, *465*, 413–426, doi:10.1016/j.ijpharm.2014.02.038.

75. Apaolaza, P.S.; del Pozo-Rodríguez, A.; Torrecilla, J.; Rodríguez-Gascón, A.; Rodríguez, J.M.; Friedrich, U.; Weber, B.H.F.; Solinís, M.A. Solid lipid nanoparticle-based vectors intended for the treatment of X-linked juvenile retinoschisis by gene therapy: In vivo approaches in Rs1h-deficient mouse model. *J. Control. Release* 2015, *217*, 273–283, doi:https://doi.org/10.1016/j.jconrel.2015.09.033.

76. Ruiz De Garibay, A.P.; Solinís, M.A.; Del Pozo-Rodríguez, A.; Apaolaza, P.S.; Shen, J.S.; Rodríguez-Gascón, A. Solid lipid nanoparticles as non-viral vectors for gene transfection in a cell model of fabry disease. *J. Biomed. Nanotechnol.* 2015, *11*, 500–511, doi:10.1166/jbn.2015.1968.

77. Rodríguez-Castejón, J.; Alarcia-Lacalle, A.; Gómez-Aguado, I.; Vicente-Pascual, M.; Aspiazu, M.Á.S.; Del Pozo-Rodríguez, A.; Rodríguez-Gascón, A. α-Galactosidase A Augmentation by Non-Viral Gene Therapy: Evaluation in Fabry Disease Mice. *Pharmaceutics* 2021, *13*, doi:10.3390/pharmaceutics13060771.

78. Torrecilla, J.; del Pozo-Rodríguez, A.; Vicente-Pascual, M.; Solinís, M.Á.; Rodríguez-Gascón, A. Targeting corneal inflammation by gene therapy: Emerging strategies for keratitis. *Exp. Eye Res.* 2018, *176*, 130–140, doi:10.1016/j.exer.2018.07.006.

79. Vicente-Pascual, M.; Albano, A.; Solinís, M.; Serpe, L.; Rodríguez-Gascón, A.; Foglietta, F.; Muntoni, E.; Torrecilla, J.; Pozo-Rodríguez, A. Del; Battaglia, L. Gene delivery in the cornea: In vitro & ex vivo evaluation of solid lipid nanoparticle-based vectors. *Nanomedicine* 2018, *13*, 1847–1864, doi:10.2217/nnm-2018-0112.

80. Vicente-Pascual, M.; Gómez-Aguado, I.; Rodríguez-Castejón, J.; Rodríguez-Gascón, A.; Muntoni, E.; Battaglia, L.; Pozo-Rodríguez, A. Del; Aspiazu, M.Á.S. Topical administration of sln-based gene therapy for the treatment of corneal inflammation by de novo il-10

production. *Pharmaceutics* 2020, *12*, 1–23, doi:10.3390/pharmaceutics12060584.

81. Dias, M.F.; Joo, K.; Kemp, J.A.; Fialho, S.L.; da Silva Cunha, A.; Woo, S.J.; Kwon, Y.J. Molecular genetics and emerging therapies for retinitis pigmentosa: Basic research and clinical perspectives. *Prog. Retin. Eye Res.* 2018, *63*, 107–131, doi:https://doi.org/10.1016/j.preteyeres.2017.10.004.

82. del Pozo-Rodríguez, A.; Torrecilla, J.; Rodríguez-Gascón, A.; Solinís, M.Á. Nonviral Delivery Systems for Gene Therapy for Retina and Posterior Segment Disease. In *Drug Delivery for the Retina and Posterior Segment Disease*; Patel, J.K., Sutariya, V., Kanwar, J.R., Pathak, Y. V, Eds.; Springer International Publishing: Cham, 2018; pp. 131–149 ISBN 978-3-319-95807-1.

83. Trigueros, S.; Domènech, E.B.; Toulis, V.; Marfany, G. In vitro gene delivery in retinal pigment epithelium cells by plasmid dna-wrapped gold nanoparticles. *Genes (Basel).* 2019, *10*, doi:10.3390/genes10040289.

84. Di Iorio, E.; Barbaro, V.; Alvisi, G.; Trevisan, M.; Ferrari, S.; Masi, G.; Nespeca, P.; Ghassabian, H.; Ponzin, D.; Palù, G. New Frontiers of Corneal Gene Therapy. *Hum. Gene Ther.* 2019, *30*, 923–945, doi:10.1089/hum.2019.026.

85. Klausner, E.A.; Peer, D.; Chapman, R.L.; Multack, R.F.; Andurkar, S. V Corneal gene therapy. *J. Control. Release* 2007, *124*, 107–133, doi:https://doi.org/10.1016/j.jconrel.2007.05.041.

86. Mashhour, B.; Couton, D.; Perricaudet, M.; Briand, P. In vivo adenovirus-mediated gene transfer into ocular tissues. *Gene Ther.* 1994, *1*, 122–126.

87. Rodríguez-Gascón, A.; del Pozo-Rodríguez, A.; Isla, A.; Solinís, M.A. Gene Therapy in the Cornea. *eLS* 2016, 1–9.

88. Alvarez-Rivera, F.; Rey-Rico, A.; Venkatesan, J.K.; Diaz-Gomez, L.; Cucchiarini, M.; Concheiro, A.; Alvarez-Lorenzo, C. Controlled Release of rAAV Vectors from APMA-Functionalized Contact Lenses for Corneal Gene Therapy. *Pharm.* 2020, *12*.

89. de la Fuente, M.; Seijo, B.; Alonso, M.J. Bioadhesive hyaluronan–chitosan nanoparticles can transport genes across the ocular mucosa and transfect ocular tissue. *Gene Ther.* 2008, *15*, 668–676, doi:10.1038/gt.2008.16.

90. Delgado, D.; Del Pozo-Rodríguez, A.; Solinís, M.Á.; Avilés-Triqueros, M.; Weber, B.H.F.; Fernández, E.; Gascón, A.R. Dextran and protamine-based solid lipid nanoparticles as potential vectors for the treatment of X-linked juvenile retinoschisis. *Hum. Gene Ther.* 2011, *23*, 345–355, doi:10.1089/hum.2011.115.

91. Bauer, D.; Lu, M.; Wasmuth, S.; Li, H.; Yang, Y.; Roggendorf, M.; Steuhl, K.P.; Heiligenhaus, A. Immunomodulation by topical particle-mediated administration of cytokine plasmid DNA suppresses herpetic stromal keratitis without impairment of antiviral defense. *Graefe's Arch. Clin. Exp. Ophthalmol.* 2006, *244*, 216–225, doi:10.1007/s00417-005-0070-z.

92. Gupta, S.; Fink, M.K.; Ghosh, A.; Tripathi, R.; Sinha, P.R.; Sharma, A.; Hesemann, N.P.; Chaurasia, S.S.; Giuliano, E.A.; Mohan, R.R. Novel Combination BMP7 and HGF Gene Therapy Instigates Selective Myofibroblast Apoptosis and Reduces Corneal Haze In Vivo. *Invest. Ophthalmol. Vis. Sci.* 2018, *59*, 1045–1057, doi:10.1167/iovs.17-23308.

93. Siene Ng, W.; Binley, K.; Song, B.; Morgan, J.E. Use of magnetic nanoparticles and oscillating magnetic field for non-viral gene transfer into mouse cornea. *Lancet* 2015,

385, S75, doi:10.1016/S0140-6736(15)60390-7.

94. Contreras-Ruiz, L.; Zorzi, G.K.; Hileeto, D.; López-García, A.; Calonge, M.; Seijo, B.; Sánchez, A.; Diebold, Y. A nanomedicine to treat ocular surface inflammation: performance on an experimental dry eye murine model. *Gene Ther.* 2013, *20*, 467–477, doi:10.1038/gt.2012.56.

95. Gupta, R.; Tandon, A.; Hansen, E.T.; Cebulko, T.C.; Hemmat, Y.J.; Fortune, J.A.; Klibanov, A.M.; Mohan, R.R. Rapid And Substantial Gene Delivery Into Cornea In Vivo And In Vitro With Linearized Polyethyleneimine Nanoparticles. *Invest. Ophthalmol. Vis. Sci.* 2011, *52*, 494.

96. Sharma, A.; Tandon, A.; Tovey, J.C.K.; Gupta, R.; Robertson, J.D.; Fortune, J.A.; Klibanov, A.M.; Cowden, J.W.; Rieger, F.G.; Mohan, R.R. Polyethylenimine-conjugated gold nanoparticles: Gene transfer potential and low toxicity in the cornea. *Nanomedicine Nanotechnology, Biol. Med.* 2011, *7*, 505–513, doi:https://doi.org/10.1016/j.nano.2011.01.006.

97. Singh, M.; Guzman-Aranguez, A.; Hussain, A.; Srinivas, C.S.; Kaur, I.P. Solid lipid nanoparticles for ocular delivery of isoniazid: evaluation, proof of concept and in vivo safety \& kinetics. *Nanomedicine* 2019, *14*, 465–491, doi:10.2217/nnm-2018-0278.

98. Mobaraki, M.; Soltani, M.; Harofte, S.Z.; Zoudani, E.L.; Daliri, R.; Aghamirsalim, M.; Raahemifar, K. Biodegradable nanoparticle for cornea drug delivery: Focus review. *Pharmaceutics* 2020, *12*, 1–26, doi:10.3390/pharmaceutics12121232.

99. Battaglia, L.; Serpe, L.; Foglietta, F.; Muntoni, E.; Gallarate, M.; Del Pozo Rodriguez, A.; Solinis, M.A. Application of lipid nanoparticles to ocular drug delivery. *Expert Opin. Drug Deliv.* 2016, *13*, 1743–1757, doi:10.1080/17425247.2016.1201059.

100. Bachu, R.D.; Chowdhury, P.; Al-Saedi, Z.H.F.; Karla, P.K.; Boddu, S.H.S. Ocular Drug Delivery Barriers—Role of Nanocarriers in the Treatment of Anterior Segment Ocular Diseases. *Pharmaceutics* 2018, *10*, doi:10.3390/pharmaceutics10010028.

101. Farooq, A. V; Shukla, D. Herpes Simplex Epithelial and Stromal Keratitis: An Epidemiologic Update. *Surv. Ophthalmol.* 2012, *57*, 448–462, doi:10.1016/j.survophthal.2012.01.005.

102. Kwon, M.S.; Carnt, N.A.; Truong, N.R.; Pattamatta, U.; White, A.J.; Samarawickrama, C.; Cunningham, A.L. Dendritic cells in the cornea during Herpes simplex viral infection and inflammation. *Surv. Ophthalmol.* 2018, *63*, 565–578, doi:10.1016/j.survophthal.2017.11.001.

103. Miraldi Utz, V.; Kaufman, A.R. Allergic Eye Disease. *Pediatr. Clin. North Am.* 2014, *61*, 607–620, doi:https://doi.org/10.1016/j.pcl.2014.03.009.

104. Boersma, P.M.; Haarsma, L.D.; Schotanus, M.P.; Ubels, J.L. TNF-R1 and FADD mediate UVB-Induced activation of K+ channels in corneal epithelial cells. *Exp. Eye Res.* 2017, *154*, 1–9, doi:https://doi.org/10.1016/j.exer.2016.11.003.

105. Lee, S.H.; Kim, K.W.; Joo, K.; Kim, J.C. Angiogenin ameliorates corneal opacity and neovascularization via regulating immune response in corneal fibroblasts. *BMC Ophthalmol.* 2016, *16*, 57, doi:10.1186/s12886-016-0235-z.

106. Kim, B.; Tang, Q.; Biswas, P.S.; Xu, J.; Schiffelers, R.M.; Xie, F.Y.; Ansari, A.M.; Scaria, P. V; Woodle, M.C.; Lu, P.; et al. Inhibition of Ocular Angiogenesis by siRNA Targeting Vascular Endothelial Growth Factor Pathway Genes: Therapeutic Strategy for Herpetic Stromal Keratitis. *Am. J. Pathol.* 2004, *165*, 2177–2185, doi:https://doi.org/10.1016/S0002-

9440(10)63267-1.

107. Darby, I.A.; Laverdet, B.; Bonté, F.; Desmoulière, A. Fibroblasts and myofibroblasts in wound healing. *Clin. Cosmet. Investig. Dermatol.* 2014, *7*, 301–311, doi:10.2147/CCID.S50046.

108. Pakyari, M.; Farrokhi, A.; Maharlooei, M.K.; Ghahary, A. Critical Role of Transforming Growth Factor Beta in Different Phases of Wound Healing. *Adv. Wound Care* 2013, *2*, 215–224, doi:10.1089/wound.2012.0406.

109. Mohan, R.; Chintala, S.K.; Jung, J.C.; Villar, W.V.L.; McCabe, F.; Russo, L.A.; Lee, Y.; McCarthy, B.E.; Wollenberg, K.R.; Jester, J. V; et al. Matrix Metalloproteinase Gelatinase B (MMP-9) Coordinates and Effects Epithelial Regeneration *. *J. Biol. Chem.* 2002, *277*, 2065–2072, doi:10.1074/jbc.M107611200.

110. Sivak, J.M.; Fini, M.E. MMPs in the eye: emerging roles for matrix metalloproteinases in ocular physiology. *Prog. Retin. Eye Res.* 2002, *21*, 1–14, doi:https://doi.org/10.1016/S1350-9462(01)00015-5.

111. Afonso, A.A.; Sobrin, L.; Monroy, D.C.; Selzer, M.; Lokeshwar, B.; Pflugfelder, S.C. Tear Fluid Gelatinase B Activity Correlates with IL-1α Concentration and Fluorescein Clearance in Ocular Rosacea. *Invest. Ophthalmol. Vis. Sci.* 1999, *40*, 2506–2512.

112. Garrana, R.M.; Zieske, J.D.; Assouline, M.; Gipson, I.K. Matrix metalloproteinases in epithelia from human recurrent corneal erosion. *Invest. Ophthalmol. Vis. Sci.* 1999, *40*, 1266–1270.

113. Coleman, C.M.; Hannush, S.; Covello, S.P.; Smith, F.J.D.; Uitto, J.; McLean, W.H.I. A novel mutation in the helix termination motif of keratin K12 in a US family with Meesmann corneal dystrophy. *Am. J. Ophthalmol.* 1999, *128*, 687–691, doi:10.1016/S0002-9394(99)00317-7.

114. Sobrin, L.; Liu, Z.; Monroy, D.C.; Solomon, A.; Selzer, M.G.; Lokeshwar, B.L.; Pflugfelder, S.C. Regulation of MMP-9 Activity in Human Tear Fluid and Corneal Epithelial Culture Supernatant. *Invest. Ophthalmol. Vis. Sci.* 2000, *41*, 1703–1709.

115. Wong, T.T.L.; Sethi, C.; Daniels, J.T.; Limb, G.A.; Murphy, G.; Khaw, P.T. Matrix Metalloproteinases in Disease and Repair Processes in the Anterior Segment. *Surv. Ophthalmol.* 2002, *47*, 239–256, doi:10.1016/S0039-6257(02)00287-4.

116. Gordon, G.M.; Ledee, D.R.; Feuer, W.J.; Fini, M.E. Cytokines and signaling pathways regulating matrix metalloproteinase-9 (MMP-9) expression in corneal epithelial cells. *J. Cell. Physiol.* 2009, *221*, 402–411, doi:https://doi.org/10.1002/jcp.21869.

117. Goktas, S.; Erdogan, E.; Sakarya, R.; Sakarya, Y.; Yılmaz, M.; Ozcimen, M.; Unlukal, N.; Alpfidan, I.; Tas, F.; Erdogan, E.; et al. Inhibition of Corneal Neovascularization by Topical and Subconjunctival Tigecycline. *J. Ophthalmol.* 2014, *2014*, 452685, doi:10.1155/2014/452685.

118. Li, Q.; Jie, Y.; Wang, C.; Zhang, Y.; Guo, H.; Pan, Z. Tryptase compromises corneal epithelial barrier function. *Cell Biochem. Funct.* 2014, *32*, 183–187, doi:https://doi.org/10.1002/cbf.2991.

119. Higuchi, A.; Kawakita, T.; Tsubota, K. IL-6 induction in desiccated corneal epithelium in vitro and in vivo. *Mol. Vis.* 2011, *17*, 2400–2406.

120. Zahir-Jouzdani, F.; Atyabi, F.; Mojtabavi, N. Interleukin-6 participation in pathology of

ocular diseases. *Pathophysiology* 2017, *24*, 123–131, doi:https://doi.org/10.1016/j.pathophys.2017.05.005.

121. Zhang, J.-M.; An, J. Cytokines, Inflammation, and Pain. *Int. Anesthesiol. Clin.* 2007, *45*.

122. Saw, V.P.J.; Offiah, I.; Dart, R.J.; Galatowicz, G.; Dart, J.K.G.; Daniels, J.T.; Calder, V.L. Conjunctival Interleukin-13 Expression in Mucous Membrane Pemphigoid and Functional Effects of Interleukin-13 on Conjunctival Fibroblasts in Vitro. *Am. J. Pathol.* 2009, *175*, 2406–2415, doi:10.2353/ajpath.2009.090579.

123. Yang, Y.-N.; Wang, F.; Zhou, W.; Wu, Z.-Q.; Xing, Y.-Q. TNF-α Stimulates MMP-2 and MMP-9 Activities in Human Corneal Epithelial Cells via the Activation of FAK/ERK Signaling. *Ophthalmic Res.* 2012, *48*, 165–170, doi:10.1159/000338819.

124. Hayashi, K.; Hooper, L.C.; Detrick, B.; Hooks, J.J. HSV immune complex (HSV-IgG: IC) and HSV-DNA elicit the production of angiogenic factor VEGF and MMP-9. *Arch. Virol.* 2009, *154*, 219–226, doi:10.1007/s00705-008-0303-7.

125. Lee, S.; Zheng, M.; Kim, B.; Rouse, B.T. Role of matrix metalloproteinase-9 in angiogenesis caused by ocular infection with herpes simplex virus. *J. Clin. Invest.* 2002, *110*, 1105–1111, doi:10.1172/JCI15755.

126. Moore, K.W.; de Waal Malefyt, R.; Coffman, R.L.; O'Garra, A. Interleukin-10 and the Interleukin-10 Receptor. *Annu. Rev. Immunol.* 2001, *19*, 683–765, doi:10.1146/annurev.immunol.19.1.683.

127. de Waal Malefyt, R.; Abrams, J.; Bennett, B.; Figdor, C.G.; de Vries, J.E. Interleukin 10(IL-10) inhibits cytokine synthesis by human monocytes: an autoregulatory role of IL-10 produced by monocytes. *J. Exp. Med.* 1991, *174*, 1209–1220, doi:10.1084/jem.174.5.1209.

128. Abrams, J.; Figdor, C.G.; De Waal Malefyt, R.; Bennett, B.; De Vries, J.E. Interleukin 10(IL-10) inhibits cytokine synthesis by human monocytes: An autoregulatory role of IL-10 produced by monocytes. *J. Exp. Med.* 1991, *174*, 1209–1220, doi:10.1084/jem.174.5.1209.

129. Ralph, P.; Nakoinz, I.; Sampson-Johannes, A.; Fong, S.; Lowe, D.; Min, H.Y.; Lin, L. IL-10, T lymphocyte inhibitor of human blood cell production of IL-1 and tumor necrosis factor. *J. Immunol.* 1992, *148*, 808 LP – 814.

130. Cassatella, M.A.; Meda, L.; Bonora, S.; Ceska, M.; Constantin, G. Interleukin 10 (IL-10) inhibits the release of proinflammatory cytokines from human polymorphonuclear leukocytes. Evidence for an autocrine role of tumor necrosis factor and IL-1 beta in mediating the production of IL-8 triggered by lipopolysaccharide. *J. Exp. Med.* 1993, *178*, 2207–2211, doi:10.1084/jem.178.6.2207.

131. Azar, D. Corneal Angiogenic Privilege: Angiogenic and Antiangiogenic Factors in Corneal Avascularity, Vasculogenesis, and Wound Healing. *Trans. Am. Ophthalmol. Soc.* 2006, *104*, 264–302.

132. Feizi, S.; Azari, A.A.; Safapour, S. Therapeutic approaches for corneal neovascularization. *Eye Vis.* 2017, *4*, 28, doi:10.1186/s40662-017-0094-6.

133. Lu, X.-X.; Zhao, S.-Z. Gene-based Therapeutic Tools in the Treatment of Cornea Disease. *Curr. Gene Ther.* 2019, *19*, 7–19, doi:10.2174/1566523219666181213120634.

134. Liu, S.; Romano, V.; Steger, B.; Kaye, S.B.; Hamill, K.J.; Willoughby, C.E. Gene-based

antiangiogenic applications for corneal neovascularization. *Surv. Ophthalmol.* 2018, *63*, 193–213, doi:10.1016/j.survophthal.2017.10.006.

135. Das, S.K.; Gupta, I.; Cho, Y.K.; Zhang, X.; Uehara, H.; Muddana, S.K.; Bernhisel, A.A.; Archer, B.; Ambati, B.K. Vimentin Knockdown Decreases Corneal Opacity. *Invest. Ophthalmol. Vis. Sci.* 2014, *55*, 4030–4040, doi:10.1167/iovs.13-13494.

136. Bargagna-Mohan, P.; Paranthan, R.R.; Hamza, A.; Zhan, C.-G.; Lee, D.-M.; Kim, K.B.; Lau, D.L.; Srinivasan, C.; Nakayama, K.; Nakayama, K.I.; et al. Corneal Antifibrotic Switch Identified in Genetic and Pharmacological Deficiency of Vimentin *. *J. Biol. Chem.* 2012, *287*, 989–1006, doi:10.1074/jbc.M111.297150.

137. Sato, Y. The vasohibin family: a novel family for angiogenesis regulation. *J. Biochem.* 2013, *153*, 5–11, doi:10.1093/jb/mvs128.

138. Maddula, S.; Davis, D.K.; Maddula, S.; Burrow, M.K.; Ambati, B.K. Horizons in Therapy for Corneal Angiogenesis. *Ophthalmology* 2011, *118*, 591–599, doi:https://doi.org/10.1016/j.ophtha.2011.01.041.

139. Liu, X.; Wang, S.; Wang, X.; Liang, J.; Zhang, Y. Recent drug therapies for corneal neovascularization. *Chem. Biol. Drug Des.* 2017, *90*, 653–664, doi:https://doi.org/10.1111/cbdd.13018.

140. Azar, D.T. Corneal angiogenic privilege: Angiogenic and antiangiogenic factors in corneal avascularity, vasculogenesis, and wound healing (An American Ophthalmological Society Thesis). *Trans. Am. Ophthalmol. Soc.* 2006, *104*, 264–302.

141. Chang, J.-H.; Garg, N.K.; Lunde, E.; Han, K.-Y.; Jain, S.; Azar, D.T. Corneal Neovascularization: An Anti-VEGF Therapy Review. *Surv. Ophthalmol.* 2012, *57*, 415–429, doi:10.1016/j.survophthal.2012.01.007.

142. Chen, H.-C.J.; Yeh, L.-K.; Tsai, Y.-J.; Lai, C.-H.; Chen, C.-C.; Lai, J.-Y.; Sun, C.-C.; Chang, G.; Hwang, T.-L.; Chen, J.-K.; et al. Expression of Angiogenesis-Related Factors in Human Corneas after Cultivated Oral Mucosal Epithelial Transplantation. *Invest. Ophthalmol. Vis. Sci.* 2012, *53*, 5615–5623, doi:10.1167/iovs.11-9293.

143. Tarui, T.; Miles, L.A.; Takada, Y. Specific Interaction of Angiostatin with Integrin α$_v$β$_3$ in Endothelial Cells *. *J. Biol. Chem.* 2001, *276*, 39562–39568, doi:10.1074/jbc.M101815200.

144. Gabison, E.; Chang, J.-H.; Hernández-Quintela, E.; Javier, J.; Lu, P.C.S.; Ye, H.; Kure, T.; Kato, T.; Azar, D.T. Anti-angiogenic role of angiostatin during corneal wound healing. *Exp. Eye Res.* 2004, *78*, 579–589, doi:https://doi.org/10.1016/j.exer.2003.09.005.

145. Albuquerque, R.J.C.; Hayashi, T.; Cho, W.G.; Kleinman, M.E.; Dridi, S.; Takeda, A.; Baffi, J.Z.; Yamada, K.; Kaneko, H.; Green, M.G.; et al. Alternatively spliced vascular endothelial growth factor receptor-2 is an essential endogenous inhibitor of lymphatic vessel growth. *Nat. Med.* 2009, *15*, 1023—1030, doi:10.1038/nm.2018.

146. Saika, S.; Yamanaka, O.; Okada, Y.; Miyamoto, T.; Kitano, A.; Flanders, K.C.; Ohnishi, Y.; Nakajima, Y.; Kao, W.W.-Y.; Ikeda, K. Effect of overexpression of pparγ on the healing process of corneal alkali burn in mice. *Am. J. Physiol. Physiol.* 2007, *293*, C75–C86, doi:10.1152/ajpcell.00332.2006.

147. Tsunoda, S.; Nakamura, T.; Sakurai, H.; Saiki, I. Fibroblast growth factor-2-induced host stroma reaction during initial tumor growth promotes progression of mouse melanoma via vascular endothelial growth factor A-dependent neovascularization. *Cancer Sci.* 2007,

98, 541–548, doi:https://doi.org/10.1111/j.1349-7006.2007.00432.x.

148. Mohan, R.R.; Tovey, J.C.K.; Sharma, A.; Schultz, G.S.; Cowden, J.W.; Tandon, A. Targeted Decorin Gene Therapy Delivered with Adeno-Associated Virus Effectively Retards Corneal Neovascularization In Vivo. *PLoS One* 2011, *6*, e26432.

149. Shin, S.H.; Kim, J.C.; Chang, S.-I.; Lee, H.; Chung, S.I. Recombinant kringle 1-3 of plasminogen inhibits rabbit corneal angiogenesis induced by angiogenin. *Cornea* 2000, *19*, 212–217, doi:10.1097/00003226-200003000-00016.

150. Yoon, K.C.; Ahn, K.Y.; Lee, J.H.; Chun, B.J.; Park, S.W.; Seo, M.S.; Park, Y.-G.; Kim, K.K. Lipid-mediated delivery of brain-specific angiogenesis inhibitor 1 gene reduces corneal neovascularization in an in vivo rabbit model. *Gene Ther.* 2005, *12*, 617–624, doi:10.1038/sj.gt.3302442.

151. Liclican, E.L.; Nguyen, V.; Sullivan, A.B.; Gronert, K. Selective Activation of the Prostaglandin E2 Circuit in Chronic Injury-Induced Pathologic Angiogenesis. *Invest. Ophthalmol. Vis. Sci.* 2010, *51*, 6311–6320, doi:10.1167/iovs.10-5455.

152. Mohan, R.R.; Tovey, J.C.K.; Sharma, A.; Tandon, A. Gene therapy in the Cornea: 2005–present. *Prog. Retin. Eye Res.* 2012, *31*, 43–64, doi:https://doi.org/10.1016/j.preteyeres.2011.09.001.

153. Clements, J.L.; Dana, R. Inflammatory Corneal Neovascularization: Etiopathogenesis. *Semin. Ophthalmol.* 2011, *26*, 235–245, doi:10.3109/08820538.2011.588652.

154. Haas, T.L. Endothelial cell regulation of matrix metalloproteinases. *Can. J. Physiol. Pharmacol.* 2005, *83*, 1–7, doi:10.1139/y04-120.

155. Zhang, X.; Lin, X.; Liu, Z.; Wu, Y.; Yang, Y.; Ouyang, W.; Li, W.; Liu, Z. Topical Application of Mizoribine Suppresses CD4+ T-cell–Mediated Pathogenesis in Murine Dry Eye. *Invest. Ophthalmol. Vis. Sci.* 2017, *58*, 6056–6064, doi:10.1167/iovs.17-22852.

156. Guzman-Aranguez, A.; Loma, P.; Pintor, J. Small-interfering RNAs (siRNAs) as a promising tool for ocular therapy. *Br. J. Pharmacol.* 2013, *170*, 730–747, doi:https://doi.org/10.1111/bph.12330.

157. Torrecilla, J.; Rodríguez-Gascón, A.; Solinís, M.Á.; del Pozo-Rodríguez, A. Lipid Nanoparticles as Carriers for RNAi against Viral Infections: Current Status and Future Perspectives. *Biomed Res. Int.* 2014, *2014*, 161794, doi:10.1155/2014/161794.

158. Remeijer, L.; Osterhaus, A.; Verjans, G. Human herpes simplex virus keratitis: the pathogenesis revisited. *Ocul. Immunol. Inflamm.* 2004, *12*, 255–285, doi:10.1080/092739490500363.

159. Keadle, T.L.; Stuart, P.M. Interleukin-10 (IL-10) ameliorates corneal disease in a mouse model of recurrent herpetic keratitis. *Microb. Pathog.* 2005, *38*, 13–21, doi:https://doi.org/10.1016/j.micpath.2004.09.003.

160. Tumpey, T.M.; Elner, V.M.; Chen, S.-H.; Oakes, J.E.; Lausch, R.N. Interleukin-10 treatment can suppress stromal keratitis induced by herpes simplex virus type 1. *J. Immunol.* 1994, *153*, 2258–2265.

161. Li, L.; Elliott, J.F.; Mosmann, T.R. IL-10 inhibits cytokine production, vascular leakage, and swelling during T helper 1 cell-induced delayed-type hypersensitivity. *J. Immunol.* 1994, *153*, 3967–3978.

162. Zhou, R.; Dean, D.A. Gene transfer of interleukin 10 to the murine cornea using

electroporation. *Exp. Biol. Med.* 2007, *232*, 362–369.

163. Parker, D.G.; Coster, D.J.; Brereton, H.M.; Hart, P.H.; Koldej, R.; Anson, D.S.; Williams, K.A. Lentivirus-mediated gene transfer of interleukin 10 to the ovine and human cornea. *Clin. Experiment. Ophthalmol.* 2010, *38*, 405–413, doi:https://doi.org/10.1111/j.1442-9071.2010.02261.x.

164. Hirsch, M.L.; Conatser, L.M.; Smith, S.M.; Salmon, J.H.; Wu, J.; Buglak, N.E.; Davis, R.; Gilger, B.C. AAV vector-meditated expression of HLA-G reduces injury-induced corneal vascularization, immune cell infiltration, and fibrosis. *Sci. Rep.* 2017, *7*, 17840, doi:10.1038/s41598-017-18002-9.

165. del Pozo-Rodríguez, A.; Delgado, D.; Solinís, M.A.; Gascón, A.R.; Pedraz, J.L. Solid lipid nanoparticles: Formulation factors affecting cell transfection capacity. *Int. J. Pharm.* 2007, *339*, 261–268, doi:10.1016/j.ijpharm.2007.03.015.

166. Ke, Y.; Wu, Y.; Cui, X.; Liu, X.; Yu, M.; Yang, C.; Li, X. Polysaccharide Hydrogel Combined with Mesenchymal Stem Cells Promotes the Healing of Corneal Alkali Burn in Rats. *PLoS One* 2015, *10*, e0119725.

167. Carpentier, G. Angiogenesis Analyzer for Image J. Available online: http://rsb.info.nih.gov/ij/macros/toolsets/Analogenesis%20Analyzer.txt (accessed on 25 March 2019).

168. Delgado, D.; Del Pozo-Rodríguez, A.; Solinís, M.Á.; Rodríguez-Gascón, A. Understanding the mechanism of protamine in solid lipid nanoparticle-based lipofection: The importance of the entry pathway. *Eur. J. Pharm. Biopharm.* 2011, *79*, 495–502, doi:10.1016/j.ejpb.2011.06.005.

169. Ruseska, I.; Fresacher, K.; Petschacher, C.; Zimmer, A. Use of Protamine in Nanopharmaceuticals — A Review. 2021.

170. Delgado, D.; Gascón, A.R.; Del Pozo-Rodríguez, A.; Echevarría, E.; Ruiz De Garibay, A.P.; Rodríguez, J.M.; Solinís, M.Á. Dextran-protamine-solid lipid nanoparticles as a non-viral vector for gene therapy: In vitro characterization and in vivo transfection after intravenous administration to mice. *Int. J. Pharm.* 2012, *425*, 35–43, doi:10.1016/j.ijpharm.2011.12.052.

171. Balazs, D.A.; Godbey, W. Liposomes for Use in Gene Delivery. *J. Drug Deliv.* 2011, *2011*, 1–12, doi:10.1155/2011/326497.

172. Delgado, D.; Gascón, A.R.; Del Pozo-Rodríguez, A.; Echevarría, E.; Ruiz De Garibay, A.P.; Rodríguez, J.M.; Solinís, M.Á. Dextran-protamine-solid lipid nanoparticles as a non-viral vector for gene therapy: In vitro characterization and in vivo transfection after intravenous administration to mice. *Int. J. Pharm.* 2012, *425*, 35–43, doi:10.1016/j.ijpharm.2011.12.052.

173. Li, J.; Chen, Q.; Zha, Z.; Li, H.; Toh, K.; Dirisala, A.; Matsumoto, Y.; Osada, K.; Kataoka, K.; Ge, Z. Ternary polyplex micelles with PEG shells and intermediate barrier to complexed DNA cores for efficient systemic gene delivery. *J. Control. Release* 2015, *209*, 77–87, doi:10.1016/j.jconrel.2015.04.024.

174. Danaei, M.; Dehghankhold, M.; Ataei, S.; Hasanzadeh Davarani, F.; Javanmard, R.; Dokhani, A.; Khorasani, S.; Mozafari, M.R. Impact of particle size and polydispersity index on the clinical applications of lipidic nanocarrier systems. *Pharmaceutics* 2018, *10*, 1–17, doi:10.3390/pharmaceutics10020057.

175. Resina, S.; Prevot, P.; Tjierry, A.R. Physico-chemical characteristics of lipoplexes influence cell uptake mechanisms and transfection efficacy. *PLoS One* 2009, *4*, doi:10.1371/journal.pone.0006058.

176. Kasai, H.; Inoue, K.; Imamura, K.; Yuvienco, C.; Montclare, J.K.; Yamano, S. Efficient siRNA delivery and gene silencing using a lipopolypeptide hybrid vector mediated by a caveolae-mediated and temperature-dependent endocytic pathway. *J. Nanobiotechnology* 2019, *17*, 1–14, doi:10.1186/s12951-019-0444-8.

177. del Pozo-Rodríguez, A.; Pujals, S.; Delgado, D.; Solinís, M.A.; Gascón, A.R.; Giralt, E.; Pedraz, J.L. A proline-rich peptide improves cell transfection of solid lipid nanoparticle-based non-viral vectors. *J. Control. Release* 2009, *133*, 52–59, doi:10.1016/j.jconrel.2008.09.004.

178. Yamada, Y.; Sato, Y.; Nakamura, T.; Harashima, H. Evolution of drug delivery system from viewpoint of controlled intracellular trafficking and selective tissue targeting toward future nanomedicine. *J. Control. Release* 2020, *327*, 533–545, doi:10.1016/j.jconrel.2020.09.007.

179. Maruggi, G.; Zhang, C.; Li, J.; Ulmer, J.B.; Yu, D. mRNA as a Transformative Technology for Vaccine Development to Control Infectious Diseases. *Mol. Ther.* 2019, *27*, 757–772, doi:10.1016/j.ymthe.2019.01.020.

180. Azkur, A.K.; Kim, B.; Suvas, S.; Lee, Y.; Kumaraguru, U.; Rouse, B.T. Blocking Mouse MMP-9 Production in Tumor Cells and Mouse Cornea by Short Hairpin (sh) RNA Encoding Plasmids. *Oligonucleotides* 2005, *15*, 72–84, doi:10.1089/oli.2005.15.72.

181. Ueta, M.; Kinoshita, S. Ocular surface inflammation is regulated by innate immunity. *Prog. Retin. Eye Res.* 2012, *31*, 551–575, doi:https://doi.org/10.1016/j.preteyeres.2012.05.003.

182. Kimura, K. [Molecular mechanism of the disruption of barrier function in cultured human corneal epithelial cells induced by tumor necrosis factor-alpha, a proinflammatory cytokine]. *Nihon. Ganka Gakkai Zasshi* 2010, *114*, 935–943.

183. Kimura, K.; Morita, Y.; Orita, T.; Haruta, J.; Takeji, Y.; Sonoda, K.-H. Protection of Human Corneal Epithelial Cells From TNF-α–Induced Disruption of Barrier Function by Rebamipide. *Invest. Ophthalmol. Vis. Sci.* 2013, *54*, 2752–2760, doi:10.1167/iovs.12-11294.

184. Ramaesh, T.; Ramaesh, K.; Riley, S.C.; West, J.D.; Dhillon, B. Effects of N-acetylcysteine on matrix metalloproteinase-9 secretion and cell migration of human corneal epithelial cells. *Eye* 2012, *26*, 1138–1144, doi:10.1038/eye.2012.135.

185. Webb, A.H.; Gao, B.T.; Goldsmith, Z.K.; Irvine, A.S.; Saleh, N.; Lee, R.P.; Lendermon, J.B.; Bheemreddy, R.; Zhang, Q.; Brennan, R.C.; et al. Inhibition of MMP-2 and MMP-9 decreases cellular migration, and angiogenesis in in vitro models of retinoblastoma. *BMC Cancer* 2017, *17*, 434, doi:10.1186/s12885-017-3418-y.

186. Swamynathan, S.; Loughner, C.L.; Swamynathan, S.K. Inhibition of HUVEC tube formation via suppression of NFκB suggests an anti-angiogenic role for SLURP1 in the transparent cornea. *Exp. Eye Res.* 2017, *164*, 118–128, doi:https://doi.org/10.1016/j.exer.2017.08.007.

187. Omerović, N.; Vranić, E. Application of nanoparticles in ocular drug delivery systems. *Health Technol. (Berl).* 2020, *10*, 61–78, doi:10.1007/s12553-019-00381-w.

188. Wong, C.W.; Metselaar, J.M.; Storm, G.; Wong, T.T. A review of the clinical applications of drug delivery systems for the treatment of ocular anterior segment inflammation. *Br. J. Ophthalmol.* 2020, 1–6, doi:10.1136/bjophthalmol-2020-315911.

189. Wang, X.; Coradin, T.; Hélary, C. Modulating inflammation in a cutaneous chronic wound model by IL-10 released from collagen-silica nanocomposites: Via gene delivery. *Biomater. Sci.* 2018, *6*, 398–406, doi:10.1039/c7bm01024a.

190. Reimondez-Troitiño, S.; Csaba, N.; Alonso, M.J.; de la Fuente, M. Nanotherapies for the treatment of ocular diseases. *Eur. J. Pharm. Biopharm.* 2015, *95*, 279–293, doi:https://doi.org/10.1016/j.ejpb.2015.02.019.

191. Dubashynskaya, N.; Poshina, D.; Raik, S.; Urtti, A.; Skorik, Y.A. Polysaccharides in Ocular Drug Delivery. *Pharmaceutics* 2020, *12*, doi:10.3390/pharmaceutics12010022.

192. Basa, B.; Jakab, G.; Kállai-Szabó, N.; Borbás, B.; Fülöp, V.; Balogh, E.; Antal, I. Evaluation of biodegradable PVA-based 3D printed carriers during dissolution. *Materials (Basel).* 2021, *14*, doi:10.3390/ma14061350.

193. Bhattarai, R.S.; Das, A.; Alzhrani, R.M.; Kang, D.; Bhaduri, S.B.; Boddu, S.H.S. Comparison of electrospun and solvent cast polylactic acid (PLA)/poly(vinyl alcohol) (PVA) inserts as potential ocular drug delivery vehicles. *Mater. Sci. Eng. C* 2017, *77*, 895–903, doi:10.1016/j.msec.2017.03.305.

194. Akbari, E.; Imani, R.; Shokrollahi, P.; Heidari keshel, S. Preparation of Nanoparticle-Containing Ring-Implanted Poly(Vinyl Alcohol) Contact Lens for Sustained Release of Hyaluronic Acid. *Macromol. Biosci.* 2021, doi:10.1002/mabi.202100043.

195. Abelson, M.B.; Udell, I.J.; Weston, J.H. Normal Human Tear pH by Direct Measurement. *Arch. Ophthalmol.* 1981, *99*, 301, doi:10.1001/archopht.1981.03930010303017.

196. Garcia-Valldecabres, M.; López-Alemany, A.; Refojo, M.F. pH Stability of ophthalmic solutions. *Optometry* 2004, *75*, 161–168, doi:10.1016/S1529-1839(04)70035-4.

197. Račić, A.; Čalija, B.; Milić, J.; Dukovski, B.J.; Lovrić, J.; Dobričić, V.; Micov, A.; Vuković, M.; Stepanović-Petrović, R.; Krajišnik, D. Formulation of olopatadine hydrochloride viscous eye drops – physicochemical, biopharmaceutical and efficacy assessment using in vitro and in vivo approaches. *Eur. J. Pharm. Sci.* 2021, 105906, doi:10.1016/j.ejps.2021.105906.

198. Stocum, D.L. Regeneration of Epidermal Structures. *Regen. Biol. Med.* 2012, *1*, 43–65, doi:10.1016/b978-0-12-384860-4.00003-4.

199. Struve, C.; Krogfelt, K.A. Role of capsule in Klebsiella pneumoniae virulence: lack of correlation between in vitro and in vivo studies. *FEMS Microbiol. Lett.* 2003, *218*, 149–154, doi:https://doi.org/10.1111/j.1574-6968.2003.tb11511.x.

200. Hulsart-Billström, G.; Dawson, J.I.; Hofmann, S.; Müller, R.; Stoddart, M.J.; Alini, M.; Redl, H.; El Haj, A.; Brown, R.; Salih, V.; et al. A surprisingly poor correlation between in vitro and in vivo testing of biomaterials for bone regeneration: Results of a multicentre analysis. *Eur. Cells Mater.* 2016, *31*, 312–322, doi:10.22203/eCM.v031a20.

201. Zheng, Y.F.; Bae, S.H.; Huang, Z.; Chae, S.U.; Jo, S.J.; Shim, H.J.; Lee, C. Bin; Kim, D.; Yoo, H.; Bae, S.K. Lack of Correlation between In Vitro and In Vivo Studies on the Inhibitory Effects of (–)-Sophoranone on CYP2C9 Is Attributable to Low Oral Absorption and Extensive Plasma Protein Binding of (–)-Sophoranone. *Pharmaceutics* 2020, *12*, doi:10.3390/pharmaceutics12040328.

202. Williams, C.S.; Watson, A.J.M.; Sheng, H.; Helou, R.; Shao, J.; DuBois, R.N. Celecoxib prevents tumor growth in vivo without toxicity to normal gut: Lack of correlation between in vitro and in vivo models. *Cancer Res.* 2000, *60*, 6045–6051.

203. De Matteis, V.; Rizzello, L. Noble Metals and Soft Bio-Inspired Nanoparticles in Retinal Diseases Treatment: A Perspective. *Cells* 2020, *9*, 679, doi:10.3390/cells9030679.

204. Masse, F.; Ouellette, M.; Lamoureux, G.; Boisselier, E. Gold nanoparticles in ophthalmology. *Med. Res. Rev.* 2019, *39*, 302–327, doi:10.1002/med.21509.

205. Sortino, S. *Light-Responsive Nanostructured Systems for Applications in Nanomedicine*; 2016; Vol. 370; ISBN 978-3-319-22941-6.

206. Remaliah, N.; Sibuyi, S.; Moabelo, K.L.; Fadaka, A.O.; Meyer, S.; Onani, M.O.; Madiehe, A.M.; Meyer, M. Multifunctional Gold Nanoparticles for Improved Diagnostic and Therapeutic Applications : A Review. *Nanoscale Res. Lett.* 2021, doi:10.1186/s11671-021-03632-w.

207. Mukherjee, P.; Bhattacharya, R.; Wang, P.; Wang, L.; Basu, S.; Nagy, J.A.; Atala, A.; Mukhopadhyay, D.; Soker, S. Antiangiogenic properties of gold nanoparticles. *Clin. Cancer Res.* 2005, *11*, 3530–3534, doi:10.1158/1078-0432.CCR-04-2482.

208. Darweesh, R.S.; Ayoub, N.M.; Nazzal, S. Gold nanoparticles and angiogenesis: Molecular mechanisms and biomedical applications. *Int. J. Nanomedicine* 2019, *14*, 7643–7663, doi:10.2147/IJN.S223941.

209. Pereira, D.V.; Petronilho, F.; Pereira, H.R.S.B.; Vuolo, F.; Mina, F.; Possato, J.C.; Vitto, M.F.; de Souza, D.R.; da Silva, L.; Paula, M.M. da S.; et al. Effects of gold nanoparticles on endotoxin-induced uveitis in rats. *Investig. Ophthalmol. Vis. Sci.* 2012, *53*, 8036–8041, doi:10.1167/iovs.12-10743.

210. Rhim, W.K.; Kim, J.S.; Nam, J.M. Lipid-gold-nanoparticle hybrid-based gene delivery. *Small* 2008, *4*, 1651–1655, doi:10.1002/smll.200800628.

211. Li, P.; Li, D.; Zhang, L.; Li, G.; Wang, E. Cationic lipid bilayer coated gold nanoparticles-mediated transfection of mammalian cells. *Biomaterials* 2008, *29*, 3617–3624, doi:10.1016/j.biomaterials.2008.05.020.

212. Mahareek, O.; Fahmi, A.; Abdur-Rahman, M.; Shemis, M. Synthesis, Characterization and Optimization of PCL - based Nanocapsules for Delivery of Anticancer Chemotheraputic Drug. *J. Sci. Res. Sci.* 2019, *36*, 412–423, doi:10.21608/jsrs.2019.57774.

SECTION 2: CONCLUSIONS

1. The revision of the state of art of the strategies employed to enhance the functionality and efficacy of IVT mRNA has evidenced that synthetic mRNA is attracting great interest as a therapeutic molecule. The main feature that has encouraged its recent expansion is the controlled expression of the nucleic acid without the risk of insertional mutagenesis or permanent genomic alteration. Other advantages include economical production, scalable manufacturing, and versatility of applications. Limiting technological issues mainly associated with delivery and stability difficulties have still to be overcome, although important advances have been done in the last years.

2. The physicochemical features of the nucleic acid-based medicinal products designed depended mainly on the ligands included, the composition of the SLNs in terms of cationic and ionizable lipids and, the preparation method of the SLNs, evaporation/emulsification, hot-melt emulsification or coacervation. The formulations with a particle size in the nanometre range, from 90 to 350 nm, and a positive superficial charge, from +18 to +50 mV, were made up by electrostatic interactions among SLNs, mRNA or pDNA, and different ligands such as dextran, hyaluronic acid and protamine. The nanovectors properly protected and released the nucleic acid, and they were efficiently internalized in ARPE-19, HEK-293 and HCE-2. Formulation-related factors had a significant impact on nucleic acid delivery, transfection efficacy and long-term stability of the nanovectors, being mRNA more sensitive to formulation changes.

3. The *in vitro* efficacy of the nucleic acid-based medicinal products designed was highly influenced by their intracellular behaviour in the target cell. Protein production was conditioned by energy-dependent or -independent entry mechanisms, determined by the type of nucleic acid delivered, the physicochemical characteristics of the nanovectors, and the cell line. The synthesis of the encoded protein was faster, and the duration of the expression shorter with mRNA than with pDNA. A thorough understanding of the intracellular behavior of nucleic acid delivery systems is a key point for the design of medicinal products specifically tailored to nucleic acid characteristics and therapeutic purpose.

4. Long-term stability studies showed that pDNA formulations storage at 4 °C maintained their transfection efficacy at least during seven months, although physicochemical changes were observed from the second month. On the contrary, mRNA vectors were more stable in terms of size and zeta potential, but transfection efficacy decreased from the first month, with different degree depending on the formulation. The mRNA medicinal products containing

only DOTAP as cationic lipid were the most effective, and the inclusion of dextran or hyaluronic acid conferred them a higher stability. Considering both the efficacy and the long-term stability, vectors prepared only with the cationic lipid DOTAP are more promising formulations for nucleic acid delivery than those containing also the non-ionizable lipid DODAP.

5. The medicinal products containing shRNA against the proangiogenic factor MMP-9 were prepared to avoid CNV by gene silencing. Formulations prepared with SLNs, protamine and dextran were able to downregulate MMP-9 expression in HCE-2 cells. The reduction of MMP-9 induced a decrease of both HCE-2 cell migration in a wound healing *in vitro* assay, and tube formation in an *in vitro* HUVEC tube formation assay. The results highlight the potential of nucleic acid delivery systems based on SLN for the treatment of CNV-associated inflammation by RNAi technology.

6. Topical instillation to mice of eye drops containing the mRNA and pDNA medicinal products encoding GFP resulted in the transfection of the outer layer of the corneal epithelium, although some of those formulations hardly transfected HCE-2 cells *in vitro*. The lack of correlation between *in vitro* and *in vivo* results highlights the necessity of performing *in vivo* studies at the earliest phases of pharmaceutical development of nucleic acid delivery systems, to accomplish an adequate selection and optimization of candidate formulations.

7. The nanovectors bearing mRNA encoding the therapeutic protein IL-10, formulated as eye drops, induced the synthesis of this anti-inflammatory cytokine in the corneal epithelium of mice, when administered by topical instillation for three days. Secreted IL-10 was even detected in the deeper layers of the epithelium. The results obtained highlight the possible contribution of non-viral gene supplementation therapy to the future clinical approach of corneal inflammation.

8. The incorporation of gold nanoparticles into mRNA and pDNA nanovectors based on SLNs resulted in a reduction of the size and polydispersion of mRNA nanovectors, whereas pDNA formulations maintained their physicochemical features. The administration to mice of mRNA encoding GFP included in these new golden lipid nanoparticles provided a higher transfection efficacy of the corneal tissue than the formulations without gold nanoparticles, in terms of fluorescence intensity. Therefore, the combination of gold nanoparticles with SLNs is of great advantage in terms of the physical properties and the transfection efficacy of the nucleic acids delivery systems.

SECTION 3: APPENDIXES

PUBLISHED WORKS

APPENDIX I:

Nanomedicines to deliver mRNA: state of the art and future perspectives

Itziar Gómez-Aguado, Julen Rodríguez-Castejón, Mónica Vicente-Pascual, Alicia Rodríguez Gascón, María Ángeles Solinís, Ana del Pozo-Rodríguez

Published in: Nanomaterials (2020)

Journal Impact Factor JCR 2020: 5.076 (Q1) 35/160

Related Categories:

CHEMISTRY, MULTIDISCIPLINARY (Q2)

MATERIALS SCIENCE, MULTIDISCIPLINARY (Q2)

NANOSCIENCE & NANOTECHNOLOGY (Q2)

PHYSICS, APPLIED (Q1)

Other quality indicators: 66 citations

Nanomedicines to deliver mRNA: state of the art and future perspectives

Abstract

The use of messenger RNA (mRNA) in gene therapy is increasing in recent years, due to its unique features compared to plasmid DNA: transient expression, no need to enter into the nucleus and no risk of insertional mutagenesis. Nevertheless, the clinical application of mRNA as therapeutic tool is limited by its instability and ability to activate immune responses; so that mRNA chemical modifications together with thedesing of suitable vehicles result essential. This manuscript includes a revision of the strategies employed to enhance in vitro transcribed (IVT) mRNA functionality and efficacy, including the optimization of its stability and translational efficiency, as well as the regulation of its immunostimulatory properties. An overview of the nanosystems designed to protect the mRNA and to overcome the intra and extracellular barriers for a successful delivery is also included. Finally, the present and future applications of mRNA nanomedicines for immunization against infectious diseases and cancer, protein replacement, gene editing, and regenerative medicine are highlighted.

Keywords: In vitro transcribed messenger RNA (IVT mRNA); gene therapy; nanomedicine; immunotherapy; infectious disease vaccines; cancer immunotherapy; CAR T cells; dendritic cells; protein replacement; gene editing

1. Introduction

According to the European Medicines Agency (EMA), a gene therapy medicinal product generally consists of a vector or delivery formulation/system containing a genetic construct engineered to express a specific transgene ('therapeutic sequence') for the regulation, repair, replacement, addition or deletion of a genetic sequence [1]. Nevertheless, scientifically it is usually accepted a broader view, and the concept of gene therapy includes the therapeutic application of products containing any nucleic acid.

Gene therapy entered clinical trials in the early 1990s. Up to date around 17 nucleic acid-based products have been approved worldwide and almost 2,700 gene therapy-based clinical trials have been completed, are ongoing or have been approved for a broad range of applications. It is expected that nucleic acid based products will have a substantial impact on the biopharmaceutical market in a near future [2]. Gene therapy has been clinically implemented primarily through two different approaches: ex vivo or in vivo. In ex vivo therapy, cells are

harvested from the patient or a donor, in vitro modified with the therapeutic nucleic acid and finally, re-infused into the patient. In vivo gene therapy is applied by direct administration of the vector containing the nucleic acid into the patient [3].

Depending on the final objective, gene therapy can be applied for gene augmentation, gene silencing, or gene editing [4]. So that, diverse nucleic acids are being used to address the development of these new medicinal products. DNA and messenger RNA (mRNA) induce protein expression, whereas small interfering RNA (siRNA), microRNA, oligonucleotides or aptamers provides posttranslational gene silencing [2]. Molecular scissor and gene editing approaches such as zinc finger nucleases (ZFNs), transcription activator-like effector nucleases (TALEN), and clustered regularly interspaced short palindromic repeats (CRISPR)-associated nuclease Cas9 (CRISPR/Cas9) are also being developed.

The specific features of synthetic mRNA make it a promising alternative to DNA based products. Firstly, mRNA does not need the machinery of the nucleus to be functional, as DNA therapies do [5–8]. Therefore, once mRNA reaches the cytoplasm, it starts translating the protein that encodes, being effective in both, mitotic and non-mitotic cells [9–11]. Secondly, mRNA has a better safety profile because unlike DNA, it does not integrate into the host genome, thereby reducing the risk of carcinogenesis and mutagenesis, [5–8,11]. In addition, it works without encoding additional genes [9]. Thirdly, the synthesis of the encoded protein is fast and its expression is temporary [6,9]. Onset of expression is usually detected within 1h after transfection with a peak in expression 5–7h later [12].Finally, the production of in vitro mRNA (IVT mRNA) is easier than the manufacturing of DNA, and it can be standardized maintaining its reproducibility [7].

Nevertheless, the use of IVT mRNA for clinical purposes has been mostly limited by its physical instability, its immunogenic capacity, and the difficulty to pass through the cellular membrane, due to the anionic nature of mRNA molecules [8,13,14]. The knowledge of mRNA structure has boosted modifications designed to improve stability and translation efficacy, and to reduce immunogenicity; however, optimized IVT mRNA has still to overcome several extracellular and intracellular barriers. As observed in figure 1, IVT mRNA has to avoid degradation from extracellular degradative agents, such as ribonucleases, and reach the target cell, cross the cytoplasmic membrane and diffuse in the cytoplasm to reach the ribosomes [7,15]. The formulation of IVT mRNA in suitable nanosystems or vectors is frequently a requirement for surpassing all these barriers. Among delivery systems for IVT mRNA non-viral vectors, and more specifically lipidic systems, are the most studied.

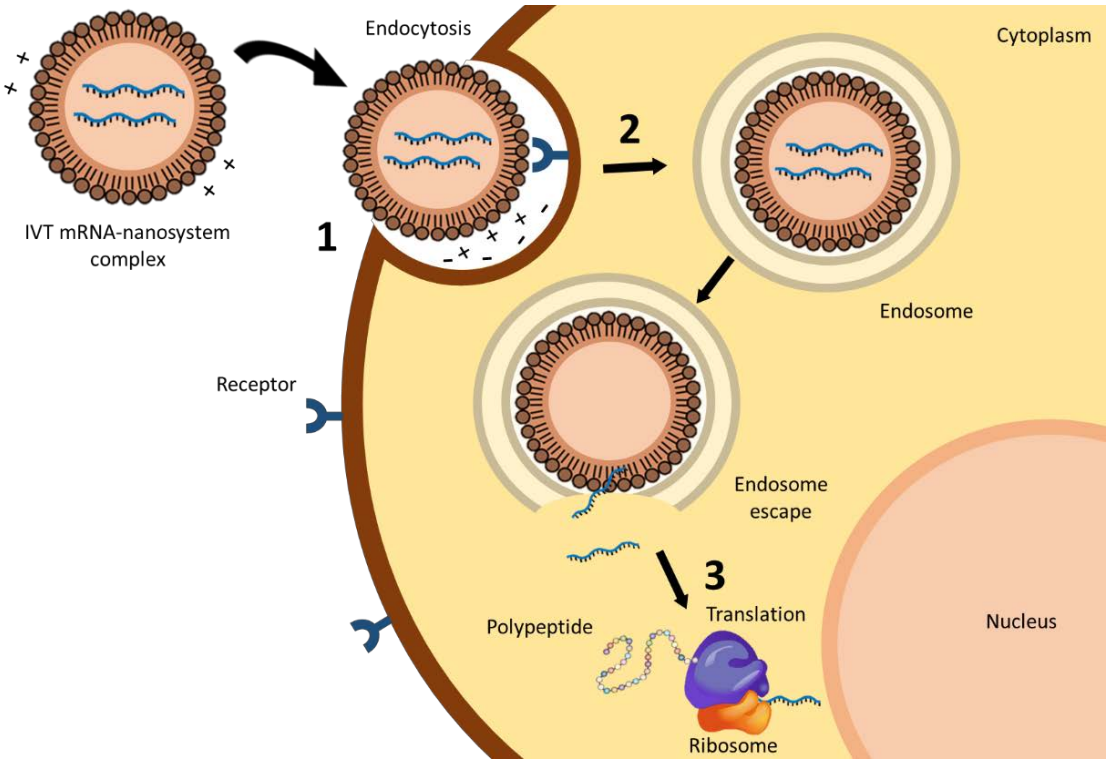

Figure 1. Intracellular barriers for IVT mRNA delivery: (1) interaction between delivery system and cell membrane, (2) endocytosis and (3) endosomal escape and liberation of the mRNA to start the translation process.

The first step for an efficient internalization of IVT mRNA is the interaction between the delivery system and the cell membrane. The attachment to the cell surface may occur through electrostatic interactions between the system and the membrane surface, which is favored for those presenting a cationic nature [16]. Cell binding can also be improved by incorporating ligands into the vectors, able to interact with specific cell surface receptors [17,18].

The main mechanism of cell entry is endocytosis. It comprises a variety of complex processes that determine the intracellular disposition of the mRNA. The vectors are included into endosomes by the invagination of the cell membrane. Endosomes mature and fuse with lysosomes, where the acidic environment and the presence of hydrolytic enzymes can degrade the vector and the nucleic acid. Therefore, the endosomal escape before degradation is considered a bottleneck for a successful mRNA therapy, and, as in the case of the cellular internalization, the delivery system plays a crucial role. The foremost proposed mechanisms of endosomal escape include endosome disruption, active transport, or fusion of the delivery system with the endosomal membrane [19]. However, Patel et al. have recently identified that late endosome/lysosome formation is essential for functional delivery of exogenously presented mRNA [20].

The present review collects the strategies accomplished to optimize the functionality and efficacy of IVT mRNA. Besides the chemical modifications in its structure, the different nanosystems and technological approaches developed for a successful IVT mRNA delivery will be described. Finally, the potential applications of mRNA nanomedicines will be discussed: vaccination against infectious diseases, cancer immunotherapy, protein replacement, gene editing, and regenerative medicine.

2. Structure of Synthetic IVT mRNA and Chemical Modifications

The production of IVT mRNA is usually carried out in cell-free systems, leading to easy standardization of clinical grade manufacturing, which can be performed under Good Manufacturing Practices (GMPs). As compared to recombinant proteins produced in eukaryotic cells, fabrication costs of IVT mRNA under GMPs are substantially lower [21]. It is important to select an efficient purification method of the IVT mRNA in order to eliminate aberrant (e.g. truncated) mRNA molecules, which are highly immunogenic contaminants and may lower translation efficiency [22].

Manufacturing of IVT mRNA by a cell-free in vitro transcription system requires a linearized DNA template which must contain a prokaryotic phage promoter sequence for the T7, T3 or SP6 RNA polimerases, the open reading frame (ORF) encoding the desired protein, the sequences corresponding to the regulatory untranslated regions (UTRs), and, optionally, to a polyadenylated A tail (poly(A) tail). [9,14,23]. When the poly(A) tail is not encoded directly in the DNA template, it can be added post-transcriptionally by enzymatic reactions with recombinant poly(A)polymerase of E. coli (E-PAP) [11,24]. Since the final IVT mRNA must be structurally similar to natural mRNA processed in the cytoplasm of eukaryotic cells, it needs also to be capping in 5’.

A synthetic IVT mRNA consists of the following five fundamental structures, which can be chemically modified in order to optimize the translation process, and the stability and regulate the immunogenicity: (a) cap in 5’; (b) 5’ UTR; (c) an ORF, which has the starting codon AUG and the stop codon (UAA,UAG,UGA); (d) 3’ UTR; and (e) poly(A) tail. Figure 2 schematizes the main chemical modifications of these structural elements.

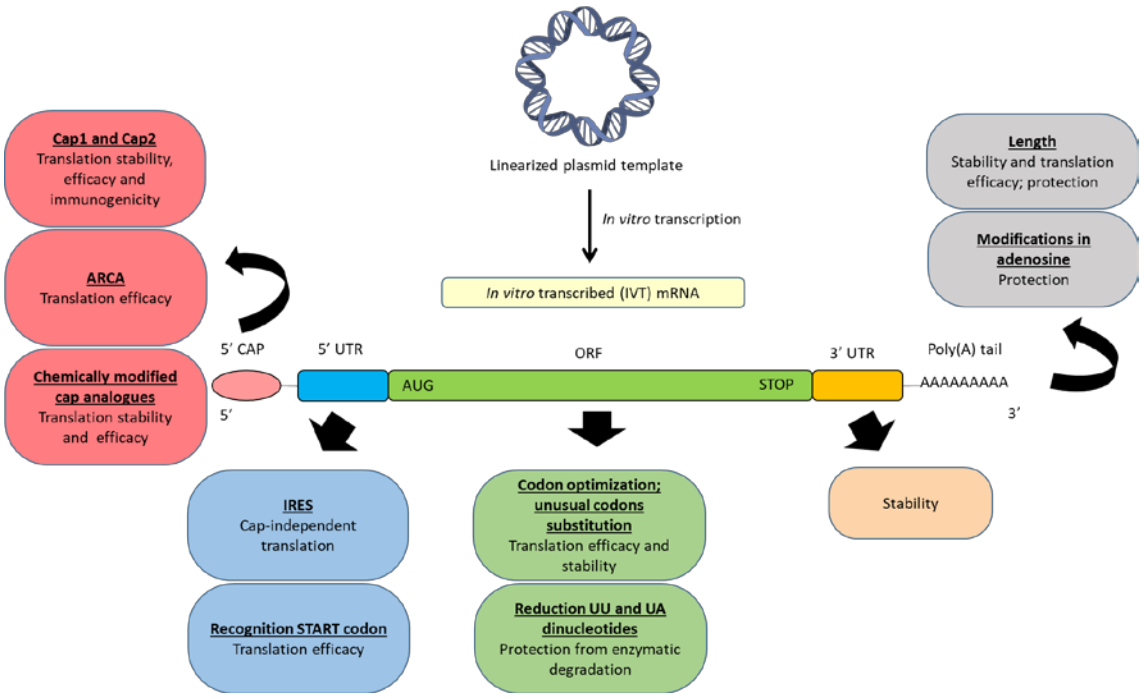

Figure 2. Representative scheme of the IVT mRNA structure and its principal modifications to improve the efficacy and the stability and to reduce the immunogenicity.

2.1. 5' cap

All eukaryotic native mRNA possess a 5' cap structure, known as cap0, formed by the union of an inverted 7-methyl guanosine (m7G) to the first nucleotide of the mRNA by a 5' to 5' triphosphate bridge during the transcription process. This capping occurs by three consecutive enzymatic reactions, when the first 20-30 nucleotides of mRNA have been transcribed in the nucleus.

Besides stabilizing the mRNA in the translation, splicing, polyadenylation and nuclear exportation processes, cap0 protects the mRNA from exonucleases. Additionally, cap0 interacts with cap binding proteins (CBP), essentials for the nuclear export of mRNA, and also with the translation initiation factor 4E (eIF4E) in the cytoplasm, crucial for the initiation of translation [11,25,26]. Moreover, it could be used as innate immune marker which differentiates the viral RNA from cellular RNA [26].

In the last years, human enzymes that form other two types of 5' cap, cap1 and cap2, have been identified [26,27]. In these cases, the m7G-specific 2'O methyltransferase (2'O MTase) methylates the second or third ribonucleotide at the 2'O or 3'O position of the riboses generating cap1 and cap2 structures, respectively. Cap1 and cap2 are less immunogenic than Cap0, and, furthermore, they enhance the translation efficiency [10]. Therefore, the introduction of cap1 or cap2 in the synthesis of IVT mRNA is a crucial factor to reduce the

immunogenicity for applications in which immune response has to be minimized [24], but the incorporation of cap0 could be more useful in therapies in which the immune response is beneficial, such as in vaccination.

In order to resemble the chemical structure of eukaryotic mRNA, synthetic mRNA transcripts can be capped after finishing the transcription (post-transcriptionally) or during the transcription (co-transcriptionally).

Post-transcriptional capping is usually carried out by using the enzyme machinery of recombinant Vaccinia Virus to perform the consecutive enzyme reactions to add the cap0, cap1 or cap2.

In co-transcriptional capping synthetic cap analogues are directly added during the transcription. This process is simpler than the enzymatic capping, but it also presents some limitations. On the one hand, all mRNA molecules obtained are not capped, because the cap analogue has to compete with the guanosine triphosphate (GTP), which is the initiator nucleotide [14,26]. As a consequence, the uncapped mRNAs are immediately digested by nucleases and can induce an immune response. An strategy to reduce the stimulation of the immune system is the removal of the triphosphates of the 5' end of uncapped IVT mRNA, by using a phosphatase [9,28]. On the other hand, there is the risk of reverse orientation of the cap analogues, which impede the binding to the CBP and the posterior translation [11,24,29]. As an alternative, an anti-reverse cap analogue (ARCA) has been developed [11,24]. ARCA consists of a methyl group in the 3'-OH of the m7G nucleotide, that enables the appropriate orientation of the cap and prevents the elongation of the mRNA along the wrong site [24,26]. Other traditional limitation of co-transcriptional capping is the inability to incorporate cap1 and cap2. However, recently, TriLink BioTechnologies have designed a new co-transcriptional capping technology, CleanCapTM, able to incorporate cap1 or cap2 in the 94% of the mRNA molecules during the transcription process [30].

Finally, it has to be also taken into account that cytosolic decapping enzymes can remove mRNA cap. In order to provide resistance to the IVT mRNA against these enzymes and, therefore, extend its half-life, chemically modified cap analogues can be used. The resulting modified mRNAs can contain a phosphorothioate, phosphorothiolate, imidiphosphate and boranophosphate, among others [31–36].

2.2. ORF

The codon composition of the region that encodes the protein sequence, known as ORF, may also influence the translation efficiency and stability of the mRNA. So that, the reduction of the

quantity of UU and UA dinucleotides in the ORF has demonstrated to protect the IVT mRNA from the decapping enzymes [37,38]. Additionally, since most amino acids are encoded by different synonymous codons, codon optimization strategies have been developed to improve the cost efficiency of recombinant protein production [39]. Codon optimization is mainly based on the substitution of multiple rare codons by other more frequent ones that encode the same amino acid. As a result, the rate and efficiency of the protein translation are increased [14,23,40]. However, the clinical application in humans is controversial, because in the last years it has been documented that synonymous mutations affect protein functions, and alterations in translation kinetics can lead to alterations in protein conformation [40–43].

2.3. Poly(A) tail

The poly(A) tail in native eukaryotic mRNA is formed by 100-250 residues of adenosine [9,24,44]. It participates in the exportation process of mRNA molecules from the nucleus, interacts with initiation factors of the translation and prevents the degradation by nucleases through the interaction with poly(A)-binding protein, providing stability [45].

The poly(A) tail can be added to IVT mRNA directly during the transcription, if the DNA template encodes the poly (T) sequence, or post-transcriptionally by enzymatic reactions with recombinant poly(A)polymerase of E. coli (E-PAP) [11,24]. The addition during transcription is preferable, because the length of the poly(A) tail is more reproducible [14,23,24].

The length of the poly(A) tail influences the stability and translation efficiency of the IVT mRNA [46,47]; although a relatively long poly(A) tail seems to be appropriate, the optimal length may vary depending on the target cell. In HeLa (epithelial human) cells the increase of adenosine residues in the poly(A) tail from 14 to 98 enhanced the protein expression [48], whereas in dendritic cells (DCs) a number of 120 adenosine residues enhances the translation efficiency, and improves the protection and the stability of the IVT mRNA [49,50].

2.4. UTRs

The ORF is limited by the UTRs in both 5’ and 3’ sides. These non-coding regions do not participate directly in the codification of the proteins, but their sequences, length and secondary structures are crucial for the regulation of the translation of the mRNA and the protein expression [51]. 5’ UTR is involved in the initiation of translation, which is considered the most intricate step among the whole process, whereas 3’ UTR has influence in mRNA stability and in the extent of protein expression [52].

The presence of the internal ribosomal entry sites (IRES) in the 5' UTR recruits the ribosome and induce a cap-independent translation initiation [53–55]. In order to improve translation efficiency, 5’ UTRs containing IRES from viral origin may be incorporated into IVT mRNA [37]. In these cases, translation is not dependent of eIF4E, as it does with cap0, and IVT mRNA expression is extended to cells where eIF4E levels are low [14]. However, the 5’ cap is still necessary for the protection of the mRNA against nucleases, and therefore, most IVT mRNAs contain both 5’ cap and IRES in their structure.

The Kozak consensus sequence, located in the 5’ UTR, also plays a major role in the initiation of the translation process. The Kozak sequence, defined as RCCAUGG, where R is a purine (A or G) was considered the preferred sequence for translation initiation in eukaryotes [56]. In this sequence, some nucleotides are more important than others; particularly the −3 and the +4 positions, relative to the adenine of the starting codon AUG. To facilitate the recognition of the starting codon AUG, G nucleotide must be in the position +4 and A/G nucleotides must be in the position -3 [57].

Regarding the 3’ UTR, the presence in this region of the specific sequences of α-globin and β-globin mRNAs improve the stability of IVT mRNA and the duration of protein expression, respectively [58,59]. In addition, the length of the 3’ UTR sequence may be modified to regulate the protein localization. For instance, in the case of CD47 protein membrane, long 3’ UTR induces the protein expression on the cell surface, whereas short 3’ UTR results in the localization of the protein in the reticulum endoplasmic [60].

2.5. Modified nucleosides

The incorporation of modified nucleosides into mRNA is a common strategy to reduce its immunostimulatory activity. Exogenous IVT mRNA induces innate immune responses by interacting with pattern recognition receptors (PRRs), including Toll-like receptors (TLRs) and cytoplasmic RNA sensors, such as retinoic acid-inducible protein I (RIG-I) [61,62]. It is known that uridine residues activate TLR7, and GU- and AU-rich RNA strands activate TLR7 and TLR8 [63,64]. However, the incorporation of modified nucleosides into the transcript, (i.e. pseudouridine (Ψ), N1-methylpseudouridine (N1mΨ), 5-methylcytidine (m5C), N6-methyladenosine (m6A), 5-methyluridine (m5U), or 2-thiouridine(s2U)), avoids the activation of TLRs [65–69]. Some of them, such as Ψ and s2U, also abolish activation of RIG-I [63]. In addition, the presence of m6A in the 5’ UTR of IVT mRNA has been proposed as an alternative to IRES, in order to favour cap-independent translation [70].

3. mRNA nanomedicines

A key challenge for the clinical application of nucleic acid medicinal products entails the availability of delivery systems specifically adapted to their features and purpose. A vehicle for mRNA therapy in addition to protect it and provide specificity to reach the target cell, must afford an adequate intracellular disposition of the nucleic acid that enables the translation process, and all of this, preventing the activation of the immune response [71,72].

Currently, around 70% of the clinical trials with nucleic acids use recombinant viruses as delivery systems, such as retroviruses, lentiviruses, adenoviruses and adeno-associated viruses (AAVs), among others [73]. Viral systems are viruses genetically modified to prevent their replication in the host cell; they present high capacity of transfection, but also oncogenic and immunogenic potential. Moreover, viral vectors present a limitation regarding the size of the nucleic acid they can transport [74]. Despite the major advances achieved in DNA delivery with viral vectors, they do not play an important role in the case of mRNA-based products [7,75–78]. Non-viral systems are safer, their production is simpler, more economical and reproducible than viral vectors, and the size of nucleic acid to be packed is not usually an obstacle. However, their efficacy of transfection is still a limitation, although it has been improved by different strategies and the efforts are still ongoing [75,77,79].

Therapeutic application of mRNA without the help of a delivery system presents important drawbacks [66]. So that, naked mRNA has been mainly applied ex vivo by using physical methods, including electroporation, microinjection and gene gun; these methods are able to disrupt the cell membrane and facilitate the entry of mRNA into the cell [80]. Electroporation consists of generating pores in a cell membrane through electric pulses. This technique has shown efficient mRNA delivery for tumour antigen loading of DCs [81]; even in some studies mRNA electroporation has been more efficient compared to that of DNA, with faster and more homogeneous protein expression in vivo [82]. Microinjection, the direct injection of mRNA into the target cell by the use of microneedles [83,84] and gene gun, in which naked mRNA is pneumatically shot into the target cell, have also been used for mRNA transfection [85–88]. In in vivo applications, intravenously administered naked mRNA is rapidly degraded by ribonucleases and the innate immune system can be activated. In contrast, local administrations, such as subcutaneous, intramuscular or intranodal, have been useful for naked mRNA delivery, especially when the activation of the immune system and a small amount of protein are required, as happens in vaccination [89].

Chemical nanocarriers are nowadays in the forefront of pharmaceutical research for mRNA delivery. Thanks to the advances in material sciences, the rapid progress of nanotechnology, and the progress in nucleic acid chemistry, an extensive work is currently ongoing to develop new systems [81]. Chemical nanocarriers are formed by synthetic or natural biocompatible components that form complexes with the mRNA, and vary in composition, size, shape and physico-chemical characteristics. In addition to the function of protecting the nucleic acid from degradation and denaturation, they all should facilitate the transfection process, being minimally toxic and immunologically responsive [90]. Moreover, these delivery systems could be also useful to programme the release profile of the active substance, improve the pharmacokinetic profile, reduce the toxicity to healthy organs/tissues and increase the blood circulation time [71,91]. As can be seen in figure 3, nanocarriers for mRNA delivery evolve into various forms, including lipidic, polymeric and polypeptidic systems, dendrimers, gold nanoparticles, and hybrid systems.

3.1. Lipid based systems

Lipid-based vectors are among the most widely used non-viral nucleic acids carriers. The main component of lipidic systems are cationic lipids, which are able to interact with the mRNA by electrostatic interactions, leading to the formation of a complex called lipoplex [78].

DOTMA (N-[1-(2,3-dioleyloxy)propyl]-N,N,N-trimethylammonium chloride) was the first synthetic cationic lipid utilized to complex IVT mRNA. The system containing the IVT mRNA luciferase condensed and delivered the nucleic acid in human, rat, mouse, xenopus (frog) and drosophila cells in vitro [92]. DOTAP (1,2-dioleoyl-3-trimethylammonium-propane) is another traditional synthetic lipid derived from DOTMA, althoug more economical to synthesize and with a greater efficacy [78]. DOTAP has been frequently combined with the zwitterionic lipid DOPE (dioleoylphosphatidylethanolamine), to prepare colloidal systems able to bind the nucleic acids. This mixture facilitates the endosomal escape under acidic pH conditions, thanks to the capacity of DOPE to modify the lipoplex from a bilayer structure to hexagonal phase II (HII), structures known to induce supramolecular arrangements which result in the fusion of lipid bilayers [7,93]. The use of DOTAP alone or in combination with the helper lipid DOPE has been applied to mRNA delivery [94,95]. More recently, ionizable lipids with lower toxicity but preserving the transfection capacity, such as 1,2-dioleoyl-3-dimethylammonium propane (DODAP) or 1,2-dioleyloxy-N,N-dimethyl-3-aminopropane (DODMA), have been developed as an alternative to conventional cationic lipids [5]. While cationic lipids present alkylated quaternary ammonium groups and retain their cationic nature regardless of the pH, ionizable lipids acquire positive charges due to the protonation of free amines as pH decreases [13]. These new lipids are neutral

at physiological pH but positively charged inside the endosome, when pH values are below its pKa. The electrostatic interactions between naturally occurring anionic lipids in endosomal membranes and the ionizable cationic lipids have been proposed as the underlying mechanism of nucleic acid release [88]. This interaction is able to promote membrane lytic nonbilayer structures such as the hexagonal HII phase, culminating in the intracellular mRNA delivery [96]. Nowadays, nanocarriers containing ionizable cationic lipids are among the leading delivery system candidates with promising applications for siRNA and mRNA delivery [78].

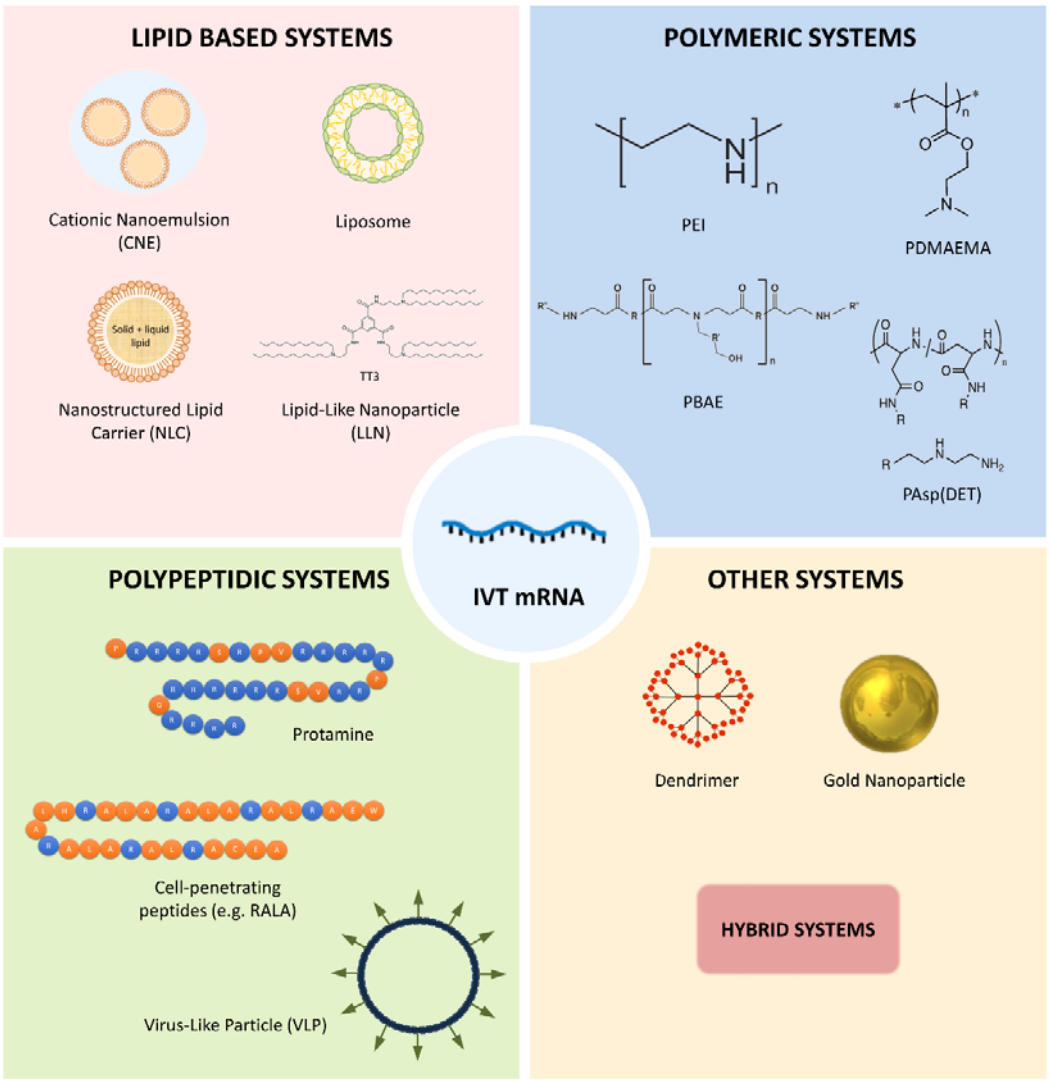

Figure 3. Representative scheme of chemical nanocarriers for the mRNA delivery.

Cationic lipids can be formulated to prepare cationic nanoemulsions (CNEs) and lipid nanoparticles (LNPs) [75]. CNEs consist of a dispersion of an oil phase stabilized by an aqueous phase containing the cationic lipid. These nanoemulsions present a droplet size distribution of about 200 nm, and are mainly used to formulate mRNA vaccines [2,9]. For instance, a self-

amplifying RNA (SAM) vaccine expressing human immunodeficiency virus (HIV) type 1 envelope formulated in a CNE induced potent immune responses in rhesus macaques [97]. Brito et al. [98] developed a well tolerated and immunogenic SAM vaccine based on CNE. This SAM vaccine elicited immune responses in a variety of animal models (including mice, rats, rabbits, and nonhuman primates) at doses much lower than those required for pDNA vaccines.

LNPs include liposomes and other lipid based nanoparticles, and are regarded as one of the most developed systems for mRNA delivery. Currently, several LNP platforms are at the forefront of clinical trials, indeed, they are clinically validated delivery systems for RNA therapy. At the beginnings, LNPs were a considerable promise for the delivery of siRNA, being their utility as agents for mRNA delivery more recent [99]. In this sense, Patisiran (ONPATTRO™), a siRNA formulated in LNP targeted to inhibit hepatic transthyretin protein, received a recent FDA approval, meaning a significant progress in the field [100]. This product contains a novel ionizable lipid, Dlin-MC3-DMA (MC3) [101], and after its success, several groups have managed to use MC3 as vehicle for transferring mRNA [102]. The previous experience in siRNA formulation is benefiting the development of mRNA nanosystems, although mRNA has a different structure which may interfere with the packing capacity of nanoparticles [99]. For an optimal mRNA release the delivery systems should contain less ionizable lipid and cholesterol and more phospholipid and polyethylene glycol (PEG) [5] than in the case of siRNA.

Liposome based formulations are amphiphilic spherical vesicles formed by one or more lipid bilayers enveloping an aqueous core with size ranging from 20 nm to a few microns. They generally contain a cationic lipid combined with: a helper lipid that support the bilayer structure and facilitates the endocytosis, cholesterol to stabilize the lipid bilayer of the LNP, and a (PEG)-lipid. PEG lends the nanoparticle a hydrating layer to improve colloidal stability, reduce protein adsorption and non-specific uptake, and prevent reticuloendothelial clearance [13,89]. Additionally, helper lipids such as DSPC (1,2-distearoyl-sn-glycero-3-phosphocholine), DOPE and POPE (1-palmitoyl-2-oleoyl-sn-glycero-3-phosphoethanolamine) are frequently used in these systems [44]. The in vivo delivery of mRNA by using this kind of lipid-based system was already evaluated in 1994 [103], demonstrating a comparable efficacy to liposome-DNA complexes in accomplishing in situ tumour transfection. That study also showed that mRNA may be considered as an alternative to pDNA as a gene transfer vector for genetic immunopotentiation applications. More recently, LNPs containing an ionizable cationic lipid, phosphatidylcholine, cholesterol, and PEG-lipid were used to encapsulate nucleoside-modified mRNA encoding the pre-membrane and envelope glycoproteins of a strain from the Zika virus [104]. An intradermal single low-dose immunization elicited potent and durable neutralizing antibody responses and

protective immunity in mice and non-human primates. SAM vaccine platform is another example of a synthetic mRNA delivered by LNPs. SAM vaccine encoding an influenza H1HA antigen from N1H1 virus, and formulated with 1,2-dilinoleyloxy-3-dimethylaminopropane, 1,2-diastearoyl-sn-glycero-3-phosphocholine, cholesterol and PEG-DMG 2000 , has demonstrated to be immunogenic in mice at low doses, and to elicit antibody responses that were comparable to licenced vaccine [104]. The use of mRNA-liposomes in cancer therapy has increased dramatically since the first study in 1999. Zhou et al. [106] used hemagglutinating virus of Japan (HVJ)-based liposomes as delivery system for the injection of the synthesized mRNA encoding gp-100 directly into the mouse spleen, and gp100 antibody and responses against B16 cells were induced. Recently, the first-in-human, open label phase I study in ovarian cancer patients has been approved. Patients will be vaccinated intravenously prior and during (neo)-adjuvant chemotherapy with a liposome formulated mRNA vaccine (W_ova1 vaccine) which includes 3 ovarian cancer- tumour-associated antigens (TAAs) RNAs (ClinicalTrials.gov Identifier: NCT04163094). CRISPR/Cas9 genome editing mediated by LNP have recently provided in vivo evidence in animal models. Finn et al. [107] developed a LNP-mediated delivery method by using a biodegradable and ionizable lipid termed LP01 to form LNPs co-formulated with both, Spy Cas9 mRNA and single guide RNA (sgRNA). A single administration of the system enabled significant editing of the mouse transthyretin gene in the liver and resulted in >97% reduction in serum protein levels that persisted for at least 12 months.

A few marketed transfection reagents (for instance MegaFectinTM, TransITTM) are cationic liposome formulations based on DOTAP, DOPE and cholesterol [89], useful for mRNA transfection. As an example, expression was obtained after the intravenous injection to mice of MegaFectinTM containing mRNA encoding red fluorescent protein [108]. Other cationic lipid-based transfection reagents commercialized have been widely used for the mRNA delivery, such as Lipofectin™, which is a mixture of DOTMA and DOPE, and LipofectamineTM, which is a mixture of DOSMA (the polycationic lipid, 2,3-dioleyloxy-N-[2(sperminecarboxamido)ethyl]-N,N-dimethyl-1-propanaminium trifluoroacetate) and DOPE [89]. However, their use is restricted to in vitro studies due to the toxicity by the positive charges, fast clearance, activation of immune response and low transfection efficacy in vivo [89,96].

Lipidoids, a new class of lipid-like delivery molecules comprising multiple hydrophilic groups and several lipid tails, were developed in 2008 as novel delivery agents for siRNA therapy [109]. Based on those results, more recently, a new class of lipid-like materials termed zwitterionic amino lipids (ZALs) have been applied for mRNA gene editing [110]. Intravenous co-delivery of

Cas9 mRNA and targeted sgRNA from a single ZAL nanoparticle enabled CRISPR/Cas gene editing in mice.

In recent years, new lipid derivate systems, known as lipid-like nanoparticles (LLNs), have been developed for mRNA delivery. N1,N3,N5-tris(2-aminoethyl)benzene-1,3,5-tricarboxamide (TT) is formed by a phenyl ring, three amide linkers and three aminolipids chains [44]. Among them, TT3 was recognized as the principal compound in the optimized formulation, which increased in 350-fold the efficacy of luciferase-mRNA transfection [111]. More recently, TT3 LLNs delivered human factor IX (hFIX) mRNA and recovered the normal levels of the protein in IX-deficient mice [111]. TT3 LLN3 were also optimized to deliver both Cas9 mRNA and sgRNA, demonstrating effective gene editing of hepatitis B virus DNA and the proprotein convertase subtilisin/kexin type 9 (*pcsk9*) gene [112].

Nanostructured lipid carriers (NLCs) are another type of LNPs used to deliver mRNA for vaccination. NLCs are colloidal structures composed by a core containing a mixture of solid and liquid lipids, resulting in an unstructured lipid matrix [113]. An important advantage of NLCs is their low toxicity respect to other lipid systems, as emulsions, which require high quantities of surfactants and cosurfactans. Additionally, production and sterilization of NLCs are less difficult and expensive than they are for other systems. Specifically, sterilization of liposomal formulations is rather difficult due to the sensitivity of phospholipids to heat and radiation [23], their production is highly cost, and batch-to batch reproducibility and large-scale manufacturing are difficult and expensive to achieve [114]. Better than for nucleic acid delivery, NLCs have been studied mainly for increasing the oral bioavailability of poorly soluble drugs [115]. Nevertheless, in a recent study [116], administration of replicating viral mRNA encoding Zika virus antigens formulated in NLCs, completely protected mice against a lethal Zika challenge; this achievement represents what might be the most potent approach to date of any Zika vaccine.

3.2. Polymeric systems

The use of polymer nanoparticles has been intensively investigated for pDNA delivery, although few studies have addressed their use for mRNA. One key advantage of polymeric systems is the possibility of modifying their chemical properties to adapt them to the active substance. The binding of cationic polymers and nucleic acids leads to the formation of poliplexes [89]. Different cationic polymers have been studied for mRNA complexation, including polyethyleneimine (PEI), polyacrylates, poly(β-amino esters) (PBAEs) and poly(aspartamides) (PAsp), among others. However, despite the significant number of polymeric materials available, polymeric systems are not as clinically advanced as lipidic systems for mRNA-based therapies.

PEI was one of the first polymers used for nucleic acid delivery; it contains a large number of amine groups in its structure conferring it a positive charge. PEI may present both a linear and a branched conformation. Linear PEI contains secondary amino groups partially protonated at physiological pH, whereas branched PEI contains primary and secondary groups, and a small amount of tertiary amines. The presence of amino groups is responsible for the strong affinity to nucleic acids, including mRNA, and the cationic charges facilitate the interaction of the lipoplexes with the cell membrane and the entry into the target cell. Moreover, amino groups allow ionization and confer high buffering ability that, although under discussion, is the responsible of the "proton sponge effect" and enables the endosomal swelling and rupture by changing the osmolarity of acidic vesicles [71]. Nevertheless, the high density of positive charges is also related to in vivo toxicity by owing interactions with extra and intracellular proteins, destabilization of lipid cellular membranes and activation of the immune system [117,118]. New PEI derivatives have been designed to improve its biocompatibility and transfection efficiency. For example, jetPEI®, a linear PEI commercialized as an in vivo transfection reagent in mice, was firstly evaluated for pDNA and siRNA transfections, and later for mRNA transfection [119]. More recently, the administration of IVT mRNA with jetPEI® by direct myocardial injection in mouse demonstrated expression of the protein in lung [120].

Polyacrilates have been also used for mRNA delivery, although with modifications in the side chain, needed to interact electrostatically with nucleic acids. One of the most studied polyacrilates is poly(2-dimethylaminoethyl methacrylate) (PDMAEMA), which presents lower affinity for mRNA than for pDNA; however, its PEGylation improves mRNA binding and transfection efficiency [121]. The development of triblock copolymers, formed by modifications in PDMAEMA structure, have demonstrated an improvement in transfection efficiency in both siRNA and mRNA systems. The modifications include: (1) the addition of amphiphilic materials, such as PEG methacrylate (PEGMA), to improve the stability and biocompatibility; (2) the incorporation of a hydrophobic butyl methacrylate segment (BMA) for fusogenicity; and (3) a pH-responsive diethylaminoethyl methacrylate (DEAEMA), to break the membrane of endosomes [71]. Triblock copolymer with PEGMA placed in the centre of copolymer chain showed high transfection efficiency and stability in macrophages and DCs, showing the potential of this system for mRNA-based vaccination approaches [122]. Oligoalkilamines grafted to an 8000 Da poly(acrylic acid) (PAA8k) scaffold complexed with chemically modified mRNA resulted in another kind of polyplexes with transfection capacity. Intravenous administration of PAA8k-luciferase mRNA systems in mice showed different luminescence signal in liver depending on their structure[123].

PBAEs are biodegradable and pH responsiveness copolymers synthetized by the addition of amines and acrylates via Michael-type reaction. The tertiary amine of its structure can electrostatically interact with the negative charge of nucleic acids. There is a broad variety of PBAEs delivery systems due to their compatibility with other polymers, such as PEG, poly (lactic acid) (PLA), and poly(ε-caprolactone) (PCL) [124]. The use of PBAEs formulated with PEG-lipid improves serum stability of mRNA after intravenous administration [125]. Recently, inhaled delivery of IVT mRNA by hyperbranched PBAEs provided uniform distribution of luciferase mRNA in the lung and protein expression lasted 24 h [126].

PAsp are synthetized by polymerization of DL-aspartic acid in orthophosporic acid medium and later addition of a nucleophilic amine [91]. The length of the aminoethylene side chain influences both the cationic charge and buffering capacity of each P(Asp) construct. For example, PAsp(DET), which is formed by the addition of 1,2-diaminoethane in the side chain to the PAsp, shows endosomal scape capabilities and biodegradability [89,127]. An odd-even effect of the amynoethylene repeated units has been described for different nucleic acid payload. PAsp containing even-numbered of amynoethylene units showed higher transfection with pDNA, whereas an odd-numbered unit produced sustained increase in mRNA expression and enhanced mRNA resistance against RNase [127,128]. PEG-PAsp polyplexes have displayed enhanced stability and lower cytotoxicity; for instance, IVT mRNA complexed with PEG-PAsp(DET) was intranasally administrated to mice for delivering brain-derived neurotrophic factor (BDNF), showing protein expression in nasal tissues for nearly two days [129]. PEG-PAsp(DET) has been also used to complex Bcl-2 IVT mRNA, being more effective than pDNA on reducing apoptosis in the liver of mice with fulminant hepatitis [130].

In addition to the most used polymers discussed above, it has been reported transfection of IVT mRNA with other kind of polyplexes. Nanoparticles formed by a core-shell structure of IVT mRNA complexed with the peptide protamine surrounded by PCL layers improved the stability of mRNA [131]. Chitosan, a biocompatible cationic glycopolymer containing amines, formulated as chitosan/hyaluronic acid nanoparticles provided successful delivery of luciferase-encoding mRNA [132]. Self-immolative polycarbonate-block-poly(α-amino)esters, also known as charge-altering releasable transporters (CARTs), have demonstrated capacity to deliver mRNA thanks to their capacity to reduce chelative electrostatic anion-binding ability with the cationic polymer and facilitate endosomal escape [133,134]. CART polymers are effective for in vivo delivery of mRNA with minimal toxicity in different cell lines and animal models via intramuscular, intratumoral, and intravenous administration. These CARTs have shown in a mouse model strong antigen-specific immune response against mRNA-encoded viral epitopes [135]. Another

biodegradable ionizable amino polyesters (APEs) synthetised via ring opening polymerization of lactones with tertiary amino-alcohols, are tissue-selective for mRNA delivery [136].

3.3. Polypeptidic systems

Polypeptides consist of one or various amino acids disposed in block or random sequences. They can provide biocompatibility and physicochemical properties to the delivery systems, thanks to the biodegradable naturally occurring monomeric units. Another advantage for nucleic acid delivery is the ability to adapt their cationic and endosomolytic properties due to their structural flexibility [71].

Protamines are a family of small peptides with arginine-rich sequence that come from fish sperm. Arginines confer positive charge, facilitating electrostatic interactions with the negative charge of the nucleic acid; in fact, protamine was described more than 50 years ago as an enhancer of RNA uptake [137]. The condensation of mRNA with protamine protects it against ribonuclease degradation, and the complex formed can activate TLRs acting as danger signals useful for vaccination [138]. Protamine-based formulations for IVT mRNA delivery are the second most used chemical system in clinical trials, although far from lipidic systems. RNActive® technology, developed by CureVac, is an mRNA vaccine platform based on protamine/mRNA complexes currently under clinical evaluation against the rabies [136] and different cancers [139,140]. RNActive® platform has been also tested preclinically against the influenza virus infection [141].

Cell-Penetrating Peptides (CPPs) have been used for nucleic acid delivery due to their capacity to overcome cell membranes. Although the mechanisms of cellular internalization are not fully known, it is thought that CPPs may promote the grouping of negatively charged glycosaminoglycans of the cell surface, triggering macropinocytosis and lateral diffusion or directly disrupting the lipid bilayer [13]. A cationic CPP containing the arginine-rich amphipathic RALA motif was used as an mRNA vector for DCs. Nanocomplexes of RALA with Ψ and m5C modified IVT mRNA elicit potent cytolytic T cell responses against the antigenic mRNA payload [142].

Artificial viral coat proteins formulated as virus-like particles (VLPs) have been used as vehicles for transfection due to their ability to assemble and protect mRNA. Li et al. [143] developed an mRNA vaccine as therapy for prostate cancer based on recombinant bacteriophage MS2 VLPs. This vaccine induced strong humoral and cellular immune responses and protected mice against prostate cancer. In other work, artificial viral coat protein consisting of an oligolysine (K12), a silk protein-like midblock S10, and a long hydrophilic random coil block C was generated and

complexed with mRNA to form rod-shaped VLPs. This system transfected cells with both EGFP and luciferase, but the efficacy was low compared to that obtained with a lipoplex transfection reagent [144]. More recently, VLPs prepared by fusing protein G of Vesicular stomatitis virus (VSV-G) with a ribosomal protein L7Ae of Archeoglobus fulgidus, resulted in efficient delivery of EGFP in human induced pluripotent stem cells (iPS cells) and monocytes [145].

3.4. Dendrimers

Dendrimers are highly branched polymeric macromolecules with well-defined uniform sizes and shapes, and adaptable surface functionalities. Their basic structure encompasses a central core, repetitive branching units, and terminal groups [146]. Modified dendrimers, derived from polyamidoamine (PAMAM) have been extensively studied for nucleic acid delivery due to their hydrophilic, biocompatible and non-immunogenic properties. Chahal et al. [147] developed a rapid-response and adjuvant-free vaccine based on a PAMAM dendrimer formulated in nanoparticles, wherein the antigens were encoded by encapsulated mRNA replicons. Intramuscular injection to mice of a single dose generated protective immunity against lethal Ebola, H1N1 influenza, and Toxoplasma gondii challenges. In a later study, this dendrimer-based nanoparticle was used to create a vaccine candidate that elicited Zika virus E protein-specific IgG responses. After immunization to mice, the authors identified a unique H-2Db-restricted epitope to which there was a CD8+ T cell response [148].

3.5. Gold nanoparticles

Gold nanoparticles (AuNPs) present features that make them an appropriate platform for nucleic acid delivery. AuNPs can be fabricated in a scalable fashion with low size dispersity, and they are easily functionalized by the formation of multifunctional monolayers and the inclusion of different moieties and targeting agents. Moreover, the in vivo toxicity and biodistribution, can be regulated by optimizing the particle size and surface functionality [149]. Yeom et al. [150] injected into mice xenograft tumours an IVT mRNA encoding Bcl-2-associated X (BAX) protein, a pro-apoptotic factor, loaded on AuNP-DNA conjugates. The mRNA released produced BAX protein, and tumour growth was inhibited.

3.6. Hybrid systems

Hybrid systems are made up of the combination of various types of materials, including lipids, polymers and peptides, among others. Thereby, the hybrid system takes advantage of all the benefits of its individual components, offering greater functionality and flexibility [14,78].

The combination of cationic lipids and peptides has been commonly studied for mRNA delivery. As an example, complexes formed by IVT mRNA, coding for the model antigen beta-

galactosidase, condensed with protamine and encapsulated in liposomes provided in vivo protein expression, activation of cytotoxic T lymphocytes and production of IgG antibodies against the antigen [151]. In another study, the administration of lipid/protamine/IVT mRNA to mice bearing human lung NCI-H460 carcinoma, demonstrated better results in both efficacy and toxicity than the equivalent formulation with pDNA [152]. Lipofectamine with CRPPR-R9, a peptide containing nine arginine residues, efficiently transfected cultured mouse cardiac fibroblasts [153]. Cationic lipids have also been combined with inorganic nanoparticles. The transfection efficacy of mRNA-DOTAP, mRNA-apatite and mRNA-DOTAP-apatite was evaluated using an mRNA encoding the luciferase enzyme, being the complex formed by mRNA-DOTAP-apatite the most effective [154].

Lipopolyplexes, the complexation of nucleic acids with cationic polymers and lipids, were among the first hybrids used for DNA and siRNA delivery, and after that for mRNA. Histidylated lipopolyplexes, synthesized by the combination of PEGylated derivative of histidylated polylysine and L-histidine-(N,N-di-n-hexadecylamine)ethylamide liposomes, incorporating a synthetic melanoma-associated antigen MART1 mRNA have been administered to mice as a mRNA cancer vaccine. The histidylated lipopolyplexes protected significantly injected mice against B16F10 melanoma tumour progression [155]. The subsequent mannosylation of the system targeted the mRNA into the DCs by the mannose receptor [156]. mRNA nanocomplexes formed with the polymer PLGA (poly(lactic-co-glycolic acid)), the cationic lipid-like compound (G0-C14) and a lipid-PEG were used to enhance the protein expression of the tumour-suppressor gene PTEN (phosphatase and tensin homolog deleted on chromosome ten). This hybrid system provided a high IVT mRNA PTEN transfection in prostate cancer cells, and led to significant inhibition of tumour growth when delivered systemically in multiple mouse models of prostate cancer [157] A hybrid polymer-lipid nanoformulation for systemic delivery to the lung was prepared by co-formulation of PBAEs with lipid-PEG. This degradable polymer–lipid nanoparticle showed both enhanced serum stability and increased in vitro potency, delivering IVT mRNA in the lungs after intravenous administration in mice [125].

A nanomicelle-based platform was prepared by mixing IVT mRNA encoding an anti-angiogenic protein (sFlt-1), with PEG-polycation block copolymers. PAsp(TEP) was selected as the cationic segment of the block copolymer and a cholesterol (Chol) moiety was attached by hydrophobic interaction. PEG-PAsp(TEP)-Chol nanosystems produced efficient protein expression in tumour tissue, and remarkable inhibition of the tumour growth [158].

Another example of multi-component delivery system is that formed with poly(glycoamidoamine) (PGAAs) brush nanoparticles. It has been used for intravenous administration of mRNA-encoding erythropoietin (EPO) in mice [159]. First, three different PGAA polymers based on tartarate, galactarate, or glucarate sugars combined with three different amine-containing monomers were prepared. Polymer-brush materials were synthetized through ring opening reactions between PGAAs and epoxides, and incorporated into LNPs. Cholesterol, DSPC and mPEG2000-DMG (1,2-dimyristoyl-sn-glycero-3-phosphoethanolamine-N-[methoxy-(polyethylene glycol)-2000]) were added via a microfluidic based mixing device to form the LNP Polymer-brush nanoparticles.

Recently, DCs have been transfected with a mRNA delivery system combining both PLA based micelles and the cationic CPP RALA. This hybrid nanoplatform offers the possibility of further multifunctionality through PLA core encapsulation [160].

4. Therapeutic Applications of mRNA

The growing knowledge of IVT mRNA design and manufacture, along with the advances in nanotechnology have conducted to broaden the potential therapeutic applications of mRNA-based medicines. According to preclinical and clinical trials, four major IVT mRNA applications can be considered: immunotherapy (including infectious diseases and cancer therapy), protein replacement, gene editing and regenerative medicine. Currently, all the clinical trials ongoing, both applying in vitro and in vivo strategies, are still in Phase I or II, with most of them focusing on immunotherapy, and especially on cancer therapy.

4.1. Immunotherapy

The induction of an immune response by using mRNA has been the main application among mRNA-based therapies, with a number of mRNA vaccines being evaluated in clinical trials against infectious diseases and multiple types of cancer. Apart from these applications, a proof of concept for prevention of type 1 diabetes in mice, by administering modified T cells redirected against diabetogenic CD8 T cells, has emerged as a new mRNA-immunotherapy application [161].

Besides the general advantages of mRNA, previously mentioned, this active substance shows specific interesting features for immunotherapy: the immunostimulatory capacity, although it can have also potential toxicity, the transient nature of the antigen and the versatility of applications, including prophylaxis, therapy and personalized vaccines [162,163]. Several preclinical studies of mRNA vaccines are showing promising perspectives. However, preclinical and human immunogenicity is often not consistent, animal studies are not predictive of human

efficacy, and there is a lack of knowledge about the targets and type of immune responses which are essential for an effective therapy. These challenges highlight the need to carry out further studies on the correlation between the immune response mechanisms in animals and in humans, as well as of a better understanding of the diseases to be treated or prevented, for the clinical success of immunotherapy [14,163].

4.1.1. mRNA vaccines against infectious diseases

mRNA vaccines are emerging as potential substitutes of conventional vaccines due to their advantages comparing with subunit, killed, live attenuated and inactivated pathogens containing vaccines, and with DNA-based vaccines [162]. Two kind of mRNA-based vaccines, SAM and non-replicating vaccines, have been developed against infectious diseases. Figure 4 shows a representative scheme of the intracellular disposition of these two types of vaccines; in both cases the translation machinery of the cell is used to produce the specific antigen [13].

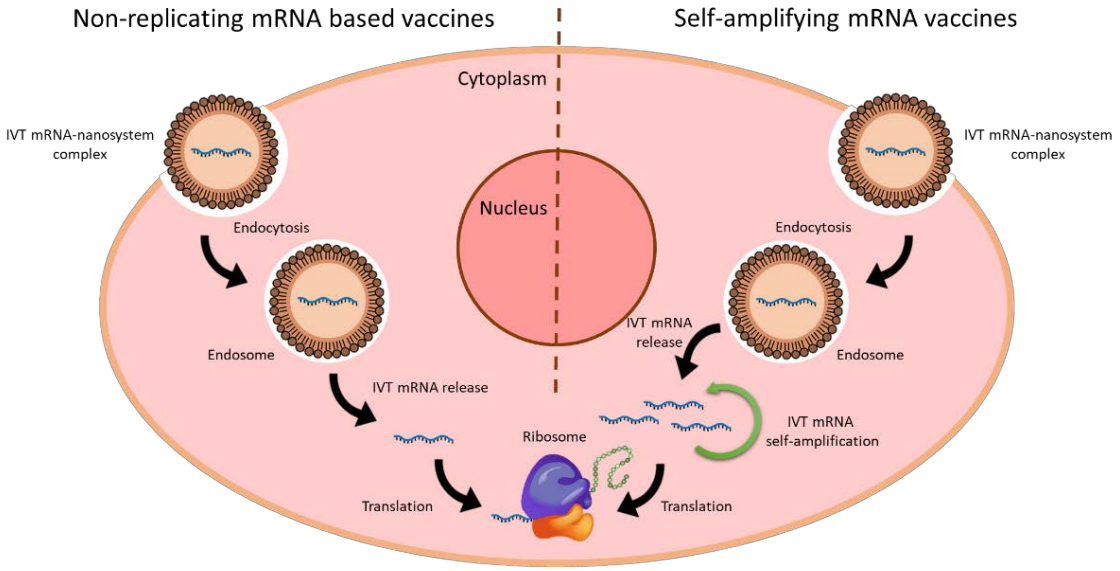

Figure 4. : Representative scheme of the difference between non-replicating mRNA-based vaccines and self-amplifying mRNA vaccines.

SAM vaccines, called replicon, contain a positive single-stranded RNA virus genome, especially from alphaviruses, where the genes encoding the replicative viral machinery are not modified, but structural genes are replaced by the sequence that encodes the antigen. Therefore, SAM vaccine IVT mRNA, contains two different ORFs, one encoding proteins for RNA capping and replication, and other encoding the target antigen. SAM vaccines show an increased efficacy thanks to the capacity of the replicon to self-replicate and amplify inside the cell, enabling a significantly higher antigen production for a given mRNA vector [14,163]. Another advantage is the capacity to encode different antigens in their sequence. This feature allows the

implementation of different therapeutic strategies such as a vaccine encoding both the antigen of interest and an immunomodulatory molecule to enhance the efficacy, a vaccine with both antigens of T and B cells to attack wide variety of pathogens, or a vaccine against multi-subunit complex antigens [164]. However, among the limitations of replicons are their large size (~10kb) and the inability to withstand many modifications of synthetic nucleotides and alterations of the sequences [13].

The first report of SAM vaccine was in 1994, and it was demonstrated that the IVT mRNA derived from the alphavirus Semliki Forest virus (SFV) activated the immune system against a heterologous antigen [165]. In later works it was reported that a single low dose of naked SFV-derived IVT-mRNA encoding respiratory syncytial virus fusion (RSV-F) protein, influenza virus hemagglutinin (HA), or louping ill virus prME produced antibody response and partial protection from lethal viral challenges in mice [166]. The development of LNP have played an important role in the improvement of the efficiency of the SAM vaccines. The administration of very low doses of LNP complexed with the RSV-F RNA replicon vaccine triggered a potent lymphocyte T and B responses in mice, and elicited a protective response against RSV in a cotton mice [167].

As can be seen in Table 1, the use of SAM vaccines are under clinical evaluation for cytomegalovirus (CMV), influenza and HIV-1 infectious diseases. AVX601, a bivalent alphavirus replicon vaccine (alphavaccine) expressing three CMV proteins (gB, pp65 and IE1) was a candidate vaccine against CMV evaluated in healthy volunteers in 2007 (NCT00439803). The vaccine was well tolerated and induced neutralizing antibody and multifunctional T cell responses against the three CMV antigens [168]. The safety and immunogenicity of another alpha vaccine (AVX502), expressing an influenza HA protein was evaluated in healthy volunteers of 18-40 years of age (NCT00440362) or 65 years of age or older (NCT00706732), respectively. The vaccine was safe and well tolerated in both trials, and, especially in the younger group, antibody and T cell responses were efficiently stimulated and persisted for the four-month study [169]. Finally, an alphavirus replicon vaccine (AVX101), in which the alphavirus structural proteins were replaced with HIV-1 subtype C gag, was administered subcutaneously in healthy HIV-1-uninfected adults for safety and immunogenicity evaluation (NCT00097838 and NCT00063778). Only low levels of binding antibodies and T-cell responses were observed at the highest doses [170].

Table 1. Clinical Trials of mRNA vaccines against infectious diseases

Infectious disease	Biological active / Encoding sequence	Strategy / Delivery system	Administration route	NCT Number / Phase
Rabies	CV7201 mRNA / Rabies virus glycoprotein (RABV-G)	*In vivo* / Polypeptide system	i.d. or i.m.	NCT02241135 / Phase I
	CV7202 mRNA / Rabies virus glycoprotein (RABV-G)	*In vivo* / Lipid nanosystem	i.m.	NCT03713086 / Phase I
Zika Virus	mRNA-1893 / Structural proteins of Zika virus	*In vivo* / Lipid nanosystem		NCT04064905 / Phase I
	mRNA-1325 / Zika virus antigen	*In vivo* / Lipid nanosystem	i.d.	NCT03014089 / Phase I
Cytomegalovirus (CMV)	mRNA-1647 and mRNA-1443 / Pentamer complex and full-length membrane-bound glycoprotein B (gB) and pp65 T-cell antigen of CMV	*In vivo* / Lipid nanosystem	i.d.	NCT03382405 / Phase I
	AVX601 / Alphavirus Replicon Vaccine Expressing gB, pp65 and IE1 proteins of CMV	*In vivo* / Viral vector	i.m. or s.c.	NCT00439803 / Phase I
hMPV and PIV3	mRNA-1653: fusion proteins of hMPV and PIV3	*In vivo* / Lipid nanosystems	i.d.	NCT03392389 / Phase I
Tuberculosis	GSK 692342 / Immunogenic fusion protein (M72) derived from Mycobacterium tuberculosis	*In vivo* / Lipid nanosytems	i.m.	NCT01669096 / Phase II
HIV-1	HIV-1 Gag and Nef	*Ex vivo* / mRNA transfected autologous DCs	i.d.	NCT00833781 / Phase I
	iHIVARNA: TriMix and HTI / APC activation molecules (CD40L+CD70+caTLR4) and HIV immunogen sequences (Gag, Pol, Vif and Nef)	*In vivo* / Naked mRNA	Inguinal intranodal	NCT02413645 and NCT02888756/ Phase I and Phase II

Table 1. Cont.

Infectious disease	Biological active / Encoding sequence	Strategy / Delivery system	Administration route	NCT Number / Phase
HIV-1	AVX101 / Alphavirus replicon vaccine expressing HIV Gag antigen	*In vivo* / Viral vector	s.c.	NCT00097838 and NCT00063778 / Phase I
Influenza	VAL-506440 / H10N8 antigen	*In vivo* / Lipid nanosystems	i.d. or i.m.	NCT03076385 / Phase I
	VAL-339851 / H7N9 antigen	*In vivo* / Lipid nanosystems	i.d. or i.m.	NCT03345043 / Phase I
	AVX502 / Alphavirus Replicon Vaccine Expressing Influenza A/Wyoming/03/2003 Hemagglutinin	*In vivo* / Viral vector	i.m. or s.c.	NCT00440362 and NCT00706732 / Phase I/II

DCs: Dendritic cells; i.d.:intradermal; i.m.:intramuscular; s.c.:subcutaneous; i.v.: intravenous; hMPV: Human metapneumovirus; PIV3: human parainfluenza virus type 3; HIV-1: Human immunodeficiency virus type 1.

Non-replicating mRNA-based vaccines are engineered to resemble fully processed mature mRNA, and are formed by an IVT mRNA containing an ORF encoding the antigen of interest. The clinical trials currently ongoing for infectious diseases with non-replicating mRNA include prophylactic vaccines directed to rabies, Zika virus, CMV, human metapneumovirus, human parainfluenza, tuberculosis and influenza viruses (Table 1). All of them use an in vivo strategy by direct intradermal, intramuscular or subcutaneous injection of vaccines, with lipid nanosystems as the most used delivery system.

The first study of immunization by non-replicating mRNA vaccines against infectious diseases was reported in 2012 by Petsch et al. [141]. Synthetized mRNA encoding different influenza virus antigens based on CureVac's RNActive® platform were administered intradermally to mice, ferret and pigs. Later on, IVT mRNA encoding an optimized non-replicating rabies virus glycoprotein (RABV-G), also formulated as RNActive® vaccine, was administered intradermally in mice and pigs [171]. In mice the vaccine provided protection against lethal intracerebral challenge infection, whereas in pigs neutral antibodies were detected. The first clinical trial of this prophylactic mRNA-based vaccine (CV7201) in healthy adults demonstrated a reasonable tolerability profile (NCT02241135). The participants received three doses of CV7201 intradermally or intramuscularly by needle-syringe or needle-free devices. Vaccine induced boostable functional antibodies against a viral antigen only when administered with a needle-

free device [171]. Based on positive results from preclinical studies in both mice and nonhuman primates [136], a new intramuscular RABV-G mRNA vaccine encapsulated in LNPs (CV7202) is being tested in clinical studies (NCT03713086).

Immunization against Zika virus by mRNA vaccination has also reached clinical evaluation, after successful preclinical results [104,173]. The safety, tolerability, and immunogenicity of two Zika vaccines containing mRNA encoding for viral antigenic proteins formulated with LNP are under clinical evaluation in healthy adults (NCT03014089, NCT04064905).

The immunogenicity of vaccines based on LNP-complexed mRNA against influenza virus was also reported in mice, ferrets, and non-human primates [174]. Subsequently, the results from two clinical trials (NCT03076385, NCT03345043) have shown that the mRNA vaccines against H10N8 and H7N9 influenza viruses, formulated as LPNs, were well tolerated and elicited robust humoral immune responses in healthy adults [175].

Two clinical trials (NCT02413645, NCT02888756) evaluated mRNA vaccines as an immunotherapeutic vaccine for HIV infection. In one of them [176] naked mRNA (iHIVARNA) was administered intranodally to redirect T-cell immunity in HIV-infected individuals to the most vulnerable viral targets. iHIVARNA combines a mRNA-encoding a novel HIV immunogen sequence (HTI) with TriMix [177], composed by three naked mRNA encoding the DC activation signals CD40L (activation stimuli CD40 ligand), CD70 (costimulatory molecule CD70) and caTLR4 (constitutively active Toll-like receptor 4). iHIVARNA administration was safe, well tolerated and induced moderate HIV-specific T-cell responses; however, the phase II study (NCT02888756) was terminated due to lack of immunogenicity.

Ex vivo strategy for vaccination is based on the use of DCs loaded with mRNA. DCs internalize and process antigens and present them to CD8+ and CD4+T cells on major histocompatibility complexes (MHCs) class I and II, respectively [162]. DCs are able to internalize naked mRNA by different endocytic ways, although electroporation improves the efficacy. A large number of clinical trials evaluate the use of ex vivo mRNA transfected DCs for cancer, due to the cell-mediated immune response. However, in the case of infectious diseases this strategy has only been used for HIV immunotherapy (NCT00833781). In this case, intradermal immunization with autologous DCs electroporated with an mRNA encoding HIV-1 Gag and Nef antigens, did not induce significant responses [178].

4.1.2. Cancer immunotherapy

Cancer immunotherapy relies on the generation of a host antitumour immune response, playing a key role cytotoxic T cells due to their capacity to recognize and kill tumour cells. The induction

of a specific immune response by mRNA vaccines begins when the antigen is expressed into the cytosol of APC cells (DC or macrophages). The resulting proteins are processed by proteasomes and presented on MHC class I molecules to CD8+T cells, activating cellular response [178]. Complementary, CD4+T helper cell responses can be triggered by fusion to the encoded antigen of different trafficking signals of lysosomal proteins residing in MHC class II processing compartments [180–182]. Cancer mRNA vaccines present important advantages. On the one band, the possibility of obtaining RNA from a tumour sample to amplify it, yielding large amounts of patient specific antigens. On the other hand, the capacity of mRNA to act as an adjuvant by providing costimulatory signals, for instance via TLR3, TLR7 and TLR8 [183].

At present, there is a great number of clinical trials using in vivo or ex vivo mRNA based immunotherapy in various cancer types (Table 2). Although they are in early stages, encouraging clinical outcomes are expected. The in vivo strategy is based on the direct administration of mRNA, naked or complexed in nanosystems, by different routes, whereas ex vivo approach is implemented by the administration of IVT mRNA modified DCs or chimeric antigen receptor (CAR) T cells.

Table 2. Clinical trials of mRNA for Cancer Immunotherapy

Type of cancer	Biological active / Encoding sequence	Strategy / Delivery system	Administration route	NCT Number / Phase
Non-small-cell lung carcinoma (NSCLC)	CV9201 / five mRNAs encoding antigens which are overexpressed or exclusively expressed in NSCLC cells	*In vivo* / Polypeptide system	i.d.	NCT00923312 / Phase I/II
	CV9202 / six mRNAs encoding antigens which are overexpressed in NSCLC compared to healthy tissue	*In vivo* / Polypeptide system	i.d.	NCT01915524 / Phase I
Metastatic NSCLC	BI 1361849 / NSCLC-associated antigens (NY-ESO-1, MAGE-C1, MAGE-C2, survivin, 5T4, and MUC-1)	*In vivo* / Polypeptide system	i.d.	NCT03164772 / Phase I and II
Esophageal Cancer and NSCLC	Personalized mRNA Tumour Vaccine / Neoantigen (tumour associated specific antigens)	*In vivo* / -	s.c.	NCT03908671 / NotA
Malignant Melanoma	mRNA coding for melanoma associated antigens	*In vivo* / Naked mRNA	s.c.	NCT00204516 / Phase I/II
Malignant Melanoma	mRNA coding melanoma associated antigens (Melan-A, Mage-A1, Mage-A3, Survivin, GP100 and Tyrosinase)	*In vivo* / Polypeptide system	i.d.	NCT00204607 / Phase I/II
	mRNA coding the unique spectrum of tumour antigens in each patient	*Ex vivo* / mRNA transfected DCs	i.d. or intranodal	NCT01278940 / Phase I/II
Malignant Melanoma III and IV	TriMix-DC encoding melamona tumour-associated antigens (MAGE-A3, MAGE-C2, tyrosinase and gp100)	*Ex vivo* / autologous TriMix-DC	i.v.	NCT01302496 / Phase II
Melanoma	mRNA-4157 / personalized cancer vaccine targeting twenty tumour-associated antigens	*In vivo* / Lipid nanosystems	i.d.	NCT03897881 / Phase II
	(RBL001; RBL002) / malignant melanoma associated antigens	*In vivo* / Naked mRNA	intranodal	NCT01684241 / Phase I

Table 2. Cont.

Type of cancer	Biological active / Encoding sequence	Strategy / Delivery system	Administration route	NCT Number / Phase
Melanoma	IVAC MUTANOME / poly-neo-epitopic personalized cancer vaccine targeting tumour-associated antigens (with or without initial treatment with RBL001/RBL002)	*In vivo* / Naked mRNA	intranodal	NCT02035956 / Phase I
	RBL001.1; RBL002.2; RBL003.1; RBL004.1 / malignant melanoma-associated antigens	*In vivo* / Lipid nanosystems	i.v.	NCT02410733 / Phase I
	mRNA encoding TriMix	*Ex vivo* / mRNA-transfected autologous DCs	i.d. and i.v.	NCT01066390 / Phase I
	mRNA encoding melanoma-associated tumour antigens (gp100 and tyrosinase) and TriMix	*Ex vivo* / mRNA-transfected autologous DCs	intranodal	NCT01530698 / Phase I/II
Melanoma Stage III or IV	mRNA encoding melanoma associated antigens (gp100 and tyrosinase)	*Ex vivo* / mRNA-transfected DCs	i.v., i.d., intranodal	NCT00243529 / Phase I/II
Metastatic Malignant Melanoma	hTERT-, survivin- and tumour cell derived mRNA + ex vivo T cell expansion	*Ex vivo* / mRNA-transfected DCs	i.d. and i.v.	NCT00961844 / Phase I/II
Uveal Melanoma	mRNA coding tumour associated antigens	*Ex vivo* / mRNA-transfected DCs	i.d. / i.v.	NCT00929019 / Phase I/II
Acute Myeloid Leukemia (AML)	mRNA coding for the Wilms' tumour protein (WT1)	*Ex vivo* / mRNA transfected autologous DCs	i.d.	NCT00834002 / Phase I
	AML-specific mRNA	*Ex vivo* / mRNA transfected autologous DCs	i.d.	NCT00514189 / Phase I
	mRNA encoding WT1, PRAME, and CMVpp65	*Ex vivo* / mRNA transfected autologous DCs	i.d.	NCT01734304 / Phase I/ II

Table 2. Cont.

Type of cancer	Biological active / Encoding sequence	Strategy / Delivery system	Administration route	NCT Number / Phase
Relapsed or Refractory AML	Autologous Anti-CD 123 CAR TCR/4-1BB-expressing T-lymphocytes / anti-CD123 chimeric antigen receptors expressing tandem TCR and 4-1BB (TCR /4-1BB) costimulatory domains	*Ex vivo* / mRNA transfected autologous CAR T cells	iv	NCT02623582 / Early Phase I
Multiple Myeloma	mRNA encoding CT7, MAGE-A3, and WT1	*Ex vivo* / mRNA-transfected autologous Langerhans-type DCs	i.d.	NCT01995708 / Phase I
Prostate Cancer	CV9104 / mRNAs encoding PSA, PSCA, PSMA, STEAP1, PAP and Mucin 1 antigens	*In vivo* / Polypeptide system	i.d.	NCT01817738 and NCT02140138 / Phase I/II and Phase II
	mRNA coding tumour associated antigens	*Ex vivo* / mRNA-transfected DCs	i.d.	NCT01278914 / Phase I/II
	mRNA extracted from Primary Prostate Cancer Tissue, combined with mRNA encoding hTERT and Survivin	*Ex vivo* / mRNA-transfected DCs	i.d.	NCT01197625 / Phase I/II
Metastatic Prostate Cancer	mRNA derived from the patient's own tumour	*Ex vivo* / mRNA-transfected autologous DCs	i.d.	NCT01153113 / Phase I/II (withdrawn)
Hormonal Refractory Prostate Cancer	CV9103 / mRNAs encoding PSA, PSCA, PSMA and STEAP1 antigens	*In vivo* / Polypeptide system	i.d.	NCT00831467 (eudract 2008-003967-37) and NCT00906243 / Phase I/II

Table 2. Cont.

Type of cancer	Biological active / Encoding sequence	Strategy / Delivery system	Administration route	NCT Number / Phase
Glioblastoma	mRNA encoding survivin, hTERT or autologous tumour stem cells derived from tumorspheres	*Ex vivo* / mRNA-transfected autologous DCs	id	NCT03548571 / Phase II/III
Ovarian Cancer	W_ova1 vaccine: 3 ovarian cancer tumour associated antigens mRNAs	*In vivo* / Lipid nanosystems	i.v.	NCT04163094 / Phase I
Recurrent Epithelial Ovarian Cancer	mRNA encoding hTERT and survivin in addition to amplified cancer stem cell mRNA	*Ex vivo* / mRNA-transfected DCs	i.d.	NCT01334047 / Phase I/II
Breast Cancer	cMet RNA CAR T cells	*Ex vivo* / mRNA transfected autologous CAR T cells	intratumoral	NCT01837602 / Phase I
Early Breast Cancer	mRNA encoding TriMix	*In vivo* / naked mRNA	intratumoral	NCT03788083 / Phase I
Triple-negative breast cancer	IVAC_WAREHOUSE_bre1_uID; IVAC MUTANOME _uID / personalized cancer vaccine targeting tumour-associated antigens	*In vivo* / Lipid nanosystems	i.v.	NCT02316457 / Phase I
Solid tumours	mRNA-4157 / personalized cancer vaccine targeting twenty tumour-associated antigens	*In vivo* / Lipid nanosystem	i.m.	NCT03313778 / Phase I
Hodgkin Lymphoma	RNA anti-CD19 CAR T cells / CD19 chimeric antigen receptors expressing tandem TCR /4-1BB costimulatory domains	*Ex vivo* / mRNA transfected autologous CAR T cells	i.v.	NCT02277522 and NCT02624258 / Early Phase I
Metastatic Pancreatic Ductal Adenocarcinoma	RNA mesothelin re-directed autologous T cell / chimeric anti-mesothelin immunoreceptor SS1	*Ex vivo* / mRNA transfected autologous CAR T cells	i.v.	NCT01897415 / Phase I

Table 2. Cont.

Type of cancer	Biological active / Encoding sequence	Strategy / Delivery system	Administration route	NCT Number / Phase
Malignant Pleural Mesothelioma	Autologous anti-mesothelin CAR T cells/ chimeric anti-mesothelin immunoreceptor	*Ex vivo* / mRNA transfected autologous CAR T cells	i.v.	NCT01355965 / Phase I
Malignant Melanoma, Breast Cancer	RNA CART-cMET / MET chimeric antigen receptors with tandem TCRζ and 4-1BB (TCRζ /4-1BB) co-stimulatory domains	*Ex vivo* / mRNA transfected autologous CAR T cells	i.v.	NCT03060356 / Early Phase I
Brain Cancer, Neoplasm Metastases	Personalized cellular vaccine / tumour associated antigen mRNA	*Ex vivo* / mRNA transfected autologous DCs	NA	NCT02808416 / Phase I
Advanced Esophageal Squamous Carcinoma, Gastric Adenocarcinoma, Pancreatic Adenocarcinoma, Colorectal Adenocarcinoma	Personalized mRNA Tumour Vaccine / Neoantigen (tumour associated specific antigens)	*In vivo* / -	s.c.	NCT03468244 / NotA
Melanoma, Colon cancer, Gastrointestinal cancer, Genitourinary cancer, hepatocellular cancer	NCI-4650 / mRNA-based, Personalized Cancer Vaccine	*In vivo* / Lipid nanosystems	i.m.	NCT03480152 / Phase I/II
Melanoma, NSCLC, Bladder Cancer, Colorectal Cancer, Triple Negative Breast Cancer, Renal Cancer, Head and Neck Cancer, Other Solid Cancers	RO7198457 / personalized cancer vaccine targeting tumour-associated antigens	*In vivo* / Lipid nanosystem	i.v.	NCT03289962 / Phase I

Table 2. Cont.

Type of cancer	Biological active / Encoding sequence	Strategy / Delivery system	Administration route	NCT Number / Phase
Relapsed/Refractory Solid Tumour Malignancies or Lymphoma, Ovarian Cancer	mRNA-2416 / OX40L	*In vivo* / Lipid nanosystems	Intratumoral	NCT03323398 / Phase I and II
Squamous Cell Carcinoma, Head and Neck Neoplasm, Cervical Neoplasm, Penile Neoplasms Malignant	human papillomavirus (HPV16) mRNA vaccine/ HPV16-derived E6, E7 tumour antigens	*In vivo* / Naked mRNA	i.d.	NCT03418480 / Phase I and II
Advanced or Metastatic Malignancies Expressing CEA (Colorectal Cancer, Breast Cancer, Lung Cancer, Pancreatic Cancer) or Stage III Colon Cancer	AVX701 / Alphaviral Replicon Particle Vaccine Expressing Carcinoembryonic Antigen Gene (CEA(6D)).	*In vivo* / Viral vector	i.m.	NCT00529984, NCT01890213 / Phase I and II, Phase I
Glioblastoma, Renal Cell Carcinoma, Sarcomas, Breast Cancers, Malignant Mesothelioma, Colorectal Tumour	mRNA encoding WT1	*Ex vivo* / mRNA-transfected autologous DCs	i.d.	NCT01291420 / Phase I/II

NA: not available; NotA: Not applicable; DCs: Dendritic cells; i.d.:intradermal; s.c.:subcutaneous; i.v.: intravenous; i.m.:intramuscular

Regardless of the strategy, mRNA vaccines can be designed to target a wide variety of antigens, including TAAs, cancer testis antigens (CTAs) and tumour-specific antigens (TSAs); all of them have been tested in clinical trials. TAAs derive from proteins that are overexpressed in cancer cells but they also occur in normal cells. CTAs are a group of TAAs that might serve as ideal targets for cancer immunotherapy because of their cancer-restricted expression and robust immunogenicity. TSAs derive from viral oncogenic proteins or from proteins produced due to somatic mutations or gene rearrangements; tumours in general acquire mutations during carcinogenesis and progression, resulting in altered proteins that may serve as neoantigens [184]. Potential neoantigen targets, which allow the design of personalized neoepitope cancer vaccines, can be identified after analysis of the entirety somatic cancer mutations in an individual tumour, called mutanome, by means of whole exome and/or next generation RNA sequencing [185].

Apart from the use of IVT mRNA to produce a specific immune response, non-coding mRNA (CV8102) has been also tested clinically as an adjuvant. CV8102 is a TLR7/8/RIG-1 agonist based on noncoding single stranded RNA, designed to modulate the tumour microenvironment after intratumoral injection. It is being evaluated alone (NCT03291002) or in combination with IMA970A, which is a new cancer vaccine for primary liver cancer based on an off-the-shelf cocktail of 16 peptides (NCT03203005).

The first mRNA cancer vaccine was developed by Conry et al. in 1995 [186]. It consisted in intramuscular injection of mRNA coding for carcinoembryonic antigen (CEA) to mice. This study showed the ability of naked mRNA to induce antitumour adaptive immune responses. However, the rapid degradation of mRNA results in low clinical efficiency. Therefore, for in vivo administration, clinical trials usually utilize mRNA formulated in delivery nanosystems. Among them, lipids are the most used followed by polypeptides, and viral vectors have been applied only in one clinical trial. In this sense, in most of the clinical trials that aim to address cancer with personalized vaccines the mRNA encoding antigens are formulated in lipid nanosystems, (NCT03897881, NCT02316457, NCT03313778, NCT03480152, NCT03289962), although naked mRNA has also been evaluated (NCT01684241, NCT02035956).

Besides the delivery system, the administration route also has a significant influence on mRNA vaccine efficacy. Multiple administration approaches have been evaluated in clinical trials to target mRNA to APC cells, from conventional vaccination routes such as intradermal, intramuscular and subcutaneous, to less common methods such as intranodal, intravenous or intratumoral. Except for CAR T Cells, intradermal route is the most widely used in both, in vivo

and ex vivo approaches. Regarding in vivo delivery, CV9201 and CV9202 (NCT00923312 and NCT01915524), based on CureVac's RNActive® technology, have been applied intradermically for the treatment of non-small cell lung carcinoma (NSCLC). CV9202, containing a sequence-optimized mRNA encoding six NSCLC-associated antigens (NY-ESO-1, MAGE-C1, MAGE-C2, survivin, 5T4, and MUC-1), was well tolerated and antigen-specific immune responses were detected [187]. Different types of prostate cancers have been addressed by intradermal administration of RNActive® vaccines (NCT01817738, NCT02140138, NCT00831467). In addition, intradermal route has been selected for in vivo strategies against metastatic NSCLC (NCT03164772), malignant melanoma (NCT00204607, NCT03897881), multiple myeloma (NCT01995708), and squamous cell carcinomas (NCT03418480).

Ex vivo therapy with transfected DCs, the most potent APC of the inmune system, is the most frequent strategy used for mRNA cancer vaccination. This method allows precise control of the cellular target and transfection efficiency, although is expensive and laborious. Electroporated DCs with mRNA demonstrated already in 1996 their capacity to induce immune response against tumour antigens [188]. Ex vivo strategies generally use intradermal and intravenous routes for DCs and CAR T cells administration, respectively. In 2006, the results of a clinical trial (NCT01278940) that evaluated the intradermal vs intranodal administration of an individualized melanoma vaccine based on mRNA transfected autologous DCs were published. The vaccine elicited in vivo T-cell responses against expressed tumour antigens, although the response rates did not suggest an advantage in applying intranodal vaccination [189]. TriMixDC-MEL are autologous DCs electroporated with synthetic mRNA TriMix together with mRNA encoding fusion proteins of a human leukocyte antigen (HLA)-class II targeting signal (DC-LAMP), and a melanoma-associated antigen (either MAGE-A3, MAGE-C2, tyrosinase or gp100). Combined intradermal and intravenous administration to patients in stage III or IV melanoma of TriMixDC-MEL resulted safe, immunogenic and showed antitumour activity [190] (NCT01066390). In a later study, patients in stage III or IV melanoma were treated with TriMixDC-MEL and the monoclonal antibody Ipilimumab (NCT01302496). This combination was well tolerated and showed a durable tumour reduction in patients with recurrent or refractory melanoma [191]. Apart from melanoma, ex vivo IVT mRNA DCs have been used for other cancers including acute myeloid leukemia (AML), multiple myeloma, prostate cancer, glioblastoma and ovarian cancer, among others (Table 2).

Adoptive T cell therapy by ex vivo IVT-mRNA based CAR T-cell administration has focused great interest thanks to the market of two viral transduced CAR-T products in 2017. Tisagenlecleucel and Axicabtagene ciloleucel were approved for the treatment of acute B-cell lymphoblastic

leukaemia and large B-cell lymphoma, respectively [192]. Ravinovich et al. [193] transfected for the first time T cells with IVT mRNA encoding CARs against CD19. Transient expression of T cells transduced by IVT mRNA offers safety features and highly efficient recombinant protein translation, but also resulted in a need of frequent injection of the CAR T cells [194]. Currently, several clinical trials with IVT mRNA CAR T cells for cancer treatment are ongoing. CAR-encoding IVT mRNA targeting the TAA mesothelin was applied against malignant mesothelioma (NCT01355965). However, due to the transient nature of CAR expression on the T cells, repeated infusions were needed, and after the third infusion, one subject developed anaphylaxis and cardiac arrest infusion. These results pointed out a safety issue owing to the potential immunogenicity of CARs derived from murine antibodies, especially when administering intermittently [195]. Application of CD19 CAR T cells targeting the inflammatory tumour microenvironment in Hodgkin's lymphoma (NCT02277522 and NCT02624258), showed transient responses [196]. Treatment of acute myeloid leukemia is being attempted by intravenous administration of CD123 CAR T cells. These cells consist of mRNA electroporated autologous T cells expressing anti-CD123 CAR linked to TCR and 4-1BB (TCR /4-1BB) costimulatory signaling domains (NCT02623582). These costimulatory domains are also included in autologous cMet RNA CAR T cells, which has been administered intratumorally in patients with breast cancer, showing good toelrability and evoking an inflammatory response within tumours [197] (NCT01837602). Currently, intravenous administration of cMet RNA CAR T cells in patients with advanced melanoma or breast carcinoma is under evaluation (NCT03060356).

4.2. Protein replacement

The application of IVT mRNA for protein replacement therapies is based on the supplementation of proteins that are infra-expressed or are not functional, as well as on the expression of foreign proteins that can activate or inhibit cellular pathways. Since the first preclinical evaluation of IVT mRNA for protein replacement in 1992 [198], several proteins have been targeted by IVT mRNA administration. In that first study, temporary reversal of diabetes insipidus was observed after hypothalamus injection of vasopressin mRNA in Brattleboro rats.

Protein replacement therapies based on IVT mRNA have been mainly directed to liver [199], lungs [200] and heart [201] because of the accessibility of these organs. However, other organs and tissues, such as skin [202], back of the eye [203] or nasal cavity [204] have been also evaluated as target sites. The main applications of this therapy are genetic and rare diseases. The therapeutic IVT mRNA encodes a missing or down-expressed protein responsible for the disease and associated to genomic defects. These are, for instance, the cases of: hemophilia B, characterized by coagulation defects due to lack of coagulation factor IX [205], Fabry disease,

associated to a deficit of alpha-galactosidase A [206], methylmalonic acidemia (MMA), caused by methylmalonyl-coenzyme A mutase (MUT) deficiency [207], propionic acidemia (PA), triggered by a deficiency in the mitochondrial enzyme propionyl-CoA carboxylase [208], acute intermittent porphyria (AIP), resultant from insufficiency of porphobilinogen deaminase [209], ornithine transcarbamylase (OTC) deficiency [210], cystic fibrosis [211] provoked by a genetic defect in the cystic fibrosis transmembrane conductance regulator (CFTR), or William-Beuren syndrome (WBS), which is related to microdeletion of approximately 26 to 28 genes on chromosome 7q11.23, including the elastin gene [202]. Nevertheless, IVT mRNA protein replacement is also useful in disease conditions that are not directly associated to a genetic defect. IVT mRNA encoding vascular endothelial growth factor-A (VEGF-A) may lead to the creation of blood vessels and improve blood supply, providing a regenerative treatment option for patients with ischemic cardiovascular disease, as well as for diabetic wound healing and other ischemic vascular diseases [212,213].

As it is observed in Table 3, several studies have demonstrated the translational potential of IVT mRNA protein replacement therapies to clinic. In addition, most of them use lipid nanomaterials as delivery systems, which reinforces the importance of an appropriate vehicle to improve the efficiency.

Moderna, a clinical-stage biotechnology company pioneering mRNA therapeutics, collaborates with AstraZeneca, a biopharmaceutical company, in two clinical trials in which a naked IVT-mRNA encoding VEGF-A (AZD8601) is locally administered in patients undergoing coronary artery bypass grafting surgery with moderately reduced systolic function (NCT03370887) and for the treatment of ulcers in diabetic patients (NCT02935712).

Table 3. Clinical trials of mRNA for protein-replacement therapies

Disease	Biological active / Encoding sequence	Strategy / Delivery system	Administration route	NCT Number / Phase
Heart Failure	AZD8601 / Vascular endothelial growth factor-A (VEGF-A)	Naked mRNA	Epicardial injection	NCT03370887 / Phase II
Ulcers associated to type II diabetes	AZD8601 / Vascular endothelial growth factor-A (VEGF-A)	Naked mRNA	Intradermal	NCT02935712/ Phase I
Propionic Acidemia	mRNA-3927 / alpha and beta subunits of the mitochondrial enzyme propionyl-CoA carboxylase	*In vivo* / Lipid nanosytems	Intravenous	NCT04159103 / Phase I and II

Table 3. Cont.

Disease	Biological active / Encoding sequence	Strategy / Delivery system	Administration route	NCT Number / Phase
Isolated Methylmalonic Acidemia	mRNA-3704 / methylmalonyl-coenzyme A mutase (MUT)	*In vivo* / Lipid nanosytems	Intravenous	NCT03810690 / Phase I and II
Ornithine Transcarbamylase Deficiency	MRT5201 / Ornithine transcarbamylase	*In vivo* / Lipid nanosystems	Intravenous	NCT03767270 / Phase I and II
Cystic Fibrosis	MRT5005 / Human Cystic Fibrosis Transmembrane Regulator protein (CFTR)	*In vivo* / Lipid nanosystems	Nebulization	NCT03375047 / Phase I and II

Moderna has also proprietary LNP formulations used as delivery systems in IVT mRNA clinical trials; specifically, for the treatment of PA and MMA, the most common organic acidemias. PA is an autosomal recessive condition caused by mutations in the PCCA and PCCB genes. These genes encode two subunits of the enzyme propionyl-CoA carboxylase (PPC). Disrupting the function of this enzyme avoids the normal breakdown of proteins and lipids at mitochondrial level. As a result, propionyl-CoA and other toxic compounds accumulates in the body [214]. MMA is also an autosomal recessive disease, which is caused by mutations in the gene coding vitamin B12-dependent enzyme MUT. MUT participates in the intermediary metabolism of proteins lipids and cholesterol inside the mitochondrial matrix and its deterioration is related to the accumulation of toxic metabolites and to the alteration of mitochondrial oxidative phosphorylation [215]. Currently there are no approved therapies to treat the underlying cause of PA or MMA; because of the complexity to reach the mitochondrial localization of PPC and MUT, no enzyme replacement therapy is available. The only effective treatment for severely affected individuals is liver transplant, although it is not a cure because patients remain at risk for disease-related complications [216]. Moderna has recently initiated two clinical trials to evaluate the safety, pharmacokinetics, and pharmacodynamics of different doses of mRNA-3927 (NCT04159103) and mRNA-3704 (NCT03810690) in patients with PA and MMA, respectively. After selection of the dose with satisfactory safety and pharmacodynamic activity, additional patients will be enrolled in a dose expansion phase to allow for further characterization.

Translate Bio, another clinical-stage mRNA therapeutics company, has initiated in the last few years two clinical trials in which synthetic mRNAs, also formulated in LNP, are administered to patients with cystic fibrosis (NCT03375047) or OTC deficiency (NCT03767270). Cystic fibrosis is

a monogenic disorder affecting approximately 1 in 2,000-3,000 newborns in the European Union and 1 in every 3,500 births in United States of America [217]. The disease is caused by genetic variance within the coding region of the CFTR, an anion channel necessary for chloride efflux from secretory epithelial cells. Over time, the resulting ion transport dysregulation induces multisystem organ failure and death [210]. The severity of cystic fibrosis varies greatly from person to person, and it is determined mainly by how much the lungs are affected. Translate Bio has developed a product known as MRT5005, composed of an IVT mRNA encoding CFTR formulated in LNP developed through its proprietary delivery platform. The results from the single-ascending dose phase of the clinical trial (NCT03375047) in 12 adult patients with cystic fibrosis, who received a single nebulization dose of either MRT5005 or placebo (3:1 randomization), show that the drug was generally well tolerated at the low and mid dose levels. Furthermore, in 4/9 of the subjects treated with MRT5005 the percent predicted forced expiratory volume (ppFEV1), a primary measure of lung function, increased [218]. The multiple-ascending dose phase of the clinical trial is ongoing.

OTC deficiency consists of the increment of the ammonia levels in the bloodstream because of disorders in ammonia detoxification and deficiencies of mitochondrial OTC in the urea cycle [219]. Current treatment consists of a protein-restricted diet for life, arginine and citrulline supplementation and currently available ammonia scavengers. However, when there is a critical OTC deficiency in neonatal form or in case of recurrent hyperammonaemia episodes, liver transplantion is the only therapeutic option [220]. Translate Bio initiated a clinical trial (NCT03767270) to evaluate safety, tolerability and pharmacokinetic/pharmacodynamics of intravenous administration of an IVT mRNA encoding OTC-LNP system (MRT5201). However, it was discontinued, because preclinical studies did not support the desired pharmacokinetic and safety profile [221]. The investors relate those preclinical results to the non-optimal features of the first-generation LNP designed to target the liver; currently, the development of novel next-generation LNP is supporting the further progress of liver disease IVT mRNA therapeutics.

4.3. Gene editing

Gene editing has recently emerged as a new therapeutic option for a numerous variety of clinical conditions. This technology uses programmable nucleases, engineered to accomplish a DNA double stranded break (DSB) in a specific target location of the genome. The repair of DSBs can be performed by two mechanisms: homologous-dependent repair (HDR) and non-homologous end joining (NHEJ). In HDR the nucleases act in presence of a donor DNA template that contains a homologous sequence to be introduced into DSB. This repair is useful to correct genomic

mutations or to insert new sequences encoding therapeutic proteins. NHEJ eliminates the target region by binding DSBs; it can be used to silence or correct an anomalous gene [222,223].

There are three main types of gene editing nucleases, composed of a target-sequence-recognizing domain and a nuclease: ZFNs, TALENs and CRISPR/Cas9.

ZFN are engineering by fusing zinc-finger DNA binding domains (Cys2-His2) with FokI nuclease as the DNA cleavage domain [224]. In a similar way, TALEN is obtained by combination of FokI nuclease and the DNA-binding domain derived from transcription activator-like effector (TALE) [CV]. In these two strategies nucleases recognize the target sequences by DNA-protein interaction. The mechanism of action of CRISPR/Cas9 is different; nuclease targeting is mediated through RNA and DNA base pairing. It requires two components: Cas9, a nuclease responsible for the DNA cleavage, and a single guide RNA (sgRNA) that directs Cas9 to cut the DNA at the target sequence [5]. The advantage of CRISPR/Cas9 is that modifying the sequence of sgRNA Cas9 can recognize any sequence of the genome. Additionally, it is possible to edit simultaneously different genes using different sgRNA [225]. However, CRISPR/Cas9 has an important challenge to consider, the complexity of delivering both sgRNA and Cas9.

Gene editing nucleases can be delivered in protein, pDNA or mRNA forms [226]. Delivery in form of mRNA offers great potential for therapeutic application. Compared to pDNA, IVT mRNA reduces the risk of genome insertion, and, since the effect is transient, the presence of the nuclease inside the cells and the risk of off-target adverse effects are limited. Compared to protein delivery, the intracellular presence of the nucleases is more consistent after mRNA expression as compared to the delivery of the nuclease itself [227]. In addition, administration of nucleases in protein form has several limitations for in vivo therapy (cellular and humoral immune response, its charge and large size are challenges for systemic administration, complex protein purification procedures for large nucleases) [226].

IVT mRNA encoding genome-editing nucleases has been mainly used ex vivo to edit T cells or hematopoietic stem and progenitor cells (HSPCs) by electroporation for research and preclinical studies [2287–230], or to generate animal models by genome editing of embryos or zygotes, by microinjection [231–234]. Co-delivery of sgRNA and Cas9 mRNA has been also evaluated in vivo in mice, mainly with LNP as delivery systems [73,110,235] . It can be achieved by encapsulation of Cas9 mRNA and sgRNA in two different delivery systems, or by co-formulation into a single nanoparticle of Cas9 mRNA and sgRNA [107]. This last strategy ensures simultaneous delivery of these two components to the same individual cell and has achieved greater editing efficiency [110].

The translation to clinic of mRNA-based gene editing is currently focused on ex vivo applications (Table 4), especially with ZFN-mRNA and TALEN-mRNA. CRISPR/Cas9-mRNA has been clinically evaluated only in one trial.

Sangamo Therapeutics, a genomic medicine company, is using a ZFN mRNA product (SB-728mR) targeting the human *CCR5* gene in several clinical trials for the treatment of ex vivo HIV-1. C-C chemokine receptor 5 (CCR5) is a co-receptor essential for HIV-1 entry into cells. The deletion of this protein makes the cells resistant to infection by the virus [236]. Electroporation of SB-728mR is under evaluation in clinical trials to disrupt CCR5 expression in autologous T cells (NCT02225665, NCT04201782), autologous CD4+ T cells (NCT02388594), autologous T cells genetically modified to express a CD4 chimeric antigen receptor (NCT03617198) or autologous CD34+ HSPCs (NCT02500849). In these studies, the cells genetically modified are reinfused intravenously to the patients. Ex vivo ZFN mRNA gene editing is also under clinical evaluation for the treatment of Sickle Cell Disease. Sickle cell disease or Sickle cell anemia is a globally widespread life-threatening hematological disorder. It is caused by mutations in the hemoglobin genes, resulting in red blood cells with abnormal sickle or crescent shape, which makes them inefficient in their ability to transport oxygen [237]. A clinical study (NCT03653247) is assessing the safety, tolerability, and efficacy of the transplantation in Sickle Cell Disease patients of autologous HSPCs electroporated ex vivo with ZFN mRNAs targeting the B-cell lymphoma/leukemia 11A (BCL11A) locus, which plays a role in the fetal to adult erythropoiesis transition [238].

TALEN-mRNA is used to generate UCART19, the first allogenic CAR T-cell therapy in clinical study, in pediatric and adult relapsed/refractory B-cell acute lymphoblastic leukemia (NCT02808442, NCT02746952). The base of this product are allogenic T cells engineered to express CARs against the leukemia antigen CD19. In addition, CAR19 T cells are treated by electroporation with TALEN-mRNA to knockout T cell receptors (TCR) and the CD52. The knockout of the TCR is intended to reduce the risk of graft-versus-host disease (GVHD) caused by donor T-cells, whereas knockout of the CD52 gene makes transplanted allogenic T-cells resistant to the lymphodepleting agent alemtuzumab [239]. Following a similar strategy, UCART019 is under evaluation in patients with relapsed or refractory CD19+ leukemia and lymphoma (NCT03166878). UCART019 is also based on allogenic CAR19 T cells, but in this case, these cells are treated by CRISPR-Cas9 mRNA electroporation to disrupt endogenous TCR and beta-2 microglobulin (B2M) genes simultaneously, in order to evade host-mediated immunity and to avoid GVHD.

Table 4. Clinical trials of mRNA for gene editing therapy

Disease	Biological active	Therapeutic mRNA	Target protein	Strategy / Delivery system	Administration route	NCT Number / Phase
HIV	SB-728mR	ZFN mRNA	CCR5	Ex vivo / Autologous CD4+ T Cells	Intravenous	NCT02388594 / Phase I
	SB-728mR	ZFN mRNA	CCR5	Ex vivo / Autologous CD4 CAR+ T cells	Intravenous	NCT03617198 / Phase I
	SB-728mR-T	ZFN mRNA	CCR5	Ex vivo / Autologous T cells	Intravenous	NCT02225665, NCT04201782, / Phase I, Phase I/II
	SB-728mR-HSPC	ZFN mRNA	CCR5	Ex vivo / Autologous CD34+ hHSPCs	Intravenous	NCT02500849 / Phase I
Sickle Cell Disease	BIVV003	ZFN mRNA	B-cell lymphoma/leukemia 11A (BCL11A)	Ex vivo / Autologous CD34 + hematopoietic stem cells (HSPC)	Intravenous	NCT03653247 / Phase I/II
B acute lymphoblastic leukemia	UCART19	TALEN mRNA	TCR and CD52	Ex vivo / Allogenic T cells	Intravenous	NCT02808442, NCT02746952, NCT02735083 / Phase I
B cell leukemia and B cell linfoma	UCART019	CRISPR/Cas9 mRNA	TCR, B2M	Ex vivo / Allogenic T cells	Intravenous	NCT03166878 / Phase I/II

4.4. Regenerative medicine and cell engineering

Regenerative medicine aims to regrow, repair or replace injured or lost cells, organs or tissues by restoring or establishing their normal function [240]. The regeneration process needs the functionality of proteins, such as growth factors, cytokines and transcription factors, which control cellular biological activity, including cell mitosis, migration or differentiation. Among the regenerative strategies, reprogramming and transdifferentiation of somatic cells into other specific lineages can help to repair cell or tissue deficits in patients. In both processes specific transcription factors are required to bind to enhancer or promoter sequences of DNA and regulate gene expression. However, the intracellular delivery of the transcription factors is quite limited by the plasmatic membrane [15,51], and the use of pDNA to express them also shows the risk of the insertion and of the consequent mutagenesis. Transfection of somatic cells with IVT mRNA encoding transcription factors has been assessed as an attractive alternative to conventional reprogramming and transdifferentiation of somatic cells [51], although research in this field is quite incipient and, up to date, it is limited to in vitro preclinical works.

Cellular reprogramming is based on the generation of induced pluripotent stem cells (iPSCs) from patient's adult somatic cells. Those iPSCs will be later differentiated into autologous specific cell types [5,15,51]. Alternatively, in the transdifferentiation or direct reprogramming process adult somatic cells are transformed into cell lineages without iPSC generation [241,242]. Figure 5 depicts the differences between cellular reprogramming and transdifferentiation. Depending on the cocktail of transcription factors expressed by the IVT mRNA and on the adult somatic cell type, reprogramming or transdifferentiation will be performed and different lineages can be obtained [153,243–246].

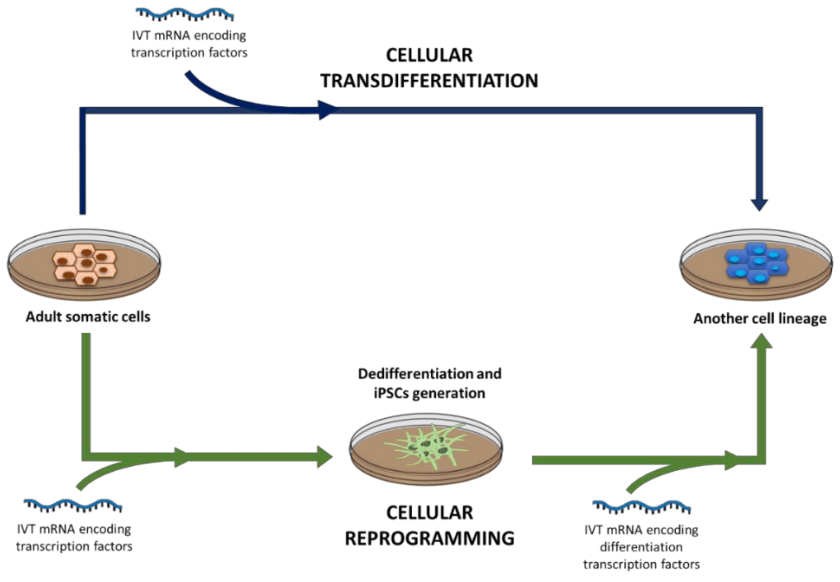

Figure 5. Representative scheme of cellular transdifferentiation and cellular reprogramming therapies.

In 2010, the first study of IVT mRNA to mediate in vitro reprogramming of somatic cells was reported. iPSCs were generated by delivering synthetic mRNA encoding four transcription factors (Oct4, Sox2, Lin28, and Nanog) to human foreskin fibroblasts [244]. In the same year, another study reported the use of IVT-mRNA encoding the following mix of transcription factors, Oct4, Sox2, Klf4, and cMyc (known as Yamanaka factors [245], to obtain iPSCs from fibroblasts [246]. In this study, additionally, the iPSCs were differentiated toward myofibers after transfection with myogenic differentiation factor (MyoD) IVT mRNA.

Transdifferentiation of somatic cells with IVT-mRNA has been mainly focused on obtaining cardiomyocytes to regenerate the cardiac tissue after a heart attack [153], and on the generation of insulin secreting β-cells for type 1 diabetes patients [247-249].

Another application of IVT mRNA in regenerative medicine is mesenchymal stem cells (MSCs) engineering. MSCs are adult stem cells that can be isolated from different sources, including bone marrow, umbilical cord, adipose tissue, liver, multiple dental tissues, and iPSCs [250]. Among their properties, MSCs show migration capacity and the ability of self-renewal and differentiation into wide range of cell lines, such as cartilage, adipocytes, and bone. In addition, MSCs secrete a huge variety of proteins which can promote the angiogenesis, reduce inflammation and improve tissue reparation. Engineering of MSC with IVT mRNA has been proposed to modulate the migratory properties of these cells, by expressing homing proteins in a brief, burst and temporary way. It is advantageous because MSCs treated with other strategies of cell surface modification (enzymatic or chemical modification and DNA-based genetic modifications) may suffer permanent changes by alterations in the cell membrane, which, in turn, result in disorders of the differentiation properties [51].

IVT mRNA-based modulation of homing MSCs to target ischemic areas has been assessed by in vitro transfection of different surface molecules, including the chemokine receptor CXCR4 [251] and the integrin α4 (ITGA4) [252]. MSCs may be also used as vehicle to target biological molecules, such as interleukins (IL), to specific tissues. In this sense, Levy et al. [253] transfected MSCs by lipofection with the IVT mRNA encoding the adhesion molecules P-selectin glycoprotein ligand-1 (PSGL-1) and Sialyl-Lewisx (SLeX), as well as, as the anti-inflammatory molecule IL-10. After intravenous administration of the engineered MSCs to C57BL/6 mice with induced ear inflammation, authors demonstrated the migration capacity of the cells and a high level of IL-10 expression in the target tissue.

5. Conclusions

Synthetic mRNA is attracting great interest as a therapeutic molecule. The main feature that has encouraged its recent expansion is the controlled expression of transgenes without the risk of insertional mutagenesis or permanent genomic alteration. Other advantages include economical production, scalable manufacturing, and versatility of applications. Limiting technological issues mainly associated with delivery and stability difficulties have still to be overcome, although important advances have been done in the last years.

Innovative progress in IVT-mRNA design as well as significant advances in nanodelivery systems are approaching its clinical translation. Unlike DNA gene therapy, non-viral vectors are at the forefront of IVT-mRNA therapy, and among them, LNP have the best prospects for mRNA-based medicines development. The combination of IVT mRNA and nanotechnology, as two powerful technological tools, is undergoing significant growth, and it is expected to play a key role in the biotechnology industry in the near future.

Gene editing, protein replacement therapy and immunotherapy have entered the early phases of clinical trials, whereas cellular reprogramming and engineering are still in preclinical stages. Immunotherapy for prophylaxis and therapy of infectious diseases has shown the high influence of the delivery system and the administration route on the efficacy. Most clinical trials are focused on cancer immunotherapy; actually, the therapeutic perspectives of this field have been broaden thanks to the beginning of the first mRNA CAR T cells clinical trials. Encouraging outcomes are expected, although the results of ongoing and future clinical research will help to define more accurately the therapeutic potential of mRNA.

References

1. European Medicines Agency. Guideline on the quality, non-clinical and clinical aspects of gene therapy medicinal products. Eur Med Agency Guidel. 2015;44(1):1–41.
2. del Pozo-Rodríguez A, Rodríguez-Gascón A, Rodríguez-Castejón J, Vicente-Pascual M, Gómez-Aguado I, Battaglia LS, et al. Gene therapy. In: Adv Biochem Eng Biotechnol. 2019.
3. Thorne B., Takeya R., Vitelli F., Swanson X. (2017) Gene Therapy. In: Kiss B., Gottschalk U., Pohlscheidt M. (eds) New Bioprocessing Strategies: Development and Manufacturing of Recombinant Antibodies and Proteins. Advances in Biochemical Engineering/Biotechnology, vol 165. Springer, Cham
4. Anguela XM, High KA. Entering the Modern Era of Gene Therapy. Annu Rev Med. 2019;70(1):273–88.
5. Hajj KA, Whitehead KA. Tools for translation: Non-viral materials for therapeutic mRNA delivery. Nat Rev Mater. 2017;2:1–17.

6. Sahin U, Karikó K, Türeci Ö. MRNA-based therapeutics-developing a new class of drugs. Nat Rev Drug Discov. 2014;13(10):759–80.

7. Meng Z, O'Keeffe-Ahern J, Lyu J, Pierucci L, Zhou D, Wang W. A new developing class of gene delivery: Messenger RNA-based therapeutics. Biomater Sci. 2017;5(12):2381–92.

8. Zarghampoor F, Azarpira N, Khatami SR, Behzad-Behbahani A, Foroughmand AM. Improved translation efficiency of therapeutic mRNA. Gene. 2019;707:231–8.

9. Zhong Z, Mc Cafferty S, Combes F, Huysmans H, De Temmerman J, Gitsels A, et al. mRNA therapeutics deliver a hopeful message. Nano Today. 2018;23:16–39.

10. Schlake T, Thess A, Thran M, Jordan I. mRNA as novel technology for passive immunotherapy. Cell Mol Life Sci. 2019;76(2):301–28.

11. Patel S, Athirasala A, Menezes PP, Ashwanikumar N, Zou T, Sahay G, et al. Messenger RNA Delivery for Tissue Engineering and Regenerative Medicine Applications. Tissue Eng - Part A. 2019;25(1–2):91–112.

12. Hecker JG. Non-Viral, Lipid-Mediated DNA and mRNA Gene Therapy of the Central Nervous System (CNS): Chemical-Based Transfection. In: Manfredsson FP, editor. Gene Therapy for Neurological Disorders: Methods and Protocols. New York, NY: Springer New York; 2016. p. 307–24.

13. Vallazza B, Petri S, Poleganov MA, Eberle F, Kuhn AN, Sahin U. Recombinant messenger RNA technology and its application in cancer immunotherapy, transcript replacement therapies, pluripotent stem cell induction, and beyond. Wiley Interdiscip Rev RNA. 2015;6(5):471–99.

14. Kowalski PS, Rudra A, Miao L, Anderson DG. Delivering the Messenger: Advances in Technologies for Therapeutic mRNA Delivery. Mol Ther. 2019;27(4):710–28.

15. Xiong Q, Lee GY, Ding J, Li W, Shi J. Biomedical applications of mRNA nanomedicine. Nano Res. 2018;11(10):5281–309.

16. del Pozo-Rodríguez A, Delgado D, Solinís MA, Gascón AR, Pedraz JL. Solid lipid nanoparticles for retinal gene therapy: Transfection and intracellular trafficking in RPE cells. Int J Pharm. 2008;360(1–2):177–83.

17. Gan L, Wang J, Zhao Y, Chen D, Zhu C, Liu J, et al. Hyaluronan-modified core-shell liponanoparticles targeting CD44-positive retinal pigment epithelium cells via intravitreal injection. Biomaterials. 2013;34(24):5978–87.

18. Apaolaza PS, del Pozo-Rodríguez A, Solinís MA, Rodríguez JM, Friedrich U, Torrecilla J, et al. Structural recovery of the retina in a retinoschisin-deficient mouse after gene replacement therapy by solid lipid nanoparticles. Biomaterials. 2016;90:40–9.

19. Stewart MP, Sharei A, Ding X, Sahay G, Langer R, Jensen KF. In vitro and ex vivo strategies for intracellular delivery. Nature. 2016;538(7624):183–92.

20. Patel S, Ashwanikumar N, Robinson E, Duross A, Sun C, Murphy-Benenato KE, et al. Boosting Intracellular Delivery of Lipid Nanoparticle-Encapsulated mRNA. Nano Lett. 2017;17(9):5711–8.

21. Steinle H, Behring A, Schlensak C, Wendel HP, Avci-Adali M. Concise Review: Application of In Vitro Transcribed Messenger RNA for Cellular Engineering and Reprogramming: Progress and Challenges. Stem Cells. 2017;35(1):68–79.

22. Karikó K, Muramatsu H, Ludwig J, Weissman D. Generating the optimal mRNA for therapy: HPLC purification eliminates immune activation and improves translation of nucleoside-modified, protein-encoding mRNA. Nucleic Acids Res. 2011;39(21):1–10.

23. Weissman D. mRNA transcript therapy. Expert Rev Vaccines. 2014;14(2):265–81.

24. Islam MA, Reesor EKG, Xu Y, Zope HR, Zetter BR, Shi J. Biomaterials for mRNA delivery. Biomater Sci. 2015;3(12):1519–33.

25. Ramanathan A, Robb GB, Chan SH. mRNA capping: Biological functions and applications. Nucleic Acids Res. 2016;44(16):7511–26.

26. Muttach F, Muthmann N, Rentmeister A. Synthetic mRNA capping. Beilstein J Org Chem. 2017;13:2819–32.

27. Werner M, Purta E, Kaminska KH, Cymerman IA, Campbell DA, Mittra B, et al. 2'-O-ribose methylation of cap2 in human: Function and evolution in a horizontally mobile family. Nucleic Acids Res. 2011;39(11):4756–68.

28. McCracken S, Fong N, Rosonina E, Yankulov K, Brothers G, Siderovski D, et al. 5'-Capping enzymes are targeted to pre-mRNA by binding to the phosphorylated carboxy-terminal domain of RNA polymerase II. Genes Dev. 1997;11(24):3306–18.

29. Fuchs A-L, Neu A, Sprangers R. A general method for rapid and cost-efficient large-scale production of 5' capped RNA. RNA. 2016;22(9):1454-1466.

30. Trilink Biotechnologies. Available online: https://www.trilinkbiotech.com/cleancap (accessed on 30 January 2020).

31. Warminski M, Kowalska J, Buck J, Zuberek J, Lukaszewicz M, Nicola C, et al. The synthesis of isopropylidene mRNA cap analogs modified with phosphorothioate moiety and their evaluation as promoters of mRNA translation. Bioorganic Med Chem Lett. 2013;23(13):3753–8.

32. Ziemniak M, Kowalska J, Lukaszewicz M, Zuberek J, Wnek K, Darzynkiewicz E, et al. Phosphate-modified analogues of m7GTP and m7Gppppm7G - Synthesis and biochemical properties. Bioorganic Med Chem. 2015;23(17):5369–81.

33. Kuhn AN, Diken M, Kreiter S, Selmi A, Kowalska J, Jemielity J, et al. Phosphorothioate cap analogs increase stability and translational efficiency of RNA vaccines in immature dendritic cells and induce superior immune responses in vivo. Gene Ther. 2010;17(8):961–71.

34. Strenkowska M, Kowalska J, Lukaszewicz M, Zuberek J, Su W, Rhoads RE, et al. Towards mRNA with superior translational activity: Synthesis and properties of ARCA tetraphosphates with single phosphorothioate modifications. New J Chem. 2010;34(5):993–1007.

35. Zytek M, Kowalska J, Lukaszewicz M, Wojtczak BA, Zuberek J, Ferenc-Mrozek A, et al. Towards novel efficient and stable nuclear import signals: Synthesis and properties of

trimethylguanosine cap analogs modified within the 5',5'-triphosphate bridge. Org Biomol Chem. 2014;12(45):9184–99.

36. Rydzik AM, Kulis M, Lukaszewicz M, Kowalska J, Zuberek J, Darzynkiewicz ZM, et al. Synthesis and properties of mRNA cap analogs containing imidodiphosphate moiety - Fairly mimicking natural cap structure, yet resistant to enzymatic hydrolysis. Bioorganic Med Chem. 2012;20(5):1699–710.

37. Al-Saif M, Khabar KSA. UU/UA dinucleotide frequency reduction in coding regions results in increased mRNA stability and protein expression. Mol Ther. 2012;20(5):954–9.

38. Mauro VP, Chappell SA. A critical analysis of codon optimization in human therapeutics. Trends Mol Med. 2014;20(11):604–13.

39. Alexaki A, Hettiarachchi GK, Athey JC, Katneni UK, Simhadri V, Hamasaki-Katagiri N, et al. Effects of codon optimization on coagulation factor IX translation and structure: Implications for protein and gene therapies. Sci Rep. 2019;9(1):1–15.

40. Presnyak V, Alhusaini N, Chen YH, Martin S, Morris N, Kline N, et al. Codon optimality is a major determinant of mRNA stability. Cell. 2015;160(6):1111–24.

41. Hunt RC, Simhadri VL, Iandoli M, Sauna ZE, Kimchi-Sarfaty C. Exposing synonymous mutations. Trends Genet. 2014;30(7):308–21.

42. McCarthy C, Carrea A, Diambra L. Bicodon bias can determine the role of synonymous SNPs in human diseases. BMC Genomics. 2017;18(1):1–11.

43. Bali V, Bebok Z. Decoding mechanisms by which silent codon changes influence protein biogenesis and function. Int J Biochem Cell Biol. 2015;64:58–74.

44. Li B, Zhang X, Dong Y. Nanoscale platforms for messenger RNA delivery. Wiley Interdiscip Rev Nanomedicine Nanobiotechnology. 2019;11(2):1–14.

45. Jalkanen AL, Coleman SJ, Wilusz J. Determinants and implications of mRNA poly(A) tail size - Does this protein make my tail look big? Semin Cell Dev Biol. 2014;34:24–32.

46. Eckmann CR, Rammelt C, Wahle E. Control of poly(A) tail length. Wiley Interdiscip Rev RNA. 2011;2(3):348–61.

47. Weill L, Belloc E, Bava FA, Méndez R. Translational control by changes in poly(A) tail length: Recycling mRNAs. Nat Struct Mol Biol . 2012;19(6):577–85.

48. Peng J, Schoenberg DR. mRNA with a <20-nt poly(A) tail imparted by the poly(A)-limiting element is translated as efficiently in vivo as long poly(A) mRNA. Rna. 2005;11(7):1131–40.

49. Holtkamp S, Kreiter S, Selmi A, Simon P, Koslowski M, Huber C, et al. Modification of antigen-encoding RNA increases stability, translational efficacy, and T-cell stimulatory capacity of dendritic cells. Blood. 2006;108(13):4009–17.

50. Mockey M, Gonçalves C, Dupuy FP, Lemoine FM, Pichon C, Midoux P. mRNA transfection of dendritic cells: Synergistic effect of ARCA mRNA capping with Poly(A) chains in cis and in trans for a high protein expression level. Biochem Biophys Res Commun. 2006;340(4):1062–8.

51. Kwon H, Kim M, Seo Y, Moon YS, Lee HJ, Lee K, et al. Emergence of synthetic mRNA: In vitro synthesis of mRNA and its applications in regenerative medicine. Biomaterials. 2018;156:172–93.

52. Matoulkova E, Michalova E, Vojtesek B, Hrstka R. The role of the 3' untranslated region in post-transcriptional regulation of protein expression in mammalian cells. RNA Biol. 2012;9(5):563–76.

53. Hellen CUT, Sarnow P. Internal ribosome entry sites in eukaryotic mRNA molecules. Genes Dev. 2001;15(13):1593–612.

54. Johnson AG, Grosely R, Petrov AN, Puglisi JD, Puglisi JD. Dynamics of IRES-mediated translation. 2017;(i).

55. Yang Y, Wang Z. IRES-mediated cap-independent translation , a path leading to hidden proteome. :1–20.

56. Kozak M. Point mutations close to the AUG initiator codon affect the efficiency of translation of rat preproinsulin in vivo. Nature. 1984;308(5956):241–6.

57. Kozak M. At least six nucleotides preceding the AUG initiator codon enhance translation in mammalian cells. J Mol Biol. 1987;196(4):947–50.

58. Jiang Y, Xu X-S, Russell JE. A Nucleolin-Binding 3' Untranslated Region Element Stabilizes -Globin mRNA In Vivo. Mol Cell Biol. 2006;26(6):2419–29.

59. Volloch V, Housman D. Stability of globin mRNA in terminally differentiating murine erythroleukemia cells. Cell. 1981;23(2):509–14.

60. Berkovits BD, Mayr C. Alternative 3' UTRs act as scaffolds to regulate membrane protein localization. Nature. 2015;522(7556):363–7.

61. Karikó K, Muramatsu H, Welsh FA, Ludwig J, Kato H, Akira S, et al. Incorporation of pseudouridine into mRNA yields superior nonimmunogenic vector with increased translational capacity and biological stability. Mol Ther. 2008;16(11):1833–40.

62. Hornung V, Ellegast J, Kim S, Brzózka K, Jung A, Kato H, et al. 5'-Triphosphate RNA Is the Ligand for RIG-I. Science (80-). 2006 Nov 10;314(5801):994 LP – 997.

63. Diebold SS, Massacrier C, Akira S, Paturel C, Morel Y, Reis e Sousa C. Nucleic acid agonists for Toll-like receptor 7 are defined by the presence of uridine ribonucleotides. Eur J Immunol. 2006;36(12):3256–67.

64. Gorden KKB, Qiu X, Battiste JJL, Wightman PPD, Vasilakos JP, Alkan SS. Oligodeoxynucleotides Differentially Modulate Activation of TLR7 and TLR8 by Imidazoquinolines. J Immunol. 2006;177(11):8164–70.

65. Karikó K, Buckstein M, Ni H, Weissman D. Suppression of RNA recognition by Toll-like receptors: The impact of nucleoside modification and the evolutionary origin of RNA. Immunity. 2005;23(2):165–75.

66. Lorenz C, Fotin-Mleczek M, Roth G, Becker C, Dam TC, Verdurmen WPR, et al. Protein expression from exogenous mRNA: Uptake by receptor-mediated endocytosis and trafficking via the lysosomal pathway. RNA Biol. 2011;8(4).

67. Svitkin Y V., Cheng YM, Chakraborty T, Presnyak V, John M, Sonenberg N. N1-methyl-pseudouridine in mRNA enhances translation through eIF2α-dependent and independent mechanisms by increasing ribosome density. Nucleic Acids Res. 2017;45(10):6023–36.

68. Andries O, Mc Cafferty S, De Smedt SC, Weiss R, Sanders NN, Kitada T. N1-methylpseudouridine-incorporated mRNA outperforms pseudouridine-incorporated mRNA by providing enhanced protein expression and reduced immunogenicity in mammalian cell lines and mice. J Control Release. 2015;217:337–44.

69. Martini PGV, Guey LT. A New Era for Rare Genetic Diseases: Messenger RNA Therapy. Hum Gene Ther. 2019;30(10):1180–9.

70. Meyer KD, Patil DP, Zhou J, Zinoviev A, Skabkin MA, Elemento O, et al. 5′ UTR m6A Promotes Cap-Independent Translation. Cell. 2015;163(4):999–1010.

71. Ulkoski D, Bak A, Wilson JT, Krishnamurthy VR. Recent advances in polymeric materials for the delivery of RNA therapeutics. Expert Opin Drug Deliv. 2019;16(11):1149-1167.

72. Rodríguez-Gascón A, del Pozo-Rodríguez A, Solinís MÁ. Development of nucleic acid vaccines: Use of self-amplifying RNA in lipid nanoparticles. Int J Nanomedicine. 2014;9(1):1833–43.

73. Gene Therapy Clinical Trials Worldwide, provided by the Journal of Gene Medicine, Jon Wiley and Sons Ltd., 2019. Available online: http://www.abedia.com/wiley/vectors.php (accessed on 13 January 2020).

74. Carvalho M, Sepodes B, Martins AP. Regulatory and Scientific Advancements in Gene Therapy: State-of-the-Art of Clinical Applications and of the Supporting European Regulatory Framework. Front Med. 2017;4:182.

75. del Pozo-Rodríguez A, Solinís MÁ, Rodríguez-Gascón A. Applications of lipid nanoparticles in gene therapy. Eur J Pharm Biopharm. 2016;109:184–93.

76. Wang Y, Rajala A, Rajala R. Lipid Nanoparticles for Ocular Gene Delivery. J Funct Biomater. 2015;6(2):379–94.

77. Yin H, Kanasty RL, Eltoukhy AA, Vegas AJ, Dorkin JR, Anderson DG. Non-viral vectors for gene-based therapy. Nat Rev Genet. 2014;15(8):541–55.

78. Guan S, Rosenecker J. Nanotechnologies in delivery of mRNA therapeutics using nonviral vector-based delivery systems. Gene Ther. 2017;24(3):133–43.

79. Rodríguez-Gascón A, del Pozo-Rodríguez A, Isla A, Solinís MA. Vaginal gene therapy. Adv Drug Deliv Rev. 2015;92(7):71–83.

80. Gascón AR, del Pozo-Rodríguez A, Solinís MA. Non-Viral Delivery Systems in Gene Therapy. In: Molina FM, editor. Gene Therapy. Rijeka: IntechOpen; 2013.

81. Van Tendeloo VFI, Ponsaerts P, Lardon F, Nijs G, Lenjou M, Van Broeckhoven C, et al. Highly efficient gene delivery by mRNA electroporation in human hematopoietic cells: Superiority to lipofection and passive pulsing of mRNA and to electroporation of plasmid cDNA for tumor antigen loading of dendritic cells. Blood. 2001;98(1):49–56.

82. Bugeon S, De Chevigny A, Boutin C, Coré N, Wild S, Bosio A, et al. Direct and efficient transfection of mouse neural stem cells and mature neurons by in vivo mRNA electroporation. Dev. 2017;144(21):3968–77.

83. Golombek S, Pilz M, Steinle H, Kochba E, Levin Y, Lunter D, et al. Intradermal Delivery of Synthetic mRNA Using Hollow Microneedles for Efficient and Rapid Production of Exogenous Proteins in Skin. Mol Ther - Nucleic Acids. 2018;11:382–92.

84. Moody SA. Microinjection of mRNAs and oligonucleotides. Cold Spring Harb Protoc. 2018;2018(12):923–32.

85. Ainger K, Avossa D, Morgan F, Hill SJ, Barry C, Barbarese E, et al. Transport and localization of exogenous myelin basic protein mRNA microinjected into oligodendrocytes. J Cell Biol. 1993;123(2):431–41.

86. Belyantseva IA. Helios® Gene Gun-Mediated Transfection of the Inner Ear Sensory Epithelium: Recent Updates. In: Sokolowski B, editor. Auditory and Vestibular Research: Methods and Protocols. New York, NY: Springer New York; 2016. p. 3–26.

87. Vassilev VB, Gil LHVG, Donis RO. Microparticle-mediated RNA immunization against bovine viral diarrhea virus. Vaccine. 2001;19(15–16):2012–9.

88. Ramezanpour M, Schmidt ML, Bodnariuc I, Kulkarni JA, Leung SSW, Cullis PR, et al. Ionizable amino lipid interactions with POPC: implications for lipid nanoparticle function. Nanoscale. 2019;11(30):14141–6.

89. Kauffman KJ, Webber MJ, Anderson DG. Materials for non-viral intracellular delivery of messenger RNA therapeutics. J Control Release. 2016;240:227–34.

90. Slivac I, Guay D, Mangion M, Champeil J, Gaillet B. Non-viral nucleic acid delivery methods. Expert Opin Biol Ther. 2017;17(1):105–18.

91. Aderibigbe BA, Ray SS. Preparation, characterization and in vitro release kinetics of polyaspartamide-based conjugates containing antimalarial and anticancer agents for combination therapy. J Drug Deliv Sci Technol. 2016;36:34–45

92. Malone RW, Felgner PL, Verma IM. Cationic liposome-mediated RNA transfection. Proc Natl Acad Sci USA. 1989;86(16):6077–81.

93. Koltover I, Salditt T, Rädler JO, Safinya CR. An inverted hexagonal phase of cationic liposome-DNA complexes related to DNA release and delivery. Science (80-). 1998;281(5373):78–81.

94. Sayour EJ, De Leon G, Pham C, Grippin A, Kemeny H, Chua J, et al. Systemic activation of antigen-presenting cells via RNA-Loaded nanoparticles. Oncoimmunology. 2017;6(1):1–14.

95. Kranz LM, Diken M, Haas H, Kreiter S, Loquai C, Reuter KC, et al. Systemic RNA delivery to dendritic cells exploits antiviral defence for cancer immunotherapy. Nature. 2016;534(7607):396–401.

96. Kulkarni JA, Cullis PR, Van Der Meel R. Lipid Nanoparticles Enabling Gene Therapies: From Concepts to Clinical Utility. Nucleic Acid Ther. 2018;28(3):146–57.

97. Bogers WM, Oostermeijer H, Mooij P, Koopman G, Verschoor EJ, Davis D, et al. Potent immune responses in rhesus macaques induced by nonviral delivery of a self-amplifying RNA vaccine expressing HIV type 1 envelope with a cationic nanoemulsion. J Infect Dis. 2015;211(6):947–55.

98. Brito LA, Chan M, Shaw CA, Hekele A, Carsillo T, Schaefer M, et al. A cationic nanoemulsion for the delivery of next-generation RNA vaccines. Mol Ther. 2014;22(12):2118–29.

99. Kauffman KJ, Dorkin JR, Yang JH, Heartlein MW, Derosa F, Mir FF, et al. Optimization of Lipid Nanoparticle Formulations for mRNA Delivery in Vivo with Fractional Factorial and Definitive Screening Designs. Nano Lett. 2015;15(11):7300–6.

100. Adams D, Gonzalez-Duarte A, O'Riordan WD, Yang CC, Ueda M, Kristen A V., et al. Patisiran, an RNAi therapeutic, for hereditary transthyretin amyloidosis. N Engl J Med. 2018;3791):11–21.

101. Zhang X, Goel V, Robbie GJ. Pharmacokinetics of Patisiran, the First Approved RNA Interference Therapy in Patients With Hereditary Transthyretin-Mediated Amyloidosis. J Clin Pharmacol. 2019.

102. Sedic M, Senn JJ, Lynn A, Laska M, Smith M, Platz SJ, et al. Safety Evaluation of Lipid Nanoparticle–Formulated Modified mRNA in the Sprague-Dawley Rat and Cynomolgus Monkey. Vet Pathol. 2018;55(2):341–54.

103. Lu D, Benjamin R, Kim M, Conry RM, Curiel DT. Optimization of methods to achieve mRNA-mediated transfection of tumor cells in vitro and in vivo employing cationic liposome vectors. Cancer Gene Ther. 1994;1(4):245–52.

104. Pardi N, Hogan MJ, Pelc RS, Muramatsu H, Andersen H, DeMaso CR, et al. Zika virus protection by a single low-dose nucleoside-modified mRNA vaccination. Nature. 2017;543(7644):248–51.

105. Hekele A, Bertholet S, Archer J, Gibson DG, Palladino G, Brito LA, et al. Rapidly produced SAM(®) vaccine against H7N9 influenza is immunogenic in mice. Emerg Microbes Infect. 2013;2(8):e52.

106. Zhou WZ, Hoon DSB, Huang SKS, Fujii S, Hashimoto K, Morishita R, et al. RNA melanoma vaccine: Induction of antitumor immunity by human glycoprotein 100 mRNA immunization. Hum Gene Ther. 1999;10(16):2719–24.

107. Finn JD, Smith AR, Patel MC, Shaw L, Youniss MR, van Heteren J, et al. A Single Administration of CRISPR/Cas9 Lipid Nanoparticles Achieves Robust and Persistent In Vivo Genome Editing. Cell Rep. 2018;22(9):2227–35.

108. Kormann MSD, Hasenpusch G, Aneja MK, Nica G, Flemmer AW, Herber-Jonat S, et al. Expression of therapeutic proteins after delivery of chemically modified mRNA in mice. Nat Biotechnol. 2011;29(2):154–9.

109. Akinc A, Zumbuehl A, Goldberg M, Leshchiner ES, Busini V, Hossain N, et al. A combinatorial library of lipid-like materials for delivery of RNAi therapeutics. Nat Biotechnol. 2008;26(5):561–9.

110. Miller JB, Zhang S, Kos P, Xiong H, Zhou K, Perelman SS, et al. Non-Viral CRISPR/Cas Gene Editing In Vitro and In Vivo Enabled by Synthetic Nanoparticle Co-Delivery of Cas9 mRNA and sgRNA. Angew Chemie - Int Ed. 2017;56(4):1059–63.

111. Li B, Luo X, Deng B, Wang J, McComb DW, Shi Y, et al. An Orthogonal Array Optimization of Lipid-like Nanoparticles for mRNA Delivery in Vivo. Nano Lett. 2015;15(12):8099–107.

112. Nagpal G, Chaudhary K, Dhanda SK, Pal G, Raghava S. Chapter 5 Potential of RNA Sequences. 2017;1632:75–90.

113. Beloqui A, Solinís MÁ, Rodríguez-Gascón A, Almeida AJ, Préat V. Nanostructured lipid carriers: Promising drug delivery systems for future clinics. Nanomedicine Nanotechnology, Biol Med. 2016;12(1):143–61.

114. Beloqui A, del Pozo-Rodríguez A, Isla A, Rodríguez-Gascón A, Solinís MÁ. Nanostructured lipid carriers as oral delivery systems for poorly soluble drugs. J Drug Deliv Sci Technol. 2017;42:144–54.

115. Beloqui A, Solinís MÁ, des Rieux A, Préat V, Rodríguez-Gascón A. Dextran–protamine coated nanostructured lipid carriers as mucus-penetrating nanoparticles for lipophilic drugs. Int J Pharm. 2014;468(1):105–11.

116. Erasmus JH, Khandhar AP, Guderian J, Granger B, Archer J, Archer M, et al. A Nanostructured Lipid Carrier for Delivery of a Replicating Viral RNA Provides Single, Low-Dose Protection against Zika. Mol Ther. 2018;26(10):2507–22.

117. Godbey WT, Wu KK, Mikos AG. Size matters: Molecular weight affects the efficiency of poly(ethylenimine) as a gene delivery vehicle. J Biomed Mater Res. 1999;45(3):268–75.

118. Lv H, Zhang S, Wang B, Cui S, Yan J. Toxicity of cationic lipids and cationic polymers in gene delivery. J Control Release. 2006;114(1):100–9.

119. Rejman J, Tavernier G, Bavarsad N, Demeester J, De Smedt SC. MRNA transfection of cervical carcinoma and mesenchymal stem cells mediated by cationic carriers. J Control Release. 2010;147(3):385–91.

120. Sultana N, Magadum A, Hadas Y, Kondrat J, Singh N, Youssef E, et al. Optimizing Cardiac Delivery of Modified mRNA. Mol Ther. 2017;25(6):1306–15.

121. Üzgün S, Nica G, Pfeifer C, Bosinco M, Michaelis K, Lutz JF, et al. PEGylation improves nanoparticle formation and transfection efficiency of messenger RNA. Pharm Res. 2011;28(9):2223–32.

122. Cheng C, Convertine AJ, Stayton PS, Bryers JD. Multifunctional triblock copolymers for intracellular messenger RNA delivery. Biomaterials. 2012;33(28):6868–76.

123. Jarzębińska A, Pasewald T, Lambrecht J, Mykhaylyk O, Kümmerling L, Beck P, et al. A Single Methylene Group in Oligoalkylamine-Based Cationic Polymers and Lipids Promotes Enhanced mRNA Delivery. Angew Chemie Int Ed. 2016;55(33):9591–5.

124. Liu Y, Li Y, Keskin D, Shi L. Poly(β-Amino Esters): Synthesis, Formulations, and Their Biomedical Applications. Adv Healthc Mater. 2019;8(2):1–24.

125. Kaczmarek JC, Patel AK, Kauffman KJ, Fenton OS, Webber MJ, Heartlein MW, et al. Polymer–Lipid Nanoparticles for Systemic Delivery of mRNA to the Lungs. Angew Chemie - Int Ed. 2016;55(44):13808–12.

126. Patel AK, Kaczmarek JC, Bose S, Kauffman KJ, Mir F, Heartlein MW, et al. Inhaled Nanoformulated mRNA Polyplexes for Protein Production in Lung Epithelium. Adv Mater. 2019;31(8):1805116.

127. Uchida S, Kataoka K. Design concepts of polyplex micelles for in vivo therapeutic delivery of plasmid DNA and messenger RNA. J Biomed Mater Res Part A. 2019;107(5):978–90.

128. Uchida H, Itaka K, Nomoto T, Ishii T, Suma T, Ikegami M, et al. Modulated protonation of side chain aminoethylene repeats in N-substituted polyaspartamides promotes mRNA transfection. J Am Chem Soc. 2014;136(35):12396–405.

129. Baba M, Itaka K, Kondo K, Yamasoba T, Kataoka K. Treatment of neurological disorders by introducing mRNA in vivo using polyplex nanomicelles. J Control Release. 2015;201:41–8.

130. Matsui A, Uchida S, Ishii T, Itaka K, Kataoka K. Messenger RNA-based therapeutics for the treatment of apoptosis-associated diseases. Sci Rep. 2015;5:1–10.

131. Palamà IE, Cortese B, D'Amone S, Gigli G. MRNA delivery using non-viral PCL nanoparticles. Biomater Sci. 2015;3(1):144–51.

132. Lallana E, Rios de la Rosa JM, Tirella A, Pelliccia M, Gennari A, Stratford IJ, et al. Chitosan/Hyaluronic Acid Nanoparticles: Rational Design Revisited for RNA Delivery. Mol Pharm. 2017 Jul 3;14(7):2422–36.

133. McKinlay CJ, Vargas JR, Blake TR, Hardy JW, Kanada M, Contag CH, et al. Charge-altering releasable transporters (CARTs) for the delivery and release of mRNA in living animals. Proc Natl Acad Sci. 2017;24;114(4):E448 LP-E456.

134. McKinlay CJ, Benner NL, Haabeth OA, Waymouth RM, Wender PA. Enhanced mRNA delivery into lymphocytes enabled by lipid-varied libraries of charge-altering releasable transporters. Proc Natl Acad Sci. 2018;26;115(26):E5859 LP-E5866.

135. Haabeth OAW, Blake TR, McKinlay CJ, Waymouth RM, Wender PA, Levy R. mRNA vaccination with charge-altering releasable transporters elicits human T cell responses and cures established tumors in mice. Proc Natl Acad Sci. 2018;25;115(39):E9153 LP-E9161.

136. Armbruster N, Jasny E, Petsch B. Advances in RNA Vaccines for Preventive Indications: A Case Study of A Vaccine Against Rabies. Vaccines. 2019 Sep 27 [cited 2020 Jan 27];7(4):132.

137. Amos H. Protamine enhancement of RNA uptake by cultured chick cells. Biochem Biophys Res Commun. 1961;5(1):1–4.

138. Scheel B, Teufel R, Probst J, Carralot JP, Geginat J, Radsak M, et al. Toll-like receptor-dependent activation of several human blood cell types by protamine-condensed mRNA. Eur J Immunol. 2005;35(5):1557–66.

139. Sebastian M, Schröder A, Scheel B, Hong HS, Muth A, von Boehmer L, et al. A phase I/IIa study of the mRNA-based cancer immunotherapy CV9201 in patients with stage IIIB/IV non-small cell lung cancer. Cancer Immunol Immunother. 2019;68(5):799–812.

140. Kübler H, Scheel B, Gnad-Vogt U, Miller K, Schultze-Seemann W, Dorp F, et al. Self-adjuvanted mRNA vaccination in advanced prostate cancer patients: A first-in-man phase I/IIa study. J Immunother Cancer. 2015;3(1):1–14.

141. Petsch B, Schnee M, Vogel AB, Lange E, Hoffmann B, Voss D, et al. Protective efficacy of in vitro synthesized, specific mRNA vaccines against influenza A virus infection. Nat Biotechnol. 2012;30(12):1210–6.

142. Udhayakumar VK, De Beuckelaer A, McCaffrey J, McCrudden CM, Kirschman JL, Vanover D, et al. Arginine-Rich Peptide-Based mRNA Nanocomplexes Efficiently Instigate Cytotoxic T Cell Immunity Dependent on the Amphipathic Organization of the Peptide. Adv Healthc Mater. 2017;6(13):1–13.

143. Li J, Sun Y, Jia T, Zhang R, Zhang K, Wang L. Messenger RNA vaccine based on recombinant MS2 virus-like particles against prostate cancer. Int J Cancer. 2014;134(7):1683–94.

144. Jekhmane S, de Haas R, da Silva Filho O, van Asbeck AH, Favretto ME, Hernandez Garcia A, et al. Virus-Like Particles of mRNA with Artificial Minimal Coat Proteins: Particle Formation, Stability, and Transfection Efficiency. Nucleic Acid Ther. 2017;27(3):159–67.

145. Zhitnyuk Y, Gee P, Lung MSY, Sasakawa N, Xu H, Saito H, et al. Efficient mRNA delivery system utilizing chimeric VSVG-L7Ae virus-like particles. Biochem Biophys Res Commun. 2018;505(4):1097–102.

146. Palmerston Mendes L, Pan J, Torchilin VP. Dendrimers as Nanocarriers for Nucleic Acid and Drug Delivery in Cancer Therapy. Molecules. 2017;22(9).

147. Chahal JS, Khan OF, Cooper CL, McPartlan JS, Tsosie JK, Tilley LD, et al. Dendrimer-RNA nanoparticles generate protective immunity against lethal Ebola, H1N1 influenza, and Toxoplasma gondii challenges with a single dose. Proc Natl Acad Sci. 2016;113(29):E4133 LP-E4142.

148. Chahal JS, Fang T, Woodham AW, Khan OF, Ling J, Anderson DG, et al. An RNA nanoparticle vaccine against Zika virus elicits antibody and CD8+ T cell responses in a mouse model. Sci Rep. 2017;7(1):252.

149. Ding Y, Jiang Z, Saha K, Kim CS, Kim ST, Landis RF, et al. Gold Nanoparticles for Nucleic Acid Delivery. Mol Ther. 2014;22(6):1075–83.

150. Yeom JH, Ryou SM, Won M, Park M, Bae J, Lee K. Inhibition of Xenograft Tumor Growth by Gold Nanoparticle-DNA Oligonucleotide Conjugates-Assisted Delivery of BAX mRNA. PLoS One. 2013;8(9):1–10.

151. Hoerr I, Obst R, Rammensee HG, Jung G. In vivo application of RNA leads to induction of specific cytotoxic T lymphocytes and antibodies. Eur J Immunol. 2000;30(1):1–7.

152. Wang Y, Su HH, Yang Y, Hu Y, Zhang L, Blancafort P, et al. Systemic delivery of modified mRNA encoding herpes simplex virus 1 thymidine kinase for targeted cancer gene therapy. Mol Ther. 2013;21(2):358–67.

153. Lee K, Yu P, Lingampalli N, Kim HJ, Tang R, Murthy N. Peptide-enhanced mRNA transfection in cultured mouse cardiac fibroblasts and direct reprogramming towards cardiomyocyte-like cells. Int J Nanomedicine. 2015;10:1841–54.

154. Zohra FT, Chowdhury EH, Akaike T. High performance mRNA transfection through carbonate apatite-cationic liposome conjugates. Biomaterials. 2009;30(23–24):4006–13.

155. Mockey M, Bourseau E, Chandrashekhar V, Chaudhuri A, Lafosse S, Le Cam E, et al. mRNA-based cancer vaccine: Prevention of B16 melanoma progression and metastasis by systemic injection of MART1 mRNA histidylated lipopolyplexes. Cancer Gene Ther. 2007;14(9):802–14.

156. Pichon C, Midoux P. Mannosylated and Histidylated LPR Technology for Vaccination with Tumor Antigen mRNA. In: Rabinovich PM, editor. Synthetic Messenger RNA and Cell Metabolism Modulation: Methods and Protocols. Totowa, NJ: Humana Press; 2013. p. 247–74.

157. Islam MA, Xu Y, Tao W, Ubellacker JM, Lim M, Aum D, et al. Restoration of tumour-growth suppression in vivo via systemic nanoparticle-mediated delivery of PTEN mRNA. Nat Biomed Eng. 2018;2(11):850–64.

158. Uchida S, Kinoh H, Ishii T, Matsui A, Tockary TA, Takeda KM, et al. Systemic delivery of messenger RNA for the treatment of pancreatic cancer using polyplex nanomicelles with a cholesterol moiety. Biomaterials. 2016;82:221–8.

159. Dong Y, Dorkin JR, Wang W, Chang PH, Webber MJ, Tang BC, et al. Poly(glycoamidoamine) Brushes Formulated Nanomaterials for Systemic siRNA and mRNA Delivery in Vivo. Nano Lett. 2016;16(2):842–8.

160. Lacroix C, Humanes A, Coiffier C, Gigmes D, Verrier B, Trimaille T. Polylactide-Based Reactive Micelles as a Robust Platform for mRNA Delivery. Pharm Res. 2020;37(2):30.

161. Fishman S, Lewis MD, Siew LK, Leenheer E De, Kakabadse D, Davies J, et al. Adoptive Transfer of mRNA-Transfected T Cells Redirected against Diabetogenic CD8 T Cells Can Prevent Diabetes. Mol Ther. 2017;25(2):456–64.

162. Pardi N, Hogan MJ, Porter FW, Weissman D. mRNA vaccines-a new era in vaccinology. Nat Rev Drug Discov. 2018;17(4):261–79.

163. Liu AM. A Comparison of Plasmid DNA and mRNA as Vaccine Technologies. Vol. 7, Vaccines . 2019.

164. Maruggi G, Zhang C, Li J, Ulmer JB, Yu D. mRNA as a Transformative Technology for Vaccine Development to Control Infectious Diseases. Mol Ther. 2019;27(4):757–72.

165. Zhou X, Berglund P, Rhodes G, Parker SE, Jondal M, Liljeström P. Self-replicating Semliki Forest virus RNA as recombinant vaccine. Vaccine. 1994;12(16):1510–4.

166. Fleeton MN, Chen M, Berglund P, Rhodes G, Parker SE, Murphy M, et al. Self-Replicative RNA Vaccines Elicit Protection against Influenza A Virus, Respiratory Syncytial Virus, and a Tickborne Encephalitis Virus. J Infect Dis. 2001;183(9):1395–8.

167. Geall AJ, Verma A, Otten GR, Shaw CA, Hekele A, Banerjee K, et al. Nonviral delivery of self-amplifying RNA vaccines. Proc Natl Acad Sci U S A. 2012;109(36):14604–9.

168. Bernstein DI, Reap EA, Katen K, Watson A, Smith K, Norberg P, et al. Randomized, double-blind, Phase 1 trial of an alphavirus replicon vaccine for cytomegalovirus in CMV seronegative adult volunteers. Vaccine. 2009;28(2):484–93.

169. AlphaVax. Available online: https://www.alphavax.com/clinical-experience.html (accessed on 30 January 2020).

170. Wecker M, Gilbert P, Russell N, Hural J, Allen M, Pensiero M, et al. Phase I Safety and Immunogenicity Evaluations of an Alphavirus Replicon HIV-1 Subtype C gag Vaccine in Healthy HIV-1-Uninfected Adults. Clin Vaccine Immunol. 2012;1;19(10):1651 LP – 1660.

171. Schnee M, Vogel AB, Voss D, Petsch B, Baumhof P, Kramps T, et al. An mRNA Vaccine Encoding Rabies Virus Glycoprotein Induces Protection against Lethal Infection in Mice and Correlates of Protection in Adult and Newborn Pigs. PLoS Negl Trop Dis. 2016;10(6):1–20.

172. Alberer M, Gnad-Vogt U, Hong HS, Mehr KT, Backert L, Finak G, et al. Safety and immunogenicity of a mRNA rabies vaccine in healthy adults: an open-label, non-randomised, prospective, first-in-human phase 1 clinical trial. Lancet. 2017;390(10101):1511–20.

173. Richner JM, Himansu S, Dowd KA, Butler SL, Salazar V, Fox JM, et al. Modified mRNA Vaccines Protect against Zika Virus Infection. Cell. 2017;168(6):1114-1125.e10.

174. Bahl K, Senn JJ, Yuzhakov O, Bulychev A, Brito LA, Hassett KJ, et al. Preclinical and Clinical Demonstration of Immunogenicity by mRNA Vaccines against H10N8 and H7N9 Influenza Viruses. Mol Ther. 2017;25(6):1316–27.

175. Feldman RA, Fuhr R, Smolenov I, (Mick) Ribeiro A, Panther L, Watson M, et al. mRNA vaccines against H10N8 and H7N9 influenza viruses of pandemic potential are immunogenic and well tolerated in healthy adults in phase 1 randomized clinical trials. Vaccine. 2019;37(25):3326–34.

176. Leal L, Guardo AC, Morón-López S, Salgado M, Mothe B, Heirman C, et al. Phase I clinical trial of an intranodally administered mRNA-based therapeutic vaccine against HIV-1 infection. AIDS. 2018;32(17).

177. Van Lint S, Renmans D, Broos K, Goethals L, Maenhout S, Benteyn D, et al. Intratumoral Delivery of TriMix mRNA Results in T-cell Activation by Cross-Presenting Dendritic Cells. Cancer Immunol Res. 2016 Feb 1;4(2):146 LP – 156.

178. Gandhi RT, Kwon DS, Macklin EA, Shopis JR, McLean AP, McBrine N, et al. Immunization of HIV-1-Infected Persons With Autologous Dendritic Cells Transfected With mRNA Encoding HIV-1 Gag and Nef: Results of a Randomized, Placebo-Controlled Clinical Trial. JAIDS J Acquir Immune Defic Syndr. 2016;71(3).

179. McNamara MA, Nair SK, Holl EK. RNA-Based Vaccines in Cancer Immunotherapy. Cools N, editor. J Immunol Res. 2015;2015:794528.

180. Kavanagh DG, Kaufmann DE, Sunderji S, Frahm N, Le Gall S, Boczkowski D, et al. Expansion of HIV-specific CD4+ and CD8+ T cells by dendritic cells transfected with mRNA encoding cytoplasm- or lysosome-targeted Nef. Blood. 2006;1;107(5):1963–9.

181. Melhem NM, Liu XD, Boczkowski D, Gilboa E, Barratt-Boyes SM. Robust CD4+ and CD8+ T cell responses to SIV using mRNA-transfected DC expressing autologous viral Ag. Eur J Immunol. 2007;1;37(8):2164–73.

182. Van Nuffel AMT, Benteyn D, Wilgenhof S, Pierret L, Corthals J, Heirman C, et al. Dendritic Cells Loaded With mRNA Encoding Full-length Tumor Antigens Prime CD4+ and CD8+ T Cells in Melanoma Patients. Mol Ther. 2012;20(5):1063–74.

183. Eisenächer K, Steinberg C, Reindl W, Krug A. The role of viral nucleic acid recognition in dendritic cells for innate and adaptive antiviral immunity. Immunobiology. 2007;212(9–10):701—714.

184. Wirth TC, Kühnel F. Neoantigen Targeting—Dawn of a New Era in Cancer Immunotherapy? Front Immunol. 2017;8:1848.

185. Sahin U, Derhovanessian E, Miller M, Kloke BP, Simon P, Löwer M, et al. Personalized RNA mutanome vaccines mobilize poly-specific therapeutic immunity against cancer. Nature. 2017;547(7662):222–6.

186. Conry RM, LoBuglio AF, Wright M, Sumerel L, Pike MJ, Johanning F, et al. Characterization of a Messenger RNA Polynucleotide Vaccine Vector. Cancer Res. 1995;55(7):1397–400.

187. Papachristofilou A, Hipp MM, Klinkhardt U, Früh M, Sebastian M, Weiss C, et al. Phase Ib evaluation of a self-adjuvanted protamine formulated mRNA-based active cancer immunotherapy, BI1361849 (CV9202), combined with local radiation treatment in patients with stage IV non-small cell lung cancer. J Immunother Cancer. 2019;7(1):38.

188. Boczkowski BD, Nair SK, Snyder D, Gilboa E. Dendritic Cells Pulsed with RNA are Potent Antigen-presenting Cells In Vitro and In Vivo. J Exp Med. 1996;184(2): 465–472.

189. Kyte JA, Mu L, Aamdal S, Kvalheim G, Dueland S, Hauser M, et al. Phase I/II trial of melanoma therapy with dendritic cells transfected with autologous tumor-mRNA. Cancer Gene Ther. 2006;13(10):905–18.

190. Wilgenhof S, Van Nuffel AMT, Benteyn D, Corthals J, Aerts C, Heirman C, et al. A phase IB study on intravenous synthetic mRNA electroporated dendritic cell immunotherapy in pretreated advanced melanoma patients. Ann Oncol. 2013;24(10):2686–93.

191. Wilgenhof S, Corthals J, Heirman C, Van Baren N, Lucas S, Kvistborg P, et al. Phase II study of autologous monocyte-derived mRNA electroporated dendritic cells (TriMixDC-MEL) plus ipilimumab in patientswith pretreated advanced melanoma. J Clin Oncol. 2016;34(12):1330–8.

192. Nogrady B. Gene therapy delivers hope. Nature, VOL 563 | S42-S43, 2018.

193. Rabinovich PM, Komarovskaya ME, Ye ZJ, Imai C, Campana D, Bahceci E, et al. Synthetic messenger RNA as a tool for gene therapy. Hum Gene Ther. 2006;17(10):1027–35.

194. Foster JB, Barrett DM, Karikó K. The Emerging Role of In Vitro-Transcribed mRNA in Adoptive T Cell Immunotherapy. Mol Ther . 2019;27(4):747–56.

195. Maus M V, Haas AR, Beatty GL, Albelda SM, Levine BL, Liu X, et al. T Cells Expressing Chimeric Antigen Receptors Can Cause Anaphylaxis in Humans. Cancer Immunol Res. 2013;1(1):26 LP – 31.

196. Svoboda J, Rheingold SR, Gill SI, Grupp SA, Lacey SF, Kulikovskaya I, et al. Nonviral RNA chimeric antigen receptor–modified T cells in patients with Hodgkin lymphoma. Blood. 2018;6;132(10):1022–6.

197. Tchou J, Zhao Y, Levine BL, Zhang PJ, Davis MM, Melenhorst JJ, et al. Safety and Efficacy of Intratumoral Injections of Chimeric Antigen Receptor (CAR) T Cells in Metastatic Breast Cancer. Cancer Immunol Res. 2017;1;5(12):1152 LP – 1161.

198. Jirikowski GF, Sanna PP, Maciejewski-Lenoir D, Bloom FE. Reversal of diabetes insipidus in Brattleboro tats: Intrahypothalamic injection of vasopressin mRNA. Science (80-). 1992;255(5047):996–8.

199. Trepotec Z, Lichtenegger E, Plank C, Aneja MK, Rudolph C. Delivery of mRNA Therapeutics for the Treatment of Hepatic Diseases. Mol Ther. 2019;27(4):794–802.

200. Sahu I, Haque AKMA, Weidensee B, Weinmann P, Kormann MSD. Recent Developments in mRNA-Based Protein Supplementation Therapy to Target Lung Diseases. Mol The. 2019;27(4):803–23.

201. Magadum A, Kaur K, Zangi L. mRNA-Based Protein Replacement Therapy for the Heart. Mol Ther. 2019;27(4):785–93.

202. Lescan M, Perl RM, Golombek S, Pilz M, Hann L, Yasmin M, et al. De Novo Synthesis of Elastin by Exogenous Delivery of Synthetic Modified mRNA into Skin and Elastin-Deficient Cells. Mol Ther - Nucleic Acids. 2018;11:475–84.

203. Patel S, Ryals RC, Weller KK, Pennesi ME, Sahay G. Lipid nanoparticles for delivery of messenger RNA to the back of the eye. J Control Release. 2019;303:91–100.

204. Baba M, Itaka K, Kondo K, Yamasoba T, Kataoka K. Treatment of neurological disorders by introducing mRNA in vivo using polyplex nanomicelles. J Control Release. 2015;201:41–8.

205. DeRosa F, Guild B, Karve S, Smith L, Love K, Dorkin JR, et al. Therapeutic efficacy in a hemophilia B model using a biosynthetic mRNA liver depot system. Gene Ther. 2016;23(10):699–707.

206. Zhu X, Yin L, Theisen M, Zhuo J, Siddiqui S, Levy B, et al. Systemic mRNA Therapy for the Treatment of Fabry Disease: Preclinical Studies in Wild-Type Mice, Fabry Mouse Model, and Wild-Type Non-human Primates. Am J Hum Genet. 2019;104(4):625–37.

207. An D, Schneller JL, Frassetto A, Liang S, Zhu X, Park JS, et al. Systemic Messenger RNA Therapy as a Treatment for Methylmalonic Acidemia. Cell Rep. 2017;21(12):3548–58.

208. Moderna [Internet]. Cambridge: Moderna, Inc; [cited 2020 Jan 30]. Available from: https://investors.modernatx.com/news-releases/news-release-details/moderna-announces-open-ind-propionic-acidemia-program-mrna-3927/.

209. Jiang L, Berraondo P, Jericó D, Guey LT, Sampedro A, Frassetto A, et al. Systemic messenger RNA as an etiological treatment for acute intermittent porphyria. Nat Med. 2018;24(12):1899–909.

210. Berraondo P, Martini PGV, Avila MA, Fontanellas A. Messenger RNA therapy for rare genetic metabolic diseases. Gut. 2019;68(7):1323–30.

211. Robinson E, MacDonald KD, Slaughter K, McKinney M, Patel S, Sun C, et al. Lipid Nanoparticle-Delivered Chemically Modified mRNA Restores Chloride Secretion in Cystic Fibrosis. Mol Ther. 2018;26(8):2034–46.

212. Carlsson L, Clarke JC, Yen C, Gregoire F, Albery T, Billger M, et al. Biocompatible, Purified VEGF-A mRNA Improves Cardiac Function after Intracardiac Injection 1 Week Post-myocardial Infarction in Swine. Mol Ther - Methods Clin Dev. 2018;9:330–46.

213. Gan L-M, Lagerström-Fermér M, Carlsson LG, Arfvidsson C, Egnell A-C, Rudvik A, et al. Intradermal delivery of modified mRNA encoding VEGF-A in patients with type 2 diabetes. Nat Commun. 2019;10(1):871.

214. Genetics Home reference. U.S. National Library of Medicine [Internet]. Bethesda: USA.gov; [cited 2020 Jan 30]. Available from: https://ghr.nlm.nih.gov/condition/propionic-acidemia.

215. Fraser JL, Venditti CP. Methylmalonic and propionic acidemias: Clinical management update. Curr Opin Pediatr. 2016;28(6):682–93.

216. Critelli K, McKiernan P, Vockley J, Mazariegos G, Squires RH, Soltys K, et al. Liver Transplantation for Propionic Acidemia and Methylmalonic Acidemia: Perioperative Management and Clinical Outcomes. Liver Transplant [Internet]. 2018;1;24(9):1260–70. Available from: https://doi.org/10.1002/lt.25304

217. Human Genomics in Global Health. Available online: https://www.who.int/genomics/public/geneticdiseases/en/index2.html#CF (accessed on 30 January 2020).

218. Zuckerman JB, McCoy K, Schechter MS, Dorgan D, Jain M, MacDonald KD, et al. Safety and Tolerability of a Single Dose of MRT5005, a Nebulized CFTR mRNA Therapeutic, in Adult CF Patients Poster presented at: North American Cystic Fibrosis Conference (NACFC); 2019 Oct 31 – Nov 2; Nashville, TN.

219. Waisbren SE, Gropman AL, Members of the Urea Cycle Disorders Consortium (UCDC), Batshaw ML. Improving long term outcomes in urea cycle disorders-report from the Urea Cycle Disorders Consortium. J Inherit Metab Dis. 2016;39(4):573–84.

220. Brassier A, Gobin S, Arnoux JB, Valayannopoulos V, Habarou F, Kossorotoff M, et al. Long-term outcomes in Ornithine Transcarbamylase deficiency: A series of 90 patients. Orphanet J Rare Dis. 2015;10(1):1–14.

221. Intrado [Internet]. Available online: https://www.globenewswire.com/news-release/2019/09/09/1913059/0/en/Translate-Bio-Announces-Pipeline-Program-Update.html (accessed on 30 January 2020).

222. Shim G, Kim D, Park GT, Jin H, Suh SK, Oh YK. Therapeutic gene editing: Delivery and regulatory perspectives. Acta Pharmacol Sin. 2017;38(6):738–53.

223. Conway A, Mendel M, Kim K, McGovern K, Boyko A, Zhang L, et al. Non-viral Delivery of Zinc Finger Nuclease mRNA Enables Highly Efficient In Vivo Genome Editing of Multiple Therapeutic Gene Targets. Mol Ther. 2019;27(4):866–77.

224. Gersbach CA, Gaj T, Barbas CF. Synthetic zinc finger proteins: The advent of targeted gene regulation and genome modification technologies. Acc Chem Res. 2014;47(8):2309–18.

225. Wang H, Yang H, Shivalila CS, Dawlaty MM, Cheng AW, Zhang F, et al. One-step generation of mice carrying mutations in multiple genes by CRISPR/cas-mediated genome engineering. Cell. 2013;153(4):910–8.

226. Zhang H-X, Zhang Y, Yin H. Genome Editing with mRNA Encoding ZFN, TALEN, and Cas9. Mol Ther 2019;10;27(4):735–46.

227. Crudele JM, Chamberlain JS. Cas9 immunity creates challenges for CRISPR gene editing therapies. Nat Commun. 2018;9(1):3497.

228. Wang J, Exline CM, DeClercq JJ, Llewellyn GN, Hayward SB, Li PW-L, et al. Homology-driven genome editing in hematopoietic stem and progenitor cells using ZFN mRNA and AAV6 donors. Nat Biotechnol. 2015;33(12):1256–63.

229. De Ravin SS, Reik A, Liu P-Q, Li L, Wu X, Su L, et al. Targeted gene addition in human CD34+ hematopoietic cells for correction of X-linked chronic granulomatous disease. Nat Biotechnol. 2016;34(4):424–9.

230. Wang J, DeClercq JJ, Hayward SB, Li PW-L, Shivak DA, Gregory PD, et al. Highly efficient homology-driven genome editing in human T cells by combining zinc-finger nuclease mRNA and AAV6 donor delivery. Nucleic Acids Res. 2015;2;44(3):e30–e30.

231. Wefers B, Panda SK, Ortiz O, Brandl C, Hensler S, Hansen J, et al. Generation of targeted mouse mutants by embryo microinjection of TALEN mRNA. Nat Protoc. 2013;8(12):2355–79.

232. Hwang WY, Fu Y, Reyon D, Maeder ML, Tsai SQ, Sander JD, et al. Efficient genome editing in zebrafish using a CRISPR-Cas system. Nat Biotechnol. 2013;31(3):227–9.

233. Wang H, Yang H, Shivalila CS, Dawlaty MM, Cheng AW, Zhang F, et al. One-Step Generation of Mice Carrying Mutations in Multiple Genes by CRISPR/Cas-Mediated Genome Engineering. Cell. 2013;153(4):910–8.

234. Watanabe M, Nakano K, Matsunari H, Matsuda T, Maehara M, Kanai T, et al. Generation of Interleukin-2 Receptor Gamma Gene Knockout Pigs from Somatic Cells Genetically Modified by Zinc Finger Nuclease-Encoding mRNA. PLoS One. 2013;8(10):e76478.

235. Miller JB, Zhang S, Kos P, Xiong H, Zhou K, Perelman SS, et al. Non-Viral CRISPR/Cas Gene Editing In Vitro and In Vivo Enabled by Synthetic Nanoparticle Co-Delivery of Cas9 mRNA and sgRNA. Angew Chemie - Int Ed. 2017;56(4):1059–63.

236. Liu J, Chang J, Jiang Y, Meng X, Sun T, Mao L, et al. Fast and Efficient CRISPR/Cas9 Genome Editing In Vivo Enabled by Bioreducible Lipid and Messenger RNA Nanoparticles. Adv Mater. 2019;31(33):1902575.

237. Samson M, Libert F, Doranz BJ, Rucker J, Liesnard C, Farber C-M, et al. Resistance to HIV-1 infection in Caucasian individuals bearing mutant alleles of the CCR-5 chemokine receptor gene. Nature. 1996;382(6593):722–5.

238. Ware RE, de Montalembert M, Tshilolo L, Abboud MR. Sickle cell disease. Lancet. 2017;390(10091):311–23.

239. Smith EC, Luc S, Croney DM, Woodworth MB, Greig LC, Fujiwara Y, et al. Strict in vivo specificity of the Bcl11a erythroid enhancer. Blood. 2016;128(19):2338–42.

240. Qasim W, Zhan H, Samarasinghe S, Adams S, Amrolia P, Stafford S, et al. Molecular remission of infant B-ALL after infusion of universal TALEN gene-edited CAR T cells. Sci Transl Med. 2017;9(374):eaaj2013.

241. Jo J-I, Gao J-Q, Tabata Y. Biomaterial-based delivery systems of nucleic acid for regenerative research and regenerative therapy. Regen Ther. 2019;11:123–30.

242. Jopling C, Boue S, Belmonte JCI. Dedifferentiation, transdifferentiation and reprogramming: Three routes to regeneration. Nat Rev Mol Cell Biol. 2011;12(2):79–89.

243. Eguizabal C, Carlos J, Belmonte I. Reprogramming : Future Directions in Regenerative Medicine. Semin Reprod Med. 2013;31:82–94.

244. Yakubov E, Rechavi G, Rozenblatt S, Givol D. Reprogramming of human fibroblasts to pluripotent stem cells using mRNA of four transcription factors. Biochem Biophys Res Commun. 2010;394(1):189–93.

245. Takahashi K, Yamanaka S. Induction of Pluripotent Stem Cells from Mouse Embryonic and Adult Fibroblast Cultures by Defined Factors. Cell. 2006;126(4):663–76.

246. Warren L, Manos PD, Ahfeldt T, Loh YH, Li H, Lau F, et al. Highly efficient reprogramming to pluripotency and directed differentiation of human cells with synthetic modified mRNA. Cell Stem Cell. 2010;7(5):618–30.

247. Corritore E, Lee Y-S, Pasquale V, Liberati D, Hsu M-J, Lombard CA, et al. V-Maf Musculoaponeurotic Fibrosarcoma Oncogene Homolog A Synthetic Modified mRNA Drives Reprogramming of Human Pancreatic Duct-Derived Cells Into Insulin-Secreting Cells. Stem Cells Transl Med. 2016;5(11):1525–37.

248. Orlando G, Gianello P, Salvatori M, Stratta RJ, Soker S, Ricordi C, et al. Cell Replacement Strategies Aimed at Reconstitution of the β-Cell Compartment in Type 1 Diabetes. Diabetes. 2014;63(5):1433 LP – 1444.

249. Koblas T, Leontovyc I, Loukotova S, Kosinova L, Saudek F. Reprogramming of Pancreatic Exocrine Cells AR42J Into Insulin-producing Cells Using mRNAs for Pdx1, Ngn3, and MafA Transcription Factors. Mol Ther - Nucleic Acids. 2016;5:e320.

250. Park JS, Suryaprakash S, Lao YH, Leong KW. Engineering mesenchymal stem cells for regenerative medicine and drug delivery. Methods. 2015;84:3–16.

251. Ryser MF, Ugarte F, Thieme S, Bornhäuser M, Roesen-Wolff A, Brenner S. mRNA Transfection of CXCR4-GFP Fusion—Simply Generated by PCR—Results in Efficient Migration of Primary Human Mesenchymal Stem Cells. Tissue Eng Part C Methods. 2008;14(3):179–84.

252. Nowakowski A, Andrzejewska A, Boltze J, Nitzsche F, Cui LL, Jolkkonen J, et al. Translation, but not transfection limits clinically relevant, exogenous mRNA based induction of alpha-4 integrin expression on human mesenchymal stem cells. Sci Rep. 2017;7(1):1–12.

253. Levy O, Zhao W, Mortensen LJ, Leblanc S, Tsang K, Fu M, et al. mRNA-engineered mesenchymal stem cells for targeted delivery of interleukin-10 to sites of inflammation. Blood. 2013/08/26. 2013;122(14):e23–32.

APPENDIX II:

Nucleic acid delivery by solid lipid nanoparticles containing switchable lipids: plasmid DNA vs messenger RNA

Itziar Gómez-Aguado, Julen Rodríguez-Castejón, Mónica Vicente-Pascual, Alicia Rodríguez-Gascón, Ana del Pozo-Rodríguez, María Ángeles Solinís Aspiazu

Published in: Molecules (2020)

Journal Impact Factor JCR 2020: 4.412 (Q2) 115/295

Related Categories:

BIOCHEMISTRY & MOLECULAR BIOLOGY (Q2)

CHEMISTRY, MULTIDISCIPLINARY (Q2)

Other quality indicators: 6 citations

Nucleic acid delivery by solid lipid nanoparticles containing switchable lipids: plasmid DNA vs messenger RNA

Abstract:

The development of safe and effective nucleic acid delivery systems remains a challenge, with solid lipid nanoparticle (SLN)-based vectors as one of the most studied systems. In this work, different SLNs were developed by combination of cationic and ionizable lipids for delivery of mRNA and pDNA. The influence of formulation factors on transfection efficacy, protein expression and intracellular disposition of the nucleic acid was evaluated in human retinal pigment epithelial cells (ARPE-19) and human embryonic kidney cells (HEK-293). A long-term stability study of the vectors was also performed. mRNA formulations induced a higher percentage of transfected cells than those containing pDNA, mainly in ARPE-19 cells, although pDNA formulations induced a greater protein production per cell in this cell line. Protein production was conditioned by energy-dependent or independent entry mechanisms depending on the cell line, SLN composition and kind of nucleic acid delivered. Vectors containing DOTAP as unique cationic lipid showed better stability after seven months, which improved with the addition of a polysaccharide to the vectors. Transfection efficacy and long-term stability of mRNA vectors were more influenced by formulation-related factors than those containing pDNA; in particular, the SLNs containing only DOTAP were the most promising formulations for nucleic acid delivery.

Keywords: gene therapy; solid lipid nanoparticles; pDNA; mRNA; cationic lipid; ionizable lipid; intracellular disposition; long-term storage

1. Introduction

With the development of RNA-based products, the potential of therapeutic targets has expanded significantly. The United States Food and Drug Administration (FDA) has authorized a number of RNA drugs targeted to various human diseases. These RNA drugs include aptamer RNAs (e.g. pegaptanib), antisense oligonucleotides (ASOs) or antisense RNAs (asRNAs) (e.g. mipomersen, eteplirsen, nusinersen, inotersen and golodirsen), and short interfering RNAs (siRNAs) (e.g. patisiran and givosiran) [1]. Additionally, the development and use of messenger RNA (mRNA) also has broad potential for the treatment of human infections, cancers and genetic disorders, by means of protein replacement therapy, vaccination and antibody therapy [2,3]. Moreover, mRNAs are a promising tool for use in the expanding area of genome editing [4,5].

Classically, all these therapeutic applications have been addressed through the administration of plasmid DNA (pDNA). However, mRNA possess specific characteristics that make it a promising alternative to pDNA [6]. From a safety point of view, mRNA is not integrated into the cell genome, and the risk of carcinogenesis and mutagenesis is much lower than with pDNA. Regarding the protein expression, it is faster and temporary (actually, the expression can be detected within 1 h after transfection [7,8]). An additional advantage is that the production and manufacturing is simpler than that of DNA, and it can be standardized while maintaining reproducibility. Finally, from a delivery point of view, mRNA must only reach the cytoplasm to interact with the cellular translation machinery, whereas pDNA requires entry into the nucleus, which is one of the most limiting steps for transfection.

Many mRNA based therapies have already entered clinical trials [9–12], although the construction of safe and effective delivery systems remains a challenge. The desired pharmacological effect will be only achieved if a sufficient number of RNA molecules access the intracellular environment. An optimal delivery system should avoid the degradation of the mRNA by serum RNases and allow it to pass through the target cell membranes. Significant attention is focused on the development of biocompatible carriers, such as lipid nanoparticles (LNPs), polymer nanoparticles, complexes formed by proteins or peptides and mRNA, among others. In particular, lipid-based nanomaterials are currently one of the most promising biomaterials that mediate effective mRNA delivery, with LNPs as the most advanced vector and the delivery vehicle of choice for mRNA [13]. Solid lipid nanoparticles (SLNs) are a kind of LNP regarded as one of the most versatile and effective non-viral vector in gene therapy [14]. Our research group has developed SLNs based on cationic lipids for pDNA administration, which have proven to be effective in different in vitro and in vivo applications, including a murine model of retinoschisis, a degenerative retinal disease [15,16]. SLNs are formed by well-tolerated physiological lipids as solid lipid core matrix dispersed in aqueous solution stabilized by surfactants, which usually includes cationic lipids that allows electrostatic interactions with nucleic acids [17,18]. One of the advantages of this versatile delivery system is that it can be reformulated depending of the features of the genetic material to be delivered. In this sense, nowadays, nanocarriers containing ionizable or switchable cationic lipids are among the leading delivery system candidates with promising applications for mRNA delivery [19]. Cationic lipids are a critical component of these lipidic systems, whose function is to interact with the mRNA leading to the formation of a lipoplex. The traditional cationic lipid DOTAP is one of the most used for mRNA delivery. This lipid is completely protonated at pH 7.4, so it has been postulated that for successful transfection, high energy is required for the separation of nucleic acid from

the lipoplex. Thus, to improve its efficacy in nucleic acid delivery, DOTAP should be combined with a helper lipid [20]; in fact, it is frequently combined with the zwitterionic lipid DOPE (dioleoylphosphatidylethanolamine). The use of ionizable lipids such as DODAP and DOBAQ is a more recent strategy; these lipids are neutral at physiological pH but become protonated in the acidic environment of the endosome. The electrostatic interactions between the lipids of the endosomal membranes and the ionizable cationic lipids promote membrane lytic nonbilayer structures such as the hexagonal HII phase, facilitating the endosomal scape and the intracellular nucleic acid delivery [21,22].

The aim of the present work was to evaluate the influence of formulation factors in the efficacy of SLNs as pDNA or mRNA delivery systems. Different non-viral vectors formulated with SLNs composed by combinations of cationic lipids and ionizable cationic lipids were characterized in terms of size, polidispersity index and zeta potential, as well as their capacity to bind protect and release the nucleic acids. The transfection efficacy was assessed in vitro in two cell models (ARPE-19 and HEK-293), and the cellular uptake and intracellular disposition of the genetic material were also evaluated. Finally, a long-term stability study of the vectors was performed.

2. Results

2.1. Size, polydispersity index and ζ-potential of SLNs and vectors

Table 1 shows the mean diameter, polydispersity index (PDI) and ζ-potential of the SLNs prepared with different combinations of cationic and ionizable lipids. SLN1, SLN2 and SLN4 showed similar particle size ranging from 185 to 211 nm, PDI values lower than 0.4, and superficial charge higher than +40 mV. However, SLN3, prepared without the cationic lipid DOTAP, presented particle size higher than 400 nm, PDI higher than 0.5, and negative surface charge of -28 mV. Considering these results, SLN3 formulation was discarded for preparing vectors.

Table 1. Physical characterization of SLNs.

SLNs	Cationic/ionizable lipid	Size (nm)	PDI	ζ-Potential (mV)
SLN1	DOTAP/-	185.1 ± 3.5	0.30 ± 0.03	+59.5 ± 1.9 $^{\&}$
SLN2	DOTAP/DODAP	208.8 ± 0.4	0.27 ± 0.01	+50.2 ± 1.1 $^{\&}$
SLN3	-/DOBAQ	423.5 ± 51.7 ***	0.57 ± 0.05	-28.0 ± 0.8 $^{\&}$
SLN4	DOTAP/DOBAQ	211.3 ± 3.5	0.36 ± 0.01	+42.4 ± 1.2 $^{\&}$

*** $p < 0.001$ with respect to SLN1, SLN2 and SLN4. $^{\&}$ $p < 0.001$ with respect to the all SLNs. SLN: solid lipid nanoparticle. PDI: polydispersity index. $n = 3$; data are expressed as mean ± standard deviation.

Table 2 shows the size, PDI and ζ-potential of the SLN-based vectors containing either CleanCap™ EGFP mRNA (5moU) or pcDNA3-EGFP plasmid , which encode the enhanced green fluorescent protein (EGFP). All vectors contained protamine (P), and some of them a polysaccharide, dextran (DX) or hyaluronic acid (HA). Particle size ranged from 176 nm to 349 nm, PDIs was lower than 0.4, and surface charge ranged from +18 to +45 mV.

Table 2. Physical characterization of SLNs-based vectors.

Nucleic acid	Vectors	Size (nm)	PDI	ζ-Potential (mV)
pcDNA3-EGFP plasmid	pDNA-DX-SLN1	176.4 ± 0.4	0.27 ± 0.01	+45.4 ± 2.7
	pDNA-DX-SLN2	165.8 ± 1.7	0.27 ± 0.01	+42.2 ± 0.9
	pDNA-DX-SLN4	211.9 ± 14.6 *	0.40 ± 0.07 ###	+32.6 ± 0.9
	pDNA-HA-SLN1	201.2 ± 1.3	0.17 ± 0.01	+29.8 ± 1.1 &&&
	pDNA-HA-SLN2	194.2 ± 0.8	0.20 ± 0.00	+35.6 ± 1.9 &
CleanCap™ EGFP mRNA (5moU)	mRNA-DX-SLN1	246.8 ± 1.3	0.39 ± 0.02	+37.2 ± 1.0
	mRNA-DX-SLN2	210.1 ± 0.8 **	0.26 ± 0.01	+36.5 ± 0.3
	mRNA-HA-SLN1	202.4 ± 2.2 **	0.35 ± 0.00	+27.5 ± 0.6
	mRNA-HA-SLN2	349.2 ± 9.9 •••	0.39 ± 0.02	+18.5 ± 0.9 •
	mRNA-P0.25-SLN1	251.6 ± 6.5	0.35 ± 0.01	+28.8 ± 0.7
	mRNA-P0.5-SLN2	233.7 ± 2.8	0.24 ± 0.00	+25.4 ± 0.6
	mRNA-P1-SLN2	261.7 ± 4.0	0.29 ± 0.02	+23.1 ± 1.3

* $p < 0.05$ with respect to pDNA-DX-SLN2. ** $p < 0.01$ with respect to mRNA-DX-SLN1, mRNA-P0.25-SLN1, mRNA-P0.5-SLN2 and mRNA-P1-SLN2. ••• $p < 0.001$ with respect to the rest of mRNA vectors. ### $p < 0.001$ with respect to the rest of pDNA vectors. & $p < 0.05$ with respect to mRNA-HA-SLN1. &&& $p < 0.001$ with respect to pDNA-DX-SLN1 and pDNA-DX-SLN2. • $p < 0.05$ with respect to mRNA-DX-SLN1 and mRNA-DX-SLN2. PDI: polydispersity index; DX: dextran; HA: hyaluronic acid; P: protamine; SLN: solid lipid nanoparticle. $n = 3$; data are expressed as mean ± standard deviation.

No significant difference in particle size, PDI or ζ-potential was observed when SLNs were labeled with Nile Red (data not shown).

2.2. Transmission Electron Microscopy (TEM) images

Figure 1 shows TEM photographs of mRNA- vectors. In all cases, except for mRNA-P-SLN2, the structure appears compact and homogenous with an external layer (black arrows) surrounding the electro-dense nucleus. When mRNA was complexed with P and SLN2 (without polysaccharide), last image in the right, a characteristic multilamellar internal structure can be observed.

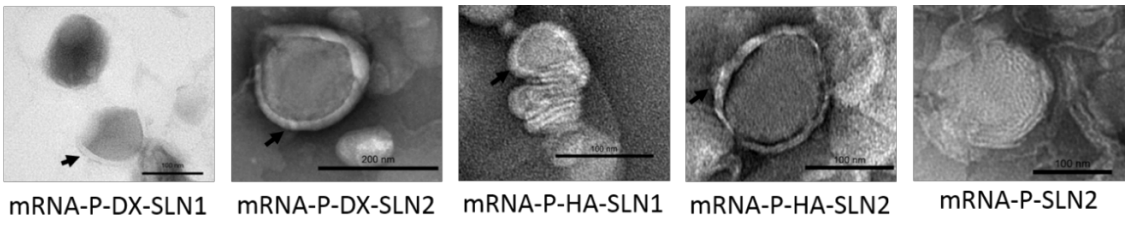

Figure 1. Images of mRNA combined with P, a polysaccharide (DX or HA) and SLN1 or SLN2, acquired by TEM. Black arrows indicate an external layer surrounding the electro-dense nucleus of the vectors.

2.3. Binding, protection and release of nucleic acids

Figure 2 shows the ability of SLN1 and SLN2 vectors to bind, protect and release the pDNA (Figure 2A) and mRNA (Figure 2B), respectively.

Regarding the binding capacity, in both gels the absence of bands on the corresponding lanes and the presence of pDNA (Figure 2A) and mRNA (Figure 2B) on the loading wells indicate that the nucleic acid was unable to migrate through the gel, and therefore, it was completely bound to the vector.

Moreover, all pDNA-based formulations were able to protect the plasmid when treated with DNase I, while free pDNA was totally degraded. After the treatment with SDS, pDNA was able to migrate from the loading wells, which demonstrates its ability to be released from SLN1 and SLN2 vectors.

In the case of mRNA-based systems, differences in the protection were detected depending on the composition of the vector. Bands corresponding to the vectors prepared with SLN1 and DX or HA were more intense, which indicates a higher protection degree of the nucleic acid. All formulations were capable to release the mRNA after the treatment with SDS.

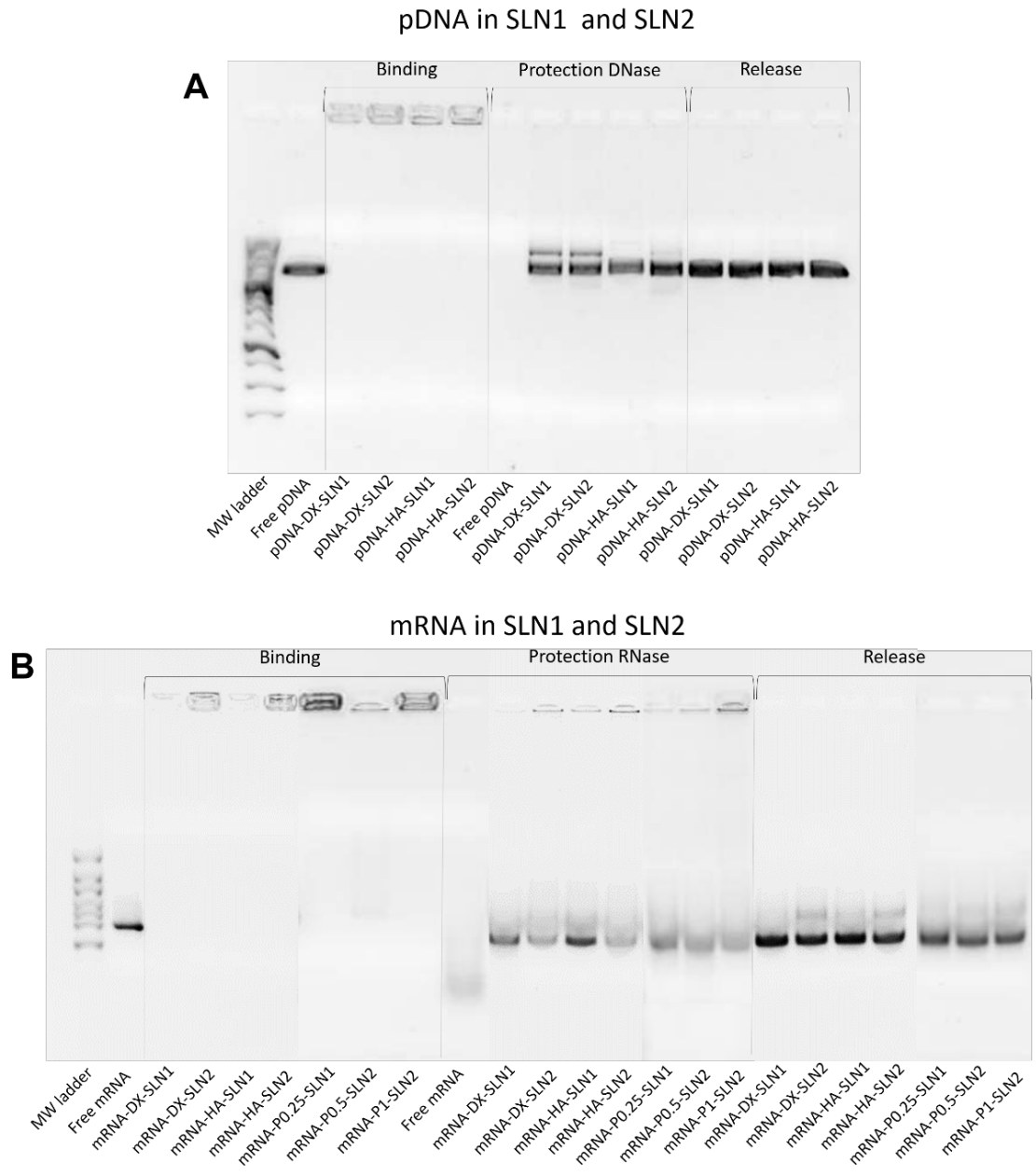

Figure 2. Binding, protection and release capacity of pDNA- and mRNA-based vectors. A: pDNA-SLN1 and pDNA-SLN2 vectors. B: mRNA-SLN1 and mRNA-SLN2 vectors.

The evaluation of the formulations prepared with SLN4 revealed a low capacity to protect the pDNA (supplementary material Figure S1), and therefore, they were excluded for following experiments.

2.4. Cell culture studies

2.4.1. Transfection efficacy and cell viability in ARPE-19 cells

Figure 3 shows the percentage of transfected cells and intensity of fluorescence of ARPE-19 cells treated with SLN1- and SLN2-based vectors at 37 °C and 4 °C.

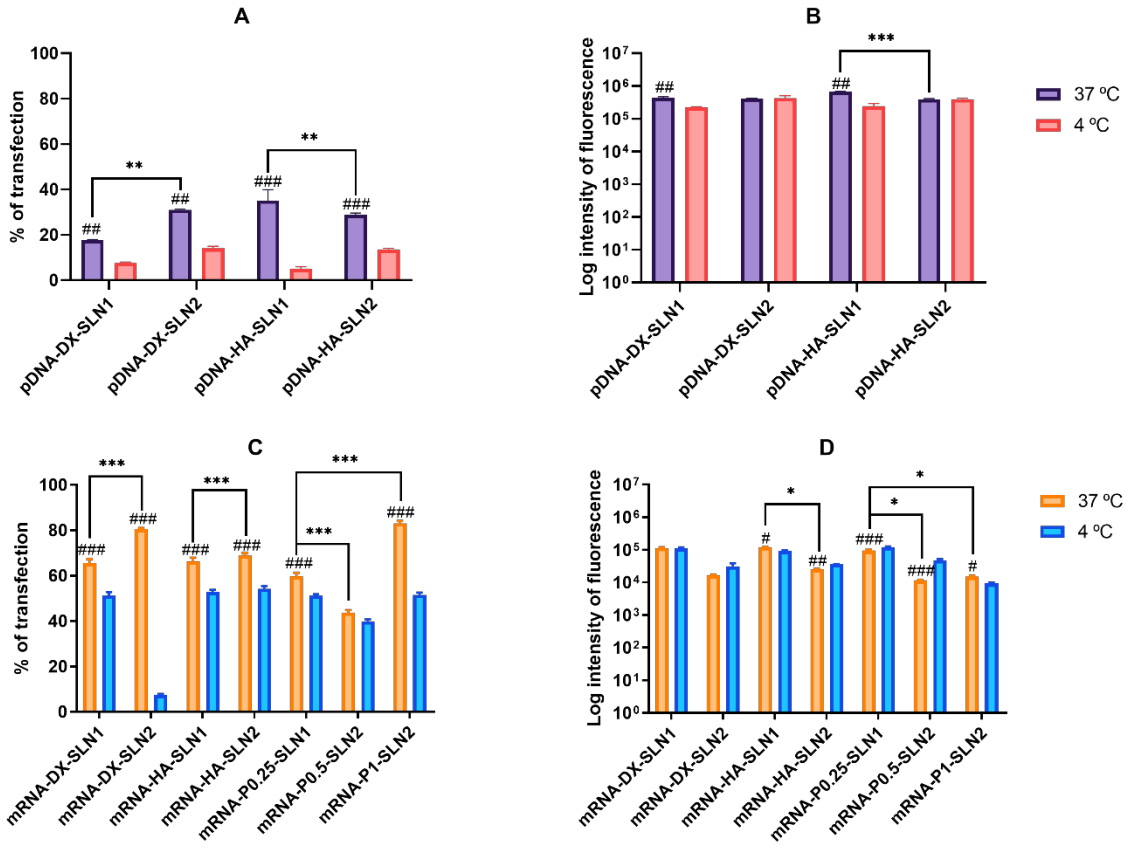

*Figure 3. Percentage of transfected cells and intensity of fluorescence of ARPE-19 cells after incubation with SLN1- and SLN2-based vectors at 37 °C and 4 °C. n = 3; data are expressed as mean ± standard deviation. A: Percentage of transfected ARPE-19 cells 72 h after treatment with pDNA vectors. B: Intensity of fluorescence of transfected ARPE-19 cells 72 h after treatment with pDNA vectors. C: Percentage of transfected ARPE-19 cells 48 h after treatment with mRNA vectors. D: Intensity of fluorescence of transfected ARPE-19 cells 48 h after treatment with mRNA vectors. # p < 0.05 with respect to the same vector at 4 °C. ## p < 0.01 with respect to the same vector at 4 °C. ### p < 0.001 with respect to the same vector at 4 °C. * p < 0.05 with respect to the other formulation. ** p < 0.01 with respect to the other formulation. *** p < 0.001 with respect to the other formulation.*

At 37 °C, pDNA-based vectors (Figure 3A) induced lower percentage of transfected cells than mRNA-based vectors (Figure 3C). However, the vectors prepared with pDNA (Figure 3B) provided higher fluorescence intensities than those containing mRNA (Figure 3D).

Regarding pDNA vectors, at 37 °C the percentage of transfected cells (Figure 3A) observed was 35% and 20% for pDNA-HA-SLN1-and pDNA-DX-SLN1, respectively. SLN2-based formulations presented a 30% of transfected cells regardless the polysaccharide used. In terms of intensity (Figure 3B), pDNA-HA-SLN1 showed the highest value ($p < 0.001$). At 4 °C, the percentage of transfected cells decreased with all formulations, ranging from 5% to 14% (Figure 3A), although the fluorescence intensity only diminished in the case of SLN1-based vectors (Figure 3B).

At 37 °C, although the highest values of transfected cells with mRNA-based vectors were observed with SLN2 formulations, in particular for mRNA-DX-SLN2 and mRNA-P1-SLN2 (Figure 3C), the vectors prepared with SLN1 were much more effective in terms of intensity of fluorescence (Figure 3D). At 4 °C, the percentage of transfected cells decreased, especially in the case of mRNA-DX-SLN2 (Figure 3C).

Cell viability, of ARPE-19 cells treated with the SLN-based vectors was around 100% at either 37 °C or 4 °C.

2.4.2. Transfection efficacy and cell viability in HEK-293 cells.

Figure 4 shows the percentage of transfected cells and intensity of fluorescence of HEK-293 cells treated with SLN1- and SLN2-based vectors at 37 °C and 4 °C.

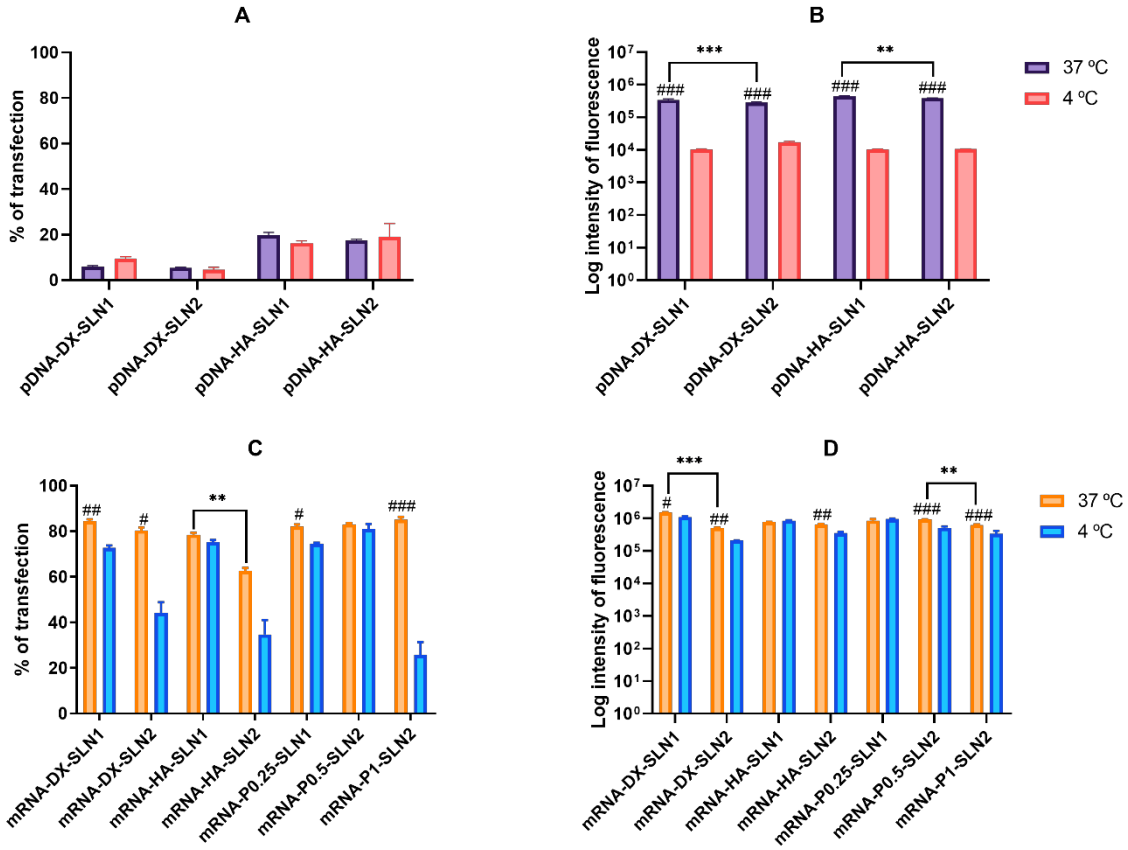

*Figure 4. Percentage of transfected cells and intensity of fluorescence of HEK-293 cells after incubation with SLN1- and SLN2-based vectors at 37 °C and 4 °C. n = 3; data are expressed as mean ± standard deviation. A: Percentage of transfected HEK-293 cells 72 h after treatment with pDNA vectors. B: Intensity of fluorescence of transfected HEK-293 cells 72 h after treatment with pDNA vectors. C: Percentage of transfected HEK-293 cells 48 h after treatment with mRNA vectors. D: Intensity of fluorescence of transfected HEK-293 cells 48 h after treatment with mRNA vectors. # p < 0.05 with respect to the same vector at 4 °C. ## p < 0.01 with respect to the same vector at 4 °C. ### p < 0.001 with respect to the same vector at 4 °C. ** p < 0.01 with respect to the other formulation. *** p < 0.001 with respect to the other formulation.*

The percentage of transfected cells with pDNA-based vectors ranged from 5% to 20% at 37 °C (Figure 4A), and, as in ARPE-19 cells, it was significantly lower than that achieved with mRNA-based vectors (60%-80%) (Figure 4C). Nevertheless, contrary to that observed in ARPE-19 cells, the vectors prepared with mRNA also provided the highest fluorescence intensities (Figure 4D).

In the case of pDNA-based vectors, at 37 °C the inclusion of HA in the formulation provided the highest percentage of transfection ($p < 0.01$). At 4 °C, the percentage of transfected cells was similar to that observed at 37 °C, but there was a drastic reduction in the fluorescence intensity for all formulations (Figure 4B).

mRNA-based vectors showed a similar percentage of transfected cells at 37 °C, over 80%, except for mRNA-HA-SLN2, which presented a percentage of 60% (Figure 4C). Intensity of fluorescence was higher for SLN1 formulations than for SLN2 (Figure 4D). At 4 °C the percentage of transfected cells decreased significantly with all formulations, except for mRNA-HA-SLN1 and mRNA-P0.5-SLN2 (Figure 4C), and the intensity of fluorescence decreased for SLN2 formulations and mRNA DX-SLN1 (Figure 4D).

Cell viability, was close to 100% and over 85% for pDNA and mRNA-based vectors, respectively, at either 37 °C or 4 °C.

2.4.3. Cellular uptake in ARPE-19 cells

Figure 5 shows the efficacy of cell internalization in ARPE-19 cells at 37 °C and 4 °C. For this study, cells were treated with the pDNA- and mRNA based vectors labelled with Nile Red, and the uptake was measured 2 hours later. The histograms showing the cellular uptake are included in supplementary material (Figure S2 and Figure S3).

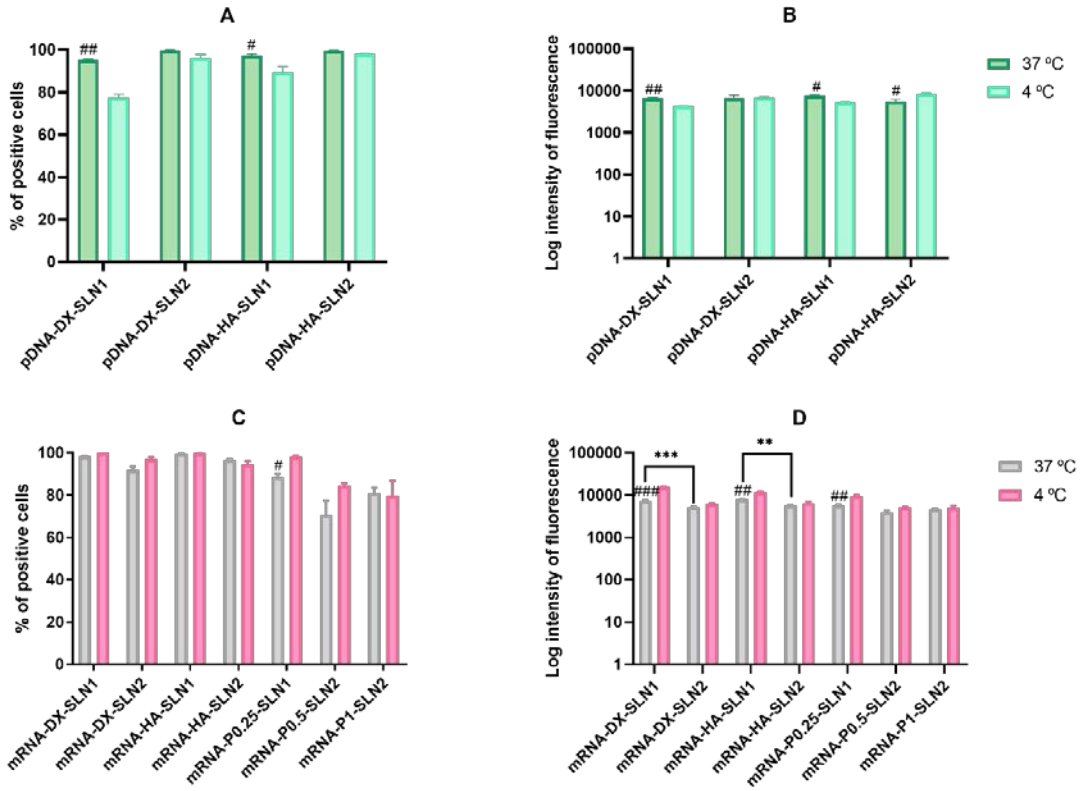

*Figure 5. Flow cytometry analysis of cellular uptake of vectors using Nile Red-labelled pDNA- and mRNA-SLNs in ARPE-19 cells at 37 °C and 4 °C. n = 3; data are expressed as mean ± standard deviation. A: Percentage of Nile Red positive ARPE-19 cells 2 h after the treatment with pDNA vectors. B: Intensity of fluorescence of Nile Red positive ARPE-19 cells 2 h after the treatment with pDNA vectors. C: Percentage of Nile Red positive ARPE-19 cells 2 h after the treatment with mRNA vectors. D: Intensity of fluorescence of Nile Red positive ARPE-19 cells 2 h after the treatment with mRNA vectors. # $p < 0.05$ with respect to the same vector at 4 °C. ## $p < 0.01$ with respect to the same vector at 4 °C. ### $p < 0.001$ with respect to the same vector at 4 °C. ** $p < 0.01$ with respect to the other formulation. *** $p < 0.001$ with respect to the other formulation.*

In the case of pDNA-based vectors, the percentage of positive cells (Figure 5A) was over 90% at 37 °C, but it decreased at 4 °C with SLN1 formulations. The intensity of fluorescence (Figure 5B) at 37 °C was also similar with all formulations. At 4 °C, the intensity also decreased for SLN1-based vectors whereas it was similar or even higher for pDNA-DX-SLN2 and pDNA-HA-SLN2, respectively (Figure 5B).

In the case of mRNA-based vectors, the percentage of positive cells (Figure 5C) at 37 °C was over 92% for mRNA-DX-SLN1, mRNA-DX-SLN2, mRNA-HA-SLN1 and mRNA-HA-SLN2, whereas it ranged from 70% to 88% for the formulations prepared without polysaccharide. The percentage of entry was similar at 4 °C, but the intensity of fluorescence increased for SLN1-based formulations (Figure 5D).

2.4.4. Cellular uptake of the vectors in HEK-293 cells

Figure 6 shows the cell uptake and intensity of fluorescence of pDNA- and mRNA-based vectors labelled with Nile Red. HEK-293 cells were treated with the vectors at both 37 °C and 4 °C, and cell uptake was measured 2 hours later. The histograms showing the cellular uptake are included in supplementary material (Figure S4 and Figure S5).

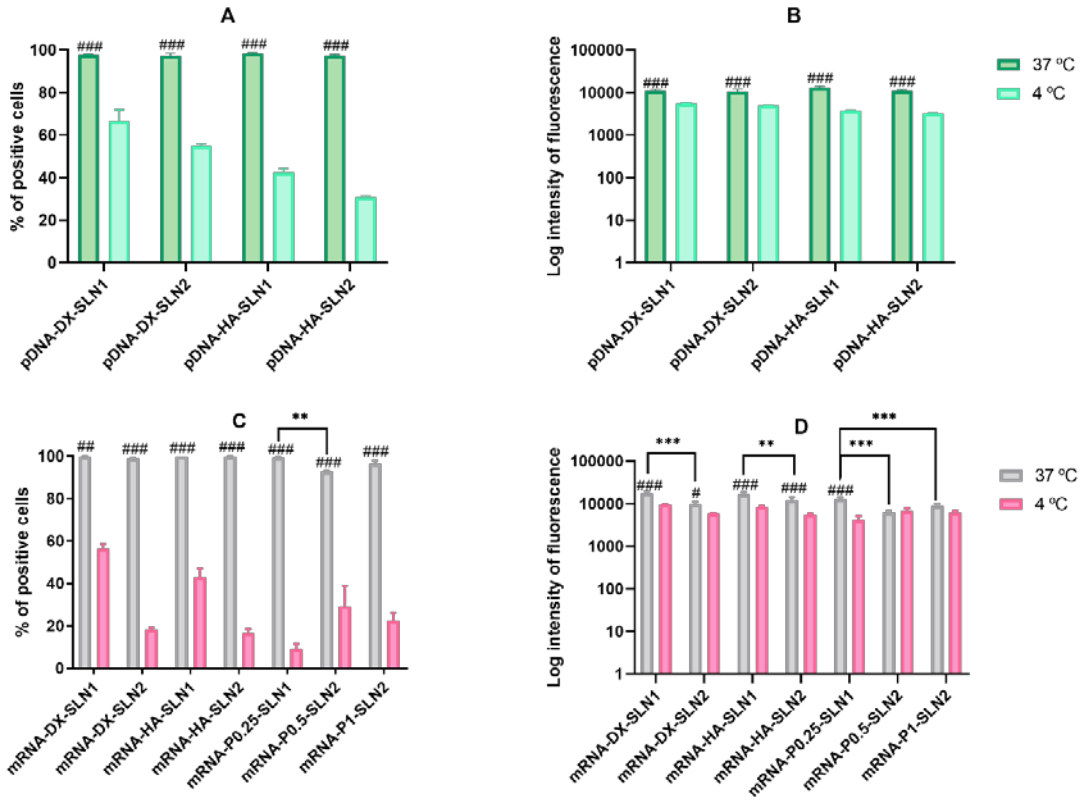

*Figure 6. Flow cytometry analysis of cellular uptake of vectors using Nile Red-labelled pDNA- and mRNA-SLNs in HEK-293 cells at 37 °C and 4 °C. n = 3; data are expressed as mean ± standard deviation. A: Percentage of Nile Red positive HEK-293 cells 2 h after the treatment with pDNA vectors. B: Intensity of fluorescence of Nile Red positive HEK-293 cells 2 h after the treatment with pDNA vectors. C: Percentage of Nile Red positive HEK-293 cells2 h after the treatment with mRNA vectors. D: Intensity of fluorescence of Nile Red positive HEK-293 cells 2 h after the treatment with mRNA vectors. # $p < 0.05$ with respect to the same vector at 4 °C. ## $p < 0.01$ with respect to the same vector at 4 °C. ### $p < 0.001$ with respect to the same vector at 4 °C. ** $p < 0.01$ with respect to the other formulation. *** $p < 0.001$ with respect to the other formulation.*

In the case of pDNA-based vectors (Figure 6A), the percentage of positive cells was near 100% at 37 °C, whereas at 4 °C the entry decreased drastically by more than a half with HA containing vectors, and around a 50% with DX containing vectors. This reduction was also observed in terms of intensity (Figure 6B).

The entry of mRNA-based vectors at 37 °C (Figure 6C) was also close to 100% with all formulations, and, as in the case of pDNA-based vectors, the entry at 4 °C decreased extremely.

The intensity of fluorescence (Figure 6D) was higher with SLN1 formulations than with SLN2 at 37 °C, and a drastic decrease on the intensity was observed at 4 °C, except for mRNA-P0.5-SLN2 and mRNA-P1-SLN2.

2.4.5. Intracellular disposition of non-viral vectors

Figure 7 shows the intracellular disposition of pDNA and mRNA in ARPE-19 and HEK-293 cells. Differences in the nucleic acid disposition depending on the formulation and on the cell line were observed.

In ARPE-19 cells, the disposition of pDNA was similar with all formulations. However, in HEK-293 cells, pDNA dots were smaller with the vectors DX-SLN1 and HA-SLN2.

In both cell lines, mRNA appeared less dispersed along the cytoplasm when formulated in the vectors prepared with SLN1. This behaviour is more noticeable in HEK-293 than in ARPE-19 cells.

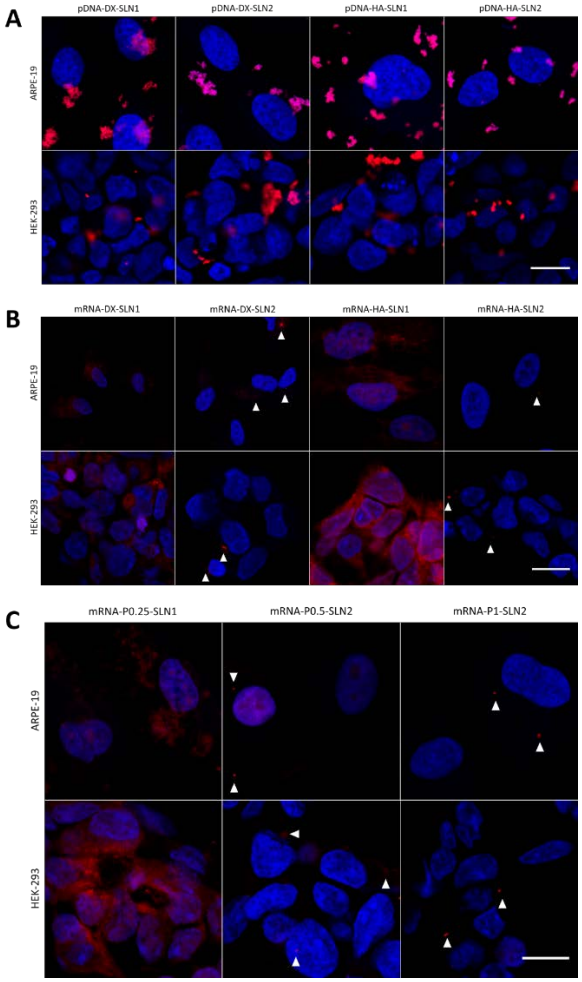

Figure 7. Fluorescence microscopy images 4 h after the addition of SLN1- and SLN2-based vectors in ARPE-19 and HEK-293 cells. A: pcDNA3-EGFP plasmid labelled with Label IT® Cy®5 vectors. B: CleanCap™ Cyanine 5 EGFP mRNA (5moU) vectors formulated with P, DX and HA. C: CleanCap™ Cyanine 5 EGFP mRNA (5moU) vectors formulated with P. Nuclei were labeled with DAPI (blue). Magnification 60×.Scale bar: 15 µm. White arrows indicate the condensed mRNA.

2.5. Long-term stability study of pDNA- and mRNA-based vectors

2.5.1. Size, polydispersity index and ζ-potential

Figure 8 and Figure 9 present the characterization data of pDNA- and mRNA-based vectors, respectively over 1, 2 3 and 7 months. The particle size and PDI of pDNA formulations increased after 2 months of storage at 4 °C (Figure 8A and 8B); the change of the size was higher for the vectors containing HA. After 2 months, the PDI of pDNA-DX-SLN1 and pDNA-DX-SLN2 increased above 0.4. ζ-potential of SLN1 vectors was maintained during the 7 months, but it decreased in the case of SLN2 formulations (Figure 8C).

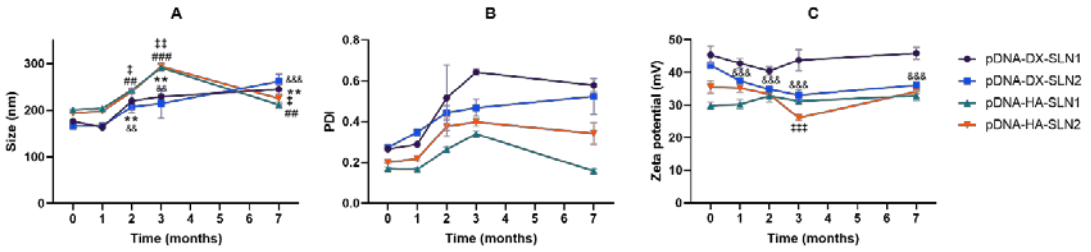

*Figure 8. Size (A), polydispersity index (B) and ζ-potential (C) of pDNA-based vectors formulated with SLN1 and SLN2 at time zero, 1, 2 and 3 months. n = 3; data are expressed as mean ± standard deviation. ** p < 0.01 with respect to mRNA-DX-SLN1 at time 0. && p < 0.01, &&& p < 0.001 with respect to pDNA-DX-SLN2 at time 0. ## p < 0.01, ### p < 0.001 with respect to pDNA-HA-SLN1 at time 0. ‡ p < 0.05, ‡‡ p < 0.01, ‡‡‡ p < 0.001 with respect to pDNA-HA-SLN2 at time 0.*

In the case of mRNA formulations, after 7 months the mean size (Figure 9A) changed significantly for mRNA-P0.5-SLN2 and mRNA-DX-SLN1; it decreased 20 nm and 40 nm, respectively. PDI values were below 0.4 during the stability study (Figure 9B). Differences were observed after 2 months in ζ-potential for mRNA-DX-SLN1, and at month 7 for all formulations except for mRNA-DX-SLN2 (Figure 9C).

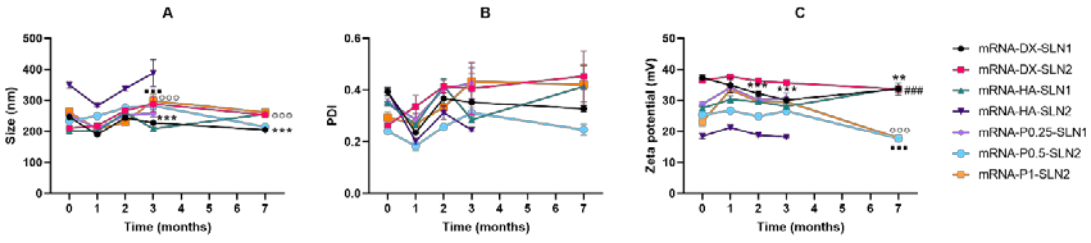

*Figure 9. Size (A), polydispersity index (B) and ζ-potential (C) of mRNA-based vectors formulated with SLN1 and SLN2 at time zero, 1, 2 and 3 months. n = 3; data are expressed as mean ± standard deviation. ** p < 0.01,*** p < 0.001 with respect to mRNA-DX-SLN1 at time 0. ### p < 0.001 with respect to mRNA-HA-SLN1 at time 0.°°° p < 0.001 with respect to mRNA-P0.5-SLN2 at time 0. ▪▪▪ p < 0.001 with respect to mRNA-P1-SLN2 at time 0.*

2.5.2. Binding, protection and release of nucleic acids

Gel electrophoresis of pDNA-based vectors were carried out at time 0 (freshly prepared; Figure 2A), and after 1, 2, and 3 months of storage at 4 °C (gel electrophoresis at month 2 is included in supplementary material Figure S6). Figure 10 shows the gel electrophoresis at month 1 (Figure 10A) and 3 months (Figure 10B). Regarding the binding, the presence of bands on the loading wells and their absence on the corresponding lanes at both, 1 and 3 months, indicates that vectors maintained the pDNA binding capacity. In comparison to time 0, pDNA-HA vectors showed two bands instead one and less intense, indicating that these vectors maintained the ability to protect the pDNA only partially. The protection ability of all vectors decreased at 2 months of storage (Figure S6), and after 3-months, all vectors lost the pDNA protection capacity, as the pDNA fragmentation indicates. One month after the preparation, the vectors were able to release the nucleic acid.

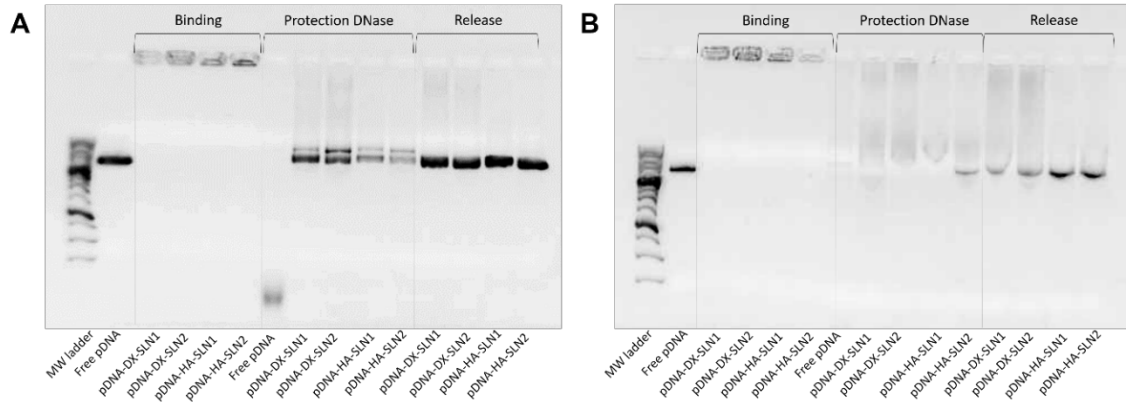

Figure 10. Long-term stability study of the binding, protection and release of pDNA-based vectors formulated with SLN1 and SLN2. A: binding, protection and release after 1 month of storage. B: binding, protection and release after 3 months of storage.

Gel electrophoresis of mRNA-based vectors were carried out at time 0 (freshly prepared, Figure 2B), and after 1, 2, and 3 months of storage at 4 °C (gel electrophoresis of 2 months is included in supplementary material Figure S7). Figure 11 shows gel electrophoresis at month 1 (Figure 11A) and month 3 (Figure 11B). After 1 and 3 months of storage, the vectors maintained their ability to completely bind the mRNA. One month after the preparation, the vectors were still able to protect the mRNA, but from 2 months (Figure S7), the nucleic acid was much less protected, regardless of the formulation.

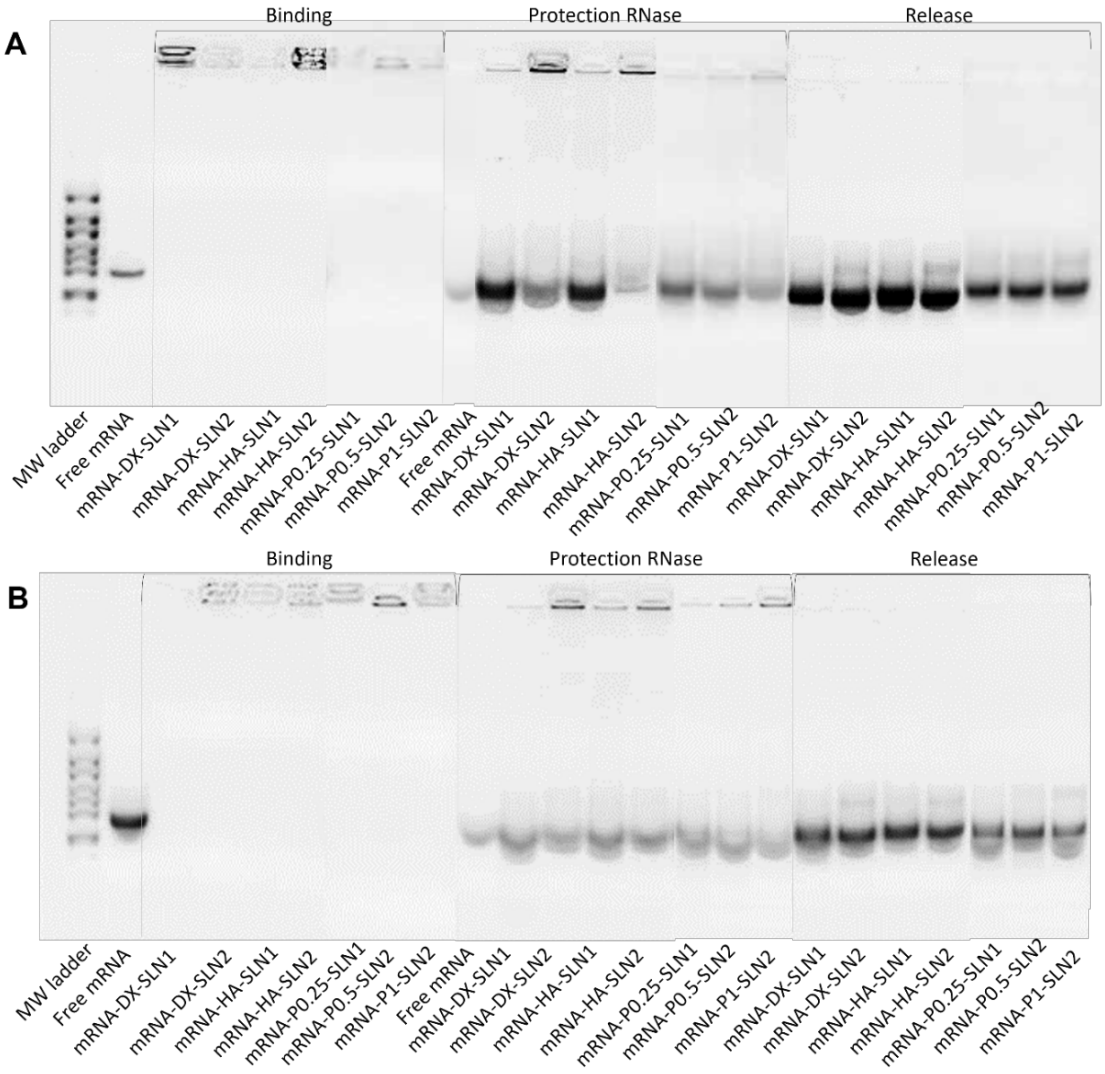

Figure 11. Long-term stability study of the binding, protection and release of mRNA-based vectors formulated with SLN1 and SLN2. A: binding, protection and release after 1 month of storage. B: binding, protection and release after 3 months of storage.

2.5.3. Transfection efficacy and cell viability

Figure 12 shows the percentage of ARPE-19 cells transfected with pDNA- based vectors, at time 0 (freshly prepared), and 1, 2, 3 and 7 months after preparation. The percentage of transfected cells with pDNA-vectors remained stable during the 7 months evaluated.

In the case of mRNA (Figure 13) the transfection efficacy of mRNA-SLN2 vectors decreased significantly during the first 3 months of storage. The percentage of transfected cells felt below 25% at month 1 in the case of mRNA-DX-SLN2 and mRNA-P1-SLN2. When the vectors were prepared with SLN1, the percentage of transfection remained over 80% for 3 months for mRNA-P0.25-SLN1, and during the 7 months evaluated for mRNA-DX-SLN1 and mRNA-HA-SLN1.

There were no differences in cell viability values during the stability study for pDNA and mRNA formulations.

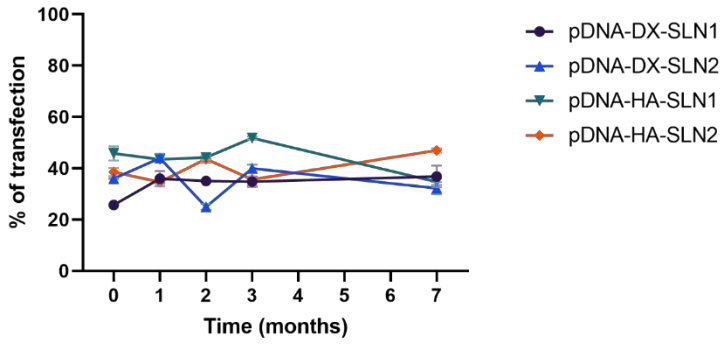

Figure 12. Percentage of ARPE-19 transfected cells after treatment with pDNA vectors after different times of storage. n = 3; data are expressed as mean ± standard deviation.

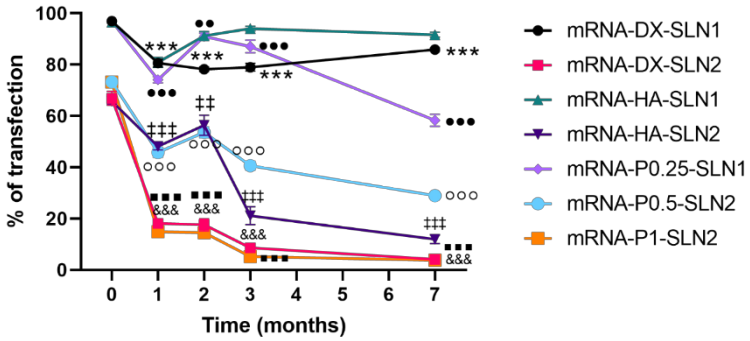

*Figure 13. Percentage of ARPE-19 transfected cells after treatment with mRNA vectors after different times of storage. n = 3; data are expressed as mean ± standard deviation. *** p < 0.001 with respect to mRNA-DX-SLN1 at time 0. &&& p < 0.001 with respect to mRNA-DX-SLN2 at time 0. ‡‡ p < 0.01, ‡‡‡ p < 0.001 with respect to mRNA-HA-SLN2 at time 0. ●● p < 0.01 and ●●● p < 0.001 with respect to mRNA-P0.25-SLN1 at time 0. °°° p < 0.001 with respect to mRNA-P0.5-SLN2 at time 0. ▪▪▪ p < 0.001 with respect to mRNA-P1-SLN2 at time 0.*

3. Discussion

The final formulations were prepared by combining the following components: SLNs, the nucleic acid (pDNA or mRNA), the cationic peptide protamine (P), and a polysaccharide, DX or HA. In our study, only the SLNs prepared with DOTAP as the only cationic lipid (SLN1) and those containing a mixture of DOTAP and DODAP (SLN2) showed physicochemical features adequate to be used as nucleic acid delivery systems.

The electrostatic interactions between the different components play a major role in the vector formation, conditioning the final structure. TEM photographs of mRNA-vectors (Figure 1) show an external layer or a corona surrounding the surface only when the polysaccharide is included in the final formulation. However, when mRNA was only complexed with P and SLN2, a

characteristic multilamellar internal structure can be observed; this structure has been also documented when the mRNA is combined with P and DOTAP as cationic lipid [23].

To prepare the nanovectors, the nucleic acid was first condensed with P, which contributes to bind and protect the genetic material at intra and extracellular level (Figure S8). Regarding DX and HA, both polysaccharides possess suitable properties to improve nucleic acid delivery. The final pDNA formulations presented a particle size and a PDI similar to the plain SLNs but lower ζ-potential. Nonetheless, mRNA-based formulations showed higher particle size and PDI values, and lower superficial charge than those prepared with pDNA. Electrophoresis on agarose gels showed that pDNA was well protected regardless of the formulation; however, the incorporation of DODAP to the SLNs resulted in a lower capacity to protect the mRNA, which indicates that the mRNA is more exposed to external agents, such as RNAses. The difference in the capacity of the vectors to protect the nucleic acid may be related to the unique structure of mRNA, which is a single-stranded molecule that folds into complex secondary and tertiary structures, and takes forms that differ from the double stranded pDNA [24].

We have evaluated the different vectors in two cell models, ARPE-19 and HEK-293 cells. These cell lines have been previously selected to study the behaviour of SLN-based vectors as pDNA delivery systems, because of their different features in terms of cell division rate (which is lower in ARPE-19 cells) and of the main endocytic processes [25]. As can be seen in Figure 3 and 4, all formulations were able to transfect both cell lines, regardless of the type of SLN, although the transfection efficacy varied depending on the cell line, on the type of nucleic acid and on the composition of the vectors. The efficacy of a nucleic acid delivery system depends on its ability to behave as a stable complex that provides protection of the genetic material against degradation, but is able to disassemble intracellularly to release it; both properties are conditioned by the physicochemical characteristics of the nanosystem. In this sense, the SLNs resulted necessary for transfection, and when cells were treated with a complex prepared with mRNA or pDNA, P, and DX or HA, the percentage of transfected cells was lower than 0.8% (data not shown).

In ARPE-19 cells at 37°C, pDNA-based vectors (Figure 3A) induced a lower percentage of transfected cells than those containing mRNA (Figure 3C), but pDNA-mediated transfected cells provided higher fluorescence intensities; namely, pDNA transfection is more effective for protein production in this cell line. In HEK-293, pDNA-based vectors (Figure 4) induced lower transfection efficacy than mRNA-vectors in terms of transfected cells and protein production. Overall, cellular uptake of all vectors, pDNA and mRNA, was over 90%, therefore, the bottleneck

for a successful pDNA transfection seems to be the nuclear entry, despite our systems contains P, which favors the transcription process and the entry of the pDNA into the nucleus thanks to their nuclear localization signals [26]. Unfortunately, an effective nuclear transport system has yet to be stablished [27]. Among pDNA vectors, the highest transfection efficacy was observed with HA-containing vectors in both cell lines, and in ARPE-19 especially with the vector pDNA-HA-SLN1. Regarding mRNA formulations, the inclusion of a polysaccharide did not have a great impact on the in vitro transfection efficacy.

Designing nanosystems to modulate intracellular nucleic acid release and stability is a key challenge to broad the therapeutic potential of nucleic acid based medicinal products. All mRNA formulations showed the highest transfection efficacy at 24-48 h, and the protein expression decreased notably at 96 h, whereas pDNA formulations showed the maximum transfection at 72-96 h; in both cases, it lasted at least 11 days (Figure S9). The synthesis of the encoded protein with mRNA is faster and its expression is temporary, which makes it a more predictable molecule than pDNA; however, mRNA provides short-term transfection. Most mRNA applications are focusing on immunotherapy, and particularly on cancer, due to the immunostimulatory capacity of mRNA together with the transient nature of the encoded antigen and the versatility of applications, including prophylaxis, therapy and personalized vaccines [28,29]. Transient expression could be also beneficial for introducing antiapoptotic factors or genome editing enzymes [27]. However, in other cases, long-term expression is required, such as in protein replacement therapy intended for the supplementation of infra-expressed and not functional proteins, or for the expression of foreign proteins [6]. Therefore, the duration of transfection should be considered and not only the rate of transfected cells and the efficiency of the protein production. In our study, although mRNA vectors were able to transfect a larger number of cells, pDNA-mediated transfection in ARPE-19 cells was the most effective in terms of the amount of protein synthetized per cell. The production of a large amount of protein, even with low percent of transfected cells, may be a desired objective in gene augmentation to produce a protein in a cell to be secreted and reach the target tissue.

All the components that form the vector determine the interaction with the target cells, and as a consequence, the internalization process, the intracellular behaviour of the genetic material and the transfection capacity [30,31]. It is well known that the degree of cellular uptake and endosomal escape of the vectors condition transfection efficiency [32]. The major entry mechanism of SLN-based vectors is the endocytosis. The two main endocytic processes are reported to be pinocytosis and phagocytosis. The former is mainly associated to nanoparticle uptake, and different pathways are involved (micropinocytosis, clathrin-mediated, caveolin

dependent or independent) [33]. The predominant entry pathway depends on the target cells and on the composition and physicochemical characteristics of the non-viral vectors [14]. The endocytosis is an energy-dependent and temperature-dependent process, and it is inhibited at 4 °C because cells consume less ATP and block the active transport at this temperature [34,35].

In ARPE-19 cells, the percentage of transfected cells decreased significantly at 4 °C for almost all formulations, and mainly for pDNA formulations and mRNA-DX-SLN2. Surprisingly, the fluorescence intensity of the vectors containing DODAP (SLN2) did not change or even increased at low temperature. The lower cellular uptake of pDNA-SLN1 formulations at 4 °C explains the decrease of the transfection efficacy of these formulations. On the contrary, the percentage of entry of pDNA-SLN2 and mRNA vectors was hardly affected at 4 °C, which reveals the presence of energy-independent mechanisms; actually, lipid exchange might occur at 4 °C and contribute to the intracellular transport of the vectors [34]. It has to be taken also in mind that due to the nature of biological systems, several dynamic processes might take place in parallel, which might turn in compete with one another [36]. The higher protein production observed at 4 °C, despite the lower number of transfected cells, indicates that in ARPE-19 cells energy-independent mechanisms are more effective to induce protein production, principally in the case of the vectors containing DODAP.

In HEK-293 cells, cell uptake and fluorescence intensity of transfection decreased drastically at 4 °C, but surprisingly, the percentage of transfected cells by the pDNA vectors was not affected. This cell line presents a high caveolae-dependent endocytic activity, and the blocking of the active transport has a very relevant influence on the uptake. In the case of mRNA vectors, the efficacy of transfection of mRNA-SLN1 vectors was less affected than the SLN2 formulations at low temperature. Taking in mind all these results, we can conclude that in HEK-293, cell energy-dependent entry mechanisms are the most effective for protein production, regardless of the kind of the SLN used for preparing the pDNA vectors, and mainly for SLN2 formulations in the case of mRNA. Therefore, protein production is favored by energy-dependent or independent mechanisms depending on the cell line, SLN composition and the nucleic acid delivered, pDNA vs mRNA. Endosomal escape is recognized as the rate limiting step for mRNA delivery [37] and ionizable lipids, such as DODAP, could facilitate this process. Nevertheless, recently, Patel et al. have reported that late endosome/lysosome formation is essential for the functional delivery of exogenously presented mRNA [38]. The balance between endosomal escaping capability and stability of translocated nucleic acids in cytoplasm is essential for an effective transfection. This balance may be modulated by an appropriate delivery system. If mRNA is easily transported and delivered into the cytoplasm, its poor stability will make that the transfection results in a short

pattern. However, if the delivery system slows down the endosomal escape and provides long-protection of mRNA, a sustained expression may be achieved. In the case of pDNA, which shows higher stability than mRNA, the limiting step in transfection would be more related to the endosomal escape than to the cytoplasmic stability [39]. It is essential that the early steps of the development of nucleic acid medicinal products include mechanistic studies in the target cell for an in depth understanding of the intracellular nucleic acid nanomedicines behavior. This knowledge will allow a properly design of the formulations specifically adapted to the nucleic acid features, clinical application and therapeutic purpose.

In the present work, the type of formulation had a greater influence on the intracellular disposition of mRNA than that of pDNA (Figure 7). mRNA appeared less dispersed along the cytoplasm with the vectors prepared only with DOTAP (SLN1). On the agarose gel (Figure 2) vectors prepared with both SLN1 and SLN2 were able to completely bind the mRNA; however, the formulations prepared with DOTAP and DODAP (SLN2) showed a lower protection degree, which is usually associated to a less condensation capacity. The differences in the intracellular disposition were related not only to the capacity of the vectors to bind, condense and protect the nucleic acid, but also to the entry mechanism and the intracellular trafficking of the vectors, which are cell line dependent processes. Unlike what happens in ARPE-19 cells, in HEK-293 cells, mRNA appeared more dispersed in the cytoplasm, which may be indicative of a higher exposure to degradation. Consequently, mRNA was most effective in ARPE-19 than in HEK-293 cells, even if a lower dose of mRNA was administered in retinal cells.

Efficacy and stability of the delivery systems should be guaranteed during storage over time. In fact, thermal stability of nucleic acid-based medicinal products is a major issue, especially relevant in the case of vaccines, since storage conditions involve a logistical problem for stockpiling and distribution, particularly in countries that lack infrastructure to maintain the cold chain [40]. We have evaluated the physicochemical characteristics and the transfection efficacy of our vectors along 7 months of storage at 4 °C. The changes detected in size, PDI, zeta potential and in the agarose gel studies did not always correlate with the transfection efficacy. pDNA formulations showed physicochemical changes from the second month, but transfection efficacy was maintained for 7 months in vitro. On the contrary, mRNA vectors were more stable in terms of size, zeta potential and in the agarose gel studies, but transfection decreased drastically from the first month with the vectors containing the SLNs prepared with DOTAP and DODAP (SLN2). The vectors prepared with mRNA and the SLNs containing only DOTAP showed a percentage of transfection higher than 80% during the first three months of storage, and it lasted for 7 months, except for the formulation prepared without polysaccharide. Therefore, in

the formulations prepared with SLN containing only DOTAP as cationic lipid (SLN1), the inclusion of a polysaccharide confers stability; in addition, it provides other beneficial properties such as stealth capacity and ability to modulate the mechanism of entry to the target cell [15,25,30]. The lower number of positive charges of the lipid DODAP is related to its lower capacity to condense the genetic material, which could be the reason of the worse stability of SLN2-based vectors, especially for mRNA. Considering not only the efficacy but also the long-term stability, vectors prepared only with the cationic lipid DOTAP seems to be the most promising formulations.

4. Materials and Methods

4.1. Materials

Precirol® ATO 5 (glyceryl palmitostearate) was generously provided by Gattefossé (Madrid, Spain), 1,2-dioleoyl-3-trimethylammonium-propane chloride salt (DOTAP) and 1,2-dioleoyl-3-dimethylammonium-propane (DODAP) were obtained from Avanti Polar-lipids, Inc. (AL, USA), and Tween 80 and dichloromethane from Panreac (Madrid, Spain). Protamine sulfate salt Grade X (P), dextran (M_w of 3.26 KDa) (DX) and Nile Red were purchased from Sigma-Aldrich (Madrid, Spain). Hyaluronic acid (M_w of 100 KDa) (HA) was acquired from Lifecore Biomedical (MN, USA).

The plasmid pcDNA3-EGFP (6.1 kb) was kindly provided by the laboratory of Professor BHF Weber (University of Regensburg, Germany), and CleanCap™ EGFP mRNA (5moU) and CleanCap™ Cyanine 5 EGFP mRNA (5moU) were purchased from TriLink BioTechnologies. All of the nucleic acids encoded green fluorescent protein (GFP). Label IT® Cy®5 Nucleic Acid Labeling Kit, was obtained from Mirus.

The materials employed for the electrophoresis on agarose gel were acquired from Bio-Rad (Madrid, Spain). Deoxyribonuclease I (DNase I) and sodium dodecyl sulphate (SDS) were obtained from Sigma-Aldrich, GelRed™ from Biotium (CA, USA) and Ambion™ RNase I from Life Technologies (ThermoFisher Scientific, Madrid, Spain).

Human Retinal Pigmented Epithelium (ARPE-19) and Human Embryonic Kidney (HEK-293) cells were purchased from American Type Culture Collection (ATCC, Manassas, VA, USA). Cell culture reagents, including Dulbecco´s Modified Eagle´s Medium/Nutrient Mixture F-12 (DMEM/F-12), fetal bovine serum, penicillin-streptomicin, and trypsin-EDTA were acquired from Life Technologies (ThermoFisher Scientific, Madrid, Spain). Eagle's Minimum Essential Medium (EMEM) was purchased from LGC Promochem (Barcelona, Spain).

Reporter lysis buffer was provided by Promega Biotech Ibérica (Madrid, Spain), and 4',6-diamidine-2'-phenylindole dihydrochloride (DAPI)-fluoromount-G by Southern Biotech (Birmingham,AL, USA). Paraformaldehyde (PFA) was obtained from Panreac, while phosphate buffered saline (PBS) and HEPES buffer were purchased from Gibco (ThermoFisher Scientific, Madrid, Spain). Lipofectamine™ 2000 Lipid-Reagent was acquired from Life Technologies (ThermoFisher Scientific, Madrid, Spain) and Cell Couniting Kit-8 (CCK-8) from Sigma-Aldrich (Madrid, Spain). 7-Amino-Actinomycin D (7-AAD) Viability Dye was provided by Beckman Coulter.

4.2. Preparation of SLNs and Vectors

Four different SLNs, SLN1, SLN2, SLN3 and SLN4, were prepared by the solvent emulsification-evaporation method previously described [41].

Table 4 shows the composition of the SLNs. SLN1 were obtained by the sonication of the oil phase containing Precirol® ATO 5 and dichloromethane in an aqueous phase of the cationic lipid DOTAP (0.4%, w/v) and Tween 80 (0.1%, w/v); whereas SLN2 contained a mixture of DOTAP (0.2% w/v) and DODAP (0.2% w/v) as cationic and ionizable lipids, respectively. SLN3 were prepared with the ionizable lipid DOBAQ (0.4%, w/v) and SLN4 with a mixture of DOTAP (0.2% w/v) and DOBAQ (0.2% w/v).

Table 4. Composition of SLNs.

Type of SLN	Cationic lipid (%)			Tween 80 (%)
	DOTAP	DODAP	DOBAQ	
SLN1	0.4			0.1
SLN2	0.2	0.2		0.1
SLN3			0.4	0.1
SLN4	0.2		0.2	0.1

SLN: solid lipid nanoparticle.

In order to elaborate SLN-based vectors, the nucleic acid (pcDNA3-EGFP plasmid, CleanCap™ EGFP mRNA (5moU)) was first mixed for 5 min with the protamine (P) solubilized in water. Then, when corresponding, an aqueous solution of a polysaccharide, dextran (DX) or hyaluronic acid (HA), was added to the previous mixture, and they were kept in contact for 15 min. Finally, the suspension of SLNs was added to the complexes. The final vectors were obtained by the electrostatic interactions between all the components. The weight ratios of the components are summarized in Table 5.

Table 5. Weight ratios of the vectors.

Name of the vector	Nucleic acid	Polysaccharide	SLN	Weight ratio (w:w:w:w)
pDNA-DX-SLN1	pDNA	DX	SLN1	DX:P:DNA:SLN1 1:2:1:5
pDNA-DX-SLN2	pDNA	DX	SLN2	DX:P:DNA:SLN2 1:2:1:5
pDNA-DX-SLN4	pDNA	DX	SLN4	DX:P:DNA:SLN4 1:2:1:5
pDNA-HA-SLN1	pDNA	HA	SLN1	HA:P:DNA:SLN1 0.5:2:1:2
pDNA-HA-SLN2	pDNA	HA	SLN2	HA:P:DNA:SLN2 0.5:2:1:5
mRNA-DX-SLN1	mRNA	DX	SLN1	DX:P:mRNA:SLN1 1:0.25:1:5
mRNA-DX-SLN2	mRNA	DX	SLN2	DX:P:mRNA:SLN2 1:1:1:5
mRNA-HA-SLN1	mRNA	HA	SLN1	HA:P:mRNA:SLN1 0.5:0.5:1:5
mRNA-HA-SLN2	mRNA	HA	SLN2	HA:P:mRNA:SLN2 0.5:1:1:5
mRNA-P-SLN1	mRNA	-	SLN1	P:mRNA:SLN1 0.25:1:5
mRNA-P0.5-SLN2	mRNA	-	SLN2	P:mRNA:SLN2 0.5:1:5
mRNA-P1-SLN2	mRNA	-	SLN2	P:mRNA:SLN2 1:1:5

DX: dextran; HA: hyaluronic acid; P: protamine; SLN: solid lipid nanoparticle.

4.3. Size, PDI and ζ-potential measurement

Size and polydispersity index (PDI) of SLNs and final vectors were measured by photon correlation spectroscopy, and ζ potential by laser doppler velocimetry, in a ζsizer Nano series-Nano ZS (Malvern Instruments, Worcestershire, UK). All samples were dilute in Milli-Q™ water (EDM Millipore, Billerica, MA, USA).

4.4. Transmission Electron Microscopy (TEM) images

SLN1, SLN2, SLN1- and SLN2-based vectors were observed by Transmission Electronic Microscopy (TEM) using electron microscopy negative staining. To this end, 10 µl of the sample were adsorbed for 60 s onto glow discharged carbon coated grids. Then, the remaining liquid was removed, via blotting on filter paper, and the staining was carried out with 2% uranyl acetate for 60 s.

Visualization of samples was performed in a Philips EM208S TEM. For acquisition of digital images an Olympus SIS purple digital camera was used. Technical and human support for TEM

was provided by the Advanced Research Facilities (SGIker) of Analytical and High Resolution Microscopy in Biomedicine at the University of the Basque Country UPV/EHU.

4.5. Agarose gel electrophoresis assay

The studies of the pDNA binding capacity, the protection from DNase I and the release from the vectors were performed in 0.7% agarose gel electrophoresis labelled with Gel Red™. The gels were run for 30 min at 120 V, and immediately they were analyzed with the Uvitec Uvidoc D-55-LCD-20 M Auto transilluminator. To evaluate binding capacity, vectors were diluted in MilliQ™ water to a final concentration of 0.03 µg pDNA/µl in the gel. The protection was analysed by the addition of 1 U DNase I/2.5 µg pDNA; mixtures were incubated at 37 °C for 30 min in a heater. Then, the samples were removed from the heater and mixed with a SDS solution (final concentration of 1%) at room temperature to release the nucleic acid. The same SDS solution was added to the vectors to unbind the plasmid in the release studies. Two controls for the integrity of the pDNA were included in the gels: 1 kb pDNA ladder from NIPPON Genetics Europe (Dueren, Germany) and untreated pcDNA3-EGFP plasmid.

In order to study the mRNA binding capacity, the protection from RNase I digestion and the release from the vectors 1.2% agarose gel electrophoresis for 60 min at 75 V containing Gel Red™ was used. The bands were analysed with Uvitec Uvidoc D-55-LCD-20 M Auto transilluminator. To evaluate binding capacity, vectors were diluted in MilliQ™ water to a final concentration of 0.12 µg/µl mRNA in the gel. The protection was analysed by the addition of 6 U RNase I/ µg mRNA; mixtures were incubated at 37 °C for 40 min in a heater. Then, the samples were removed from the heater and mixed with a SDS solution (final concentration of 1%) at room temperature to release the nucleic acid. The same SDS solution was added to the vectors to unbind the plasmid in the release studies. RiboRuler High Range RNA Ladder and untreated CleanCap™ EGFP mRNA (5moU) as controls were included as controls in the gels to compare the integrity of the mRNA.

4.6. Cell culture studies

In vitro cell studies were carried out in two cell lines: Human Retinal Pigmented Epithelial (ARPE-19) and Human Embryonic Kidney (HEK-293) cells. ARPE-19 were maintained in culture in Dulbecco's Modified Eagle Medium:Nutrient Mixture F-12 (DMEM / F-12), and HEK-293 cells were cultured in Eagle's Minimum Essential Medium (EMEM). Both mediums were supplemented with 10% fetal bovine serum and 1% penicillin and streptomycin antibiotic. Cells cultures were incubated at 37 °C in a 5% CO_2 air atmosphere, changing the medium every 2 or 3 days and subcultured every 7 days.

4.6.1. Transfection efficacy and cell viability

pDNA and mRNA vectors were prepared 24 h and 72 h before their addition, respectively, and maintained at 4 °C before their use. ARPE-19 cells were cultured at a density of 60,000 cells per well in 12-well plates 72h before the addition of the vectors, in order to ensure the formation of a cell monolayer. HEK-293 cells were cultured at a density of 150,000 cells per well in 24-well plates 24h before the addition of the vectors, when a 75-85% confluence was reached. Then, part of the medium was removed, leaving the enough volume to cover the cells, and a total volume of 75 µl of each vector diluted in HBS (equivalent to 2.5 µg or 1.5 µg of pDNA or mRNA, respectively), were added to each well. The dose of mRNA to be added to the cells was optimised in order to better detect differences in the transfection efficacy (supplementary material Figure S10). After incubation for 4 hours at 37ºC in a 5% CO_2 air atmosphere, vectors were removed and cells were refreshed with 1 ml of complete medium. Cells were kept growing during 72h in the pDNA experiments, and during 48 h in the mRNA experiments.

In order to analyze transfection efficacy and cell viability cells were washed with 500 µl of PBS and then detached by incubation with 500 µl of trypsin-EDTA for 10 min. Thereafter, the cell suspension was centrifuged at 1,000 rpm for 5 min. The supernatant was discarded and the pellet of cells was resuspended in 500 µl of PBS.

In both cell lines, the percentage of transfected cells and intensity of fluorescence, indicative of the amount of EGFP produced, and the cell viability were measured using a CytoFLEX flow cytometer (Beckman Coulter, Brea, CA). For each sample 10,000 events were collected. Transfection efficacy was measured at 525 nm (FITC), andcell viability was determined at 610 nm (ECD) after addition of 7-Amino-Actinomycin D (7-AAD) Viability Dye to the samples. 7-AAD labels fluorescently dead cells..

The effect of temperature on cell transfection was studied by incubation of ARPE-19 and HEK-293 cells at 4 °C for 30 min prior to the addition of the vectors. The cells were maintained 4 h at 4 °C and then, cells were treated as explained above.

4.6.2. Cellular uptake

The internalization of the vectors was studied in ARPE-19 and HEK-293 cells, by using SLNs labelled with the fluorescent dye Nile Red (λ = 590 nm) to prepare the vectors, according to a previously reported method [42]. . For this purpose, when preparing SLNs, Nile Red was dissolved in dichloromethane together with Precirol® ATO 5.

Two hours after the addition of 75 µl of the vectors, the culture medium was retired and cells were detached from plates, as described in section 4.6.1. for the cytometry analysis of

transfected cells. The entrance of the vectors was analysed using a CytoFLEX flow cytometer (Beckman Coulter, Brea, CA) at 610 nm (ECD). For each sample, 10,000 events were collected.

In addition, the effect of temperature on cell uptake was studied by incubation of ARPE-19 and HEK-293 cells at 4 °C for 30 min prior to the addition of the vectors. Once the Nile Red-labelled vectors were added to cell cultures, the cells were maintained at 4 °C for additional 2 h. Finally, the cells were collected to evaluate the vector uptake by flow cytometry, as described above.

4.6.3. Intracellular disposition

To evaluate the intracellular location of the vectors, 35,000 cells and 150,000 cells of ARPE-19 and HEK-293, respectively, were seeded in Millicell EZ slides (Millipore) with 1 ml per well at 37 °C and 5 % CO_2 air atmosphere 24 h before experiment.

For mRNA assays, 75 µl of vector equivalent to 0.8 µg of CleanCap™ Cyanine 5 EGFP mRNA (5moU) as nucleic acid was added to each well. For pDNA assays pcDNA3-EGFP plasmid was labelled with Label IT® Cy®5, following manufacturer's instructions, and. 75 µl of vector equivalent to 2.5 µg of pcDNA3-EGFP plasmid was added to each well. After 4 hours, the slides were washed with PBS and fixed with PFA 4%. DAPI-fluoromount-G™ was used as the mounting fluid, to label the nuclei. The slides were then were examined under a Zeiss LSM800 confocal microscope.

4.7. Long-term stability study of pDNA- and mRNA-based vectors

pDNA- and mRNA-based vectors were stored at 4 °C during 7 months. Both, pDNA- and mRNA-based vectors were elaborated with 2.5 µg of nucleic acid. Vectors were characterized at different times (1, 2, 3 and 7 months) in terms of size, PDI and ζ potential, as described in section 4.3.; and the binding, protection and release capacity of the nucleic acids from the delivery system. The percentage of transfection was also quantified in ARPE-19 at the different storage times.

4.8. Statistical analysis

Results are reported as mean values ± standard deviation (S.D.). Statistical analysis was performed using IBM® SPSS® Statistics 25 (IBM, NY, USA). The normal distribution of samples was assessed by the Shapiro–Wilk test, and homogeneity of variance by the Levene test. The different formulations were compared with ANOVA and Student's t-test. Differences were considered statistically significant at $p < 0.05$.

5. Conclusions

The present work shows that formulation-related factors have a greater influence on nucleic acid delivery, transfection efficiency and long-term stability of mRNA vectors than pDNA vectors. The formulations prepared with DOTAP as unique cationic lipid showed a better stability profile during storage than those containing also the ionizable lipid DODAP; moreover, the addition of a polysaccharide to DOTAP formulations improved the long-term stability.

The therapeutic potential of the nucleic acid based medicinal products designed is also highly conditioned by the intracellular behavior of the nucleic acid nanomedicines in the target cell. Protein production was conditioned by energy-dependent or independent entry mechanisms depending on the cell line, SLN composition and kind of nucleic acid delivered. On the one hand, mRNA vectors were able to transfect a larger number of cells, and the protein expression was faster and less permanent than that obtained with pDNA vectors; therefore, these mRNA systems may be interesting for immunization or gene editing applications. On the other hand, pDNA formulations were the most effective in terms of production of encoded protein in retinal cells, which would be interesting for protein replacement therapy when the therapeutic objective is to produce a protein in a cell to be secreted and reach the target tissue.

References

1. Yu, A.-M.; Choi, Y.H.; Tu, M.-J. RNA Drugs and RNA Targets for Small Molecules: Principles, Progress, and Challenges. Pharmacol. Rev. 2020, 72, 862–898, doi:10.1124/pr.120.019554.
2. Pardi, N.; Hogan, M.J.; Porter, F.W.; Weissman, D. mRNA vaccines-a new era in vaccinology. Nat. Rev. Drug Discov. 2018, 17, 261–279, doi:10.1038/nrd.2017.243.
3. Kowalski, P.S.; Rudra, A.; Miao, L.; Anderson, D.G. Delivering the Messenger: Advances in Technologies for Therapeutic mRNA Delivery. Mol. Ther. 2019, 27, 710–728, doi:10.1016/j.ymthe.2019.02.012.
4. Liu, J.; Chang, J.; Jiang, Y.; Meng, X.; Sun, T.; Mao, L.; Xu, Q.; Wang, M. Fast and Efficient CRISPR/Cas9 Genome Editing In Vivo Enabled by Bioreducible Lipid and Messenger RNA Nanoparticles. Adv. Mater. 2019, 31, 1902575, doi:10.1002/adma.201902575.
5. Miller, J.B.; Zhang, S.; Kos, P.; Xiong, H.; Zhou, K.; Perelman, S.S.; Zhu, H.; Siegwart, D.J. Non-Viral CRISPR/Cas Gene Editing In Vitro and In Vivo Enabled by Synthetic Nanoparticle Co-Delivery of Cas9 mRNA and sgRNA. Angew. Chemie - Int. Ed. 2017, 56, 1059–1063, doi:10.1002/anie.201610209.
6. Gómez-Aguado, I.; Rodríguez-Castejón, J.; Vicente-Pascual, M.; Rodríguez-Gascón, A.; Solinís, M.Á.; Del Pozo-Rodríguez, A. Nanomedicines to deliver mRNA: State of the art and future perspectives. Nanomaterials 2020, 10, doi:10.3390/nano10020364.

7. Sahin, U.; Karikó, K.; Türeci, Ö. MRNA-based therapeutics-developing a new class of drugs. Nat. Rev. Drug Discov. 2014, 13, 759–780, doi:10.1038/nrd4278.

8. Zhong, Z.; Mc Cafferty, S.; Combes, F.; Huysmans, H.; De Temmerman, J.; Gitsels, A.; Vanrompay, D.; Portela Catani, J.; Sanders, N.N. mRNA therapeutics deliver a hopeful message. Nano Today 2018, 23, 16–39, doi:10.1016/j.nantod.2018.10.005.

9. Anderson, E.J.; Rouphael, N.G.; Widge, A.T.; Jackson, L.A.; Roberts, P.C.; Makhene, M.; Chappell, J.D.; Denison, M.R.; Stevens, L.J.; Pruijssers, A.J.; et al. Safety and Immunogenicity of SARS-CoV-2 mRNA-1273 Vaccine in Older Adults. N. Engl. J. Med. 2020, doi:10.1056/NEJMoa2028436.

10. Papachristofilou, A.; Hipp, M.M.; Klinkhardt, U.; Früh, M.; Sebastian, M.; Weiss, C.; Pless, M.; Cathomas, R.; Hilbe, W.; Pall, G.; et al. Phase Ib evaluation of a self-adjuvanted protamine formulated mRNA-based active cancer immunotherapy, BI1361849 (CV9202), combined with local radiation treatment in patients with stage IV non-small cell lung cancer. J. Immunother. Cancer 2019, 7, 38, doi:10.1186/s40425-019-0520-5.

11. Sebastian, M.; Papachristofilou, A.; Weiss, C.; Früh, M.; Cathomas, R.; Hilbe, W.; Wehler, T.; Rippin, G.; Koch, S.D.; Scheel, B.; et al. Phase Ib study evaluating a self-adjuvanted mRNA cancer vaccine (RNActive®) combined with local radiation as consolidation and maintenance treatment for patients with stage IV non-small cell lung cancer. BMC Cancer 2014, 14, 748, doi:10.1186/1471-2407-14-748.

12. Bahl, K.; Senn, J.J.; Yuzhakov, O.; Bulychev, A.; Brito, L.A.; Hassett, K.J.; Laska, M.E.; Smith, M.; Almarsson, Ö.; Thompson, J.; et al. Preclinical and Clinical Demonstration of Immunogenicity by mRNA Vaccines against H10N8 and H7N9 Influenza Viruses. Mol. Ther. 2017, 25, 1316–1327, doi:https://doi.org/10.1016/j.ymthe.2017.03.035.

13. Samaridou, E.; Heyes, J.; Lutwyche, P. Lipid nanoparticles for nucleic acid delivery: Current perspectives. Adv. Drug Deliv. Rev. 2020, doi:10.1016/j.addr.2020.06.002.

14. del Pozo-Rodríguez, A.; Solinís, M.Á.; Rodríguez-Gascón, A. Applications of lipid nanoparticles in gene therapy. Eur. J. Pharm. Biopharm. 2016, 109, 184–193, doi:10.1016/j.ejpb.2016.10.016.

15. Apaolaza, P.S.; del Pozo-Rodríguez, A.; Torrecilla, J.; Rodríguez-Gascón, A.; Rodríguez, J.M.; Friedrich, U.; Weber, B.H.F.; Solinís, M.A. Solid lipid nanoparticle-based vectors intended for the treatment of X-linked juvenile retinoschisis by gene therapy: In vivo approaches in Rs1h-deficient mouse model. J. Control. Release 2015, 217, 273–283, doi:https://doi.org/10.1016/j.jconrel.2015.09.033.

16. Apaolaza, P.S.; del Pozo-Rodríguez, A.; Solinís, M.A.; Rodríguez, J.M.; Friedrich, U.; Torrecilla, J.; Weber, B.H.F.; Rodríguez-Gascón, A. Structural recovery of the retina in a retinoschisin-deficient mouse after gene replacement therapy by solid lipid nanoparticles. Biomaterials 2016, 90, 40–49, doi:https://doi.org/10.1016/j.biomaterials.2016.03.004.

17. Ramamoorth, M.; Narvekar, A. Non viral vectors in gene therapy - An overview. J. Clin. Diagnostic Res. 2015, 9, GE01–GE06, doi:10.7860/JCDR/2015/10443.5394.

18. Paliwal, R.; Paliwal, S.R.; Kenwat, R.; Kurmi, B. Das; Sahu, M.K. Solid lipid nanoparticles: a review on recent perspectives and patents. Expert Opin. Ther. Pat. 2020, 30, 179–194, doi:10.1080/13543776.2020.1720649.

19. Guan, S.; Rosenecker, J. Nanotechnologies in delivery of mRNA therapeutics using nonviral vector-based delivery systems. Gene Ther. 2017, 24, 133–143, doi:10.1038/gt.2017.5.

20. Balazs, D.A.; Godbey, W. Liposomes for Use in Gene Delivery. J. Drug Deliv. 2011, 2011, 1–12, doi:10.1155/2011/326497.

21. Ramezanpour, M.; Schmidt, M.L.; Bodnariuc, I.; Kulkarni, J.A.; Leung, S.S.W.; Cullis, P.R.; Thewalt, J.L.; Tieleman, D.P. Ionizable amino lipid interactions with POPC: implications for lipid nanoparticle function. Nanoscale 2019, 11, 14141–14146, doi:10.1039/C9NR02297J.

22. Sayour, E.J.; De Leon, G.; Pham, C.; Grippin, A.; Kemeny, H.; Chua, J.; Huang, J.; Sampson, J.H.; Perez, L.S.; Flores, C.; et al. Systemic activation of antigen-presenting cells via RNA-Loaded nanoparticles. Oncoimmunology 2017, 6, 1–14, doi:10.1080/2162402X.2016.1256527.

23. Siewert, C.D.; Haas, H.; Cornet, V.; Nogueira, S.S.; Nawroth, T.; Uebbing, L.; Ziller, A.; Al-Gousous, J.; Radulescu, A.; Schroer, M.A.; et al. Hybrid Biopolymer and Lipid Nanoparticles with Improved Transfection Efficacy for mRNA. Cells 2020, 9, 1–19, doi:10.3390/cells9092034.

24. Lorenz, C.; Fotin-Mleczek, M.; Roth, G.; Becker, C.; Dam, T.C.; Verdurmen, W.P.R.; Brock, R.; Probst, J.; Schlake, T. Protein expression from exogenous mRNA: Uptake by receptor-mediated endocytosis and trafficking via the lysosomal pathway. RNA Biol. 2011, 8, doi:10.4161/rna.8.4.15394.

25. Delgado, D.; Gascón, A.R.; Del Pozo-Rodríguez, A.; Echevarría, E.; Ruiz De Garibay, A.P.; Rodríguez, J.M.; Solinís, M.Á. Dextran-protamine-solid lipid nanoparticles as a non-viral vector for gene therapy: In vitro characterization and in vivo transfection after intravenous administration to mice. Int. J. Pharm. 2012, 425, 35–43, doi:10.1016/j.ijpharm.2011.12.052.

26. Delgado, D.; Del Pozo-Rodríguez, A.; Solinís, M.Á.; Rodríguez-Gascón, A. Understanding the mechanism of protamine in solid lipid nanoparticle-based lipofection: The importance of the entry pathway. Eur. J. Pharm. Biopharm. 2011, 79, 495–502, doi:10.1016/j.ejpb.2011.06.005.

27. Uchida, S.; Kataoka, K. Design concepts of polyplex micelles for in vivo therapeutic delivery of plasmid DNA and messenger RNA. J. Biomed. Mater. Res. Part A 2019, 107, 978–990, doi:10.1002/jbm.a.36614.

28. Fishman, S.; Lewis, M.D.; Siew, L.K.; Leenheer, E. De; Kakabadse, D.; Davies, J.; Ziv, D.; Margalit, A.; Karin, N.; Gross, G.; et al. Adoptive Transfer of mRNA-Transfected T Cells Redirected against Diabetogenic CD8 T Cells Can Prevent Diabetes. Mol. Ther. 2017, 25, 456–464, doi:https://doi.org/10.1016/j.ymthe.2016.12.007.

29. Van Hoecke, L.; Roose, K. How mRNA therapeutics are entering the monoclonal antibody field. J. Transl. Med. 2019, 17, 54, doi:10.1186/s12967-019-1804-8.

30. Apaolaza, P.S.; Delgado, D.; Pozo-Rodríguez, A. Del; Gascón, A.R.; Solinís, M.Á. A novel gene therapy vector based on hyaluronic acid and solid lipid nanoparticles for ocular diseases. Int. J. Pharm. 2014, 465, 413–426, doi:10.1016/j.ijpharm.2014.02.038.

31. Delgado, D.; Del Pozo-Rodríguez, A.; Solinís, M.Á.; Avilés-Triqueros, M.; Weber, B.H.F.; Fernández, E.; Gascón, A.R. Dextran and protamine-based solid lipid nanoparticles as potential vectors for the treatment of X-linked juvenile retinoschisis. Hum. Gene Ther. 2011, 23, 345–355, doi:10.1089/hum.2011.115.

32. Li, J.; Chen, Q.; Zha, Z.; Li, H.; Toh, K.; Dirisala, A.; Matsumoto, Y.; Osada, K.; Kataoka, K.; Ge, Z. Ternary polyplex micelles with PEG shells and intermediate barrier to complexed DNA cores for efficient systemic gene delivery. J. Control. Release 2015, 209, 77–87, doi:10.1016/j.jconrel.2015.04.024.

33. Danaei, M.; Dehghankhold, M.; Ataei, S.; Hasanzadeh Davarani, F.; Javanmard, R.; Dokhani, A.; Khorasani, S.; Mozafari, M.R. Impact of particle size and polydispersity index on the clinical applications of lipidic nanocarrier systems. Pharmaceutics 2018, 10, 1–17, doi:10.3390/pharmaceutics10020057.

34. Resina, S.; Prevot, P.; Tjierry, A.R. Physico-chemical characteristics of lipoplexes influence cell uptake mechanisms and transfection efficacy. PLoS One 2009, 4, doi:10.1371/journal.pone.0006058.

35. Kasai, H.; Inoue, K.; Imamura, K.; Yuvienco, C.; Montclare, J.K.; Yamano, S. Efficient siRNA delivery and gene silencing using a lipopolypeptide hybrid vector mediated by a caveolae-mediated and temperature-dependent endocytic pathway. J. Nanobiotechnology 2019, 17, 1–14, doi:10.1186/s12951-019-0444-8.

36. del Pozo-Rodríguez, A.; Pujals, S.; Delgado, D.; Solinís, M.A.; Gascón, A.R.; Giralt, E.; Pedraz, J.L. A proline-rich peptide improves cell transfection of solid lipid nanoparticle-based non-viral vectors. J. Control. Release 2009, 133, 52–59, doi:10.1016/j.jconrel.2008.09.004.

37. Yamada, Y.; Sato, Y.; Nakamura, T.; Harashima, H. Evolution of drug delivery system from viewpoint of controlled intracellular trafficking and selective tissue targeting toward future nanomedicine. J. Control. Release 2020, 327, 533–545, doi:10.1016/j.jconrel.2020.09.007.

38. Patel, S.; Ashwanikumar, N.; Robinson, E.; Duross, A.; Sun, C.; Murphy-Benenato, K.E.; Mihai, C.; Almarsson, Ö.; Sahay, G. Boosting Intracellular Delivery of Lipid Nanoparticle-Encapsulated mRNA. Nano Lett. 2017, 17, 5711–5718, doi:10.1021/acs.nanolett.7b02664.

39. Uchida, H.; Itaka, K.; Nomoto, T.; Ishii, T.; Suma, T.; Ikegami, M.; Miyata, K.; Oba, M.; Nishiyama, N.; Kataoka, K. Modulated protonation of side chain aminoethylene repeats in N-substituted polyaspartamides promotes mRNA transfection. J. Am. Chem. Soc. 2014, 136, 12396–12405, doi:10.1021/ja506194z.

40. Maruggi, G.; Zhang, C.; Li, J.; Ulmer, J.B.; Yu, D. mRNA as a Transformative Technology for Vaccine Development to Control Infectious Diseases. Mol. Ther. 2019, 27, 757–772, doi:10.1016/j.ymthe.2019.01.020.

41. del Pozo-Rodríguez, A.; Delgado, D.; Solinís, M.A.; Gascón, A.R.; Pedraz, J.L. Solid lipid nanoparticles: Formulation factors affecting cell transfection capacity. Int. J. Pharm. 2007, 339, 261–268, doi:10.1016/j.ijpharm.2007.03.015.

42. Vicente-Pascual, M.; Albano, A.; Solinís, M.; Serpe, L.; Rodríguez-Gascón, A.; Foglietta, F.; Muntoni, E.; Torrecilla, J.; Pozo-Rodríguez, A. Del; Battaglia, L. Gene delivery in the cornea: In vitro & ex vivo evaluation of solid lipid nanoparticle-based vectors. Nanomedicine 2018, 13, 1847–1864, doi:10.2217/nnm-2018-0112.

APPENDIX III:

MMP-9 downregulation with lipid nanoparticles for inhibiting corneal neovascularization by gene silencing

Josune Torrecilla, **Itziar Gómez-Aguado**, Mónica Vicente-Pascual, Ana del Pozo-Rodríguez, María Ángeles Solinís and Alicia Rodríguez-Gascón

Published in: Nanomaterials (2019)

Journal Impact Factor JCR 2019: 4.324 (Q2) 89/314

Related Categories:

MATERIALS SCIENCE, MULTIDISCIPLINARY (Q2)

NANOSCIENCE & NANOTECHNOLOGY (Q2)

Other quality indicators: 9 citations

MMP-9 downregulation with lipid nanoparticles for inhibiting corneal neovascularization by gene silencing

Abstract:

Gene silencing targeting proangiogenic factors have been shown to be a useful strategy in the treatment of corneal neovascularization (CNV). Among interference RNA (RNAi) molecules, short-hairpin RNA (shRNA) is a plasmid-coded RNA able to down-regulate the expression of the desired gene. It is continuously produced in the host cell, inducing a durable gene silencing effect. The aim of this work was to develop a solid lipid nanoparticle (SLN)-based shRNA delivery system to downregulate metalloproteinase 9 (MMP-9), a proangiogenic factor, in corneal cells for the treatment of CNV associated with inflammation. The nanovectors were prepared using a solvent emulsification-evaporation technique, and after physicochemical evaluation, they were evaluated in different culture cell models. Transfection efficacy, cell internalization, cell viability, the effect on MMP-9 expression, and cell migration were evaluated in human corneal epithelial cells (HCE-2). The inhibition of tube formation using human umbilical vein endothelial cells (HUVEC) was also assayed. The non-viral vectors based on SLN were able to downregulate the MMP-9 expression in HCE-2 cells via gene silencing, and, consequently, to inhibit cell migration and tube formation. These results demonstrate the potential of lipid nanoparticles as gene delivery systems for the treatment of CNV-associated inflammation by RNAi technology.

Keywords: gene therapy; solid lipid nanoparticles; MMP-9; corneal inflammation; HCE-2 cells; capillary tube formation; RNAi; shRNA

1. Introduction

Corneal inflammation, or keratitis, may be caused by many underlying illnesses, including dry eye, eyelid injuries, physical and chemical traumas, and microbial infections (the major cause of corneal inflammation development) [1]. In developing countries, herpes simplex virus type I is the leading cause of keratitis-associated infectious blindness [2]. Common symptoms of keratitis are local pain, tearing, photophobia, blurry vision and ocular redness. When keratitis becomes chronic, visual disturbances occur and often results in tissue damage that leads to corneal ulceration, corneal wound healing, and even perforation, causing visual impairment and blindness [3].

Matrix metalloproteinases (MMPs) are a group of enzymes with a key role in the different phases of the corneal inflammation, from the onset of the epithelial defect to its resolution [4,5]. Among the enzymes included in this group, MMP-9 is one of the primary extracellular matrix

remodeling enzymes that participate in pathological conditions of the cornea, including corneal neovascularization (CNV) [6]. Although neovascularization is part of the repair process of extensive damage to the eye surface [7], it can lead to compromised visual acuity because the cornea loses its avascularity feature. Current treatment options for CNV include the topical application of nonsteroidal or corticosteroidal anti-inflammatory agents, immunosuppressive drugs or surgical interventions such as photodynamic therapy cauterization and β-irradiations [8]. However, the limited efficacy and adverse effects restrict the current treatment therapies [9]. For instance, the rise of intraocular pressure is a complication of topical corticosteroid applications with drugs such as dexamethasone or prednisolone [10] while long-term treatment with immunosuppressants increases the risk of infection and some blood diseases [11]. Therefore, the development of alternative strategies becomes necessary, gene therapy being a hot issue of modern medical research work. The treatment of CNV based on gene therapy can be tackled by two different approaches: gene supplementation to express an antiangiogenic factor, and gene suppression to inhibit the synthesis of a proangiogenic factor. This latter option can be carried out by interference RNA (RNAi) technology [12]. Among RNAi molecules, short-hairpin RNA (shRNA), also called expressed RNAi activator, is a plasmid-coded RNA. In contrast to other forms of RNAi [13,14], shRNA is continuously produced in the host cell and therefore induces a more lasting gene silencing effect. To be effective, shRNA must enter the cell and reach the nucleus, which is a major challenge to the design of a suitable delivery system. In fact, the success of gene therapy is strongly dependent on the development of safe and efficacious delivery systems that are able not only to reach the target cell, but also to provide an adequate intracellular disposition of the genetic material.

The cornea is a well-suited tissue for the application of gene-based therapies due to its easily accessible and immune-privileged status [15]. However, a historically poor transfection efficiency after topical instillation has hampered the development of gene delivery in the cornea, and the direct administration of the vectors into the corneal stroma is often used in preclinical studies. The design and evaluation of more efficient systems for nucleic acid delivery would promote the advance of gene therapy for corneal diseases, and the development of clinical trials, which are very scarce [16,17]. Most studies that evaluated gene delivery into the cornea have used viral vectors [18,19], which are well-established and effective, but apart from the technological drawbacks in terms of production and the limited size of the genetic material, they can induce oncogenicity and an immune response, mainly after repeated administrations [9]. Non-viral vectors offer a safer, more attractive alternative to viral vectors for corneal gene delivery due to their easy generation, ability to transport large nucleic acids or multiple genes,

and more versatility for DNA conjugation. In this sense, our research group showed the potential of lipidic non-viral systems to efficiently transfect ocular tissues, including the corneal epithelium [20–22]. Lipid nanoparticles, which are at the forefront of the rapidly developing field of nanotechnology, present a high potential in biomedical application, such as the administration of chemotherapeutic drugs or nucleic acids [23,24]. Actually, solid lipid nanoparticles (SLNs) are regarded as one of the most effective non-viral vectors for gene therapy with additional advantages such as biocompatibility and the ease of large-scale production [25]. In addition, cationic SLNs present several advantages that make them appropriate for corneal gene therapy, since they interact with negatively charged mucus on the ocular surface after topical administration [26]. The mucoadhesive properties favor the retention time and, therefore, corneal permeation through endocytic uptake by the corneal epithelial cells.

Considering this situation, the aim of this work was to develop an SLN-based shRNA delivery system to downregulate MMP-9 in corneal cells using RNAi technology as a gene suppression therapy for the treatment of CNV-associated inflammation.

2. Materials and methods

2.1. Materials

Precirol® ATO 5 was a gift by Gattefossé (Madrid, Spain), DOTAP (1,2-dioleoyl-3-trimethylammonium-propane chloride salt) was purchased from Avanti Polar-lipids, Inc. (Alabaster, AL, USA), Tween 80 and dichloromethane were obtained from Panreac (Madrid, Spain). Nile Red, protamine sulfate salt Grade X (P), dextran (M_w of 3.26 KDa) (DX), deoxyribonuclease I (DNase I), sodium dodecyl sulfate (SDS), human insulin solution, and the Cell Counting Kit-8 (CCK-8) were obtained from Sigma-Aldrich (Madrid, Spain). The plasmid encoding a short-hairpin interference RNA against MMP-9 (p-shRNA-MMP-9; 4993 bp) and the plasmid encoding both a short-hairpin interference RNA against MMP-9 and the green fluorescent protein (GFP) (p-shRNA-MMP-9-GFP; 6675 bp) were obtained from GeneCopeia (Rockville, MD, USA). GelRed™ was obtained from Biotium (Fremont, CA, USA), and the materials used in electrophoresis on agarose gel were purchased from Bio-Rad (Madrid, Spain).

The human corneal epithelial (HCE-2) cell line and human umbilical vein endothelial cells (HUVEC) were supplied by American Type Culture Collection (ATCC, Manassas, VA, USA). For the cell culture, Dulbecco's Modified Eagle's Medium/Nutrient Mixture F-12 with Gluta MAX™ (DMEM/F-12 with GlutaMAX), Medium 200, Large vessel Endothelial Supplement (LVES), fetal bovine serum (FBS), and penicillin-streptomycin were acquired from Life Technologies (Thermo Fisher Scientific, Madrid, Spain). Epidermal growth factor (EGF) was obtained from Miltenyi

Biotec (Madrid, Spain), and Trypsin-EDTA (ethylenediaminetetraacetic acid) from Lonza (Basel, Switzerland). Recombinant human tumor necrosis factor alpha (TNF-α) was obtained from Peprotech (London, UK), the Reporter Lysis Buffer (RLB) was purchased in Promega Biotech Iberica (Madrid, Spain), and the Micro BCA™ Protein Assay Kit and Geltrex® LDEV-Free Reduced Growth Factor Basement Membrane Matrix from Thermo Scientific (Madrid, Spain).

Paraformaldehyde (PFA) was purchased from Panreac (Madrid, Spain) and phosphate buffered saline (PBS) and 4-(2-hydroxyethyl) piperazine-1-ethanesulfonic acid (HEPES) buffer was purchased from Gibco (Thermo Fisher Scientific, Madrid, Spain). Transfectin® was acquired from Bio-Rad (Madrid, Spain). Enzyme-Linked Immuno Sorbent Assay (ELISA) for MMP-9 with the Duo Set Ancillary reagent kit was purchased from R&D Systems (Minneapolis, MN, USA).

The goat monoclonal anti-hMMP-9 antibody and Alexa Fluor 568-conjugated donkey anti-goat IgG were obtained from Abcam (Cambridge, MA, USA), and 4',6-Diamidine-2'-phenylindole dihydrochloride (DAPI) Fluoromount-G® was obtained from SouthernBiotech (Birmingham, AL, USA).

2.2. Methods

2.2.1. Elaboration of the p-shRNA-MMP-9-bearing vectors

Different formulations based on SLN, dextran (DX), protamine (P), and plasmids (p-shRNA-MMP-9 or p-shRNA-MMP-9-GFP) were prepared as previously described [27]. First, SLNs were prepared with Precirol® ATO 5 (Gattefossé, Madrid, Spain), DOTAP, and Tween 80, by using a solvent emulsification-evaporation technique. The final nanocarriers were formed by the addition of a complex previously prepared with P, p-shRNA-MMP-9, and DX. The vectors were formed with the following component ratios (*w/w*), expressed as DX/P/p-shRNA-MMP-9/SLN: 1/2/1/5, 1/1/1/5, 2/1/1/5 and 2/0.5/1/5.

2.2.2. The characterization of the vectors

The plasmid, the complex of DX, P and the plasmid (component ratios (w/w) 2:1:1, respectively), and the final vector were subjected to electron microscopy negative staining for visualization. The vector suspension (10 μL) was adhered onto glow-discharged carbon coated grids for 60 s. The liquid remaining was removed by blotting on filter paper and the samples were stained with 2% uranyl acetate for 60 s. A JEOL JEM 1400 Plus transmission electron microscope (TEM, Tokyo, Japan) was used to obtain digital images.

The Correlation Spectroscopy (PCS) technique was used to measure the particle size and the polydispersity index and Laser Doppler Velocimetry (LDV) was used to measure the ζ-potential

of the vectors. These measurements were carried out in a ZetaSizer Nano ZS (Malvern Panalytical, Malvern, UK). We analyzed the ability of the nanocarriers to bind the DNA, to protect it against DNase I digestion, and to release it by electrophoresis on 1% agarose gel containing Gel Red™ (30 min at 120 V). An Uvidoc D-55-LCD-20 M Auto transilluminator (Uvitec, Cambridge, UK) was used to analyze the gels. The vectors were diluted in MilliQ™ water (Merck Millipore, Madrid, Spain) up to a final concentration of 0.03 µg DNA/µL. To evaluate the capacity of the plasmid to be released, the vectors were treated with 4% sodium dodecyl sulfate (SDS) solution. For DNase I protection evaluation, a concentration of 1 U DNase I/2.5 µg DNA was added to the vectors and then the mixtures were incubated 30 min at 37 °C. Afterward, the p-shRNA-MMP-9 was released from the SLNs with SDS. An untreated 1-kb DNA ladder from NIPPON Genetics Europe (Dueren, Germany) was added as a molecular weight (MW) control.

2.2.3. Cell culture conditions

The HCE-2 cell line was maintained in DMEM/F-12 GlutaMAX medium supplemented with 15% (*v*/*v*) heat-inactivated fetal bovine serum (FBS), insulin (4 mg/mL), EGF (10 ng/mL), and penicillin–streptomycin (1%). Cells were incubated with 5% CO_2 at 37 °C and subcultured every 7 days using trypsin/EDTA. Cells from passages 1 to 4 were used to perform all in vitro assays.

2.2.4. In vitro transfection assays

For in vitro transfection, cells were seeded on 24-well plates at a density of 1×10^5 cells/well and were allowed to adhere overnight. Cells were transfected with the vectors at a plasmid dose of 2.5 µg and maintained for 30 min at 37 °C and 5% CO_2. Four hours after the addition of the vectors, the media were replaced, and the cell culture was allowed to grow up to 72 h at 37 °C and 5% CO_2.

2.2.4.1. Percentage of transfected cells and GFP production

To evaluate the rate of cells transfected, the vectors were prepared with the p-shRNA-MMP-9-GFP plasmid. The percentage of transfected cells was measured using a CytoFLEX (Beckman Coulter, Indianapolis, IN, USA) flow cytometer. Cells were rinsed with PBS (three times), separate from plates, and resuspended in PBS. Finally, samples were evaluated by flow cytometry at 525 nm collecting 1×10^4 events per sample. The amount of intracellular GFP, in terms of relative fluorescence units (RFU)/mg total protein, was quantified by fluorometry. To do that, the culture media were substituted with 300 mL of 1× reported lysis buffer (RLB) and frozen. The cells were then scraped and centrifuged at 4 °C and 12,000× *g* for 2 min. The GFP fluorescence in the supernatant was measured by using a Glomax™ Multi-Detection System (Promega Biotech

Iberica, Madrid, Spain). The fluorescence was corrected by the amount of protein, quantified by a Micro BCA™ Protein Assay kit (Thermo Scientific, Madrid, Spain).

2.2.4.2. Silencing of MMP-9

In order to know the capacity of the nanocarriers bearing the p-shRNA-MMP-9 plasmid to downregulate the MMP-9, we transfected HCE-2 cells using the same protocol described above. A p-shRNA-scramble (shRNAscr) plasmid and a naked p-shRNA-MMP-9 plasmid were used as negative controls. The silencing activity was evaluated at 72 h by measuring the MMP-9 secreted to the culture medium, and by detecting the MMP-9 at an intracellular level. The amount of MMP-9 secreted by the cells was measured in the culture medium by an ELISA kit (R&D Systems, Minneapolis, MN, USA).

The presence of MMP-9 in HCE-2 was evaluated by immunocytochemistry. For this purpose, untreated and transfected cells were seeded in 24-well plates with cover glasses in the bottom that were previously treated with the attachment factor protein (Thermo Fisher Scientific, Madrid, Spain). After adequate washing in PBS, the cells were blocked and permeabilized with PB buffer, 0.3% Triton X-100, 10% donkey serum for 30 min. A goat monoclonal anti-MMP-9 antibody in PBS buffer (2.5% donkey serum, 0.1% triton X-100) was then added and maintained for 1 h. After 3 more washes with PBS, the cells were dyed with the secondary antibody Alexa Fluor 568-conjugated donkey anti-goat IgG for 1 h in the dark. Finally, the nuclei were dyed with the mounting media DAPI Fluoromount-G® **(**SouthernBiotech, Birmingham, AL, USA). The specificity of the staining was controlled by incubating cells without the primary antibody. The images were obtained with an inverted fluorescence microscope (Nikon TMS, Izasa Scientific, Madrid, Spain) at 40× magnification. Intracellular MMP-9 was also evaluated in HCE-2 cells previously stimulated with 10 ng of TNF-α, a proinflammatory mediator, for 6 h.

2.2.5. Cell viability

We measured the viability of the HCE-2 cells treated with the nanocarriers with the CCK-8 assay following the manufacturer's protocol. In short, the cells were seeded in a 96-well plate at a density of 1×10^3 cells/well and incubated overnight at 37 °C in a CO_2 incubator followed by transfection with the different vectors. CCK-8 reactive solution was added to each well, incubated at 37 °C for 4 h. Finally, the absorbance was measured in a microplate reader at 450 nm.

2.2.6. Cellular uptake of non-viral vectors

The internalization of the vectors by the HCE-2 cells was studied using a CytoFLEX flow cytometer. For this purpose, SLNs were labeled with the fluorescent Nile Red dye (λ = 590 nm)

as previously described [28]. The cells were treated with the nanosystems for 2 h, resuspended in PBS and analyzed by flow cytometry at 610 nm, collecting 1×10^4 events per sample.

2.2.7. Intracellular disposition of the vectors

In order to know the intracellular disposition of the plasmid, cells were seeded at a density of 100,000 cells and 1 mL per well and incubated at 37 °C and 5% CO_2 for 24 h in Millicell EZ slides (Merck Millipore, Madrid, Spain). Then, they were then treated with vectors containing the plasmid labeled with ethidium monoazide (EMA; Dro Byosystems S.L., San Sebastian, Spain). After 4, 12, and 24 h, the slides were rinsed with PBS and fixed with 4% PFA. Nuclei were labeled with DAPI Fluoromount-G® (SouthernBiotech, Birmingham, AL, USA), and images were captured with the inverted fluorescence microscope (Nikon TMS, Izasa Scientific, Madrid, Spain)

2.2.8. Cell migration assay

The effect of the formulations on the migration of HCE-2 cells was studied using a wound healing assay. For this purpose, HCE-2 cells were grown to confluence in 24-well plates coated with attachment factor containing gelatin (substrate of MMP-9) and a linear wound was created with a pipette tip. Afterward, cultures were rinsed twice with PBS to remove detached cells and 1 mL of fresh serum-free medium was added. Untreated cells, cells treated with the vector (corresponding to a plasmid dose of 2.5 µg), and cells stimulated with 10 ng of TNF-α were allowed to migrate at 37 °C under 5% CO_2. After 4 h, the medium was changed by a 1 mL complete medium. The wound width was measured at 7 different points at 7, 24, and 48 h. The relative distance filled was calculated with the formula: $m = (1 - n_t/r) \times 100\%$, where m is the migration, n_t is the width of the scratch at time t, and r is the initial width of the scratch [29]. Blank nanoparticles were also assayed.

2.2.9. HUVEC tube formation assay

The HUVEC cell line was employed to evaluate whether MMP-9 downregulation is able to inhibit capillary tube formation. HUVEC cells were seeded onto Geltrex® LDEV-Free Reduced Growth Factor Basement Membrane Matrix in 96-well plates and the culture medium was replaced with conditioned culture medium from HCE-2 cells untreated or treated with vector III, TNF-α, or TNF-α plus vector III. The plates were incubated at 37 °C, and tube formation was evaluated after 15 h of incubation under an optic inverted microscope. Morphometric measurements in captured images were obtained using the ImageJ software (National Institutes of Health, Bethesda, MA, USA) [30].

2.2.10. Statistical analysis

Significant differences between groups were analyzed with IBM SPSS Statistics for Windows, Version 23.0. (IBM Corp, Armonk, NY, USA). Normal distribution data were assessed by the Shapiro–Wilk test, and homogeneity of variance using the Levene test. The formulations were compared with the ANOVA test. Results are expressed as mean ± standard deviation and p values of less than 0.05 were regarded as statistically significant.

3. Results

3.1. Characterization

Figure 1 shows images of the p-shRNA-MMP-9 plasmid, the DX:P:p-shRNA-MMP-9 complex, and the DX:P:p-shRNA-MMP-9:SLN vector, acquired by TEM. We can observe that the plasmid, in dark, appears highly condensed after the binding to protamine and dextran. The picture also shows the spherical shape of the final vector.

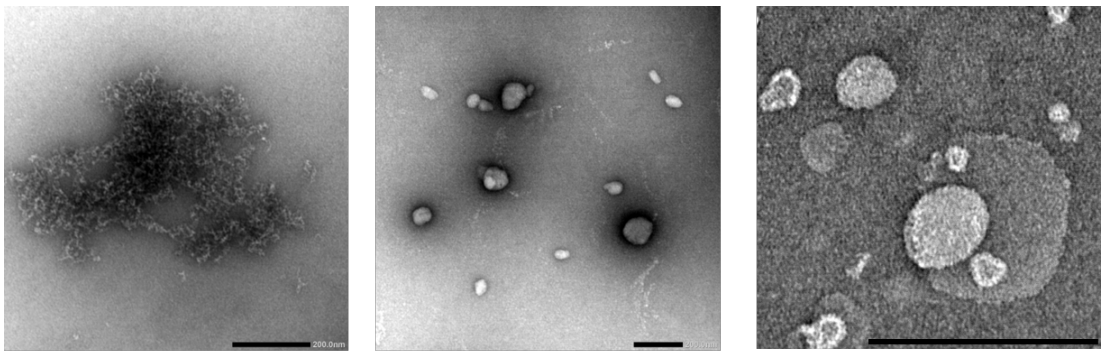

p-shRNA-MMP-9 DX:P:p-shRNA-MMP-9 DX:P:p-shRNA-MMP-9:SLN

Figure 1. The images of p-shRNA-MMP-9, DX:P:p-shRNA-MMP-9 complex (w/w ratios 2:1:1), and DX:P:p-shRNA-MMP-9:SLN vector (w/w ratios 2:1:1:5), acquired by Transmission Electronic Microscopy (TEM). Scale bar: 200 nm. DX: dextran; P: protamine.

The particle size of the vectors (Table 1) was in the range of nanometers, ranging from 182 to 216 nm, and all had a positive surface charge (+36.1 to +45.7 mV). Vector II presented a significantly higher particle size and a lower surface charge than the other vectors. The polydispersity index (PdI) was similar and under 0.30 in all cases, which indicates the homogeneity of the particle size.

Table 1. The characterization of nanovectors bearing the p-shRNA-MMP-9 plasmid. Size (nm), Zeta potential (mV), and polydispersity index are presented as mean ± SD (n = 3).

Vector	DX:P:p-shRNA-MMP-9:SLN Ratio	Size (nm)	ZP (mV)	PdI
I	1:2:1:5	186 ± 5	+40.7 ± 1.0 **	0.21 ± 0.01
II	1:1:1:5	216 ± 4 *	+36.1 ± 1.0 *	0.28 ± 0.02
III	2:1:1:5	190 ± 3	+45.1 ± 1.2	0.22 ± 0.01
IV	2:0.5:1:5	189 ± 4	+42.8 ± 0.8 **	0.21 ± 0.01
V	3:1:1:5	182 ± 2	+45.7 ± 1.4	0.23 ± 0.01

* $p < 0.05$ with respect to the other formulations. ** $p < 0.05$ with respect to formulations II, III, and V. Abbreviations: DX: dextran; SLN: solid lipid nanoparticle; MMP: metalloproteinase; P: protamine; ZP: ζ-potential; PdI: polydispersity index.

To analyze the ability of the vectors to bind, protect, and release p-shRNA-MMP-9 plasmid, an agarose gel was conducted. The absence of bands in lanes 2–6 in Figure 2 indicates that all vectors were able to completely bind the p-shRNA-MMP-9. The gel also shows that formulations I to III (lanes 8–10, respectively) protected the plasmid more efficiently than formulations IV and V (lanes 11 and 12, respectively). After the treatment of the nanosystems with SDS, the plasmid was effectively released (lanes 13 to 17).

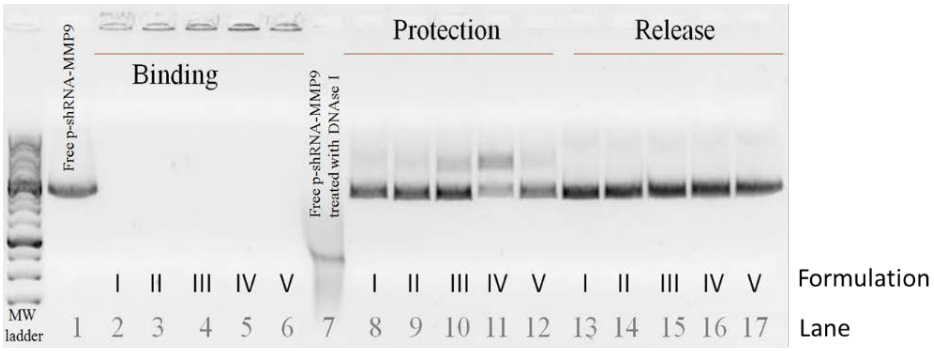

Figure 2. The agarose gel electrophoresis study of the capacity of the vectors to bind, protect, and release the p-shRNA-MMP-9. Lane 1: free p-shRNA-MMP-9; lanes 2 to 6: binding; lane 7: free p-shRNA-MMP-9 treated with DNase I; lanes 8 to 12: vectors treated with DNase I; lanes 13 to 17: vectors treated with SDS (induced release). Molecular weight (MW) ladder corresponds to the 1 kb DNA ladder from NIPPON Genetics Europe (Dueren, Germany).

3.2. In Vitro transfection and cell viability

The percentage of HCE-2 transfected cells and the amount of GFP (expressed as RFUs corrected by the total amount of protein) were measured 72 h after the addition of vectors. The percentage of transfected cells ranged from 3.5% to 5.6%, and the vector that presented the highest transfection efficacy, expressed as both RFUs and percentage of cells transfected, was vector III (Figure 3). With all formulations, cell viability was always higher than 90%; no difference was detected compared to the untreated cells.

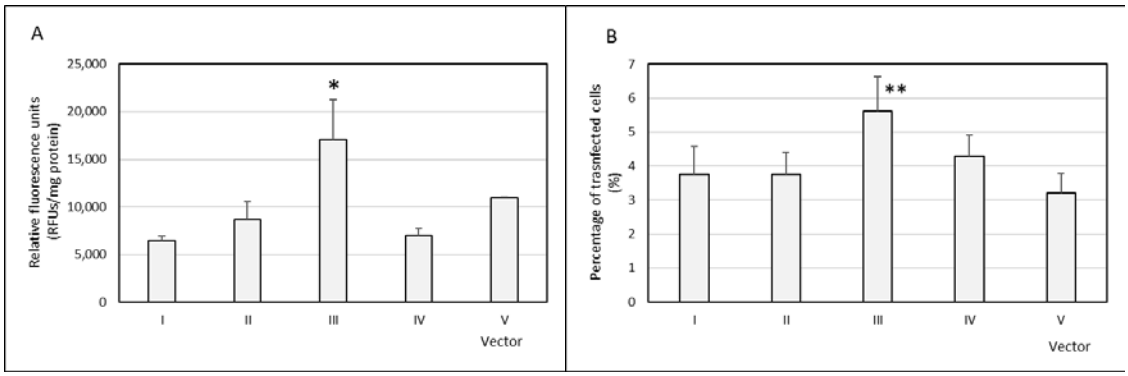

*Figure 3. The transfection efficacy of the vectors in human corneal epithelial (HCE)-2 cells. (A) Relative fluorescence units per mg of protein (RFUs/mg protein) of the transfected cells. (B) Percentage of transfected cells (n = 4). Data are expressed as mean ± standard deviation. * p < 0.05 with respect to the other formulations. ** p < 0.05 with respect to formulations I, II, and V.*

To evaluate the silencing capacity of the nanoformulations, we quantified the MMP-9 secreted by the HCE-2 cells both untreated and treated with the vectors. Figure 4 shows that only vector III was able to significantly decrease the amount of MMP-9 secreted by the cells, with a silencing effect close to 30%. Cell viability was close to 100%, and no difference was detected compared to the untreated cells. Based on these results, vector III was selected for further experiments.

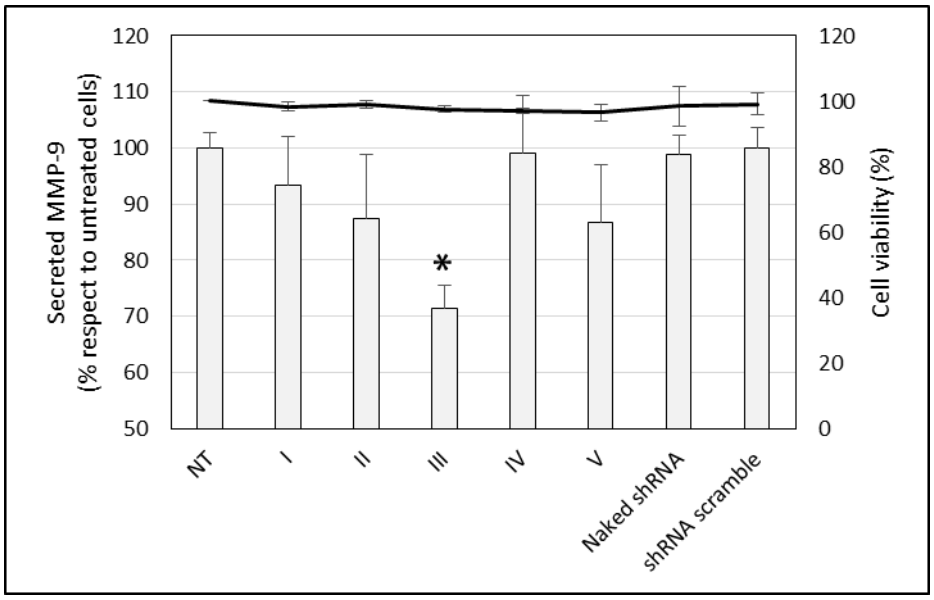

*Figure 4. The secreted MMP-9 levels (bars, expressed as a percentage with respect to untreated cells) and viability (line) of HCE-2 cells treated with the vectors and naked p-shRNA-MMP-9. Data are expressed as mean ± SD of 4 experiments. NT: non-treated cells. * p < 0.05 with respect to NT cells.*

Figure 5A shows that the stimulation of HCE-2 cells with TNF-α significantly increased the levels of secreted MMP-9. The addition of vector III to non-stimulated and TNF-α-stimulated HCE-2 cells induced a decrease of about 20% in the secretion of MMP-9 levels to the culture medium.

The intracellular expression of the metalloproteinase (Figure 5B) confirmed the silencing effect of the vector.

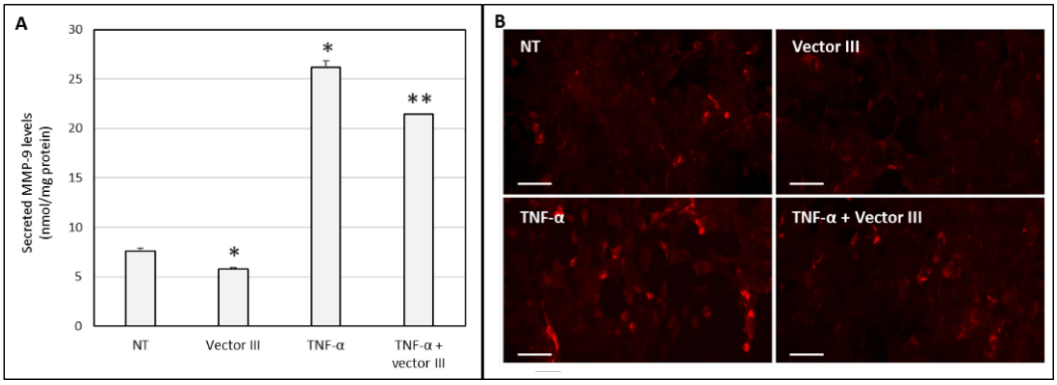

*Figure 5. (A) The secreted MMP-9 levels in HCE-2 cells untreated and treated with vector III, TNF-α, or both. (B) Fluorescence images of immunostained MMP-9 in HCE-2 cells untreated and treated with vector III, TNF-α, or both. NT: non-treated cells. * $p < 0.05$ respect to non-treated cells (NT), ** $p < 0.05$ respect to TNF-α. Scale bar: 60 µm.*

3.3. Cellular uptake and intracellular trafficking

Flow cytometry histograms (Figure 6) show that vector III was efficiently internalized by the HCE-2 cells. A fluorescence microscopy photograph confirmed the high uptake degree of the nanosystems.

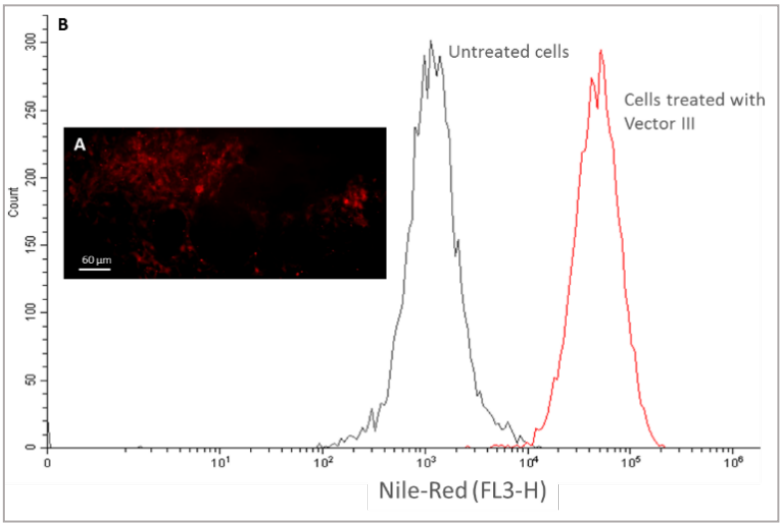

Figure 6. The uptake of the vector III in HCE-2 cells 2 h after transfection with Nile Red-labelled vector containing p-shRNA-MMP-9 against MMP-9. (A) Fluorescence microscopy image (40×); (B) flow cytometry histograms.

Figure 7 shows the fluorescence microscopy images captured at 4, 12, and 24 h post-addition of the vector III prepared with EMA-labelled DNA. As can be seen, the approach of the plasmid to the nucleus was increasing over time.

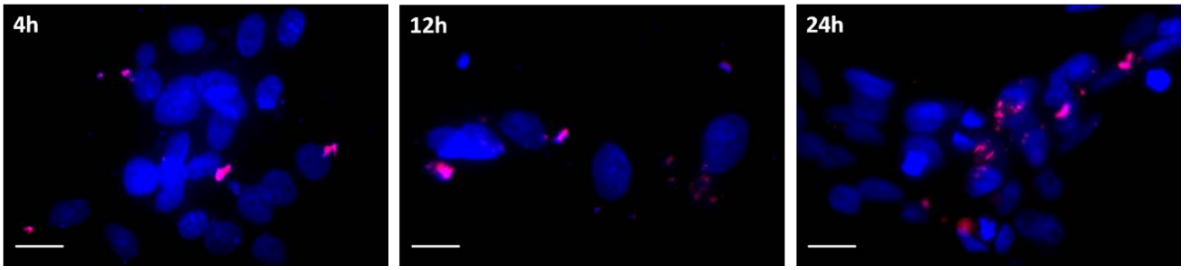

Figure 7. The fluorescence microscopy images of HCE-2 cells at different times after addition of vector III (4, 12, and 24 h). Ethidium monoazide (EMA)-labelled DNA (red) and nuclei stained with DAPI fluoromount-G® (SouthernBiotech, Birmingham, AL, USA) (blue). Scale bar: 20 µm.

3.4. Migration assay

Figure 8 shows that vector III was able to reduce HCE-2 cell migration. While at 48 h, untreated cells reduced the wound width close to 100%, cells treated with vector III (stimulated and non-stimulated with TNF-α) produced a closure of only about 70%.

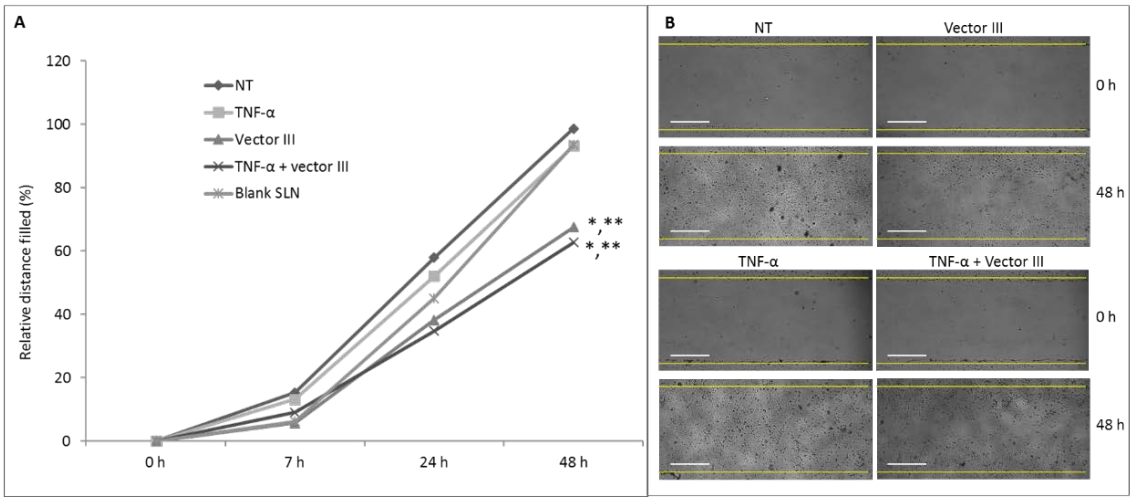

*Figure 8. The effect of vector III on HCE-2 cell migration. (A) The evolution of the distance between cells of the edge of the wound; the mean data of reduction of the wound width from the 4 replicates (measures) in each condition. (B) Phase contrast representative images (4×). NT: non-treated cells. Statistics at 48 h. * p < 0.05 respect to NT, ** p < 0.05 respect to cells treated with TNF-α. Scale bar: 60 µm.*

3.5. HUVEC tube formation assay

Figure 9 shows representative images of HUVEC cells treated with culture medium from HCE-2 untreated or treated with TNF-α, vector III, or TNF-α plus vector III. Both the photographs and the morphometric measurement show the inhibition of the tube formation, in terms of total master segment length, the number of meshes, total segment length, and total length (Figure 9B).

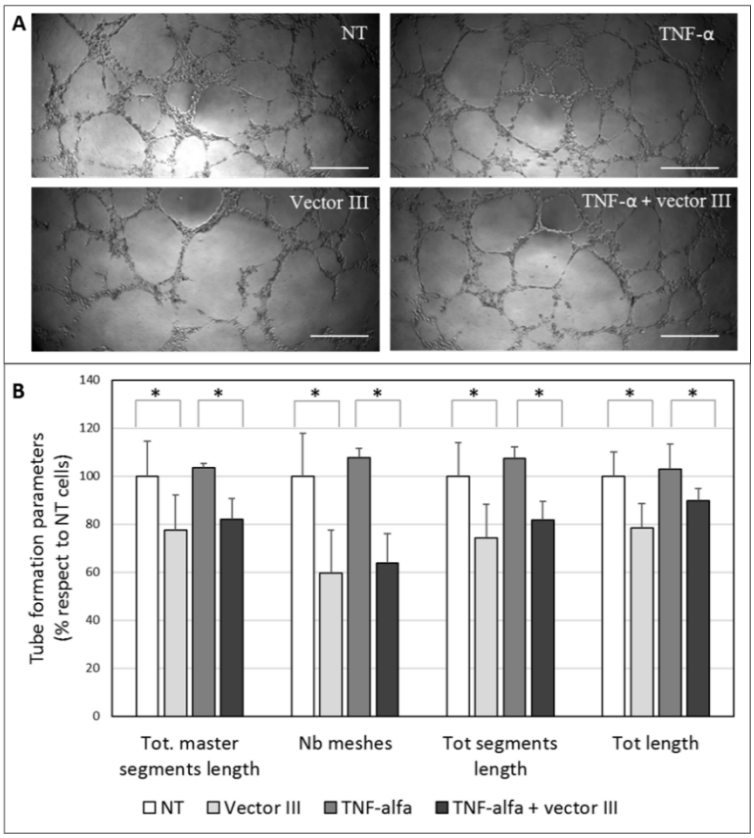

*Figure 9. (A) The representative images obtained in the tube formation assay in human umbilical vein endothelial cells (HUVECs) and (B) the quantification of tube formation. Data were normalized relative to the values of non-treated cells (NT). * $p < 0.05$. Scale bar: 60 µm.*

4. Discussion

Among the different strategies used in the treatment of CNV-associated inflammation, gene silencing has been shown to be useful for targeting proangiogenic factors. In a previous study [31], two plasmids encoding shRNA targeted against MMP-9 were effective to inhibit MMP-9 enzyme expression after intrastromal injection into the cornea of mice, stopping angiogenesis and decreasing the severity of herpetic keratitis. The authors concluded that the in vivo therapeutic application depends on the availability of efficient vehicles to deliver the RNAi to the target cells with low toxicity and in a method suitable for repeated administrations. In this regard, in the present work, we have developed vectors containing a shRNA against MMP-9 to be useful for the treatment of CNV. The systems are composed of SLNs, protamine, and dextran. The protamine has shown to increase the transfection efficacy of non-viral vectors due to its high ability to condense the genetic material, and therefore, to protect it from degradation, facilitate the entry into the nucleus, and to enhance transcription [32–34]. A polysaccharide, dextran, was also included because it is biocompatible and has demonstrated to contribute to nucleic acid delivery; moreover, it shows low cytotoxicity, is easily subject to chemical modification, have stealth properties, and is widely used for pharmaceutical and biomedical

applications [35,36]. For the formation of the vectors, the complex dextran-protamine-plasmid is adsorbed on the nanoparticle surface, playing the electrostatic interactions between the components a fundamental role. The plasmid is highly condensed by the protamine and the cationic lipid, and dextran modulates these interactions, conditioning the final structure (Figure 1) and the physicochemical characteristics of the vectors.

All nanosystems that we prepared showed suitable features for transfection: particle size in the range of nanometers, and the ability to bind, release, and protect the p-shRNA-MMP-9 against nucleases. It is important to consider that the transfection success of a non-viral system depends on the equilibrium between the capacity to condense and release the DNA [37]. This balance is conditioned by the nature and proportion of the components in the vector, which bind the genetic material by electrostatic interactions, as mentioned above. Accordingly, vector IV, which was prepared with the lowest proportion of protamine, provided the lowest protection against DNase I.

All vectors were able to transfect HCE-2 cells, with vector III being the most efficacious in terms of percentage of cells transfected and the amount of protein expressed as well. The higher efficacy of vector III was confirmed when we measured the protein MMP-9, secreted by the HCE-2 cells. This vector was able to induce a decrease of approximately 30% in the amount of MMP-9 protein synthesized by the cells. The effect of the vector is related to extensive internalization and to the ability of the plasmid to be released in the cytoplasm close to the nuclear membrane, as Figures 6 and 7 show.

Once we demonstrated the efficacy in silencing MMP-9 in HCE-2 cells, an SLN-based vector was evaluated in TNF-α stimulated cells. TNF-α is a proinflammatory mediator that plays an important role in a variety of corneal diseases [38]. It disrupts the barrier function of human corneal epithelial cells and contributes to ocular inflammation [39,40]. TNF-α is reportedly elevated in corneas from individuals suffering keratitis [40], and this cytokine has been shown to stimulate MMP-9 activity in HCE cells [6]. We confirmed the increase in MMP-9 levels after the stimulation of the HCE-2 cells with TNF-α and the ability of the SLN-based vector to reduce the production of the MMP-9 in TNF-α-induced cells. These results indicate the suitability of TNF-α induced HCE-2 cells as an in vitro model to evaluate new formulations based on the MMP-9 downregulation for CNV.

MMPs are enzymes that are capable of cleaving numerous extracellular matrix proteins, which facilitates the migration of corneal epithelial cells to the underlying stroma [41–44]. Actually, the increased production and activity of MMPs are related to a more migratory and invasive cell

phenotype [45,46]; conversely, the reduction of MMP-9 in HCE cells inhibits cell migration [47]. The suppression of the production of MMP-9 in the ocular surface contributed to the improvement in the corneal barrier function in a model of dry eye mice [48]. In our study, vector III was able to decrease the migration of HCE-2 cells. This effect can be related to the inhibition of MMP-9 production. MMP-9 degrades type IV collagen and gelatin substrates [49], and, therefore, a decrease in MMP-9 levels will result in a lower capacity to degrade the gelatin, used in this study as extracellular matrix protein. This strategy may be clinically helpful for the treatment of corneal diseases in which MMP-9 activity and inflammatory cytokines are upregulated.

As mentioned above, MMP-9 has also been revealed to play an important role in angiogenesis and, specifically, in angiogenesis associated with herpetic keratitis [50]. Corneal avascularity relies on the balance between proangiogenic and antiangiogenic factors. When the counterbalance between both kinds of factors shifts toward proangiogenic factors, new blood vessels grow from pre-existing vasculature at the pericorneal plexus [51]. In response to a stimulus such as an injury, the corneal epithelial cells release angiogenic growth factors that bind to receptors on the vascular endothelial cells of pericorneal vessels [9], and although CNV occurs in the corneal stroma, it is regulated by corneal epithelium-expressed factors. Vector III was able to partially suppress the tube formation in an in vitro HUVEC tube formation assay. Morphometric measurements revealed that total master segment length, the number of meshes, total segments length, and total length decreased when the HUVEC cells were supplemented with the conditioned culture medium from HCE-2 cells treated with the vector. The magnitude of the inhibition of the tube formation was in the same order as the reduction of the secreted MMP-9 levels by the HCE-2 cells. The effect of our vector was observed also for TNF-α-stimulated cells. We previously showed, in rabbit corneal explants, the ability of SLN to transfect different layers of the cornea [20]. Therefore, we expect that after the in vivo topical administration of the vector, MMP-9 downregulation could have effects not only in epithelial cells, but also in stromal keratocytes and even vascular endothelial cells, which are also involved in CNV, contributing to the total effect.

In conclusion, we demonstrated the ability of non-viral vectors based on SLN to downregulate MMP-9 expression in HCE-2 cells by gene silencing and, consequently, to inhibit cell migration and tube formation. These results highlight the potential of lipid nanoparticles as gene delivery systems for the treatment of CNV-associated inflammation by RNAi technology. The next step to assess the potential of this new vector will be to move towards in vivo studies.

References

1. Torrecilla, J.; del Pozo-Rodríguez, A.; Vicente-Pascual, M.; Solinís, M.Á.; Rodríguez-Gascón, A. Targeting corneal inflammation by gene therapy: Emerging strategies for keratitis. Exp. Eye Res. 2018, 176, 130–140.
2. Kwon, M.S.; Carnt, N.A. Truong, N.R.; Pattamatta, U.; White, A.J.; Samarawickrama, C.; Cunningham, A.L. Dendritic cells in the cornea during Herpes simplex viral infection and inflammation. Surv. Ophthalmol. 2018, 63, 565–578.
3. Lee, S.H.; Kim, K.W.; Joo, K.; Kim, J.C. Angiogenin ameliorates corneal opacity and neovascularization via regulating immune response in corneal fibroblasts. BMC Ophthalmol. 2016, 16, 57.
4. Sivak, J.M.; Fini, M.E. MMPs in the eye: Emerging roles for matrix metalloproteinases in ocular physiology. Prog. Retin. Eye Res. 2002, 21, 1–14.
5. Mohan, R.; Chintala, S.K.; Jung, J.C.; Villar, W.V.; McCabe, F.; Russo, L.A.; Lee, Y.; McCarthy, B.E.; Wollenberg, K.R.; Jester, J.V.; et al. Matrix metalloproteinase gelatinase B (MMP-9) coordinates and effects epithelial regeneration. J. Biol. Chem. 2002, 277, 2065–2072.
6. Yang, Y.N.; Wang, F.; Zhou, W.; Wu, Z.Q.; Xing, Y.Q. TNF-α stimulates MMP-2 and MMP-9 activities in human corneal epithelial cells via the activation of FAK/ERK signaling. Ophthalmic Res. 2012, 48, 165–170.
7. Feizi, S.; Azari, A.A.; Safapour, S. Therapeutic approaches for corneal neovascularization. Eye Vis. 2017, 4, 28.
8. Lu, X.X.; Zhao, S.Z. Gene-based therapeutic tools in the treatment of Cornea Disease. Curr. Gene Ther. 2018, doi:10.2174/1566523219666181213120634.
9. Liu, S.; Romano, V.; Steger, B.; Kaye, S.B.; Hamill, K.J.; Willoughby, C.E. Gene-based antiangiogenic applications for corneal neovascularization. Surv. Ophthalmol. 2018, 63, 193–213.
10. Kersey, J.P.; Broadway, D.C. Corticosteroid-induced glaucoma: A review of the literature. Eye 2006, 20, 407–416.
11. O'Doherty, M.; Murphy, C.C. Update on immunosuppressive therapy for corneal transplantation. Int. Ophthalmol. Clin. 2010, 5, 113–122.
12. Guzman-Aranguez, A.; Loma, P.; Pintor, J. Small-interfering RNAs (siRNAs) as a promising tool for ocular therapy. Br. J. Pharmacol. 2013, 170, 730–747.
13. Torrecilla, J.; Rodríguez-Gascón, A.; Solinís, M.Á.; Del Pozo-Rodríguez, A. Lipid nanoparticles as carriers for RNAi against viral infections: Current status and future perspectives. BioMed Res. Int. 2014, 2014, 161794. Available online: https://www.hindawi.com/journals/bmri/2014/161794/ (accessed on 25 March 2019).
14. Jin, X.; Sun, T.; Zhao, C.; Zheng, Y.; Zhang, Y.; Cai, W.; He, Q.; Taira, K.; Zhang, L.; Zhou, D. Strand antagonism in RNAi: An explanation of differences in potency between intracellularly expressed siRNA and shRNA. Nucleic Acids Res. 2012, 40, 1797–1806.

15. Rodríguez-Gascón, A.; del Pozo-Rodríguez, A.; Isla, A. Gene Therapy in the Cornea; In: eLS; John Wiley Sons, Ltd.: Chichester, UK, 2016. Available online: https://onlinelibrary.wiley.com/doi/abs/10.1002/9780470015902.a0024274 (accessed on 25 March 2019).

16. ClinicalTrials.gov. Available online: https://clinicaltrials.gov/ (accessed on 8 March 2019).

17. Gene Therapy Clinical Trials Worldwide. Available online: http://www.abedia.com/wiley/ (accessed on 8 March 2019).

18. Mohan, R.R.; Sinha, S.; Tandon, A.; Gupta, R.; Tovey, J.C.; Sharma, A. Efficacious and safe tissue-selective controlled gene therapy approaches for the cornea. PLoS ONE 2011, 6, e18771.

19. Rodier, J.T.; Tripathi, R.; Fink, M.K.; Sharma, A.; Korampally, M.; Gangopadhyay, S.; Giuliano, E.A.; Sinha, P.R.; Mohan, R.R. Linear Polyethylenimine-DNA Nanoconstruct for Corneal Gene Delivery. J. Ocul. Pharmacol. Ther. 2019, 35, 23–31.

20. Vicente-Pascual, M.; Albano, A.; Solinís, M.Á.; Serpe, L.; Rodríguez-Gascón, A.; Foglietta, F.; Muntoni, E.; Torrecilla, J.; Pozo-Rodríguez, A.D.; Battaglia, L. Gene delivery in the cornea: In vitro & ex vivo evaluation of solid lipid nanoparticle-based vectors. Nanomedicine 2018, 13, 1847–1864.

21. Delgado, D.; del Pozo-Rodríguez, A.; Solinís, M.Á.; Avilés-Triqueros, M.; Weber, B.H.; Fernández, E.; Gascón, A.R. Dextran and Protamine-Based Solid Lipid Nanoparticles as Potential Vectors for the Treatment of X-Linked Juvenile Retinoschisis. Hum. Gene Ther. 2012, 23, 345–355.

22. Apaolaza, P.S.; Del Pozo-Rodríguez, A.; Solinís, M.A.; Rodríguez, J.M.; Friedrich, U.; Torrecilla, J.; Weber, B.H.; Rodríguez-Gascón, A. Structural recovery of the retina in a retinoschisin-deficient mouse after gene replacement therapy by solid lipid nanoparticles. Biomaterials 2016, 90, 40–49.

23. Tapeinos, C.; Marino, A.; Battaglini, M.; Migliorin, S.; Brescia, R.; Scarpellini, A.; De Julián Fernández, C.; Prato, M.; Drago, F.; Ciofani, G. Stimuli-responsive lipid-based magnetic nanovectors increase apoptosis in glioblastoma cells through synergic intracellular hyperthermia and chemotherapy. Nanoscale 2019, 11, 72–88.

24. Mukherjee, S.; Ray, S.; Thakur, R.S. Solid lipid nanoparticles: A modern formulation approach in drug delivery system. Indian J. Pharm. Sci. 2009, 71, 349–358.

25. Del Pozo-Rodríguez, A.; Solinís, M.Á.; Rodríguez-Gascón, A. Applications of lipid nanoparticles in gene therapy. Eur. J. Pharm. Biopharm. 2016, 109, 184–193.

26. Battaglia, L.; Serpe, L.; Foglietta, F.; Muntoni, E.; Gallarate, M.; Del Pozo Rodriguez, A.; Solinis, M.A. Application of lipid nanoparticles to ocular drug delivery. Expert Opin. Drug Deliv. 2016, 13, 1743–1757.

27. Torrecilla, J.; Del Pozo-Rodríguez, A.; Solinís, M.Á.; Apaolaza, P.S.; Berzal-Herranz, B.; Romero-López, C.; Berzal-Herranz, A.; Rodríguez-Gascón, A. Silencing of hepatitis C virus replication by a non-viral vector based on solid lipid nanoparticles containing a shRNA

targeted to the internal ribosome entry site (IRES). Colloid Surf. B Biointerfaces 2016, 146, 808–817.

28. Torrecilla, J.; Del Pozo-Rodríguez, A.; Apaolaza, P.S.; Solinís, M.Á.; Rodríguez-Gascón, A. Solid lipid nanoparticles as non-viral vector for the treatment of chronic hepatitis C by RNA interference. Int. J. Pharm. 2015, 479, 181–188.

29. Ke, Y.; Wu, Y.; Cui, X.; Liu, X.; Yu, M.; Yang, C.; Li, X. Polysaccharide hydrogel combined with mesenchymal stem cells promotes the healing of corneal alkali burn in rats. PLoS ONE 2015, 10, e0119725.

30. Carpentier, G. Angiogenesis Analyzer for Image J. Available online: http://rsb.info.nih.gov/ij/macros/toolsets/Analogenesis%20Analyzer.txt (accessed on 25 March 2019).

31. Azkur, A.K.; Kim, B.; Suvas, S.; Lee, Y.; Kumaraguru, U.; Rouse, B.T. Blocking mouse MMP-9 production in tumor cells and mouse cornea by short hairpin (sh) RNA encoding plasmids. Oligonucleotides 2005, 15, 72–84.

32. Ruiz de Garibay, A.P.; Solinís, M.A.; del Pozo-Rodríguez, A.; Apaolaza, P.S.; Shen, J.S.; Rodríguez-Gascón, A. Solid lipid nanoparticles as non-viral vectors for gene transfection in a cell model of Fabry disease. J. Biomed. Nanotechnol. 2015, 11, 500–511.

33. Apaolaza, P.S.; Delgado, D.; Del Pozo-Rodríguez, A.; Rodríguez-Gascón, A.; Solinís, M.Á. A novel gene therapy vector based on hyaluronic acid and solid lipid nanoparticles for ocular diseases. Int. J. Pharm. 2014, 465, 413–426.

34. Delgado, D.; Del Pozo-Rodríguez, A.; Solinís, M.Á.; Rodríguez-Gascón, A. Understanding the mechanism of protamine in solid lipid nanoparticle-based lipofection: The importance of the entry pathway. Eur. J. Pharm. Biopharm. 2011, 79, 495–502.

35. Delgado, D.; Gascón, A.R.; Del Pozo-Rodríguez, A.; Echevarría, E.; Ruiz de Garibay, A.P.; Rodríguez, J.M.; Solinís, M.Á. Dextran-protamine-solid lipid nanoparticles as a non-viral vector for gene therapy: In vitro characterization and in vivo transfection after intravenous administration to mice. Int. J. Pharm. 2012, 425, 35–43.

36. Apaolaza, P.S.; Del Pozo-Rodríguez, A.; Torrecilla, J.; Rodríguez-Gascón, A.; Rodríguez, J.M.; Friedrich, U.; Weber, B.H.; Solinís, M.A. Solid lipid nanoparticle-based vectors intended for the treatment of X-linked juvenile retinoschisis by gene therapy: In vivo approaches in Rs1h-deficient mouse model. J. Control. Release 2015, 217, 273–283.

37. del Pozo-Rodríguez, A.; Delgado, D.; Solinís, M.A.; Gascón, A.R.; Pedraz, J.L. Solid lipid nanoparticles: Formulation factors affecting cell transfection capacity. Int. J. Pharm. 2007, 339, 261–268.

38. Ueta, M.; Kinoshita, S. Ocular surface inflammation is regulated by innate immunity. Prog. Retin. Eye Res. 2012, 31, 551–575.

39. Kimura, K. Molecular mechanism of the disruption of barrier function in cultured human corneal epithelial cells induced by tumor necrosis factor-alpha, a proinflammatory cytokine. Nihon. Ganka Gakkai Zasshi 2010, 114, 935–943.

40. Kimura, K.; Morita, Y.; Orita, T.; Haruta, J.; Takeji, Y.; Sonoda, K.H. Protection of human corneal epithelial cells from TNF-α- induced disruption of barrier function by rebamipide. Investig. Ophthalmol. Vis. Sci. 2013, 54, 2752–2760.

41. Li, Q.; Jie, Y.; Wang, C.; Zhang, Y.; Guo, H.; Pan, Z. Tryptase compromises corneal epithelial barrier function. Cell Biochem. Funct. 2014, 32, 183–187.

42. Goktas, S.; Erdogan, E.; Sakarya, R.; Sakarya, Y.; Yılmaz, M.; Ozcimen, M.; Unlukal, N.; Alpfidan, I.; Tas, F.; Erdogan, E.; et al. Inhibition of corneal neovascularization by topical and subconjunctival tigecycline. J. Ophthalmol. 2014, 2014, 452685. Available online: https://www.hindawi.com/journals/joph/2014/452685/ (accessed on 25 March 2019).

43. Gordon, G.M.; Ledee, D.R.; Feuer, W.J.; Fini, M.E. Cytokines and signaling pathways regulating matrix metalloproteinase-9 (MMP-9) expression in corneal epithelial cellsy. J. Cell. Physiol. 2009, 221, 402–411.

44. Mohan, R.R.; Tovey, J.C.K.; Sharmaa, A.; Tandon, A. Gene Therapy in the Cornea: 2005-present. Prog. Retin. Eye Res. 2012, 31, 43–64.

45. Clements, J.L.; Dana, R. Inflammatory corneal neovascularization: Etiopathogenesis. Semin. Ophthalmol. 2011, 26, 235–245.

46. Haas, T.L. Endothelial cell regulation of matrix metalloproteinases. Can. J. Physiol. Pharmacol. 2005, 83, 1–7.

47. Ramaesh, T.; Ramaesh, K.; Riley, S.C.; West, J.D.; Dhillon, B. Effects of N-acetylcysteine on matrix metalloproteinase-9 secretion and cell migration of human corneal epithelial cells. Eye 2012, 26, 1138–1144.

48. Zhang, X.; Lin, X.; Liu, Z.; Wu, Y.; Yang, Y.; Ouyang, W.; Li, W.; Liu, Z. Topical application of mizoribine suppresses CD4+ T-cell-mediated pathogenesis in murine dry eye. Investig. Ophthalmol. Vis. Sci. 2017, 58, 6056–6064.

49. Webb, A.H.; Gao, B.T.; Goldsmith, Z.K.; Irvine, A.S.; Saleh, N.; Lee, R.P.; Lendermon, J.B.; Bheemreddy, R.; Zhang, Q.; Brennan, R.C.; et al. Inhibition of MMP-2 and MMP-9 decreases cellular migration, and angiogenesis in in vitro models of retinoblastoma. BMC Cancer 2017, 17, 434.

50. Lee, S.; Zheng, M.; Kim, B.; Rouse, B.T. Role of matrix metalloproteinase-9 in angiogenesis caused by ocular infection with herpes simplex virus. J. Clin. Investig. 2002, 110, 1105–1111.

51. Swamynathan, S.; Loughner, C.L.; Swamynathan, S.K. Inhibition of HUVEC tube formation via suppression of NFκB suggests an anti-angiogenic role for SLURP1 in the transparent cornea. Exp. Eye Res. 2017, 164, 118–128.

APPENDIX IV:

mRNA-based nanomedicinal products to address corneal inflammation by interleukin-10 supplementation

Itziar Gómez-Aguado, Julen Rodríguez-Castejón, Marina Beraza-Millor, Mónica Vicente-Pascual, Alicia Rodríguez-Gascón, Sara Garelli, Luigi Battaglia, Ana del Pozo-Rodríguez and María Ángeles Solinís

Published in: Pharmaceutics (2021)

Journal Impact Factor JCR 2020: 6.321 (Q1) 29/276

Category: PHARMACOLOGY & PHARMACY (Q1)

mRNA-based nanomedicinal products to address corneal inflammation by interleukin-10 supplementation

Abstract

The anti-inflammatory cytokine Interleukin-10 (IL-10) is considered an efficient treatment for corneal inflammation, in spite of its short half-life and poor eye bioavailability. In the present work, mRNA-based nanomedicinal products based on solid lipid nanoparticles (SLNs) were developed in order to produce IL-10 to treat corneal inflammation. mRNA encoding green fluorescent protein (GFP) or human IL-10 was complexed with different SLNs and ligands. After, physicochemical characterization, transfection efficacy, intracellular disposition, cellular uptake and IL-10 expression of the nanosystems were evaluated in vitro in human corneal epithelial (HCE-2) cells. Energy-dependent mechanisms favoured HCE-2 transfection, whereas protein production was influenced by energy-independent uptake mechanisms. Nanovectors with a mean particle size between 94 and 348 nm and a positive superficial charge were formulated as eye drops containing 1% (w/v) of polyvinyl alcohol (PVA) with 7.1–7.5 pH. After three days of topical administration to mice, all formulations produced GFP in the corneal epithelium of mice. SLNs allowed the obtaining of a higher transfection efficiency than naked mRNA. All formulations produce IL-10, and the interleukin was even observed in the deeper layers of the epithelium of mice depending on the formulation. This work shows the potential application of mRNA-SLN-based nanosystems to address corneal inflammation by gene augmentation therapy.

Keywords: messenger RNA; solid lipid nanoparticles; interleukin-10; corneal inflammation; polyvinyl alcohol; topical administration; gene augmentation; transfection; corneal epithelium; advanced therapies

---

1. Introduction

The eye is considered the perfect target for gene therapy due to its physiological features: it is easy to access and examine, it has a well-defined anatomy and it is relatively immune privileged. Moreover, from an experimental point of view, in the same subject, one eye can be used as a control, whereas the other eye can be used as the experimental target [1–3]. Currently, 47 clinical trials restricted to “ocular diseases” are registered in the database of Gene Therapy Clinical Trials Worldwide [4], all of them targeting retinal degenerative diseases, except one, which concerns corneal opacity. The cornea is a transparent tissue localized in the anterior segment of the eye, which contributes to eyesight by focusing a visual image through light refraction. Several factors can damage this tissue and provoke corneal inflammation or keratitis,

such as infections, dry eye, eyelid disorders, physical and chemical damage, and a wide variety of underlying diseases [5]. Current treatments of corneal inflammation are based on corticosteroids, which require repeated topical applications and have been associated with multiple adverse effects, such as infectious keratitis, increased intraocular pressure, and cataracts [6]. Alternatively, the topical administration of IL-10, an anti-inflammatory cytokine, has been suggested as an effective treatment for corneal inflammation [7]. However, the short half-life and poor eye bioavailability of IL-10 limit its therapeutic use. Therefore, IL-10 ocular delivery may be better attempted by gene therapy, with the aim of inducing IL-10 *de novo* synthesis in corneal cells [8].

In the last few decades, a wide range of reagents and techniques suitable to transfer nucleic acids into cells have been developed, in order to modulate both *in vitro* and *in vivo* gene expression. Particularly, mRNA therapeutics present several advantages: since mRNA does not need to enter inside the cell nucleus in order to exert its effect, protein translation is faster than in the case of DNA; furthermore, mRNA expression is temporary and it owns a safe profile with no risk of insertion-related mutagenesis, as it does not incorporate into the genome of the host [9]. Additionally, the production and manufacturing of mRNA is easy to scale up in a cost-effective, standardized, and reproducible way. However, mRNA instability is one of its major vulnerabilities [10], which makes the development of suitable delivery systems necessary. Delivery systems should be able to protect mRNA against RNase degradation, and to ensure its intracellular delivery inside the cytoplasm of the target cell [11]. In this context, different strategies and efforts for advances in nanotechnology and material sciences are still ongoing [9]. Presently, non-viral vectors are at the frontline of mRNA therapy, in contrast to DNA-based gene therapy; particularly, lipid-based vectors are among the most extensively used non-viral nucleic acid delivery platforms. Indeed, mRNA therapy has gained much attention after its application in the vaccination against the SARS-CoV-2 [12-14]. It should be noted that during the COVID-19 pandemic, the first vaccines approved for distribution and use against the SARS-CoV-2 by the European Medicines Agency (EMA) and the United States Food and Drug Administration (FDA) were based on mRNA encapsulated in lipid nanoparticles (LNs) [15,16]. These mRNA vaccines have been well-tolerated and have demonstrated approximately 95% efficacy against COVID-19, with few adverse events [17,18].

Among lipid-based systems, liposomes and solid lipid nanoparticles (SLNs) have been suggested as up-and-coming non-viral ocular drug delivery systems. [10,20]. Liposomes were introduced as carriers for the delivery of nucleic acids for gene therapy over two decades ago and, to date, they still represent the most widely studied vectors for gene delivery. Liposomes used for gene

delivery are typically nanometric and are defined by a spherical vesicle with an aqueous internal cavity enclosed by a lipid bilayer membrane. However, these systems are not devoid of stability and efficacy issues [21,22]. SLNs were more recently developed with the aim of, among other things, addressing the above issues underlying liposome gene transfection [23]. SLNs are spherical particles with a solid lipid core matrix, which is stabilized by surfactants in an aqueous dispersion, and are usually composed of well-tolerated physiological lipids [24–27]. In addition, SLNs have demonstrated to be effective for ocular topical drug administration [28]. This administration route shows several advantages: it is non-invasive, drug absorption into the systemic circulation is minimized, first pass metabolism is prevented, and formulations are easy to administer. However, the main issue of conventional ocular drug delivery systems relies on the poor retention onto the ocular surface, due to corneal clearance; as a consequence, the amount of drug that is able to cross the cornea and access the ocular structures is small. Therefore, an effective ocular drug delivery system should increase corneal retention time and improve drug permeation through the cornea [29]. SLNs possess a nanometer sized-range, lipophilic properties, and usually positive surface charges. This makes them suitable for topical drug administration by improving corneal permeation and retention [30,31]. Previously, our research group has used a gene augmentation strategy to induce IL-10 production into the cornea by the administration of SLNs containing plasmid DNA (pDNA) [32]. However, mRNA could be an alternative therapeutic option to tackle corneal inflammation, thanks to its high efficacy, safety profile, and versatility for fast protein production.

The aim of this experimental work is the development of SLNs containing mRNA as non-viral vectors, to be used as a genetic supplementation strategy for the *de novo* production of IL-10 in corneal cells. Additionally, vectors prepared with plasmid DNA (pDNA) were evaluated for comparison purposes. Formulations containing mRNA or pDNA encoding green fluorescent protein (GFP) or IL-10 were characterized from a physico-chemical point of view, and then evaluated for internalization and transfection properties, both *in vitro* by using human corneal epithelial (HCE-2), and *in vivo* after administration to mice by ocular instillation.

2. Materials and methods

2.1. Materials

1,2-Dioleoyl-3-trimethylammonium-propane chloride salt (DOTAP) was obtained from Avanti Polar-lipids, Inc. (Alabaster, AL, USA). Precirol® ATO 5 (glyceryl palmitostearate) was kindly provided by Gattefossé (Madrid, Spain). Tween 80 and dichloromethane were purchased from Panreac (Madrid, Spain) and sodium behenate from Nu-Chek Prep (Eleysian, AL, USA). Sigma-

Aldrich (Madrid, Spain) provided protamine sulfate salt from salmon (Grade X) (P), dextran (Mn of 3260 Da) (DX), DEAE-dextran, Nile Red and partially hydrolyzed polyvinyl alcohol (PVA) 9,000–10,000 Da M_w. Lifecore Biomedical (Chaska, MN, USA) supplied hyaluronic acid (HA) (M_w of 100 KDa).

CleanCap™ EGFP mRNA (5moU) and CleanCap™ Cyanine 5 EGFP mRNA (5moU) were acquired from TriLink BioTechnologies (San Diego, CA, USA). Both of the nucleic acids encode green fluorescent protein (GFP). mRNA encoding human IL-10 was customized by TriLink BioTechnologies. Professor BHF Weber laboratory (University of Regensburg, Germany) kindly provided plasmid pcDNA3-EGFP (6.1 kb) encoding GFP. Plasmid pUNO1-hIL10 (3.7 kb), which encodes human IL-10, was acquired by InvivoGen (San Diego, CA, USA). Label IT® Cy®5 Nucleic Acid Labeling Kit was obtained from Mirus Bio (Madison, WI, USA).

Materials used on agarose gel in an electrophoresis assay were acquired from Bio-Rad (Madrid, Spain). Ambion™ RNase I was purchased from Life Technologies (Thermo Fisher Scientific, Madrid, Spain), Deoxyribonuclease I (DNase I) and sodium dodecyl sulfate (SDS) from Sigma-Aldrich and GelRed™ from Biotium (Fremont, CA, USA).

Human Corneal Epithelial (HCE-2) cells were purchased from American Type Culture Collection (ATCC, Manassas, VA, USA). Cell culture reagents, including Dulbecco's Modified Eagle´s Medium/Nutrient Mixture F-12 with GlutaMAX™ (DMEM/F-12 with GlutaMAX™), fetal bovine serum (FBS), Penicillin-Streptomycin, Trypsin/EDTA and Attachment Factor were acquired from Life Technologies (Thermo Fisher Scientific, Madrid, Spain), whereas epidermal Growth Factor (EGF) and human insulin solution were obtained from Myltenyi Biotec (Madrid, Spain) and Sigma-Aldrich (Madrid, Spain), respectively. The DuoSet Ancillary reagent kit and Enzyme-linked immunoassay (ELISA) for IL-10 were obtained from R&D Systems (Minneapolis, MN, USA).

Reporter lysis buffer was provided by Promega Biotech Ibérica (Madrid, Spain). Paraformaldehyde (PFA) was obtained from Panreac, while 40,6-diamidine-20-phenylindole dihydrochloride (DAPI)-fluoromount-G was purchased from Southern Biotech (Birmingham, AL, USA). Phosphate buffered saline (PBS) and HEPES buffered solution were obtained from Gibco (Thermo Fisher Scientific, Madrid, Spain) and Lipofectamine™ 2000 Lipid-Reagent was acquired from Life Technologies (Thermo Fisher Scientific, Madrid, Spain). The 7-Amino-Actinomycin D (7-AAD) Viability Dye was acquired from Beckman Coulter (Brea, CA, USA).

Antibodies used for immunoassay, Anti-GFP polyclonal antibody and goat anti-Rabbit IgG (H+L) Cross-Adsorbed Secondary Antibody Alexa Fluor 488, were provided by Life Technologies (Thermo Fisher Scientific, Madrid, Spain), except rabbit Anti-IL-10 antibody, which was obtained

from Abcam (Cambridge, UK). Sakura Finetek Europe (Alphen aan den Rijn, The Netherlands) supplied Tissue-Tek® O.C.T.-compound.

Other chemicals, unless detailed, were reagent grade from Panreac (Barcelona, Spain) and Sigma-Aldrich (Madrid, Spain).

2.2. Formulation of SLNs and vectors

Three different techniques were used in order to prepare SLNs: solvent evaporation/emulsification (SLN_{EE}), hot-melt emulsification (SLN_{HM}) and coacervation (SLN_C).

SLN_{EE} were elaborated as previously reported [33], with the solid lipid Precirol® ATO 5 and the cationic lipid DOTAP, stabilized by the surfactant Tween 80. Briefly, SLN_{EE} were obtained by the sonication (Branson Sonifier 250, Danbury) of the organic phase (Precirol® ATO 5 dissolved in dichloromethane 5% w/v) in the aqueous phase, containing the cationic lipid DOTAP (0.4% w/v) and Tween 80 (0.1% w/v). SLNs' precipitation occurred upon dichloromethane evaporation.

SLN_{HM} was produced as a SLN_{EE} with minor modifications. Briefly, DOTAP (0.4% w/v) and Tween 80 (0.1% w/v) were dissolved in water. This aqueous solution and Precirol® ATO 5 were heated in a bain-marie. When both phases were led to 80 °C and lipids melted, the aqueous solution was added to the Precirol® ATO 5. The emulsion was obtained by sonication (Branson Sonifier 250, Danbury) for 30 min at 50 W. SLNs were obtained by cooling the obtained nanoemulsion on ice for 30 min.

SLN_C were composed of behenic acid as the lipid matrix, coated by the suspending agent PVA 9000 and the cationizing agent DEAE-dextran, as previously described [32]. Briefly, sodium behenate and PVA 9000 were dissolved in water under hot agitation, and when the solution reached 80 °C and became translucent, NaOH was added. Then, when the solution turned completely transparent DEAE-dextran was added drop by drop, turning the mixture turbid. Later, HCl was rapidly added and when the suspension turned white, it was cooled under stirring in a water bath. The final product underwent a re-melting process, by heating again and cooling by agitation in a water bath.

When required, Nile Red was incorporated in the preparation of all SLNs to label them. In the case of SLN_{EE}, Nile Red was dissolved in the dichloromethane of the organic phase, whereas in SLN_{HM} Nile Red was dissolved in dichloromethane and added during the first 30 s of the sonication step. Finally, in the case of SLN_C, a solution of dichloromethane containing Nile Red was added during the re-melting step.

In order to prepare SLN-based vectors, an aqueous solution of protamine (P) was added to the nucleic acid, mRNA or pDNA. Then, a solution of polysaccharide, dextran (DX) or hyaluronic acid (HA) dissolved in water was added. Finally, the SLN suspension was added to the previous complexes and incubated for 20 min. Electrostatic interactions between negative and positive charges of the components led to the formation of the final vectors, in which complexes were adsorbed on the surface of the cationic SLNs.

The weight ratios of the components of the formulations are summarized in Table 1.

Table 1. Weight ratios of the formulations.

Name of the vector	Weight ratio
mRNA-DX-SLN_{EE}	DX:P:mRNA:SLN_{EE} 1:0.25:1:5
mRNA-HA-SLN_{EE}	HA:P:mRNA:SLN_{EE} 0.5:0.5:1:5
mRNA-DX-SLN_{HM}	DX:P:mRNA:SLN_{HM} 1:0.25:1:5
mRNA-HA-SLN_{HM}	HA:P:mRNA:SLN_{HM} 0.5:0.5:1:5
mRNA-SLN_{C}	P:mRNA:SLN_{C} 2:1:10
mRNA-HA-SLN_{C}	HA:P:mRNA:SLN_{C} 0.5:2:1:10
pDNA-DX-SLN_{HM}	DX:P:pDNA:SLN_{HM} 1:2:1:5
pDNA-HA-SLN_{HM}	HA:P:pDNA:SLN_{HM} 0.5:2:1:5

SLN: Solid Lipid Nanoparticle. DX: dextran. HA: hyaluronic acid. P: protamine.

In order to obtain viscous formulations suitable for ocular delivery to animal models, an aqueous solution of PVA (85,000–124,000 M_w) was incorporated into the above mentioned vectors. The final concentration of PVA was 1% (w/v).

2.3. Characterization of SLNs and vectors: size, polydispersity Index and ζ-potential measurements

The mean size and polydispersity index (PDI) of 3 batches of SLNs and vectors were measured by Dynamic Light Scattering (DLS) and ζ-potential was determined by Laser Doppler Velocimetry (LDP). These measurements were carried out in a ZetaSizer Nano ZS (Malvern Panalytical, Malvern, UK) after the appropriate dilution of the samples in Milli-Q™ water (EDM Millipore, MA, USA).

2.4. Agarose gel electrophoresis assay

Studies of mRNA binding capacity, protection from RNase I digestion and release from the vectors were performed in a 1.2% agarose gel electrophoresis labelled with GelRed™. The gel ran for 60 min at 75 V, then it was immediately analyzed with the Uvitec Uvidoc D-55-LCD-20 M Auto transilluminator (Cambridge, UK). In order to evaluate binding capacity, vectors were

diluted in MilliQ™ water to a final concentration of 0.12 µg mRNA/µL in the gel. Protection from RNase I digestion was analyzed by the addition of 6 U RNase I/µg mRNA; mixtures were incubated at 37 °C for 40 min in a heater. Then, the samples were removed from the heater and mixed with an SDS solution (final concentration of 1%), at room temperature. The same SDS solution was added to the vectors to unbind the mRNA in the release studies. Two controls for the integrity of the mRNA were included in the assay: RiboRuler High Range RNA Ladder and untreated CleanCap™ EGFP mRNA (5moU).

In order to study the pDNA binding capacity, protection against DNase I digestion and release from the vectors, 0.7% agarose gel electrophoresis with GelRed™ was used. The gel was analyzed with the Uvitec Uvidoc D-55-LCD-20 M Auto transilluminator (Cambridge, UK) after running for 30 min at 120 V. The binding capacity was evaluated by adding vectors diluted in MilliQ™ water to a final concentration of 0.03 µg pDNA/µL in the gel. For DNAse I protection, the same concentration was exposed to 1 U DNase I/2.5 µg pDNA and then incubated at 37 °C for 30 min in a heater. The samples were removed from the heater and mixed with an SDS solution (4%) to a final concentration of 1% at room temperature. The same SDS solution was added to the vectors to unbind the plasmid in the release studies. Two controls for the integrity of the pDNA were included in the gels: 1 kb pDNA ladder from NIPPON Genetics Europe (Dueren, Germany) and untreated pcDNA3-EGFP plasmid.

2.5. pH measurement

Crison Basic 20 pH meter (Crison Instruments, Barcelona, Spain) was employed to determine the pH of the vectors. Measures were carried out in triplicate and the pH meter was calibrated daily.

2.6. Cell culture studies

Human corneal epithelial (HCE-2) cell line was used in order to perform *in vitro* studies. HCE-2 cell line was maintained in a DMEM/F-12 GlutaMAX™ medium, which was supplemented with 15% (v/v) heat-inactivated fetal bovine serum (FBS), insulin (4 mg/mL), Epidermal Growth Factor (EGF) (10 ng/mL), and Penicillin–Streptomycin (1% v/v) and incubated at 37 °C with 5% CO_2. Cells were sub-cultured once a week using Trypsin/EDTA in flasks earlier treated with Attachment Factor. The medium was renewed every 2 days. Cells from passages 1 to 4 were used to perform all *in vitro* assays.

2.6.1. Transfection efficacy and cell viability

mRNA-based vectors were prepared 72 h before their addition and maintained at 4 °C before their use.

After incubation with Attachment Factor, the cells were cultured on 24-well plates for 72 h at a density of 70,000 cells/well, until the cells were adhered and were able to create a monolayer. Later, part of the medium was removed, leaving enough volume to cover the cells, and a total volume of 75 µL of each vector diluted in Hank's Balanced Salt solution (HBS) (equivalent to 2.5 µg) was added to each well for 4 h in the incubator at 37 °C in a 5% CO_2. The medium containing the vectors was removed after the incubation time, and the cells were refreshed with 1 mL of the complete medium. The cells were kept growing during 48 h or 72 h in the case of mRNA- or pDNA-vectors, respectively.

The percentage of transfected cells and intensity of fluorescence, indicative of the amount of GFP produced, as well as cell viability, were measured using a CytoFLEX flow cytometer (Beckman Coulter). For this purpose, the cells were washed with 500 µL of PBS and then detached by incubation with 300 µL of Trypsin/EDTA for 5 min. After the centrifugation of cell suspension at 1000 rpm for 5 min, the supernatant was removed, and the pellet of cells was resuspended in 500 µL of PBS. Ten thousand events were collected for each sample. Transfection efficacy was measured at 525 nm (FITC) [34], and cell viability was determined at 610 nm (ECD), after the addition of 7-Amino-Actinomycin D (7-AAD) Viability Dye to the samples. The percentage of transfected cells was calculated counting the positive fluorescent GFP cells over the total cells. The intensity of fluorescence represented the mean of the intensity of fluorescence per labelled cell, which is correlated with gene expression and protein production [35–37].

The effect of temperature on cell transfection was studied by the incubation of HCE-2 cells at 4 °C for 30 min, prior to the addition of the vectors. The cells were maintained for 4 h at 4 °C, and then the cells were treated as explained above.

2.6.2. Cellular uptake

The internalization of the vectors by the HCE-2 cells was studied by using vectors containing SLNs labelled with the fluorescent Nile Red dye (λ = 590 nm), as previously described [8] and as explained above. The vectors were prepared 72 h before their addition. For this purpose, a total volume of 75 µL of each vector diluted in HBS (equivalent to 2.5 µg of nucleic acid) was added to each well; then, the cells were incubated for 2 h at 37 °C in a 5% CO_2. Once the incubation time had finished, the culture medium was removed and the cells were detached from the plates, as described in Section 2.6.1., for the cytometry analysis of transfected cells. The entrance of the vectors was analyzed by using a CytoFLEX flow cytometer (Beckman Coulter) at 610 nm (ECD). For each sample, 10,000 events were collected.

Additionally, the effect of temperature on cellular uptake was studied by the incubation of cells at 4 °C for 30 min before the incorporation of the vectors. Once the Nile Red-labelled vectors were added to the cell cultures, the cells were maintained at 4 °C for an additional 2 h. Finally, the cells were collected to evaluate the vector uptake by flow cytometry, as described above. In this case, the percentage of positive cells corresponds to the cells that have uptaken vectors labelled with Nile Red over the total cells.

2.6.3. Intracellular disposition of the vectors

A density of 150,000 cells in 1 mL per well was seeded in Millicell EZ slides (Millipore) and incubated at 37 °C and 5% CO_2 for 24 h. Then, they were treated with 75 µL of vector equivalent to 0.8 µg of CleanCap™ Cyanine 5 EGFP mRNA (5moU) as nucleic acid. After 4 h, the slides were washed with PBS, fixed with PFA 4% and covered with the mounting fluid DAPI-fluoromount-G™, used to label the nuclei. Then, a Leica DM IL LED Fluo inverted microscope (Leica Microsystems CMS GmbH, Wetzlar, Germany) was used to analyze the slides.

2.6.4. Quantification of IL-10

To measure the levels of IL-10 expressed by the cells aft er the addition of the complexes, an Enzyme-linked Immunosorbent Assay (ELISA) kit was carried out. The secreted and intracellular IL-10 were quantified 48 h and 72 h after the addition of the mRNA- and pDNA-bearing vectors encoding human IL-10, respectively. For the secreted IL-10, the medium of each well was removed and centrifuged at 12,000 g for 2 min. For the intracellular IL-10, the cells were washed with 300 µL of PBS twice, and then 400 µL of reporter lysis buffer 1× was added. Finally, the plate was frozen to complete the lysis of cell culture. After thawing, each well was detached by a scrapper and the lysate was centrifuged at 12,000 g for 2 min at 4 °C. A total of 100 µL of each sample was added to a 96-well plate that was covered with the corresponding capture antibody; then the assay was performed according to the manufacturer's instructions.

2.7. In Vivo studies

Five-week-old male BALB/cOlaHsd mice, with a weight ranging between 20 and 25 g (Envigo), were employed for the *in vivo* studies.

The use of the mice (license M20/2018/142) was approved by The Animal Experimentation Ethics Committee of the University of the Basque Country UPV/EHU following the Spanish and European Union (EU) laws. All the procedures were followed in accordance. The animals were accommodated under controlled temperature, humidity, and 12 h day-night cycles, with food and water ad libitum access.

The mice were anesthetized with 1-2% isoflurane (IsoFlo, Abbott, Madrid, Spain) in air, at a flow rate of 0.5–1 L/min with the aim of preventing distress during experimental manipulation.

The mice were humanely euthanatized by cervical dislocation, and then their eyes were removed. After the enucleation, the eyes were washed in a physiological saline solution, fixed with 4% PFA during 30 min and washed with PBS for 5 min. Then, the eyes were immersed in 30% sucrose in PBS at 4 °C until the eyes precipitated. Then, half of the volume was removed and substituted with Tissue-Tek® O.C.T.™ and shaken at room temperature for 2 h. Finally, the eyeballs were stored in 100% Tissue-Tek® O.C.T.™ to freeze at 80 °C for future studies.

2.7.1. Topical administration

The formulations described in Table 1, as well as naked mRNA encoding GFP or human IL-10, were viscosized with 1% PVA (85,000-124,000 M_w), and administered to the mice by eye drop instillation. The administration of the nanosystems was carried out in 2 doses over 3 days. In each dose, 3 instillations of 2.5 µL at 3 min intervals were carried out, administering a final dose of 4.5 µg of nucleic acid per day.

2.7.2. Evaluation of gene expression

The mice were sacrificed 24 h or 48 h after the last dose depending on the formulation administered. For GFP expression studies, the mice were sacrificed at 48 h, except in the case of mRNA-HA-SLN_{EE} formulation, where the mice were sacrificed both at 24 h and 48 h. For IL-10 expression studies, the mice were sacrificed at 24 h. Then, the eyeballs were extracted, fixed and histologically evaluated by sections of 14 µm on a cryostat (Cryocut 3000, Leica, Bensheim, Germany).

In order to evaluate the gene expression, two different transfection studies were carried out. In the first one, vectors contained the nucleic acid that encodes GFP, whereas in the second one vectors were bearing the nucleic acid that encodes IL-10. Both transfections were evaluated qualitatively by immunofluorescence. Sections were washed with a PB buffer. The samples were blocked and permeabilized employing a solution of 20% PB, 0.3% Triton X-100, 10% goat serum, and water q.s. 100%. Then, the respective primary antibody, anti-GFP or anti-IL-10, was added and incubated for 24 h at 4 °C. Secondary antibody goat anti-rabbit IgG Alexa Fluor 488 was added in both transfection assays after washing for 30 min protected from light. Finally, after washing and drying the samples, they were mounted with DAPI-Fluoromount-G. Tissue sections were examined by a Zeiss LSM800 confocal microscope (ZEISS microscopy, Oberkochen, Germany). The overlapping of fluorescence emission spectra was avoided by sequential acquisition. Six sections for each cornea were analyzed as representations of the entire tissue.

2.8. Data analysis

IBM SPSS Statistics 26 (IBM) software was used to perform the statistical analysis, and the Saphiro–Wilk test and Levene test were employed for the evaluation of homogeneity and variance, and normal distribution of samples, respectively. Student's t-test was used to compare means from two independent groups and ANOVA for multiple comparisons, followed by Bonferroni or T3 Dunnet post-hoc, depending on the results of the Levene test of homogeneity of variances. $p < 0.05$ was considered statistically significant. Data are shown as mean ± standard deviation (SD).

3. Results

3.1. Size and ζ-potential of SLNs and vectors

Table 2 shows the average size, polydispersity index (PDI), and ζ-potential of the SLNs. The particle size ranged from 93.3 to 307.8 nm and PDI values were lower than 0.3. The superficial particle charge ranged from +21.1 to +68.5 mV. Significant differences ($p < 0.001$) were observed in terms of particle size and superficial charge among all SLNs. SLN_C showed the highest particle size and the lowest superficial charge, whereas SLN_{HM} showed the smallest size and the highest superficial charge. The Particle Size Distribution Intensity Diagram of SLN_{HM} has been included as an example in Supplementary Material (Supplementary Material Figure S1).

Table 2. Physical characterization of solid lipid nanoparticles (SLNs).

SLNs	Size (nm)	PDI	ζ-Potential (mV)
SLN_{EE}	198.7 ± 2.0	0.26 ± 0.01	+57.8 ± 1.7
SLN_{HM}	93.3 ± 0.4	0.28 ± 0.01	+68.5 ± 0.7
SLN_C	307.8 ± 3.5	0.17 ± 0.01	+21.1 ± 0.8

DX: dextran; HA: hyaluronic acid SLN_{EE}: solid lipid nanoparticle prepared by emulsification-evaporation method. SLN_{HM} solid lipid nanoparticle prepared by hot-melt emulsification method. SLN_C: solid lipid nanoparticle prepared by coacervation method. PDI: polydispersity index. Data are expressed as mean ± standard deviation; $n = 3$.

Table 3 shows the size, PDI, and ζ-potential of the SLN-based vectors containing CleanCap™ EGFP mRNA (5moU) or IL-10 mRNA customized by TriLink BioTechnologies. All formulations were prepared with protamine (P). Moreover, an aqueous solution of polysaccharide, either dextran (DX) or hyaluronic acid (HA), was incorporated into the SLN_{EE} and SLN_{HM} vectors. Since SLN_C vectors contain DEAE-dextran in their composition, only HA was used to prepare the mRNA-HA-SLN_C vector. The particle size of vectors containing EGFP mRNA ranged from 132.3 to 348.4 nm, PDIs were lower than 0.4, and the surface charge ranged from +9.5 to +43.9 mV. A PDI value less than 0.4 is related to the homogeneity in the size of the particles of the sample and it

demonstrates a monodisperse sample population, which is considered acceptable for drug delivery [38]. Significant differences ($p < 0.001$) in terms of size were observed in both mRNA-SLN_{HM} formulations and mRNA-HA-SLN_C with respect to the rest of the formulations. Regarding the superficial charge, significant differences ($p < 0.001$) were observed between SLN_C vectors (with the lowest superficial charge), as well as mRNA-DX-SLN_{EE} (with the highest superficial charge), with respect to the rest of the formulations. Particle Size Distribution Intensity Diagram of mRNA-HA-SLN_{HM} bearing CleanCap™ EGFP mRNA (5moU) has been included as an example in Supplementary Material (Supplementary Material Figure S2).

IL-10 mRNA vectors showed a smaller particle size than those prepared with GFP mRNA, ranging from 116.9 to 283.9 nm, with a PDI lower than 0.3 and a superficial charge from +19.4 to +49.2 mV. Significant differences ($p < 0.001$) were observed between the vectors prepared with different SLNs with respect to the rest of the formulations in terms of particle size. Regarding the superficial charge, significant differences ($p < 0.001$) were observed between mRNA-SLN_C and mRNA-HA-SLN_C with respect to the others.

Table 3. Physical characterization of mRNA-based vectors.

	Size (nm)	PDI	ζ-Potential (mV)
CleanCap™ EGFP mRNA (5moU)			
mRNA-DX-SLN_{EE}	241.7 ± 4.8	0.29 ± 0.01	+43.9 ± 0.25
mRNA-HA-SLN_{EE}	287.2 ± 1.8	0.36 ± 0.01	+37.7 ± 0.3
mRNA-DX-SLN_{HM}	132.3 ± 1.9	0.25 ± 0.01	+38.0 ± 1.3
mRNA-HA-SLN_{HM}	132.4 ± 1.6	0.20 ± 0.01	+32.7 ± 0.3
mRNA-SLN_C	292.0 ± 1.2	0.17 ± 0.02	+9.5 ± 0.4
mRNA-HA-SLN_C	348.4 ± 2.9	0.26 ± 0.01	+13.2 ± 0.6
IL-10 mRNA			
mRNA-DX-SLN_{EE}	180.1 ± 1.1	0.21 ± 0.00	+49.2 ± 0.3
mRNA-HA-SLN_{EE}	199.4 ± 0.7	0.21 ± 0.00	+46.3 ± 0.1
mRNA-DX-SLN_{HM}	116.9 ± 0.9	0.25 ± 0.00	+42.1 ± 2.0
mRNA-HA-SLN_{HM}	121.3 ± 1.0	0.24 ± 0.00	+41.7 ± 0.2
mRNA-SLN_C	242.8 ± 1.7	0.25 ± 0.01	+19.4 ± 0.9
mRNA-HA-SLN_C	283.9 ± 4.6	0.26 ± 0.02	+19.5 ± 1.6

DX: dextran; HA: hyaluronic acid; SLN_{EE}: solid lipid nanoparticle prepared by emulsification-evaporation method. SLN_{HM}: solid lipid nanoparticle prepared by hot-melt emulsification method. SLN_C: solid lipid nanoparticle prepared by coacervation method. PDI: polydispersity index. Data are expressed as mean ± standard deviation; $n = 3$.

Table 4 shows the size, PDI, and ζ-potential of the SLN-based vectors containing either plasmid pcDNA3-EGFP or plasmid pUNO1-hIL10. Only SLN_{HM} were employed. All formulations were

prepared with P, DX or HA, and SLNs. The particle size of the vectors bearing pcDNA3-EGFP plasmid ranged from 94.5 to 204.0 nm, PDIs were lower than 0.3, and the surface charge ranged from +26.3 to +43.9 mV. Significant differences ($p < 0.001$) were noticed with regard to particle size and ζ-potential between formulations. In the case of pUNO1-hIL10 vectors, the particle size ranged from 101.1 to 193.7 nm, PDIs were less than 0.3 except for pDNA-HA-SLN_{HM}, which was 0.48. The superficial charge ranged from +41.4 to +44.7 mV. Significant differences ($p < 0.001$) were reported in terms of size between formulations.

Table 4. Physical characterization of pDNA-based vectors.

	Size (nm)	PDI	ζ-Potential (mV)
Plasmid pcDNA3-EGFP			
pDNA-DX-SLN_{HM}	94.5 ± 1.0	0.27 ± 0.00	+43.9 ± 1.01
pDNA-HA-SLN_{HM}	204.0 ± 2.8	0.25 ± 0.01	+26.3 ± 0.1
Plasmid pUNO1-hIL10			
pDNA-DX-SLN_{HM}	101.1 ± 1.1	0.27 ± 0.00	+44.7 ± 0.6
pDNA-HA-SLN_{HM}	193.7 ± 15.1	0.48 ± 0.01	+41.4 ± 0.2

DX: dextran; HA: hyaluronic acid SLN_{EE}: solid lipid nanoparticle prepared by emulsification-evaporation method. SLN_{HM}: solid lipid nanoparticle prepared by hot-melt emulsification method. SLN_C: solid lipid nanoparticle prepared by coacervation method. PDI: polydispersity index. Data are expressed as mean ± standard deviation; $n = 3$.

No significant differences in particle size, PDI, or ζ-potential was observed when SLNs were labelled with Nile Red (data not shown).

3.2. Agarose gel electrophoresis assay

Figure 1 shows the ability of SLN_{HM} and SLN_C vectors to bind, protect, and release mRNA (Figure 1A) and the capacity of SLN_{HM} vectors to bind, protect, and release pDNA (Figure 1B).

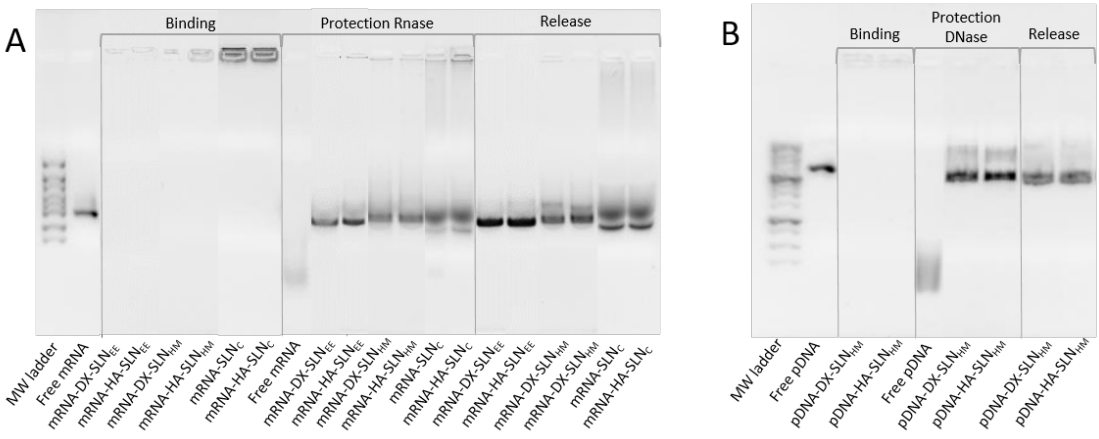

Figure 1. Binding, protection and release capacity of mRNA- and pDNA-based vectors. (A) mRNA-SLN_{HM} and mRNA-SLN_C; (B) pDNA-SLN_{HM}. DX: dextran; HA: hyaluronic acid; SLN_{EE}: solid lipid nanoparticle

prepared by emulsification-evaporation method. SLN_{HM}: solid lipid nanoparticle prepared by hot-melt emulsification method. SLN_C: solid lipid nanoparticle prepared by coacervation method.

Regarding the binding capacity, the absence of bands in both gels and the presence of mRNA (Figure 1A) and pDNA (Figure 1B) on the loading wells indicate that nucleic acid was completely bound to the vector and unable to migrate through the gel.

Differences in the protection capacity were observed according to the formulation. Bands in the lanes corresponding to vectors prepared with SLN_{EE} and SLN_{HM} were more intense and less faded than those prepared with SLN_C; these data indicate a higher protection degree of the nucleic acid. Moreover, the presence of the two bands in the SLN_C lanes indicates a lower capacity of protection.

In the case of pDNA vectors, both formulations were capable of protecting the nucleic acid against DNase I digestion. All formulations were able to release pDNA after the treatment with SDS.

3.3. pH measurement

Table 5 shows the pH values of mRNA- and pDNA-based vectors formulated as eye drops (1% PVA in HBS (Hanks' Balanced Salt solution) pH= 7.4). The pH values ranged from 7.13 to 7.44 and did not show significant differences depending on the formulations.

Table 5. pH measurements of mRNA- and pDNA-based vectors.

Sample	pH
mRNA-DX-SLN_{EE}	7.31 ± 0.04
mRNA-HA-SLN_{EE}	7.20 ± 0.16
mRNA-DX- SLN_{HM}	7.31 ± 0.04
mRNA-HA- SLN_{HM}	7.44 ± 0.21
mRNA-SLN_C	7.08 ± 0.29
mRNA-HA-SLN_C	7.13 ± 0.11
pDNA-DX- SLN_{HM}	7.39 ± 0.06
pDNA-HA-SLN_{HM}	7.53 ± 0.02

DX: dextran; HA: hyaluronic acid; SLN_{EE}: solid lipid nanoparticle prepared by emulsification-evaporation method. SLN_{HM}: solid lipid nanoparticle prepared by hot-melt emulsification method. SLN_C: solid lipid nanoparticle prepared by coacervation method.

3.4. Cell culture studies

3.4.1. Transfection efficacy and cell viability

Figure 2 shows the percentage of transfection and intensity of fluorescence of HCE-2 cells treated with the vectors containing mRNA GFP or pDNA at 37 °C and 4 °C.

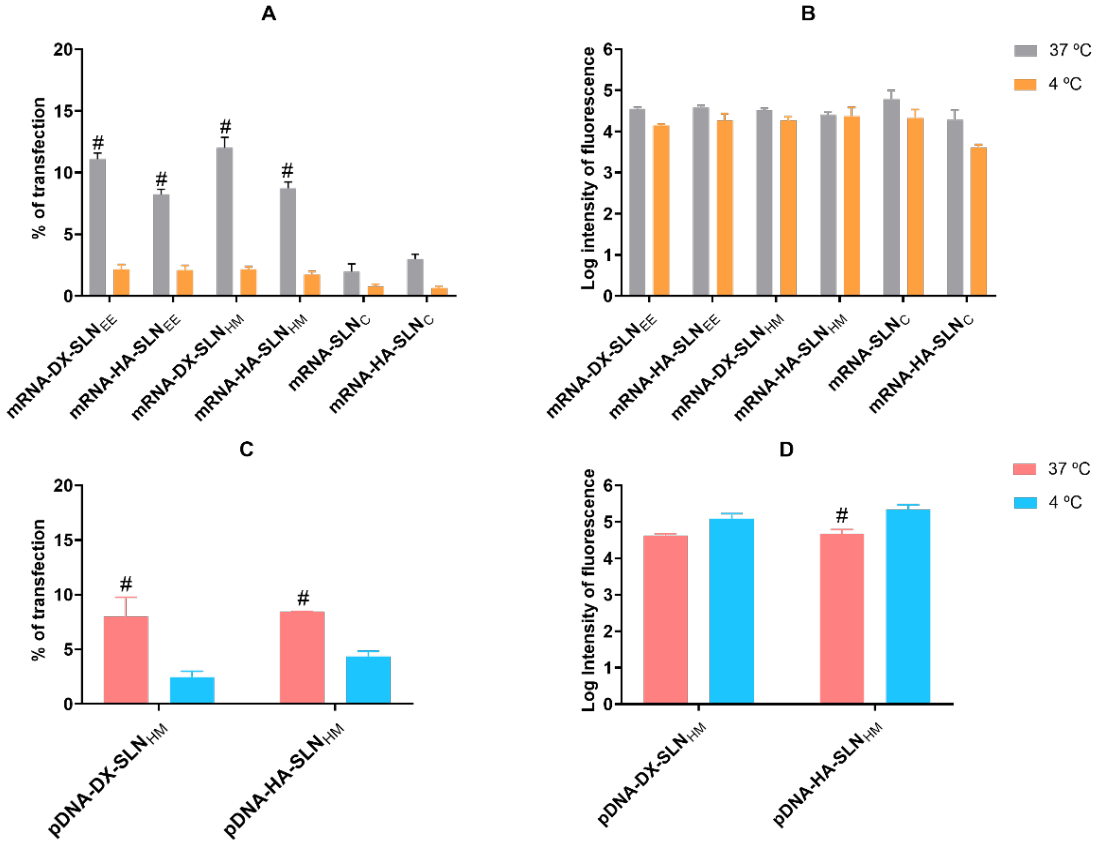

Figure 2. Flow cytometry analysis of transfection efficacy and intensity of fluorescence of HCE-2 cells after the addition of SLN_{EE}, SLN_{HM} and SLN_C vectors at 37 °C and 4 °C. Percentage of transfection values correspond to the positive fluorescent GFP cells over the total cells. Log of intensity of fluorescence indicates the average intensity of fluorescence per labeled cell. Data are expressed as mean ± standard deviation; n = 3. (A) Percentage of transfected HCE-2 cells at 37 °C and 4 °C 48 h after administration of mRNA-based vectors. (B) Log of intensity of fluorescence of transfected HCE-2 cells 48 h after administration of mRNA-based vectors. (C) Percentage of transfected HCE-2 cells at 37 °C and 4 °C 72 h after administration of pDNA-based vectors. (D) Log of intensity of fluorescence of transfected HCE-2 cells 72 h after administration of pDNA-based vectors. # $p < 0.05$ with respect to the same vector at 4 °C. DX: dextran; HA: hyaluronic acid; SLN_{EE}: solid lipid nanoparticle prepared by emulsification-evaporation method. SLN_{HM}: solid lipid nanoparticle prepared by hot-melt emulsification method. SLN_C: solid lipid nanoparticle prepared by coacervation method.

Amongst the mRNA-based formulations at 37 °C, the transfection percentage was higher with the vectors prepared with SLN_{EE} and SLN_{HM} (Figure 2A) than with the vectors prepared with SLN_C. No significant differences were found between nanocarriers prepared with SLN_{EE} and SLN_{HM}. With respect to the influence of temperature, the percentage of transfection decreased

significantly at 4 °C in all cases. Conversely, the fluorescent intensity (Figure 2B) was similar regardless of the vectors employed and the operating temperature.

In the case of pDNA-based vectors, the percentage of transfected cells was similar with the two formulations, approximately 8%. At 4 °C, the transfection efficacy was lower, although the intensity of the fluorescence of pDNA-HA-SLN_{HM} increased significantly.

Cell viability at 37 °C was approximately 98% for SLN_{EE} and SLN_{HM}, and 90% for SLN_C at 4 °C, cell viability was approximately 98% for all formulations.

3.4.2. Cellular uptake

Figure 3 shows the efficacy of cellular uptake in HCE-2 cells at 37 °C and 4 °C after the addition of mRNA- and pDNA-based vectors labelled with Nile Red. Cell internalization was measured 2 h after the addition of the vectors to the cells cultures.

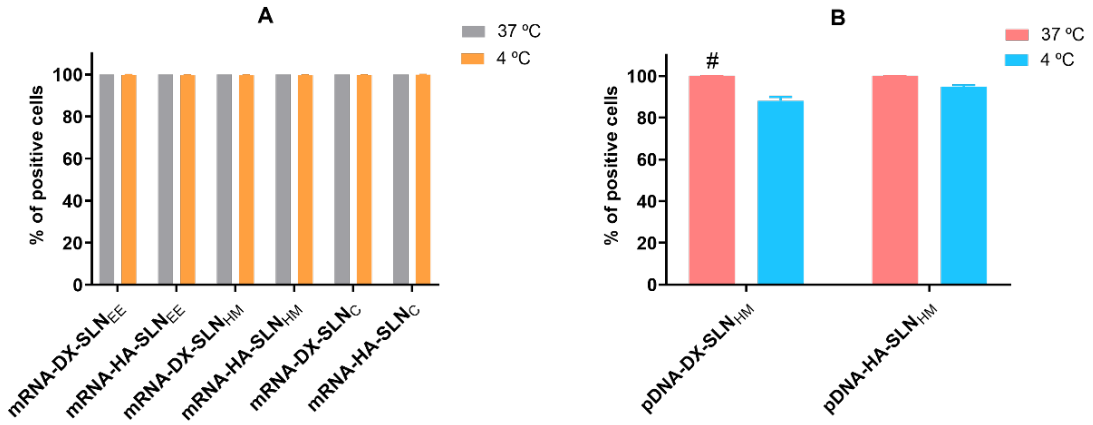

Figure 3. Cellular uptake of vectors using Nile-Red labelled SLNs in HCE-2 cells at 37 °C and 4 °C analyzed by flow cytometry. Percentage of positive cells correspond to the cells which have uptaken the vectors labeled with Nile Red over the total cells. Data are expressed as mean ± standard deviation; n = 3. (A) Percentage of Nile Red positive HCE-2 cells 2 h after the addition of mRNA-based vectors. (B) Percentage of Nile Red positive HCE-2 cells 2 h after the addition of pDNA-based vectors. # $p < 0.05$ with respect to the same vector at 4 °C. DX: dextran; HA: hyaluronic acid; SLN_{EE}: solid lipid nanoparticle prepared by emulsification-evaporation method. SLN_{HM}: solid lipid nanoparticle prepared by hot-melt emulsification method. SLN_C: solid lipid nanoparticle prepared by coacervation method.

In the case of mRNA-based vectors, the percentage of positive cells (Figure 3A) was over 99% at both temperatures. In the case of pDNA vectors, the percentage of positive cells was over 99% at 37 °C. In contrast, the percentage of positive cells at 4 °C decreased to 88% for pDNA-DX-SLN_{HM}.

3.4.3. Intracellular disposition of the vectors

Figure 4 shows the intracellular disposition of mRNA and pDNA in HCE-2 cells, represented by the red fluorescence signal. Depending on the formulation, a difference in the disposition of nucleic acid was observed.

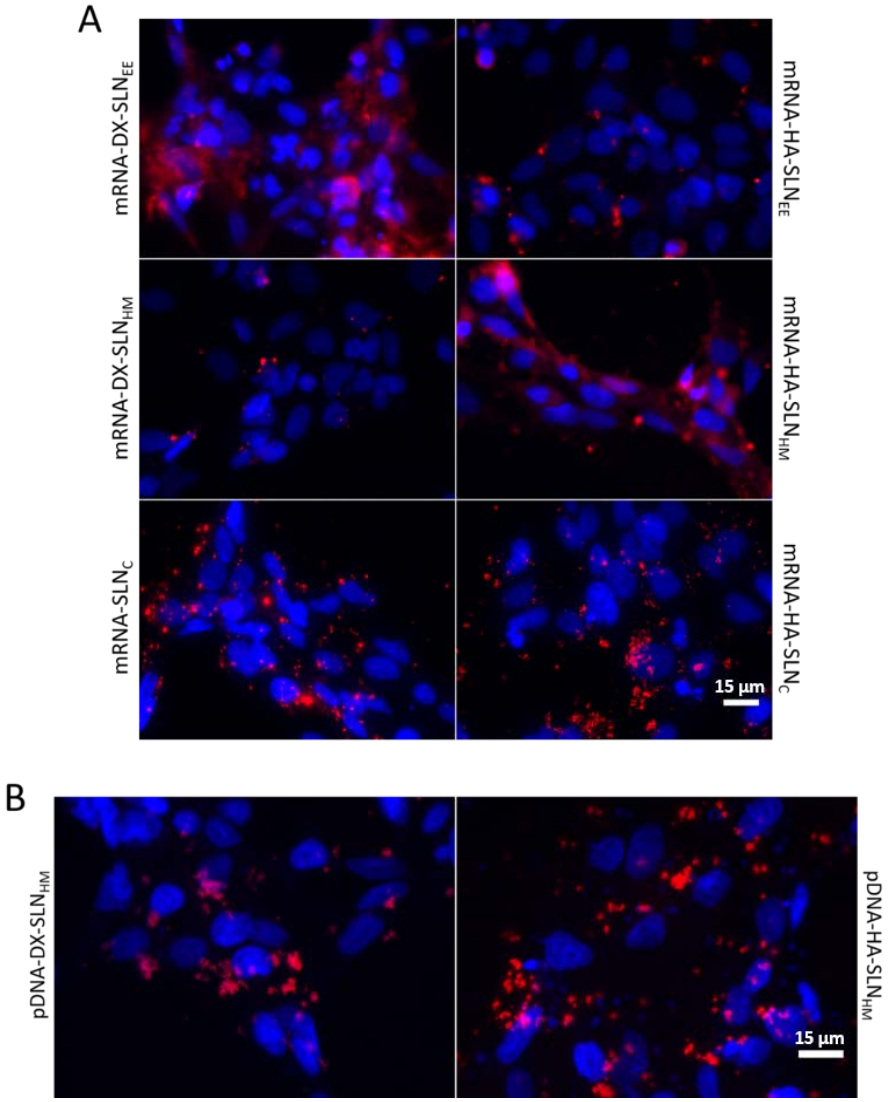

*Figure 4. Confocal microscopy analysis of intracellular disposition of mRNA- and pDNA-based vectors 4 h after their addition in HCE-2 cells. (**A**) CleanCap™ Cyanine 5 EGFP mRNA (5moU) vectors formulated with P, DX and HA. (**B**) pcDNA3-EGFP plasmid labeled with Label IT® Cy®5 vectors. Blue: nuclei labeled with DAPI. Red: fluorescence signal of nucleic acid labeled with Cy®5. Magnification 60×. Scale bar: 15 µm. DX: dextran; HA: hyaluronic acid; SLN$_{EE}$: solid lipid nanoparticle prepared by emulsification-evaporation method. SLN$_{HM}$: solid lipid nanoparticle prepared by hot-melt emulsification method. SLN$_{C}$: solid lipid nanoparticle prepared by coacervation method.*

The mRNA appeared dispersed along the cytoplasm when formulated in DX-SLN$_{EE}$ and HA-SLN$_{H}$ (Figure 4A). However, in the case of the remaining vectors, it appears as dots, indicating that it is more condensed.

The pDNA in the cells treated with the vectors appeared highly condensed and near the nucleus (Figure 4B); no difference in the disposition of the pDNA was observed between the two nanocarriers.

3.4.4. Quantification of IL-10

Figure 5 shows the levels of secreted and intracellular IL-10 in HCE-2 cells 48 h and 72 h after the addition of mRNA- and pDNA-based vectors, respectively. The mRNA-vectors induced greater secretion of IL-10 than did the pDNA-based vectors. The basal production of non-treated cells was not detectable. In the case of the mRNA-based vectors, SLN_{EE} formulations were the most effective, while SLN_C vectors showed the lowest secreted IL-10 levels.

Intracellular levels of the cytokine were close to 10 pg/mL with all formulations except pDNA-HA-SLN_{HM}, reaching 30 pg/mL (Supplementary Material S3).

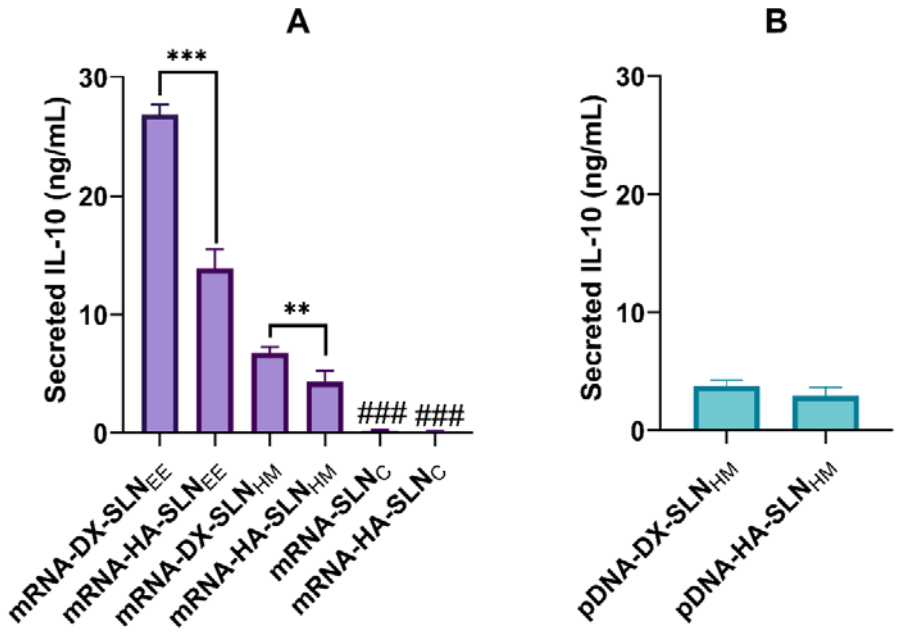

*Figure 5. Levels of secreted IL-10 by HCE-2 cells after the administration of SLN-based vectors bearing IL-10 mRNA and pUNO1-hIL10 plasmid. (A) Concentration of secreted IL-10 48 h after the administration of mRNA-based vectors. (B) Concentration of secreted IL-10 72 h after the administration of pDNA-based vectors. ### $p < 0.001$ with respect to the mRNA-SLN_{EE} and mRNA-SLN_C formulations. ** $p < 0.01$ with respect to the other formulation. *** $p < 0.001$ with respect to the other formulation. DX: dextran; HA: hyaluronic acid; SLN_{EE}: solid lipid nanoparticle prepared by emulsification-evaporation method. SLN_{HM}: solid lipid nanoparticle prepared by hot-melt emulsification method. SLN_C: solid lipid nanoparticle prepared by coacervation method.*

3.5. In Vivo Studies

3.5.1. In Vivo transfection with mRNA and pDNA encoding GFP

Vectors bearing CleanCap™ EGFP mRNA (5moU) or plasmid pcDNA3-EGFP combined with PVA were topically administered as eye drops to mice in order to assess the capacity of transfection in the corneal epithelium. Figure 6 shows representative images of the corneas 48 h after being transfected with the different vectors. A 48 h time interval between administration of the formulations and animal sacrifice was initially used, in order to compare the effects of fast acting mRNA and slow acting pDNA vectors.

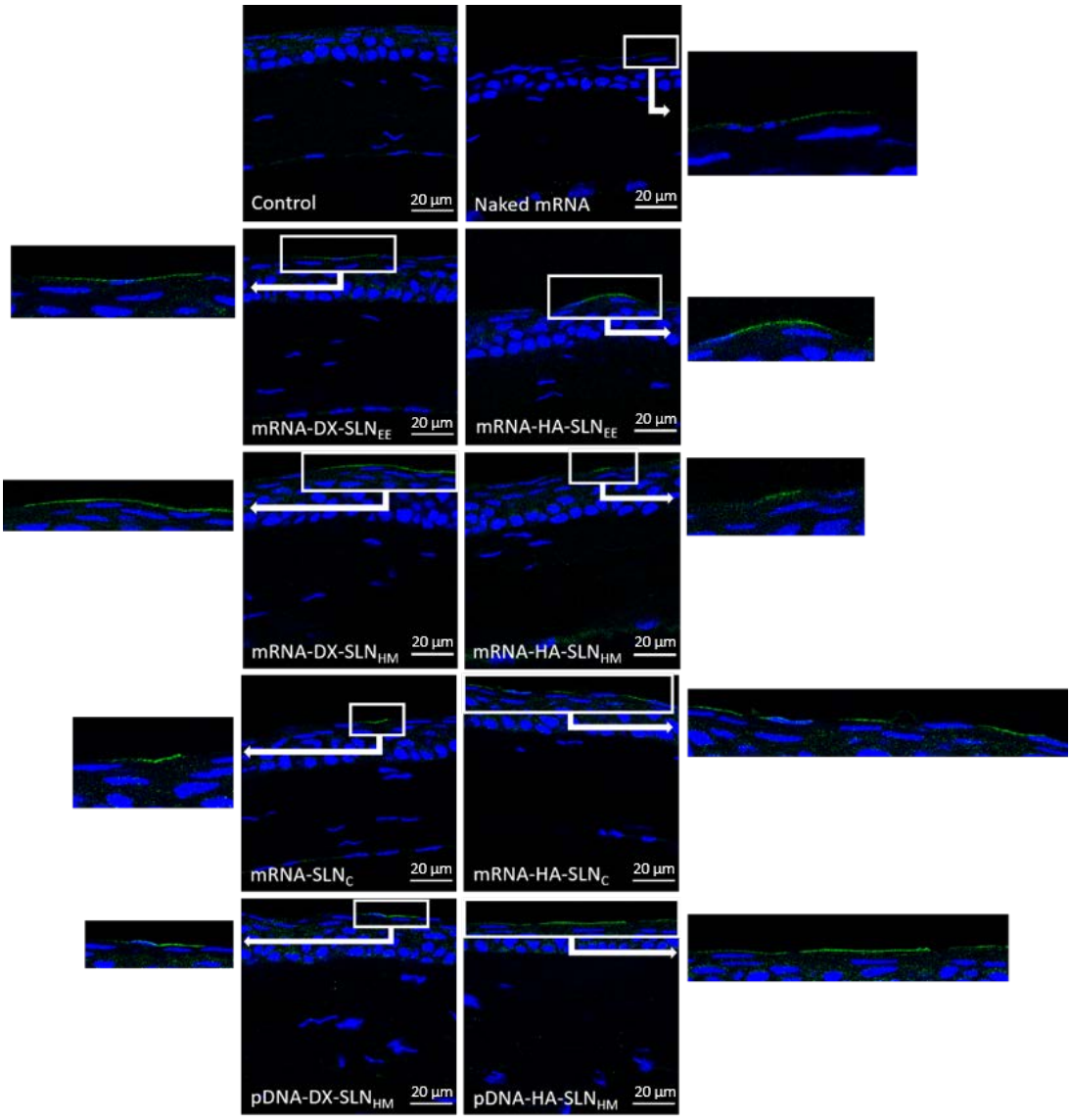

Figure 6. In vivo corneal transfection in mice 48 h after the administration of mRNA- and pDNA-vectors encoding GFP with the viscosifier PVA (63×). Blue: nuclei stained with DAPI. Green: GFP detected by immunofluorescence with the secondary antibody labeled with Alexa Fluor 488. Scale bar: 20 µm. DX: dextran; HA: hyaluronic acid; SLN$_{EE}$: solid lipid nanoparticle prepared by emulsification-evaporation method. SLN$_{HM}$: solid lipid nanoparticle prepared by hot-melt emulsification method. SLN$_{C}$: solid lipid nanoparticle prepared by coacervation method.

GFP was detected in 100% of the sections analyzed. All formulations were able to transfect and produce GFP in the corneal epithelium. GFP produced by naked mRNA was difficult to observe, whereas the intensity of fluorescence of GFP was higher when mRNA was formulated in the vectors.

GFP produced by mRNA-DX-SLN_{EE} and mRNA-DX-SLN_{HM} was localized continuously along the epithelium surface. In the case of mRNA-HA-SLN_{EE}, mRNA-HA-SLN_{HM}, and mRNA-SLN_{C}, uninterrupted segments of GFP were observed. In contrast, GFP in the corneas transfected with mRNA-HA-SLN_{C} was localized discontinuously.

Regarding transfection of the corneas with the nanocarriers prepared with pDNA, GFP was detected in a wider area with pDNA-HA-SLN_{HM} than with pDNA-DX-SLN_{HM}. pDNA-based formulations were used as controls for the mRNA-based ones; naked pDNA (GFP and IL-10) was previously evaluated [32].

Furthermore, by analyzing the corneas of the mice treated with selected formulations (mRNA-HA-SLN_{EE}) after 24 h, it was observed that GFP was detected in a larger surface area and with a higher intensity of fluorescence than after 48 h (Supplementary Material S4). Considering these promising results with mRNA-based vectors, indicating a faster onset of action than initially expected, the corneas treated with the vectors bearing mRNA-IL-10 were evaluated at 24 h post administration. Indeed, a 24 h timeframe, which is required because a quick expression of IL-10 would help to deal with the progression of the inflammatory disease, would be too short for pDNA expression.

3.5.2. In vivo transfection with mRNA encoding human IL-10

mRNA vectors encoding IL-10 viscosized with PVA were administered to mice as eye drops. The transfection efficacy of vectors was analyzed qualitatively 24 h after the last administration (Figure 7).

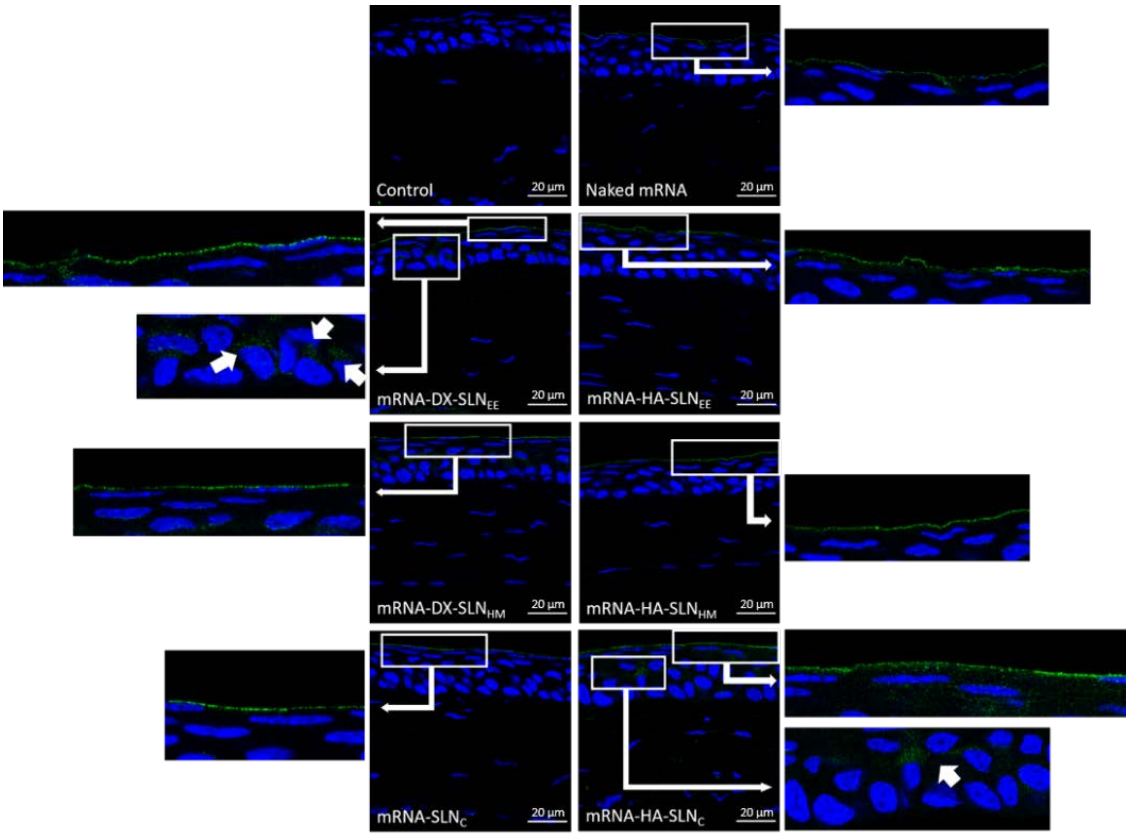

Figure 7. In vivo corneal transfection in mice 24 h after the administration of mRNA-vectors encoding human IL-10 with the viscosifier PVA (63×). Blue: nuclei stained with DAPI. Green: IL-10 detected by immunofluorescence with the secondary antibody labeled with Alexa Fluor 488. Scale bar: 20 µm. DX: dextran; HA: hyaluronic acid; SLN_{EE}: solid lipid nanoparticle prepared by emulsification-evaporation method. SLN_{HM}: solid lipid nanoparticle prepared by hot-melt emulsification method. SLN_{C}: solid lipid nanoparticle prepared by coacervation method.

IL-10 was observed continuously along the corneal epithelium in all analyzed sections. The intensity of the fluorescence signal was higher when the corneas were treated with the nanosystems than in the case of the naked mRNA. Slight differences were found among the different vectors, although with mRNA-DX-SLN_{EE} and mRNA-HA-SLN_{C}, IL-10 was also detected in deeper corneal layers underlying the epithelium (arrows in magnification).

4. Discussion

The development of new nanomedicine products for mRNA-based therapies has emerged as an attractive and promising tool in the field of advanced therapies. In this study, we have developed nanovectors based on SLNs for nucleic acid delivery. Three different methods were used to prepare the SLNs: SLN_{EE}, prepared by evaporation/emulsification, SLN_{HM} obtained by hot-melt emulsification, and SLN_{C} prepared by coacervation.

The preparation method influenced the physicochemical features of the SLNs, in terms of particle size and surface charge. In particular, SLN_{EE} and SLN_{HM}, made up with the same chemical

components but prepared by different methods, varied in particle size. Indeed, it ranged from 90 nm in the case of the hot emulsification procedure, which avoids the use of organic solvents, but involves a high operating temperature, to 200 nm in the case of the evaporation/solvent method. The solvent-free coacervation method, which exploits different compositions compared to the previously mentioned techniques, led to the highest particle size.

The final vectors were made up by electrostatic interactions among SLN, nucleic acid (mRNA or pDNA), and different ligands. Differences regarding the physicochemical characteristics of the SLN may lead to variations in the arrangement of the remaining components, since they are adsorbed on the SLN's surface to form the final vector. Therefore, the transfection capacity can be influenced. Firstly, the genetic material was condensed with P, which contributes to binding and protecting the nucleic acid extra and intracellularly due to its cationic character [39,40]. Secondly, if required, HA or DX were added; these polysaccharides influence the interactions with the target cells and the intracellular disposition of the nucleic acid [41–43]. An additional advantage of the inclusion of one of these polysaccharides is long-term stability for mRNA-SLN-based formulations [33].

For corneal transfection, small-sized particles between 10 and 1000 nm reduce eye irritability after topical administrations. Moreover, they show mucoadhesive properties, which help to prolong the residence time and, consequently, to increase the drug bioavailability in the ocular tissues [29,44]. The vectors prepared in our work showed a mean size lower than 300 nm and a positive superficial charge, which facilitates cellular uptake [30] and prolongs the retention time at the corneal epithelium, thanks to the electrostatic interactions with the negatively charged ocular surface [45].

A successful transfection depends upon the balance between the protection provided by the nanosystem to the nucleic acid against degradation, and its capacity to unpack and release the same inside the cell. The preparation method and the composition of the formulations, especially the presence of different ligands, have an important influence on the mRNA condensation and consequently, on the binding, protection, and release from the vector. Electrophoresis on agarose gel (Figure 1) showed that the SLNc vectors presented a weak protection capacity against external agents, and a low release ability. In the case of mRNA-SLN_{EE} and mRNA-SLN_{HM} vectors, differences in the condensation degree were observed (Figure 4). Nevertheless, both formulations protected and released the mRNA effectively (Figure 1). By contrast, no differences in condensation, protection, release capacity, and intracellular

disposition of the genetic material were observed in pDNA vectors. Therefore, mRNA seems to be more sensitive to the formulation-related factors than does pDNA.

The interaction between the formulation components and target cells condition the internalization process, and therefore, the intracellular disposition, the endosomal escape and, consequently, the transfection capacity of the systems [41,43,46]. The multi-component nanosystem developed in this work could be adapted to overpass the limiting barriers at the intracellular level, providing an appropriate nucleic acid packaging in the target cells. Endocytosis is the most common mechanism used by SLNs to enter inside the cells. It is an energy- and temperature-dependent process, associated with endosomal/lysosomal pathways of cellular trafficking. Depending on the lipid composition and the physicochemical characteristics of the non-viral vector, the predominant pathway may be different [47,48]. It is well-known that all energy-dependent uptake mechanisms are inhibited by cold temperatures [49]. In the present work, the influence of temperature (37 °C vs. 4 °C) on cellular uptake and transfection efficacy was studied in the HCE-2 cells. Cellular uptake remained stable at both temperatures, which indicates that not only energy-dependent but also energy-independent entry mechanisms are undertaken. Conversely, the percentage of transfected cells decreased significantly at 4 °C, whereas the intensity of fluorescence, indicative of the amount of protein produced by transfected cells, remained almost stable. Therefore, at cold temperatures the few transfected cells are able to produce a higher amount of protein. These results show that the transfection of HCE-2 cells is favoured by energy-dependent mechanisms, although the production of protein seems to be more efficient when the vectors are taken up by energy-independent mechanisms.

The transfection capacity of mRNA- and pDNA-based vectors was similar in terms of transfected cells and intensity of fluorescence (Figure 2). Contrarily to pDNA, mRNA bypasses one of most limiting steps: it does not need to reach the nucleus to transfect, and therefore, it is expected to lead to a faster transfection rate. Noteworthy, our results seem to indicate that the bottleneck for a successful transfection in corneal epithelial cells is before the nuclear entry; as a consequence, the intra-cytoplasmic behaviour of our nanosystems seems to be the limiting step for the transfection.

Transfection studies with the nanovectors bearing pDNA or mRNA encoding the anti-inflammatory cytokine IL-10 were also carried out in HCE-2 cells. The IL-10 was measured in the culture media and at the intracellular level. The mRNA vectors most efficient in terms of IL-10 production were those containing the SLNs prepared by the solvent/evaporation method. For

the same kind of SLNs (SLN_{EE} or SLN_{HM}), those containing DX were more effective than those containing HA. The mRNA-vectors, including the SLNs prepared by coacervation, hardly produced IL-10. The levels of IL-10 secreted by cells treated with the vectors prepared with SLN_{HM} and either mRNA or pDNA were similar (Figure 5). It is expected that levels over 0.8 ng/mL of IL-10 would exert the anti-inflammatory effect [50]. In previous works, we showed that SLNs-based systems bearing pDNA were able to produce up to 10 ng/mL of IL-10 in HCE-2 cells [8]. In our case, the IL-10 levels obtained with mRNA-SLN_{EE} were higher; in particular, the most effective formulation, mRNA-DX-SLN_{EE}, showed IL-10 levels almost three-folds higher.

The formulation of nanodelivery systems plays a crucial role in the development of medicinal products based on gene therapy, and specifically, in ocular gene therapy. An optimal ophthalmic drug formulation should comply to an adequate bioavailability, an increased permeability, an improved stability against degradation, a prolonged retention on the eye surface, and an augmented interaction with the cornea and targeted delivery [51]. Indeed, due to the pseudoplastic properties of the tear fluid, the inclusion of thickening agents could be advantageous in order to increase the corneal retention time and ocular bioavailability [52]. For the *in vivo* studies, the thickening agent PVA was added to the vectors. The non-ionic and synthetic biodegradable hydrophilic polymer PVA [53] is approved by the FDA for use in ophthalmic formulations [54]. PVA has been widely used because of its muco-mimetic properties, high water retention capacity, oxygen permeability, and low toxicity [55]. These properties confer to our nanosystems the ability to increase the residence time, and consequently improve the ocular bioavailability, reducing the drainage from lachrymal fluid [56,57]. In early studies, our group showed that the combination of SLN-based vectors with PVA provided a higher retention on the cornea [32]. Ophthalmic formulations should have the pH of the lacrimal fluid, or a pH within the range of the ocular comfort range, in order to ensure a good tolerance [58,59]. The ocular pH ranges from 6.6 to 7.8; it is reported that a pH value of an ocular preparation ranged outside 5.0-8.5 causes extra lachrymation and decreases the ocular residence time [60]. Our formulations showed pH values within the ocular tolerance range, from 7.1 to 7.5 (Table 5).

In vivo studies in mice were first carried out to evaluate the formulations containing mRNA or pDNA for GFP expression. Since GFP, once produced, remains at the intracellular level, it allowed us to identify the corneal layers where transfection occurs, after the instillation on the mice ocular surface with these vectors. Since the cornea is a complex structure, mRNA-delivery systems are engineered to induce the therapeutic protein expression in the cornea, specifically in the stratified and renewable epithelial layer, where a high number of cells can be transfected.

Another alternative could be the transfection of the innermost layer of the cornea, the endothelial layer, associated with a difficult accessibility. Indeed, this layer contains a low number of cells that do not undergo division and gene expression could be maintained for longer times. To this aim, DNA could be most advantageous, since it provides a more persistent transgene production than mRNA. However, although we have previously shown the capacity of DNA-based formulations to transfect the cornea [8], mRNA possesses several advantages that could make it a better option for corneal inflammation management. Indeed, mRNA shows a better safety profile than DNA; the encoded protein is earlier produced, and its expression is transitory, which makes the behaviour of this molecule easier to predict. Moreover, taking into account that the corneal epithelium only needs 7 to 14 days to achieve a complete renewal [61], a short-term expression of the protein is required.

All mRNA-based formulations included in this experimental work transfected the cornea *in vivo* and showed a higher intensity of fluorescence than naked mRNA. Thus, the SLNs resulted necessary to obtain a high transfection efficiency. These formulations were able to transfect only the epithelial cells but not the inner layers of the cornea, regardless of their different particle size. The intensity of fluorescence of GFP observed in the HCE-2 cells *in vitro*, representative of the protein production, was similar for all formulations, and it seems to correlate better with the *in vivo* results than with the percentage of transfected cells *in vitro*. Nevertheless, the lack of a strict correlation between *in vitro* and *in vivo* studies [62–65] highlights the necessity to perform the latter ones at the earliest phases of the pharmaceutical development process, in order to perform adequate selection and optimization of candidate formulations.

Finally, we evaluated the capacity of our formulations to induce the production of the anti-inflammatory cytokine IL-10 [51]. In view of the fact that IL-10 is a secreted protein, it may be produced in the epithelial corneal cells and diffuse through the cornea to reach deeper layers. Moreover, for corneal inflammation management, a quick expression of IL-10 would help to deal with the progression of the disease. In this context, we administered the formulations for 3 days and, 24 h after the last administration, the presence of IL-10 in the cornea was assessed. When mice were treated with an mRNA-DX-SLN_{EE} vector, the best performing formulation in *in vitro* experiments in HCE-2 cells (Figure 5), the interleukin was even observed in the deeper layers of the epithelium (Figure 7). mRNA-HA-SLN_C vectors also showed a high capacity to produce IL-10, despite the low efficacy observed *in vitro*. It should be considered that the transfection efficacy of the nanovectors could be increased in inflamed corneas, as the histological structure of corneal layers would be altered and disorganized, resulting in a potentially increased

permeation of the nanosystems into the tissue. Within this concern, in previous studies with SLN-based nanosystem containing pDNA as the nucleic acid, vectors prepared with the polysaccharide HA showed the highest transfection efficacy [32]. pDNA and mRNA differ not only in their physico-chemical characteristics, but also in terms of their intracellular barriers to overcome in order to achieve protein production. Our results confirm the necessity of the adaptation of the nanovector to the target cells and to the nature of the nucleic acid, in order to obtain an effective transfection.

5. Conclusions

The nature of the nucleic acid and the target cell are key points for the design and optimization of nanosystems aimed at ocular gene delivery, with mRNA being more sensitive to the formulation-related factors than pDNA. Nanomedicinal products design is based, initially, on *in vitro* studies. We have demonstrated that the HCE-2 cells' transfection is favoured by energy-dependent mechanisms, but the production of protein is more efficient when the vectors are taken up by energy-independent mechanisms. However, the lack of correlation observed between *in vitro* and *in vivo* assays has highlighted the necessity to perform *in vivo* studies at the earliest phases of the pharmaceutical development of nucleic acid delivery systems. In the present work, SLNs allowed the ability to obtain a high transfection efficiency *in vivo*. Therefore, topical administration to mice of eye drops containing mRNA formulated in SLNs has shown to be a feasible strategy to tackle corneal inflammation by *de novo* fast IL-10 production from corneal epithelial cells.

References

1. del Pozo-Rodríguez, A.; Torrecilla, J.; Rodríguez-Gascón, A.; Solinís, M.Á. Nonviral Delivery Systems for Gene Therapy for Retina and Posterior Segment Disease BT. In *Drug Delivery for the Retina and Posterior Segment Disease*; Patel, J.K., Sutariya, V., Kanwar, J.R., Pathak, Y.V., Eds.; Springer International Publishing: Cham, Switzerland, 2018; pp. 131–149 ISBN 978-3-319-95807-1.
2. Trigueros, S.; Domènech, E.B.; Toulis, V.; Marfany, G. In vitro gene delivery in retinal pigment epithelium cells by plasmid dna-wrapped gold nanoparticles. Genes 2019, 10, doi:10.3390/genes10040289.
3. Di Iorio, E.; Barbaro, V.; Alvisi, G.; Trevisan, M.; Ferrari, S.; Masi, G.; Nespeca, P.; Ghassabian, H.; Ponzin, D.; Palù, G. New Frontiers of Corneal Gene Therapy. Hum. Gene Ther. 2019, 30, 923–945, doi:10.1089/hum.2019.026.
4. Gene Therapy Clinical Trials Worldwide. Provided by Journal of Gene Medicine, John Wileys and Sons LTD. 2021. Available online: https://a873679.fmphost.com/fmi/webd/GTCT (accessed on 31 May 2021).

5. Torrecilla, J.; del Pozo-Rodríguez, A.; Vicente-Pascual, M.; Solinís, M.Á.; Rodríguez-Gascón, A. Targeting corneal inflammation by gene therapy: Emerging strategies for keratitis. Exp. Eye Res. 2018, 176, 130–140, doi:10.1016/j.exer.2018.07.006.

6. Beeken, L.J.; Ting, D.S.J.; Sidney, L.E. Potential of mesenchymal stem cells as topical immunomodulatory cell therapies for ocular surface inflammatory disorders. Stem Cells Transl. Med. 2021, 10, 39–49, doi:10.1002/sctm.20-0118.

7. Ghasemi, H.; Ghazanfari, T.; Yaraee, R.; Owlia, P.; Hassan, Z.M.; Faghihzadeh, S. Roles of IL-10 in Ocular Inflammations: A Review. Ocul. Immunol. Inflamm. 2012, 20, 406–418, doi:10.3109/09273948.2012.723109.

8. Vicente-Pascual, M.; Albano, A.; Solinís, M.; Serpe, L.; Rodríguez-Gascón, A.; Foglietta, F.; Muntoni, E.; Torrecilla, J.; Pozo-Rodríguez, A.D.; Battaglia, L. Gene delivery in the cornea: In vitro & ex vivo evaluation of solid lipid nanoparticle-based vectors. Nanomedicine 2018, 13, 1847–1864, doi:10.2217/nnm-2018-0112.

9. Gómez-Aguado, I.; Rodríguez-Castejón, J.; Vicente-Pascual, M.; Rodríguez-Gascón, A.; Solinís, M.Á.; del Pozo-Rodríguez, A. Nanomedicines to Deliver mRNA: State of the Art and Future Perspectives. Nanomaterials 2020, 10, 364, doi:10.3390/nano10020364.

10. Damase, T.R.; Sukhovershin, R.; Boada, C.; Taraballi, F.; Pettigrew, R.I.; Cooke, J.P. The Limitless Future of RNA Therapeutics. Front. Bioeng. Biotechnol. 2021, 9, 1–24, doi:10.3389/fbioe.2021.628137.

11. Del Pozo-Rodríguez, A.; Alicia Rodríguez-Gascón; Rodríguez-Castejón, J.; Vicente-Pascual, M.; Gómez-Aguado, I.; Battaglia, L.S.; Solinís, M.Á. Gene Therapy. In Advances in Biochemical Engineering/Biotechnology; Springer: Berlin/Heidelberg, Germany, 2019; Volume 171, pp. 321–368 ISBN 978-3-030-40464-2.

12. May, M. After COVID-19 successes, researchers push to develop mRNA vaccines for other diseases. Nat. Med. 2021, 27, 930–932, doi:10.1038/s41591-021-01393-8.

13. Igyártó, B.Z.; Jacobsen, S.; Ndeupen, S. Future considerations for the mRNA-lipid nanoparticle vaccine platform. Curr. Opin. Virol. 2021, 48, 65–72, doi:10.1016/J.COVIRO.2021.03.008.

14. Chakraborty, C.; Sharma, A.R.; Bhattacharya, M.; Lee, S.-S. From COVID-19 to Cancer mRNA Vaccines: Moving From Bench to Clinic in the Vaccine Landscape. Front. Immunol. 2021, 12, 1–17, doi:10.3389/fimmu.2021.679344.

15. U.S. Department of Health and Human Services. Food and Drug Administration. COVID-19 Vaccines. Available online: https://www.fda.gov/emergency-preparedness-and-response/coronavirus-disease-2019-covid-19/covid-19-vaccines (accessed on 22 July 2021).

16. European Medicines Agency. Science Medicines Health. COVID-19 vaccines. Available online: https://www.ema.europa.eu/en/human-regulatory/overview/public-health-threats/coronavirus-disease-covid-19/treatments-vaccines/covid-19-vaccines (accessed on 22 July 2021).

17. Gediz Erturk, A.; Sahin, A.; Ay, E.B.; Pelit, E.; Bagdatli, E.; Kulu, I.; Gul, M.; Mesci, S.; Eryilmaz, S.; Yildirim, T.; et al. molecules A Multidisciplinary Approach to Coronavirus Disease (COVID-19). Molecules 2021, 26, doi:10.3390/molecules26123526.

18. Paganelli, R.; Frasca, D.; Nisini, R.; Bajaj, V.; Gadi, N.; Spihlman, A.P.; Wu, S.C.; Choi, C.H.; Moulton, V.R. Aging, Immunity, and COVID-19: How Age Influences the Host Immune Response to Coronavirus Infections? Front. Physiol. 2020, 11, 1793, doi:10.3389/fphys.2020.571416.

19. del Pozo-Rodríguez, A.; Solinís, M.Á.; Rodríguez-Gascón, A. Applications of lipid nanoparticles in gene therapy. Eur. J. Pharm. Biopharm. 2016, 109, 184–193, doi:10.1016/j.ejpb.2016.10.016.

20. Wang, Y.; Rajala, A.; Rajala, R.V.S. Lipid Nanoparticles for Ocular Gene Delivery. J. Funct. Biomater. 2015, 6, 379–394.

21. Barba, A.A.; Bochicchio, S.; Dalmoro, A.; Lamberti, G. Lipid delivery systems for nucleic-acid-based-drugs: From production to clinical applications. Pharmaceutics 2019, 11, 5–7, doi:10.3390/pharmaceutics11080360.

22. Mehnert, W.; Mader, K. Advances in the Cognitive Neuroscience of Neurodevelopmental Disorders: Views from Child Psychiatry and Medical Genetics. Neurodev. Disord. 2020, 47, 165–196, doi:10.7551/mitpress/4945.003.0031.

23. Müller, R.H.; Radtke, M.; Wissing, S.A. Solid lipid nanoparticles (SLN) and nanostructured lipid carriers (NLC) in cosmetic and dermatological preparations. Adv. Drug Deliv. Rev. 2002, 54, 131–155, doi:10.1016/S0169-409X(02)00118-7.

24. Yadav, N.; Khatak, S.; Sara, U.S. Solid lipid nanoparticles—A review. Int. J. Appl. Pharm. 2013, 5, 8–18, doi:10.9790/3013-26103444.

25. Ramamoorth, M.; Narvekar, A. Non viral vectors in gene therapy—An overview. J. Clin. Diagnostic Res. 2015, 9, GE01–GE06, doi:10.7860/JCDR/2015/10443.5394.

26. Trucillo, P.; Campardelli, R. Production of solid lipid nanoparticles with a supercritical fluid assisted process. J. Supercrit. Fluids 2019, 143, 16–23, doi:10.1016/j.supflu.2018.08.001.

27. Chattopadhyay, P.; Shekunov, B.Y.; Yim, D.; Cipolla, D.; Boyd, B.; Farr, S. Production of solid lipid nanoparticle suspensions using supercritical fluid extraction of emulsions (SFEE) for pulmonary delivery using the AERx system. Adv. Drug Deliv. Rev. 2007, 59, 444–453, doi:10.1016/j.addr.2007.04.010.

28. Singh, M.; Guzman-Aranguez, A.; Hussain, A.; Srinivas, C.S.; Kaur, I.P. Solid lipid nanoparticles for ocular delivery of isoniazid: Evaluation, proof of concept and in vivo safety & kinetics. Nanomedicine 2019, 14, 465–491, doi:10.2217/nnm-2018-0278.

29. Mobaraki, M.; Soltani, M.; Harofte, S.Z.; Zoudani, E.L.; Daliri, R.; Aghamirsalim, M.; Raahemifar, K. Biodegradable nanoparticle for cornea drug delivery: Focus review. Pharmaceutics 2020, 12, 1–26, doi:10.3390/pharmaceutics12121232.

30. Battaglia, L.; Serpe, L.; Foglietta, F.; Muntoni, E.; Gallarate, M.; Del Pozo Rodriguez, A.; Solinis, M.A. Application of lipid nanoparticles to ocular drug delivery. Expert Opin. Drug Deliv. 2016, 13, 1743–1757, doi:10.1080/17425247.2016.1201059.

31. Bachu, R.D.; Chowdhury, P.; Al-Saedi, Z.H.F.; Karla, P.K.; Boddu, S.H.S. Ocular Drug Delivery Barriers—Role of Nanocarriers in the Treatment of Anterior Segment Ocular Diseases. Pharmaceutics 2018, 10, 28, doi:10.3390/pharmaceutics10010028.

32. Vicente-Pascual, M.; Gómez-Aguado, I.; Rodríguez-Castejón, J.; Rodríguez-Gascón, A.; Muntoni, E.; Battaglia, L.; Del Pozo-Rodríguez, A.; Aspiazu, M.Á.S. Topical Administration of SLN-Based Gene Therapy for the Treatment of Corneal Inflammation by De Novo IL-10 Production. Pharmaceutics 2020, 12, 1–23, doi:10.3390/pharmaceutics12060584.

33. Gómez-Aguado, I.; Rodríguez-Castejón, J.; Vicente-Pascual, M.; Rodríguez-Gascón, A.; Del Pozo-Rodríguez, A.; Solinís Aspiazu, M.Á. Nucleic Acid Delivery by Solid Lipid Nanoparticles Containing Switchable Lipids: Plasmid DNA vs. Messenger RNA. Molecules 2020, 25, doi:10.3390/molecules25245995.

34. Sloot, Y.J.E.; Rabold, K.; Ulas, T.; De Graaf, D.M.; Heinhuis, B.; Händler, K.; Schultze, J.L.; Netea, M.G.; Smit, J.W.A.; Joosten, L.A.B.; et al. Interplay between thyroid cancer cells and macrophages: Effects on IL-32 mediated cell death and thyroid cancer cell migration. Cell. Oncol. 2019, 42, 691–703, doi:10.1007/s13402-019-00457-9.

35. Tsai, Y.-C.; Tsai, T.-H.; Chang, C.-P.; Chen, S.-F.; Lee, Y.-M.; Shyue, S.-K. Linear correlation between average fluorescence intensity of green fluorescent protein and the multiplicity of infection of recombinant adenovirus. J. Biomed. Sci. 2015, 22, 31, doi:10.1186/s12929-015-0137-z.

36. Sandhu, K.S.; Al-Rubeai, M. Monitoring of the Adenovirus Production Process by Flow Cytometry. Biotechnol. Prog. 2008, 24, 250–261, doi:https://doi.org/10.1021/bp070198s..

37. Xu, X.; Lambrecht, A.D.; Xiao, W. Chapter 13—Yeast Survival and Growth Assays. Methods Mol. Biol. 2014, 1163, 33–44, doi:10.1007/978-1-4939-0799-1.

38. Mahareek, O.; Fahmi, A.; Abdur-Rahman, M.; Shemis, M. Synthesis, Characterization and Optimization of PCL-based Nanocapsules for Delivery of Anticancer Chemotheraputic Drug. J. Sci. Res. Sci. 2019, 36, 412–423, doi:10.21608/jsrs.2019.57774.

39. Delgado, D.; Del Pozo-Rodríguez, A.; Solinís, M.Á.; Rodríguez-Gascón, A. Understanding the mechanism of protamine in solid lipid nanoparticle-based lipofection: The importance of the entry pathway. Eur. J. Pharm. Biopharm. 2011, 79, 495–502, doi:10.1016/j.ejpb.2011.06.005.

40. Ruseska, I.; Fresacher, K.; Petschacher, C.; Zimmer, A. Use of protamine in nanopharmaceuticals—a review. Nanomaterials 2021, 11, doi:10.3390/nano11061508

41. Delgado, D.; Gascón, A.R.; Del Pozo-Rodríguez, A.; Echevarría, E.; Ruiz De Garibay, A.P.; Rodríguez, J.M.; Solinís, M.Á. Dextran-protamine-solid lipid nanoparticles as a non-viral vector for gene therapy: In vitro characterization and in vivo transfection after intravenous administration to mice. Int. J. Pharm. 2012, 425, 35–43, doi:10.1016/j.ijpharm.2011.12.052.

42. Apaolaza, P.S.; del Pozo-Rodríguez, A.; Torrecilla, J.; Rodríguez-Gascón, A.; Rodríguez, J.M.; Friedrich, U.; Weber, B.H.F.; Solinís, M.A. Solid lipid nanoparticle-based vectors intended for the treatment of X-linked juvenile retinoschisis by gene therapy: In vivo approaches in Rs1h-deficient mouse model. J. Control. Release 2015, 217, 273–283, doi:10.1016/j.jconrel.2015.09.033.

43. Apaolaza, P.S.; Delgado, D.; Pozo-Rodríguez, A. Del; Gascón, A.R.; Solinís, M.Á. A novel gene therapy vector based on hyaluronic acid and solid lipid nanoparticles for ocular diseases. Int. J. Pharm. 2014, 465, 413–426, doi:10.1016/j.ijpharm.2014.02.038.

44. Omerović, N.; Vranić, E. Application of nanoparticles in ocular drug delivery systems. Health Technol. 2020, 10, 61–78, doi:10.1007/s12553-019-00381-w.

45. Wong, C.W.; Metselaar, J.M.; Storm, G.; Wong, T.T. A review of the clinical applications of drug delivery systems for the treatment of ocular anterior segment inflammation. Br. J. Ophthalmol. 2020, 1–6, doi:10.1136/bjophthalmol-2020-315911.

46. Li, J.; Chen, Q.; Zha, Z.; Li, H.; Toh, K.; Dirisala, A.; Matsumoto, Y.; Osada, K.; Kataoka, K.; Ge, Z. Ternary polyplex micelles with PEG shells and intermediate barrier to complexed DNA cores for efficient systemic gene delivery. J. Control. Release 2015, 209, 77–87, doi:10.1016/j.jconrel.2015.04.024.

47. Al Khafaji, A.S.; Donovan, M.D. Endocytic uptake of solid lipid nanoparticles by the nasal mucosa. Pharmaceutics 2021, 13, doi:10.3390/pharmaceutics13050761.

48. Manzanares, D.; Ceña, V. Endocytosis: The nanoparticle and submicron nanocompounds gateway into the cell. Pharmaceutics 2020, 12, 1–22, doi:10.3390/pharmaceutics12040371.

49. Nagai, N.; Ogata, F.; Otake, H.; Nakazawa, Y.; Kawasaki, N. Energy-dependent endocytosis is responsible for drug transcorneal penetration following the instillation of ophthalmic formulations containing indomethacin nanoparticles. Int. J. Nanomedicine 2019, 14, 1213–1227, doi:10.2147/IJN.S196681.

50. Wang, X.; Coradin, T.; Hélary, C. Modulating inflammation in a cutaneous chronic wound model by IL-10 released from collagen-silica nanocomposites: Via gene delivery. Biomater. Sci. 2018, 6, 398–406, doi:10.1039/c7bm01024a.

51. Reimondez-Troitiño, S.; Csaba, N.; Alonso, M.J.; de la Fuente, M. Nanotherapies for the treatment of ocular diseases. Eur. J. Pharm. Biopharm. 2015, 95, 279–293, doi:10.1016/j.ejpb.2015.02.019.

52. Dubashynskaya, N.; Poshina, D.; Raik, S.; Urtti, A.; Skorik, Y.A. Polysaccharides in Ocular Drug Delivery. Pharmaceutics 2020, 12, 22, doi:10.3390/pharmaceutics12010022.

53. Basa, B.; Jakab, G.; Kállai-Szabó, N.; Borbás, B.; Fülöp, V.; Balogh, E.; Antal, I. Evaluation of biodegradable PVA-based 3D printed carriers during dissolution. Materials 2021, 14, doi:10.3390/ma14061350.

54. Bhattarai, R.S.; Das, A.; Alzhrani, R.M.; Kang, D.; Bhaduri, S.B.; Boddu, S.H.S. Comparison of electrospun and solvent cast polylactic acid (PLA)/poly(vinyl alcohol) (PVA) inserts as

potential ocular drug delivery vehicles. Mater. Sci. Eng. C 2017, 77, 895–903, doi:10.1016/j.msec.2017.03.305.

55. Akbari, E.; Imani, R.; Shokrollahi, P.; Heidari keshel, S. Preparation of Nanoparticle-Containing Ring-Implanted Poly(Vinyl Alcohol) Contact Lens for Sustained Release of Hyaluronic Acid. Macromol. Biosci. 2021, 21, 2100043, doi:10.1002/mabi.202100043.

56. Hao, J.; Wang, X.; Bi, Y.; Teng, Y.; Wang, J.; Li, F.; Li, Q.; Zhang, J.; Guo, F.; Liu, J. Fabrication of a composite system combining solid lipid nanoparticles and thermosensitive hydrogel for challenging ophthalmic drug delivery. Colloids Surfaces B Biointerfaces 2014, 114, 111–120, doi:10.1016/j.colsurfb.2013.09.059.

57. Battaglia, L.; Gallarate, M.; Serpe, L.; Foglietta, F.; Muntoni, E.; del Pozo Rodriguez, A.; Angeles Solinis Aspiazu, M. Ocular delivery of solid lipid nanoparticles. In Lipid Nanocarriers for Drug Targeting; Elsevier, 2018; pp. 269–312 ISBN 9780128136874.

58. Abelson, M.B.; Udell, I.J.; Weston, J.H. Normal Human Tear pH by Direct Measurement. Arch. Ophthalmol. 1981, 99, 301, doi:10.1001/archopht.1981.03930010303017.

59. Garcia-Valldecabres, M.; López-Alemany, A.; Refojo, M.F. pH Stability of ophthalmic solutions. Optometry 2004, 75, 161–168, doi:10.1016/S1529-1839(04)70035-4.

60. Račić, A.; Čalija, B.; Milić, J.; Dukovski, B.J.; Lovrić, J.; Dobričić, V.; Micov, A.; Vuković, M.; Stepanović-Petrović, R.; Krajišnik, D. Formulation of olopatadine hydrochloride viscous eye drops—physicochemical, biopharmaceutical and efficacy assessment using in vitro and in vivo approaches. Eur. J. Pharm. Sci. 2021, 105906, doi:10.1016/j.ejps.2021.105906.

61. Stocum, D.L. Regeneration of Epidermal Structures. Regen. Biol. Med. 2012, 1, 43–65, doi:10.1016/b978-0-12-384860-4.00003-4.

62. Struve, C.; Krogfelt, K.A. Role of capsule in Klebsiella pneumoniae virulence: Lack of correlation between in vitro and in vivo studies. FEMS Microbiol. Lett. 2003, 218, 149–154, doi:10.1111/j.1574-6968.2003.tb11511.x.

63. Hulsart-Billström, G.; Dawson, J.I.; Hofmann, S.; Müller, R.; Stoddart, M.J.; Alini, M.; Redl, H.; El Haj, A.; Brown, R.; Salih, V.; et al. A surprisingly poor correlation between in vitro and in vivo testing of biomaterials for bone regeneration: Results of a multicentre analysis. Eur. Cells Mater. 2016, 31, 312–322, doi:10.22203/eCM.v031a20.

64. Zheng, Y.F.; Bae, S.H.; Huang, Z.; Chae, S.U.; Jo, S.J.; Shim, H.J.; Lee, C. Bin; Kim, D.; Yoo, H.; Bae, S.K. Lack of Correlation between In Vitro and In Vivo Studies on the Inhibitory Effects of (–)-Sophoranone on CYP2C9 Is Attributable to Low Oral Absorption and Extensive Plasma Protein Binding of (–)-Sophoranone. Pharmaceutics 2020, 12, 328, doi:10.3390/pharmaceutics12040328.

65. Williams, C.S.; Watson, A.J.M.; Sheng, H.; Helou, R.; Shao, J.; DuBois, R.N. Celecoxib prevents tumor growth in vivo without toxicity to normal gut: Lack of correlation between in vitro and in vivo models. Cancer Res. 2000, 60, 6045–6051.

WORKS UNDER REVIEW

APPENDIX V:

mRNA delivery technologies: towards clinical translation

Itziar Gómez-Aguado, Julen Rodríguez-Castejón, Marina Beraza-Millor, Alicia Rodríguez-Gascón, Ana del Pozo-Rodríguez, María Ángeles Solinís

Under review in: International Review of Cell and Molecular Biology

Journal Impact Factor JCR 2020: 6.813 (Q1) 54/295

Related Categories:

BIOCHEMISTRY & MOLECULAR BIOLOGY (Q1)

CELL BIOLOGY (Q1)

mRNA delivery technologies: towards clinical translation

Abstract:

Messenger RNA (mRNA)-therapies have recently taken a huge step towards clinic thanks to the first mRNA-based medicinal products marketed. mRNA features for clinical purposes are improved by chemical modifications, but the inclusion in a delivery system is a regular requirement. mRNA nanomedicines must be designed for the specific therapeutic purpose, protecting the nucleic acid and facilitating the overcoming of biological barriers. Polymers, polypeptides, and cationic lipids are the main used materials to design mRNA delivery systems. Among them, lipid nanoparticles (LNPs) are the most advanced ones, and currently they are at the forefront of preclinical and clinical evaluation in several fields, including immunotherapy (against infectious diseases and cancer), protein replacement, gene editing and regenerative medicine. This chapter includes an overview on mRNA delivery technologies, with special interest in LNPs, and the most recent advances in their clinical application. Liposomes are the mRNA delivery technology with the highest clinical translation among LNPs, whereas the first clinical trial of a therapeutic mRNA formulated in exosomes has been recently approved for protein replacement therapy. The first mRNA products approved by the regulatory agencies worldwide are LNP-based mRNA vaccines against viral infections, specifically against the 2019 coronavirus disease (COVID-19). The clinical translation of mRNA-therapies for cancer is mainly focused on three strategies: anti-cancer vaccination by means of delivering cancer antigens or acting as an adjuvant, mRNA-engineered chimeric antigen receptors (CARs) and T-cell receptors (TCRs), and expression of antibodies and immunomodulators. Cancer immunotherapy and, more recently, COVID-19 vaccines spearhead the advance of mRNA clinical use.

Keywords: messenger RNA (mRNA); gene therapy; nanomedicine; cancer immunotherapy; vaccines; COVID-19; lipid nanoparticles; liposomes; nucleic acid delivery; clinical trials.

1. Introduction

Nucleic acid medicinal products are making great progress, leading the way in the development of advanced therapies. These medicines can be applied for gene augmentation, gene silencing, or gene editing [1]. DNA has been classically studied to induce protein expression; however, due to the recent advance in understanding the structure of the messenger RNA (mRNA) and its role in genetic processes, and due to the progress on delivery carriers, mRNA is being studied for several applications, such as vaccination against infectious diseases, cancer immunotherapy, protein replacement, gene editing or regenerative medicine [2,3]. In fact, after many years of

research, in 2020 mRNA medicinal products reached the clinic worldwide in the form of mRNA-based vaccines for the prevention of Coronavirus Disease Pandemic (COVID-19) [4,5].

Synthetic mRNA presents several characteristics that support its use as an alternative to DNA. In contrast to DNA, mRNA molecules do not need to reach the nucleus to start the protein translation; therefore, mRNA is more effective to express the target protein, and it can be functional in mitotic and non-mitotic cells [6–12] Moreover, mRNA does not integrate into the host genome, which makes this molecule safer than DNA [7–12]. From the point of view of large-scale production, mRNA synthesis is fast, easy to standardize with high reproducibility and inexpensive [8]. Finally, protein expression is initiated earlier with mRNA; the protein can be detected since the first hour after transfection, and the maximum level of expression is usually observed after 5-7 h [13].

Clinical application of mRNA can be implemented in vivo or ex vivo. In the latter case, cells are extracted from the patient and modified with the nucleic acid in the laboratory before being reinfused into the patient. In the former, the nucleic acid is administered into the patient via the routes commonly used for conventional drugs [14,15]. However, the use of synthetic mRNA for clinical purposes, both ex vivo and in vivo, needs to overcome important limitations to result effective: physical instability, immunogenicity and entry into the cell, which is difficult due to the high molecular weight, the anionic nature and the hydrosolubility of the nucleic acid [16]. Chemical modifications of mRNA structure improve stability and translation efficacy, and reduce immunogenicity, but the inclusion of synthetic mRNA in properly designed delivery systems is frequently essential for overcoming all these barriers. The most studied systems for mRNA delivery are non-viral vectors, and more specifically lipidic systems.

The aim of this work is to review the main mRNA delivery techniques, with special focus on lipid-based systems, and the recent and near future clinical applications of mRNA medicines.

2. Synthetic mRNA

2.1. Synthetic mRNA structure

Synthetic mRNA mimics the structure of natural mRNA and is formed by a single strand consisting of five basic structures (Figure 1): 5’ Cap, 5’ untranslated region (UTR), an open reading frame (ORF), 3’ UTR, and a polyadenylated tail (poly(A) tail).

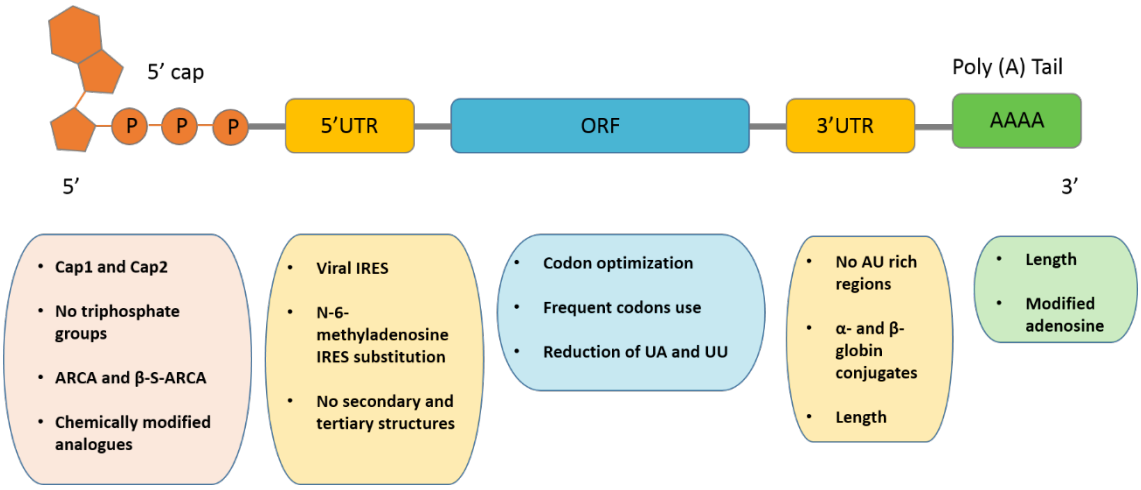

Figure 1. Scheme of synthetic mRNA structure scheme including the main modifications to improve its stability, translation efficacy and immunogenicity. 5' UTR: 5' untranslated region. 3' UTR: 3' untranslated region. ORF: open reading frame. Poly(A) tail: polyadenylated tail. A: adenine. P: phosphate. UA: uridine-adenine dinucleotides. UU: uridine-uridine dinucleotides. ARCA: anti-reverse cap analogue. β-S-ARCA: ARCA-β sulphured. IRES: internal ribosomal entry sites.

5'Cap structure is formed by an inverted 7-methyl guanosine (m7G) connected to the first transcribed RNA nucleotide by a 5' to 5' triphosphate bridge. This structure is known as cap0, and its functions include: mRNA stabilization in cellular processes (translation, splicing, polyadenylation or nuclear exportation), protection from exonucleases, interaction with cap binding proteins (CBPs), participation in nuclear exportation and in binding to the translation initiation factor 4E (eIF4E) [3,17].

The ORF is the most crucial component of mRNA molecule because it consists of the nucleotide sequence encoding the target protein, and the codon composition influences the translation efficiency and the stability of the nucleic acid.

UTRs are non-coding regions located at 5' and 3' sides of ORF. They do not directly contribute to protein expression but they contain specific regulatory elements that modulate mRNA replication, stability and translation efficiency. In cooperation with RNA binding proteins, they can slow down mRNA decay and improve transfection efficacy [18]. In general, UTRs regulate protein expression depending on three structural parameters: sequence, length and secondary structure [19].

The 5' UTR is an important element for ribosome recruitment and for choosing the start codon. [19,20]. Moreover, it is a key regulatory factor in the initiation of protein translation as it presents two major domains: Kozak sequence and the internal ribosomal entry sites (IRES). In eukaryotes, Kozak consensus sequence is represented by the nucleotides RCCAUGG, where R is a purine nucleotide, adenine (A) or guanine (G). In this structure, the initiation codon AUG is

included. In order to facilitate the recognition of the starting codon, an A or G nucleotide must be in the position -3 respect to the A of AUG, and a G in the position +4 [21–23]. IRES is responsible for the recruitment of the ribosome, and it allows a cap-independent translation initiation process. [24–27].

The 3' UTR sequence plays an important role in protein translation, particularly in stabilizing mRNA [19]. The stability and translation efficiency of mRNA is highly conditioned by the presence of AU rich elements in 3' UTR. AU rich sequences are present in mRNA molecules with a high rate of degradation [3,28].

In eukaryotes, the poly(A) tail decorates the 3' end of mature mRNA. It consists of a 100-250 adenosine residues chain. It is well known that its sequence plays a key role in regulating stability and translation aspects of mRNA [29]. In this sense, it presents several functions, such as interaction with initiation translation factors, protection from nucleases and mRNA exportation from the nucleus. It slows down the degradation process of RNA exonucleases, which increases the stability, in vivo half-life and the translation efficiency of mRNA [30].

Synthetic mRNA is usually produced by a cell-free transcription system, which requires a linearized DNA template. Since its first successful report in 1990 [31] in vitro transcription technology of mRNA has matured [32]. mRNA can be transcribed from a linearized DNA plasmid or a PCR product [33,34]]. The DNA contains a promoter which is recognized by a bacteriophage RNA polymerase such as T7, T3 or SP6 [35]. In addition to the ORF sequence, it may also contain the sequences that encode UTRs. The poly(A) tail and the 5' Cap can be incorporated during the transcription process or post-transcriptionally. At the end of the process, the DNA template is degraded by DNases [36]. The use of cell-free systems can be carried out under Good Manufacturing Practices (GMPs), and it allows for easy standardization of clinical grade manufacturing. As a consequence, fabrication of synthetic mRNA under GMPs is more economical than production of recombinant proteins in eukaryotic cells [37].

Once the mRNA is transcribed, a set of purification steps should be done to remove aberrant molecules, which are associated to immunogenicity [38]. In particular, double stranded RNA (dsRNA) contaminants are similar to viral RNA replication intermediaries, and are considered pathogen-associated molecular patterns (PAMPs) [30], so they can promote the production of type I interferon (IFN-1) [8]. Purification processes include concentration, precipitation, and extraction and chromatography techniques (high performance liquid chromatography (HPLC), affinity and anion exchange) and size exclusion columns [38,39] may be applied. In addition to purification methods and in order to downregulate the production of dsRNA, in vitro

transcription process can be adjusted. Most recommended strategies include modified nucleosides, reduction of the Mg^{+2} concentration, which is needed for the elongation process, or the use of thermostable T7 RNA polymerase [38,40].

2.2. Synthetic mRNA modifications

The design of the mRNA may include specific modifications aimed at improving stability, reducing immunogenicity and maximizing protein-producing potential. Table 1 summarizes the main chemical modifications of mRNA and the purpose of these modifications.

Table 1. Main modifications of mRNA structure.

Modified structure	Modification	Purpose
5' Cap	Cap1 and cap2	Efficacy, translation stability and immunogenicity
	Elimination of triphosphate groups	Stability, recognition by ribosomes and initiation of translation
	ARCA (anti-reverse cap analogue)	Translation efficacy
	β-S-ARCA	Translation efficacy
	Chemically modified analogues (imidiphosphate, phosphorothiate, boranophosphate)	Efficacy and translation stability. Decapping protection
5' UTR	Viral IRES	Translation efficacy and cap-independent translation
	m6A IRES substitution	Cap-independent translation
	No secondary or tertiary structures	Stability and translation efficacy
ORF	Codon optimization and frequent codons use	Stability and translation efficacy
	Reduction of UA and UU dinucleotides	Stability
3' UTR	No AU rich regions	Stability
	α- and β-globin conjugates	Translation efficacy and stability
	Length	Location of the expressed protein
Poly A tail	Length	Stability, translation efficacy and protection
	Adenosine modifications	Protection
Modified nucleotides	Pseudouridine, N'methylpseudouridine, N-methyladenosine, 2-thiouridine	Immunogenicity, stability

circRNAs	Incorporation of IRES or m6A modification to 5' UTR	Stability and avoid immune system

5' UTR: 5' untranslated region; 3' UTR: 3' untranslated region; ORF: open reading frame; A: adenine; P: phosphate; UA: uridine-adenine dinucleotides; UU: uridine-uridine dinucleotides. ARCA: anti-reverse cap analogue; β-S-ARCA: ARCA-β sulphured; IRES: internal ribosomal entry sites; circRNAs: circular RNAs

The incorporation of modified nucleosides into mRNA is a common strategy to optimize protein expression efficiency and to reduce its immunostimulatory activity. mRNA interacts with cytoplasmic sensors, such as retinoic acid-inducible protein I (RIG-I) [41,42], which is responsible of blocking the translational machinery. Specifically, uridine (U)-rich regions interact with RIG-I. It has been documented that the U depletion in mRNA molecules leads to an improvement of protein expression [43]. Alternatively, RIG-I activation can be also abolished with the incorporation into the transcript of the modified nucleosides pseudouridine (Ψ) or 2-thiouridine (s2U) [44]. Modified nucleosides (Ψ, s2U, N1-methylpseudouridine (N1mΨ), 5-methylcytidine (m5C), N6-methyladenosine (m6A), or 5-methyluridine (m5U)) can also avoid the activation of Toll-like receptors (TLRs), which is responsible of the innate immune responses associated to the administration of exogenous mRNA [45–49].

Apart from the use of modified nucleosides, in 5' Cap region cap0 can be replaced by cap1 or cap2 by means of the methylation of the second or third ribonucleotide at the 2'O or 3'O position of the riboses, respectively. The objective of this modification is reducing the immunogenicity and enhancing the translation efficiency [50]. This methylation can be performed enzymatically by the enzyme m7G-specific 2'O methyltransferase (2'O MTase). Alternatively, addition of cap1 and cap2 during transcription is simpler than enzymatic capping; however, this process usually results in not capped molecules, which are immunostimulant, and immediately digested by nucleases. This limitation can be avoided by applying two different strategies. On the one hand, the use of a phosphatase to eliminate the triphosphates of the 5' end of uncapped mRNA [6,51] reduces the immunogenicity. On the other hand, co-transcriptional capping technology CleanCap™, developed by TriLink BioTechnologies, is able to incorporate cap1 or cap2 in the 94% of the mRNA molecules [52,53]. Other drawback during the capping process is the possibility of the cap analogues being arranged in reverse orientation, resulting in the inability to bind to the CBP [9,54,55]. This effect can be avoided by using anti-reverse cap analogue (ARCA) [9,55], which is a methyl group in the 3'-OH of the m7G nucleotide. ARCA enables the appropriate orientation of the cap, and prevents the elongation of the mRNA along the wrong site [55,56]. The substitution of an S group at β-position of the triphosphate bridge results in a new modification known as β-S-ARCA, which leads to in high affinity of the cap to EIF4E and low susceptibility to the decapping complex DCP1/DCP2 [57–59]. Removal of cap by this complex

inhibits the translation initiation and makes the mRNA to be committed to full degradation by exonucleases [60,61]. Chemically modified cap analogues, such as phosphorothioate, phosphorothiolate, imidiphosphate and boranophosphate, among others [58,61–66], are usually incorporated to synthetic mRNA to get protected from decapping.

mRNA can be also optimized by modifications in the UTRs. Namely, IRES viral sequences can be included in 5' UTR segments as a strategy to improve translation efficacy. These viral IRES can begin the translation process without cap0, and are able to start translation in cells with low levels of translation initiation factors. Thus, the incorporation of IRES viral sequences represents a feasible strategy to improve translation rate on cells in which it is normally low [67]. Other possibility to favour cap-independent translation is the insertion of the modified nucleoside m6A in the 5' UTR as an alternative to IRES [22,67–69]. Regarding 3' UTR modifications, the presence in this structure of the specific sequence of α-globin mRNA improves the stability of synthetic mRNA, whereas the addition of the sequence corresponding to the β-globin mRNA extends the protein expression [70–72]. Moreover, the localization of the protein expressed may be modulated depending on the length of the 3' UTR sequence. For example, the CD47 protein membrane is expressed on the cell surface when the 3' UTR of the mRNA is long, but the same protein appears in the reticulum endoplasmic when the 3' UTR is short [28,73]. In addition, AU rich sequences in 3' UTR can induce repression of translation, decapping and cleavage, which finally lead to mRNA decay. Thus, it is recommended to avoid this structure [74,75].

ORF sequence or codons are frequently optimized to increase the rate and efficiency of the protein translation [35,36,76]. Codon optimization can be conducted by using more frequent codons for each amino acid instead of multiple rare codons. However, this strategy can affect protein functions, and alterations in translation kinetics can lead to alterations in protein conformation [76–79]. Dicodon optimization is other alternative to regulate the ORF because some pairs of codons work together better than others [80]. A third approach is to include in the ORF sequence the same proportion of each codon that is naturally found in the highly expressed proteins of the target species and cells [30]. Finally, it is important to reduce the frequency of UU and UA dinucleotides, as it has been reported that a high proportion of both enhances mRNA decay [81].

A relatively long poly(A) tail is appropriate to optimize stability and translation efficiency of the mRNA [45,46], although the optimal length may be different depending on the cell type. In human epithelial (HeLa) cells, a poly(A) tail composed by 98 residues has shown to increase protein expression [82]. However, in dendritic cells (DCs), the translation efficiency was

improved with 120 adenosine residues [83,84], and in human primary T cells, efficient translation was achieved with a poly-A tail longer than 300 nucleotides [33]. In terms of stability, long poly(A) tails are preferable: 120 adenosine-long molecules provide more stable mRNAs and more efficient translation processes than shorter ones [33]. Apart from the tail length, it is also important to mention that mRNA stability can be increased by the incorporation of adenosine analogues inside the poly(A) tail sequence, which protect mRNA from 3'-exonuclease degradation [3] (e.g. 8-azaadenosine and 3'-deoxyadenosine).

mRNA secondary structures play a major role in the translation process, stability and immunogenicity. Highly stable secondary structures in 5' UTR and hairpin loops hamper ribosome entry and scanning, interfere in the elongation step and are recognized as PAMPs [22,30,67,69]. Recently, Wesselhoeft et al.[85] have documented that circular RNAs (circRNAs) are an alternative to linearized mRNA. CircRNAs are a class of single-stranded non-coding RNA transcripts that are closed by covalent interactions through a splicing process called back-splicing, forming a loop-like structure. Thousands of circRNAs have been found in eukaryotic cells and they are preserved across species. Unlike linear mRNA, circRNAs are very stable against degradation by exonucleases thanks to the circular structure [86,87] In addition, it has been demonstrated that unmodified exogenous circRNA is able to bypass cellular RNA sensors, such as RIG-I and TLRs, and, therefore, immune response is avoided [85]. Not many endogenous circRNAs have shown to induce protein expression, but exogenous circRNAs can be engineered to enable protein translation through the incorporation of IRES or the m6A modification to the 5' UTR region[85,88,89].

3. mRNA delivery systems

Chemical modifications improve the features of mRNA for clinical purposes, but even so, the therapeutic effect of the naked nucleic acid is limited. For an effective delivery of mRNA in the target tissues or organs, it must be protected from extracellular agents, mainly ribonucleases, and prevent the activation of the immune system (except in vaccination). In addition to this, mRNA has to overcome the cellular mechanisms that tackle with external nucleic acid molecules including cytosolic and endosomic receptors; for example, pattern recognition receptors, which are specifically involved in the recognition of non-self RNA and the subsequent activation of pro-inflammatory pathways [10,35,90].

Naked mRNA has been administered as a direct injection principally for the prevention or treatment of infectious diseases; the presence of naked mRNA stimulates the immune response and activates the antigen presentation process [91]. Depending on the clinical application, the

preferred routes of administration include subcutaneous, intradermal, intranodular, intramuscular, intratumoral and intravenous injection [8]. Nevertheless, the efficacy of naked mRNA is limited, because the nucleic acid is exposed to further degradation after injection [8]. Indeed, the half-life of naked mRNA after intravenous administration has been shown to be less than 5 min, with a 10% reduction in serum after 5 min and 1% one hour later.

Transfection efficacy of naked mRNA can be improved by using physical administration methods. They are based on the direct disruption of cell membranes, which allows the internalization of naked mRNA. Nucleic acids present high molecular weight and they are negatively charged and highly soluble in water due to the presence of the phosphate group in their backbone. All these features confer the impossibility to diffuse passively through the cell membranes, contrary to small, neutral and hydrophobic molecules [92]. The most common physical methods are electroporation, sonoporation, gene gun and microinjection [8,93,94]. Electroporation and sonoporation form pores in the cell membranes using electric pulses or ultrasounds, respectively. As a consequence, permeability increase transiently and the entrance of the nucleic acid is allowed [95]. Electroporation has been applied as a therapeutic strategy in malignant, infectious and autoimmune diseases. Specifically, the most common clinical use of mRNA electroporation is related with antigen-presenting DCs carrying tumour-associated antigens (TAAs) alone or in combination with immunomodulatory molecules [96]. Gene gun, also known as particle bombardment method, pushes mRNA molecules coated with gold particles into target cells by using pressurized helium gas. However, the gene gun is not widely used in large animals and humans [8]. Lastly, microinjection consists of the direct injection of the nucleic acid by microneedles. It has been mainly used to study development in the oocyte and early embryo [97,98].

The inclusion of synthetic mRNA in a delivery system is a regular requirement for a successful therapy. In addition to the protection from extracellular agents, once the mRNA reaches the target cell, the delivery system also promotes overcoming of the cell membrane and several intracellular barriers, as it is observed in Figure 2. Firstly, the delivery system interacts with the negative charges of the target cell membrane through electrostatic interactions. Thus, cationic systems are preferred [24]. Moreover, the interaction between the delivery system and cell surface receptors can be favoured by the incorporation of different ligands. Then, the delivery systems start to be surrounded by invaginations that cell membrane produces during the endocytosis process, which is the principal mechanism of cellular entry [92]. Once inside the cell, nucleic acids enter in endosome-lysosome pathway. The nucleic acid moves gradually from early to late endosomes where pH decreases, until reaching the lysosomes, in which the acidic pH and

the presence of digestive enzymes can degrade mRNA [99]. Taking into account the importance of the endosomal escape, numerous strategies are being studied with the aim of boosting the endosomal escape before nucleic acid degradation, including “proton sponge” effect, pore-forming effect, membrane fusion, and photochemical disruption [100–102]. In “proton sponge” effect, ionisable moieties of the delivery systems are protonated during endosomal acidification. Consequently, and in order to equilibrate the charge and the increase of the osmotic pressure, chloride ions are transported into the endosome until endosomal membrane is ruptured [103]. Pore formation in the endosomal membrane consists of the dynamic interplay between a membrane tension that opens the pore and a line tension that closes it. The use of peptides with high affinity for the pore edge, reduces the line tension of the membrane and maintain the pore radius stable [104]. Membrane fusion is based on the destabilization of the endosomal membrane by the presence of fusogenic peptides [105]. Photochemical disruption is produced by small light-sensitive molecules that generate reactive oxidative substances after light exposition that destroy the endosomal membrane [106].

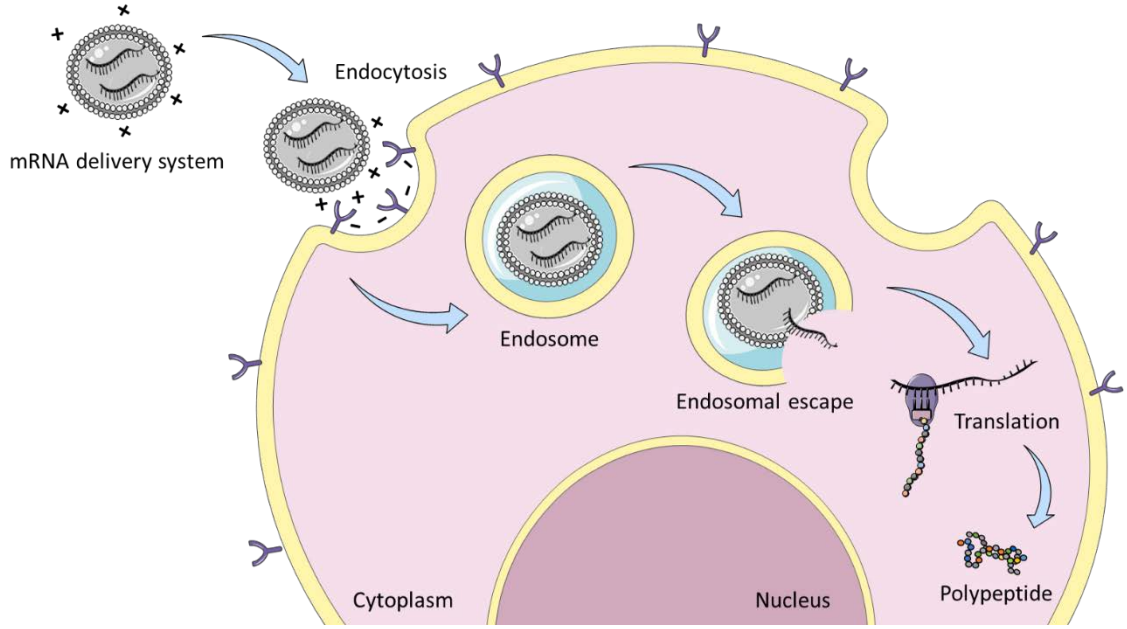

Figure 2. Intracellular barriers for mRNA delivery system: interaction between mRNA delivery system and cell membrane, endocytosis, endosome incorporation, endosomal escape and release to cytoplasm to start translation process.

Hence, for a successful mRNA therapy, the design of suitable mRNA delivery systems specifically adapted to the characteristics of the nucleic acid and the therapeutic objective, is essential. A formulation designed to administer mRNA must address a number of requirements to obtain the maximum therapeutic effect: protection of the genetic material, specificity to produce

targeted delivery, and appropriate intracellular disposition to favour endosomal escape and to allow the translation process; all this without activating the immune response [100,107].

Nucleic acid delivery systems are classically divided in viral and non-viral vectors. Unlike the progress experienced with viral vectors in DNA therapies, these delivery systems do not have a significant impact in the case of mRNA-based therapies. Non-viral vectors offer a safer, cheaper and more versatile alternative to viral vectors. In addition, they can transport nucleic acids of large size and are easier to produce. Although non-viral vectors do not have the natural capacity of viruses to pass through cellular barriers, the advances in nanotechnology and material sciences have led to safe and effective mRNA-medicinal products. Vaccines against severe acute respiratory syndrome coronavirus-2 (SARS-CoV-2) (Moderna mRNA-1273 and Pfizer/BioNTech BNT162b2) are clear examples of this [108–111].

The incorporation of mRNA in nanocarriers is at the forefront in mRNA therapeutics [100]. Chemical methods, and in particular organic nanocarriers, made up by synthetic or natural biocompatible materials, depict the most widely used non-viral gene carriers [112,113]. A large number of synthetic or natural-derived materials have been designed for mRNA therapeutics, such as lipids, lipid-like materials, polymers, inorganic particles, protein derivatives, and dendrimers; among them, lipids and lipid-derived materials are the most commonly used materials for mRNA delivery [114,115].

The first successful transfection of pDNA using the cationic polymer polyl-L-ysine (PLL) was reported in 1987 [116], but the use of cationic polymers for nucleic acid delivery has increased dramatically in the few recent years. The combination of negative charges of mRNA and cationic polymers leads to the formation of polyplexes. Polymers present several advantages as nucleic acid delivery systems: high stability, and ease of preparation, purification and chemical modification. Moreover, they protect mRNA from ribonucleases, favour cellular uptake and endosomal escape. These advantages provide polyplexes high efficacy both in vitro and in vivo [100]. A large number of polymers have been studied for mRNA complexation, including polyethylenimine (PEI) [115,117,118], polyacrylates [119,120], poly(β-amino) esters (PBAEs) [121–123], poly(aspartamides) (PAsp) [124,125] and chitosan [126–128]. However, the clinical use of polymers is less extended than that of lipid-based systems for mRNA delivery [24].

Polypeptides are made up by one or more different aminoacids organised in block or random sequences. The possibility of adapting their cationic and endosomolytic properties makes them interesting to use as nucleic acid delivery systems [119]. Polypeptidic systems include protamine, cell penetrating peptides (CPPs), and virus-like particles (VLPs). The positive charges

of arginine groups of protamine interact with the negative charges of nucleic acids by electrostatic interactions leading to tight association in nanoparticles. Protamine protects the naked mRNA with the additional advantage of acting as an adjuvant to induce immune responses, due to the ability of this peptide to activate the TLR7/8 signal [129–131]. Taking into account these properties, protamine-based systems have been applied when the activation of innate immune responses is needed, including infectious diseases and cancer [100]. For example, RNActive® vaccine is an mRNA-based vaccine technology developed by CureVac, which uses sequence-optimized, unmodified mRNA complexed with the protamine. RNActive® vaccine composed by 50% free mRNA and 50% the complexed mRNA-protamine in a weight ratio of 2:1, has been under clinical evaluation against some cancers, such as melanoma [132], prostate cancer [133] and non-small cell lung cancer [134], with promising results. The use of CPPs is based on their capacity to enter inside the cells in an efficiently and safety way, without interrupting the integrity of cell membranes. Among them, nanosystems formulated with the amphipathic RALA motif, rich in arginine peptides, are the most used CPPs [135]. VLPs are structures similar to viruses, which simulate the organization and conformation of authentic native viruses, but without viral pathogenicity, as they do not contain virus genome. Recently, in a preclinical study in mice with a mRNA vaccine encoding SARS-CoV-2 formulated in VLPs, a potent antiviral-like immune response was detected after intramuscular administration [136].

Dendrimers are nanoscale hyperbranched macromolecules with homogeneous and well-defined tree-like structure formed by a central core, inner branches and functional groups in the surface [95,137]. Polyamidoamine (PAMAM) and polypropylenimine-based dendrimers have been widely used as nucleic acids delivery systems, due to their hydrophilic, biocompatible and non-immunogenic properties [35]. Chahal et al. developed an adjuvant-free vaccine based on a PAMAM dendrimer containing antigens encoded by mRNA [138]. This study showed that, after the intramuscular injection of a single dose into mice, the vaccine generated protective immunity against lethal Ebola, H1N1 influenza, and *Toxoplasma gondii* challenges. Later, the same dendrimer-system was used as vaccine candidate to produce Zika virus E protein-specific IgG responses [139].

Gold nanoparticles (AuNPs) show interesting biomedical application due to their stability, inertness and reduced cytotoxicity. In addition, they are highly biocompatibility, their surface modification is easy and they have the ability to conjugate with biological ligands, including polymers or nucleic acids. Yeom et al. (Yeom et al., 2013) evaluated the effect on mouse xenograft tumour growth of intratumoral production of the proapoptotic factor Bcl-2-associated X protein (BAX). For that purpose, they injected in the xenograft tumour an mRNA encoding BAX,

loaded in AuNP-DNA oligonucleotide conjugates. BAX protein was produced and, consequently, tumour growth was inhibited.

3.1. Lipid-based nanocarriers

As mentioned above, lipid-based systems are the most used for mRNA delivery, both in preclinical and clinical evaluation. Lipids and lipid-like materials are usually formulated as colloidal systems, which in combination with mRNA form the lipoplexes. Colloidal systems involve nanoemulsions and LNPs [140], and these latter include liposomes, solid lipid nanoparticles (SLNs), nanostructured lipid carriers (NLCs) and exosomes. Additionally, hybrid systems have been included in this group, as they consist of lipids combined with other components. Figure 3 shows a representative scheme of the structures of the different lipid-based nanocarriers used for mRNA delivery.

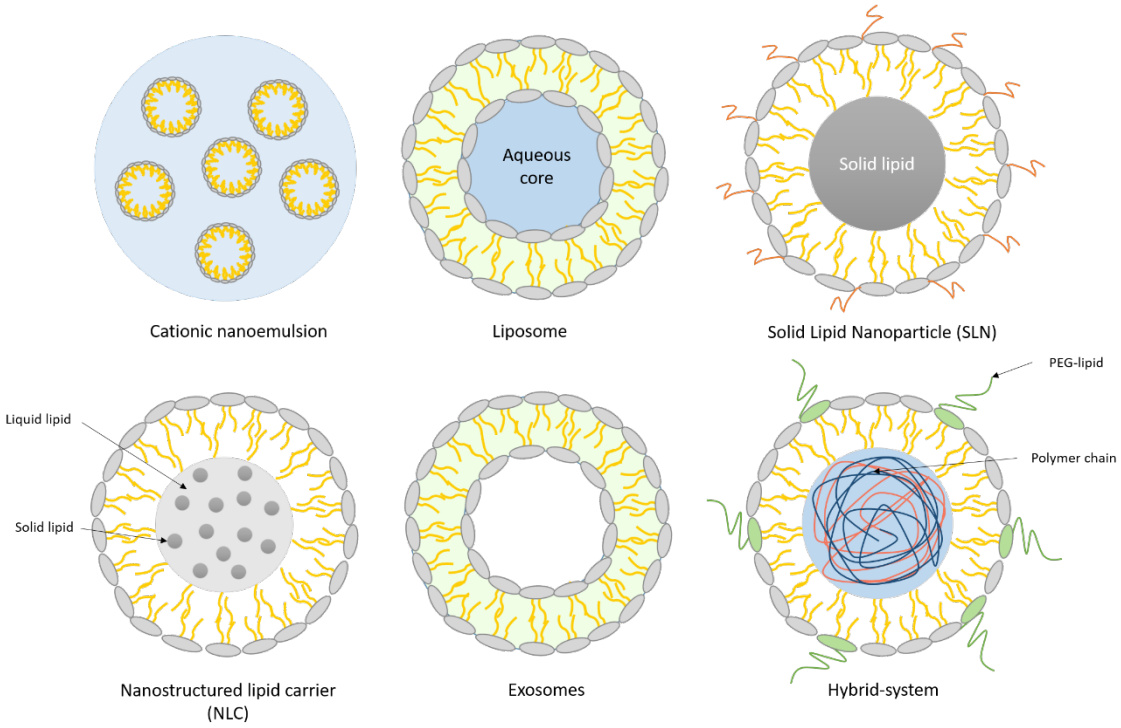

Figure 3. Scheme of the structures of the different lipid-based nanocarriers used for mRNA delivery. PEG: Polyethylene glycol.

The components most frequently used in lipid-based systems are cationic lipids. Positive charges of cationic lipids interact with the negative charges of mRNA by electrostatic interactions leading to lipoplexes [95]. The structure of cationic lipids consists of a positive charged headgroup and a hydrophobic chain joined by a linker (Figure 4). Concretely, the alkylated quaternary ammonium group confers the positive charge to the cationic lipids, which remains constant and pH-independent [35,141]. Cationic lipids have been widely used in lipoplexes for mRNA delivery.

The first cationic lipid used for mRNA delivery was N-[1-(2,3-dioleyloxy)propyl]-N,N,N-trimethylammonium chloride (DOTMA). The system was able to deliver mRNA encoding luciferase in human, rat, mouse, xenopus (frog) and drosophila cells in vitro. Later, DOTMA was commercialized in combination with 1,2- dioleoyl-sn-glycero-3-phosphoethanolamine (DOPE) as Lipofectamine, one of the most commercialised transfection reagents [142]. Additionally, 1,2-dioleoyl-3- trimethylammonium- propane (DOTAP), a biodegradable derivate of DOTMA, has been also used for mRNA delivery studies alone or in combination with DOTMA and other materials.

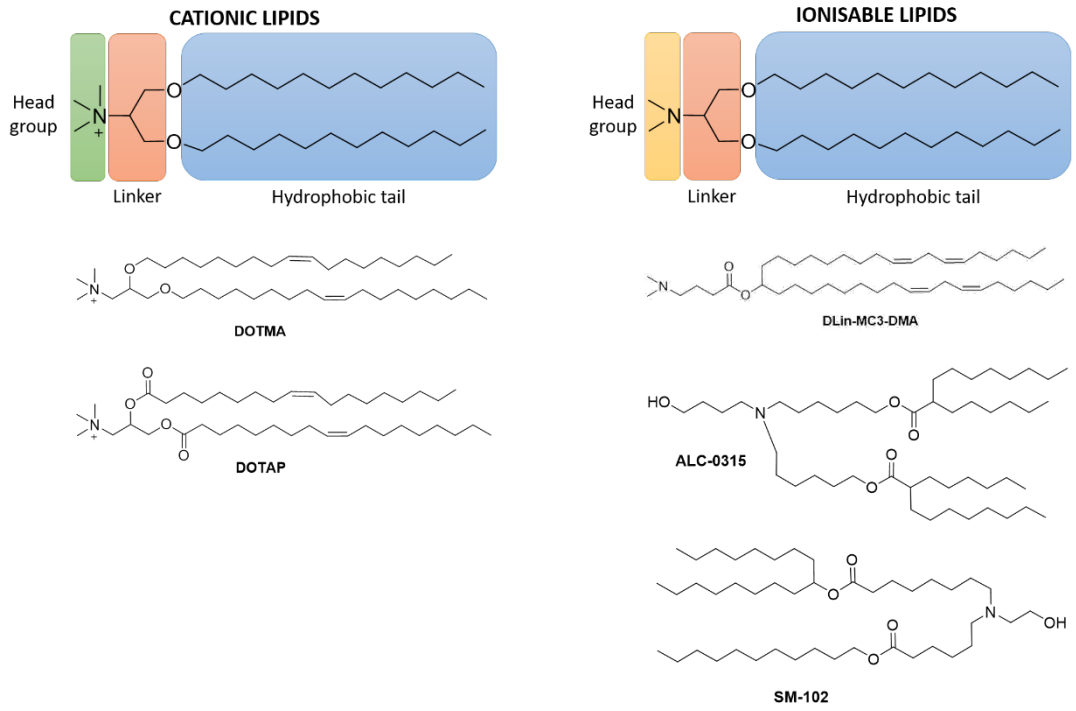

Figure 4: Differences in the chemical structure of cationic and ionisable lipids. DOTMA: N-[1-(2,3-dioleyloxy)propyl]-N,N,N-trimethylammonium chloride; DOTAP: 1,2- dioleoyl-3- trimethylammonium-propane; DLin-MC3-DMA: 6Z,9Z,28Z,31Z)- heptatriaconta-6,9,28,31- tetraen-19- yl 4-(dimethylamino) butanoate; ALC-0315: 2-hexyl-decanoic acid, 1,1'-[[(4-hydroxybutyl)imino]di-6,1-hexanediyl] ester; SM-102: 8-[(2-hydroxyethyl)[6-oxo-6-(undecyloxy)hexyl]amino]-octanoic acid, 1-octylnonyl ester.

Cationic lipids have demonstrated high delivery efficacy, but in several in vitro and in vivo studies they have shown toxicity and immunogenicity. Moreover, they present short circulation half-life, and unspecific association to negatively charged cellular and extracellular components, [90]. In fact, these systems have produced liver damage and increase of the IFN-γ response in mice [143–145]. Moreover, cationic lipids have low efficiency in the endosomal escape process, one of the major key challenges in nucleic acid delivery. Recently, ionisable lipids have been developed as an alternative to traditional cationic lipids.

Ionisable lipids present advantageous features for nucleic acid delivery due to their structure. Ionisable lipids are made up by three different structures: a tertiary amine in the head group, a linker and a hydrophobic tail (Figure 4). The tertiary amine confers the capacity to remain neutral at physiological pH, but becomes positive because of the protonation of the amine at acidic pH environment, when pH values are below its pKa. This pH-dependent feature is crucial and advantageous for the endosomal escape, since the acidic environment of the endosomes induces the protonation of the lipids, provokes the destabilization of membrane and, consequently, the release of the mRNA into the cytoplasm [92]. Moreover, their administration in vivo is advantageous due to their lower capacity to interact with the negative membranes, which improves their biocompatibility [100]. Ionisable lipids, originally developed for DNA delivery, and later for short interfering RNA (siRNA) delivery, have also been studied for mRNA therapeutics [114]. In this sense, the incorporation of the ionisable lipid (6Z,9Z,28Z,31Z)-heptatriaconta-6,9,28,31- tetraen-19-yl 4-(dimethylamino) butanoate (DLin-MC3-DMA; MC3) in Onpattro, the first siRNA drug approved by the FDA, has opened the door for its use in mRNA therapy. Different MC3-based LNPs have been studied in mRNA therapies, including protein replacement [54,146–150] and antiviral therapies [151]. It should be highlighted that Pfizer/BioNTech and Moderna mRNA vaccines developed to fight against COVID-19 pandemic, contain ionisable lipids. More specifically, Pfizer/BioNTech's vaccine is formulated with the ionisable lipid ALC-0315, whereas Moderna's is formulated with the ionisable lipid SM-102 [152]. These vaccines were the first mRNA therapies to receive the Emergency Use Authorization from United States Food and Drug Administration (FDA) [4] and Conditional Approval by the European Medicines Agency (EMA) [5]. Additionally, they are the only mRNA vaccines against SARS-CoV-2 that have been in use in patients during 2021 [152].

Apart from cationic and ionisable lipids, lipid-like materials have been also tested for the delivery of mRNA in vivo. Lipid-like materials are made up by multiple lipidic tails and different hydrophilic groups. Some examples of them are: 1,1′-((2-(4-(2-((2-(bis(2-hydroxydodecyl) amino)ethyl) (2- hydroxydodecyl)amino)ethyl) piperazin-1- yl)ethyl)azanediyl) bis(dodecan-2-ol) (C12-200) [153], tetrakis(8- methylnonyl) 3,3′,3″,3‴-(((methylazanediyl) bis(propane-3,1 diyl))bis (azanetriyl))tetrapropionate (306Oi10) [154], 3,6- bis(4-(bis(2-hydroxydodecyl)amino)butyl)piperazine- 2,5- dione (cKK- E12)[155], and N1,N3,N5- tris(3-(didodecylamino)propyl)benzene-1,3,5- tricarboxamide (TT3). Among them, TT3 has demonstrated capacity to deliver mRNA encoding the human factor IX and to recover the normal levels of the protein in IX-deficient mice [156]. Moreover, a biodegradable analogue of TT3, specifically hexa(octan-3- yl) 9,9′,9″,9‴,9⁗,9⁗′-((((benzene-1,3,5- tricarbonyl)ris(azanediyl)) tris

(propane-3,1- diyl)) tris(azanetriyl)) hexanonanoate (FTT5), further enhanced the efficacy of in vivo delivery of mRNA encoding human factor VIII [157].

Another type of lipids applied for mRNA delivery are zwitteronic ionisable lipids. These lipids change their conformation at acidic pH, transforming into an inverted hexagonal phase (HII), which destabilizes the endosome membrane and triggers the delivery of the nucleic acid into the cytoplasm [114]. They have demonstrated effective protein expression and efficient genome editing in vivo [158].

Among lipid-based colloidal systems, cationic nanoemulsions are formed by an oil phase dispersion stabilized with a surfactant in an aqueous solution with droplets size of 200 nm. DOTAP is the cationic lipid most frequently used to obtain cationic nanoemulsions [130]. These systems have been mainly applied for mRNA vaccination. Concretely, Brito et al. developed a well-tolerated self-amplifying RNA (SAM) vaccine formulated in a cationic nanoemulsion, for the synthesis of antigens of respiratory syncytial virus (RSV), human immunodeficiency virus (HIV), and human cytomegalovirus (CMV). This vaccine demonstrated induced immune responses in multiple animals at lower doses than required for pDNA vaccines [159]. Moreover, a SAM vaccine encoding HIV type 1 envelope based on cationic nanoemulsion produced potent immune responses in rhesus macaques [160]. Currently, the first time-in-human study has entered to the clinic (NCT04062669) to evaluate the safety, reactogenicity and immunogenicity of an experimental rabies glycoprotein G SAM vaccine, formulated in a cationic emulsion, after intramuscular administration.

Liposomes are spherical vesicles containing unilamellar or multilamellar phospholipid bilayers, enclosing an aqueous core in which mRNA can be encapsulated. The interaction between hydrophilic and hydrophobic groups induces the formation of the vesicles [10]. Liposomes have been widely used because they are biodegradable, easy to formulate, present high efficacy and low toxicity [161]. They are usually formed by a cationic lipid together with a helper lipid, cholesterol and a polyethylene glycol-lipid (PEG-lipid). The incorporation of these components can improve the stability of formulation, the efficacy of the nucleic acid delivery, tolerability, biodistribution and transfection efficacy [10,100,162]. For example, DOPE is a phospholipid used to adopt an inverted hexagonal H(II) phase, and destabilize the endosomal membranes [163,164]. DSPC (1,2-distearoyl-sn-glycero-3-phosphocholine), and POPE (1-palmitoyl-2-oleoylsn- glycero-3-phosphoethanolamine) are also helper lipids commonly used in these systems to stabilize the lipid bilayer of the structure [165]. Cholesterol modulates the integrity and rigidity of the membrane, and thus, increases the stability of the particle [10,100,162]. PEG-

lipids prevent particle aggregation and enhance its stability. In order to connect with specific ligands and reach the target tissue, PEG-lipids can be used as linkers. The effects of PEG-lipids depend on their properties (e.g. lipid tail length, lipid tail saturation, and lipid charge), and their proportion in the liposomes. For example, in a recent study, the saturated alkyl chain of PEG2000-1,2-dimyristoyl-sn-glycerol-3-methoxypolyethylene glycol (DMG) and PEG2000-1,2-Distearoyl-sn-glycerol, methoxypolyethylene glycol (DSG) affected the circulation time and efficacy of siRNA, resulting more effective the formulation containing PEG2000-DSG [166]. The administration of liposome-mRNA complexes was reported almost 30 years ago (Lu et al., 1994). The transfection of tumour cells in vitro and in vivo employing cationic mRNA-liposomes demonstrated their potential utility as an alternative to pDNA immunotherapy. Currently, nucleoside-modified mRNA encoding the pre-membrane and envelope glycoproteins of a strain from Zika virus was encapsulated in liposomes formed with the ionisable lipid phosphatidylcoline, cholesterol, and a PEG-lipid. Potent and durable neutralizing antibody responses and protective immunity were observed in mice and non-human primates after intradermal administration of a 50 µg dose [167]. Additionally, the administration of synthetic SAM-liposomes encoding influenza H1HA antigen from N1H1 virus showed antibody responses comparable to the licensed vaccine [168]. In 1999 Zhou et al. administered for the first time mRNA-liposomes for cancer therapy in a mouse-melanoma model, and since then, its application has increased drastically [169]. In this study, hemagglutinating virus of Japan (HVJ)-based liposomes containing mRNA encoding human melanoma-associated antigen glycoprotein 100 (gp100) were administered by direct injection into the mouse spleen. Both antibody expression and cellular immune responses were induced. Liposomes have also been applied for clustered regularly interspaced short palindromic repeats (CRISPR)-associated nuclease Cas9 (CRISPR/Cas9) delivery. Finn et al. [170] formulated LNPs composed by a biodegradable and ionisable lipid termed LP01, Spy Cas9 mRNA, and a single RNA guide (sgRNA). A single systemic administration to mice of the formulation produced significant editing of the mouse transthyretin (*Ttr*) gene in the liver, resulting in >97% reduction of TTR serum protein levels that persisted for at least 12 months. Currently, most clinical trials with liposomes complexed with mRNA are focused on cancer therapy, including ovarian cancer (NCT04163094), pediatric high-grade gliomas and adult glioblastoma (NCT00024648) and neoplasms (NCT04573140).

Recent advances in the development of novel vaccine strategies to address the COVID-19 pandemic have been made, thanks to the design of appropriate LNPs. Toward this end, LNPs for mRNA vaccines developed by Pfizer/BioNTech and Moderna have been clinically rolled out to hundreds of millions of patients around the world. These vaccines contain modified mRNA

encoding the viral Spike (S) glycoprotein of SARS-CoV-2 encapsulated in LNPs. Both Pfizer/BioNTech's vaccine and Moderna's vaccine consist of LNPs formulated by the combination of four chemical components: an ionisable cationic lipid, a neutral phospholipid, cholesterol and a lipid-anchored polymer. Specifically, Pfizer/BioNTech's vaccine is formulated with the ionisable lipid ALC-0315, cholesterol, DSPC, and PEG-lipid ALC-0159, whereas Moderna's is formulated with the ionisable lipid SM-102, cholesterol, DSPC, and PEG2000-DMG [152]. These formulations are very similar to the liposomes ones. However, which makes them different from liposomes is that the LNPs of these vaccines present lipids in the core instead of water [171]. Both vaccines have been well-tolerated and have demonstrated approximately 95% efficacy against COVID-19, with few adverse effects after intramuscular administration [172,173].

SLNs are regarded as one of the most effective lipid-based colloidal systems in gene therapy [174]. SLNs are spherical nanometric particles formed by an aqueous dispersion stabilized by surfactants surrounding a solid lipid core matrix. They are usually made of well-tolerated physiological lipids [175–178]. Initially, SLNs were developed with a view to address the efficacy and safety limitations that liposomes present [179]. In this sense, SLNs show good stability and they can be sterilised and lyophilised. Moreover, the versatility of SLNs confers to them the capacity to be functionalized incorporating specific ligands, taking into account the features of the nucleic acid and the target cell [180–182]. SLNs have demonstrated efficacy as nucleic acid delivery systems in vitro and in vivo, mainly for pDNA delivery in lysosomal storage disorders [183,184], various types of cancer [185–188] and ocular pathologies (Apaolaza et al., 2016; Torrecilla et al., 2018; Vicente-Pascual et al., 2018, 2020). More recently, SLN-based vectors have been assessed as delivery systems of mRNA. Gómez-Aguado et al. [193] showed that formulation-related factors have a more significant impact on mRNA vectors than on pDNA vectors in terms of nucleic acid delivery, transfection efficacy and long-term stability during storage. In another study, SLN-based vectors bearing mRNA encoding intereleukin-10 (IL-10) were evaluated in vitro and in vivo [194]. The study showed the capacity of SLNs to transfect human corneal epithelial (HCE-2) cells in vitro, and the capacity to transfect and produce IL-10 in the corneal epithelium of mice after topical administration as eye drops. Currently, there is no clinical trial comprising SLNs and mRNA under evaluation.

Nanostructured lipid carriers (NLCs) are a type of LNPs formed by a mixture of solid and liquid lipids, leading to a hybrid formulation between oil-in-water emulsions and SLNs [161]. Their use is advantageous comparing with liposomes due to their low toxicity, their easy and low cost production and the possibility to be sterilized [195]. NLCs have been principally used to improve

the oral bioavailability of poorly soluble drugs [196]. However, NLCs are currently being evaluated for the delivery of mRNA vaccines. Concretely, the administration of NLCs containing a replicating viral mRNA encoding Zika virus antigens reported a complete protection of mice against a lethal Zika infection [197]. For the time being, no NLC-based formulation has entered clinic evaluation.

Exosomes are extracellular vesicles naturally secreted by numerous cells with a size range of 50-100 nm. They are emerging as promising natural carriers due to their role in the cell-cell communication process by exchanging proteins, lipids and nucleic acids to the recipient cells [198]. The interest of exosomes has increased as nucleic acid delivery systems due to their natural biocompatibility and minimal immune clearance [198]. Skog et al. demonstrated the capacity of exosomes to deliver mRNA to recipient cells and translate into a therapeutic protein. Exosomes were collected from glioblastoma cells and were transduced with mRNA encoding luciferase from Gaussia (Gluc). Cell-derived microvesicles with Gluc mRNA were used to treat human brain microvascular endothelial cells (HBMVEC) in vitro, resulting in an increase of Gluc activity [199]. However, the use of these systems is hampered by the difficulties of large-scale production, isolation and purification [90]. Yang et al. proposed a cellular-nanoporation strategy, which consists of generating pores in membranes by using electrical nanochannels, to promote mRNA insertion. This method increased the exosome production by 50-fold and exosomal mRNA loading by 10^3-fold comparing with bulk electroporation [200]. Additionally, the development of exosomes that expose specific targeting ligands on their surface is ongoing [201]. More recently, mRNA-loaded exosomes have entered into clinical evaluation for the treatment of homozygous familial hypercholesterolemia (HoFH), providing a new therapeutic approach for patients suffering this disease. This first-in-human study is aimed to evaluate the safety and preliminary effectiveness of exosome-based LDL receptor mRNA nanoplatform in HoFH (NCT05043181).

To conclude, the mixture of lipids with other materials, including polymers and peptides, among others, are defined as hybrid systems. As an advantage, these systems present all the benefits of each individual component in terms of stability, functionality and improved transfection efficacy [90]. Lipid-polymer hybrid nanoparticles, also known as lipopolyplexes, are formed by polymeric material surrounded by a lipid and/or lipid-PEG layer [202]. The efficacy of transfection of this nanosystem is influenced by the nature of the polymer [203]. Moreover, the combination of cationic lipid with peptides has been widely used for mRNA delivery, and significant suppression responses have been reported. For example, the systemic administration of lipid/protamine/synthetic mRNA encoding herpes simplex virus 1-thymidine kinase (HSV1-tk)

to H460 xenograft-bearing nude mice produced higher efficacy and lower toxicity than the equivalent formulation with DNA [204]. In another example, an intratumoural injection of a liposome-protamine complex containing IL-22 Binding Protein (IL-22BP) mRNA produced successful transfection into C26 colon carcinoma in vitro and in vivo with good safety profile [205]. Presently, there is no clinical trial under evaluation with this type of systems.

4. Clinical Applications of mRNA

The attention placed over decades on mRNA design and the development of nucleic acid-based nanomedicines for therapeutic purposes is finally bearing fruit. mRNA therapeutics have dramatically changed the approach to the treatment of many diseases, with special interest in immunotherapy (treatment of infectious diseases and various types of cancer) and in protein replacement. Although most clinical trials using mRNA as active substance are focused on these fields, gene editing is a more recent clinical application of mRNA.

Gene editing is a novel therapeutic strategy that has increased in the recent years due to the different clinical conditions that can be applied for. This technology requires the action of engineered and programmable nucleases that generate a double stranded break (DSB) in the DNA by cleaving the double strand of DNA in a specific place of the genome. Two pathways can accomplish repair of DSBs: homolog-dependent repair (HDR) and non-homologous end joining (NHEJ). In the case of HDR, nucleases need a donor DNA that act as template containing a homologous sequence that will be introduced into DSB. This strategy is suitable when the repair of genomic mutations or the insertion of new therapeutic sequences are required. In contrast, NHEJ removes the specific sequence by joining DSBs in order to inactivate or correct an aberrant gene [206,207].

Zinc finger nucleases (ZFNs), transcription activator-like effector nucleases (TALENs) and CRISPR/Cas9 are the main editing technologies used. For gene editing, these nucleases can be delivered in protein, pDNA or mRNA forms [208]. mRNA delivery provides higher capability for therapeutic application compared to pDNA; since its expression is temporary, the effects of nuclease inside the cells are limited, and the possible risk of genome insertion is low. Moreover, the presence of nuclease is more consistent when it is expressed from mRNA than when the delivery of the nuclease is produced in protein form [209]. Indeed, the administration of nuclease itself presents some limitations in vivo, such as, the activation of cellular and humoral response, challenging size and superficial charge for intravenous administration and protein purification process for large nucleases [208].

As it observed in Table 2, clinical translation of mRNA-based gene editing is focused on ex vivo strategies that primarily use ZFN-mRNA. TALEN-mRNA has been evaluated only in one clinical trial. For in vivo application of CRISPR/Cas9-mRNA technology, intravenous administration of lipid nanosystems has also been evaluated. The corneal delivery of CRISPR/Cas9-mRNA in one clinical trial can be considered outstanding. There are hardly any clinical trials with nucleic acids [194,210] in cornea, and this strategy expands treatment options for a viral disease that severely limits the quality of life of patients suffering from it.

Regenerative medicine by cellular reprogramming and engineering with mRNA has just reached the clinical phase. Regenerative medicine consists of regrowing, repairing or replacing damaged or lost cells, organs or tissues, with the aim of recovering or restoring their natural activity [211]. The transfection of somatic cells bearing mRNA encoding transcription factors is overcoming the conventional reprogramming and transdifferentiation strategies with somatic cells [29]. However, it is mainly limited to in vitro preclinical works, and only one clinical trial is ongoing in phase I/II (NCT02407470). Researchers have demonstrated that adipose tissue-derived mesenchymal stem cells (AD-MSCs) can be transdifferentiated into adipose tissue-derived hematopoietic stem cells (AD-HSCs) by transfection of small RNAs to the early region 1A (E1A)-like inhibitor of differentiation 1 (EID1) in the presence of specific cytokines. The purpose of the clinical trial is to evaluate the effectiveness and safety of a combination of patient's own AD-MSCs transdifferentiated into AD-HSCs and rabbit antithymoglobulin (polyclonal antibody) for the treatment of severe aplastic anaemia. MSCs engineering is another strategy of regenerative medicine, in which mRNA can be used to modulate the migratory properties of these cells, by expressing homing proteins in a brief, burst and temporary way. Once in the target tissue, MSCs have ability of self-renewal and differentiation into a wide range of cell lines, such as cartilage, adipocytes, and bone [29,212]. Clinical application of mRNA-mediated engineered MSCs is already a reality. Indeed, a clinical trial (NCT04524962) has started recruiting patients to study the effect of RNA-engineered allogeneic MSCs (Descartes-30) in acute respiratory distress syndrome and COVID-19. Descartes-30 expresses a unique combination of DNases to eliminate extracellular networks of neutrophils, which are a key element of inflammation and coagulation in acute respiratory distress syndrome.

Table 2. Clinical trials of mRNA for gene editing therapy.

Disease	Biological active	Therapeutic mRNA	Target protein	Delivery system	Administration route	Clinical trial phase	Clinical trial identifier
Acquired immunodeficiency syndrome (AIDS) caused by HIV	SB-728mR	ZFN mRNA	CCR5	Ex vivo transfected autologous CD4+ T cells	Intravenous	Phase I	NCT02388594
	SB-728mR	ZFN mRNA	CCR5	Ex vivo transfected autologous CD4+ CAR-T cells	Intravenous	Phase I	NCT03617198
	SB-728mR-T	ZFN mRNA	CCR5	Ex vivo transfected autologous T cells	Intravenous	Phase I and I/II	NCT04201782, NCT02225665
	SB-728mR-HSPC	ZFN mRNA	CCR5	Ex vivo transfected autologous CD34+ hHSPCs	Intravenous	Phase I	NCT02500849
Sickle Cell Disease	BIVV003	ZFN mRNA	B-cell lymphoma/leukemia 11A (BCL11A)	Ex vivo transfected autologous CD34 + hematopoietic stem cells (HSPC)	Intravenous	Phase I/II	NCT03653247
Transfusion-Dependent Beta-thalassemia	ST-400	ZFN mRNA	B-cell lymphoma/leukemia 11A (BCL11A)	Ex vivo transfected autologous CD34+ hematopoietic stem/progenitor cells	Intravenous	Phase I/II	NCT03432364
B cell acute lymphoblastic leukaemia	UCART19	TALEN mRNA	TCR and CD52	Ex vivo transfected allogenic T cells	Intravenous	Phase I	NCT02808442, NCT02746952, NCT02735083
B cell leukaemia and B cell lymphoma	UCART019	CRISPR/Cas9 mRNA	TCR, B2M	Ex vivo transfected allogenic T cells	Intravenous	Phase I/II	NCT03166878

Table 2. Cont.

Disease	Biological active	Therapeutic mRNA	Target protein	Delivery system	Administration route	Clinical trial phase	Clinical trial identifier
Herpetic Stromal Keratitis	BD111	CRISPR/Cas9 mRNA	Herpes simplex virus type I	NA	Corneal injection	Phase I/II	NCT04560790
Hereditary Transthyretin Amyloidosis	NTLA-2001	CRISPR/Cas9 mRNA	Transthyretin	Lipid nanosystem	Intravenous	Phase I	NCT04601051
Hereditary Angioedema	NTLA-2002	CRISPR/Cas9 mRNA	Kallikrein B1	Lipid nanosystem	Intravenous	Phase I/II	NCT05120830

B2M: β-2 microglobulin; CAR: chimeric antigen receptor; CCR5: CC chemokine receptor type 5; CRISPR/Cas9: clustered regularly interspaced short palindromic repeats/caspase 9; HIV: human immunodeficiency virus; NA: not available; TALEN: transcription activator-like effector nucleases; ZFN: Zinc finger nucleases.

4.1. Immunotherapy

Triggering an immune response has been the main objective of mRNA-based therapies, resulting in a steady increase in clinical trials that evaluate immunotherapy with mRNA for infectious diseases and different types of cancer [32]. Besides those applications, a proof of concept by administering mRNA-transfected T cells against diabetogenic CD8+ T cells in mice offers a new approach for the treatment of type 1 diabetes [213].

Recently, antibodies expression through mRNA for passive immunization has opened a wide range of opportunities for vaccination. The field of monoclonal antibodies (mAbs) is rapidly growing; however, the high cost of manufacturing and purification processes greatly limits their use. Given that situation, the pharmaceutical industry needs a more cost-effective synthesis and an appropriate delivery of mAbs. mRNA technology has come out as a highly attractive platform for any protein expression, being a suitable strategy for antibody production in vivo [214,215]. In 2021 Moderna announced positive phase I results (NCT03829384) for the first systemic mRNA therapeutic (mRNA-1944) encoding an antibody (CHKV-24) with activity against chikungunya virus. Interim analysis of 38 healthy participants who received intravenous mRNA-1944, showed that the vaccine was well tolerated with mild to moderate adverse effects, and that the vaccination produced CHKV-24 IgG with neutralising activity at titres predicted to be therapeutically relevant [216]. Although there have been few studies with mRNA encoding antibodies and further optimization is needed, this promising field is advancing rapidly.

mRNA possesses attractive features that make it an excellent choice for immunotherapy, for instance, innate immunogenicity, transient expression of the antigen of interest and versatility of application (prophylaxis, therapy and personalized vaccines). The safety profile and the simple, fast and cost-effective synthesis of mRNA vaccines make them advantageous over conventional subunit, killed and live attenuated virus vaccines and DNA-based vaccines. [32,217].

In general, mRNA vaccines are classified as non-replicating or SAM. Figure 5 outlines the differences between these two types of mRNA vaccines. Non-replicating mRNA vaccines only encode the immunogen of interest, avoiding the expression of other encoded proteins that could induce undesired immune responses [218]. SAM constructs, also known as replicons, encode not only the target antigen, but also an RNA-dependent RNA polymerase (RDRP) complex. The sequence that encodes de RDRP complex is derived from a positive single stranded RNA virus genome, generally alphaviruses, where the genes that encode the replicative machinery of the virus are not modified, but structural genes are replaced by the sequence that

encodes the immunogen. The ability of the replicons to self-amplify increases the efficacy and duration of the expression of the constructs and the consequent production of the encoded immunogen, and usually a lower dose is needed compared to non-replicating mRNA vaccines [219]. Additionally, SAM constructs allow the incorporation of multiple genes, enabling the expression of both the target antigen and immunomodulatory molecules to enhance potency [220]. The transient self-replication generates double-stranded RNA and, thus, SAM tends to activate innate immune pathways. It is well known that SAMs activate IFN-I response via binding to TLRs 3, 7 and 8, and via melanoma differentiation-associated protein 5 (MDA5), RIG-I, protein kinase R (PKR), and 2'-5'oligoadenylate synthetase (OAS). This contributes to the enhanced immunogenicity of SAM vaccines. However, IFN-I activation can lead to inhibition of translation and degradation of the mRNA compromising the potency of the vaccine [219,221]. In addition, SAM can bear only few modifications of synthetic nucleotides and sequence alterations without losing self-replicating activity [32,35], and the production and stability is challenging since they are larger than non-replicating mRNA vaccines (≈ 9.3 vs 2.2 Kb) [218].

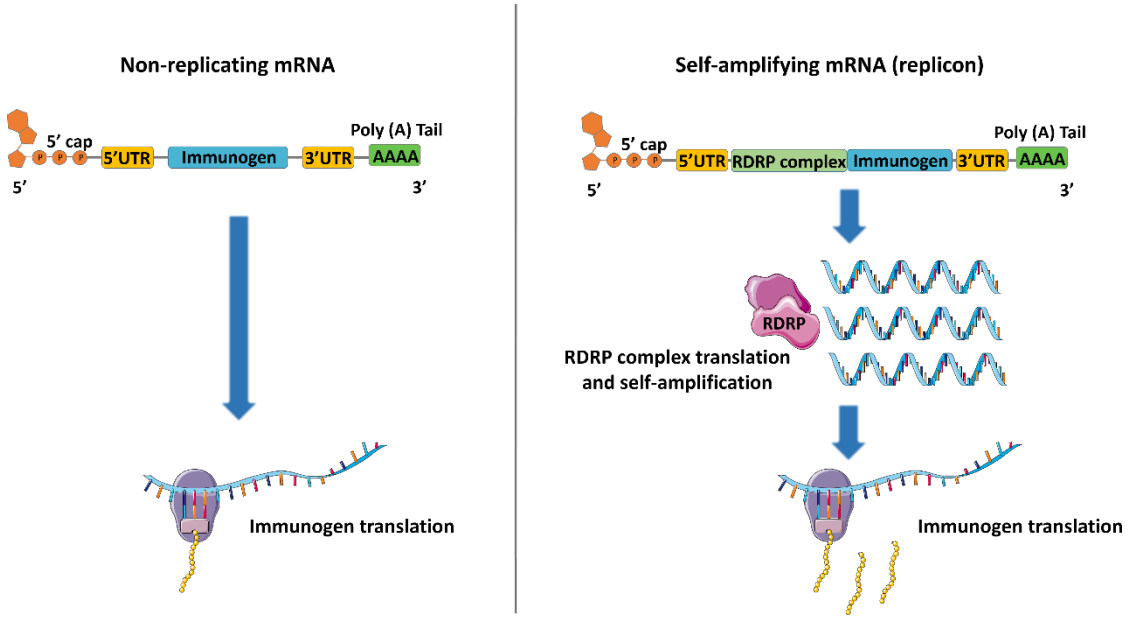

Figure 5. Non-replicating and self-amplifying (replicon) mRNA constructs. Non-replicating mRNA constructs are composed of a coding sequence (immunogen) flanked by 5' and 3' untranslated regions (UTR), a 5' Cap and a 3' polyadenylated tail (Poly (A) Tail). Additionally, self-amplifying mRNA constructs encode a RNA-dependent RNA polymerase (RDRP) complex to amplify the immunogen sequence.

For the development of a vaccine, there are two important steps to take in consideration. Firstly, an antigen from the target pathogen must be identified, and secondly, a delivery system capable of producing a strong humoral and cellular immunity must be developed [222]. Stimulation of a specific or adaptive immune response by mRNA vaccines begins when the antigen is expressed by the ribosome in the cytosol of antigen-presenting cells (APCs), such as DCs. The expressed

antigen is processed by the proteasome complex and presented on the cell surface to cytotoxic CD8+ T cells by major histocompatibility complex (MHC) class I proteins, activating cellular response. Additionally, secreted antigens can be taken up by cells, degraded inside endosomes and displayed to CD4+ helper T cells by MHC class II proteins. CD4+ helper T cells can stimulate B cells (humoral response) to produce neutralising antibodies and can secrete cytokines to activate phagocytic macrophages [223,224].

4.1.1. mRNA vaccines against infectious diseases

Vaccination is the most effective prophylactic measure to provide protection against a wide variety of infectious agents. There are currently about 24 mRNA-based vaccines under clinical evaluation for infectious diseases, excluding those developed for SARS-CoV-2. The majority of targeted infectious agents are viruses (e.g., rabies virus, Zika virus, CMV, human metapneumovirus and parainfluenza virus type 3 (hMPV/PIV3), influenza virus, chikungunya virus, RSV and HIV). mRNA-based vaccines under evaluation are mainly administered by intradermal, intramuscular or subcutaneous injection, being taken up by immune or non-immune cells and translated into antigens, which are presented to T and B cells. Furthermore, structure of the mRNA and the delivery platform greatly condition the immunogenicity and efficacy of the vaccine. Table 3 shows clinical trials of mRNA vaccines against infectious diseases apart from COVID-19.

One of the most attractive candidates for mRNA-based vaccination is influenza virus. This was the target of the first demonstration of immunization against an infectious disease by a non-replicating mRNA vaccine, reported in 2012 by Petsch et al. [225]. RNActive® mRNA encoding haemagglutinin from the PR8 H1N1 influenza virus strain was administered by intradermal injections to mice, ferret and pigs. The vaccine induced immunity against H1N1 and H5N1 strains. In ferrets and pigs, mRNA vaccines induced immunological correlates of protection and protective effects similar to those of a licensed influenza vaccine, and although complete protection from virus replication was not achieved in pigs, the virus was cleared more quickly as compared to the licensed vaccine. In addition, vaccination protected the mice against a lethal viral dose. Since then, different delivery systems, non-replicating and SAM mRNAs and target antigens have been evaluated against influenza virus [226–230]. After the successful results in mice, ferrets and non-human primates of two LNP-formulated mRNA vaccines encoding hemagglutinin proteins of H10N8 or H7N9 [231], Moderna has completed two phase I clinical trials (NCT03076385, NCT03345043) in which the safety and immunogenicity were evaluated. The administration of two intramuscular doses of the vaccines was well tolerated and elicited robust humoral immune responses in healthy adults [232].

CureVac has also applied its platform RNActive® to develop an unmodified mRNA vaccine (CV7201) against the rabies virus glycoprotein. Preclinical studies in mice and pigs showed that two intradermal doses of 80 μg of the vaccine administered with an interval of 21 days, induced high neutralising antibody titres and elicited antigen-specific CD4+ and CD8+T cell responses [233]. In a phase I clinical trial (NCT02241135), the administration route (intradermal or intramuscular) and the administration device (needle-syringe or a needle-free device) were evaluated. The administration route did not affect the immune response, but only with the needle-free system, functional antibodies were produced. Nevertheless, the humoral response resulted to have a short-life and the incidence of adverse effects was high [234]. To overcome those issues, CureVac used Acuitas Therapeutics' LNPs as delivery system of the mRNA for a new rabies vaccine CV7202 [235]. Results of the phase I clinical trial (NCT03713086) showed that two intramuscular doses of 1 μg or 2 μg of the vaccine were well tolerated and produced high neutralising antibody titres [236].

The development of an effective vaccine for the RSV has faced numerous challenges. For instance, in 1968, a formalin-inactivated RSV vaccine candidate caused vaccine-associated enhanced disease (VAED) in children, resulting in severe bronchiolitis or pneumonia cases and two fatalities [237]. Currently, Moderna is evaluating three mRNA-LNP vaccines encoding the prefusion F protein (mRNA-1172, mRNA-1777 and mRNA-1345); the three candidates differ in the type of LNPs (mRNA-1172 uses Merck's proprietary LNPs and mRNA-177 and mRNA-1345 Moderna's LNPs) and mRNA structure. In a phase I clinical trial, mRNA-1777 elicited a robust humoral response with neutralising antibodies, CD4+ T cell response to F protein and no serious adverse effects [238]. mRNA-1345 is being evaluated in a phase I study in RSV-seropositive patients (NCT04528719) and in a phase II/III clinical trial in adults that are at least 60 years old (NCT05127434). In addition, Moderna has also evaluated his candidate mRNA-1653 against hMPV/PIV3 in healthy adults (NCT03392389). An interim analysis demonstrated that the intramuscular administration of the mRNA-1653 vaccine was generally well-tolerated at all dose levels and a single dose of mRNA-1653 boosted serum neutralization titres against both hMPV and PIV3 [239]. Consequently, a phase I clinical trial is recruiting participants to evaluate the same vaccine in healthy adults (18-49 years old) and children (12-59 months old) with serological evidence of prior exposure to hMPV and PIV3 (NCT04144348).

Table 3. Clinical trials of mRNA vaccines against infectious diseases apart from COVID-19.

Infectious disease	Biological active	Encoded protein	Delivery system	Administration route	Clinical trial phase	Clinical trial identifier
Influenza	mRNA-1440 (VAL-506440)	Hemagglutinin from influenza A H10N8 strain	Lipid nanosystem	Intramuscular	Phase I	NCT03076385
	mRNA-1851 (VAL-339851)	Hemagglutinin from influenza A H7N9 strain	Lipid nanosystem	Intramuscular	Phase I	NCT03345043
	AVX502	H3 hemagglutinin from A/Wyoming/03/2003 H3N2 strain	Virus-like replicon particles	Intramuscular Subcutaneous	Phase I/II	NCT00440362, NCT00706732
	mRNA-1010	Influenza A (H1N1, H3N2), Influenza B (Yamagata lineage, Victoria lineage)	NA	Intramuscular	Phase I/II	NCT04956575
Rabies	CV7201	Rabies virus glycoprotein (RABV-G)	Polypeptide system (RNActive®)	Intradermal Intramuscular	Phase I	NCT02241135
	CV7202	Rabies virus glycoprotein (RABV-G)	Lipid nanosystem	Intramuscular	Phase I	NCT03713086
	GSK3903133A	Rabies glycoprotein G (RG)	Cationic nanoemulsion	Intramuscular	Phase I	NCT04062669
Respiratory syncytial virus (RSV)	mRNA-1345	Prefusion F glycoprotein	Lipid nanosystem	Intramuscular	Phase I and II/III	NCT04528719, NCT05127434
hMPV / PIV3	mRNA-1653	Fusion proteins of hMPV and PIV3	Lipid nanosystem	Intramuscular	Phase I	NCT03392389, NCT04144348

Table 3. Cont.

Infectious disease	Biological active	Encoded protein	Delivery system	Administration route	Clinical trial phase	Clinical trial identifier
Zika Virus	mRNA-1325	Structural proteins of Zika virus	Lipid nanosystem	Intramuscular	Phase I	NCT03014089
	mRNA-1893	Structural proteins of Zika virus	Lipid nanosystem	Intramuscular	Phase I and II	NCT04064905, NCT04917861
Chikungunya	mRNA-1944	Chikungunya antibody (CHKV-24 IgG)	Lipid nanosystem	Intravenous	Phase I	NCT03829384
	mRNA-1388 (VAL-181388)	Full native structural polyprotein (C-E3-E2-6k-E1)	Lipid nanosystem	Intramuscular	Phase I	NCT03325075
Human immunodeficiency virus 1 (HIV-1)	*Ex vivo* mRNA electroporated autologous DCs	HIV-1 Gag and Nef	Autologous DCs	Intradermal	Phase I/II	NCT00833781
	iHIVARNA-01	HIVACAT T cell immunogen (HTI) - TriMix	Naked mRNA	Intranodal	Phase I and II	NCT02413645, NCT02888756
	AVX101	HIV-1 C Gag antigen	Virus-like replicon particles	Subcutaneous	Phase I	NCT00097838, NCT00063778
	Core-g28v2 60mer mRNA vaccine (mRNA-1644) and eOD-GT8 60mer mRNA vaccine (mRNA-1644v2-Core)	NA	NA	Intramuscular	Phase I	NCT05001373

Table 3. Cont.

Infectious disease	Biological active	Encoded protein	Delivery system	Administration route	Clinical trial phase	Clinical trial identifier
Cytomegalovirus (CMV)	mRNA-1647	Pentamer complex and full-length membrane-bound glycoprotein B (gB) of CMV	Lipid nanosystem	Intramuscular	Phase I, II and III	NCT03382405, NCT05105048, NCT04232280, NCT04975893, NCT05085366
	mRNA-1443	pp65 T cell antigen of CMV	Lipid nanosystem	Intramuscular	Phase I	NCT03382405
	AVX601	gB, pp65 and IE1 proteins of CMV	Virus-like replicon particles	Intramuscular Subcutaneous	Phase I	NCT00439803
Tuberculosis	GSK 692342	Immunogenic fusion protein (M72) derived from Mycobacterium tuberculosis	Lipid nanosystem	Intramuscular	Phase I and II	NCT00730795, NCT01669096, NCT01424501, NCT00397943, NCT01755598, NCT00621322, NCT01262976, NCT00950612, NCT00600782, NCT01098474, NCT00707967

DCs: dendritic cells; hMPV / PIV3: human metapneumovirus and parainfluenza virus type 3; NA: not available.

Successful preclinical results of immunization against Zika virus with mRNA vaccines prompted two phase I clinical trials (NCT03014089, NCT04064905) to evaluate the safety, tolerability and immunogenicity of two Zika mRNA-LNP vaccine candidates, mRNA-1325 and mRNA-1893. mRNA-1325 was designed to encode structural proteins of the Zika virus inside the cells to make VLPs that are later secreted. mRNA-1893 relies on the same strategy but it contains a sequence distinct from mRNA-1325 with improved immunogenicity and production of Zika VLPs [240]. Interim results of the clinical trial with mRNA-1893 (NCT04064905) showed that the vaccine was well tolerated and induced seroconversion in 94 and 100% of seronegative participants in 10 μg and 30 μg dose groups, respectively [241]. A phase II clinical trial is recruiting adult participants living in endemic and non-endemic flavivirus (virus genus to which the Zika virus belongs) areas to evaluate safety, tolerability and immunogenicity of two dose levels of mRNA-1893 (NCT04917861).

The same strategy has been employed for the development of a vaccine against chikungunya virus, mRNA-1388 (VAL-181388). mRNA-1388 vaccine consists of a single mRNA encapsulated in LNPs encoding the full native structural polyprotein (C-E3-E2-6k-E1) which assemble into VLPs and are released from transfected cells. The structural proteins are naturally processed into C and E proteins. The E proteins on these VLPs are the main target of neutralizing and protective antibodies. Meanwhile the C protein provides structure to the VLP and contains T cell epitopes that induce immune responses [240]. mRNA-1388 has been evaluated in a phase I clinical trial (NCT03325075). Results showed that the vaccine was safe and well tolerated at all dose levels, and produced a 100% seroconversion in all subjects treated with two doses of 100 μg of mRNA-1388 [242].

Two clinical trials evaluated mRNA vaccines for HIV infection. In a phase I trial (NCT02413645), three doses of the naked mRNA (iHIVARNA-01) were injected by intranodal administration in HIV-infected individuals under stable combined antiretroviral therapy. iHIVARNA-01 was composed by an mRNA encoding HIVACAT T-cell Immunogen (HTI) in combination with TriMix. HTI is a novel HIV immunogen sequence that encodes HIV-1 target epitopes in Gag, Pol, Vif and Nef. TriMix is a combination of mRNAs encoding APCs activation signals CD40L (CD40 ligand), CD70 (costimulatory molecule ligand of CD27) and caTLR4 (constitutively active TLR4). iHIVARNA-01 was well tolerated and induced moderate HIV-specific T cells responses [243], promoting a phase II clinical trial (NCT02888756), which was terminated owing to a lack of immunogenicity [244].

Although the majority of mRNA vaccines against infectious diseases use non-replicating mRNA constructs, SAM vaccines are under clinical evaluation for CMVs, influenza virus, rabies virus and HIV. AVX601, a bivalent alphavirus replicon vaccine (alphavaccine) expressing three CMV proteins (gB, pp65 and IE1), was a vaccine candidate against CMV evaluated in healthy volunteers in 2007 (NCT00439803). The vaccine was well tolerated and induced neutralising antibodies and multifunctional T cell responses against the three CMV antigens [245]. The safety and immunogenicity of another alphavaccine (AVX502), expressing the H3 haemagglutinin from the A/Wyoming H3N2 strain was evaluated in healthy volunteers of 18-40 (NCT00440362) or 65 years old or older (NCT00706732), respectively. The vaccine was safe and well tolerated in both trials, and, especially in the younger group, antibody and T cell responses were efficiently stimulated and persisted for the four-month study [246]. In other study, an alphavaccine (AVX101) in which the alphavirus structural proteins were replaced with HIV-1 subtype C gag was administered subcutaneously in healthy HIV-1-uninfected adults, for safety and immunogenicity evaluation (NCT00097838, NCT00063778). Only low levels of binding antibodies and T cell responses were observed with the highest doses [247]. The SAM vaccine candidates mentioned above use VLPs as delivery system. Alternatively, a SAM vaccine against rabies virus, formulated in a cationic nanoemulsion and administered by intramuscular route, is under evaluation in a phase I clinical trial (NCT04062669).

Although being viruses the main infectious pathogens targeted by mRNA vaccines, other pathogens, such as *mycobacterium tuberculosis* or *plasmodium falciparum* are also candidates to be tackled with this kind of vaccination. For example, an mRNA-LNP vaccine encoding the immunogenic fusion protein M72 derived from *mycobacterium tuberculosis* was evaluated in phase I and phase II clinical trials (see clinical trial identifiers in Table 3). In a phase II study (NCT01669096), two intramuscular injections of the vaccine showed an acceptable safety profile and resulted immunogenic in a study involving a small population of healthy adults [248].

mRNA-loaded DCs have been used as ex vivo therapeutic approaches for vaccination. DCs internalize naked mRNA by different endocytic ways, although electroporation improves efficacy. Ex vivo strategy is well described for cancer immunotherapy, and will be further discussed. However, for infectious diseases, it has only been used for HIV immunotherapy in a phase I/II clinical trial (NCT00833781). Intradermal administration to HIV-1-infected subjects with autologous DCs electroporated with mRNA encoding HIV-1 Gag and Nef antigens did not induce significant responses. The authors concluded that DC vaccination should be optimised to elicit stronger and long-lasting immune responses to be effective as an HIV-1 therapeutic vaccine. [249].

- mRNA Vaccines Against SARS-CoV-2

Since December 2019, the global pandemic caused by the SARS-CoV-2 has extremely limited life-quality and has caused significant loss of life worldwide. Against this backdrop, researchers and pharmaceutical industry have made a great effort to develop effective vaccines to combat the SARS-CoV-2, shifting the focus from conventional inactivated virus- and protein-based vaccines to newer technologies such as DNA and mRNA.

Neutralising antibodies against SARS-CoV-2 found in patients who have overcome the disease mainly target epitopes within the S protein, located on the surface of the virus [250]. Therefore, most vaccine candidates against SARS-CoV-2 induce an immune response against the S protein. In fact, the S protein plays a critical role for the cellular infection; the receptor-binding domain (RBD) of S1 subunit of S protein interacts with human angiotensin-converting enzyme 2 (ACE2) on the host cell surface, followed by membrane fusion mediated by the S2 subunit [251].

Seizing the moment and taking advantage of the need for a vaccine to evade SARS-CoV-2 and mitigate its effects in society, mRNA-based vaccines have found the time to take a giant leap forward. Actually, by 18 June 2021, 287 SARS-CoV-2 vaccine candidates were under evaluation, 185 in preclinical development and 102 in clinical trials. Among those in clinical trials, 19 were mRNA-based vaccines. Generally, the mRNA vaccines encode the full-length S or its RBD. Table 4 summarises some of the mRNA-based vaccines against SARS-CoV-2 in clinical stages.

To date, two mRNA vaccines have been approved, BNT162b2 (Comirnaty®) and mRNA-1273 (Spikevax). BNT162b2, developed by Pfizer/BioNTech, received emergency authorisation from the Medicines and Healthcare products Regulatory Agency (MHRA) in the United Kingdom [252], from the FDA in the United States [253], and from the EMA in the European Union [254] on December 2020, becoming the first mRNA drug approved for human use. Pfizer and BioNTech collaborated to develop two promising mRNA vaccine candidates: BNT162b1 and BNT62b2. Both of them use LNPs formulated with the Acuitas Therapeutics' ionisable lipid ALC-0315 and a nucleoside-modified mRNA to enhance mRNA translation. BNT162b1 encodes a secreted trimerized version of the S antigen's RBD.

Table 4. Examples of clinical trials of mRNA vaccines against SARS-CoV-2

Vaccine	Encoded protein	Delivery system	Administration route	Clinical trial phase	Clinical trial identifier
BNT162b2	Full-length transmembrane prefusion spike	Lipid nanosystem	Intramuscular	Phase III	NCT04800133, NCT04713553
				Phase IV	NCT05057182, NCT05057169
mRNA-1273	Full-length transmembrane prefusion spike	Lipid nanosystem	Intramuscular	Phase III	NCT04811664, NCT04470427
				Phase IV	NCT04952402, NCT04978038
mRNA-1273.351	Full-length transmembrane prefusion spike of the SARS-CoV-2 B.1.351 variant	Lipid nanosystem	Intramuscular	Phase I	NCT04785144
mRNA-1273.211	Proteins encoded by mRNA-1273 + mRNA-1271.351	Lipid nanosystem	Intramuscular	Phase II	NCT04405076
mRNA-1283	RBD and N-terminal domain of spike	Lipid nanosystem	Intramuscular	Phase II	NCT05137236
CVnCoV	Full-length transmembrane prefusion spike	Lipid nanosystem	Intramuscular	Phase II/III	NCT04652102
ARCoV	RBD of secreted spike	Lipid nanosystem	Intramuscular	Phase III	NCT04847102
LNP-nCoVsaRNA	Full-length transmembrane prefusion spike	Lipid nanosystem	Intramuscular	Phase I	ISRCTN17072692
ARCT-021	Full-length transmembrane prefusion spike	Lipid nanosystem	Intramuscular	Phase II	NCT04728347, NCT04668339

RBD: receptor-binding domain.

BNT62b2 encodes the full-length S antigen stabilised in its prefusion conformation. Both vaccines induced high antibody and neutralising titres and a robust CD4+ and CD8+ response with mild to moderate adverse effects after two 30 μg intramuscular doses administered 21 days apart. However, only the BNT62b2 vaccine advanced to phase II/III trials owing to its safer profile [110,255]. In phase III clinical trials, BNT62b2 showed 95% effectiveness at preventing COVID-19 disease [108].

One week after the approval of Pfizer/BioNTech's BNT162b2 vaccine, Moderna's mRNA-1273 vaccine was also authorised in the USA. mRNA-1273 consists of LNPs formulated with the ionisable lipid SM-102 encapsulating a nucleoside-modified mRNA that encodes the prefusion stabilised full-length S antigen. mRNA-1273 showed extraordinary efficacy and was well tolerated in clinical trials. Vaccination induced binding and neutralising antibody titres equivalent to convalescent serum samples, and S protein-specific CD4+ T cell responses [256,257]. In phase III clinical trials, two intramuscular doses of 100 μg of the vaccine administered 28 days apart, were 94.1% effective in preventing symptomatic infection and 100% in preventing severe COVID-19 disease [257].

CureVac has also developed an mRNA vaccine against SARS-CoV-2, CVnCoV. This vaccine uses LNPs formulated with the Acuitas Therapeutics' ionisable lipid ALC-0315 to encapsulate an unmodified mRNA encoding the full-length S protein stabilised in a prefusion conformation. Although in a phase I clinical study (NCT04449276) [258] injections of 12 μg of the vaccine generated neutralising antibodies similar to those in patients recovered from COVID-19, CVnCoV resulted in 47% efficacy in phase IIb/III trials (NCT04652102) [259], which was attributed to emerging SARS-CoV-2 variants (e.g., B.1.1.7, B.1.351, P1 and B.1.617.2). CureVac, in collaboration with GSK, is developing a second-generation mRNA vaccine candidate, CV2CoV. mRNA from CV2CoV has been optimized to enhance translation and immunogenicity relative to CVnCoV by using a 5' UTR from the human hydroxysteroid 17-β-dehydrogenase 4 gene and a 3' UTR from the human proteasome 20S subunit β3 gene. Preclinical results have shown that vaccination with CV2CoV induces high titres of neutralising antibodies and significant cross-neutralisation of the B.1.1.7 and B.1.351 variants [260].

Since the emergence of different SARS-CoV-2 variants, the efficacy of current vaccines against new variants has been of great concern. Pfizer/BioNTech and Moderna have sent a message of hope by assuring that their BNT62b2 and mRNA-1273 vaccines provide protection against B.1.1.7 and B.1.351 variants. Moreover, it is also reassuring to know that flexibility of mRNA vaccines enables the reformulation of the vaccines to better protect against other variants [261–

263]. In this regard, Moderna has modified its mRNA-1273 vaccine to develop two other new vaccines: mRNA-1273.351 encoding the S protein of the B.1.351 variant, and mRNA-1273.211, a mix of mRNA-1273 and mRNA-1273.351. The safety and immunogenicity of a single booster dose of these vaccines have been evaluated in a phase II clinical trial (NCT04405076). An interim analysis showed that the vaccines were safe and well tolerated, and that all boosters increased neutralization titres against various variants, including B.1.351, P.1. and B.1.617.2 [264].

In November 2021, a new SARS-CoV-2 variant emerged, B.1.1.529 (Omicron), and it expanded rapidly throughout the world. This variant consists of over 30 mutations within the S protein, and efficacy of current mRNA vaccines targeting the S protein have been questioned. A study has recently demonstrated that patients treated with the current posology (two doses) of BNT62b2 and mRNA-1273 vaccines did not show neutralising activity against the Omicron variant, but a third dose did. This finding suggested that a third dose is required to provide robust neutralising antibody responses against the Omicron lineage [265]. In fact, Pfizer and BioNTech have recently announced the necessity of three doses of the vaccine to neutralize the Omicron variant [266], and evaluation of reactogenicity and immune response of the third dose of BNT62b2 is ongoing in phase IV clinical trials (NCT05057182, NCT05057169). A third dose of mRNA-1273 is also being evaluated in clinical trials (NCT04978038).

SAM vaccines are also under development for SARS-CoV-2. The Imperial College London and Acuitas Therapeutics have developed a SAM vaccine based on LNPs, LNP-nCoVsaRNA. This vaccine encodes the full-length S protein and replication machinery from the genome of Venezuelan equine encephalitis virus [267]. LNP-nCoVsaRNA is being evaluated in a phase I clinical trial (ISRCTN17072692) with a dose ranging from 0.1 to 1 µg, the lowest dose of all mRNA vaccine candidates. Moreover, two phase II clinical trials (NCT04728347, NCT04668339) are evaluating another SAM vaccine encapsulated in LNPs, ARCT-021 (LUNAR-COV-19) [268].

4.1.2. Cancer immunotherapy

Cancer immunotherapy with mRNA harnesses the ability of the nucleic acid to deliver genetic information and its innate immunostimulatory activity to achieve a therapeutic effect. mRNA in cancer immunotherapy can be employed with different purposes, which can be summarized in three strategies, as it is depicted in Figure 6. On the one hand, mRNA can be used for anti-cancer vaccination to deliver cancer antigens to APCs, such as DCs, for the presentation on MHC class I and II, and to exert an adjuvant function by stimulating innate immune system through binding to pattern recognition receptors expressed by APCs (TLRs 3, 7 and 8, RIG-1, MDA5). On the other hand, mRNA is used to engineer T cells and natural killer (NK) cells with antigen receptors such

as chimeric antigen receptors (CARs) and T-cell receptors (TCRs). Finally, mRNA can express mAbs and immunomodulatory proteins (TLRs, chemokine receptors, co-stimulatory ligands, cytokines, chemokines) in different cells [269]. Most of the above strategies can be addressed both in vivo and ex vivo, and there are currently a large number of clinical trials evaluating them (Table 5).

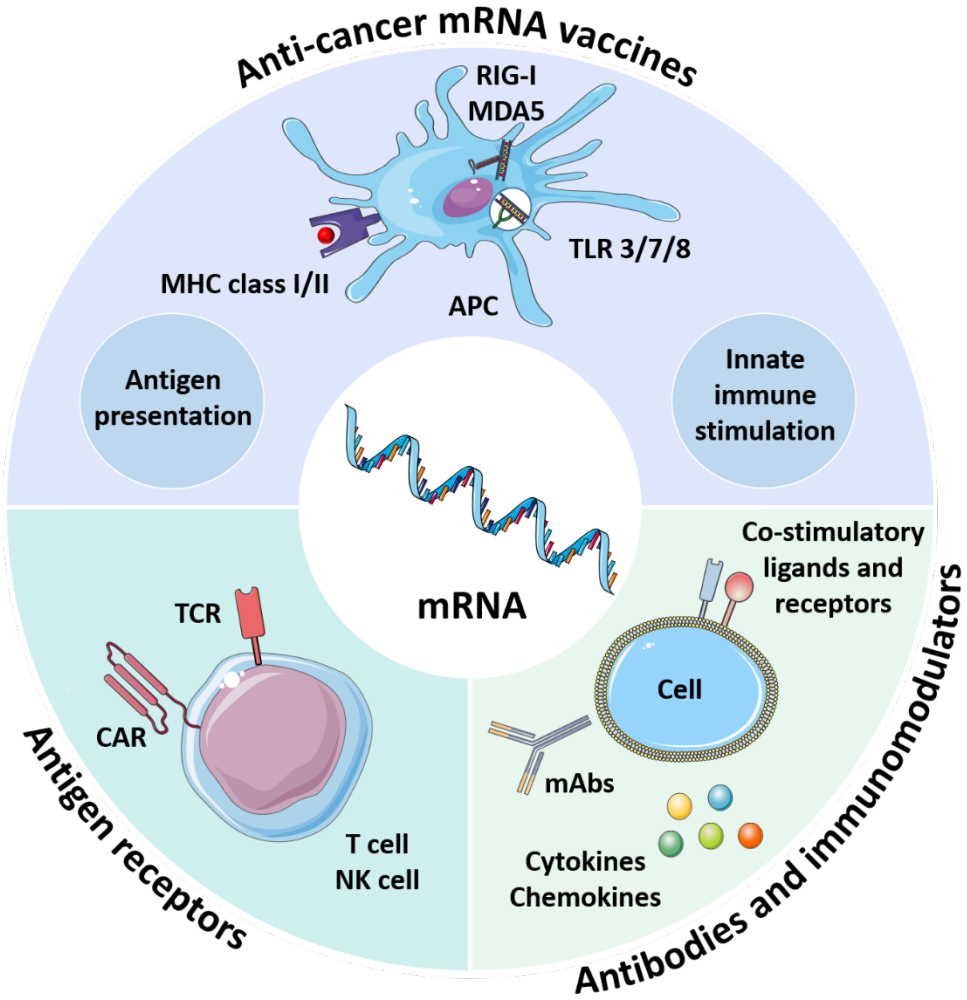

Figure 6. Strategies for cancer immunotherapy with mRNA. mRNA can be employed for anti-cancer vaccination, by means of delivering cancer antigens to antigen-presenting cell (APCs) and stimulating innate immune system (top); to provide immune cells with antigen receptors (bottom left), and to express antibodies and immunomodulators in various cells (bottom right). MHC: major histocompatibility complex; CAR: chimeric antigen receptor; TCR: T-cell receptor; NK: natural killer; mAbs: monoclonal antibodies; TLR: Toll-like receptor; RIG-I: retinoic acid-inducible gene 1; MDA5: melanoma differentiation-associated protein 5.

- Anti-cancer mRNA vaccines

In general, cancer vaccination is based on the induction of tumour-specific T-cell responses capable of fighting tumour cells, by providing cancer antigens in order to achieve an

immunostimulating effect. Additionally, some cancer vaccines also trigger B-cell activation against the tumour [141]. mRNA is an attractive candidate for cancer vaccination as it encodes the full or partial sequence of antigens at the same time that it can induce innate immune-activation. Target antigens can be either TAAs or truly tumour-specific antigens (TSAs). TAAs include proteins that are abnormally expressed in tumours compared with normal tissues, such as differentiation antigens, overexpressed antigens or cancer/testis antigens. TSAs derive from viral oncogenic proteins or from proteins produced as a consequence of somatic mutations or gene rearrangements, known as neoantigens. Neoantigens represent a perfect target for cancer vaccination since they are highly tumour-specific. Therefore, neoantigens have higher probability of inducing high-affinity T-cell responses avoiding the central tolerance that can happen with TAAs owing to their self-antigen nature [270,271]. Neoantigens can be identified by analysing the entire somatic cancer mutations in an individual tumour (called mutatome), allowing the design of personalized neoepitope cancer vaccines [272].

Table 5. Examples of clinical trials of mRNA for cancer immunotherapy.

Vaccine type (Name)	Type of cancer	Administration route	Clinical trial phase	Clinical trial identifier
Anti-cancer mRNA vaccines				
WT1 mRNA DCs	AML, CML, MM	Intradermal	Phase II	NCT00965224, NCT01686334
hTERT/LAMP-1 mRNA DCs (GRNVAC1)	AML	Intradermal	Phase II	NCT00510133
HCMV pp65/LAMP mRNA DCs	Glioblastoma, astrocytoma, GCG, GM	Intradermal	Phase II	NCT02366728, NCT03688178
PSA, PAP, surviving, nTERT mRNA DCs	Prostatic neoplasm	Intradermal	Phase II	NCT01446731
HCMV pp65-shLAMP or pp65-flLAMP mRNA DCs	GM, glioblastoma, MG, astrocytoma, GBM	Under the skin	Phase II	NCT02465268
Tyrosinase, gp100 mRNA DCs	Melanoma	Intradermal, intravenous	Phase II	NCT02285413
Tumour mRNA DCs	Uveal melanoma	Intravenous	Phase III	NCT01983748
Total tumour mRNA and CD40L mRNA DCs (AGS-003/Rocapuldencel-T)	Renal cell carcinoma	Intradermal	Phase II and III	NCT00678119, NCT01582672
MAGE-A3, MAGE-C2, tyrosinase and gp100 mRNA and TriMix (CD70, CD40L, caTLR4) mRNA DCs	Melanoma	Intradermal, intravenous	Phase II	NCT01302496, NCT01676779
TAA mRNA and TriMix (CD70, CD40L, caTLR4) mRNA (ECI-006)	Melanoma	Intranodal	Phase I	NCT03394937
HPV16 antigens mRNA-LPX (BNT113)	HPV16+ and PD-L1+ HNSCC	Intravenous	Phase II	NCT04534205
NY-ESO-1, MAGE-A3, tyrosinase and TPTE mRNA-LPX (BNT111)	Melanoma	Intravenous	Phase II	NCT04526899
Tumour neoantigens mRNA-LPX (RO7198457)	Melanoma	Intravenous	Phase II	NCT03815058
Tumour neoantigens mRNA-LNP (mRNA-4157)	Melanoma	Intramuscular	Phase II	NCT03897881

Table 5. Cont

Vaccine type (Name)	Type of cancer	Administration route	Clinical trial phase	Clinical trial identifier
Antigen receptors				
Anti-BCMA CAR-T cells (Descartes-08)	MM	Intravenous	Phase I/II	NCT03448978
Anti-mesothelin CAR-T cells	Malignant pleural mesothelioma, metastatic PDAC	Intravenous	Phase I	NCT01355965, NCT01897415
cMET redirected CAR-T cells	Metastatic breast cancer, TNBC	Intratumoral	Phase I	NCT01837602
NKG2D-ligand targeting CAR-NK cells	Solid tumours	Intravenous	Phase I	NCT03415100
Immunomodulators				
IL-12 mRNA-LNP (MEDI1191)	Solid tumours	Intratumoral	Phase I	NCT03946800
OX40L, IL-23 and IL-36γ mRNA-LNP (mRNA-2752)	Relapsed/refractory solid tumour malignancies or lymphoma, TNBC, HNSCC, Non-Hodgkin lymphoma, urothelial cancer	Intratumoral	Phase I	NCT03739931
scIL-12, IL-15sushi, IFNα and GM-CSF mRNA (SAR441000)	Metastatic neoplasms	Intratumoral	Phase I	NCT03871348
OX40L mRNA-LNP (mRNA-2416)	Relapsed/refractory solid tumour malignancies or lymphoma, ovarian cancer	Intratumoral	Phase I/II	NCT03323398
CD70, CD40L, caTLR4 mRNA (TriMix)	Breast cancer	Intratumoral	Phase I	NCT03788083

AML: acute myeloid leukemia, BMCA: B cell maturation antigen, CAR: chimeric antigen receptor, CD40L: CD40 ligand, cMET: protein kinase, CML: chronic myeloid leukemia, DCs: dendritic cells, GBM: glioblastoma multiforme of brain, GCG: giant cell glioblastoma, GM: glioblastoma multiforme, GM-CSF: granulocyte-macrophage colony stimulating factor, HCMV: human cytomegalovirus, HNSCC: head and neck squamous cell carcinoma, HPV: human papilloma virus, hTERT: telomerase reverse transcriptase, IFN: interferon, IL: interleukin, LAMP: lysosome-associated membrane glycoprotein, LNP: lipid nanoparticle, LPX: lipoplex, MAGE: melanoma-associated antigen, MG: malignant glioma, MM: multiple myeloma, NK: natural killer, NKG2D: Natural killer group 2D, NY-ESO-1: New York esophageal squamous cell carcinoma-1, OX40L: OX40 ligand, PAP: prostatic acid phosphatase, PDAC: pancreatic ductal adenocarcinoma, PD-L1 programmed cell death ligand 1, PSA: prostate-specific antigen, TAA: tumour-associated antigen, TLR: toll-like receptor, TNBC: triple-negative breast cancer, TPTE: transmembrane phosphatase with tensin homology, WT1: Wilm's tumour protein 1.

Anti-cancer vaccination with mRNA can be performed by loading the mRNA encoding the desired antigen ex vivo on autologous DCs or by administering it in vivo. For the development of mRNA-based DC vaccines, early studies focused on ex vivo loading of mRNA into DCs to later reinfuse the transfected ones into patients by subcutaneous, intranodal or intravenous administration. DCs can be pulsed with bulk mRNA extracted from autologous tumours or with synthetic mRNA encoding defined TAAs [273]. However, expressed antigen is presented on MHC class I rather than on class II molecules of the DCs, resulting in generally weak T-cell responses. Different strategies have been employed to improve MHC class II antigen presentation. For example, the fusion of the vaccine antigen to lysosome-associated membrane proteins (LAMPs) or to MHC class I cytoplasmic and transmembrane domain, that direct the antigen through lysosomal compartments to enhance MHC class II antigen presentation [274–276]. In phase I clinical trials (NCT02529072, NCT00626483, NCT00639639), mRNA-transfected DC vaccines encoding carcinoembryogenic antigen (CEA) fused to LAMP-1 were evaluated in glioblastoma multiforme patients, and prolongation of overall survival was observed [277–279]. CEA/LAMP-1 mRNA DC vaccines are now being evaluated in glioblastoma patients in combination with varilumab, a fully human mAb that targets CD27 (NCT03688178), and routine chemotherapy (NCT02465268) in phase II clinical trials. Other strategies to enhance T-cell responses of mRNA-trasfected DC vaccines is the co-transfection of DCs with mRNA encoding immunostimulatory ligands, receptors or cytokines [280–283]. Rocapuldencel-T, consisting on autologous tumour mRNA-transfected DCs co-transfected with an mRNA encoding CD40L, is one of the most clinically advanced DC vaccines. However, in a phase III clinical trial (NCT01582672), Rocapuldencel-T did not improve the overall survival of patients with metastatic renal cell carcinoma treated with sunitinib [284]. In a phase II clinical study with 39 pretreated melanoma patients (NCT01302496), DCs vaccines transfected with mRNAs encoding four TAAs (melanoma-associated antigen (MAGE)-A3, MAGE-C2, tyrosinase or gp100) fused to an MHC class II targeting signal and TriMix were evaluated in combination with the mAb ipilimumab. The vaccine was well tolerated, in 12 out of 15 patients T-cell responses were detected, and complete and partial responses were observed after 36 months follow-up in eight and in seven patients, respectively [285,286].

Direct injection of the mRNA represents the simplest way of delivering mRNA-based cancer vaccines. Injected mRNA is taken up by local cells, including APCs, and translated in the cytoplasm. Intradermal and intranodal administration of naked mRNA has shown to efficiently induce T-cell responses in humans [287–289]. Intranodal injection facilitates the delivery of the vaccine directly at the site of activated T-cells to be uptaken by residing APCs. The feasibility and

safety of direct injection of mRNA vaccines against cancer were first demonstrated in a phase I/II clinical trial in 15 patients with metastatic melanoma, after the intradermal administration of naked autologous tumour mRNA extracted from each patient's growing metastasis, in combination with granulocyte macrophage colony-stimulating factor (GM-CSF) as adjuvant [290]. Although an increase in antitumor humoral immune response was seen in some patients, clinical effectiveness was not shown. In another phase I/II clinical trial, the feasibility, safety, and immunological and clinical response of an intradermal mRNA-based vaccine using GM-CSF as adjuvant was assessed in 30 patients with stage IV renal cell cancer [289]. The mRNA vaccine administered encoded the TAAs mucin 1 (MUC1), CEA, human epidermal growth factor receptor 2 (Her-2/neu), telomerase, surviving and melanoma-associated antigen 1 (MAGE-A1). The vaccine was well tolerated with no severe side effects and induced clinical responses (stable disease in 15 patients and one partial response). In addition, induction of CD4+ and CD8+ T cell responses was shown for several TAAs in 12 out of 17 patients. The safety and tolerability of intranodal injection of mRNA was firstly evaluated in a phase I study of 29 advanced melanoma patients (NCT01684241). In 6 out of 13 patients, T-cell responses were observed against the encoded antigen (New York esophageal squamous cell carcinoma-1 and tyrosinase), and new lesions only appeared in 8 of the 29 participants [269]. In another phase I clinical study including 20 patients with resected melanoma (NCT03394937), the safety and immunogenicity of ECI-006 vaccine administered intranodally was evaluated. ECI-006 vaccine contained a combination of TriMix and mRNAs encoding for melanoma-specific TAAs (tyrosinase, gp100, MAGE-A3, MAGE-C2, and PRAME). The vaccine was generally well tolerated and demonstrated to be immunogenic in a proportion of patients [287]. Nevertheless, the study was terminated due to the expiry of the study medication.

Formulation of mRNA vaccines with peptides, polymers or cationic/ionisable lipids to protect the genetic material and improve uptake by APCs have gained much attention in recent years. One of the most clinically advanced formulations in cancer mRNA vaccination is based on protamine. Protamine-mRNA vaccine was first evaluated in 21 metastatic melanoma patients after intradermal administration. The vaccine encoded MART-1, tyrosinase, gp100, MAGE-A1, MAGE-A3 and surviving with GM-CSF either alone or in combination with keyhole limpet hemocyanin as adjuvant (NCT00204607) [132]. The study demonstrated the safety and feasibility of protamine-mRNA formulations for cancer vaccination. Since then, several clinical trials are underway or have been carried out with protamine-complexed mRNA vaccines (e.g. NCT01817738, NCT00923312, NCT03164772). The intravenous administration to mice of negative to neutral charged mRNA lipoplexes (mRNA-LPX) have shown to target to APCs resident

in lymphoid organs, and the induction of strong local and systemic immune modulation. In addition, in mouse tumour models, RNA-LPX vaccines induced strong effector and memory T-cell responses against the encoded TSAs or TAAs, and mediated tumour growth control or rejection, and improvement of survival [291–293]. In a phase I clinical trial, 119 patients with melanoma were treated by intravenous administration of an RNA-LPX vaccine, which targets four non-mutated TAAs that are prevalent in melanoma (NCT02410733). The vaccine alone or in combination with checkpoint-inhibitor antagonistic anti-reprogrammed cell death protein-1 (PD-1) antibody, mediated durable objective responses (measurable responses). Vaccination also induced strong CD4+ and CD8+ T cell immunity against the vaccine antigens. The antigen-specific cytotoxic T-cell responses in some responders reached magnitudes typically reported for adoptive T-cell therapy (the transfer of T-cells to a patient) [294]. The same vaccine will be evaluated in a randomized phase II clinical trial in combination with the antagonistic anti-PD-1 antibody cemiplimab (NCT04526899). The same platform encoding other tumour type specific TAAs is being evaluated in various phase I and I/II clinical trials in patients with triple negative breast cancer (TNBC; NCT02316457), ovarian cancer (NCT04163094) and prostate cancer (NCT04382898).

Although SAM vaccines have been extensively studied for infectious diseases, the advance of this type of vaccines for cancer immunotherapy is more limited. Currently, there are two ongoing phase I/II clinical trials using SAM personalized neoantigen vaccines against non-small cell lung cancer, colorectal cancer, gastroesophageal adenocarcinoma, urothelial carcinoma, solid tumours, and pancreatic ductal adenocarcinoma (NCT03639714, NCT03953235), although results have not yet been published.

Personalized cancer vaccines based on mRNAs encoding neoantigens represent an important step forward in cancer immunotherapy. The fast production and easy and cost-effective manufacturing of mRNA allows the “on demand” design of vaccines. This approach was evaluated in a first-in-human trial (NCT02035956) in patients with metastatic melanoma, who were treated with intranodal injection of neoantigen-specific mRNA vaccines encoding 20 patient-unique mutations (IVAC MUTANOME). Patients tolerated well the vaccine and showed CD4+ and CD8+ T-cell responses against neoepitopes. In addition, cumulative rate of recurrences was significantly reduced [288]. Since this first report, several clinical trials are testing mRNA-LNPs encoding TSAs. In a phase I clinical trial, mRNA-LNPs encoding specific neoantigens were administered intramuscularly to four gastrointestinal cancer patients (NCT03480152). It was seen that the vaccine is safe and induced mutation-specific T-cell responses. However, no objective clinical responses were observed in the four patients [295]. mRNA-4157, a lipid-

encapsulated mRNA encoding neoantigens, has been evaluated alone in participants with resected solid tumours and in combination with pembrolizumab in participants with unresectable solid tumours (NCT03313778). Intramuscular vaccination was well tolerated and clinical responses were observed in 6 out of the 20 patients treated with the combination [296]. Consequently, a phase II trial (NCT03897881) is ongoing to further evaluate the efficacy of the personalized vaccine mRNA-4157 and pembrolizumab in patients with high-risk melanoma. An individualized neoantigen-specific immunotherapy (iNeST) program, in which patients are treated with their "on demand" manufactured individualized cancer mutations, is testing in various tumour types (e.g., melanoma, non-small cell lung cancer, colorectal cancer) in phase I and II clinical trials (NCT03289962, NCT03815058, NCT04486378).

- Antigen receptors

Another immunotherapy strategy in cancer is the adoptive cell transfer (the transfer of cells to a patient) of engineered T cells with tumour-specific antigen receptors such as T cell receptors or CARs. This approach is of relevant interest since two DNA-based CAR-T cells products were marketed in 2017-2018, tisagenlecleucel (Kymriah) and axicabtagene ciloleucel (Yescarta), for acute B-cell lymphoblastic leukaemia and large B-cell lymphoma, respectively [297,298]. Generation of CAR-T cells with mRNA is mainly accomplished by electroporation, unlike classical CAR-T cells, which are transfected using viral vectors to deliver the DNA that encodes the CAR. Transient expression of T cells transduced by mRNA offers safety features and highly efficient recombinant protein translation, but repeated administrations are needed [299]. Several phase I clinical trials are evaluating mRNA CAR-T cells against various antigens. Mesothelin-directed mRNA CAR-T cells were evaluated in two phase I clinical trials (NCT01355965, NCT01897415). However, repeated infusions of the mRNA CAR-T cells were needed, and one patient experienced anaphylactic shock after the third infusion. These results pointed out a safety issue owing to the potential immunogenicity of CARs derived from murine antibodies, especially when administering intermittently [300]. CD19-directed mRNA CAR-T cells are the most advanced. Application of CD19 CAR-T cells in pediatric and adult patients with Hodgkin's lymphoma (NCT02624258, NCT02277522) was well tolerated and showed transient responses [301]. Treatment of acute myeloid leukemia (AML) is being attempted by CD123 mRNA CAR-T cells (NCT02623582), but no anti-tumour effect has been demonstrated [302]. The intratumoral administration of protein kinase Met (cMet)-directed mRNA CAR-T cells to breast cancer patients have shown good tolerance and capacity to evoke an inflammatory response within tumours (NCT01837602) [303]. A phase I/II clinical trial is also evaluating mRNA CAR-T cells for the treatment of multiple myeloma (NCT03448978).

Apart from T cells, other type of cells can be modified with mRNA CARs, such as γδ T cells, NKT cells and NK cells [304–308]. In a phase I clinical trial (NCT03415100), intraperitoneal treatment with NKG2D-Ligand targeted CAR-NK cells resulted in clinical activity in patients with colorectal and liver metastatic tumour sites [309].

- Antibodies and immunomodulators

Other approaches for cancer immunotherapy with mRNA comprise the expression of antibodies and immunomodulators (cytokines and co-stimulatory ligands and receptors). mAbs in cancer treatment are employed to target tumour cells and for the modulation of immune responses, and most of the approved recombinant mAbs are administered intravenously. One of the strategies for encoding anti-cancer antibodies with mRNA is the encapsulation of the mRNA in delivery systems targeting the liver to achieve a high protein production and to release the expressed mAbs into the circulation [310]. This approach is being evaluated in preclinical studies for breast cancer and different lymphomas, among others [311,312]. Nevertheless, ex vivo transfection of DCs with mRNA encoding mAbs have taken a step forward compared to in vivo production of mAbs with mRNA. In fact, in a phase I clinical trial, subjects with metastatic melanoma were vaccinated with an intradermal injection of DCs transfected ex vivo with mRNA encoding melanoma TAAs (MART, MAGE-3, gp100 and tyrosinase), and co-administered with DCs transfected ex vivo with mRNA encoding soluble human GITR-L and/or anti-CTLA-4 mAb (NCT01216436). However, the clinical trial was terminated because the principal investigator retired.

Unlike mRNA-encoded mAbs, mRNA-based immunomodulators have successfully entered clinical testing. The immunomodulators expressed with mRNA for cancer immunotherapy include cytokines and stimulatory ligands and receptors. Several cytokines have been proposed for cancer immunotherapy (e.g., IL-2, IL-15, IL-12, IFNα, GM-CSF) with different immunomodulatory properties [313]. Delivery of cytokines with mRNA is being tested in various clinical trials, by administering the mRNA encoding a single cytokine or a combination or mRNAs encoding different cytokines. The cytokines delivered via mRNA that are under clinical evaluation include IL-12 (MEDI1191) in patients with solid tumours (NCT03946800), a mixture of IL-36, IL-23 and OX40L (mRNA-2752) in patients with relapsed solid tumours or lymphoma (NCT03739931) [314], and a combination of IL-12 single chain, IL-15sushi, GM-CSF and IFNα (SAR441000) in metastatic neoplasm patients (NCT03871348). The three vaccines are administered intratumorally, and MEDI1191 and mRNA-2752 are formulated in LNPs.

mRNA can also be used to express stimulatory ligands and receptors on the surface of cells, providing a strong activation of immune signals. This strategy can be achieved by ex vivo modification of T cells, or by in vivo administration of mRNAs encoding for immune-stimulatory ligands or receptors, or a combination of both [315–317]. In a phase I clinical trial, the intratumoral administration of TriMix is being evaluated in early breast cancer patients (NCT03788083) [318]. Moreover, mRNA-LNP encoding OX40L (mRNA-2416) entered a phase I/II clinical trial to evaluate dose escalation and efficacy after intratumoral injection, alone and in combination with durvalumab, in participants with advanced malignancies, such as refractory solid tumours, lymphoma and ovarian cancer (NCT03323398). OX40L alone proved to be safe and showed pro-inflammatory activity in tumour lesions [319].

4.2. Protein Replacement Therapy

The main objective of protein replacement therapy with mRNA is to restore missing, down-expressed or non-functional proteins, responsible for the target disease. Due to the easy accessibility via the bloodstream, protein replacement therapies with mRNA have been targeted to express proteins mainly in the liver [320], lungs [321] and heart [322]. Nevertheless, the skin [323], the back of the eye [147] and neuronal tissue through the nasal cavity [324] have been also proposed as tissues for protein synthesis. The first preclinical study of mRNA administration for protein replacement purposes was carried out in 1992, where the injection of mRNA encoding vasopressin in the hypothalamus of Brattleboro rats resulted in a reversal of diabetes insipidus for up to 5 days [325]. Since then, different genetic diseases have been proposed to be treated with mRNA-based protein replacement therapy: haemophilia B [326], Fabry disease [327], methylmalonic acidemia [328], propionic acidemia [329], acute intermittent porphyria [330], ornithine transcarbamylase (OTC) deficiency [331], cystic fibrosis [332], William-Beuren syndrome [323], glycogen storage disease type III (GSDIII) [333] and familial hypercholesterolemia [334]. Nevertheless, it can also be employed to treat disease conditions without a genetic basis. In those cases, the therapy is based on the administration of an mRNA sequence encoding foreign proteins capable of activating or inhibiting cellular pathways. For instance, the expression of vascular endothelial growth factor-A (VEFG-A) with mRNA can induce the creation of new blood vessels in patients suffering ischemic cardiovascular disease, providing a regenerative effect due to the improved blood supply [335]. Recently, it has been completed a phase II clinical trial evaluating safety of epicardial injection of VEGF-A mRNA (AZD8601) in patients with moderately decreased left ventricular function undergoing elective coronary artery bypass surgery (NCT03370887) [336], but results are not yet available. The same treatment can be applied with healing purposes of diabetic wounds and other ischemic vascular

diseases [337]. In a phase I study (NCT02935712), safety and potential therapeutic effects of intradermal administration of AZD8601 was assessed. The study showed that intradermal AZD8601 was well tolerated and led to local functional VEGF-A protein expression and transient skin blood flow enhancement in men with type 2 diabetes mellitus, demonstrating the therapeutic potential for regenerative angiogenesis.

Table 6 summarizes the clinical trials with mRNA for protein replacement therapies. As it can be observed, mRNA is being evaluated in clinical trials for both, genetic diseases and illnesses without a genetic basis. Most of the biologicals under evaluation are formulated in lipidic carriers, including the first study with exosomes (NCT05043181).

Moderna has also developed mRNA-based therapies formulated in LNPs to be used in protein replacement therapies. The safety and clinical activity of intravenous doses of mRNA-3927 in LNPs is being evaluated in clinical trials for the treatment of propionic acidemia (NCT04159103, NCT05130437). This is an autosomal recessive inherited disease caused by mutations in the gene that encodes the enzyme propionyl-CoA carboxylase, leading to the accumulation of propionyl-CoA and other toxic compounds at mitochondrial level [338]. Additionally, Moderna started a phase I and II clinical trial to evaluate an intravenous LNP formulation containing mRNA-3704 (NCT03810690) that encodes the enzyme deficient in patients with methylmalonic acidemia. This disease is caused by mutations in the gene encoding the vitamin B12-dependent enzyme methylmalonyl CoA mutase [339]. The clinical trial was withdrawn before the start of dosing due to a business decision and not due to safety or efficacy reasons; however, another clinical trial is recruiting participants to evaluate the pharmacologically optimized biological active mRNA-3705 (NCT04899310).

In the las few years, Translate Bio, another clinical-stage mRNA therapeutics company, has started two clinical trials for the treatment of ornithine transcarbamylase (OTC) deficiency and cystic fibrosis. OTC deficiency is characterized by the increase of ammonium levels in the blood caused by disorders in ammonium detoxification and deficiencies of mitochondrial OTC in the urea cycle. Currently, liver transplantation is the only therapeutic option for severe cases of the disease [340]. Translate Bio initiated a clinical trial (NCT03767270) to evaluate the safety, tolerability and pharmacokinetic/pharmacodynamics of a product (MRT5201) consisting of an mRNA encoding OTC in LNPs, after intravenous administration. Nevertheless, the clinical trial was discontinued because preclinical studies did not support the expected pharmacokinetic and safety profile, mainly related to non-optimal featured of the first-generation LNPs targeting the liver [341]. Arcturus Therapeutics, Inc. is evaluating the safety, tolerability and pharmacokinetics

of the intravenous administration of an mRNA-LNP formulation, ARCT-810, in healthy adults (NCT04416126) and in stable adults with OTC deficiency (NCT04442347).

Additionally, Translate Bio has developed a biological active, named MRT5005, for the treatment of cystic fibrosis, a monogenic disorder that affects approximately 70,000 people worldwide. It is caused by genetic variance within the coding region of the cystic fibrosis transmembrane conductance regulator (CFTR), an anion channel necessary for chloride efflux from secretory epithelial cells. Consequently, ion transport dysregulation happens leading to multisystem organ failure and death. Currently, around 300 different mutations have been described, and disease severity varies greatly from person to person which is mainly determined by the degree of the lung affectation [332]. MRT5005 is an inhaled medicinal product based on the delivery of an mRNA encoding CFTR by LNPs. Single- (8, 16 and 24 mg) and multiple-ascending doses (five once-weekly doses of 8, 12 and 16 mg) of MRT5005 are being evaluated in a phase I/II clinical trial (NCT03375047) in patients with cystic fibrosis. Interim data analysis showed that a single dose of the product was well tolerated at low and mid doses. In 4 out of 9 patients treated with MRT5005 the percent predicted forced expiratory volume in 1 second ($ppFEV_1$), a primary measure of lung function, were higher than expected based on known variability of $ppFEV_1$ [342]. A second interim analysis of the clinical trial has announced results of a new dose of the single-ascending dose group (20 mg), and results of the multiple-ascending dose group. In both cases, treatment-emergent adverse events were considered mild to moderate, and no marked increases in $ppFEV_1$ were observed. In the 20 mg single-ascending dose group just a serious adverse event, a pulmonary exacerbation 22 days after the dose, was observed. In the multiple-ascending dose group, three patients experienced transient, mild to moderate febrile reaction after the first dose; one of them discontinued due to the febrile reaction, but in the other two, the adverse effect did not recur with subsequent dosing [343].

GSDIII is caused by a deficiency of a glycogen debranching enzyme, resulting glycogen accumulation in the liver and muscle. Consequently, patients suffer hepatomegaly, hypoglycemia, hyperlipidemia, cirrhosis and myopathy [333]. Unfortunately, no therapies are approved for GSDIII. Protein replacement therapy with mRNA has been proposed to restore the deficient enzyme. An mRNA-LNP formulation (UX053) encoding glycogen debranching enzyme, demonstrated reductions in glycogen content in the liver in multiple models of the disease. Subsequently, a phase I/II clinical trial is evaluating the safety, tolerability and pharmacokinetics of intravenous administrations of UX053 in patients with GSDIII (NCT04990388).

Table 6. Clinical trials of mRNA for protein replacement therapies.

Disease	Biological active	Encoded protein	Delivery system	Administration route	Clinical trial phase	Clinical trial identifier
Heart Failure	AZD8601	Vascular endotelial growth factor-A (VEGF-A)	Naked mRNA	Epicardial injection	Phase II	NCT03370887
Ulcers associated with type II diabetes	AZD8601	Vascular endotelial growth factor-A (VEGF-A)	Naked mRNA	Intradermal	Phase I	NCT02935712
Propionic Acidemia	mRNA-3927	α and β subunits of the mitochondrial enzyme propionyl-CoA carboxylase	Lipid nanosystem	Intravenous	Phase I/II	NCT04159103, NCT05130437
Isolated Methylmalonic Acidemia	mRNA-3704	Methylmalonyl-coenzyme A mutase (MUT)	Lipid nanosystem	Intravenous	Phase I/II	NCT03810690
	mRNA-3705	Methylmalonyl-coenzyme A mutase (MUT)	Lipid nanosystem	Intravenous	Phase I/II	NCT04899310
Ornithine Transcarbamylase Deficiency	MRT5201	Ornithine transcarbamylase	Lipid nanosystem	Intravenous	Phase I/II	NCT03767270
	ARCT-810	Ornithine transcarbamylase	Lipid nanosystem	Intravenous	Phase I	NCT04416126, NCT04442347
Cystic Fibrosis	MRT5005	Human cystic fibrosis transmembrane regulator protein (CFTR)	Lipid nanosystem	Respiratory tract (Nebulization)	Phase I/II	NCT03375047
Glycogen Storage Disease Type III	UX053	Glycogen debranching enzyme	Lipid nanosystem	Intravenous	Phase I/II	NCT04990388
Familial Hypercholesterolemia	Low Density Lipoprotein Receptor mRNA Exosomes	Low-density lipoprotein receptor	Exosome	Intravenous Intraperitoneal	Phase I	NCT05043181

5. Conclusions

mRNA has come a long way to finally demonstrate its great potential with the recent approval of two mRNA-based vaccines. Its multiple applications have enabled the development of therapies for a myriad of pathologies, with the number of clinical trials increasing dramatically in recent years. Nevertheless, mRNA chemical modifications together with the design of suitable vehicles adapted to its features and therapeutic purpose are key points to ensure clinical success. LNPs are the most advanced mRNA delivery systems, with liposomes being the main clinical translatable delivery technology. COVID-19 vaccines, as the first mRNA-based medicinal products marketed worldwide, and cancer immunotherapy are leading the way in the clinical use of mRNA. It represents a new therapeutic approach applicable to a wide variety of pathologies, and although it still has a long way to go, mRNA is here to stay.

References:

1. Anguela, X.M.; High, K.A. Entering the modern era of gene therapy. Annu. Rev. Med. 2019, 70, 273–288, doi:10.1146/annurev-med-012017-043332.
2. Shuai, Q.; Zhu, F.; Zhao, M.; Yan, Y. mRNA delivery via non-viral carriers for biomedical applications. Int. J. Pharm. 2021, 607, 121020, doi:10.1016/j.ijpharm.2021.121020.
3. Xiong, Q.; Lee, G.Y.; Ding, J.; Li, W.; Shi, J. Biomedical applications of mRNA nanomedicine. Nano Res. 2018, 11, 5281–5309, doi:10.1007/s12274-018-2146-1.
4. U.S. Food and Drug Administration COVID-19 Vaccines Available online: https://www.fda.gov/emergency-preparedness-and-response/coronavirus-disease-2019-covid-19/covid-19-vaccines (accessed on Dec 30, 2021).
5. European Medicines Agency COVID-19 vaccines Available online: https://www.ema.europa.eu/en/human-regulatory/overview/public-health-threats/coronavirus-disease-covid-19/treatments-vaccines/covid-19-vaccines (accessed on Dec 30, 2021).
6. Zhong, Z.; Mc Cafferty, S.; Combes, F.; Huysmans, H.; De Temmerman, J.; Gitsels, A.; Vanrompay, D.; Portela Catani, J.; Sanders, N.N. mRNA therapeutics deliver a hopeful message. Nano Today 2018, 23, 16–39, doi:10.1016/j.nantod.2018.10.005.
7. Zarghampoor, F.; Azarpira, N.; Khatami, S.R.; Behzad-Behbahani, A.; Foroughmand, A.M. Improved translation efficiency of therapeutic mRNA. Gene 2019, 707, 231–238, doi:10.1016/j.gene.2019.05.008.
8. Xu, S.; Yang, K.; Li, R.; Zhang, L. Mrna vaccine era—mechanisms, drug platform and clinical prospection; 2020; Vol. 21; ISBN 1886183031.
9. Patel, S.; Athirasala, A.; Menezes, P.P.; Ashwanikumar, N.; Zou, T.; Sahay, G.; Bertassoni, L.E. Messenger RNA Delivery for Tissue Engineering and Regenerative Medicine Applications. Tissue Eng. Part A 2019, 25, 91–112, doi:10.1089/ten.tea.2017.0444.

10. Hajj, K.A.; Whitehead, K.A. Tools for translation: Non-viral materials for therapeutic mRNA delivery. Nat. Rev. Mater. 2017, 2, 1–17, doi:10.1038/natrevmats.2017.56.

11. Meng, Z.; O'Keeffe-Ahern, J.; Lyu, J.; Pierucci, L.; Zhou, D.; Wang, W. A new developing class of gene delivery: Messenger RNA-based therapeutics. Biomater. Sci. 2017, 5, 2381–2392, doi:10.1039/c7bm00712d.

12. Sahin, U.; Karikó, K.; Türeci, Ö. MRNA-based therapeutics-developing a new class of drugs. Nat. Rev. Drug Discov. 2014, 13, 759–780, doi:10.1038/nrd4278.

13. Björklund, T. Non-Viral, Lipid-Mediated DNA and mRNA Gene Therapy of the Central Nervous System (CNS): Chemical-Based Transfection. In; 2016; Vol. 1382, pp. 41–56 ISBN 9781493932719.

14. Thorne, B.; Takeya, R.; Vitelli, F.; Swanson, X. Gene Therapy. In New Bioprocessing Strategies: Development and Manufacturing of Recombinant Antibodies and Proteins; Kiss, B., Gottschalk, U., Pohlscheidt, M., Eds.; Springer International Publishing: Cham, 2018; pp. 351–399 ISBN 978-3-319-97110-0.

15. Alnasser, S.M. Review on mechanistic strategy of gene therapy in the treatment of disease. Gene 2021, 769, 145246, doi:10.1016/j.gene.2020.145246.

16. Ramanathan, A.; Robb, G.B.; Chan, S.H. mRNA capping: Biological functions and applications. Nucleic Acids Res. 2016, 44, 7511–7526, doi:10.1093/nar/gkw551.

17. Jang, S.K.; Paek, K.Y. Cap-dependent translation is mediated by 'RNA looping' rather than 'ribosome scanning.' RNA Biol. 2016, 13, 1–5, doi:10.1080/15476286.2015.1107700.

18. Schlake, T.; Thess, A.; Fotin-Mleczek, M.; Kallen, K.J. Developing mRNA-vaccine technologies. RNA Biol. 2012, 9, 1319–1330, doi:10.4161/rna.22269.

19. Matoulkova, E.; Michalova, E.; Vojtesek, B.; Hrstka, R. The role of the 3' untranslated region in post-transcriptional regulation of protein expression in mammalian cells. RNA Biol. 2012, 9, 563–576, doi:10.4161/rna.20231.

20. Hinnebusch, A.G.; Ivanov, I.P.; Sonenberg, N. Translational control by 5'-untranslated regions of eukaryotic mRNAs. 2016, 352.

21. Kozak, M. Point mutations close to the AUG initiator codon affect the efficiency of translation of rat preproinsulin in vivo. Nature 1984, 308, 241–246, doi:10.1038/308241a0.

22. Kozak, M. Structural features in eukaryotic mRNAs that modulate the initiation of translation. J. Biol. Chem. 1991, 266, 19867–19870, doi:10.1016/s0021-9258(18)54860-2.

23. Kozak, M. At least six nucleotides preceding the AUG initiator codon enhance translation in mammalian cells. J. Mol. Biol. 1987, 196, 947–950, doi:10.1016/0022-2836(87)90418-9.

24. Gómez-Aguado, I.; Rodríguez-Castejón, J.; Vicente-Pascual, M.; Rodríguez-Gascón, A.; Solinís, M.Á.; Del Pozo-Rodríguez, A. Nanomedicines to deliver mRNA: State of the art and future perspectives. Nanomaterials 2020, 10, doi:10.3390/nano10020364.

25. Hellen, C.U.T.; Sarnow, P. Internal ribosome entry sites in eukaryotic mRNA molecules. Genes Dev. 2001, 15, 1593–1612, doi:10.1101/gad.891101.

26. Johnson, A.G.; Grosely, R.; Petrov, A.N.; Puglisi, J.D.; Puglisi, J.D. Dynamics of IRES-mediated translation. 2017.

27. Yang, Y.; Wang, Z. IRES-mediated cap-independent translation, a path leading to hidden proteome. J. Mol. Cell Biol. 2019, 11, 911–919, doi:10.1093/jmcb/mjz091.

28. Mayr, C. Regulation by 3'-Untranslated Regions. Annu. Rev. Genet. 2017, 51, 171–194, doi:10.1146/annurev-genet-120116-024704.

29. Kwon, H.; Kim, M.; Seo, Y.; Moon, Y.S.; Lee, H.J.; Lee, K.; Lee, H. Emergence of synthetic mRNA: In vitro synthesis of mRNA and its applications in regenerative medicine. Biomaterials 2018, 156, 172–193, doi:10.1016/j.biomaterials.2017.11.034.

30. Linares-Fernández, S.; Lacroix, C.; Exposito, J.Y.; Verrier, B. Tailoring mRNA Vaccine to Balance Innate/Adaptive Immune Response. Trends Mol. Med. 2020, 26, 311–323, doi:10.1016/j.molmed.2019.10.002.

31. Wolff, J.A.; Malone, R.W.; Williams, P.; Chong, W.; Acsadi, G.; Jani, A.; Felgner, P.L. Direct gene transfer into mouse muscle in vivo. Science (80-.). 1990, 247, 1465–1468, doi:10.1126/science.1690918.

32. Pardi, N.; Hogan, M.J.; Porter, F.W.; Weissman, D. mRNA vaccines-a new era in vaccinology. Nat. Rev. Drug Discov. 2018, 17, 261–279.

33. Grier, A.E.; Burleigh, S.; Sahni, J.; Clough, C.A.; Cardot, V.; Choe, D.C.; Krutein, M.C.; Rawlings, D.J.; Jensen, M.C.; Scharenberg, A.M.; et al. pEVL: A Linear Plasmid for Generating mRNA IVT Templates With Extended Encoded Poly(A) Sequences. Mol. Ther. - Nucleic Acids 2016, 5, e306, doi:10.1038/mtna.2016.21.

34. Oh, S.; Kessler, J.A. Design, Assembly, Production, and Transfection of Synthetic Modified mRNA. Methods 2018, 133, 29–43, doi:10.1016/j.ymeth.2017.10.008.

35. Kowalski, P.S.; Rudra, A.; Miao, L.; Anderson, D.G. Delivering the Messenger: Advances in Technologies for Therapeutic mRNA Delivery. Mol. Ther. 2019, 27, 710–728, doi:10.1016/j.ymthe.2019.02.012.

36. Weissman, D. mRNA transcript therapy. Expert Rev. Vaccines 2014, 14, 265–281, doi:10.1586/14760584.2015.973859.

37. Steinle, H.; Behring, A.; Schlensak, C.; Wendel, H.P.; Avci-Adali, M. Application of In Vitro Transcribed Messenger RNA for Cellular Engineering and Reprogramming: Progress and Challenges. Stem Cells 2017, 35, 68–79, doi:10.1002/stem.2402.

38. Baiersdörfer, M.; Boros, G.; Muramatsu, H.; Mahiny, A.; Vlatkovic, I.; Sahin, U.; Karikó, K. A Facile Method for the Removal of dsRNA Contaminant from In Vitro-Transcribed mRNA. Mol. Ther. - Nucleic Acids 2019, 15, 26–35, doi:10.1016/j.omtn.2019.02.018.

39. Karikó, K.; Muramatsu, H.; Ludwig, J.; Weissman, D. Generating the optimal mRNA for therapy: HPLC purification eliminates immune activation and improves translation of

nucleoside-modified, protein-encoding mRNA. Nucleic Acids Res. 2011, 39, 1–10, doi:10.1093/nar/gkr695.

40. Mu, X.; Greenwald, E.; Ahmad, S.; Hur, S. An origin of the immunogenicity of in vitro transcribed RNA. Nucleic Acids Res. 2018, 46, 5239–5249, doi:10.1093/nar/gky177.

41. Karikó, K.; Muramatsu, H.; Welsh, F.A.; Ludwig, J.; Kato, H.; Akira, S.; Weissman, D. Incorporation of pseudouridine into mRNA yields superior nonimmunogenic vector with increased translational capacity and biological stability. Mol. Ther. 2008, 16, 1833–1840, doi:10.1038/mt.2008.200.

42. Hornung, V.; Kato, H.; Poeck, H.; Akira, S.; Conzelmann, K.; Schlee, M. 5′-Triphosphate RNA Is the Ligand for RIG-I. Science (80-.). 2010, 994, 1–5.

43. Vaidyanathan, S.; Azizian, K.T.; Haque, A.K.M.A.; Henderson, J.M.; Hendel, A.; Shore, S.; Antony, J.S.; Hogrefe, R.I.; Kormann, M.S.D.; Porteus, M.H.; et al. Uridine Depletion and Chemical Modification Increase Cas9 mRNA Activity and Reduce Immunogenicity without HPLC Purification. Mol. Ther. - Nucleic Acids 2018, 12, 530–542, doi:10.1016/j.omtn.2018.06.010.

44. Diebold, S.S.; Massacrier, C.; Akira, S.; Paturel, C.; Morel, Y.; Reis e Sousa, C. Nucleic acid agonists for Toll-like receptor 7 are defined by the presence of uridine ribonucleotides. Eur. J. Immunol. 2006, 36, 3256–3267, doi:10.1002/eji.200636617.

45. Karikó, K.; Buckstein, M.; Ni, H.; Weissman, D. Suppression of RNA recognition by Toll-like receptors: The impact of nucleoside modification and the evolutionary origin of RNA. Immunity 2005, 23, 165–175, doi:10.1016/j.immuni.2005.06.008.

46. Lorenz, C.; Fotin-Mleczek, M.; Roth, G.; Becker, C.; Dam, T.C.; Verdurmen, W.P.R.; Brock, R.; Probst, J.; Schlake, T. Protein expression from exogenous mRNA: Uptake by receptor-mediated endocytosis and trafficking via the lysosomal pathway. RNA Biol. 2011, 8, doi:10.4161/rna.8.4.15394.

47. Svitkin, Y. V.; Cheng, Y.M.; Chakraborty, T.; Presnyak, V.; John, M.; Sonenberg, N. N1-methyl-pseudouridine in mRNA enhances translation through eIF2α-dependent and independent mechanisms by increasing ribosome density. Nucleic Acids Res. 2017, 45, 6023–6036, doi:10.1093/nar/gkx135.

48. Andries, O.; Mc Cafferty, S.; De Smedt, S.C.; Weiss, R.; Sanders, N.N.; Kitada, T. N1-methylpseudouridine-incorporated mRNA outperforms pseudouridine-incorporated mRNA by providing enhanced protein expression and reduced immunogenicity in mammalian cell lines and mice. J. Control. Release 2015, 217, 337–344, doi:10.1016/j.jconrel.2015.08.051.

49. Martini, P.G.V.; Guey, L.T. A New Era for Rare Genetic Diseases: Messenger RNA Therapy. Hum. Gene Ther. 2019, 30, 1180–1189, doi:10.1089/hum.2019.090.

50. Schlake, T.; Thess, A.; Thran, M.; Jordan, I. mRNA as novel technology for passive immunotherapy. Cell. Mol. Life Sci. 2019, 76, 301–328, doi:10.1007/s00018-018-2935-4.

51. McCracken, S.; Fong, N.; Rosonina, E.; Yankulov, K.; Brothers, G.; Siderovski, D.; Hessel, A.; Foster, S.; Shuman, S.; Bentley, D.L. 5′-Capping enzymes are targeted to pre-mRNA by binding

to the phosphorylated carboxy-terminal domain of RNA polymerase II. Genes Dev. 1997, 11, 3306–3318, doi:10.1101/gad.11.24.3306.

52. Henderson, J.M.; Ujita, A.; Hill, E.; Yousif-Rosales, S.; Smith, C.; Ko, N.; McReynolds, T.; Cabral, C.R.; Escamilla-Powers, J.R.; Houston, M.E. Cap 1 Messenger RNA Synthesis with Co-transcriptional CleanCap® Analog by In Vitro Transcription. Curr. Protoc. 2021, 1, doi:10.1002/cpz1.39.

53. TriLink BioTechnologies CleanCap Technology: Leading the way in mRNATM Available online: https://www.trilinkbiotech.com/cleancap (accessed on Dec 30, 2021).

54. Zhao, W.; Hou, X.; Vick, O.G.; Dong, Y.; Wu, L.; Zhang, J.; Watanabe, W.; Burki, T.; Sonneveld, S.; Verhagen, B.M.P.; et al. A new developing class of gene delivery: Messenger RNA-based therapeutics. Adv. Drug Deliv. Rev. 2021, 9, 1–10, doi:10.1039/c7bm00712d.

55. Islam, M.A.; Reesor, E.K.G.; Xu, Y.; Zope, H.R.; Zetter, B.R.; Shi, J. Biomaterials for mRNA delivery. Biomater. Sci. 2015, 3, 1519–1533, doi:10.1039/c5bm00198f.

56. Muttach, F.; Muthmann, N.; Rentmeister, A. Synthetic mRNA capping. Beilstein J. Org. Chem. 2017, 13, 2819–2832, doi:10.3762/bjoc.13.274.

57. Warminski, M.; Kowalska, J.; Nowak, E.; Kubacka, D.; Tibble, R.; Kasprzyk, R.; Sikorski, P.J.; Gross, J.D.; Nowotny, M.; Jemielity, J. Structural Insights into the Interaction of Clinically Relevant Phosphorothioate mRNA Cap Analogs with Translation Initiation Factor 4E Reveal Stabilization via Electrostatic Thio-Effect. ACS Chem. Biol. 2021, 16, 334–343, doi:10.1021/acschembio.0c00864.

58. Kuhn, A.N.; Diken, M.; Kreiter, S.; Selmi, A.; Kowalska, J.; Jemielity, J.; Darzynkiewicz, E.; Huber, C.; Türeci, Ö.; Sahin, U. Phosphorothioate cap analogs increase stability and translational efficiency of RNA vaccines in immature dendritic cells and induce superior immune responses in vivo. Gene Ther. 2010, 17, 961–971, doi:10.1038/gt.2010.52.

59. Kowalska, J.; Zuberek, J.; Darzynkiewicz, Z.M.; Lukaszewicz, M.; Darzynkiewicz, E.; Jemielity, J. The first examples of mRNA cap analogs bearing boranophosphate modification. Nucleic Acids Symp. Ser. (Oxf). 2008, 289–290, doi:10.1093/nass/nrn146.

60. Chang, C. Te; Bercovich, N.; Loh, B.; Jonas, S.; Izaurralde, E. The activation of the decapping enzyme DCP2 by DCP1 occurs on the EDC4 scaffold and involves a conserved loop in DCP1. Nucleic Acids Res. 2014, 42, 5217–5233, doi:10.1093/nar/gku129.

61. Pelletier, J.; Schmeing, T.M.; Sonenberg, N. The multifaceted eukaryotic cap structure. Wiley Interdiscip. Rev. RNA 2021, 12, 1–24, doi:10.1002/wrna.1636.

62. Warminski, M.; Kowalska, J.; Buck, J.; Zuberek, J.; Lukaszewicz, M.; Nicola, C.; Kuhn, A.N.; Sahin, U.; Darzynkiewicz, E.; Jemielity, J. The synthesis of isopropylidene mRNA cap analogs modified with phosphorothioate moiety and their evaluation as promoters of mRNA translation. Bioorganic Med. Chem. Lett. 2013, 23, 3753–3758, doi:10.1016/j.bmcl.2013.05.001.

63. Ziemniak, M.; Kowalska, J.; Lukaszewicz, M.; Zuberek, J.; Wnek, K.; Darzynkiewicz, E.; Jemielity, J. Phosphate-modified analogues of m7GTP and m7Gppppm7G - Synthesis and

biochemical properties. Bioorganic Med. Chem. 2015, 23, 5369–5381, doi:10.1016/j.bmc.2015.07.052.

64. Strenkowska, M.; Kowalska, J.; Lukaszewicz, M.; Zuberek, J.; Su, W.; Rhoads, R.E.; Darzynkiewicz, E.; Jemielity, J. Towards mRNA with superior translational activity: Synthesis and properties of ARCA tetraphosphates with single phosphorothioate modifications. New J. Chem. 2010, 34, 993–1007, doi:10.1039/b9nj00644c.

65. Zytek, M.; Kowalska, J.; Lukaszewicz, M.; Wojtczak, B.A.; Zuberek, J.; Ferenc-Mrozek, A.; Darzynkiewicz, E.; Niedzwiecka, A.; Jemielity, J. Towards novel efficient and stable nuclear import signals: Synthesis and properties of trimethylguanosine cap analogs modified within the 5′,5′-triphosphate bridge. Org. Biomol. Chem. 2014, 12, 9184–9199, doi:10.1039/c4ob01579g.

66. Rydzik, A.M.; Kulis, M.; Lukaszewicz, M.; Kowalska, J.; Zuberek, J.; Darzynkiewicz, Z.M.; Darzynkiewicz, E.; Jemielity, J. Synthesis and properties of mRNA cap analogs containing imidodiphosphate moiety - Fairly mimicking natural cap structure, yet resistant to enzymatic hydrolysis. Bioorganic Med. Chem. 2012, 20, 1699–1710, doi:10.1016/j.bmc.2012.01.013.

67. Vivinus, S.; Baulande, S.; Zanten, M. Van; Campbell, F.; Topley, P.; Ellis, J.H.; Dessen, P. An element within the 5 H untranslated region of human Hsp70 mRNA which acts as a general enhancer of mRNA translation. 2001, 1917, 1908–1917.

68. Meyer, K.D.; Patil, D.P.; Zhou, J.; Zinoviev, A.; Skabkin, M.A.; Elemento, O.; Pestova, T. V.; Qian, S.B.; Jaffrey, S.R. 5′ UTR m6A Promotes Cap-Independent Translation. Cell 2015, 163, 999–1010, doi:10.1016/j.cell.2015.10.012.

69. Kozak, M. An analysis of vertebrate mRNA sequences: Intimations of translational control. J. Cell Biol. 1991, 115, 887–903, doi:10.1083/jcb.115.4.887.

70. Jiang, Y.; Xu, X.-S.; Russell, J.E. A Nucleolin-Binding 3′ Untranslated Region Element Stabilizes β-Globin mRNA In Vivo. Mol. Cell. Biol. 2006, 26, 2419–2429, doi:10.1128/mcb.26.6.2419-2429.2006.

71. Volloch, V.; Housman, D. Stability of globin mRNA in terminally differentiating murine erythroleukemia cells. Cell 1981, 23, 509–514, doi:10.1016/0092-8674(81)90146-X.

72. Ross, J.; Sullivan, T.D. Half-lives of beta and gamma globin messenger RNAs and of protein synthetic capacity in cultured human reticulocytes. Blood 1985, 66, 1149–1154, doi:10.1182/blood.v66.5.1149.1149.

73. Berkovits, B.D.; Mayr, C. Alternative 3′ UTRs act as scaffolds to regulate membrane protein localization. Nature 2015, 522, 363–367, doi:10.1038/nature14321.

74. Koh, W.S.; Porter, J.R.; Batchelor, E. Tuning of mRNA stability through altering 3′-UTR sequences generates distinct output expression in a synthetic circuit driven by p53 oscillations. Sci. Rep. 2019, 9, 1–8, doi:10.1038/s41598-019-42509-y.

75. Gergen, J.; Petsch, B. mRNA-Based Vaccines and Mode of Action. 2020, doi:10.1007/82_2020_230.

76. Presnyak, V.; Alhusaini, N.; Chen, Y.H.; Martin, S.; Morris, N.; Kline, N.; Olson, S.; Weinberg, D.; Baker, K.E.; Graveley, B.R.; et al. Codon optimality is a major determinant of mRNA stability. Cell 2015, 160, 1111–1124, doi:10.1016/j.cell.2015.02.029.

77. Hunt, R.C.; Simhadri, V.L.; Iandoli, M.; Sauna, Z.E.; Kimchi-Sarfaty, C. Exposing synonymous mutations. Trends Genet. 2014, 30, 308–321, doi:10.1016/j.tig.2014.04.006.

78. McCarthy, C.; Carrea, A.; Diambra, L. Bicodon bias can determine the role of synonymous SNPs in human diseases. BMC Genomics 2017, 18, 1–11, doi:10.1186/s12864-017-3609-6.

79. Bali, V.; Bebok, Z. Decoding mechanisms by which silent codon changes influence protein biogenesis and function. Int. J. Biochem. Cell Biol. 2015, 64, 58–74, doi:10.1016/j.biocel.2015.03.011.

80. Alexaki, A.; Kames, J.; Holcomb, D.D.; Athey, J.; Santana-Quintero, L. V.; Lam, P.V.N.; Hamasaki-Katagiri, N.; Osipova, E.; Simonyan, V.; Bar, H.; et al. Codon and Codon-Pair Usage Tables (CoCoPUTs): Facilitating Genetic Variation Analyses and Recombinant Gene Design. J. Mol. Biol. 2019, 431, 2434–2441, doi:10.1016/j.jmb.2019.04.021.

81. Al-Saif, M.; Khabar, K.S.A. UU/UA dinucleotide frequency reduction in coding regions results in increased mRNA stability and protein expression. Mol. Ther. 2012, 20, 954–959, doi:10.1038/mt.2012.29.

82. Peng, J.; Schoenberg, D.R. mRNA with a <20-nt poly(A) tail imparted by the poly(A)-limiting element is translated as efficiently in vivo as long poly(A) mRNA. Rna 2005, 11, 1131–1140, doi:10.1261/rna.2470905.

83. Holtkamp, S.; Kreiter, S.; Selmi, A.; Simon, P.; Koslowski, M.; Huber, C.; Türeci, Ö.; Sahin, U. Modification of antigen-encoding RNA increases stability, translational efficacy, and T-cell stimulatory capacity of dendritic cells. Blood 2006, 108, 4009–4017, doi:10.1182/blood-2006-04-015024.

84. Mockey, M.; Gonçalves, C.; Dupuy, F.P.; Lemoine, F.M.; Pichon, C.; Midoux, P. mRNA transfection of dendritic cells: Synergistic effect of ARCA mRNA capping with Poly(A) chains in cis and in trans for a high protein expression level. Biochem. Biophys. Res. Commun. 2006, 340, 1062–1068, doi:10.1016/j.bbrc.2005.12.105.

85. Wesselhoeft, R.A.; Kowalski, P.S.; Parker-Hale, F.C.; Huang, Y.; Bisaria, N.; Anderson, D.G. RNA Circularization Diminishes Immunogenicity and Can Extend Translation Duration In Vivo. Mol. Cell 2019, 74, 508-520.e4, doi:10.1016/j.molcel.2019.02.015.

86. Barrett, S.P.; Salzman, J. Circular RNAs: Analysis, expression and potential functions. Dev. 2016, 143, 1838–1847, doi:10.1242/dev.128074.

87. Kristensen, L.S.; Andersen, M.S.; Stagsted, L.V.W.; Ebbesen, K.K.; Hansen, T.B.; Kjems, J. The biogenesis, biology and characterization of circular RNAs. Nat. Rev. Genet. 2019, 20, 675–691, doi:10.1038/s41576-019-0158-7.

88. Wesselhoeft, R.A.; Kowalski, P.S.; Anderson, D.G. Engineering circular RNA for potent and stable translation in eukaryotic cells. Nat. Commun. 2018, 9, 2629, doi:10.1038/s41467-018-05096-6.

89. Yang, Y.; Fan, X.; Mao, M.; Song, X.; Wu, P.; Zhang, Y.; Jin, Y.; Yang, Y.; Chen, L.-L.; Wang, Y.; et al. Extensive translation of circular RNAs driven by N 6-methyladenosine. Cell Res. 2017, 27, 626–641, doi:10.1038/cr.2017.31.

90. Ibba, M.L.; Ciccone, G.; Esposito, C.L.; Catuogno, S.; Giangrande, P.H. Advances in mRNA non-viral delivery approaches. Adv. Drug Deliv. Rev. 2021, 177, 113930, doi:10.1016/J.ADDR.2021.113930.

91. Pardi, N.; Hogan, M.J.; Porter, F.W.; Weissman, D. mRNA vaccines-a new era in vaccinology. Nat. Rev. Drug Discov. 2018, 17, 261–279, doi:10.1038/nrd.2017.243.

92. Schlich, M.; Palomba, R.; Costabile, G.; Mizrahy, S.; Pannuzzo, M.; Peer, D.; Decuzzi, P. Cytosolic delivery of nucleic acids: The case of ionizable lipid nanoparticles. Bioeng. Transl. Med. 2021, 6, 1–16, doi:10.1002/btm2.10213.

93. Mohammad, R. Key considerations in formulation development for gene therapy. Drug Discov. Today 2021, doi:10.1016/j.drudis.2021.08.013.

94. Mirón-Barroso, S.; Domènech, E.B.; Trigueros, S. Nanotechnology-Based Strategies to Overcome Current Barriers in Gene Delivery. Int. J. Mol. Sci. 2021, 22, 8537, doi:10.3390/ijms22168537.

95. Sharma, D.; Arora, S.; Singh, J.; Layek, B. A review of the tortuous path of nonviral gene delivery and recent progress. Int. J. Biol. Macromol. 2021, 183, 2055–2073, doi:10.1016/j.ijbiomac.2021.05.192.

96. Campillo-Davo, D.; De Laere, M.; Roex, G.; Versteven, M.; Flumens, D.; Berneman, Z.N.; Van Tendeloo, V.F.I.; Anguille, S.; Lion, E. The Ins and Outs of Messenger RNA Electroporation for Physical Gene Delivery in Immune Cell-Based Therapy. Pharmaceutics 2021, 13, 396, doi:10.3390/pharmaceutics13030396.

97. Jones, V.A.S.; Bucher, M.; Hambleton, E.A.; Guse, A. Microinjection to deliver protein, mRNA, and DNA into zygotes of the cnidarian endosymbiosis model Aiptasia sp. Sci. Rep. 2018, 8, 16437, doi:10.1038/s41598-018-34773-1.

98. Lane, M.; Mis, E.K.; Khokha, M.K. Microinjection of Xenopus tropicalis Embryos. Cold Spring Harb. Protoc. 2021, doi:10.1101/pdb.prot107644.

99. De Haes, W.; Van Mol, G.; Merlin, C.; De Smedt, S.C.; Vanham, G.; Rejman, J. Internalization of mRNA lipoplexes by dendritic cells. Mol. Pharm. 2012, 9, 2942–2949, doi:10.1021/mp3003336.

100. Meng, C.; Chen, Z.; Li, G.; Welte, T.; Shen, H. Nanoplatforms for mRNA Therapeutics. Adv. Ther. 2021, 4, 1–23, doi:10.1002/adtp.202000099.

101. Selby, L.I.; Cortez-Jugo, C.M.; Such, G.K.; Johnston, A.P.R. Nanoescapology: progress toward understanding the endosomal escape of polymeric nanoparticles. WIREs Nanomedicine and Nanobiotechnology 2017, 9, e1452, doi:https://doi.org/10.1002/wnan.1452.

102. Varkouhi, A.K.; Scholte, M.; Storm, G.; Haisma, H.J. Endosomal escape pathways for delivery of biologicals. J. Control. Release 2011, 151, 220–228, doi:https://doi.org/10.1016/j.jconrel.2010.11.004.

103. Behr, J.-P. The proton sponge: A trick to enter cells the viruses did not exploit. Chimia (Aarau). 1997, 51, 34–36.

104. Huang, H.W.; Chen, F.-Y.; Lee, M.-T. Molecular Mechanism of Peptide-Induced Pores in Membranes. Phys. Rev. Lett. 2004, 92, 198304, doi:10.1103/PhysRevLett.92.198304.

105. Du, Z.; Munye, M.M.; Tagalakis, A.D.; Manunta, M.D.I.; Hart, S.L. The Role of the helper lipid on the DNA transfection efficiency of lipopolyplex formulations. Sci. Rep. 2014, 4, doi:10.1038/srep07107.

106. Berg, K.; Kristian Selbo, P.; Prasmickaite, L.; Tjelle, T.E.; Sandvig, K.; Moan, J.; Gaudernack, G.; Fodstad, Ø.; Kjølsrud, S.; Anholt, H.; et al. Photochemical Internalization. Cancer Res. 1999, 59, 1180 LP – 1183.

107. Patel, P.; Ibrahim, N.M.; Cheng, K. The Importance of Apparent pKa in the Development of Nanoparticles Encapsulating siRNA and mRNA. Trends Pharmacol. Sci. 2021, 42, 448–460, doi:10.1016/j.tips.2021.03.002.

108. Polack, F.P.; Thomas, S.J.; Kitchin, N.; Absalon, J.; Gurtman, A.; Lockhart, S.; Perez, J.L.; Pérez Marc, G.; Moreira, E.D.; Zerbini, C.; et al. Safety and Efficacy of the BNT162b2 mRNA Covid-19 Vaccine. N. Engl. J. Med. 2020, 383, 2603–2615, doi:10.1056/NEJMoa2034577.

109. Baden, L.R.; El Sahly, H.M.; Essink, B.; Kotloff, K.; Frey, S.; Novak, R.; Diemert, D.; Spector, S.A.; Rouphael, N.; Creech, C.B.; et al. Efficacy and Safety of the mRNA-1273 SARS-CoV-2 Vaccine. N. Engl. J. Med. 2020, 384, 403–416, doi:10.1056/NEJMoa2035389.

110. Mulligan, M.J.; Lyke, K.E.; Kitchin, N.; Absalon, J.; Gurtman, A.; Lockhart, S.; Neuzil, K.; Raabe, V.; Bailey, R.; Swanson, K.A.; et al. Phase I/II study of COVID-19 RNA vaccine BNT162b1 in adults. Nature 2020, 586, 589–593, doi:10.1038/s41586-020-2639-4.

111. Jackson, L.A.; Anderson, E.J.; Rouphael, N.G.; Roberts, P.C.; Makhene, M.; Coler, R.N.; McCullough, M.P.; Chappell, J.D.; Denison, M.R.; Stevens, L.J.; et al. An mRNA Vaccine against SARS-CoV-2 — Preliminary Report. N. Engl. J. Med. 2020, 383, 1920–1931, doi:10.1056/NEJMoa2022483.

112. Wadhwa, A.; Aljabbari, A.; Lokras, A.; Foged, C.; Thakur, A. Opportunities and challenges in the delivery of mrna-based vaccines. Pharmaceutics 2020, 12, doi:10.3390/pharmaceutics12020102.

113. del Pozo-Rodríguez, A.; Rodríguez-Gascón, A.; Rodríguez-Castejón, J.; Vicente-Pascual, M.; Gómez-Aguado, I.; Battaglia, L.S.; Solinís, M.Á. Gene Therapy. In Current Applications of Pharmaceutical Biotechnology; Silva, A.C., Moreira, J.N., Lobo, J.M.S., Almeida, H., Eds.; Springer International Publishing: Cham, 2020; pp. 321–368 ISBN 978-3-030-40464-2.

114. Hou, X.; Zaks, T.; Langer, R.; Dong, Y. Lipid nanoparticles for mRNA delivery. Nat. Rev. Mater. 2021, 0123456789, doi:10.1038/s41578-021-00358-0.

115. Weng, Y.; Li, C.; Yang, T.; Hu, B.; Zhang, M.; Guo, S.; Xiao, H.; Liang, X.J.; Huang, Y. The challenge and prospect of mRNA therapeutics landscape. Biotechnol. Adv. 2020, 40, doi:10.1016/j.biotechadv.2020.107534.

116. Wu, G.Y.; Wu, C.H. Receptor-mediated in vitro gene transformation by a soluble DNA carrier system. J. Biol. Chem. 1987, 262, 4429–4432, doi:10.1016/S0021-9258(18)61209-8.

117. Jere, D.; Jiang, H.; Arote, R.; Kim, Y.; Choi, Y.; Cho, M.; Akaike, T.; Cho, C. Degradable polyethylenimines as DNA and small interfering RNA carriers. Expert Opin. Drug Deliv. 2009, 6, 827–834, doi:10.1517/17425240903029183.

118. Chiper, M.; Tounsi, N.; Kole, R.; Kichler, A.; Zuber, G. Self-aggregating 1.8 kDa polyethylenimines with dissolution switch at endosomal acidic pH are delivery carriers for plasmid DNA, mRNA, siRNA and exon-skipping oligonucleotides. J. Control. Release 2017, 246, 60–70, doi:10.1016/j.jconrel.2016.12.005.

119. Ulkoski, D.; Bak, A.; Wilson, J.T.; Krishnamurthy, V.R. Recent advances in polymeric materials for the delivery of RNA therapeutics. Expert Opin. Drug Deliv. 2019, 16, 1149–1167, doi:10.1080/17425247.2019.1663822.

120. Shuai, Q.; Zhu, F.; Zhao, M.; Yan, Y. mRNA delivery via non-viral carriers for biomedical applications. Int. J. Pharm. 2021, 607, 121020, doi:10.1016/j.ijpharm.2021.121020.

121. Wahane, A.; Waghmode, A.; Kapphahn, A.; Dhuri, K.; Gupta, A.; Bahal, R. Role of lipid-based and polymer-based non-viral vectors in nucleic acid delivery for next-generation gene therapy. Molecules 2020, 25, doi:10.3390/molecules25122866.

122. Patel, A.K.; Kaczmarek, J.C.; Bose, S.; Kauffman, K.J.; Mir, F.; Heartlein, M.W.; DeRosa, F.; Langer, R.; Anderson, D.G. Inhaled Nanoformulated mRNA Polyplexes for Protein Production in Lung Epithelium. Adv. Mater. 2019, 31, 1805116, doi:10.1002/adma.201805116.

123. Kaczmarek, J.C.; Patel, A.K.; Kauffman, K.J.; Fenton, O.S.; Webber, M.J.; Heartlein, M.W.; DeRosa, F.; Anderson, D.G. Polymer–Lipid Nanoparticles for Systemic Delivery of mRNA to the Lungs. Angew. Chemie - Int. Ed. 2016, 55, 13808–13812, doi:10.1002/anie.201608450.

124. Uchida, H.; Miyata, K.; Oba, M.; Ishii, T.; Suma, T.; Itaka, K.; Nishiyama, N.; Kataoka, K. Odd–Even Effect of Repeating Aminoethylene Units in the Side Chain of N-Substituted Polyaspartamides on Gene Transfection Profiles. J. Am. Chem. Soc. 2011, 133, 15524–15532, doi:10.1021/ja204466y.

125. Miyata, K.; Oba, M.; Nakanishi, M.; Fukushima, S.; Yamasaki, Y.; Koyama, H.; Nishiyama, N.; Kataoka, K. Polyplexes from Poly(aspartamide) Bearing 1,2-Diaminoethane Side Chains Induce pH-Selective, Endosomal Membrane Destabilization with Amplified Transfection and Negligible Cytotoxicity. J. Am. Chem. Soc. 2008, 130, 16287–16294, doi:10.1021/ja804561g.

126. McCullough, K.C.; Bassi, I.; Milona, P.; Suter, R.; Thomann-Harwood, L.; Englezou, P.; Démoulins, T.; Ruggli, N. Self-replicating Replicon-RNA Delivery to Dendritic Cells by Chitosan-nanoparticles for Translation In Vitro and In Vivo. Mol. Ther. - Nucleic Acids 2014, 3, e173, doi:10.1038/mtna.2014.24.

127. McKinlay, C.J.; Vargas, J.R.; Blake, T.R.; Hardy, J.W.; Kanada, M.; Contag, C.H.; Wender, P.A.; Waymouth, R.M. Charge-altering releasable transporters (CARTs) for the delivery and release of mRNA in living animals. Proc. Natl. Acad. Sci. 2017, 114, E448 LP-E456, doi:10.1073/pnas.1614193114.

128. McKinlay, C.J.; Benner, N.L.; Haabeth, O.A.; Waymouth, R.M.; Wender, P.A. Enhanced mRNA delivery into lymphocytes enabled by lipid-varied libraries of charge-altering releasable transporters. Proc. Natl. Acad. Sci. 2018, 115, E5859 LP-E5866, doi:10.1073/pnas.1805358115.

129. Kallen, K.-J.; Heidenreich, R.; Schnee, M.; Petsch, B.; Schlake, T.; Thess, A.; Baumhof, P.; Scheel, B.; Koch, S.D.; Fotin-Mleczek, M. A novel, disruptive vaccination technology. Hum. Vaccin. Immunother. 2013, 9, 2263–2276, doi:10.4161/hv.25181.

130. Wang, Y.; Zhang, Z.; Luo, J.; Han, X.; Wei, Y.; Wei, X. mRNA vaccine: a potential therapeutic strategy. Mol. Cancer 2021, 20, 1–23, doi:10.1186/s12943-021-01311-z.

131. Scheel, B.; Teufel, R.; Probst, J.; Carralot, J.P.; Geginat, J.; Radsak, M.; Jarrossay, D.; Wagner, H.; Jung, G.; Rammensee, H.G.; et al. Toll-like receptor-dependent activation of several human blood cell types by protamine-condensed mRNA. Eur. J. Immunol. 2005, 35, 1557–1566, doi:10.1002/eji.200425656.

132. Weide, B.; Pascolo, S.; Scheel, B.; Derhovanessian, E.; Pflugfelder, A.; Eigentler, T.K.; Pawelec, G.; Hoerr, I.; Rammensee, H.-G.; Garbe, C. Direct Injection of Protamine-protected mRNA: Results of a Phase 1/2 Vaccination Trial in Metastatic Melanoma Patients. J. Immunother. 2009, 32, 498–507, doi:10.1097/CJI.0b013e3181a00068.

133. Kübler, H.; Scheel, B.; Gnad-Vogt, U.; Miller, K.; Schultze-Seemann, W.; Dorp, F.; Parmiani, G.; Hampel, C.; Wedel, S.; Trojan, L.; et al. Self-adjuvanted mRNA vaccination in advanced prostate cancer patients: A first-in-man phase I/IIa study. J. Immunother. Cancer 2015, 3, 1–14, doi:10.1186/s40425-015-0068-y.

134. Papachristofilou, A.; Hipp, M.M.; Klinkhardt, U.; Früh, M.; Sebastian, M.; Weiss, C.; Pless, M.; Cathomas, R.; Hilbe, W.; Pall, G.; et al. Phase Ib evaluation of a self-adjuvanted protamine formulated mRNA-based active cancer immunotherapy, BI1361849 (CV9202), combined with local radiation treatment in patients with stage IV non-small cell lung cancer. J. Immunother. Cancer 2019, 7, 38, doi:10.1186/s40425-019-0520-5.

135. Udhayakumar, V.K.; De Beuckelaer, A.; McCaffrey, J.; McCrudden, C.M.; Kirschman, J.L.; Vanover, D.; Van Hoecke, L.; Roose, K.; Deswarte, K.; De Geest, B.G.; et al. Arginine-Rich Peptide-Based mRNA Nanocomplexes Efficiently Instigate Cytotoxic T Cell Immunity Dependent on the Amphipathic Organization of the Peptide. Adv. Healthc. Mater. 2017, 6, 1–13, doi:10.1002/adhm.201601412.

136. Lu, J.; Lu, G.; Tan, S.; Xia, J.; Xiong, H.; Yu, X.; Qi, Q.; Yu, X.; Li, L.; Yu, H.; et al. A COVID-19 mRNA vaccine encoding SARS-CoV-2 virus-like particles induces a strong antiviral-like immune response in mice. Cell Res. 2020, 30, 936–939, doi:10.1038/s41422-020-00392-7.

137. Dammes, N.; Peer, D. Paving the Road for RNA Therapeutics. Trends Pharmacol. Sci. 2020, 41, 755–775, doi:10.1016/j.tips.2020.08.004.

138. Chahal, J.S.; Khan, O.F.; Cooper, C.L.; McPartlan, J.S.; Tsosie, J.K.; Tilley, L.D.; Sidik, S.M.; Lourido, S.; Langer, R.; Bavari, S.; et al. Dendrimer-RNA nanoparticles generate protective immunity against lethal Ebola, H1N1 influenza, and Toxoplasma gondii challenges with a single dose. Proc. Natl. Acad. Sci. 2016, 113, E4133 LP-E4142, doi:10.1073/pnas.1600299113.

139. Chahal, J.S.; Fang, T.; Woodham, A.W.; Khan, O.F.; Ling, J.; Anderson, D.G.; Ploegh, H.L. An RNA nanoparticle vaccine against Zika virus elicits antibody and CD8+ T cell responses in a mouse model. Sci. Rep. 2017, 7, 252, doi:10.1038/s41598-017-00193-w.

140. Pozo-Rodríguez, A. del; Alicia Rodríguez-Gascón; Rodríguez-Castejón, J.; Vicente-Pascual, M.; Gómez-Aguado, I.; Battaglia, L.S.; Solinís, M.Á. Gene Therapy. In Advances in biochemical

engineering/biotechnology; 2019; Vol. 171, pp. 321–368 ISBN 0724-6145 (Print)r0724-6145 (Linking).

141. Zhao, Z.; Zheng, L.; Chen, W.; Weng, W.; Song, J.; Ji, J. Delivery strategies of cancer immunotherapy: Recent advances and future perspectives. J. Hematol. Oncol. 2019, 12.

142. Malone, R.W.; Felgner, P.L.; Verma, I.M. Cationic liposome-mediated RNA transfection [cationic lipid vesicies/N-[1-(2,3-dioleyloxy)propyl]-NNN-timethylammonium chloride (DOTMA)/translationj. Proc. Natl. Acad. Sci. USA 1989, 86, 6077–6081.

143. Platanias, L.C. Mechanisms of type-I- and type-II-interferon-mediated signalling. Nat. Rev. Immunol. 2005, 5, 375–386, doi:10.1038/nri1604.

144. Ma, Z.; Li, J.; He, F.; Wilson, A.; Pitt, B.; Li, S. Cationic lipids enhance siRNA-mediated interferon response in mice. Biochem. Biophys. Res. Commun. 2005, 330, 755–759, doi:https://doi.org/10.1016/j.bbrc.2005.03.041.

145. Landesman-Milo, D.; Peer, D. Toxicity profiling of several common RNAi-based nanomedicines: a comparative study. Drug Deliv. Transl. Res. 2014, 4, 96–103, doi:10.1007/s13346-013-0158-7.

146. Nabhan, J.F.; Wood, K.M.; Rao, V.P.; Morin, J.; Bhamidipaty, S.; LaBranche, T.P.; Gooch, R.L.; Bozal, F.; Bulawa, C.E.; Guild, B.C. Intrathecal delivery of frataxin mRNA encapsulated in lipid nanoparticles to dorsal root ganglia as a potential therapeutic for Friedreich's ataxia. Sci. Rep. 2016, 6, 20019, doi:10.1038/srep20019.

147. Patel, S.; Ryals, R.C.; Weller, K.K.; Pennesi, M.E.; Sahay, G. Lipid nanoparticles for delivery of messenger RNA to the back of the eye. J. Control. Release 2019, 303, 91–100, doi:10.1016/j.jconrel.2019.04.015.

148. Jain, R.; Frederick, J.P.; Huang, E.Y.; Burke, K.E.; Mauger, D.M.; Andrianova, E.A.; Farlow, S.J.; Siddiqui, S.; Pimentel, J.; Cheung-Ong, K.; et al. MicroRNAs Enable mRNA Therapeutics to Selectively Program Cancer Cells to Self-Destruct. Nucleic Acid Ther. 2018, 28, 285–296, doi:10.1089/nat.2018.0734.

149. Ryals, R.C.; Patel, S.; Acosta, C.; McKinney, M.; Pennesi, M.E.; Sahay, G. The effects of PEGylation on LNP based mRNA delivery to the eye. PLoS One 2020, 15, 1–17, doi:10.1371/journal.pone.0241006.

150. Zhang, H.; Leal, J.; Soto, M.R.; Smyth, H.D.C.; Ghosh, D. Aerosolizable Lipid Nanoparticles for Pulmonary Delivery of mRNA through Design of Experiments. Pharmaceutics 2020, 12, doi:10.3390/pharmaceutics12111042.

151. Zhang, M.; Sun, J.; Li, M.; Jin, X. Modified mRNA-LNP Vaccines Confer Protection against Experimental DENV-2 Infection in Mice. Mol. Ther. - Methods Clin. Dev. 2020, 18, 702–712, doi:10.1016/j.omtm.2020.07.013.

152. Andresen, J.L.; Fenton, O.S. Nucleic acid delivery and nanoparticle design for COVID vaccines. MRS Bull. 2021, 46, 1–8, doi:10.1557/s43577-021-00169-2.

153. Love, K.T.; Mahon, K.P.; Levins, C.G.; Whitehead, K.A.; Querbes, W.; Dorkin, J.R.; Qin, J.; Cantley, W.; Qin, L.L.; Racie, T.; et al. Lipid-like materials for low-dose, in vivo gene silencing. Proc. Natl. Acad. Sci. 2010, 107, 1864–1869, doi:10.1073/pnas.0910603106.

154. Whitehead, K.A.; Dorkin, J.R.; Vegas, A.J.; Chang, P.H.; Veiseh, O.; Matthews, J.; Fenton, O.S.; Zhang, Y.; Olejnik, K.T.; Yesilyurt, V.; et al. Degradable lipid nanoparticles with predictable in vivo siRNA delivery activity. Nat. Commun. 2014, 5, 4277, doi:10.1038/ncomms5277.

155. Dong, Y.; Love, K.T.; Dorkin, J.R.; Sirirungruang, S.; Zhang, Y.; Chen, D.; Bogorad, R.L.; Yin, H.; Chen, Y.; Vegas, A.J.; et al. Lipopeptide nanoparticles for potent and selective siRNA delivery in rodents and nonhuman primates. Proc. Natl. Acad. Sci. 2014, 111, 3955–3960, doi:10.1073/pnas.1322937111.

156. Li, B.; Luo, X.; Deng, B.; Wang, J.; McComb, D.W.; Shi, Y.; Gaensler, K.M.L.; Tan, X.; Dunn, A.L.; Kerlin, B.A.; et al. An Orthogonal Array Optimization of Lipid-like Nanoparticles for mRNA Delivery in Vivo. Nano Lett. 2015, 15, 8099–8107, doi:10.1021/acs.nanolett.5b03528.

157. Xinfu, Z.; Weiyu, Z.; N., N.G.; Chengxiang, Z.; Chunxi, Z.; Jingyue, Y.; Shi, D.; Xucheng, H.; Wenqing, L.; Justin, J.; et al. Functionalized lipid-like nanoparticles for in vivo mRNA delivery and base editing. Sci. Adv. 2021, 6, eabc2315, doi:10.1126/sciadv.abc2315.

158. Liu, S.; Cheng, Q.; Wei, T.; Yu, X.; Johnson, L.T.; Farbiak, L.; Siegwart, D.J. Membrane-destabilizing ionizable phospholipids for organ-selective mRNA delivery and CRISPR–Cas gene editing. Nat. Mater. 2021, 20, 701–710, doi:10.1038/s41563-020-00886-0.

159. Brito, L.A.; Chan, M.; Shaw, C.A.; Hekele, A.; Carsillo, T.; Schaefer, M.; Archer, J.; Seubert, A.; Otten, G.R.; Beard, C.W.; et al. A cationic nanoemulsion for the delivery of next-generation RNA vaccines. Mol. Ther. 2014, 22, 2118–2129, doi:10.1038/mt.2014.133.

160. Bogers, W.M.; Oostermeijer, H.; Mooij, P.; Koopman, G.; Verschoor, E.J.; Davis, D.; Ulmer, J.B.; Brito, L.A.; Cu, Y.; Banerjee, K.; et al. Potent immune responses in rhesus macaques induced by nonviral delivery of a self-amplifying RNA vaccine expressing HIV type 1 envelope with a cationic nanoemulsion. J. Infect. Dis. 2015, 211, 947–955, doi:10.1093/infdis/jiu522.

161. Aldosari, B.N.; Alfagih, I.M.; Almurshedi, A.S. Lipid nanoparticles as delivery systems for RNA-based vaccines. Pharmaceutics 2021, 13, 1–29, doi:10.3390/pharmaceutics13020206.

162. Kim, J.; Eygeris, Y.; Gupta, M.; Sahay, G. Self-assembled mRNA vaccines. Adv. Drug Deliv. Rev. 2021, 170, 83–112, doi:https://doi.org/10.1016/j.addr.2020.12.014.

163. Koltover, I.; Salditt, T.; Rädler, J.O.; Safinya, C.R. An inverted hexagonal phase of cationic liposome-DNA complexes related to DNA release and delivery. Science (80-.). 1998, 281, 78–81, doi:10.1126/science.281.5373.78.

164. Kauffman, K.J.; Dorkin, J.R.; Yang, J.H.; Heartlein, M.W.; DeRosa, F.; Mir, F.F.; Fenton, O.S.; Anderson, D.G. Optimization of Lipid Nanoparticle Formulations for mRNA Delivery in Vivo with Fractional Factorial and Definitive Screening Designs. Nano Lett. 2015, 15, 7300–7306, doi:10.1021/acs.nanolett.5b02497.

165. Li, B.; Zhang, X.; Dong, Y. Nanoscale platforms for messenger RNA delivery. Wiley Interdiscip. Rev. Nanomedicine Nanobiotechnology 2019, 11, 1–14, doi:10.1002/wnan.1530.

166. Zhu, X.; Tao, W.; Liu, D.; Wu, J.; Guo, Z.; Ji, X.; Bharwani, Z.; Zhao, L.; Zhao, X.; Farokhzad, O.C.; et al. Surface de-PEGylation controls nanoparticle-mediated siRNA delivery in vitro and in vivo. Theranostics 2017, 7, 1990–2002, doi:10.7150/thno.18136.

167. Pardi, N.; Hogan, M.J.; Pelc, R.S.; Muramatsu, H.; Andersen, H.; DeMaso, C.R.; Dowd, K.A.; Sutherland, L.L.; Scearce, R.M.; Parks, R.; et al. Zika virus protection by a single low-dose

nucleoside-modified mRNA vaccination. Nature 2017, 543, 248–251, doi:10.1038/nature21428.

168. Hekele, A.; Bertholet, S.; Archer, J.; Gibson, D.G.; Palladino, G.; Brito, L.A.; Otten, G.R.; Brazzoli, M.; Buccato, S.; Bonci, A.; et al. Rapidly produced SAM(®) vaccine against H7N9 influenza is immunogenic in mice. Emerg. Microbes Infect. 2013, 2, e52, doi:10.1038/emi.2013.54.

169. Zhou, W.Z.; Hoon, D.S.B.; Huang, S.K.S.; Fujii, S.; Hashimoto, K.; Morishita, R.; Kaneda, Y. RNA melanoma vaccine: Induction of antitumor immunity by human glycoprotein 100 mRNA immunization. Hum. Gene Ther. 1999, 10, 2719–2724, doi:10.1089/10430349950016762.

170. Finn, J.D.; Smith, A.R.; Patel, M.C.; Shaw, L.; Youniss, M.R.; van Heteren, J.; Dirstine, T.; Ciullo, C.; Lescarbeau, R.; Seitzer, J.; et al. A Single Administration of CRISPR/Cas9 Lipid Nanoparticles Achieves Robust and Persistent In Vivo Genome Editing. Cell Rep. 2018, 22, 2227–2235, doi:10.1016/j.celrep.2018.02.014.

171. Schoenmaker, L.; Witzigmann, D.; Kulkarni, J.A.; Verbeke, R.; Kersten, G.; Jiskoot, W.; Crommelin, D.J.A. mRNA-lipid nanoparticle COVID-19 vaccines: Structure and stability. Int. J. Pharm. 2021, 601, 120586, doi:10.1016/j.ijpharm.2021.120586.

172. Gediz Erturk, A.; Sahin, A.; Ay, E.B.; Pelit, E.; Bagdatli, E.; Kulu, I.; Gul, M.; Mesci, S.; Eryilmaz, S.; Yildirim, T.; et al. molecules A Multidisciplinary Approach to Coronavirus Disease (COVID-19). 2021, doi:10.3390/molecules26123526.

173. Bajaj, V.; Gadi, N.; Spihlman, A.P.; Wu, S.C.; Choi, C.H.; Moulton, V.R. Aging, Immunity, and COVID-19: How Age Influences the Host Immune Response to Coronavirus Infections? Front. Physiol. 2021, 11, doi:10.3389/fphys.2020.571416.

174. Solinís, M.Á.; del Pozo-Rodríguez, A.; Apaolaza, P.S.; Rodríguez-Gascón, A. Treatment of ocular disorders by gene therapy. Eur. J. Pharm. Biopharm. 2015, 95, 331–342, doi:https://doi.org/10.1016/j.ejpb.2014.12.022.

175. Yadav, N.; Khatak, S.; Singh Sara, U.V. Solid lipid nanoparticles- A review. Int. J. Appl. Pharm. 2013, 5, 8–18, doi:10.9790/3013-26103444.

176. Ramamoorth, M.; Narvekar, A. Non viral vectors in gene therapy - An overview. J. Clin. Diagnostic Res. 2015, 9, GE01–GE06, doi:10.7860/JCDR/2015/10443.5394.

177. Trucillo, P.; Campardelli, R. Production of solid lipid nanoparticles with a supercritical fluid assisted process. J. Supercrit. Fluids 2019, 143, 16–23, doi:10.1016/j.supflu.2018.08.001.

178. Chattopadhyay, P.; Shekunov, B.Y.; Yim, D.; Cipolla, D.; Boyd, B.; Farr, S. Production of solid lipid nanoparticle suspensions using supercritical fluid extraction of emulsions (SFEE) for pulmonary delivery using the AERx system. Adv. Drug Deliv. Rev. 2007, 59, 444–453, doi:10.1016/j.addr.2007.04.010.

179. Müller, R.H.; Radtke, M.; Wissing, S.A. Solid lipid nanoparticles (SLN) and nanostructured lipid carriers (NLC) in cosmetic and dermatological preparations. Adv. Drug Deliv. Rev. 2002, 54, 131–155, doi:10.1016/S0169-409X(02)00118-7.

180. Delgado, D.; del Pozo-Rodríguez, A.; Angeles Solinís, M.; Bartkowiak, A.; Rodríguez-Gascón, A. New gene delivery system based on oligochitosan and solid lipid nanoparticles: 'In vitro'

and 'in vivo' evaluation. Eur. J. Pharm. Sci. 2013, 50, 484–491, doi:https://doi.org/10.1016/j.ejps.2013.08.013.

181. Apaolaza, P.S.; Delgado, D.; Pozo-Rodríguez, A. Del; Gascón, A.R.; Solinís, M.Á. A novel gene therapy vector based on hyaluronic acid and solid lipid nanoparticles for ocular diseases. Int. J. Pharm. 2014, 465, 413–426, doi:10.1016/j.ijpharm.2014.02.038.

182. Apaolaza, P.S.; del Pozo-Rodríguez, A.; Torrecilla, J.; Rodríguez-Gascón, A.; Rodríguez, J.M.; Friedrich, U.; Weber, B.H.F.; Solinís, M.A. Solid lipid nanoparticle-based vectors intended for the treatment of X-linked juvenile retinoschisis by gene therapy: In vivo approaches in Rs1h-deficient mouse model. J. Control. Release 2015, 217, 273–283, doi:https://doi.org/10.1016/j.jconrel.2015.09.033.

183. Ruiz De Garibay, A.P.; Solinís, M.A.; Del Pozo-Rodríguez, A.; Apaolaza, P.S.; Shen, J.S.; Rodríguez-Gascón, A. Solid lipid nanoparticles as non-viral vectors for gene transfection in a cell model of fabry disease. J. Biomed. Nanotechnol. 2015, 11, 500–511, doi:10.1166/jbn.2015.1968.

184. Rodríguez-Castejón, J.; Alarcia-Lacalle, A.; Gómez-Aguado, I.; Vicente-Pascual, M.; Aspiazu, M.Á.S.; Del Pozo-Rodríguez, A.; Rodríguez-Gascón, A. α-Galactosidase A Augmentation by Non-Viral Gene Therapy: Evaluation in Fabry Disease Mice. Pharmaceutics 2021, 13, doi:10.3390/pharmaceutics13060771.

185. De, K. Decapeptide Modified Doxorubicin Loaded Solid Lipid Nanoparticles as Targeted Drug Delivery System against Prostate Cancer. Langmuir 2021, 37, 13194–13207, doi:10.1021/acs.langmuir.1c01370.

186. Ma, Y.; Zhang, X.; Xu, X.; Shen, L.; Yao, Y.; Yang, Z.; Liu, P. STAT3 Decoy Oligodeoxynucleotides-Loaded Solid Lipid Nanoparticles Induce Cell Death and Inhibit Invasion in Ovarian Cancer Cells. PLoS One 2015, 10, e0124924.

187. Granja, A.; Lima-Sousa, R.; Alves, C.G.; de Melo-Diogo, D.; Pinheiro, M.; Sousa, C.T.; Correia, I.J.; Reis, S. Mitoxantrone-loaded lipid nanoparticles for breast cancer therapy – Quality-by-design approach and efficacy assessment in 2D and 3D in vitro cancer models. Int. J. Pharm. 2021, 607, 121044, doi:https://doi.org/10.1016/j.ijpharm.2021.121044.

188. del Pozo-Rodríguez, A.; Solinís, M.Á.; Rodríguez-Gascón, A. Applications of lipid nanoparticles in gene therapy. Eur. J. Pharm. Biopharm. 2016, 109, 184–193, doi:10.1016/j.ejpb.2016.10.016.

189. Apaolaza, P.S.; del Pozo-Rodríguez, A.; Solinís, M.A.; Rodríguez, J.M.; Friedrich, U.; Torrecilla, J.; Weber, B.H.F.; Rodríguez-Gascón, A. Structural recovery of the retina in a retinoschisin-deficient mouse after gene replacement therapy by solid lipid nanoparticles. Biomaterials 2016, 90, 40–49, doi:https://doi.org/10.1016/j.biomaterials.2016.03.004.

190. Torrecilla, J.; del Pozo-Rodríguez, A.; Vicente-Pascual, M.; Solinís, M.Á.; Rodríguez-Gascón, A. Targeting corneal inflammation by gene therapy: Emerging strategies for keratitis. Exp. Eye Res. 2018, 176, 130–140, doi:10.1016/j.exer.2018.07.006.

191. Vicente-Pascual, M.; Albano, A.; Solinís, M.; Serpe, L.; Rodríguez-Gascón, A.; Foglietta, F.; Muntoni, E.; Torrecilla, J.; Pozo-Rodríguez, A. Del; Battaglia, L. Gene delivery in the cornea: In vitro & ex vivo evaluation of solid lipid nanoparticle-based vectors. Nanomedicine 2018, 13, 1847–1864, doi:10.2217/nnm-2018-0112.

192. Vicente-Pascual, M.; Gómez-Aguado, I.; Rodríguez-Castejón, J.; Rodríguez-Gascón, A.; Muntoni, E.; Battaglia, L.; Pozo-Rodríguez, A. Del; Aspiazu, M.Á.S. Topical administration of sln-based gene therapy for the treatment of corneal inflammation by de novo il-10 production. Pharmaceutics 2020, 12, 1–23, doi:10.3390/pharmaceutics12060584.

193. Gómez-Aguado, I.; Rodríguez-Castejón, J.; Vicente-Pascual, M.; Rodríguez-Gascón, A.; Pozo-Rodríguez, A. Del; Solinís Aspiazu, M.Á. Nucleic Acid Delivery by Solid Lipid Nanoparticles Containing Switchable Lipids: Plasmid DNA vs. Messenger RNA. Molecules 2020, 25, doi:10.3390/molecules25245995.

194. Gómez-Aguado, I.; Rodríguez-Castejón, J.; Beraza-Millor, M.; Vicente-Pascual, M.; Rodríguez-Gascón, A.; Garelli, S.; Battaglia, L.; del Pozo-Rodríguez, A.; Solinís, M.Á. mRNA-Based Nanomedicinal Products to Address Corneal Inflammation by Interleukin-10 Supplementation. Pharmaceutics 2021, 13, 1472, doi:10.3390/pharmaceutics13091472.

195. Beloqui, A.; Solinís, M.Á.; Rodríguez-Gascón, A.; Almeida, A.J.; Préat, V. Nanostructured lipid carriers: Promising drug delivery systems for future clinics. Nanomedicine Nanotechnology, Biol. Med. 2016, 12, 143–161, doi:https://doi.org/10.1016/j.nano.2015.09.004.

196. Beloqui, A.; del Pozo-Rodríguez, A.; Isla, A.; Rodríguez-Gascón, A.; Solinís, M.Á. Nanostructured lipid carriers as oral delivery systems for poorly soluble drugs. J. Drug Deliv. Sci. Technol. 2017, 42, 144–154, doi:https://doi.org/10.1016/j.jddst.2017.06.013.

197. Erasmus, J.H.; Khandhar, A.P.; Guderian, J.; Granger, B.; Archer, J.; Archer, M.; Gage, E.; Fuerte-Stone, J.; Larson, E.; Lin, S.; et al. A Nanostructured Lipid Carrier for Delivery of a Replicating Viral RNA Provides Single, Low-Dose Protection against Zika. Mol. Ther. 2018, 26, 2507–2522, doi:10.1016/j.ymthe.2018.07.010.

198. Valadi, H.; Ekström, K.; Bossios, A.; Sjöstrand, M.; Lee, J.J.; Lötvall, J.O. Exosome-mediated transfer of mRNAs and microRNAs is a novel mechanism of genetic exchange between cells. Nat. Cell Biol. 2007, 9, 654–659, doi:10.1038/ncb1596.

199. Skog, J.; Würdinger, T.; van Rijn, S.; Meijer, D.H.; Gainche, L.; Curry, W.T.; Carter, B.S.; Krichevsky, A.M.; Breakefield, X.O. Glioblastoma microvesicles transport RNA and proteins that promote tumour growth and provide diagnostic biomarkers. Nat. Cell Biol. 2008, 10, 1470–1476, doi:10.1038/ncb1800.

200. Yang, Z.; Shi, J.; Xie, J.; Wang, Y.; Sun, J.; Liu, T.; Zhao, Y.; Zhao, X.; Wang, X.; Ma, Y.; et al. Large-scale generation of functional mRNA-encapsulating exosomes via cellular nanoporation. Nat. Biomed. Eng. 2020, 4, 69–83, doi:10.1038/s41551-019-0485-1.

201. Luan, X.; Sansanaphongpricha, K.; Myers, I.; Chen, H.; Yuan, H.; Sun, D. Engineering exosomes as refined biological nanoplatforms for drug delivery. Acta Pharmacol. Sin. 2017, 38, 754–763, doi:10.1038/aps.2017.12.

202. Guevara, M.L.; Persano, S.; Persano, F. Lipid-Based Vectors for Therapeutic mRNA-Based Anti-Cancer Vaccines. Curr. Pharm. Des. 2019.

203. Zhao, W.; Zhang, C.; Li, B.; Zhang, X.; Luo, X.; Zeng, C.; Li, W.; Gao, M.; Dong, Y. Lipid Polymer Hybrid Nanomaterials for mRNA Delivery. Cell. Mol. Bioeng. 2018, 11, 397–406, doi:10.1007/s12195-018-0536-9.

204. Wang, Y.; Su, H.H.; Yang, Y.; Hu, Y.; Zhang, L.; Blancafort, P.; Huang, L. Systemic delivery of modified mRNA encoding herpes simplex virus 1 thymidine kinase for targeted cancer gene therapy. Mol. Ther. 2013, 21, 358–367, doi:10.1038/mt.2012.250.

205. Zhang, R.; Men, K.; Zhang, X.; Huang, R.; Tian, Y.; Zhou, B.; Yu, C.; Wang, Y.; Ji, X.; Hu, Q.; et al. Delivery of a Modified mRNA Encoding IL-22 Binding Protein (IL-22BP) for Colon Cancer Gene Therapy. J. Biomed. Nanotechnol. 2018, 14, 1239–1251, doi:10.1166/jbn.2018.2577.

206. Conway, A.; Mendel, M.; Kim, K.; McGovern, K.; Boyko, A.; Zhang, L.; Miller, J.C.; DeKelver, R.C.; Paschon, D.E.; Mui, B.L.; et al. Non-viral Delivery of Zinc Finger Nuclease mRNA Enables Highly Efficient In Vivo Genome Editing of Multiple Therapeutic Gene Targets. Mol. Ther. 2019, 27, 866–877, doi:10.1016/j.ymthe.2019.03.003.

207. Shim, G.; Kim, D.; Park, G.T.; Jin, H.; Suh, S.K.; Oh, Y.K. Therapeutic gene editing: Delivery and regulatory perspectives. Acta Pharmacol. Sin. 2017, 38, 738–753.

208. Zhang, H.X.; Zhang, Y.; Yin, H. Genome Editing with mRNA Encoding ZFN, TALEN, and Cas9. Mol. Ther. 2019, 27, 735–746, doi:10.1016/j.ymthe.2019.01.014.

209. Crudele, J.M.; Chamberlain, J.S. Cas9 immunity creates challenges for CRISPR gene editing therapies. Nat. Commun. 2018, 9, 3497, doi:10.1038/s41467-018-05843-9.

210. Rodríguez-Gascón, A.; Pozo-Rodríguez, A.; Isla, A.; Solinís, M.A. Gene Therapy in the Cornea. In eLS; Wiley, 2016; pp. 1–9.

211. Jo, J.-I.; Gao, J.-Q.; Tabata, Y. Biomaterial-based delivery systems of nucleic acid for regenerative research and regenerative therapy. Regen. Ther. 2019, 11, 123–130, doi:10.1016/j.reth.2019.06.007.

212. Park, J.S.; Suryaprakash, S.; Lao, Y.H.; Leong, K.W. Engineering mesenchymal stem cells for regenerative medicine and drug delivery. Methods 2015, 84, 3–16.

213. Fishman, S.; Lewis, M.D.; Siew, L.K.; De Leenheer, E.; Kakabadse, D.; Davies, J.; Ziv, D.; Margalit, A.; Karin, N.; Gross, G.; et al. Adoptive Transfer of mRNA-Transfected T Cells Redirected against Diabetogenic CD8 T Cells Can Prevent Diabetes. Mol. Ther. 2017, 25, 456–464, doi:10.1016/j.ymthe.2016.12.007.

214. Van Hoecke, L.; Roose, K. How mRNA therapeutics are entering the monoclonal antibody field. J. Transl. Med. 2019, 17.

215. Deal, C.E.; Carfi, A.; Plante, O.J. Advancements in mRNA encoded antibodies for passive immunotherapy. Vaccines 2021, 9, 1–16, doi:10.3390/vaccines9020108.

216. August, A.; Attarwala, H.Z.; Himansu, S.; Kalidindi, S.; Lu, S.; Pajon, R.; Han, S.; Lecerf, J.-M.; Tomassini, J.E.; Hard, M.; et al. A phase 1 trial of lipid-encapsulated mRNA encoding a monoclonal antibody with neutralizing activity against Chikungunya virus. Nat. Med. 2021, 27, 2224–2233, doi:10.1038/s41591-021-01573-6.

217. Liu, M.A. A comparison of plasmid DNA and mRNA as vaccine technologies. Vaccines 2019, 7, 37.

218. Kowalzik, F.; Schreiner, D.; Jensen, C.; Teschner, D.; Gehring, S.; Zepp, F. Mrna-based vaccines. Vaccines 2021, 9, 390.

219. Blakney, A.K.; Ip, S.; Geall, A.J. An update on self-amplifying mRNA vaccine development. Vaccines 2021, 9, 1–26, doi:10.3390/vaccines9020097.

220. Maruggi, G.; Zhang, C.; Li, J.; Ulmer, J.B.; Yu, D. mRNA as a Transformative Technology for Vaccine Development to Control Infectious Diseases. Mol. Ther. 2019, 27, 757–772, doi:10.1016/j.ymthe.2019.01.020.

221. Rodríguez-Gascón, A.; del Pozo-Rodríguez, A.; Solinís, M.Á. Development of nucleic acid vaccines: Use of self-amplifying RNA in lipid nanoparticles. Int. J. Nanomedicine 2014, 9, 1833–1843.

222. Park, K.S.; Sun, X.; Aikins, M.E.; Moon, J.J. Non-viral COVID-19 vaccine delivery systems. Adv. Drug Deliv. Rev. 2021, 169, 137–151, doi:10.1016/j.addr.2020.12.008.

223. Heine, A.; Juranek, S.; Brossart, P. Clinical and immunological effects of mRNA vaccines in malignant diseases. Mol. Cancer 2021, 20, 1–20.

224. Chaudhary, N.; Weissman, D.; Whitehead, K.A. mRNA vaccines for infectious diseases: principles, delivery and clinical translation. Nat. Rev. Drug Discov. 2021, 20, 817–838.

225. Petsch, B.; Schnee, M.; Vogel, A.B.; Lange, E.; Hoffmann, B.; Voss, D.; Schlake, T.; Thess, A.; Kallen, K.J.; Stitz, L.; et al. Protective efficacy of in vitro synthesized, specific mRNA vaccines against influenza A virus infection. Nat. Biotechnol. 2012, 30, 1210–1216, doi:10.1038/nbt.2436.

226. Freyn, A.W.; Ramos da Silva, J.; Rosado, V.C.; Bliss, C.M.; Pine, M.; Mui, B.L.; Tam, Y.K.; Madden, T.D.; de Souza Ferreira, L.C.; Weissman, D.; et al. A Multi-Targeting, Nucleoside-Modified mRNA Influenza Virus Vaccine Provides Broad Protection in Mice. Mol. Ther. 2020, 28, 1569–1584, doi:10.1016/j.ymthe.2020.04.018.

227. Brazzoli, M.; Magini, D.; Bonci, A.; Buccato, S.; Giovani, C.; Kratzer, R.; Zurli, V.; Mangiavacchi, S.; Casini, D.; Brito, L.M.; et al. Induction of Broad-Based Immunity and Protective Efficacy by Self-amplifying mRNA Vaccines Encoding Influenza Virus Hemagglutinin. J. Virol. 2016, 90, 332–344, doi:10.1128/jvi.01786-15.

228. Magini, D.; Giovani, C.; Mangiavacchi, S.; MacCari, S.; Cecchi, R.; Ulmer, J.B.; De Gregorio, E.; Geall, A.J.; Brazzoli, M.; Bertholet, S. Self-amplifying mRNA vaccines expressing multiple conserved influenza antigens confer protection against homologous and heterosubtypic viral challenge. PLoS One 2016, 11, doi:10.1371/journal.pone.0161193.

229. Vogel, A.B.; Lambert, L.; Kinnear, E.; Busse, D.; Erbar, S.; Reuter, K.C.; Wicke, L.; Perkovic, M.; Beissert, T.; Haas, H.; et al. Self-Amplifying RNA Vaccines Give Equivalent Protection against Influenza to mRNA Vaccines but at Much Lower Doses. Mol. Ther. 2018, 26, 446–455, doi:10.1016/j.ymthe.2017.11.017.

230. Zhuang, X.; Qi, Y.; Wang, M.; Yu, N.; Nan, F.; Zhang, H.; Tian, M.; Li, C.; Lu, H.; Jin, N. MRNA vaccines encoding the HA protein of influenza a H1N1 virus delivered by cationic lipid nanoparticles induce protective immune responses in mice. Vaccines 2020, 8, doi:10.3390/vaccines8010123.

231. Bahl, K.; Senn, J.J.; Yuzhakov, O.; Bulychev, A.; Brito, L.A.; Hassett, K.J.; Laska, M.E.; Smith, M.; Almarsson, Ö.; Thompson, J.; et al. Preclinical and Clinical Demonstration of Immunogenicity by mRNA Vaccines against H10N8 and H7N9 Influenza Viruses. Mol. Ther. 2017, 25, 1316–1327, doi:10.1016/j.ymthe.2017.03.035.

232. Feldman, R.A.; Fuhr, R.; Smolenov, I.; (Mick)Ribeiro, A.; Panther, L.; Watson, M.; Senn, J.J.; Smith, M.; Almarsson, Örn; Pujar, H.S.; et al. mRNA vaccines against H10N8 and H7N9 influenza viruses of pandemic potential are immunogenic and well tolerated in healthy adults in phase 1 randomized clinical trials. Vaccine 2019, 37, 3326–3334, doi:10.1016/j.vaccine.2019.04.074.

233. Schnee, M.; Vogel, A.B.; Voss, D.; Petsch, B.; Baumhof, P.; Kramps, T.; Stitz, L. An mRNA Vaccine Encoding Rabies Virus Glycoprotein Induces Protection against Lethal Infection in Mice and Correlates of Protection in Adult and Newborn Pigs. PLoS Negl. Trop. Dis. 2016, 10, e0004746, doi:10.1371/journal.pntd.0004746.

234. Alberer, M.; Gnad-Vogt, U.; Hong, H.S.; Mehr, K.T.; Backert, L.; Finak, G.; Gottardo, R.; Bica, M.A.; Garofano, A.; Koch, S.D.; et al. Safety and immunogenicity of a mRNA rabies vaccine in healthy adults: an open-label, non-randomised, prospective, first-in-human phase 1 clinical trial. Lancet 2017, 390, 1511–1520, doi:10.1016/S0140-6736(17)31665-3.

235. Lutz, J.; Lazzaro, S.; Habbeddine, M.; Schmidt, K.E.; Baumhof, P.; Mui, B.L.; Tam, Y.K.; Madden, T.D.; Hope, M.J.; Heidenreich, R.; et al. Unmodified mRNA in LNPs constitutes a competitive technology for prophylactic vaccines. npj Vaccines 2017, 2, 29, doi:10.1038/s41541-017-0032-6.

236. Aldrich, C.; Leroux–Roels, I.; Huang, K.B.; Bica, M.A.; Loeliger, E.; Schoenborn-Kellenberger, O.; Walz, L.; Leroux-Roels, G.; von Sonnenburg, F.; Oostvogels, L. Proof-of-concept of a low-dose unmodified mRNA-based rabies vaccine formulated with lipid nanoparticles in human volunteers: A phase 1 trial. Vaccine 2021, 39, 1310–1318, doi:10.1016/j.vaccine.2020.12.070.

237. Kim, H.W.; Canchola, J.G.; Brandt, C.D.; Pyles, G.; Chanock, R.M.; Jensen, K.; Parrott, R.H. Respiratory syncytial virus disease in infants despite prior administration of antigenic inactivated vaccine. Am. J. Epidemiol. 1969, 89, 422–434, doi:10.1093/oxfordjournals.aje.a120955.

238. Aliprantis, A.O.; Shaw, C.A.; Griffin, P.; Farinola, N.; Railkar, R.A.; Cao, X.; Liu, W.; Sachs, J.R.; Swenson, C.J.; Lee, H.; et al. A phase 1, randomized, placebo-controlled study to evaluate the safety and immunogenicity of an mRNA-based RSV prefusion F protein vaccine in healthy younger and older adults. Hum. Vaccines Immunother. 2021, 17, 1248–1261, doi:10.1080/21645515.2020.1829899.

239. Shaw, C.; Lee, H.; Knightly, C.; Kalidindi, S.; Zaks, T.; Smolenov, I.; Panther, L. 2754. Phase 1 Trial of an mRNA-Based Combination Vaccine Against hMPV and PIV3. Open Forum Infect. Dis. 2019, 6, S970–S970, doi:10.1093/ofid/ofz360.2431.

240. Moderna Inc. Item 16. Form 10-K Summary Available online: https://www.sec.gov/Archives/edgar/data/1682852/000168285219000009/moderna10-k12312018.htm (accessed on Jan 5, 2022).

241. Moderna Inc. Moderna Highlights Opportunity of mRNA Vaccines at its First Vaccines Day Available online: https://investors.modernatx.com/news-releases/news-release-details/moderna-highlights-opportunity-mrna-vaccines-its-first-vaccines (accessed on Jan 3, 2022).

242. Shaw, C.; Panther, L.; August, A.; Zaks, T.; Smolenov, I.; Bart, S.; Watson, M. Safety and immunogenicity of a mRNA-based chikungunya vaccine in a phase 1 dose-ranging trial. Int. J. Infect. Dis. 2019, 79, 17, doi:10.1016/j.ijid.2018.11.058.

243. Leal, L.; Guardo, A.C.; Morón-López, S.; Salgado, M.; Mothe, B.; Heirman, C.; Pannus, P.; Vanham, G.; van den Ham, H.J.; Gruters, R.; et al. Phase I clinical trial of an intranodally administered mRNA-based therapeutic vaccine against HIV-1 infection. AIDS 2018, 32, 2533–2545, doi:10.1097/QAD.0000000000002026.

244. De Jong, W.; Aerts, J.; Allard, S.; Brander, C.; Buyze, J.; Florence, E.; Van Gorp, E.; Vanham, G.; Leal, L.; Mothe, B.; et al. IHIVARNA phase IIa, a randomized, placebo-controlled, double-blinded trial to evaluate the safety and immunogenicity of iHIVARNA-01 in chronically HIV-infected patients under stable combined antiretroviral therapy. Trials 2019, 20, 361, doi:10.1186/s13063-019-3409-1.

245. Bernstein, D.I.; Reap, E.A.; Katen, K.; Watson, A.; Smith, K.; Norberg, P.; Olmsted, R.A.; Hoeper, A.; Morris, J.; Negri, S.; et al. Randomized, double-blind, Phase 1 trial of an alphavirus replicon vaccine for cytomegalovirus in CMV seronegative adult volunteers. Vaccine 2009, 28, 484–493, doi:10.1016/j.vaccine.2009.09.135.

246. AlphaVax AlphaVax Clinical Experience Available online: https://www.alphavax.com/clinical-experience.html (accessed on Dec 8, 2021).

247. Wecker, M.; Gilbert, P.; Russell, N.; Hural, J.; Allen, M.; Pensiero, M.; Chulay, J.; Chiu, Y.L.; Karim, S.S.A.; Burke, D.S. Phase I safety and immunogenicity evaluations of an alphavirus replicon HIV-1 subtype C gag vaccine in healthy HIV-1-uninfected adults. Clin. Vaccine Immunol. 2012, 19, 1651–1660, doi:10.1128/CVI.00258-12.

248. van den Berg, R.A.; De Mot, L.; Leroux-Roels, G.; Bechtold, V.; Clement, F.; Coccia, M.; Jongert, E.; Evans, T.G.; Gillard, P.; van der Most, R.G. Adjuvant-associated peripheral blood mRNA profiles and kinetics induced by the adjuvanted recombinant protein candidate tuberculosis vaccine M72/AS01 in Bacillus Calmette-Guérin-vaccinated adults. Front. Immunol. 2018, 9, doi:10.3389/fimmu.2018.00564.

249. Gandhi, R.T.; Kwon, D.S.; Macklin, E.A.; Shopis, J.R.; McLean, A.P.; McBrine, N.; Flynn, T.; Peter, L.; Sbrolla, A.; Kaufmann, D.E.; et al. Immunization of HIV-1-infected persons with autologous dendritic cells transfected with mRNA encoding HIV-1 Gag and Nef: Results of a randomized, placebo-controlled clinical trial. J. Acquir. Immune Defic. Syndr. 2016, 71, 246–253, doi:10.1097/QAI.0000000000000852.

250. Du, L.; He, Y.; Zhou, Y.; Liu, S.; Zheng, B.J.; Jiang, S. The spike protein of SARS-CoV - A target for vaccine and therapeutic development. Nat. Rev. Microbiol. 2009, 7, 226–236.

251. Tang, T.; Bidon, M.; Jaimes, J.A.; Whittaker, G.R.; Daniel, S. Coronavirus membrane fusion mechanism offers a potential target for antiviral development. Antiviral Res. 2020, 178, 104792.

252. Medicines & Healthcare products Regulatory Agency Regulatory approval of Pfizer/BioNTech vaccine for COVID-19 Available online: https://www.gov.uk/government/publications/regulatory-approval-of-pfizer-biontech-vaccine-for-covid-19 (accessed on Jan 2, 2022).

253. US Food & Drug Administration FDA Approves First COVID-19 Vaccine Available online: https://www.fda.gov/news-events/press-announcements/fda-approves-first-covid-19-vaccine (accessed on Jan 2, 2022).

254. European Medicines Agency Comirnaty Available online: https://www.ema.europa.eu/en/medicines/human/EPAR/comirnaty#authorisation-details-section (accessed on Jan 2, 2022).

255. Walsh, E.E.; Frenck, R.W.; Falsey, A.R.; Kitchin, N.; Absalon, J.; Gurtman, A.; Lockhart, S.; Neuzil, K.; Mulligan, M.J.; Bailey, R.; et al. Safety and Immunogenicity of Two RNA-Based Covid-19 Vaccine Candidates. N. Engl. J. Med. 2020, 383, 2439–2450, doi:10.1056/nejmoa2027906.

256. Jackson, L.A.; Anderson, E.J.; Rouphael, N.G.; Roberts, P.C.; Makhene, M.; Coler, R.N.; McCullough, M.P.; Chappell, J.D.; Denison, M.R.; Stevens, L.J.; et al. An mRNA Vaccine against SARS-CoV-2 — Preliminary Report. N. Engl. J. Med. 2020, 383, 1920–1931, doi:10.1056/NEJMoa2022483.

257. Baden, L.R.; El Sahly, H.M.; Essink, B.; Kotloff, K.; Frey, S.; Novak, R.; Diemert, D.; Spector, S.A.; Rouphael, N.; Creech, C.B.; et al. Efficacy and Safety of the mRNA-1273 SARS-CoV-2 Vaccine. N. Engl. J. Med. 2021, 384, 403–416, doi:10.1056/nejmoa2035389.

258. Kremsner, P.; Mann, P.; Bosch, J.; Fendel, R.; Gabor, J.J.; Kreidenweiss, A.; Kroidl, A.; Leroux-Roels, I.; Leroux-Roels, G.; Schindler, C.; et al. Phase 1 Assessment of the Safety and Immunogenicity of an mRNA- Lipid Nanoparticle Vaccine Candidate Against SARS-CoV-2 in Human Volunteers. medRxiv 2020, 2020.11.09.20228551, doi:10.1101/2020.11.09.20228551.

259. Kremsner, P.G.; Ahuad Guerrero, R.A.; Arana-Arri, E.; Aroca Martinez, G.J.; Bonten, M.; Chandler, R.; Corral, G.; De Block, E.J.L.; Ecker, L.; Gabor, J.J.; et al. Efficacy and safety of the CVnCoV SARS-CoV-2 mRNA vaccine candidate in ten countries in Europe and Latin America (HERALD): a randomised, observer-blinded, placebo-controlled, phase 2b/3 trial. Lancet Infect. Dis. 2021, 0, doi:10.1016/S1473-3099(21)00677-0.

260. Roth, N.; Schön, J.; Hoffmann, D.; Thran, M.; Thess, A.; Mueller, S.O.; Petsch, B.; Rauch, S. CV2CoV, an enhanced mRNA-based SARS-CoV-2 vaccine candidate, supports higher protein expression and improved immunogenicity in rats. bioRxiv 2021, 2021.05.13.443734, doi:10.1101/2021.05.13.443734.

261. Burki, T. Understanding variants of SARS-CoV-2. Lancet (London, England) 2021, 397, 462, doi:10.1016/S0140-6736(21)00298-1.

262. Xie, X.; Liu, Y.; Liu, J.; Zhang, X.; Zou, J.; Fontes-Garfias, C.R.; Xia, H.; Swanson, K.A.; Cutler, M.; Cooper, D.; et al. Neutralization of SARS-CoV-2 spike 69/70 deletion, E484K and N501Y variants by BNT162b2 vaccine-elicited sera. Nat. Med. 2021, 27, 620–621, doi:10.1038/s41591-021-01270-4.

263. Muik, A.; Wallisch, A.K.; Sänger, B.; Swanson, K.A.; Mühl, J.; Chen, W.; Cai, H.; Maurus, D.; Sarkar, R.; Türeci, Ö.; et al. Neutralization of SARS-CoV-2 lineage B.1.1.7 pseudovirus by BNT162b2 vaccine–elicited human sera. Science (80-.). 2021, 371, 1152–1153, doi:10.1126/science.abg6105.

264. Choi, A.; Koch, M.; Wu, K.; Chu, L.; Ma, L.Z.; Hill, A.; Nunna, N.; Huang, W.; Oestreicher, J.; Colpitts, T.; et al. Safety and immunogenicity of SARS-CoV-2 variant mRNA vaccine boosters in healthy adults: an interim analysis. Nat. Med. 2021, 27, 2025–2031, doi:10.1038/s41591-021-01527-y.

265. Edara, V.-V.; Manning, K.E.; Ellis, M.; Lai, L.; Foster, S.L.; Floyd, K.; Davis-Gardner, M.E.; Nyhoff, L.E.; Bechnak, S.; Alaaeddine, G.; et al. mRNA-1273 and BNT162b2 mRNA vaccines have reduced neutralizing 1 activity against the SARS-CoV-2 Omicron variant. bioRxiv 2021, 2021.12.20.473557, doi:10.1101/2021.12.20.473557.

266. Pfizer Inc.; BioNTech SE Pfizer and BioNTech Provide Update on Omicron Variant Available online: https://www.pfizer.com/news/press-release/press-release-detail/pfizer-and-biontech-provide-update-omicron-variant (accessed on Dec 8, 2021).

267. McKay, P.F.; Hu, K.; Blakney, A.K.; Samnuan, K.; Brown, J.C.; Penn, R.; Zhou, J.; Bouton, C.R.; Rogers, P.; Polra, K.; et al. Self-amplifying RNA SARS-CoV-2 lipid nanoparticle vaccine candidate induces high neutralizing antibody titers in mice. Nat. Commun. 2020, 11, 1–7, doi:10.1038/s41467-020-17409-9.

268. de Alwis, R.; Gan, E.S.; Chen, S.; Leong, Y.S.; Tan, H.C.; Zhang, S.L.; Yau, C.; Low, J.G.H.; Kalimuddin, S.; Matsuda, D.; et al. A single dose of self-transcribing and replicating RNA-based SARS-CoV-2 vaccine produces protective adaptive immunity in mice. Mol. Ther. 2021, 29, 1970–1983, doi:10.1016/j.ymthe.2021.04.001.

269. Beck, J.D.; Reidenbach, D.; Salomon, N.; Sahin, U.; Türeci, Ö.; Vormehr, M.; Kranz, L.M. mRNA therapeutics in cancer immunotherapy. Mol. Cancer 2021, 20, 69.

270. Liu, W.; Tang, H.; Li, L.; Wang, X.; Yu, Z.; Li, J. Peptide-based therapeutic cancer vaccine: Current trends in clinical application. Cell Prolif. 2021, 54, e13025.

271. Hollingsworth, R.E.; Jansen, K. Turning the corner on therapeutic cancer vaccines. npj Vaccines 2019, 4.

272. Blass, E.; Ott, P.A. Advances in the development of personalized neoantigen-based therapeutic cancer vaccines. Nat. Rev. Clin. Oncol. 2021, 18, 215–229.

273. Filin, I.Y.; Kitaeva, K. V.; Rutland, C.S.; Rizvanov, A.A.; Solovyeva, V. V. Recent Advances in Experimental Dendritic Cell Vaccines for Cancer. Front. Oncol. 2021, 11, 3863.

274. Wu, T.C.; Guarnieri, F.G.; Staveley-O'Carroll, K.F.; Viscidi, R.P.; Levitsky, H.I.; Hedrick, L.; Cho, K.R.; August, J.T.; Pardoll, D.M. Engineering an intracellular pathway for major histocompatibility complex class II presentation of antigens. Proc. Natl. Acad. Sci. U. S. A. 1995, 92, 11671–11675, doi:10.1073/pnas.92.25.11671.

275. Bonehill, A.; Heirman, C.; Tuyaerts, S.; Michiels, A.; Breckpot, K.; Brasseur, F.; Zhang, Y.; van der Bruggen, P.; Thielemans, K. Messenger RNA-Electroporated Dendritic Cells Presenting MAGE-A3 Simultaneously in HLA Class I and Class II Molecules. J. Immunol. 2004, 172, 6649–6657, doi:10.4049/jimmunol.172.11.6649.

276. Kreiter, S.; Selmi, A.; Diken, M.; Sebastian, M.; Osterloh, P.; Schild, H.; Huber, C.; Türeci, Ö.; Sahin, U. Increased Antigen Presentation Efficiency by Coupling Antigens to MHC Class I Trafficking Signals. J. Immunol. 2008, 180, 309–318, doi:10.4049/jimmunol.180.1.309.

277. Batich, K.A.; Mitchell, D.A.; Healy, P.; Herndon, J.E.; Sampson, J.H. Once, Twice, Three Times a Finding: Reproducibility of Dendritic Cell Vaccine Trials Targeting Cytomegalovirus in Glioblastoma. Clin. Cancer Res. 2020, 26, 5297–5303.

278. Peters, K.B.; Archer, G.E.; Norberg, P.; Xie, W.; Threatt, S.; Lipp, E.S.; Herndon, J.E.; Healy, P.; Congdon, K.; Sanchez-Perez, L.; et al. Safety of nivolumab in combination with dendritic cell

vaccines in recurrent high-grade glioma. J. Clin. Oncol. 2019, 37, e13526–e13526, doi:10.1200/jco.2019.37.15_suppl.e13526.

279. Vlahovic, G.; Archer, G.E.; Reap, E.; Desjardins, A.; Peters, K.B.; Randazzo, D.; Healy, P.; Herndon, J.E.; Friedman, A.H.; Friedman, H.S.; et al. Phase I trial of combination of antitumor immunotherapy targeted against cytomegalovirus (CMV) plus regulatory T-cell inhibition in patients with newly-diagnosed glioblastoma multiforme (GBM). . J. Clin. Oncol. 2016, 34, e13518–e13518, doi:10.1200/jco.2016.34.15_suppl.e13518.

280. Dannull, J.; Nair, S.; Su, Z.; Boczkowski, D.; DeBeck, C.; Yang, B.; Gilboa, E.; Vieweg, J. Enhancing the immunostimulatory function of dendritic cells by transfection with mRNA encoding OX40 ligand. Blood 2005, 105, 3206–3213, doi:10.1182/blood-2004-10-3944.

281. Tcherepanova, I.Y.; Adams, M.D.; Feng, X.; Hinohara, A.; Horvatinovich, J.; Calderhead, D.; Healey, D.; Nicolette, C.A. Ectopic expression of a truncated CD40L protein from synthetic post-transcriptionally capped RNA in dendritic cells induces high levels of IL-12 secretion. BMC Mol. Biol. 2008, 9, 90, doi:10.1186/1471-2199-9-90.

282. Daneshmandi, S.; Pourfathollah, A.A.; Forouzandeh-Moghaddam, M. Enhanced CD40 and ICOSL expression on dendritic cells surface improve anti-tumor immune responses; effectiveness of mRNA/chitosan nanoparticles. Immunopharmacol. Immunotoxicol. 2018, 40, 375–386, doi:10.1080/08923973.2018.1510959.

283. Bonehill, A.; Tuyaerts, S.; Van Nuffel, A.M.T.; Heirman, C.; Bos, T.J.; Fostier, K.; Neyns, B.; Thielemans, K. Enhancing the t-cell stimulatory capacity of human dendritic cells by co-electroporation with CD40L, CD70 and constitutively active TLR4 encoding mRNA. Mol. Ther. 2008, 16, 1170–1180, doi:10.1038/mt.2008.77.

284. Figlin, R.A.; Tannir, N.M.; Uzzo, R.G.; Tykodi, S.S.; Chen, D.Y.T.; Master, V.; Kapoor, A.; Vaena, D.; Lowrance, W.; Bratslavsky, G.; et al. Results of the ADAPT Phase 3 Study of Rocapuldencel-T in Combination with Sunitinib as First-Line Therapy in Patients with Metastatic Renal Cell Carcinoma. Clin. Cancer Res. 2020, 26, 2327–2335, doi:10.1158/1078-0432.CCR-19-2427.

285. Wilgenhof, S.; Corthals, J.; Heirman, C.; Van Baren, N.; Lucas, S.; Kvistborg, P.; Thielemans, K.; Neyns, B. Phase II study of autologous monocyte-derived mRNA electroporated dendritic cells (TriMixDC-MEL) plus ipilimumab in patientswith pretreated advanced melanoma. J. Clin. Oncol. 2016, 34, 1330–1338, doi:10.1200/JCO.2015.63.4121.

286. De Keersmaecker, B.; Claerhout, S.; Carrasco, J.; Bar, I.; Corthals, J.; Wilgenhof, S.; Neyns, B.; Thielemans, K. TriMix and tumor antigen mRNA electroporated dendritic cell vaccination plus ipilimumab: Link between T-cell activation and clinical responses in advanced melanoma. J. Immunother. Cancer 2020, 8, 329, doi:10.1136/jitc-2019-000329.

287. Arance Fernandez, A.M.; Baurain, J.-F.; Vulsteke, C.; Rutten, A.; Soria, A.; Carrasco, J.; Neyns, B.; De Keersmaecker, B.; Van Assche, T.; Lindmark, B. A phase I study (E011-MEL) of a TriMix-based mRNA immunotherapy (ECI-006) in resected melanoma patients: Analysis of safety and immunogenicity. J. Clin. Oncol. 2019, 37, 2641–2641, doi:10.1200/jco.2019.37.15_suppl.2641.

288. Sahin, U.; Derhovanessian, E.; Miller, M.; Kloke, B.P.; Simon, P.; Löwer, M.; Bukur, V.; Tadmor, A.D.; Luxemburger, U.; Schrörs, B.; et al. Personalized RNA mutanome vaccines mobilize poly-specific therapeutic immunity against cancer. Nature 2017, 547, 222–226, doi:10.1038/nature23003.

289. Rittig, S.M.; Haentschel, M.; Weimer, K.J.; Heine, A.; Muller, M.R.; Brugger, W.; Horger, M.S.; Maksimovic, O.; Stenzl, A.; Hoerr, I.; et al. Intradermal vaccinations with RNA coding for TAA generate CD8 and CD4 immune responses and induce clinical benefit in vaccinated patients. Mol. Ther. 2011, 19, 990–999, doi:10.1038/mt.2010.289.

290. Weide, B.; Carralot, J.-P.; Reese, A.; Scheel, B.; Eigentler, T.K.; Hoerr, I.; Rammensee, H.-G.; Garbe, C.; Pascolo, S. Results of the First Phase I/II Clinical Vaccination Trial With Direct Injection of mRNA. J. Immunother. 2008, 31, 180–188, doi:10.1097/CJI.0b013e31815ce501.

291. Kranz, L.M.; Diken, M.; Haas, H.; Kreiter, S.; Loquai, C.; Reuter, K.C.; Meng, M.; Fritz, D.; Vascotto, F.; Hefesha, H.; et al. Systemic RNA delivery to dendritic cells exploits antiviral defence for cancer immunotherapy. Nature 2016, 534, 396–401, doi:10.1038/nature18300.

292. Grunwitz, C.; Salomon, N.; Vascotto, F.; Selmi, A.; Bukur, T.; Diken, M.; Kreiter, S.; Türeci, Ö.; Sahin, U. HPV16 RNA-LPX vaccine mediates complete regression of aggressively growing HPV-positive mouse tumors and establishes protective T cell memory. Oncoimmunology 2019, 8, e1629259, doi:10.1080/2162402X.2019.1629259.

293. Salomon, N.; Vascotto, F.; Selmi, A.; Vormehr, M.; Quinkhardt, J.; Bukur, T.; Schrörs, B.; Löewer, M.; Diken, M.; Türeci, Ö.; et al. A liposomal RNA vaccine inducing neoantigen-specific CD4+ T cells augments the antitumor activity of local radiotherapy in mice. Oncoimmunology 2020, 9, doi:10.1080/2162402X.2020.1771925.

294. Sahin, U.; Oehm, P.; Derhovanessian, E.; Jabulowsky, R.A.; Vormehr, M.; Gold, M.; Maurus, D.; Schwarck-Kokarakis, D.; Kuhn, A.N.; Omokoko, T.; et al. An RNA vaccine drives immunity in checkpoint-inhibitor-treated melanoma. Nature 2020, 585, 107–112, doi:10.1038/s41586-020-2537-9.

295. Cafri, G.; Gartner, J.J.; Zaks, T.; Hopson, K.; Levin, N.; Paria, B.C.; Parkhurst, M.R.; Yossef, R.; Lowery, F.J.; Jafferji, M.S.; et al. mRNA vaccine–induced neoantigen-specific T cell immunity in patients with gastrointestinal cancer. J. Clin. Invest. 2020, 130, 5976–5988, doi:10.1172/JCI134915.

296. Burris, H.A.; Patel, M.R.; Cho, D.C.; Clarke, J.M.; Gutierrez, M.; Zaks, T.Z.; Frederick, J.; Hopson, K.; Mody, K.; Binanti-Berube, A.; et al. A phase I multicenter study to assess the safety, tolerability, and immunogenicity of mRNA-4157 alone in patients with resected solid tumors and in combination with pembrolizumab in patients with unresectable solid tumors. J. Clin. Oncol. 2019, 37, 2523–2523, doi:10.1200/jco.2019.37.15_suppl.2523.

297. Maude, S.L.; Laetsch, T.W.; Buechner, J.; Rives, S.; Boyer, M.; Bittencourt, H.; Bader, P.; Verneris, M.R.; Stefanski, H.E.; Myers, G.D.; et al. Tisagenlecleucel in Children and Young Adults with B-Cell Lymphoblastic Leukemia. N. Engl. J. Med. 2018, 378, 439–448, doi:10.1056/NEJMoa1709866.

298. Neelapu, S.S.; Locke, F.L.; Bartlett, N.L.; Lekakis, L.J.; Miklos, D.B.; Jacobson, C.A.; Braunschweig, I.; Oluwole, O.O.; Siddiqi, T.; Lin, Y.; et al. Axicabtagene Ciloleucel CAR T-Cell Therapy in Refractory Large B-Cell Lymphoma. N. Engl. J. Med. 2017, 377, 2531–2544, doi:10.1056/NEJMoa1707447.

299. Foster, J.B.; Barrett, D.M.; Karikó, K. The Emerging Role of In Vitro-Transcribed mRNA in Adoptive T Cell Immunotherapy. Mol. Ther. 2019, 27, 747–756.

300. Maus, M. V.; Haas, A.R.; Beatty, G.L.; Albelda, S.M.; Levine, B.L.; Liu, X.; Zhao, Y.; Kalos, M.; June, C.H. T cells expressing chimeric antigen receptors can cause anaphylaxis in humans. Cancer Immunol. Res. 2013, 1, 26–31, doi:10.1158/2326-6066.CIR-13-0006.

301. Svoboda, J.; Rheingold, S.R.; Gill, S.I.; Grupp, S.A.; Lacey, S.F.; Kulikovskaya, I.; Suhoski, M.M.; Joseph Melenhorst, J.; Loudon, B.; Mato, A.R.; et al. Nonviral RNA chimeric antigen receptor–modified T cells in patients with Hodgkin lymphoma. Blood 2018, 132, 1022–1026, doi:10.1182/blood-2018-03-837609.

302. Cummins, K.D.; Frey, N.; Nelson, A.M.; Schmidt, A.; Luger, S.; Isaacs, R.E.; Lacey, S.F.; Hexner, E.; Melenhorst, J.J.; June, C.H.; et al. Treating Relapsed / Refractory (RR) AML with Biodegradable Anti-CD123 CAR Modified T Cells. Blood 2017, 130, 1359–1359, doi:10.1182/blood.V130.Suppl_1.1359.1359.

303. Tchou, J.; Zhao, Y.; Levine, B.L.; Zhang, P.J.; Davis, M.M.; Melenhorst, J.J.; Kulikovskaya, I.; Brennan, A.L.; Liu, X.; Lacey, S.F.; et al. Safety and efficacy of intratumoral injections of chimeric antigen receptor (CAR) T cells in metastatic breast cancer. Cancer Immunol. Res. 2017, 5, 1152–1161, doi:10.1158/2326-6066.CIR-17-0189.

304. Harrer, D.C.; Simon, B.; Fujii, S. ichiro; Shimizu, K.; Uslu, U.; Schuler, G.; Gerer, K.F.; Hoyer, S.; Dörrie, J.; Schaft, N. RNA-transfection of γ/δ T cells with a chimeric antigen receptor or an α/β T-cell receptor: A safer alternative to genetically engineered α/β T cells for the immunotherapy of melanoma. BMC Cancer 2017, 17, 551, doi:10.1186/s12885-017-3539-3.

305. Ang, W.X.; Ng, Y.Y.; Xiao, L.; Chen, C.; Li, Z.; Chi, Z.; Tay, J.C.K.; Tan, W.K.; Zeng, J.; Toh, H.C.; et al. Electroporation of NKG2D RNA CAR Improves Vγ9Vδ2 T Cell Responses against Human Solid Tumor Xenografts. Mol. Ther. - Oncolytics 2020, 17, 421–430, doi:10.1016/j.omto.2020.04.013.

306. Simon, B.; Wiesinger, M.; März, J.; Wistuba-Hamprecht, K.; Weide, B.; Schuler-Thurner, B.; Schuler, G.; Dörrie, J.; Uslu, U. The Generation of CAR-Transfected Natural Killer T Cells for the Immunotherapy of Melanoma. Int. J. Mol. Sci. 2018, 19, 2365, doi:10.3390/ijms19082365.

307. Boissel, L.; Betancur, M.; Lu, W.; Wels, W.S.; Marino, T.; Van Etten, R.A.; Klingemann, H. Comparison of mRNA and lentiviral based transfection of natural killer cells with chimeric antigen receptors recognizing lymphoid antigens. Leuk. Lymphoma 2012, 53, 958–965, doi:10.3109/10428194.2011.634048.

308. Shimasaki, N.; Fujisaki, H.; Cho, D.; Masselli, M.; Lockey, T.; Eldridge, P.; Leung, W.; Campana, D. A clinically adaptable method to enhance the cytotoxicity of natural killer cells against B-cell malignancies. Cytotherapy 2012, 14, 830–840, doi:10.3109/14653249.2012.671519.

309. Xiao, L.; Cen, D.; Gan, H.; Sun, Y.; Huang, N.; Xiong, H.; Jin, Q.; Su, L.; Liu, X.; Wang, K.; et al. Adoptive Transfer of NKG2D CAR mRNA-Engineered Natural Killer Cells in Colorectal Cancer Patients. Mol. Ther. 2019, 27, 1114–1125, doi:10.1016/j.ymthe.2019.03.011.

310. Guevara, M.L.; Persano, F.; Persano, S. Advances in Lipid Nanoparticles for mRNA-Based Cancer Immunotherapy. Front. Chem. 2020, 8, 589959.

311. Thran, M.; Mukherjee, J.; Pönisch, M.; Fiedler, K.; Thess, A.; Mui, B.L.; Hope, M.J.; Tam, Y.K.; Horscroft, N.; Heidenreich, R.; et al. mRNA mediates passive vaccination against infectious

agents, toxins, and tumors. EMBO Mol. Med. 2017, 9, 1434–1447, doi:10.15252/emmm.201707678.

312. Rybakova, Y.; Kowalski, P.S.; Huang, Y.; Gonzalez, J.T.; Heartlein, M.W.; DeRosa, F.; Delcassian, D.; Anderson, D.G. mRNA Delivery for Therapeutic Anti-HER2 Antibody Expression In Vivo. Mol. Ther. 2019, 27, 1415–1423, doi:10.1016/j.ymthe.2019.05.012.

313. Waldmann, T.A. Cytokines in cancer immunotherapy. Cold Spring Harb. Perspect. Biol. 2018, 10, a028472, doi:10.1101/cshperspect.a028472.

314. Patel, M.R.; Bauer, T.M.; Jimeno, A.; Wang, D.; LoRusso, P.; Do, K.T.; Stemmer, S.M.; Maurice-Dror, C.; Geva, R.; Zacharek, S.; et al. A phase I study of mRNA-2752, a lipid nanoparticle encapsulating mRNAs encoding human OX40L, IL-23, and IL-36γ, for intratumoral (iTu) injection alone and in combination with durvalumab. J. Clin. Oncol. 2020, 38, 3092–3092, doi:10.1200/jco.2020.38.15_suppl.3092.

315. Levin, N.; Weinstein-Marom, H.; Pato, A.; Itzhaki, O.; Besser, M.J.; Eisenberg, G.; Peretz, T.; Lotem, M.; Gross, G. Potent Activation of Human T Cells by mRNA Encoding Constitutively Active CD40. J. Immunol. 2018, 201, 2959–2968, doi:10.4049/jimmunol.1701725.

316. Weinstein-Marom, H.; Levin, N.; Pato, A.; Shmuel, N.; Sharabi-Nov, A.; Peretz, T.; Eisenberg, G.; Lotem, M.; Itzhaki, O.; Besser, M.J.; et al. Combined Expression of Genetic Adjuvants Via mRNA Electroporation Exerts Multiple Immunostimulatory Effects on Antitumor T Cells. J. Immunother. 2019, 42, 43–50, doi:10.1097/CJI.0000000000000252.

317. Haabeth, O.A.W.; Blake, T.R.; McKinlay, C.J.; Tveita, A.A.; Sallets, A.; Waymouth, R.M.; Wender, P.A.; Levy, R. Local delivery of OX40L, CD80, and CD86 mRNA kindles global anticancer immunity. Cancer Res. 2019, 79, 1624–1634, doi:10.1158/0008-5472.CAN-18-2867.

318. Van Lint, S.; Renmans, D.; Broos, K.; Goethals, L.; Maenhout, S.; Benteyn, D.; Goyvaerts, C.; Du Four, S.; Van Der Jeught, K.; Bialkowski, L.; et al. Intratumoral delivery of TriMix mRNA results in T-cell activation by cross-presenting dendritic cells. Cancer Immunol. Res. 2016, 4, 146–156, doi:10.1158/2326-6066.CIR-15-0163.

319. Jimeno, A.; Gupta, S.; Sullivan, R.; Do, K.T.; Akerley, W.L.; Wang, D.; Teoh, D.; Schalper, K.; Zacharek, S.J.; Sun, J.; et al. Abstract CT032: A phase 1/2, open-label, multicenter, dose escalation and efficacy study of mRNA-2416, a lipid nanoparticle encapsulated mRNA encoding human OX40L, for intratumoral injection alone or in combination with durvalumab for patients with advanc.; American Association for Cancer Research (AACR), 2020; pp. CT032–CT032.

320. Trepotec, Z.; Lichtenegger, E.; Plank, C.; Aneja, M.K.; Rudolph, C. Delivery of mRNA Therapeutics for the Treatment of Hepatic Diseases. Mol. Ther. 2019, 27, 794–802.

321. Sahu, I.; Haque, A.K.M.A.; Weidensee, B.; Weinmann, P.; Kormann, M.S.D. Recent Developments in mRNA-Based Protein Supplementation Therapy to Target Lung Diseases. Mol. Ther. 2019, 27, 803–823, doi:10.1016/j.ymthe.2019.02.019.

322. Magadum, A.; Kaur, K.; Zangi, L. mRNA-Based Protein Replacement Therapy for the Heart. Mol. Ther. 2019, 27, 785–793, doi:10.1016/j.ymthe.2018.11.018.

323. Lescan, M.; Perl, R.M.; Golombek, S.; Pilz, M.; Hann, L.; Yasmin, M.; Behring, A.; Keller, T.; Nolte, A.; Gruhn, F.; et al. De Novo Synthesis of Elastin by Exogenous Delivery of Synthetic

Modified mRNA into Skin and Elastin-Deficient Cells. Mol. Ther. - Nucleic Acids 2018, 11, 475–484, doi:10.1016/j.omtn.2018.03.013.

324. Baba, M.; Itaka, K.; Kondo, K.; Yamasoba, T.; Kataoka, K. Treatment of neurological disorders by introducing mRNA in vivo using polyplex nanomicelles. J. Control. Release 2015, 201, 41–48, doi:10.1016/j.jconrel.2015.01.017.

325. Jirikowski, G.F.; Sanna, P.P.; Maciejewski-Lenoir, D.; Bloom, F.E. Reversal of diabetes insipidus in Brattleboro tats: Intrahypothalamic injection of vasopressin mRNA. Science (80-.). 1992, 255, 996–998, doi:10.1126/science.1546298.

326. DeRosa, F.; Guild, B.; Karve, S.; Smith, L.; Love, K.; Dorkin, J.R.; Kauffman, K.J.; Zhang, J.; Yahalom, B.; Anderson, D.G.; et al. Therapeutic efficacy in a hemophilia B model using a biosynthetic mRNA liver depot system. Gene Ther. 2016, 23, 699–707, doi:10.1038/gt.2016.46.

327. Zhu, X.; Yin, L.; Theisen, M.; Zhuo, J.; Siddiqui, S.; Levy, B.; Presnyak, V.; Frassetto, A.; Milton, J.; Salerno, T.; et al. Systemic mRNA Therapy for the Treatment of Fabry Disease: Preclinical Studies in Wild-Type Mice, Fabry Mouse Model, and Wild-Type Non-human Primates. Am. J. Hum. Genet. 2019, 104, 625–637, doi:10.1016/j.ajhg.2019.02.003.

328. An, D.; Schneller, J.L.; Frassetto, A.; Liang, S.; Zhu, X.; Park, J.S.; Theisen, M.; Hong, S.J.; Zhou, J.; Rajendran, R.; et al. Systemic Messenger RNA Therapy as a Treatment for Methylmalonic Acidemia. Cell Rep. 2017, 21, 3548–3558, doi:10.1016/j.celrep.2017.11.081.

329. Jiang, L.; Park, J.S.; Yin, L.; Laureano, R.; Jacquinet, E.; Yang, J.; Liang, S.; Frassetto, A.; Zhuo, J.; Yan, X.; et al. Dual mRNA therapy restores metabolic function in long-term studies in mice with propionic acidemia. Nat. Commun. 2020, 11, 1–10, doi:10.1038/s41467-020-19156-3.

330. Jiang, L.; Berraondo, P.; Jericó, D.; Guey, L.T.; Sampedro, A.; Frassetto, A.; Benenato, K.E.; Burke, K.; Santamaría, E.; Alegre, M.; et al. Systemic messenger RNA as an etiological treatment for acute intermittent porphyria. Nat. Med. 2018, 24, 1899–1909, doi:10.1038/s41591-018-0199-z.

331. Prieve, M.G.; Harvie, P.; Monahan, S.D.; Roy, D.; Li, A.G.; Blevins, T.L.; Paschal, A.E.; Waldheim, M.; Bell, E.C.; Galperin, A.; et al. Targeted mRNA Therapy for Ornithine Transcarbamylase Deficiency. Mol. Ther. 2018, 26, 801–813, doi:10.1016/j.ymthe.2017.12.024.

332. Robinson, E.; MacDonald, K.D.; Slaughter, K.; McKinney, M.; Patel, S.; Sun, C.; Sahay, G. Lipid Nanoparticle-Delivered Chemically Modified mRNA Restores Chloride Secretion in Cystic Fibrosis. Mol. Ther. 2018, 26, 2034–2046, doi:10.1016/j.ymthe.2018.05.014.

333. Jauze, L.; Monteillet, L.; Mithieux, G.; Rajas, F.; Ronzitti, G. Challenges of Gene Therapy for the Treatment of Glycogen Storage Diseases Type I and Type III. Hum. Gene Ther. 2019, 30, 1263–1273, doi:10.1089/hum.2019.102.

334. Li, Z.; Zhao, P.; Zhang, Y.; Wang, J.; Wang, C.; Liu, Y.; Yang, G.; Yuan, L. Exosome-based Ldlr gene therapy for familial hypercholesterolemia in a mouse model. Theranostics 2021, 11, 2953–2965, doi:10.7150/THNO.49874.

335. Carlsson, L.; Clarke, J.C.; Yen, C.; Gregoire, F.; Albery, T.; Billger, M.; Egnell, A.C.; Gan, L.M.; Jennbacken, K.; Johansson, E.; et al. Biocompatible, Purified VEGF-A mRNA Improves Cardiac

Function after Intracardiac Injection 1 Week Post-myocardial Infarction in Swine. Mol. Ther. - Methods Clin. Dev. 2018, 9, 330–346, doi:10.1016/j.omtm.2018.04.003.

336. Anttila, V.; Saraste, A.; Knuuti, J.; Jaakkola, P.; Hedman, M.; Svedlund, S.; Lagerström-Fermér, M.; Kjaer, M.; Jeppsson, A.; Gan, L.M. Synthetic mRNA Encoding VEGF-A in Patients Undergoing Coronary Artery Bypass Grafting: Design of a Phase 2a Clinical Trial. Mol. Ther. - Methods Clin. Dev. 2020, 18, 464–472, doi:10.1016/j.omtm.2020.05.030.

337. Gan, L.-M.; Lagerström-Fermér, M.; Carlsson, L.G.; Arfvidsson, C.; Egnell, A.-C.; Rudvik, A.; Kjaer, M.; Collén, A.; Thompson, J.D.; Joyal, J.; et al. Intradermal delivery of modified mRNA encoding VEGF-A in patients with type 2 diabetes. Nat. Commun. 2019, 10, 871, doi:10.1038/s41467-019-08852-4.

338. García-Cazorla, A. Propionic Acidemia. Encycl. Mov. Disord. 2010, 485–488, doi:10.1016/B978-0-12-374105-9.00373-7.

339. Ohura, T. Methylmalonic acidemia. Tanpakushitsu Kakusan Koso. 1988, 33, 579–584.

340. Brassier, A.; Gobin, S.; Arnoux, J.B.; Valayannopoulos, V.; Habarou, F.; Kossorotoff, M.; Servais, A.; Barbier, V.; Dubois, S.; Touati, G.; et al. Long-term outcomes in Ornithine Transcarbamylase deficiency: A series of 90 patients. Orphanet J. Rare Dis. 2015, 10, 58.

341. Translate Bio Inc. Translate Bio Announces Pipeline Program Update Available online: https://investors.translate.bio/node/7121/ (accessed on Jan 3, 2022).

342. Zuckerman, J.; McCoy, K.; Schechter, M..; Dorgan, D.; Jain, M.; MacDonald, K.; Callison, C.; Walker, S.; Bodie, S.; Barbier, A.; et al. Safety and Tolerability of a Single Dose of MRT5005, a Nebulized CFTR mRNA Therapeutic, in Adult CF Patients. Pediatr. Pulmonol. 2019, 54, 350.

343. Translate Bio Inc. Results from Second Interim Data Analysis from Ongoing Phase 1 / 2 Clinical Trial of MRT5005 in Patients with Cystic Fibrosis (CF) was generally consistent with that previously reported for the 8 , 16 and 24 mg dose groups. Available online: https://investors.translate.bio/node/7886 (accessed on Jan 3, 2022).


PATENT

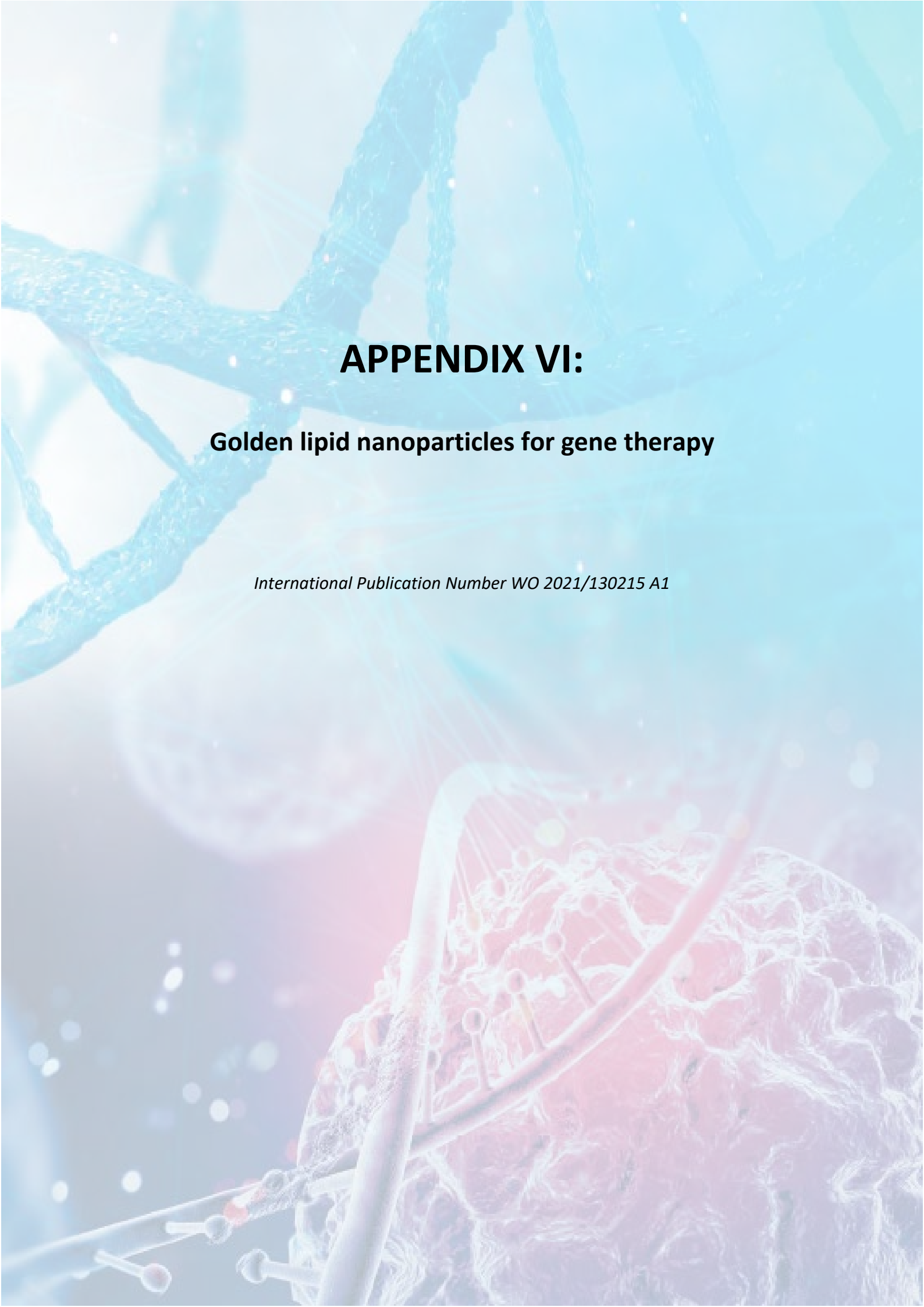

APPENDIX VI:

Golden lipid nanoparticles for gene therapy

International Publication Number WO 2021/130215 A1

(12) INTERNATIONAL APPLICATION PUBLISHED UNDER THE PATENT COOPERATION TREATY (PCT)

(19) World Intellectual Property Organization
International Bureau

(43) International Publication Date
01 July 2021 (01.07.2021)

WIPO | PCT

(10) International Publication Number
WO 2021/130215 A1

(51) International Patent Classification:
A61K 9/51 (2006.01) *C12N 15/87* (2006.01)
A61K 48/00 (2006.01) *B82Y 5/00* (2011.01)

(21) International Application Number:
PCT/EP2020/087608

(22) International Filing Date:
22 December 2020 (22.12.2020)

(25) Filing Language: English

(26) Publication Language: English

(30) Priority Data:
19383183.1 23 December 2019 (23.12.2019) EP

(71) Applicant: **UNIVERSIDAD DEL PAÍS VASCO/EUSKAL HERRIKO UNIBERTSITATEA** [ES/ES]; Barrio Sarriena, s/n, E-48940 Leioa, Vizcaya (ES).

(72) Inventors: **DEL POZO RODRÍGUEZ, Ana**; FACULTAD DE FARMACIA/FARMAZIA FAKULTATEA UPV/EHU, Paseo de la Universidad, 7, E-01006 Vitoria-Gasteiz (ES). **RODRÍGUEZ GASCÓN, Alicia**; FACULTAD DE FARMACIA/FARMAZIA FAKULTATEA UPV/EHU, Paseo de la Universidad, 7, E-01006 Vitoria-Gasteiz (ES). **GÓMEZ AGUADO, Itziar**; FACULTAD DE FARMACIA/FARMAZIA FAKULTATEA UPV/EHU, Paseo de la Universidad, 7, E-01006 Vitoria-Gasteiz (ES). **VICENTE PASCUAL, Mónica**; FACULTAD DE FARMACIA/FARMAZIA FAKULTATEA UPV/EHU, Paseo de la Universidad, 7, E-01006 Vitoria-Gasteiz (ES). **SOLINÍS ASPIAZU, María Ángeles**; FACULTAD DE FARMACIA/FARMAZIA FAKULTATEA UPV/EHU, Paseo de la Universidad, 7, E-01006 Vitoria-Gasteiz (ES).

(74) Agent: **ABG INTELLECTUAL PROPERTY LAW, S.L.**; Avda. de Burgos, 16D, Edificio EUROMOR, E-28036 Madrid (ES).

(81) Designated States *(unless otherwise indicated, for every kind of national protection available)*: AE, AG, AL, AM, AO, AT, AU, AZ, BA, BB, BG, BH, BN, BR, BW, BY, BZ, CA, CH, CL, CN, CO, CR, CU, CZ, DE, DJ, DK, DM, DO, DZ, EC, EE, EG, ES, FI, GB, GD, GE, GH, GM, GT, HN, HR, HU, ID, IL, IN, IR, IS, IT, JO, JP, KE, KG, KH, KN, KP, KR, KW, KZ, LA, LC, LK, LR, LS, LU, LY, MA, MD, ME, MG, MK, MN, MW, MX, MY, MZ, NA, NG, NI, NO, NZ, OM, PA, PE, PG, PH, PL, PT, QA, RO, RS, RU, RW,

(54) Title: GOLDEN LIPID NANOPARTICLES FOR GENE THERAPY

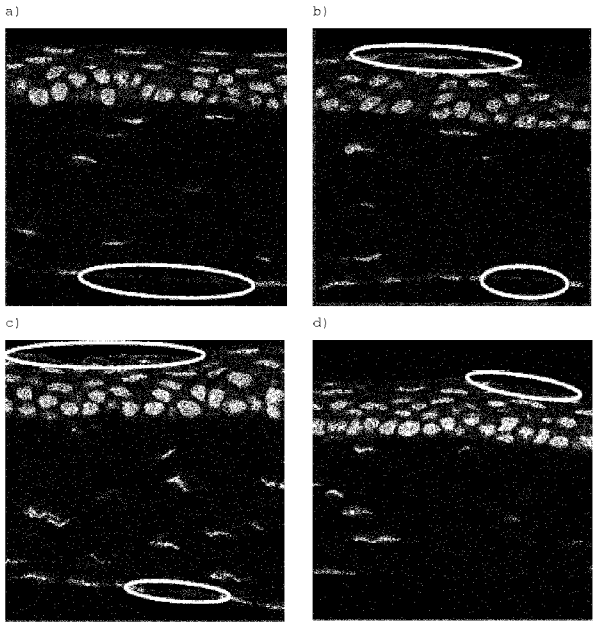

Figure 3

(57) Abstract: The invention provides solid lipid nanoparticles (SLNs) which comprise gold, and are useful as vectors for the transfection of different types of nucleic acids. Different methods for obtaining such SLNs are also disclosed.

WO 2021/130215 A1

[Continued on next page]

SA, SC, SD, SE, SG, SK, SL, ST, SV, SY, TH, TJ, TM, TN, TR, TT, TZ, UA, UG, US, UZ, VC, VN, WS, ZA, ZM, ZW.

(84) **Designated States** *(unless otherwise indicated, for every kind of regional protection available)*: ARIPO (BW, GH, GM, KE, LR, LS, MW, MZ, NA, RW, SD, SL, ST, SZ, TZ, UG, ZM, ZW), Eurasian (AM, AZ, BY, KG, KZ, RU, TJ, TM), European (AL, AT, BE, BG, CH, CY, CZ, DE, DK, EE, ES, FI, FR, GB, GR, HR, HU, IE, IS, IT, LT, LU, LV, MC, MK, MT, NL, NO, PL, PT, RO, RS, SE, SI, SK, SM, TR), OAPI (BF, BJ, CF, CG, CI, CM, GA, GN, GQ, GW, KM, ML, MR, NE, SN, TD, TG).

Published:

— *with international search report (Art. 21(3))*

— *before the expiration of the time limit for amending the claims and to be republished in the event of receipt of amendments (Rule 48.2(h))*

EUSKERAZKO BERTSIOA

1. ATALA: SARRERA

1. SARRERA

1.1. Gene-terapiako sendagaiak

Medikamentuen Europako Agentziaren (EMA ingelesezko sigletan) arabera, gene terapiako sendagaitzat hartzen da, sekuentzia genetiko ezagun bat erregulatzeko, konpontzeko, eransteko edo ezabatzeko helburuarekin administratzen den produktu bat, zeinak transgene (sekuentzia terapeutikoa) espezifiko bat adierazten duen osagai genetikoa garraiatzen duena, eta bektore, askapen-formulazio edo sistema batez osatuta dagoena [1]. Hala ere, zientifikoki kontzeptu zabalagoa onartu ohi da, eta gene-terapiak edozein azido nukleiko duten produktuen aplikazio terapeutikoa barne hartzen du.

Gene-terapia erabiltzen denean, azido nukleikoen transferentzia klinikoa bi modutan egin ohi da: *ex vivo* edo *in vivo* (1. irudia). *Ex vivo* gene-terapian, zelulak pazientetik edo emaile batetik atera ondoren, laborategian *in vitro* modifikatzen dira azido nukleiko terapeutikoarekin, eta jarraian, pazienteari administratzen zaizkio. *In vivo* gene-terapian, aldiz, azido nukleiko terapeutikoa duen bektorea pazienteri zuzenean administratzen zaio [2].

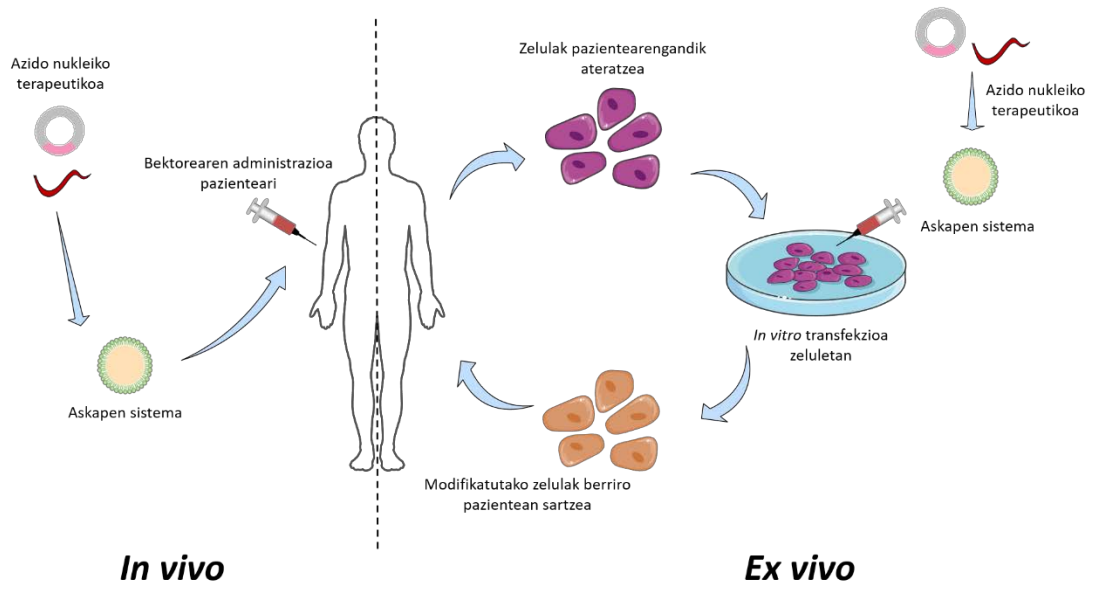

1. irudia. Gene-terapiaren in vivo eta ex vivo erabileraren eskema adierazgarria.

Tratamenduaren helburuaren arabera, gene-terapia gehikuntza genikorako, genea isiltzeko edo editatzeko erabili daiteke (2. Irudia) [3]. Horretarako, azido nukleiko mota desberdinak erabiltzen dira sendagai berrien garapena bideratzeko. DNAek eta RNA mezulariek (RNAm) proteinak adierazten dituzte; interferentzia RNA txikiek (siRNA ingelesezko sigletan), mikroRNAek, oligonukleotidoek edota aptameroek, aldiz, itzulpen prozesuaren gene-isiltzea ahalbidetzen dute [4]. Guraize molekularretan edo nukleasetan oinarritutako estrategiak ere

garatzen ari dira; hala nola, zink-hatz nukleasak (ZFN ingelesezko sigletan), transkripzio-aktibatzaile moduko nukleasak (TALEN ingelesezko sigletan), eta aldizka banandutako sekuentzia palindromiko motzak elkartuta dituzten nukleasak (CRISPR/Cas9 ingelesezko sigletan).

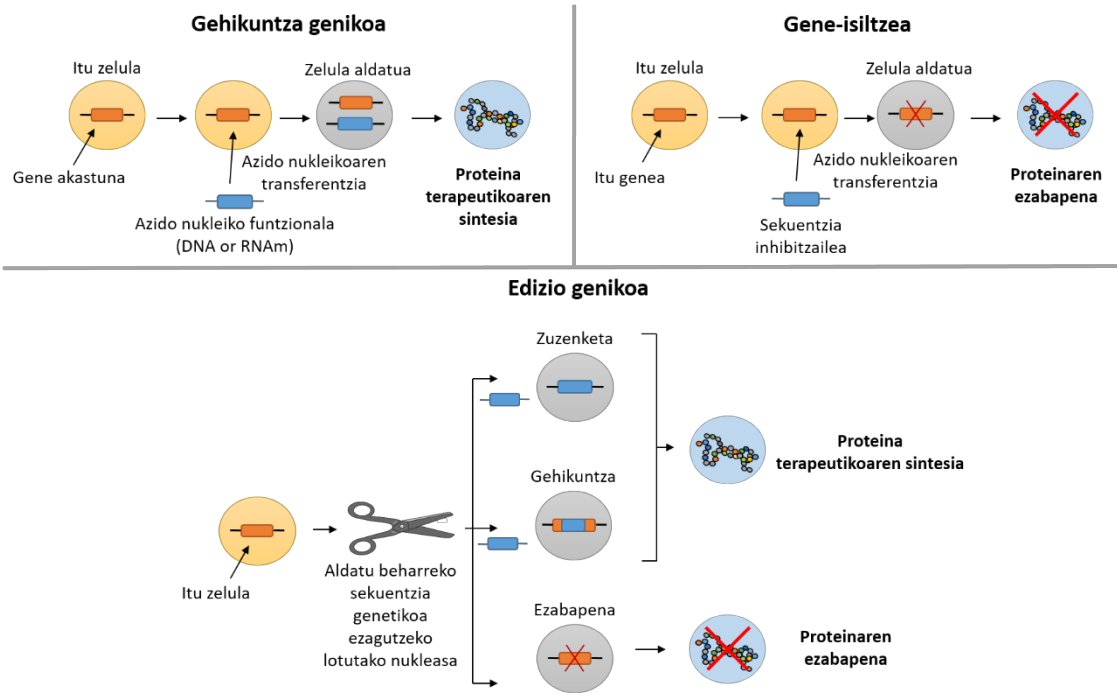

2. irudia. Gene-terapiaren estrategia desberdinen eskema adierazgarria, tratamenduaren helburuaren arabera.

Gehikuntza genikoa proteina terapeutikoa adierazten duen azido nukleikoaren (DNA edo RNAm) kopia funtzionalen administrazioa da. Tradizionalki, gehikuntza proteikoa DNA plasmidikoaren (DNAp) bidez zuzendua izan da, baina RNAm-ren bidezko terapiak arreta handia irabazi du azken urteetan eta, haren ezaugarri espezifikoei esker, DNAp-n oinarritutako terapiaren aurrean etorkizun handiko alternatiba bihurtu da. Lehenik, RNAm-k ez du nukleoaren makineria behar funtzionala izateko, DNAp bidezko terapiak ordea, bai [5–8]. Beraz, behin RNAm zitoplasmara iristean, kodetzen duen proteinaren itzulpena hasten da, eta zelula mitotikoetan eta ez-mitotikoetan eraginkorra da [9–11]. Bigarrenik, RNAm-k segurtasun-profil hobea du, ez baita ostalariaren genoman integratzen, eta, horrela, kartzinogenesi eta mutagenesi arriskuak murrizten dira [5–8,11]. Hirugarrenik, RNAm-k kodetzen duen proteinaren sintesia azkarra da eta bere adierazpena behin-behinekoa [6,9]. Proteinaren adierazpena transfektatu eta lehen orduan detektatu daiteke, adierazpen maximoa 5-7 ordu geroago lortzen da [12]. Azkenik, *in vitro* transkribatutako RNAm-aren (IVT RNAm) ekoizpena DNArena baino errazagoa da, eta estandarizatu daiteke bere erreproduzigarritasuna mantenduz [7].

Izan ere, RNAm bidezko terapiak arreta handia irabazi du SARS-CoV-2 koronabirusaren aurkako txertaketan aplikatu ondoren [13–15]. Nabarmentzekoa da COVID-19aren pandemian, EMAk eta Ameriketako Estatu Batuetako Elikagaien eta Sendagaien Administrazioak (FDA) SARS-CoV-2aren aurka onartutako lehen txertoak RNAm eta nanopartikula lipidikoetan oinarritutakoak izan zirela [16,17]. RNAm txerto horiek ondo onartu dira eta COVID-19aren aurkako % 95eko eraginkortasuna erakutsi dute, albo-ondorio gutxirekin [18,19].

Hala ere, IVT RNAm-ren erabilera klinikoa mugatua izan da bere ezegonkortasun fisikoagatik, bere immunogenizitateagatik eta zelulen mintza zeharkatzeko zailtasunengatik, RNAm molekulen izaera anionikoa dela eta [8,20,21]. RNAm-ren egitura ezagutzeak hainbat aldaketak bultzatu ditu itzulpenaren egonkortasuna eta eraginkortasuna hobetzeko eta immunogenizitatea murrizteko; hala ere, optimizatua dagoen IVT RNAm-k, kanpoko eta barneko hainbat zelula-hesiak gainditu behar ditu oraindik.

Azido nukleikoak nanosistema egokietan formulatzea sarritan beharrezkoa da kanpoko eta barneko zelula-hesiak gainditzeko. Hirugarren irudiak adierazten duenez, azido nukleikodun nanosistemek hainbat oztopo gainditu behar dituzte zelularen barnean bere ituraino iristeko: kanpoko zelularen ingurunea eta mintz zelularra gainditzea, zelula barnetik barreiatzea, besikula endozitikoetatik (endosometatik) ihes egitea, eta DNAren kasuan baita nukleo-mintza zeharkatzea ere [7,22].

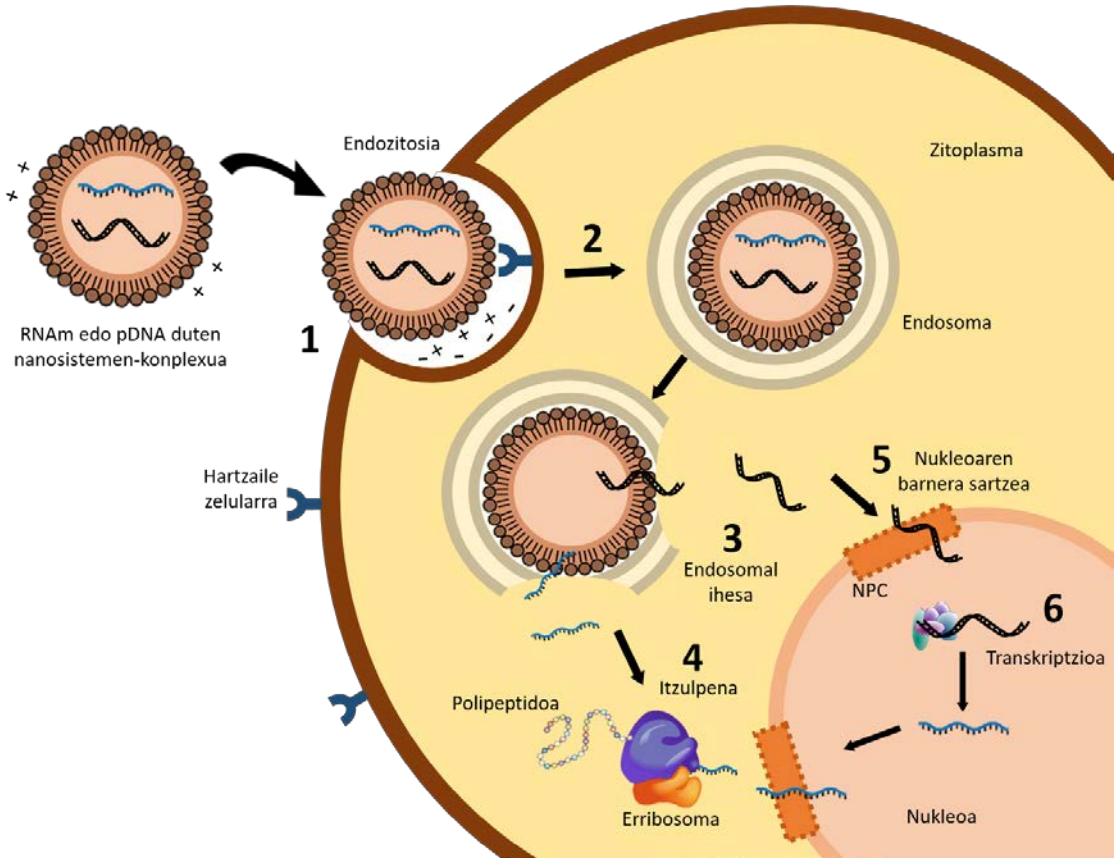

3. irudia. Azido nukleikoak administratzeko oinarritutako askapen sistemek zelula-barnean gainditu beharreko hesiak: (1) askapen sistemen eta mintz zelularren arteko elkarrekintza, (2) endozitosia, (3) endosometatik ihesa eta azido nukleikoaren askapena zitoplasman, (4) RNAm-ren itzulpena, (5) nukleoaren barnera sartzea, eta (6) DNAren transkripzioa RNAm lortzeko, zitoplasman askatu eta RNAm-ren itzulpena. Moldatua: I Gómez-Aguado, J. Rodríguez-Castejón, M. Vicente-Pascual, et al. Nanomedicines to Deliver mRNA: State of the Art and Future Perspectives. Nanomaterials 2020, 10, 364; https://doi.org/10.3390/nano10020364.

Azido nukleikoaren internalizazio eraginkor baten lehen urratsa askapen sistemaren eta mintz zelularraren arteko elkarrekintzan datza. Zelularen gainazalarekiko atxikimendua nanosistemaren eta zelula-mintzaren azaleraren arteko elkarrekintza elektrostatikoen bidez gerta daiteke, zeina izaera kationikoa aurkezten duten sistemei faboratuta dagoen [23]. Elkarrekintza hori bektoreetan estekatzaile desberdinak gehituz hobe daiteke, zelula-mintzaren gainazaleko hartzaileekin lotzeko gaitasuna handitzeko [24,25].

Zelulan sartzeko mekanismo nagusia endozitosi prozesua da. Material genetikoak zelularen barnean duen igarobidea baldintzatzen duten prozesu konplexuen multzoa da. Bektoreak mintz zelularraren inbaginazioaren ondorioz sortutako endosomaren barnean geratzen dira. Endosomak lisosomarekin bat egiten du, eta bertako entzima hidrolitikoek bektorea eta azido nukleikoa degradatu ditzakete. Degradazioa ekiditeko, endosomatik ihes egitea ezinbestekoa da, eta hori ahalbidetzeko, internalizazio zelularraren kasuan bezala, askapen-sistemak berebiziko paper erabakigarria jokatzen du. Endosometatik ihesa eman dadin proposaturiko

mekanismo nagusienak endosomaren haustura, garraio aktiboa, edo askapen sistemaren eta endosomaren mintzaren arteko fusioa dira [26]. Hala ere, Patel et al.ek berriki identifikatu dute endosoma/lisosoma berantiarren formazioa funtsezkoa dela RNAm exogenoaren askapen funtzionala lortzeko [27].

1.1.1. Azido nukleikoak administratzeko askapen sistemak

Azido nukleikodun produktuak klinikan aplikatzeko, funtsezko erronka da askapen sistemak terapiaren helburu espezifikoetara egokitzea. Garraiatzaileak material genetikoaren babesa eta itu-zelulara heltzeko espezifikotasuna bermatu behar ditu. Horrez gain, garraiatzaileak azido nukleikoari zelula-barneko disposizio egokia eman behar dio itzulpen prozesua ahalbidetzearren. Hori guztia erantzun immunologikoa aktibatu gabe [28,29].

Gaur egun, azido nukleikoak administratzeko sistemekin egindako entsegu klinikoen %70etan birus birkonbinatuak erabiltzen dituzte askapen sistema gisa; hala nola, retrobirusak (RV), lentibirusak (LV), adenobirusak (AdV) eta birus adenoasoziatuak (AAV), besteak beste [30]. Sistema biralak genetikoki eraldatutako birusak dira, ostalariaren zeluletan erreplikaziorako gaitasuna saihesteko; transfekzio ahalmen handia dute, baina baita potentzial onkogenikoa eta immunogenikoa ere. Gainera, bektore biralek garraiatu dezaketen azido nukleikoaren tamaina mugatua da [31]. Bektore biralekin DNAren askapenean aurrerapen handiak lortu badira ere, haiek ez dute paper garrantzitsua jokatzen RNAm-dun produktuen kasuan [7,32–35]. Sistema ez-biralak birusak baino seguruagoak, ekonomikoagoak eta gaitzesgarriagoak dira, ekoizpen sinpleagoa dute eta bildu beharreko azido nukleikoen tamaina ez da oztopo izaten normalean. Hala ere, haien transfekzio eraginkortasuna oraindik muga bat da, nahiz eta estrategia desberdinekin nabarmenki hobetu den eta ahaleginak egiten ari diren hura hobetzeko [32,34,36].

Askapen sistema baten laguntzarik gabeko azido nukleikoen aplikazio terapeutiko zuzenak, desabantaila garrantzitsuak aurkezten ditu [37]. Azido nukleiko biluziak *ex vivo* aplikatu dira nagusiki metodo fisikoak erabiliz; besteak beste, elektroporazioa, mikroinjekzioa eta gene pistola (gene gun ingelesez). Metodo horiek zelula-mintza desegiteko gai dira, zelulan material genetikoaren sarrera errazteko [38]. Elektroporazioa pultsu elektrikoen bidez zelula-mintzetan poroak sortzean datza. Teknika honek RNAm-ren askapen eraginkorra erakutsi du zelula dendritikoetan (DC ingelesezko sigletan) tumore-antigenoak kargatzeko [39], besteak beste. Gainera, RNAm-ren elektroporazioa DNArena baino eraginkorragoa dela demonstratu da entsegu batzuetan, *in vivo* proteinaren adierazpen azkarragoak eta homogeneoagoak lortzen baitira [40]. Mikroinjekzioa itu-zeluletan mikro-orratzen bidezko azido nukleikoen injekzio

zuzenean datza [41,42], eta gene pistola, aldiz, material genetiko biluzia itu-zeluletara pneumatikoki tiro eginez administratzen da [43–46]. Azido nukleikoen aplikazioa *in vivo* ebaluatu izan da, administrazio sistemikoa eta tokiko-administrazioa erabiliz. Nukleasek bena-barneko administrazioaren bitartez emandako azido nukleiko biluziak degradatzen dituzte eta berezko sistema immunea aktiba dezakete. Tokiko injekzioak; hala nola, azalpeko injekzioa, muskulu barneko injekzioa edo nodulu barruko injekzioa, berriz, baliagarriak izan dira RNAm biluzia askatzeko, batez ere sistema immunologikoa aktibatzea eta proteina kopuru txikia behar direnean, txertaketan gertatzen den bezala [47].

Gaur egun, nanogarraiatzaile kimikoak RNAm askapen sistemen ikerkuntza farmazeutikoaren abangoardian daude, DNA-aren askapenean oinarritutako sistemekin konparatuz, non sistema biralak erabilienak diren. Zientzia materialetan, nanoteknologian eta azido nukleikoen kimikan izandako aurrerapenei esker, gaur egun lan ugari egiten ari dira sistema berriak garatzearren [39]. Nanogarraiatzaile kimikoak osagai biokimiko sintetiko edo naturalen bidez eratuta daude, eta konposizioan, tamainan, forman eta ezaugarri fisiko-kimiko desberdinak dituzten sistema desberdinak aurki daitezke. Azido nukleikoak degradaziotik eta denaturalizaziotik babesteaz gain, sistema kimikoek transfekzio prozesua erraztu beharko lukete, aldi berean toxikotasuna eta erantzun immunologikoak ahalik eta gehien minimizatuz [48]. Gainera, askapen sistema horiek baliagarriak izan litezke substantzia aktiboaren askapen-profila programatzeko, profil farmakozinetikoa hobetzeko, organo/ehun osasuntsuen toxikotasuna murrizteko eta odol-zirkulazioan mantentzen diren denbora handitzeko [28,49]. Laugarren irudian ikus daitekeen bezala, azido nukleikoen garraiatzaileek hainbat forma biltzen dituzte, besteak beste, sistema lipidikoak, polimerikoak eta polipeptidikoak, dendrimeroak, urrezko nanopartikulak eta sistema hibridoak. Azido nukleikoen ezaugarrietara egokitutako askapen sistemen espezifikoen diseinua beharrezkoa da material genetikoa babesteko eta zelula-barneko disposizio egokia izateko, azkenik, transfekzio prozesua faboratu ahal izateko. Ezagutzan aurrera egin ahala eta nanomaterial berriak diseinatzeko lanabes berrien erabilgarritasuna handitzen den heinean, formulazio-estrategia berriek profil farmakologikoak hobetuko dituztela espero da, horrela, RNAm-ren erabilgarritasuna zabalduz.

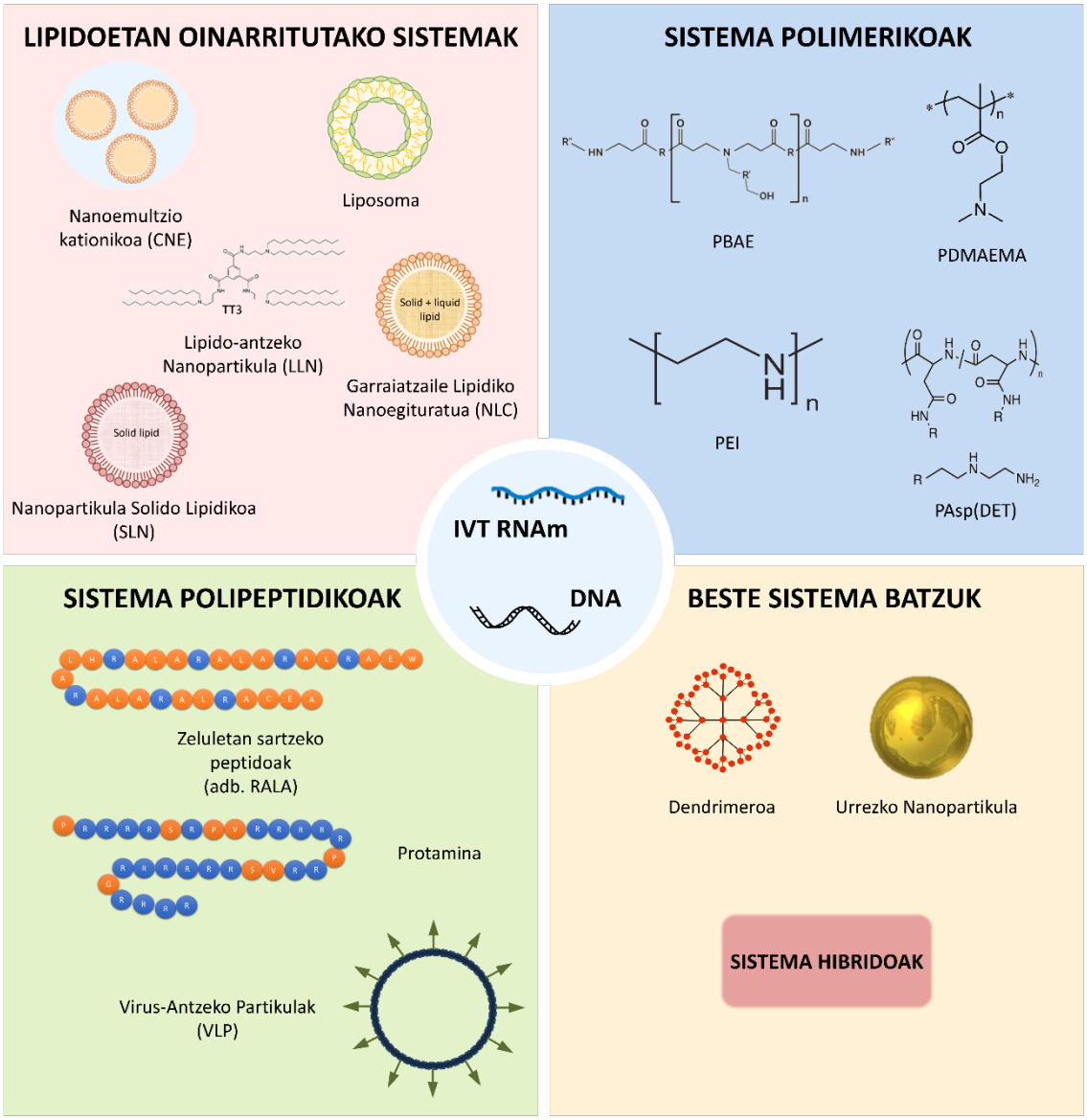

4. irudia. Azido nukleikoen askapenerako nanogarraiatzaile kimikoen eskema. PBAE: poly(β-amino ester); PDMAEMA: poly(2-dimethylaminoethyl methacrylate); PEI: polyethyleneimine; PAsp(DET) 1,2-diaminoethane poly(aspartamide). Moldatua: I Gómez-Aguado, J. Rodríguez-Castejón, M. Vicente-Pascual, et al. Nanomedicines to Deliver mRNA: State of the Art and Future Perspectives. Nanomaterials 2020, 10, 364; https://doi.org/10.3390/nano10020364.

Horien artean, lipidoetan oinarritutako azido nukleikoen askapenerako bektore erabilienak garraiatzaile ez-biralak dira. Sistema lipidikoen osagai nagusiak lipido kationikoak dira, zeinak elkarrekintza elektrostatikoen bidez azido nukleikoekin interakzionatzeko gai diren, lipoplex izeneko konplexuak eratuz [35].

DOTMA (N-[1-(2,3-dioleyloxy)propyl]-N,N,N-trimethylammonium chloride) azido nukleikoen askapenerako lipido kationiko erabilienetako bat da, IVT RNAm konplexatzeko erabili zen lehen lipido kationiko sintetikoa hain zuzen ere [50]. DOTAP (1,2-dioleoyl-3-trimetylammonium-propane) DOTMA-ren deribatua den beste lipido sintetiko tradizional bat da, sintetizatzeko

merkeago dena eta eraginkortasun handiagoa aurkezten duena [35]. DOTAP DOPE (dioleoylphosphatidylethanolamina) lipido zwitterionikoarekin maiz konbinatu izan da, sistema koloidalak prestatzeko. Bi lipido horien arteko nahasketak endosomatik ihesa errazten du pH baldintza azidoetan, DOPEk duen gaitasunari esker lipoplexoren egitura bigeruzetatik modu hexagonal (HII) batera aldatzeko, bigeruza lipidikoen fusioa eragiten dituen eraldaketa supramolekularra eraginez [7,51]. DOTAP bakarrik edo DOPE lipido-laguntzailearekin konbinatuta erabili izan da DNAren eta RNAm-ren askapenerako [52–55].

Berrikiago, toxikotasun baxuagoko baina transfekzio gaitasuna kontserbatzen duten lipido ionizagarriak garatu dira lipido kationiko konbentzionalen alternatiba gisa, hala nola, 1,2-dioleoyl-3-dimetilio-propane (DODAP) edo 1,2-dioleyloxy-N, N-dimetil-3-aminopropane (DODMA) [5]. Lipido kationikoek izaera kationikoa mantentzen duten amonio talde kuaternarioak dauzkate haien egituran; lipido ionizagarriak; aldiz, karga positiboak lortzen dituzte haien egituran dauden amina libreak protonatzean pH gutxitzen den heinean [20]. Lipido berri hauek pH fisiologikoan neutroak dira baina modu positiboan kargatzen dira endosoma barruan daudenean, pH balioak pKa-renak baino baxuagoak direnean, hain zuzen ere.

Endosomen mintzan dauden lipido anionikoen eta lipido ionizagarrien arteko naturalki gertatzen diren elkarrekintza elektrostatikoak azido nukleikoen askapenaren azpi-mekanismo gisa proposatu dira [46]. Elkarrekintza hauek HII egiturak sustatzeko gai dira, azido nukleikoaren askapena zelula barnean eragiten [56].

Gaur egun, lipido kationiko ionizagarriak dituzten nanogarraiatzaileak askapen sistemen hautagai nagusien artean daude, siRNA-ren eta RNAm-ren administraziorako etorkizun handiko aplikazioarekin [35]. 5. irudiak azido nukleiko askapen sistemak formulatzeko gehien erabiltzen diren lipido kationikoen eta ionizagarrien egitura kimikoa erakusten du.

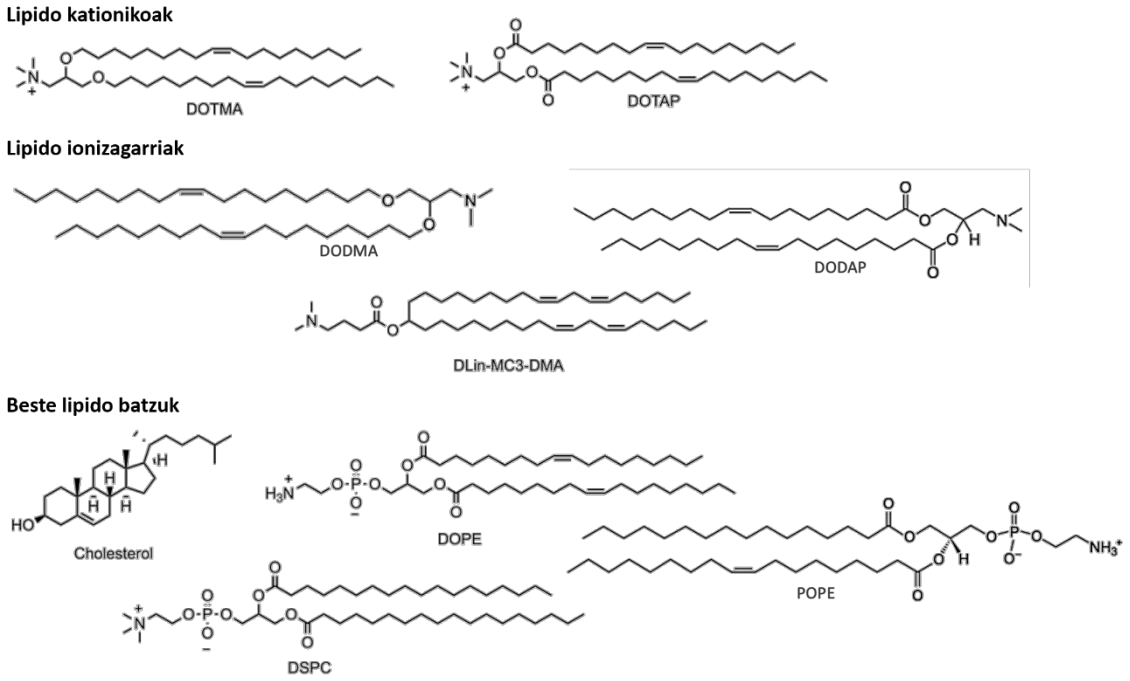

5. irudia. Azido nukleikoak administratzeko askapen sistemak formulatzeko gehien erabilitako lipido kationikoen eta ionizagarrien egitura kimikoa. DOTMA: N-[1-(2,3-dioleyloxy)propyl]-N,N,N-trimethylammonium chloride; DOTAP: 1,2-dioleoyloxy-3-(trimethylammonium)propane); DODMA: 1,2-dioleyloxy-N,N-dimethyl-3-aminopropane; DODAP: 1,2-dioleoyl-3-dimethylammoniumpropane; DOPE: dioleoylphosphatidylethanolamine; DSPC: 1,2-distearoyl-sn-glycero-3-phosphocholine; POPE: 1-palmitoyl-2-oleoylsn- glycero-3-phosphoethanolamine.

Normalean, lipido kationikoak nanopartikula lipidikoetan (LNP ingelesezko sigletan) formulatzen dira. LNPak klinikan gehien aztertutako bektore ez-biralak dira, eta liposomak eta lipidoetan oinarritutako beste nanopartikulak barne hartzen ditu. Gaur egun, hainbat LNPak entsegu klinikoen abangoardian daude, eta terapian RNAm-ren askapen sistema gisa baliozkotu dira. Hasiera batean, LNPak etorkizun handikoak ziren siRNA askapen terapietarako, eta ondorioz, haien erabilgarritasuna RNAm askapen terapiarako aztertzen hasi ziren [57]. Zentzu honetan, Patisiran-ek (ONPATTRO™), transthyretin proteina hepatikoa inhibitzen duen LNPetan formulatutako siRNA-k, FDAren onarpena jaso zuen 2018an. Honek aurrerapen esanguratsuak eragin zituen ezaguera arlo honetan [58]. Produktu honek lipido ionizagarri berri batez osatua dago, Dlin-MC3-DMA (MC3), hain zuzen ere [59]. Lortutako arrakastaren ondorioz, hainbat talde MC3 garraiatzaile gisa erabiltzen hasi dira RNAm-ren transfektziorako [60]. siRNA formulazioan izandako aurreko esperientziak RNAm nanosistemen garapenari lagundu dio, nahiz eta RNAm-ren egitura desberdina izateak nanopartikulak konplexatzeko gaitasuna oztopatu dezakeen [57].

Duela bi hamarkada baino gehiago, liposomak azido nukleikoen garraiatzaile gisa aurkeztu ziren eta, oraindik ere, gehien aztertu diren gene-terapiarako garraiatzaileak dira. Liposomak , nukleo urtsua inguratzen duten besikula anfifiliko esferikoak dira, bikapa lipidiko bat edo gehiagoz

osatua eta tamaina 20nm-tik mikretara dutenak. Normalean lipido kationikoz eta konposatu hauen konbinazioez osatuta daude: (a) lipido-laguntzaile bat, bikaparen egitura eusteko, hala nola, DSPC (1,2-distearoyl-sn-glycero-3-phosphocholine), DOPE eta POPE (1-palmitoyl-2-oleoylsn-glycero-3-phosphoethanolamine) [61], (b) kolesterola, LNParen bikapa lipidikoa egonkortzeko, eta (c) polietilen glikol (PEG)-lipidoa. PEG-k nanopartikularen egonkortasun koloidala hobetzen duen geruza hidratatzaile osatzen du, proteinen adsortzioa eta berariazkoa ez den sarrera murrizten duena, eta aklaramendu erretikuloendoteliala eragozten duena [20,48].

RNAm-ren askapenerako horrelako sistema lipidikoak erabiltzen zituzten formulazioak 1994an jada ebaluatu ziren [62], eta demostratu zen hauen eraginkortasuna liposoma-DNA konplexuekin lortutakoaren antzekoa zela *in situ* tumor transfekzioa eragiten. Ikerkuntza horrek RNAm DNAp-ren alternatiba izan zitekeela erakutsi zuen gene-immunopotentziatzio aplikazioetan. Berrikiago, lipido kationiko ionizagarria, fosfatidilkolina, kolesterola eta PEG-lipidoa zuten LNPak, Zika birusen andui baten aurre-mintza eta glikoproteinen estalkia kodetzen zuten RNAm enkapsulatzeko erabili ziren [63]. Dermis-barneko dosi gutxiko administrazio bakarrak erantzun eraginkorra eta iraunkorra lortu zuen saguetan eta gizakiak ez diren primateetan antigorputz erantzunak neutralizatuz eta babes erantzunak sortuz. Autoanplifikatzen diren txertoak (Self-amplifying txertoak, SAM ingelesezko sigletan) LNPren bidez RNAm sintetikoa askatzeko beste adibide bat dira. H1HA influenza birusen antigenoa kodetzen zuen SAM txertoak, 2-dilinoleyloxy-3-dimethylaminopropane, 1,2-diastearoyl-sn-glycero-3-phosphocholine, kolesterola eta PEG-DMG2000-rekin osatua, saguetan demostratu du dosi baxuetan immunogenikoa dela, eta baimendutako txertoarekin konparatuz antigorputz erantzun konparagarriak lortu dituela [64]. 1999an lehen ikerketa egin zenetik, RNAm-dun liposomen erabilerak gora egin du minbiziaren tratamenduan. Zhou et al.ek [65] Japoniako birus hemaglutinatzailean (HVJ) oinarritutako liposomak erabili zituzten glikoproteina 100 (gp100) antigenoa kodetzen zuen RNAm sintetizatzeko. Saguaren barean egindako injekzio zuzenak gp100ren antigorputzaren adierazpena eta B16 zelulen kontrako erantzunak eragin zituen. Duela gutxi, obulutegiko minbizia duten pazienteen lehengo giza-entsegu irekia (1. fasea) onetsi da. Pazienteek bena-barneko injekzioa jasoko dute hasieran, eta entseguaren bitartean kimioterapia-laguntzailea liposometan formulatuta dagoen RNAm txertoa (W_ova1 vaccine), zeinak hiru obulutegiko minbizia-tumoreari lotutako antigenoa (TAAs) kodetzen duen (ClinicalTrials.gov Identifier: NCT04163094).

Duela gutxi, CRISPR/Cas9 sisteman oinarritutako LNPak *in vivo* animalia ereduetan frogatu egin dira. Finn et al.ek [66] LNPn oinarritutako askapen metodoa garatu zuten, LP01 deituriko lipido

biodegradagarri eta ionizagarriaren bidez. Saguei emandako LNPtan oinarritutako CRISPR/Cas9ren administrazio sistemiko bakar batek, transtirretinaren (*Ttr*) edizio geniko esanguratsua eragin zuen saguetako gibelean, gutxienez 12 hilabetez iraun zuen TTR proteina serikoaren kontzentrazioak %97 baino gehiago murriztea eragin zuena.

Nanopartikula solido lipidikoak (SLNak) gene terapiako lipidoetan oinarritutako sistema koloidal eraginkorrenetako bat dira [67]. SLNak liposomek daukaten eraginkortasun eta segurtasun mugak zuzentzeko asmoarekin garatu ziren, nagusiki [68]. SLNak nanometroko partikula esferikoak dira, eta surfaktante geruza nukleo solido lipidikoa inguratzen duen dispertsio urtsu batez osatuta daude, zeinak normalen ondo toleratzen diren lipido fisiologikoz osatuak dauden [69–72]. SLNek egonkortasun ona eskaintzen dute, eta esterilizatu eta liofilizatu daitezke. Gainera, SLNak erraz funtzionalizatu daitezke berariazko estekatzaileak lotzen, material genetikoaren eta itu-zelularen ezaugarriak kontuan hartuz [73–75]. SLNen efizientzia azido nukleikoen askapen sistema gisa *in vitro* eta *in vivo* frogatua izan da, batez ere, DNAp askatzeko biltegiratze lisosomaleko gaitzetan [76,77], hainbat minbizi motetan [32] eta begiko gaitzetan [75,78–80].

1.2. Kornea-hanturaren tratamendurako gene-terapian oinarritutako estrategia berriak

Begia oso organo espezializatua da, non egitura indibidual bakoitzak elkarrekin lan egiten duen ikusmen-informazioa antzemateko eta prozesatzeko. Bi konpartimentuetan banatzen da: aurreko eta atzeko segmentuetan [81]. Kornea begiaren aurreko segmentuan aurkitzen den ehun gardena da, ikusmenari laguntzen diona ikusmen-irudi bat argiaren errefrakzioaren bidez enfokatzen. Kornea hiru geruzek eta bi mintzek osatzen dute: kanpoko epitelio estratifikatua eta erdiko estroma geruza Bowman-en mintz gardenak banatzen ditu, eta Descemet-en mintz basalak estroma eta barneko endotelioa bereizten ditu (6. irudia). Malko film batek kornearen aurreko gainazal ganbila estaltzen du, eta atzeko gainazal ahurra, berriz, umore urtsuarekin kontaktu zuzenean dago. Korneak eta esklerotikak begiaren kanpoko geruza osoa osatzen dute.

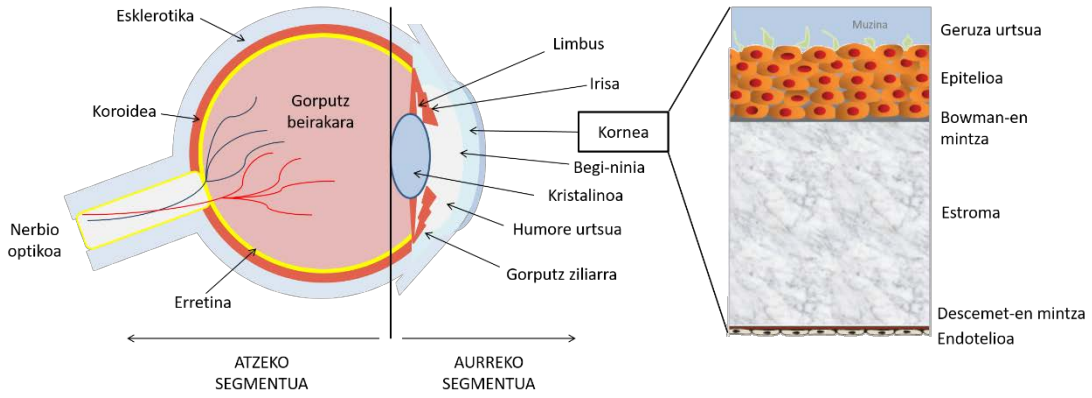

6. irudia. Giza begiaren eta kornearen irudikapena.

Begiak gene-terapiarako itu egokia izateko abantaila garrantzitsuak aurkezten ditu bere ezaugarri fisiologikoengatik: erraz aztertu daiteke, ondo definitutako anatomia du eta ikuspuntu immunologiko batetik isolatutako egitura da. Gainera, ikuspuntu esperimentaletik, pertsona berean, begi bat kontrol gisa erabil daiteke, eta beste begia, berriz, helburu esperimental gisa [82–84]. Gainera, korneako epitelioaren kokapen anatomikoak ahalbidetzen du azido nukleikodun sistemen administrazioa zuzenezko instilazio topiko ez-inbaditzailearen bidez egitea. Azkenik, korneak ikusmen azterketa ez-inbaditzailea eta azkarra errazten du, ohiko prozedura oftalmologikoen bidez, pazientearentzako arriskurik gabe [85].

1994an korneako gene-terapiaren lehen azterketa argitaratu zen [86]. Bertan, gene-terapia modu arrakastatsuan erabili zen, kornea hantura tratatzeko, kornea-ehunak transfektatu ondoren, erreplikazio eskaseko AdVen bidez. Ikerketa gehienek bektore biralak erabiltzen dituzte kornea transfektatzeko, bereziki, RVk, LVk, AdVk eta AAVk. Hala ere, bektore biralen aplikazioa gaixotasun inflamatorietan mugatuta dago, birus bektoreek immunitate- eta hantura-erantzunak sortzen baitituzte [78]. Gainera, bektore biralen administraziorako metodo inbaditzaileak erabili dira, batez ere: estroma-barnekoa, linbo-barnekoa, ganbera-barnekoa edo korneako epitelioa kendu ondorengoa [67,87,88]. Aitzitik, sistema ez-biralek etorkizun oparoko aukera erakutsi dute korneako gene-terapian, baita administrazio topikoaren ondoren ere [89–92]. Besteak beste, nanopartikula magnetikoak [93], azido hialuroniko/kitosanorekin prestatutako nanopartikulak [89], gelatinazko eta kondroitin sulfatozko nanopartikula hibridoak [94], polietilenimina [95], urrezko nanopartikulak [91], polietileniminaz konjugatutako urrezko nanopartikulak [96] eta SLNak [90], bektore ez-biral gisa probatu dira korneako gene-terapian. SLNek begiko administrazio topikorako eraginkorrak direla erakutsi dute [97].

Begiko administrazio topikoak hainbat abantaila ditu: ez da inbaditzailea, farmakoaren xurgapena zirkulazio sistemikoan minimizatu egiten da, lehen-iragaite metabolismoa saihesten

da eta formulazioak erraz administratzen dira. Hala ere, begietan administratzeko farmakoen askapen-sistema konbentzionalen arazo nagusia begiko azaleran atxikimendu txikia izatea da, kornea-aklaramenduarengatik; ondorioz, kornea zeharkatzen eta begietako egituretara sartzen den farmako kopurua eskasa da. Beraz, askapen sistema eraginkor batek farmakoaren egote denbora handitu beharko luke kornean eta iragazkortasuna hobetu [98]. SLNek ezaugarri egokiak dituzte kornearen iragazkortasuna eta kornea-atxikimendua hobetzeko begiko administrazio topikoaren ondoren, hala nola, tamaina nanometrikoa, propietate lipofilikoak eta gainazaleko karga positiboa normalean [99,100].

Korneari kalte egin diezaioketen eta kornea-hantura edo keratitisa eragin dezaketen hainbat faktore daude, hala nola infekzioak, begi-lehorra, betazaletako gaitzak, kalte fisiko eta kimikoak eta azpiko gaixotasun ugari [78]. Infekzioak kornea-hanturaren kausa nagusia dira, zehazki, herpes sinplex 1 birusak (HSB-1) eragindakoak, 1.5 milioi inguruko intzidentziarekin, eta urtero 40,000 itsutasun-kasu berri sortu dituena [101]. Garapen bidean dauden herrialdeetan, HSB-1k eragindako infekzioa keratitisari lotutako itsutasun kausa nagusia da [102].

Keratitis kasu batzuk faktore ezezagunen ondorio diren arren, arrisku-faktore nagusiek korneako gainazaleko geruzaren edozein haustura edo alterazioa eragiten dute. Gainera, keratitis-arriskua ukipen-lenteen erabilerarekin areagotu egiten da, baita gaixotasunek eragindako immunitate-sistemaren alterazioen ondorioz, Hartutako Immuno-Eskasiaren Sindromean (HIESa) adibidez; edo medikamentuen erabileraren ondorioz ere bai, hala nola, kortikoideak edo kimioterapia [103,104].

Keratitisaren jatorria edozein dela ere, sintoma arrunten artean begiko mina, ikusmen lausoa, fotofobia, malko-jarioa eta begiak gorritzea daude. Gainera, kornearen hantura kronikoak ikusmen-nahasmenduak eragiten ditu, eta, askotan, ehuna suntsitzea eragiten du, kornea ultzeratzera, orbaintzera eta, are, zulatzera ere eramaten duena, azkenik ikusmen-desgaitasuna eta itsutasuna eragiten [105].

1.2.1. Hantura-prozesua

Hantura-prozesua zauriak sendatzeko prozesu konplexu eta aktiboa da, eta hantura-estimuluaren erantzuna modulatzen duten hainbat molekulek parte hartzen dute. Molekula hauek zelulaz kanpoko matrizearen (ECM ingelesezko sigletan) proteinak, zitokinak eta hazkunde-faktoreak dira, besteak beste. Hantura-prozesuan, gainjar daitezkeen hiru fase daude: hantura-fasea, ugaltze-fasea eta ehuna birmoldatzeko edota heltze-fasea. Hasieran, neutrofiloak eta makrofagoak zauriaren inguruan errekrutatzen dira kimiokinei erantzunez. Hurrengo fasean, ECM-ren deposizioa gertatzen da, zeinak matrize barneko zelula ugalketa eta

proliferazioa osatzen duen; bestak beste, odol-hodi berriak sortzea, fibroblastoen proliferazioa eta ECM-ren eraketa. Kornea-osotasunaren alterazioak korneako keratozito kieszente normalak fibroblastoetan edota miofibroblastoetan bereiztea eragiten du [106]. Azkenik, estroma-matrizearen degradazioa gertatzen da entzima proteolitikoen ondorioz, baita erregresio baskularra, granulazio-ehunaren birmoldaketa eta ECM osagaien eraketa berria ere [107,108].

Matrizearen metaloproteinasak (MMP) hantura prozesuaren fase guztietan giltzarri diren entzima multzo bat dira [109–113]. ECM birmoldatzen, hesi epitelialaren funtzioan eta zelula epitelialen korneatik azpiko estromaren migrazioan parte hartzen dute [110,114–118].

Sistema immunitarioko zelulek hantura-prozesua kontrolatzen eta zelulen egoera fisiologiko mantentzen duten zitokinak eta proteina proinflamatorioak edo antiinflamatorioak ekoizten eta jariatzen dituzte [119,120]. Begiaren gainazala baldintza fisiologikoetan mantentzen duten pertsona osasuntsuen malkoetan hogeita bost zitokina inguru antzeman dira [119]. Zitokina horien barruan honako hauek aurki ditzakegu: interferoi-gamma (IFN-γ), beta hazkunde eraldatzailearen faktorea (TGF-β), interleukinak (IL), eta erantzun immune zelularrean eta umorezkoan parte hartzen duten kimiokinak (zitokina txikiak) [121]. Zitokina proinflamatorioen artean interleukina 13 (IL-13), IL-6, IL-1b eta tumore-nekrosiaren alfa faktorea (TNF-α) daude. Molekula hauek kornea-hanturan parte hartzen dute, faktore angiogenikoak areagotzen, hala nola hazkunde endotelial baskularraren faktorea (VEGF) eta MMP-9 [116,120,122–125]. Hanturaren aurkako zitokinen taldean, berriz, IL-10 gailentzen da monokinen ekoizpenaren inhibizioan; eta baita IL-1, IL-6, IL-8 eta TNF-alfa ere [126–130].

1.2.2. Hantura eta kornearen neobaskularizazioa

Angiogenesia ehunak ugaltzeko, garatzeko eta zauriak sendatzeko ezinbesteko prozesua da. Hala ere, estroma abaskularra mantentzea kornearen garapenerako eta fisiologiarako garrantzi handikoa da; horretarako faktore angiostatiko mailak faktore angiogenikoenak baino altuagoak mantendu behar dira. Kornean estimulu patologiko ugari izateak berezko oreka alda dezake, eta korneako edozein geruzatan angiogenesia eta kornearen neobaskularizazioa (CNV ingelesezko sigletan) sustatu. Hantura-prozesuak desoreka eragin dezake faktore angiogenikoen eta antiangiogenikoen artean, CNV eragiten [131]. Neobaskularizazioa begi-azaleko kalte zabalak konpontzeko prozesuaren parte bada ere [132], ikusmen-zorroztasuna arriskuan jar dezake, korneak abaskularitatea galtzen baitu.

CNV tratatzeko egungo aukeren artean hanturaren aurkako agente ez-esteroideoen edo kortikosteroideoen aplikazio topikoa, farmako immunosupresoreak edo interbentzio kirurgikoak daude, hala nola kauterizazio-terapia fotodinamikoa eta irradiazioak [133]. Hala ere,

eraginkortasun mugatuak eta ondorio kaltegarriek murriztu egiten dituzte gaur egungo terapiak [134]. Horren ondorioz, beharrezkoa da estrategia terapeutiko berriak bilatzea.

1.2.3. Gene-terapiaren aplikazioa kornea-hanturan

Kornea-hantura tratatzeko gene-terapiaren estrategia nagusiak neobaskularizaziora nahiz hanturazko bitartekarietara bideratzen dira [135,136]. Gene-isiltzea siRNA-ren bidez eta DNAp-n oinarritutako gehikuntza genikoa aztertu dira.

1.2.3.1. Kornearen neobaskularizaziora zuzendutako gene-terapia

Gene-terapian oinarritutako CNV-aren tratamendua bi ikuspegi desberdinen bidez landu daiteke: faktore antiangiogeniko bat adierazteko osagarri genetikoaren bidez edota faktore proangiogeniko baten sintesia inhibitzeko gene-isiltzearen bidez [112]. Berrikuspen batek itu-geneen eta CNV tratatzeko balizko bektoreen ikuspegi zabal eta osoa aurkezten du [134]. 1. taulak CNV-an inplikatutako faktore antiangiogeniko eta proangiogeniko nagusiak laburbiltzen ditu.

1. taula. Kornearen neobaskularizazioan inplikatutako faktore antiangiogeniko eta angiogeniko nagusiak

Faktore antiangiogenikoak	Faktore angiogenikoak
Vasohibin-1 [137]	Hazkunde endotelial baskularraren faktorea (VEGF) [138,139]
Endostatina [140–142]	Zelula-azaleraren mintzari lotutako VEGF 1 hartzailea (baita sflt-1 bezala ezagutua ere) [138]
Angiostatina [143,144]	Zelula-azaleraren mintzari lotutako VEGF 2 hartzailea (sVEGFR2) [145]
Peroxisomak ugaltzearen ondorioz aktibatutako gamma hartzailea (PPARγ) [146]	Fibroblastoen hazkunde faktorea (FGF) [147]
Dekorina [148]	Angiogenina [105,149]
Garunaren angiogenesi espezifikoaren inhibitzailea 1 [150]	Prostaglandinak [151]

Faktore proangiogenikoen artean, MMP-9 korneako baldintza patologikoetan (CNV barne) parte hartzen duen zelulaz kanpoko matrizea birmoldatzeko entzima nagusietako bat da [123]. MMP-ak zelulaz kanpoko matrizeko proteina ugari zatitzeko gai diren entzimak dira, eta horri esker, zelula epitelialak korneatik azpiko estromara migratzen dira eta CNV sortzen da [116–118,152]. MMP-en ekoizpenaren eta aktibitatearen hazkundea zelula-fenotipo migratzailearekin eta inbaditzailearekin erlazionatzen da [153,154]. Izan ere, begi-gainazalean MMP-9 sintesia

ezabatzeak kornea-hesiaren funtzioa hobetzen lagundu zuen begi lehorrea zuten saguen eredu batean [155]. MMP-9 faktore proangiogenikoaren ezabapena CNV-ri lotutako hantura tratatzeko estrategia ere izan liteke.

Gene-isiltzea interferentziako RNA-ren (RNAi) teknologiaren bidez gauza daiteke [156]. RNAi molekulen artean, shRNA (RNAi aktibatzaile gisa ere ezaguna), plasmido batek kodetutako RNA mota bat da. Beste RNAi forma batzuetan ez bezala [87,157], shRNA zelula ostalarian etengabe ekoizten da eta, beraz, gene-isiltze iraunkorragoa eragiten du.

1.2.3.2. Hantura-bitartekariei zuzendutako gene-terapia

Ikerketa askok gene-terapiak hanturaren aurkako bitartekari espezifikoak adierazteko duen gaitasuna ebaluatu dute, hantura garatzen duten korneako gaixotasunak tratatzeko estrategia gisa; hala nola, keratitis herpetikoa . Kontuan izan behar da HSB-1ek mindutako korneetatik %10 inguruk kornea-transplante behar dutela [158]. HSB-1 genomarekin lotutako estrategia berriak aztertzen ari diren arren, gene-terapian oinarritutako HBS keratitisaren (HSK ingelesezko sigletan) aurkako estrategia gehienak hantura-prozesu tratatzera bideratuta daude [157].

HSK errepikariaren patogenesian, IL-10 zitokina immunoerregulatzaileak funtsezko zeregina du [159]. Ikerketa baten arabera, HSBk eragindako infekzioaren ondoren, estromako keratitis nekrotizatzailearen garapena oztopatu zen eta kornea-arazoren larritasuna inhibitu egin zen, IL-10 birkonbinatzailearen kornea-barneko injekzioa administratu zenean [160]. Hala ere, IL-10ren erdi-bizitza laburra eta bioerabilgarritasun urria direla eta, begiko instilazio topikoaren ondoren, administrazio errepikatuak beharrezkoak dira efektu terapeutikoa lortzeko [161]. Alternatiboki, etengabeko IL-10ren gehikuntza genikoaren bitartez lor liteke. Adibidez, IL-10 adierazpen indartsua lortu zen elektroporazioaren bidez kornea murinetan [162].

Halaber, IL-10 garraiatzen duten bektore biralek ardien eta gizakien korneak *in vitro* eta *ex vivo* transfektatzeko erabili dira, eta AdV bektoreek LV bektoreek baino eraginkortasun handiagoa lortu zuten [163]. Berrikiago, giza G-antigeno leukozitarioa (HLA-G), molekula immunomodulatzailea eta antiinflamatorioa, AAV bektore batean garatu eta untxietan probatu zen. Bektoreen administrazioarekin hau demostratu zen: CNV-aren prebentzioa, traumak eragindako T linfozito infiltrazioaren inhibizioa (horietako batzuk CD8+ ziren) eta miofibroblastoen eraketaren murrizketa esanguratsua injekzio estroma barneko bakar baten ondoren [164]. IL-10 kodetzen duen DNAp eta SLNetan oinarritutako bektore ez-biralak, *in vitro* eta *ex vivo* ere aztertu ziren untxi-korneako explanteetan. Bertan, bektoreek korneako zenbait geruza transfektatzeko gaitasuna erakutsi zuten, nanosistemaren konposizioaren arabera [79]. Gainera, beste ikerketa batek gehikuntza genikoa wild type saguen kornean eta IL-10 knockout

saguen kornean IL-10ren ekoizpena eragin zuela frogatu du, IL-10 DNAp-dun SLNak administratu ondoren [80]. RNAm kornea-hanturari aurre egiteko aukera terapeutikoa izan liteke, duen eraginkortasun handia, segurtasun-profila eta proteinak azkar ekoizteko moldakortasuna dela eta.

2. METODOAK

Atal honetan, laburki azaltzen dira tesi osoan erabilitako metodo nagusiak. Metodologia espezifikoa modu zehatzean azalduta dago eranskinetan.

2.1. SLNen eta bektoreen prestaketa

Hiru teknika desberdin erabili ziren SLNak prestatzeko eta metodo bakoitzak haien ezaugarrietan duen eragina ebaulatzeko: disolbatzailearen emultsifikazioa/lurrunketa, urtze bero bidezko emultsifikazioa eta koazerbazioa.

Disolbatzailearen emultsifikazioa/lurrunketa bidez prestatutako SLNak (SLN_{EE}) prestatzeko fase oliotsua eta fase urtsua sonikatu ziren, aurretik gure ikerketa taldeak jakinarazi bezala [165], fase oliotsua eta fase urtsuaren bitarteko sonikazioaren ondorioz lortu ziren. Fase oliotsua Precirol® ATO5 lipido solidoa diklorometano disolbatzaile organikoan disolbatuz prestatu zen. Fase urtsua, bestalde, DOTAP lipido kationikoa edo DOTAP eta lipido ionizatua (DODAP edo DOBAQ) eta Tween 80 tentsioaktiboa nahasten prestatu zen. Fase urtsua fase oliotsuan gehitu eta emultsifikatu egin zen 50 W-ra 30 segundoz sonikatuz. SLN_{EE}-ak diklorometanoa lurrundu eta gero lortu ziren.

Urtze bero bidezko emultsifikazio teknikak (SLN_{HM}) disolbatzaile organikoa erabiltzea saihesten du. Kasu horretan, DOTAP eta Tween 80 tentsioaktiboaren disoluzio urtsua Precirol® ATO 5 lipido solidoarekin nahastu zen, 50 W-ra 30 minutuz sonikatuz. SLN_{HM}-ak 30 minutuz hoztu ondoren lortu ziren.

Azkenik, koazerbazio metodoan SLNen (SLN_C) nukleo lipidikoa azido behenikoz betetzen da, zeina PVA 9000 esekidura eszipientearekin eta DEAE-dextrano eszipiente kationikoarekin inguratuta dagoen, aurretik jakinarazi bezala [80]. Kasu honetan, sodio behenatoa eta PVA 9000 ur berotan irabiatuz disolbatu ziren, eta soluzioa 80° C-ra iristean eta zeharrargi bihurtzean, NaOH gehitu zen. Ondoren, soluzioa erabat garden bihurtzean DEAE-dextranoa tantaz tanta gehitu zen, soluzioa erabat arre bilakatu arte. Geroago, HCl gehitu zen eta esekidura zuritu zenean, ur-bainuan hozten utzi zen, irabiatzen zen bitartean. SLN_C-ak lortzeko, azkeneko produktua berriro urtu, berotu eta hoztu zen ur bainuan.

2. taulan doktorego-tesi honetan zehar erabilitako SLNen konposizioa eta prestakuntza metodoa laburbiltzen dira.

2. taula. Doktorego-tesi honetan erabilitako SLNen konposizioa era prestakuntza metodoa.

SLN mota	Lipido kationikoa (%)			Behenato sodikoa (%)(w/v)	PVA 9000 (%) (w/v)	DEAE-dextranoa (%) (w/v)	Tween 80 (%)
	DOTAP	DODAP	DOBAQ				
$SLN1_{EE}$	0.4						0.1
$SLN2_{EE}$	0.2	0.2					0.1
$SLN3_{EE}$			0.4				0.1
$SLN4_{EE}$	0.2		0.2				0.1
$SLN1_{HM}$	0.4						0.1
SLN_C				2.1	1.05	0.33	

$SLN1_{EE}$: DOTAP lipido kationikoa duen eta disolbatzailearen emultsifikazioa/lurrunketa bidez prestatutako SLN; $SLN2_{EE}$: DOTAP lipidoa kationikoa eta DODAP lipido ionizagarria duen disolbatzailearen emultsifikazioa/lurrunketa bidez prestatutako SLN; $SLN3_{EE}$: DOBAQ lipido ionizagarria duen disolbatzailearen emultsifikazioa/lurrunketa bidez prestatutako SLN; $SLN4_{EE}$: DOTAP lipidoa kationikoa eta DOBAQ lipido ionizagarria duen disolbatzailearen emultsifikazioa/lurrunketa bidez prestatutako SLN; $SLN1_{HM}$: DOTAP lipido kationikoa duen urtze bero bidezko emultsifikazioarekin prestatutako SLN. SLN_C: koazerbazio metodoarekin prestatutako SLN.

Bektoreek osagai hauek zituzten: SLNk, azido nukleikoa, protamina (P), eta, aukeran, polisakarido bat eta urrezko nanopartikulak (AuNPk). Lehenik, azido nukleikoa (DNAp, RNAm edo urkila motzeko interferentziako RNA-ren plasmidoa (shRNA-p)) protaminadun disoluzio urtsu batekin nahastu zen, eta jarraian, polisakaridoaren (dextranoa (DX) edo azido hialuronikoa (AH)) disoluzio urtsua aurreko disoluziora gehitu zen. Azkenik, SLNen esekidura konplexura gehitu zen. Osagai guztiak nahastu ondoren, interakzio elektrostatikoek bektoreak sortzea ahalbidetu zuten

DNAp-dun bektoreak prestatzeko, proteina berde fluoreszentea (GFP ingelesezko sigletan) kodifikatzen duen pcDNA3-EGFP plasmidoa eta giza IL-10 kodifikatzen duen pUNO1-hIL10 plasmidoa erabili ziren. RNAm-dun bektoreen kasuan, GFP kodetzen duen CleanCap™ EGFP (5moU) RNAm eta giza IL-10 kodetzen duen RNAm erabili ziren. Azkenik, shRNA-p-rekin entseguak egiteko, MMP-9ren aurka kodetzen duen shRNA-p (shRNA-p-MMP-9) erabili zen, eta baita MMP-9ren zein GFParen aurka kodetzen duen shRNA-p (shRNA-p-MMP-9-GFP) ere.

3. taulan doktorego-tesi honetan erabilitako formulazioen konposizioa laburbiltzen da.

3. taula. Doktorego-tesi honetan erabilitako bektore ezberdinen konposizioa.

Eranskina	Bektorearen izena	Azido nukleikoa			Estekatzailea				Agente kationikoa			
		DNAp	RNAm	shRNA-p	P	DX	AH	AuNP	DOTAP	DODAP	DOBAQ	DEAE-dextran
II	DNAp-DX-SLN1$_{EE}$	X			X	X			X			
II	DNAp-DX-SLN2$_{EE}$	X			X	X			X	X		
II	DNAp-DX-SLN4$_{EE}$	X			X	X			X		X	
II	DNAp-AH-SLN1$_{EE}$	X			X		X		X			
II	DNAp-AH-SLN2$_{EE}$	X			X		X		X	X		
II eta IV	mRNA-DX-SLN1$_{EE}$		X		X	X			X			
II	mRNA-DX-SLN2$_{EE}$		X		X	X			X	X		
II eta IV	mRNA-AH-SLN1$_{EE}$		X		X		X		X			
II	mRNA-AH-SLN2$_{EE}$		X		X		X		X	X		
II	mRNA-P-SLN1$_{EE}$		X		X				X			
II	mRNA-P0.5-SLN2$_{EE}$		X		X				X	X		
II	mRNA-P1-SLN2$_{EE}$		X		X				X	X		
III	DX:P:shRNA-p-MMP-9:SLN1$_{EE}$			X	X	X			X			
IV	mRNA-DX-SLN1$_{HM}$		X		X	X			X			
IV	mRNA-AH-SLN1$_{HM}$		X		X		X		X			
IV	mRNA-SLN$_{C}$		X		X							X
IV	mRNA-AH-SLN$_{C}$		X		X		X					X
IV	DNAp-DX-SLN1$_{HM}$	X			X	X			X			
IV	DNAp-AH-SLN1$_{HM}$	X			X		X		X			
VI	DNAp-DX-SLN1$_{EE}$_Au	X			X	X		X	X			
VI	DNAp-AH-SLN1$_{EE}$_Au	X			X		X	X	X			

VI	mRNA-DX-SLN1$_{EE}$_Au	X	X		X		X		X
VI	mRNA-AH-SLN1$_{EE}$_Au	X	X			X	X		X

P: protamina; DX: dextranoa; AH: azido hialuronikoa; Au: urrea; AuNP: urrezko nanopartikulak; SLN1$_{EE}$: DOTAP lipido kationikoa duen eta disolbatzailearen emultsifikazioa/lurrunketa bidez prestatutako SLN; SLN2$_{EE}$: DOTAP lipidoa kationikoa eta DODAP lipido ionizagarria duen disolbatzailearen emultsifikazioa/lurrunketa bidez prestatutako SLN; SLN4$_{EE}$: DOTAP lipidoa kationikoa eta DOBAQ lipido ionizagarria duen disolbatzailearen emultsifikazioa/lurrunketa bidez prestatutako SLN; SLN1$_{HM}$: DOTAP lipido kationikoa duen urtze bero bidezko emultsifikazioarekin prestatutako SLN. SLN$_C$: koazerbazio metodoarekin prestatutako SLN.

2.2. SLNen eta bektoreen karakterizazio fisiko-kimikoa

2.2.1. Tamaina, PDI eta ζ-potentziala

Laginak Milli-Q™ uretan diluitu ondoren, SLNen eta bektoreen tamaina eta polidispertsio indizea (PDI) argi dispertsio dinamikoaren ("Dynamic Light Scattering (DLS)" ingelesezko sigletan) bidez zehaztu ziren. Gainazaleko karga edo ζ-potentzialari dagokionez, laser doppler abiadura-neurgailuaren ("Laser doppler velocimetry (LDV)" ingelesezko sigletan) erabiliz zehaztu zen. Neurketa guztiak Zetasizer Nano series Nano ZS (Malvern Instruments, Worcershire, UK) ekipoan burutu ziren. Formulazioak hirukoiztuta aztertu ziren. Emaitzetan batezbestekoa ± desbideratze estandarra adierazten dira.

2.2.2. Transmisio Mikroskopio Elektronikoaren (TEM) irudiak

SLNetan oinarritutako bektoreen gainazaleko ezaugarriak transmisio mikroskopio elektronikoaren (TEM ingelesezko sigletan) (Philips EM208S TEM) bidez aztertu ziren, laginak tindatu ondoren. Horretarako, laginaren 10 µL karbono goriz estalitako saretetan adsorbatu ziren 60 segundoz. Ondoren, gainerako likidoa kendu zen, iragazki-paperean lehortu zen, eta % 2ko uranilo-azetatoarekin tindatu zen 60 segundoz. Euskal Herriko Unibertsitateko (Leioa, Euskadi, Espainia) ikerkuntzarako zerbitzu orokorren (SGIker) barruan dagoen “Mikroskopia Analitikoa eta Bereizmen Handikoa Biomedikuntzan” zerbitzuak, laguntza teknikoa eta giza laguntza eman zuen TEM erabiltzeko.

2.2.3. Agarosa gel-elektroforesi entsegua

Bektoreen gaitasuna azido nukleikoak lotzeko, babesteko eta askatzeko ebaluatu zen. DNAp-n oinarritutako bektoreen azterketa Gel Red™-rekin tindatutako %0.7 agarosa zuen gel-elektroforesian egin zen. Ehun eta hogei V-ko eremu elektrikoa aplikatu zen 30 minutuz. Ondoren, gelak Uvitec Uvidoc D-55-LCD-20 M Auto transiluminatzailean aztertu ziren. Lotura aztertzeko, bektoreak Milli-Q™ uretan diluitu ziren putzu bakoitzean 0.03 µg DNAp/µL kontzentrazioa lortu arte. Babesa ebaluatzeko, 1 U DNasa I/2.5 µg DNAp gehitu ziren eta berogailuan 37 °C-ra 30 minutuz inkubatu zen. Ondoren, bektoreak sodio lauril sulfato (SDS) soluzio batekin nahastu ziren %1 SDS kontzentrazioa lortu arte. Azkenik, askapen aztertzeko, SDS soluzioa bektoreei gehitu zitzaien. DNAp 1 kb markagailua (NIPPON Genetics Europe, Dueren, Germany) eta tratatu gabeko pcDNA3-EGFP plasmidoa kontrol bezala erabili ziren DNAp-ren osotasuna konparatzeko.

RNAm-n oinarritutako bektoreen azterketa Gel Red™-rekin tindatutako %1.2 agarosa gel-elektroforesian egin zen. Hirurogeita hamabost V-ko eremu elektrikoa aplikatu zen 60 minutuz. Ondoren, gelak Uvitec Uvidoc D-55-LCD-20 M Auto transiluminatzailean aztertu ziren. Lotura

aztertzeko, bektoreak Milli-Q™ uretan diluitu ziren, putzu bakoitzean 0.12 µg RNAm/µL kontzentrazioa lortu arte. Babesa aztertzeko, 6 U RNasa I/1 µg RNAm-ri gehituz eta berogailuan 37 °C-ra 40 minutuz inkubatuz burutu zen. Ondoren, laginak berogailutik kendu eta SDS soluzio batekin nahastu ziren %1 SDS kontzentrazioa lortu arte. Askapena ebaluatzeko, SDS soluzio bera gehitu zitzaien. RiboRuler High Range RNA markagailua eta tratatu gabeko CleanCap™ EGFP mRNA (5moU) kontrol bezala erabili ziren RNAm-ren osotasuna konparatzeko.

2.3. Zelula-kulturekin egindako entseguak

In vitro entseguak lau zelula-lerroetan burutu ziren:

- Giza Erretinako Pigmentatutako Epitelioko zelulak (ARPE-19 ingelesezko sigletan). ARPE-19 zelulak Dulbecco's Modified Eagle Medium:Nutrient Mixture F-12 (DMEM/F-12) hazkuntza-medioan mantendu ziren, %10 behi serum fetal inaktibatuarekin (FBS) eta %1 penizilina/estreptomizina (PEST) antibiotikoekin.
- Giza-Enbrioietako Giltzurrun zelulak (HEK-293 ingelesezko sigletan). HEK-293 zelulak Eagle's Minimum Essential Medium (EMEM) hazkuntza-medioan mantendu ziren, %10 FBSarekin eta %1 PEST antibiotikoekin.
- Giza Korneaklo Epitelioko zelulak (HCE-2 ingelesezko sigletan). HCE-2 zelulak DMEM/F-12 GlutaMAX hazkuntza-medioan mantendu ziren, %15 FBSarekin, intsulinarekin (4mg/mL), hazkunde epidermiko faktorearekin (EGF) (10 ng/mL) eta 1% PEST antibiotikoekin.
- Giza Zilbor-zain Endotelioko Zelulak (HUVEC ingelesezko sigletan). HUVEC zelulak Medium 200 medioan mantendu ziren, serum baxuko hazkunde gehigarriekin (LSGS).

Zelula-kultura guztiak %5 CO_2-dun atmosferan kultibatu ziren 37 °C-tan. Medio aldaketa 2-3 egunez behin burutu zen eta zelula pasea astean behin.

2.3.1. Gene-isiltzearen eraginkortasuna

2.3.1.1. Transfektatutako zelulen ehunekoa eta GFPren produkzioa

Transfektatutako zelulen ehunekoa ebaluatzeko, bektoreak shRNA-p-MMP-9-GFP plasmidoarekin prestatu ziren. Plasmido horrek aldi berean MMP-9 isilarazten eta GFP proteina kodetzen du. Bektoreak zeluletara gehitu eta lau ordura, hazkuntza-medioa medio freskoarekin ordezkatu zen, eta kultibo zelularra %5 CO_2-dun atmosferan eta 37 °C-tan 72 orduz mantendu zen kuantifikazioa egin aurretik. GFP adierazi zuten zelulen ehunekoa CytoFlex fluxu-zitometroan aztertu zen. Zelulak PBSrekin hiru aldiz garbitu ziren, putzuetatik jaso eta PBSan berreseki ziren. Azkenik, 10,000 zelula aztertu ziren lagin bakoitzeko FITC kanala erabiliz (fluoreszentziaren igorpena 525 nm-ko luzeran irakurtzen du).

Zelula-barneko GFP kopurua fluorimetriaz aztertu zen, fluoreszentzia erlatibo unitateen (RFU) eta proteina totalaren kantitatearen (mg) arteko ratioa kalkulatuz. Horretarako, hazkuntza-medioa 300 mL 1× reported lysis indargetzailearekin (RLB) ordezkatu zen eta plakak izoztu ziren. Zelulak arraskatu ondoren zentrifugatu ziren (4 °C, 12,000× *g*, 2 minutuz). GFP-fluoreszentzia Glomax™ Multi-Detection System (Promega Biotech Iberica, Madrid, Spain) gailuaren bitartez aztertu zen. Fluoreszentiza, proteína kantitakearen arabea zuzendu zen. Proteina kuantifikatzeko Micro BCA™ Protein Assay kita erabili zen (Thermo Scientific, Madrid, Spain).

2.3.1.2. MMP-9aren isiltzea

HCE-2 zelulak transfektatu ziren ebaluatzeko nolakoa zen shRNA-p-MMP-9 plasmidoa zeramaten nanobektoreen gaitasuna MMP-9 kodifikatzen duen genea isiltzeko . shRNA-p-scramble (shRNAscr) plasmidoa eta shRNA-p-MMP-9 plasmido biluzia kontrol negatibo bezala erabili ziren. Isilarazteko aktibitatea bektoreak gehitu eta 72 ordu geroago aztertu zen. Hazkuntza-medioan jariatutako MMP-9 kopurua ELISA kit (R&D Systems, Minneapolis, MN, AEB) baten bitartez neurtu zen.

Zelula-barneko MMP-9 immunozitokimikaren bitartez ebaluatu zen. Horretarako, zelulak 24 putzuko plateretan erein ziren, aurretik finkapen faktorea zuten estalkietan. PBSrekin garbitu ondoren, zelulak PB indargetzailearekin (% 0,3 Triton X-100, % 10 asto-seruma) blokeatu eta iragazkortu ziren 30 minutuz. Anti-MMP-9 ahuntz antigorputz monoklonala PB indargetzailean (% 2.5 asto-seruma, % 0.1 triton X-100) gehitu eta ordu batez mantendu zen. PBSrekin hiru garbiketa gehiago egin ondoren, zelulak anti-ahuntzaren IgG aurkako Alexa Fluor 568 konjugatutako asto antigorputz sekundarioaz tindatuak izan ziren, ordu batez iluntasunean. Azkenik, zelulen nukleoak DAPI-Fluoromount-G™ muntaketa medioarekin tindatu ziren. Fluoreszentziaren berezitasuna antigorputzik gabe inkubatutako zelulekin kontrolatu zen. Irudiak fluoreszentzia alderantzikatuko mikroskopio batekin (Nikon TMS, Izasa Scientific, Madrid, Spain) 40× magnifikazioarekin lortu ziren. Zelula-barneko MMP-9 HCE-2 zeluletan ere ebaluatu zen, aurrez estimulatuko 10 ng TNF-α bitartekari proinflamatorioaren bitartez sei orduz.

2.3.1.3. Zelulen migrazio-entsegua

Zauria sendatzeko entsegua erabili zen HCE-2 zelulen migrazioan formulazioek zuten eragina aztertzeko. Horretarako, HCE-2 zelulak konfluentzia lortu arte gelatina (MMP-9-ren substratua) eta atxikimendu faktorea zuten 24 putzuko plaketan hazi ziren, eta zauri lineal bat egin zen pipeta-punta batekin. Ondoren, zelula-kulturak PBSrekin bi aldiz garbitu ziren, itsatsita ez zeuden zelulak kentzeko eta serum-gabeko hazkuntza-medio berria gehitu zen. Tratatu gabeko

zelulak, bektoreekin tratatutako zelulak (2.5 µg-ko plasmido dosia dagozkionak) eta 10 ng TNF-α-z estimulatutako zelulak %5 CO_2-dun atmosferan eta 37 °C-tan mantendu ziren lau orduz. Ondoren, medioa hazkuntza-medio berri mL batekin ordezkatu zen. Zauriaren luzera 7, 24 eta 48 ordu eta gero neurtu zen. Distantzia erlatiboa formula honekin kalkulatu zen: *m = (1−nt/r) × %100*, non m migrazioa den, nt arraskaren luzera t denboran, eta r arraskaren hasierako zabalera [166]. Nanopartikula biluziak ere ebaluatu ziren.

2.3.1.4. Hodi kapilarrak eratzeko entsegua HUVEC zeluletan

HUVEC zelula-lerroa erabili zen MMP-9-k hodi kapilarren eraketa inhibitzeko duen gaitasuna aztertzeko. HUVEC zelulak Geltrex®-en gainean jarri ziren, 96 putzuko plaketan, eta HCE-2 zelulen hazkuntza-medioarekin ordezkatu ziren. Plakan, tratatu gabeko zelulak, DX:P:shRNA-p-MMP-9:$SLN1_{EE}$ bektorea, TNF-α eta TNF-α gehi DX:P:shRNA-p-MMP-9:$SLN1_{EE}$. bektoreak gehitu ziren. Plakak 37 °C-tan inkubatu ziren, eta hodien formazioa 15 ordura mikroskopio optiko alderantzikatuarekin ebaluatu zen. Irudien neurketa morfometrikoak ImageJ softwarea (National Institute of Health, Bethesda, Ma, AEB) erabiliz lortu ziren [167].

2.3.2. Gehikuntza genikoaren eraginkortasuna

2.3.2.1. GFP transfekzioaren eraginkortasuna

Transfektatutako zelulen ehunekoa eta fluoreszentzia-intentsitatea, RNAm-n eta DNAp-n oinarritutako bektoreak gehitu eta 48 eta 72 ordura aztertu ziren CytoFLEX fluxu-ziometroa erabiliz, hurrenez hurren. Aztertu aurretik, zelulak %5 CO_2-dun atmosferan eta 37 °C-tan mantendu ziren. Zelulak PBSrekin garbitu ziren eta plaketatik Trypsin/EDTAren inkubazio bidez askatu ziren. Zelula-suspentsioa zentrifugatu ondoren, gainjalkina kendu eta zelulak PBSn berreseki ziren. Lagin bakoitzeko 10,000 zelula aztertu ziren FITC kanala erabiliz (525 nm). Transfektatutako zelulen ehunekoa eta fluoreszentzia-intentsitatea kalkulatzeko, zelula guztietatik fluoreszentzia positiboa zutenak zenbatu ziren. Tenperaturak zelulen transfekzioan duen eragina ere aztertu zen. Horretarako, zelulak bektoreak gehitu aurretik eta ondoren 4° C-tan inkubatu ziren.

2.3.2.2. IL-10 transfekzioaren eraginkortasuna

Jariautako eta zelula-barneko IL-10 DuoSet® ELISA kitaren bidez neurtu zen. Jariatutako IL-10 kuantifikatzeko, putzu bakoitzeko medioa hartu eta zentrifugatu zen. Zelula-barneko IL-10 kuantifikatzeko, zelulak PBSrekin bi aldiz garbitu ziren, eta ondoren, 400 µL 1× RLB gehitu zitzaien. Azkenik, plakak izozkailuan sartu ziren zelulen lisia gerta zedin. Ondoren, putzu bakoitza arraska batekin altxatu eta lisatua zentrifugatu zen. 96 putzuko plakan baten putzuetan, aldez

aurretik antigorputzarekin estalita zeudenak, lagin bakoitzeko 100 µL gehitu ziren. Ondoren, fabrikatzaileak agindutakoaren arabera jarraitu zen.

2.3.3. Zelulen bideragarritasuna

Gene-isiltzea aztertzeko, HCE-2 zelulen bideragarritasuna CCK-8rekin neurtu zen, fabrikatzailearen protokoloa jarraituz. Laburbilduz, zelulak 96 putzuko plaka batean jarri ziren, 1×10^3 zelula/putzuko dentsitatean, eta 37° C-tan inkubatu ziren gau osoan %5 CO_2-dun inkubagailuan. Hurrengo egunean, bektore desberdinen transfekzioa burutu zen: putzu bakoitzari CCK-8 soluzio erreaktiboa gehitu zitzaion, eta 37 ° C-tan lau orduz inkubatu ziren. Azkenik, absorbantzia mikroplaken irakurgailuan 450 nm-tara neurtu zen.

Gehikuntza genikoa ebaluatzeko, RNAm-n eta DNAp-n oinarritutako bektoreak gehitu eta 48 eta 72 ordura aztertu ziren CytoFLEX fluxu-ziometroaren bitartez, hurrenez hurren. Aztertu aurretik, zelulak %5 CO_2-dun atmosferan eta 37 °C-tan mantendu ziren. Zelulak PBSrekin garbitu eta plaketatik Trypsin/EDTArekin askatu ziren. Zelulen zentrifugazioaren ondoren, gainjalkina kendu eta zelulak PBSn berreseki ziren. Lagin bakoitzeko 10,000 zelula aztertu ziren ECD kanala erabiliz (610 nm) 7-amino-actinomycin D (7-AAD) bideragarritasun tindagaia laginetan gehitu ondoren. Tenperaturak zelulen bideragarritasunean duen eragina ere aztertu zen. Horretarako, zelulak bektoreak gehitu aurretik eta ondoren 4 ° C-tan inkubatu ziren.

2.3.4. Bektoreen internalizazioa

Bektoreen internalizazioa aztertzeko SLNak Nile Red tindagai (λ = 590 nm) fluoreszentearekin prestatu ziren, lehen esan bezala [79]. Bektoreak gehitu eta bi orduz %5 CO_2-dun atmosferan eta 37 °C-tan inkubatu ziren. Ondoren, hazkuntza-medioa kendu, PBSrekin garbitu eta zelulak putzuetatik Trypsin/EDTArekin askatu ziren. Bektoreen sarrera CytoFLEX fluxu-zitometroa (Beckman Coulter) erabiliz aztertu zen. Lagin bakoitzeko 10,000 zelula aztertu ziren ECD kanala erabiliz (610 nm). Gainera, tenperaturak zelulen internalizazioan duen eragina aztertu zen. Horretarako, zelulak bektoreak gehitu aurretik eta ondoren 4 ° C-tan inkubatu ziren.

2.3.5. Bektoreen zelula barneko disposizioa

Zelulak Millicell EZ portetan (Millipore) erein eta %5 CO_2-dun atmosferan eta 37 °C-tan 24 orduz inkubatu ziren. Orduan, CleanCap™ Cyanine 5 EGFP RNAm (5mou) edo pcDNA3-EGFP Label IT® Cy®5-rekin tindatutako plasmidoa zuten bektoreak gehitu ziren. Lau ordu eta gero, zelulak PBSrekin garbitu, %4 PFArekin finkatu eta DAPI-fluoromunt-G™ muntaketa-medioaz estali ziren nukleoak tindatzeko. Azkenik, Leica DM IL LED Fluo alderantzikatu mikroskopioa (Leica Microsystems CMS GmbH, Wetzlar, Alemania) erabili zen portak aztertzeko.

2.4. *In vivo* entseguak

In vivo entseguetarako bost asteko BALB/COlaHsd saguak (Envigo) erabili ziren, 20 eta 25 g arteko pisua zutenak. Saguen erabilera Euskal Herriko Unibertsitateko (UPV/EHU) Animalien Esperimentazio Etika Batzordeak onetsi zuen (M20/2018/142), Espainiako eta Europar Batasuneko (EB) legeei jarraiki. Prozedura guztiak protokoloen arabera jarraitu ziren. Animaliak tenperaturaren, hezetasunaren eta 12 orduko gau-eguneko zikloen arabera egokitu ziren, jateko eta edateko aukera libre emanez.

Manipulazio esperimentalaren larritasuna saihestearren, saguak airean %1 eta %2 isofluranarekin (IsoFlo, Abbott, Madril, Espainia) anestesiatu ziren, 0,5–1 L/min arteko abiaduran.

Saguak gizalegez eutanasiatu ziren dislokazio zerbikalaren bidez, eta ondoren, begiak kendu zitzaizkien. Begi-enukleazioaren ondoren, begiak gatz-soluzio fisiologiko batean garbitu, %4 PFArekin 30 minutuz finkatu eta PBSrekin 5 minutuz garbitu ziren. Gero, begiak %30eko sukrosa zuen PBS soluzioan sartu ziren eta 4 °C-tan egon ziren harik eta begiak prezipitatu arte. Ondoren, bolumen erdia Tissue-Tek® O.C.T.™-rekin ordezkatu, eta giro-tenperaturan irabiaketan mantendu ziren bi orduz. Azkenean, begiak %100 Tissue-Tek® O.C.T. ™-ean eta -80° C-tan gorde ziren etorkizuneko ikasketetarako.

2.4.1. Bektoreen administrazioa

4. taulan deskribatutako formulazioak, %1 PVA-rekin (85,000 – 124,000 M_w) biskosizatu ziren, eta saguei begi instilazio-tanten bitartez administratu zitzaien. Horietaz gain GFP edo giza IL-10 kodetuta daramaten RNAm biluziak ere administratu ziren,. Nanosistemen administrazioa bi dosietan hiru egun zehar egin zen. Dosi bakoitzean, 2.5 µL bolumeneko hiru instilazio burutu ziren hiru minututan zehar, egunero 4.5 µg azido nukleiko administratuz.

4. taula. In vivo entseguan begi-tanta bezala administrazio topikorako aztertutako formulazioak

Formulazioak	GFP azterketa	IL-10 azterketa
Naked GFP mRNA	X	
Naked IL-10 mRNA		X
mRNA-DX-SLN1$_{EE}$	X	X
mRNA-AH-SLN1$_{EE}$	X	X
mRNA-DX-SLN1$_{HM}$	X	X
mRNA-AH-SLN1$_{HM}$	X	X
mRNA-SLN$_{C}$	X	X
mRNA-AH-SLN$_{C}$	X	
DNAp-DX-SLN1$_{HM}$	X	
DNAp-AH-SLN1$_{HM}$	X	
mRNA-DX-SLN1$_{EE}$_Au	X	
mRNA-AH-SLN1$_{EE}$_Au	X	

DX: dextranoa; AH: azido hialuronikoa; Au: urrea; SLN1$_{EE}$: DOTAP lipido kationikoa duen eta disolbatzailearen emultsifikazioa/lurrunketa bidez prestatutako SLN. SLN1$_{EE}$: DOTAP lipidoa kationikoa eta DODAP lipido ionizagarria duen disolbatzailearen emultsifikazioa/lurrunketa bidez prestatutako SLN. SLN1$_{HM}$: DOTAP lipido kationikoa duen urtze bero bidezko emultsifikazioarekin prestatutako SLN. SLN$_{C}$: koazerbazio metodoarekin prestatutako SLN.

2.4.2. Gene-adierazpenaren ebaluazioa

Gene-adierazpena honako hauek neurtuz ebaluatu zen:

- Ekoiztutako GFPrem presentziazelula-barnean.
- Jariatutako IL-10.

Bi transfekzioak immunofluoreszentzia bidez kualitatiboki ebaluatu ziren. Begiak histologikoki aztertu ziren kriostatoarekin (Cryocut 3000, Leica, Bensheim, Alemania) 14 µm lodierako ebaketetan. Ebaketak %20 PB buffer,%0.3 Triton X-100, %10 ahuntz serum eta %100ra iristeko nahikoa ur zuen indargetzailearekin blokeatu eta permeabilizatu ziren. Ondoren, entsegu bakoitzaren antigorputza(antiGFP edo anti-IL-10), gehitu eta 24 orduz 4 °C-tan inkubatu ziren. Hurrengo egunean, laginak garbitu ondoren, untxiaren aurkako IgG Alexa Fluor 488 ahuntz serumean dagoen antigorputz sekundarioa gehitu zen argitik babestuta 30 minutuz. Azkenik, laginak garbitu eta lehortu ondoren, DAPI-Fluoromount-G™ medio muntaketaz estali ziren. Ehun-sekzioak Zeiss LSM800 mikroskopio konfokalaren (ZEISS microscopy, Oberkochen, Alemania) bitartez aztertu ziren. Fluoreszentzia-emisioren espektro gainezarpena eskuratze sekuentzialari esker saihestu zen. Kornea bakoitzeko sei atal aztertu ziren ehun osoaren irudikapen gisa. Euskal Herriko Unibertsitateko (Leioa, Euskadi, Espainia) ikerkuntza zerbitzu orrokorren (SGIker) barruan dagoen “Mikroskopia Analitikoa eta Bereizmen Handikoa

Biomedikuntzan" zerbitzuak, laguntza teknikoa eta giza laguntza eman zuen mikroskopio konfokalaren erabilerako.

2.5. Data analisia

Datu esperimentalen analisia IBM SPSS Statistics 26 (IBM) software informatikoaren bidez egin zen. Saphiro–Wilk eta Levene probak homozedastizitatea eta aldakortasuna ebaluatzeko, eta laginen banaketa normala ebaluatzeko erabili ziren, hurrenez hurren. Student's t testa bi talde independenteen batez bestekoa konparatzeko eta ANOVA konparaketa anitz egiteko erabili ziren. Ondoren, Levene testean lortutako bariantzaren homogeneotasunaren arabera Bonferroni edo T3 Dunnet post-hoc testak aplikatu ziren. $p<0.05$ balioak estatistikoki adierazgarritzat jo ziren.

3. HIPOTESIA ETA HELBURUAK

3.1. Hipotesia

Gene-terapia geneen espresioa aldatuz gaixotasunak tratatzeko, sendatzeko edo prebenitzeko estrategia terapeutiko berritzailea da. Oraingoz, geneen adierazpena erregulatzeko helburuz azido nukleikoak askatzeko estrategia terapeutiko berritzaileak garatu dira. Estrategia hauetako bat, azido nukleiko baten (DNA edo RNAm) kopia funtzionalak administratzean datza, zeluletan proteina terapeutiko bat adieraztearren. Honi gehikuntza genikoa deritzo. Eskuarki, gehikuntza genikoa DNAp-ren bidez zuzendua izan da. Hala ere, azken urteetan RNAm-ren erabilera gene-terapiarako interes handia irabazten ari da haren ezaugarri espezifikoei esker, DNAp terapiaren aurrean etorkizun handiko beste aukera bat bilakatuz. Lehenik eta behin, askapenaren ikuspuntutik, RNAm-k ez du nukleoaren makineriaren beharrik funtzionala izateko, DNAp bidezko terapiak ordea, bai. Beraz, behin RNAm zitoplasmara iristean, kodetzen duen proteinaren itzulpena hasten da, eta zelula mitotikoetan eta ez-mitotikoetan eraginkorra da. Bigarrenik, segurtasunaren ikuspuntutik, RNAm ez da ostalariaren genoman integratzen, eta horren ondorioz, DNArekin lotutako kartzinogenesi eta mutagenesi arriskuak murrizten dira. Hirugarrenik, RNAm-k kodetzen duen proteinaren sintesia azkarra da eta bere adierazpena behin-behinekoa. Azkenik, IVT RNAm-aren ekoizpena DNAren fabrikazioa baino azkarragoa da, eta estandarizatu daiteke bere erreproduzigarritasuna mantenduz. Hala ere, IVT RNAm-k muga batzuk aurkezten ditu: immunogenizitatea, ezegonkortasuna fluido biologikoetan eta hainbat kanpoko eta barneko zelula-hesiak gainditzeko zailtasunak, besteak beste. Arazo hauek gainditzeko, askapen sistema bakoitzak azido nukleikoari, administrazio bideari eta itu-zelulari bereziki egokituta egon behar du.

LNPak azido nukleikoen askapenean oinarritutako sistema aurreratuenetakoak dira. Zentzu honetan, COVID-19ren pandemiak LNPetan oinarritutako lehen RNAm txertoaren onarpena bultzatu du. SLNak LNP mota bat dira. SLNak nukleo lipidiko solido batez osatutako partikulak dira, tentsioaktibo-geruza batez inguratuta daudenak. Eskala handian erraz ekoitzi daitezke; gainera, autoklabatu, esterilizatu edo liofilizatu daitezke, eta fluido biologikoetan eta biltegiratzean egonkorrak dira. SLNen gaitasuna azido nuklearrak degradaziotik babesteko, zelulen internalizazioa eta endosometatik ihesa errazteko, zitoplasman askatzeko eta nukleoaren sarrera sustatzeko ederki frogatua izan da. Askapen sistema honen beste abantaila bat bere gainazalean estekatzaileak erantsi daitezkeela da, itu-zeluletara material genetikoa bideratzea ahalbidetzen dutenak, tratamenduaren efikazia eta segurtasuna handituz.

SLNek azido nukleikoen askapenean etorkizun oparoko emaitzak erakutsi dituzte, begietako gaixotasunen alorrean batik bat. SLNek dituzten ezaugarriek (tamaina nanometrikoa, propietate lipofilikoak eta gainazal-karga positiboa) gai egiten dituzte begietako administrazio topikorako, baita kornearen iragazkortasuna eta atxikipena hobetzeko ere.

Gene-terapia begietako gaitzen tratamendurako aukera eraginkor gisa proposatua izan da, korneako asalduretan erabiltzekohain zuzen ere; haren gardentasunari, ongi mugatua duen anatomiari, eskuragarritasunari, azterketa ez-inbaditzaileari, administrazio errazari eta ikuspuntu immunologiko batetik isolatutako egitura izateari esker, batik bat. Hainbat faktorek (infekzioak, begi lehorra, betazalen nahasmendua, kalte fisiko eta kimikoak, adibidez) kornearen hantura edo keratitisa eragin dezakete. Kornearen hantura kronikoak ikusmen-asaldura eragiten du, eta sarritan ehunen suntsipena gertatzen da, kornean ultzerak, orbainak eta perforazioak sortuz eta azkenik ikusmen-urritasuna eta itsutasuna eragiten. Gainera, CNV faktore proangiogenikoen eta antiangiogenikoen arteko desorekaren ondorioz hantura-prozesuan gerta daiteke. Neobaskularizazioak begi-azalerari kalte egin diezaioke konponketa-prozesuan. Kornea-hanturaren aurkako gaur egungo tratamenduak kortikoideen erabileran dautza batez ere. Hala ere, haien erabilera mugatuta dago eragin ez desiragarrien eta efektuaren iraupen laburraren ondorioz. Hori dela eta, kornea-hantura tratatzeko estrategia terapeutiko berriak beharrezkoak dira. Zentzu honetan, IL-10 antiinflamatorioaren administrazio topikoa tratamendu eraginkor gisa proposatu egin da, nahiz eta bere begi-bioerabilgarritasun baxuak eta erdi-bizitza laburrak haren erabilera terapeutikoa mugatzen duten. Horregatik, azido nukleikoen askapenean oinarritutako gehikuntza genikoa etorkizun handiko estrategia izan liteke *de novo* IL-10 korneako zeluletan adierazteko hanturakontrako erantzunak lortzearren. Gainera, CNVri lotutako hantura MMP-9 faktore proangiogenikora bideratutako gene-isiltzearen bitartez tratatu daiteke. Izan ere, MMP-9 faktorea kornearen baldintza patologikoetan parte hartzen duten zelulaz kanpoko matrizea birmoldatzeko entzima nagusietako bat.

3.2. Helburuak

Tesi honen helburu nagusia DNAp edo RNAm duten SLNetan oinarritutako azido nukleikoen askapen-sistemak garatzea eta ebaluatzea zen, gehikuntza genikoa estrategiaren bitartez kornearen hantura tratatzeko. Helburu hori lortzeko, hurrengo urratsak gauzatu ziren.

1. IVT RNAm-ren funtzionalitatea eta eraginkortasuna hobetzeko erabilitako estrategien berrikusketa egin zen, baita haren egonkortasunaren optimizazioa, itzulpen-eraginkortasuna eta ezaugarri immunoestimulatzaileen berrikuspena ere (I. eranskina). Horretaz gain, estrategia teknologikoen eta IVT RNAm-n arrakastatsuak izan diren askapen-

nanosistemen gainikuspegia garatu zen eta halaber, RNAm-an oinarritutako terapien aplikazio potentzialen deskribapena (V. eranskina).

2. SLN desberdinetan oinarritutako azido nukleikoen askapen formulazioen diseinua, optimizazioa, karakterizazio fisiko-kimikoa, epe luzeko egonkortasuna eta *in vitro* ebaluazioa zelula-kulturetan (II. eranskina).

3. Kornea-hantura zuzentzeko SLNetan oinarritutako formulazioen diseinua, optimizazioa, karakterizazio fisiko-kimikoa eta *in vitro* ebaluazioa giza korneako epitelio zeluletan (HCE-2) (III. eta IV. eranskinak).

4. DNAp edo RNAm duten SLNetan oinarritutako formulazioen *in vivo* ebaluazioa saguen korneako epitelioan, instilazio bidezko administrazio topikoaren ondoren. Formulazioen transfekzio-eraginkortasuna, IL-10 sortzeko gaitasuna eta zitokina terapeutiko horren banaketa korneako ehunetan ebaluatu ziren (IV. eranskina).

5. Nanopartikula inorganikoak dituzten lipidoetan oinarritutako azido nukleikoen askapen nanobektore berrien diseinua, optimizazioa, karakterizazio fisiko-kimikoa, *in vitro* azterketa eta transfekzio gaitasunaren *in vivo* ebaluazioa saguetan begiko administrazio topikoa eta gero (VI. eranskina).

4. EMAITZAK ETA EZTABAIDA

Azido nukleikodun askapen sistema seguruen eta eraginkorren garapenak erronka izaten jarraitzen du, lipidoetan oinarritutako sistemak etorkizun handieneko bektore ez-biralak izanik. Horien artean, SLNak gene-terapiarako sistemarik moldakorrenetakoak eta eraginkorrenetakoak dira. Doktorego-tesi honetan, DNA eta RNAm duten SLNetan oinarritutako askapen sistemak optimizatu eta ebaluatu ziren, kornea-hanturari aurre egitearren. Alde batetik, SLNak formulatzeko erabiltzen diren lipido kationiko eta ionizagarri ezberdinen eragina ebaluatu zen; beste aldetik, nanopartikulak prestatzeko hainbat teknika aztertu ziren.

Formulazioak osagai hauek konbinatuz prestatu ziren: SLNak, azido nukleiko bat (DNAp, RNAm edo shRNA-p), protamina peptido kationikoa, eta polisakarido bat -DX edo AH. Azkenik, azido nukleikoak administratzeko nanobektore berri bat garatu zen AuNPak formulazioan gehituz. Osagaien arteko elkarrekintza elektrostatikoek zeregin garrantzitsua dute bektorearen eraketan, hauen azken egitura baldintzatzen baitute. Nanobektoreak prestatzeko, lehenbizi azido nukleikoa protaminarekin kondentsatu zen, zelularen kanpoaldean zein barnean material genetikoa batzen eta babesten laguntzeko [168,169]. Bigarrenik, behar izanez gero, polisakarido bat gehitu zen, DX edo AH. Bi polisakaridoek propietate egokiak dituzte azido nukleikoen askapena hobetzeko, zitotoxikotasun txikia dute eta kimikoki eralda daitezke. DX polianioi biobateragarria da, eta beste osagai biologiko batzuekiko elkarrekintzak oztopatzen ditu, serumaren proteinak kasu. AHak propietate mukoitsasgarriak eta helbideratzeko propietateak ditu [74,75,170]. Azkenik, SLNak aldez aurretik prestatutako konplexuarekin nahastu ziren. SLNak beharrezkoak dira transfekziorako. Izan ere, azido nukleikoa, P, eta DX edo AH zeramaten konplexuak zeluletara gehitu eta gero, zelula transfektatuen ehunekoa %0.8 baino txikiagoa lortu zen.

Ondoren, lan honetan lortutako emaitzak hurrengo ataletan laburbiltzen eta eztabaidatzen dira.

4.1. Lipido kationikoak eta ionizagarriak: azido nukleikodun SLNetan oinarritutako formulazioen *in vitro* karakterizazioa eta epe luzerako egonkortasuna

Doktorego-tesiaren lehen atalean, SLNak prestatzeko disolbatzailearen emultsifikazioa/lurrunketa metodoa (SLN_{EE}) erabili zen. Lipido kationikoen eta lipido ionizagarrien arteko konbinazioek SLNen ezaugarri fisiko-kimikoetan eta transfekzio-eraginkortasunean duten eragina ebaluatu zen.

DOTAP RNAm eta DNA administratzeko gehien erabilitako lipido kationikoa da. Lipido hau pH 7.4n erabat protonatuta dago; beraz, azido nukleikoak lipoplexetik bereizteko energia handia

behar du transfekzioak arrakasta izan dezan. Horrela, azido nukleikoen askapen eraginkortasuna hobetzeko, DOTAP lipidoa beste lipido laguntzaile batekin konbinatzeza beharrezkoa da [171]. Lipido ionizagarrien erabilera estrategia berriagoa da, hala nola, DODAP eta N-(4-carboxibencil)-N,N-dimetil-2,3-bis(oleoyloxy)propan-1-aminioa (DOBAQ). Lipido hauek neutroak dira pH fisiologikoan, baina endosomaren ingurune azidoan daudenean protonatzen dira. Endosomen mintzaren lipidoen eta lipido kationiko ionizagarrien arteko elkarrekintza elektrostatikoek mintzaren egitura hexagonala (HII) eratzea eragiten dute, azido nukleikoak endosometatik ihes egitea eta zelulen barnean askatzea erraztuz [46,54].

5. taulak SLNen batezbesteko diametroa, PDI eta ζ-potentziala erakusten ditu. SLN partikulen tamaina 185.1 nm eta 423.5 nm artekoa izan zen, PDI 0.4 baino txikiagoa, $SLN3_{EE}$ partikulen kasuan izan ezik, eta zeta potentziala -28.0 mV eta +59.5 mV artekoa.

5. taula. Nanopartikula solido lipidikoen (SLN) karakterizazio fisikoa.

SLN mota	(%) Lipido kationikoa			Tamaina (nm)	PDI	ζ-Potentziala (mV)
	DOTAP	DODAP	DOBAQ			
$SLN1_{EE}$	X			185.1 ± 3.5	0.30 ± 0.03	+59.5 ± 1.9
$SLN2_{EE}$	X	X		208.8 ± 0.4	0.27 ± 0.01	+50.2 ± 1.1
$SLN3_{EE}$			X	423.5 ± 51.7	0.57 ± 0.05	-28.0 ± 0.8
$SLN4_{EE}$	X		X	211.3 ± 3.5	0.36 ± 0.01	+42.4 ± 1.2

$SLN1_{EE}$: DOTAP lipido kationikoa duen eta disolbatzailearen emultsifikazioa/lurrunketa bidez prestatutako SLN; $SLN2_{EE}$: DOTAP lipidoa kationikoa eta DODAP lipido ionizagarria duen disolbatzailearen emultsifikazioa/lurrunketa bidez prestatutako SLN; $SLN3_{EE}$: DOBAQ lipido ionizagarria duen disolbatzailearen emultsifikazioa/lurrunketa bidez prestatutako SLN; $SLN4_{EE}$: DOTAP lipidoa kationikoa eta DOBAQ lipido ionizagarria duen disolbatzailearen emultsifikazioa/lurrunketa bidez prestatutako SLN; $SLN1_{HM}$: DOTAP lipido kationikoa duen urtze bero bidezko emultsifikazioarekin prestatutako SLN. SLN_C: koazerbazio metodoarekin prestatutako SLN. PDI: polidispertsitate indizea. Datuak batezbesteko ± desbiderapen estandar adierazten dira; *n* = 3.

5. taulan ikus daitekeenez, $SLN3_{EE}$ bektoreek, lipido kationiko bezala DOBAQ baino ez dutenak osagai bezala, 400 nm-tik gorako partikula tamaina izan zuten, 0.5-tik gorako PDI eta gainazaleko karga negatiboa (-28 mV). $SLN3_{EE}$ partikulek ez zuten ezaugarri fisiko-kimiko egokiak adierazi (tamaina handiegia, PDI zabalegia eta gainazaleko karga negatiboa). Horren ondorioz, $SLN3_{EE}$ partikulekin bektoreak prestatzeko asmoa baztertu zen.

SLNak karakterizatu eta gero, bektoreak GFP kodetzen zuen RNAm edo DNArekin prestatu ziren. 6. taulak SLNetan oinarritutako bektoreen tamaiana eta ζ-potentziala erakusten du. DNAp-dun formulazioek SLN leunen tamaina eta PDI antzekoa zuten baina ζ-potentzial txikiagoa erakutsi

zuten. RNAm-dun formulazioek, berriz, tamaina eta PDI handiagoak erakutsi zituzten, eta DNAp-dun formulazioek baino gainazaleko karga txikiagoa.

Table 6. SLN_{EE}-tan oinarritutako bektoreen karakterizazio fisikoa.

Azido nukleikoa	Bektoreak	Tamaina (nm)	PDI	ζ-potentziala (mV)
pcDNA3-EGFP plasmidoa	DNAp-DX-$SLN1_{EE}$	176.4 ± 0.4	0.27 ± 0.01	+45.4 ± 2.7
	DNAp-DX-$SLN2_{EE}$	165.8 ± 1.7	0.27 ± 0.01	+42.2 ± 0.9
	DNAp-DX-$SLN4_{EE}$	211.9 ± 14.6	0.40 ± 0.07	+32.6 ± 0.9
	DNAp-AH-$SLN1_{EE}$	201.2 ± 1.3	0.17 ± 0.01	+29.8 ± 1.1
	DNAp-AH-$SLN2_{EE}$	194.2 ± 0.8	0.20 ± 0.00	+35.6 ± 1.9
CleanCap™ EGFP RNAm (5moU)	RNAm-DX-$SLN1_{EE}$	246.8 ± 1.3	0.39 ± 0.02	+37.2 ± 1.0
	RNAm-DX-$SLN2_{EE}$	210.1 ± 0.8	0.26 ± 0.01	+36.5 ± 0.3
	RNAm-AH-$SLN1_{EE}$	202.4 ± 2.2	0.35 ± 0.00	+27.5 ± 0.6
	RNAm-AH-$SLN2_{EE}$	349.2 ± 9.9	0.39 ± 0.02	+18.5 ± 0.9
	RNAm-P0.25-$SLN1_{EE}$	251.6 ± 6.5	0.35 ± 0.01	+28.8 ± 0.7
	RNAm-P0.5-$SLN2_{EE}$	233.7 ± 2.8	0.24 ± 0.00	+25.4 ± 0.6
	RNAm-P1-$SLN2_{EE}$	261.7 ± 4.0	0.29 ± 0.02	+23.1 ± 1.3

P: protamina; DX: dextranoa; AH: azido hialuronikoa; $SLN1_{EE}$: DOTAP lipido kationikoa duen eta disolbatzailearen emultsifikazioa/lurrunketa bidez prestatutako SLN. $SLN2_{EE}$: DOTAP lipidoa kationikoa eta DODAP lipido ionizagarria duen disolbatzailearen emultsifikazioa/lurrunketa bidez prestatutako SLN. $SLN4_{EE}$: DOTAP lipidoa kationikoa eta DOBAQ lipido ionizagarria duen disolbatzailearen emultsifikazioa/lurrunketa bidez prestatutako SLN. PDI: polidispertsitate indizea. Datuak batezbesteko ± desbiderapen estandar adierazten dira; *n* = 3.

Transfekzioaren arrakasta, nanosistemak azido nukleikoaren degradazioaren aurka ematen duen babesaren eta hura zelula barruan askatzeko duen gaitasunaren arteko orekaren araberakoa da. Bektorearen gaitasuna azido nukleikoa lotzeko, babesteko eta askatzeko agarosa-gelean elektroforesi bidez aztertu zen. Emaitzek agerian utzi zuten DOTAP eta DOBAQ nahasketarekin prestatutako formulazioek ($SLN4_{EE}$) DNAp babesteko gaitasun txikia erakutsi zutela. Ondorioz, $SLN4_{EE}$-n oinarritutako bektoreak hurrengo entseguetarako baztertu ziren. DODAP lipidoarekin formulatutako SLNek ($SLN2_{EE}$) okerrago babestu zuten RNAm DNAp baino. Horrek RNAm kanpoko agenteen eraginpean geratzen dela adierazten du, hala nola RNasak. Bektoreek azido nukleikoak babesteko duten gaitasun desberdina RNAm-ren kate bakarreko egiturarekin lotuta egon daiteke. Izan ere, RNAm kate bikoitzeko DNAp-aren konformazioetatik desberdintzen duten bigarren eta hirugarren mailako egitura konplexuetan tolesten da [37].

Azterketa fisiko-kimikoen ondoren, DNAp-dun eta RNAm-dun bektoreen transfekzio gaitasuna eta zelula-sarrera bi zelula-lerroetan ebaluatu ziren: ARPE-19 eta HEK-293 zeluletan. Zelula-lerro horiek lehenago erabili izan dira DNAp-dun SLNetan oinarritutako askapen sistemen portaera

aztertzeko, zelula-banaketa tasa desberdina baitute (ARPE-19 zeluletan txikiagoa izanda) eta prozesu endozitiko nagusiei dagokienez ezaugarri desberdinak baitutuzte[172]. Formulazio guztiak bi zelula-lerroak transfektatzeko gai izan ziren, SLN mota edozein izanda ere, nahiz eta transfekzioaren eraginkortasuna aldatu egin zen zelula-lerroaren, azido nukleiko motaren eta bektoreen konposizioaren arabera.

Tenperaturak bektoreen transfekzioan eta zelula-sarreran zuen eragina ere aztertu zen. Bektorea osatzen duten osagai guztiek itu-zelulekiko interakzioa zehazten dute eta, beraz, baita internalizazio-prozesua, material genetikoaren portaera intrazelularra eta transfekzio-gaitasuna ere [74,90]. Zelulen internalizazio-mailak eta bektoreen endosometatik ihes egitea transfekzioaren eraginkortasuna baldintzatzen dute [173]. SLNetan oinarritutako bektoreen sartzeko mekanismo nagusia endozitosia da. Prozesu endozitiko nagusiak pinozitosia eta fagozitosia dira. Lehenengoa, nanopartikulen bilketari lotuta dago batez ere, eta hainbat sarbidek esku hartzen dute (mikropinozitosia, klatrina bidezkoa, kabeola bidezkoa edo independentea) [174]. Sartzeko bide nagusia itu-zelularen eta bektore ez-biralen konposizioaren eta ezaugarri fisiko-kimikoen araberakoa da [32]. Endozitosia energiaren eta tenperaturaren mendeko prozesua da, eta 4 °C-tan inhibitzen da zelulek ATP gutxiago kontsumitzen dutelako eta tenperatura horretan garraio aktiboa blokeatzen delako [175,176].

ARPE-19 zeluletan eta 37 °C-tan, DNAp-dun bektoreek (7.A irudia) RNAm-dun (7.C irudia) baino zelula transfektatuen ehuneko txikiagoa eragin zuten. Hala ere, DNAp-rekin transfektatutako zelulek fluoreszentzia-intentsitate handiagoak erakutsi zituzten (7.B eta 7.D irudiak); hau da, zelula-lerro horrek DNAp bidezko transfekzioak protein ekoizpen eraginkorragoa lortu zuen. HEK-293 zeluletan (8. irudia), DNAp-n oinarritutako bektoreek RNAm bektoreek baino transfekzio-eraginkortasun txikiagoa eragin zuten, zelula transfektatu kopuruari eta protein ekoizpenari dagokienez. DNAp-dun bektoreen artean, bi zelula-lerroetan transfekzio-eraginkortasun handiena AH zuten bektoreekin ikusi zen, eta ARPE-19 zeluletan, DNAp, AH eta $SLN1_{EE}$ zituen bektorearekin bereziki. RNAm formulazioei dagokienez, polisakarido bat sartzeak ez zuen eragin handirik izan *in vitro* transfekzioaren eraginkortasunean.

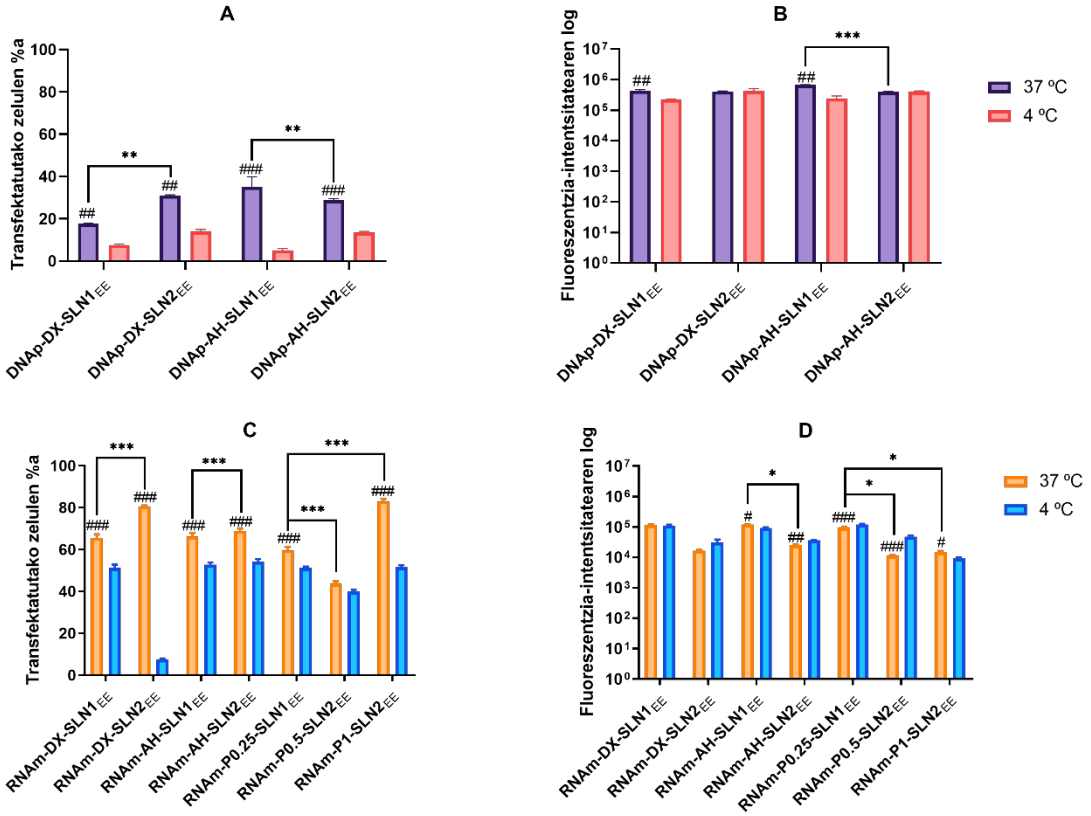

*7. irudia. ARPE-19 zelula transfektatuen ehunekoaren eta fluoreszentzia-intentsitatearen fluxu-zitometria bidezko analisia, SLN1EE eta SLN2EE bektoreekin 37 °C eta 4 °C-tan inkubatu ondoren. Transfekzio-ehunekoaren balioak zelula guztietatik GFP zelula fluoreszente positiboei dagozkie. Fluoreszentzia-intentsitatearen logaritmoak markatutako zelula bakoitzeko fluoreszentziaren batezbesteko intentsitatea adierazten du. A: DNAp bektoreekin tratatu eta 72 ordura transfektatutako ARPE-19 zelulen ehunekoa. B: DNAp bektoreekin tratatu eta 72 ordura transfektatutako ARPE-19 zelulen fluoreszentzia-intentsitatearen logaritmoa. C: RNAm bektoreekin tratatu eta 48 ordura transfektatutako ARPE-19 zelulen ehunekoa. D: RNAm bektoreekin tratatu eta 48 ordura transfektatutako ARPE-19 zelulen fluoreszentzia-intentsitatearen logaritmoa. Datuak batezbesteko ± desbiderapen estandar adierazten dira; n = 3. # p<0.05 4 °C-ko bektore berarekiko. ## p<0.01 4 °C-ko bektore berarekiko. ### p<0.001 4 °C-ko bektore berarekiko. * p<0.05 beste formulazioarekiko. ** p<0.01 beste formulazioarekiko. *** p<0.001 beste formulazioarekiko. P: protamina; DX: dextranoa; AH: azido hialuronikoa; $SLN1_{EE}$: DOTAP lipido kationikoa duen disolbatzailearen emultsifikazioa/lurrunketa bidez prestatutako SLN. $SLN2_{EE}$: DOTAP lipido kationikoa eta DODAP lipido ionizagarria duen disolbatzailearen emultsifikazioa/lurrunketa bidez prestatutako SLN.*

Oro har, DNAp-dun eta RNAm-dun bektore guztien internalizazioa % 90etik gorakoa izan zen 37 °C-tan. Beraz, DNAp bektoreekin lortutako zelula transfekzio ehunekoa baxuagoa zelula barneko hesiek eragindako oztopoen ondorioa dira. DNAp-ren transfekzio arrakastatsu baterako oztoporik nagusiena sarrera nuklearra dela dirudi, nahiz eta gure sistemek protamina duten, zeinak transkripzio-prozesua eta DNAp-ren sarrera nukleoan errazten duen kokapen nuklearraren seinaleei esker [168].

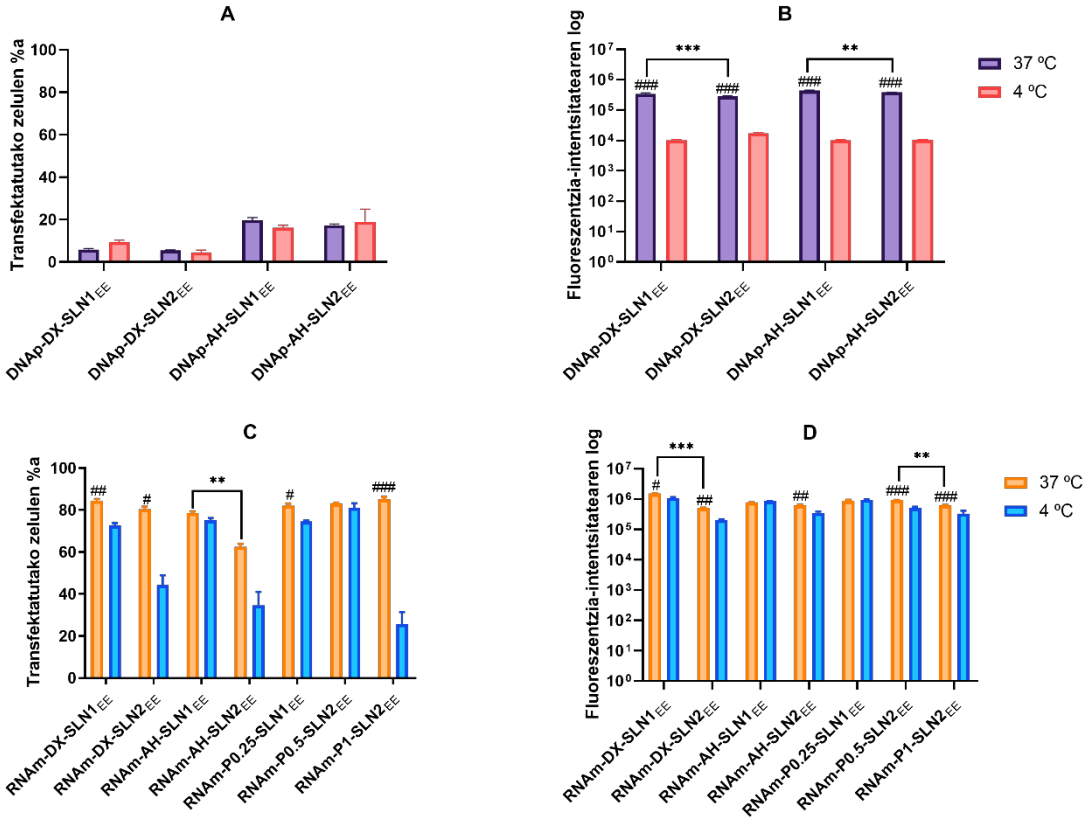

*8. irudia. HEK-293 zelula transfektatuen ehunekoa eta fluoreszentzia-intentsitatea, $SLN1_{EE}$ eta $SLN2_{EE}$ bektoreekin 37 ° C eta 4 ° C-tan inkubatu ondoren. Transfekzio-ehunekoaren balioak zelula guztien aldean GFPko zelula fluoreszente positiboei dagozkie. Fluoreszentzia-intentsitatearen logaritmoak markatutako zelula bakoitzeko fluoreszentziaren batezbesteko intentsitatea adierazten du. A: DNAp bektoreekin tratatu eta 72 ordura transfektatutako HEK-293 zelulen ehunekoa. B: DNAp bektoreekin tratatu eta 72 ordura transfektatutako HEK-293 zelulen fluoreszentzia-intentsitatearen logaritmoa. C: RNAm bektoreekin tratatu eta 48 ordura transfektatutako HEK-293 zelulen ehunekoa. D: RNAm bektoreekin tratatu eta 48 ordura transfektatutako HEK-293 zelulen fluoreszentzia-intentsitatearen logaritmoa. Datuak batezbesteko ± desbiderapen estandar adierazten dira; n = 3. # p<0.05 4 °C-ko bektore berarekiko. ## p<0.01 4 °C-ko bektore berarekiko. ### p<0.001 4 °C-ko bektore berarekiko. ** p<0.01 beste formulazioarekiko. *** p<0.001 beste formulazioarekiko. P: protamina; DX: dextranoa; AH: azido hialuronikoa; $SLN1_{EE}$: DOTAP lipido kationikoa duen disolbatzailearen emultsifikazioa/lurrunketa bidez prestatutako SLN. $SLN2_{EE}$: DOTAP lipido kationikoa eta DODAP lipido ionizagarria duen disolbatzailearen emultsifikazioa/lurrunketa bidez prestatutako SLN.*

4 °C-tan, ARPE-19 zelula transfektatuen ehunekoa nabarmen jaitsi zen ia formulazio guztiekin, eta DNAp formulazioekin batez ere. DNAp-$SLN1_{EE}$ formulazioarekin 4 °C-tan lortutako zelula-internalizazio baxua formulazio horren transfekzio-eraginkortasun baxua azaltzen du. Aitzitik, DNAp-$SLN2_{EE}$ eta RNAm bektoreen sarrera-ehunekoa ez zen ia aldatu 4 °C-tan, horrek energia-menpekoak ez diren sarrera mekanismoak erabiltzen direla erakusten duelarik. Kontuan izan behar da, halaber, sistema biologikoen izaera dela eta, hainbat prozesu dinamiko paraleloan gerta daitezkeela, elkarren artean lehian aritu daitezkeenak [177]. Zelula transfektatu gutxiago egon arren, 4 °C-tan ARPE-19 zeluletan behatutako protein ekoizpen handiagoak adierazten du

energia-menpekoak ez diren mekanismoak eraginkorragoak direla proteinen ekoizpena eragiteko, batez ere DODAP duten bektoreen kasuan.

HEK-293 zeluletan, zelula-internalizazioa izugarri murriztu zen 4 °C-tan. Zelula-lerro horrek kabeola-mendeko aktibitate endozitiko handia du, eta garraio aktiboaren blokeoak internalizazioan eragin handia du. DNAp bektoreen kasuan, transfekzioaren fluoreszentzia-intentsitatea ere nabarmenki jaitsi zen 4 °C-tan, baina transfektatutako zelulen ehunekoa ez zen aldatu (8. Irudia). RNAm bektoreen kasuan, bai transfekzioaren ehunekoa bai fluoreszentzia-intentsitatea jaitsi egin ziren tenperatura baxuan, baina RNAm-SLN1$_{EE}$ bektoreen eragina SLN2$_{EE}$ formulazioena baino txikiagoa izan zen. Emaitza horiek guztiak kontuan hartuta, ondoriozta dezakegu HEK-293 zeluletan energia mendeko sarrera-mekanismoak eraginkorrenak direla, DNAp bektoreak prestatzeko erabiltzen den SLN mota edozein dela ere, eta batez ere RNAm duten SLN2$_{EE}$ formulazioetan. Onartzen da RNAm-ren askapen-abiadura mugatzen duen oztopo nagusienetako bat endosomoetatik ihes egitea dela [178], eta lipido ionizagarriek, hala nola DODAP lipidoak, prozesu hori erraztu lezakete. Hala ere, duela gutxi, Patel et al.ek jakinarazi zuten endosoma/lisosoma berantiarrak sortzea ezinbestekoa zirela RNAm exogenoaren askapen funtzionala lortzeko [27]. Endosometatik ihes egitearen gaitasunaren eta zitoplasman translokatutako azido nukleikoen egonkortasunaren arteko oreka funtsezkoa da transfekzio eraginkorra lortzeko. Ezinbestekoa da azido nukleikoetan oinarritutako sendagaien garapenaren lehen urratsetan itu-zeluleetako azterketa mekanistikoak egitea, azido nukleikodun nanomedikamentuen portaera intrazelularra sakon ulertzearren. Ezagutza horri esker, azido nukleikoaren, aplikazio klinikoaren eta helburu terapeutikoaren ezaugarrietara egokitutako formulazioegokian diseinatu ahal izango da.

Lan honetan, formulazioaren konpozisioak eragin handiago izan zuen RNAm-ren dispozisio intrazelularrean DNAp-renean baino. 9. irudian ikus daitekeenez, RNAm-SLN1$_{EE}$ bektorea zitoplasman sakabanatuta agertzen zen, bereziki HEK-293 zeluletan, eta horrek degradazioarekiko esposizio handiagoaren adierazle izan daiteke. Hau, RNAm ARPE-19 zeluletan HEK-293 zeluletan baino eraginkorragoa izatearen arrazoia izan liteke. RNAm-SLN2$_{EE}$ bektoreen kasuan, azido nukleikoa ia ez zen hauteman eta bi zelula-lerroetan oso kondentsatuta zegoen. Agarosa-gelean, SLN2$_{EE}$ partikulekin prestatutako formulazioek babes-maila txikiagoa erakutsi zuten, eta horrek zerikusia izan dezake zitoplasma zelularrean ikusitako RNAm kantitate txikiagoarekin. Zelula-barneko dispozisioaren desberdintasunak azido nukleikoa batzeko, kondentsatzeko eta bektoreek babesteko duten gaitasunarekin ez ezik, bektoreen sarrera-mekanismoarekin eta zirkulazio intrazelularrarekin ere zerikusia zuten. Izan ere, azken hauek zelula-lerroaren mendeko prozesuak dira.

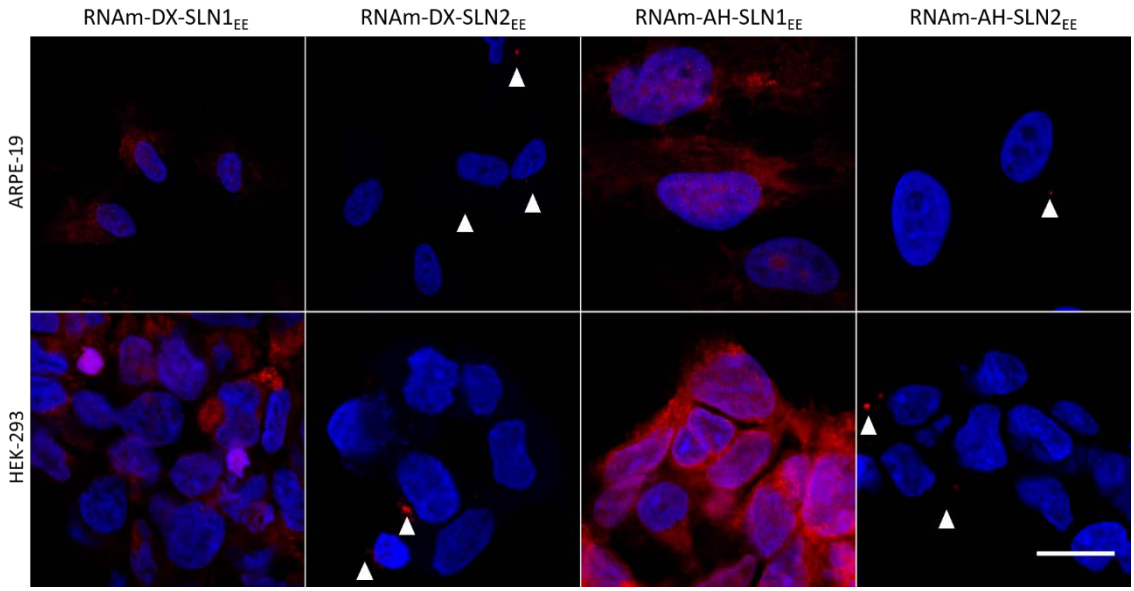

9. irudia. Fluoreszentzia-mikroskopiako irudiak ARPE-19 eta HEK-293 zeluletan $SLN1_{EE}$n eta $SLN2_{EE}$n oinarritutako RNAm bektoreak gehitu eta 4 ordura. Bektoreak CleanCap™ Cyanine 5 EGFP RNAm (5moU) P, DX edo AH bidez formulatuta daude. Nukleoak DAPIrekin (urdina) markatu ziren. 60 × handiagotua. Eskala-barra: 15 µm. Triangelu zuriek RNAm kondentsatua adierazten dute. DX: dextranoa; AH: azido hialuronikoa; $SLN1_{EE}$: DOTAP lipido kationikoa duen disolbatzailearen emultsifikazioa/lurrunketa bidez prestatutako SLN; $SLN2_{EE}$: DOTAP lipido kationikoa eta DODAP lipido ionizagarria duen disolbatzailearen emultsifikazioa/lurrunketa bidez prestatutako SLN.

Administrazio-sistemen eraginkortasuna eta egonkortasuna bermatu behar dira biltegiratuta mantentzen diren bitartean. Izan ere, azido nukleikoetan oinarritutako sendagaien egonkortasun termikoa garrantzitsua da, biltegiratze-baldintzak arazo logistikoa baitira biltegiratzeko eta banatzeko momentuan, batez ere hotz-kateari eusteko, azpiegiturarik ez duten herrialdeetan [179]. Doktorego-tesi honetan 4 °C-tan zazpi hilabeteetan zehar biltegiratuta egon ziren nanobektoreen ezaugarri fisiko-kimikoen eta transfekzioa-eraginkortasunaren azterketak ARPE-19 zeluletan egin ziren.

DNAp formulazioek aldaketa fisiko-kimikoak erakutsi zituzten bigarren hilabetetik aurrera, baina transfekzioaren eraginkortasuna zazpi hilabetez mantendu zen *in vitro*. Aitzitik, RNAm bektoreak egonkorragoak izan ziren ezaugarri fisiko-kimikoei dagokienez, baina transfekzioa izugarri jaitsi zen $SLN2_{EE}$ zuten bektoreekin lehen hilabetetik aurrera. DODAP lipidoaren karga positiboen kopuru txikiagoa material genetikoa kondentsatzeko gaitasun txikiagoarekin lotuta dago, eta hori $SLN2_{EE}$ partikuletan oinarritutako bektoreen egonkortasun baxuagoaren arrazoia izan daiteke, RNAm duten formulazioetan bereziki. RNAm eta $SLN1_{EE}$ bidez prestatutako bektoreek % 80tik gorako zelula transfekzioa erakutsi zuten entseguaren zazpi hilabeteetan zehar, polisakaridorik gabe prestatutako formulazioak izan ezik. Horrenbestez, $SLN1_{EE}$ formulazioetan polisakarido bat sartzeak, RNAm administratzeko lehen aipatutako propietate onuragarriez gain;

hala nola, osagai biologikoekiko interakzioak oztopatzeko gaitasuna eta itu-zelulara sartzeko mekanismoa modulatzeko gaitasuna, egonkortasuna ere ematen du [74,75,172].

SLNak lipido ionizagarri batekin formulatzeak azido nukleikoa kondentsatzeko eta babesteko ahalmena aldatu zuen. Lipido ionizagarriek endosomatik ihesa errazten duten arren, nanobektoreetan sartzeak ez zuen beti transfekzioaren eraginkortasuna hobetu. Epe-luzeko eraginkortasuna eta egonkortasuna kontuan hartuta, bazirudien DOTAP lipido kationikoarekin soilik prestatutako bektoreak DNAp eta RNAm administratzeko formulazio etorkizun oparokonak zirela. Horren ondorioz, DOTAP lipido kationikoa zeramaten SLNak; hau da $SLN1_{EE}$, hurrengo entseguetarako hautatu ziren.

4.2. SLNtan oinarritutako formulazioen ebaluazioa *in vitro* HCE-2 zeluletan, korneako hantura tratatzeko duten gaitasuna aztertzeko

4.2.1. MMP-9ren gene-isiltzea

Lehenago aipatu den bezala, kornearen neobaskularizazioa (CNV) prozesu inflamatorioa ematen den bitartean faktore angiogenikoen eta antiangiogenikoen arteko desorekaren ondorioz gerta daiteke [131]. Neobaskularizazioak begi-azaleran kalteak eragin ditzake eta ikusmen-zolitasunean eragina izan dezake, korneak bere baskulartasun eza galtzen baitu [132]. CNVari lotutako hanturaren aurkako tratamenduan erabilitako estrategien artean, faktore proangiogenikoetara zuzendutako gene-isiltzea baliagarria dela frogatu da [180]. Faktore proangiogeniko horietako bat MMP-9 da, korneako baldintza patologikoetan parte hartzen duen zelulaz kanpoko matrizea birmoldatzeko entzima nagusietako bat [123].

Doktorego-tesiaren bigarren zati honetan $SLN1_{EE}$, P, DX eta shRNA-p-MMP-9-rekin formulatutako bektoreak garatu ziren. shRNA-ei RNAi aktibatzaile adierazia ere esaten zaie. Hauek siRNA ekoizteko nukleoan transkibatu behar diren plasmidoak dira, gene baten adierazpenaren murrizten dutenak. Protamina eta DX proportzio desberdinetan zuten bektoreak prestatu ziren. shRNA-p-MMP-9 duten nanosistemek ezaugarri egokiak erakutsi zituzten transfekziorako: partikula tamaina nanometroen tartean (182 nm-tik 216 nm-ra), gainazaleko karga kationikoa (+36,1 mV-tik +45,7 mV-ra) eta baita shRNA-p-MMP-9 batzeko, askatzeko eta nukleasen aurka babesteko gaitasuna ere. Nanobektoreak HCE-2 zelulak transfektatzeko gai izan ziren, eta DX:P:shRNA-p-MMP-9:$SLN1_{EE}$ 2:1:1:5 (w:w:w:w) proportzioan prestatutako bektorea, zelula transfektatuen ehunekoari (% 5.6) eta adierazitako proteina kantitateari dagokionez eraginkorrena izan zen. Bektore horrek HCE-2 zelulek sintetizatutako MMP-9a %30 gutxitzea eragin zuen. Bektorearen efektua internalizazio handiarekin eta plasmidoa zitoplasman mintz nuklearretik gertu askatzeko gaitasunarekin erlazionatuta zegoen.

HCE-2 zeluletan MMP-9 isilarazteko eraginkortasuna frogatu ondoren, SLNetan oinarritutako bektoreak TNF-α bidez estimulatutako zeluletan ebaluatu ziren. TNF-α hanturazko bitartekaria da, eta zeregin garrantzitsua du korneako hainbat gaitzetan [181]. HCE zelulen hesi-funtzioa aldatzen du eta begietako hanturan laguntzen du [182,183]. Dirudienez, keratitisa duten pertsonen korneak TNF-α kontzentrazio altua du [183], eta zitokina horrek HCE zeluletan MMP-9aren jarduera estimulatzen duela frogatu da [123]. HCE-2 zelulak TNF-α-rekin estimulatu ondoren, MMP-9 kontzentrazioak handitu ziren, eta demonstratu zen SLNetan oinarritutako bektoreak gai zirela TNF-α bidez estimulatutako zeluletan MMP-9ren ekoizpena murrizteko . Emaitza hauek adierazten dute TNF-α bidez estimulatutako HCE-2 zelulen egokitasuna *in vitro* eredu gisa erabiltzeko, MMP-9ren erregulazioan oinarritutako formulazio berriak ebaluatzeko.

MMPak zelula kanpoko matrizeko proteina ugari bereizteko gai diren entzimak dira, eta zelula epitelialak korneatik azpiko estromara migratzea errazten dute [67,116–118,152]. Izan ere, MMPen ekoizpena eta aktibitatea handitzean zelula-fenotipo migratzaileago eta inbaditzaileagoarekin lotuta dago [153,154]; aitzitik, MMP-9ren murrizketak HCE zelulen migrazioa inhibitzen du [184]. 10. irudian DX:P:shRNA-p-MMP9:SLN1$_{EE}$ bektoreak daukan efektua HCE-2 zelulen migrazioan, zauriak sendatzeko *in vitro* saiakuntza batean. Bektorea zelulen migrazioa murrizteko gai izan zen. Efektu hori MMP-9ren ekoizpenaren inhibizioarekin lotuta egon daiteke. MMP-9ak IV motako kolagenoa eta gelatina substratuak degradatzen ditu [185], eta horrek, aldi berean, HCE zelulen migrazioa errazten du. MMP-9ren maila murrizteak gelatina (zelulaz kanpoko matrizeko proteina) degradatzeko gaitasuna eta korneako zelula epitelialen migrazioa txikiagotzen ditu.

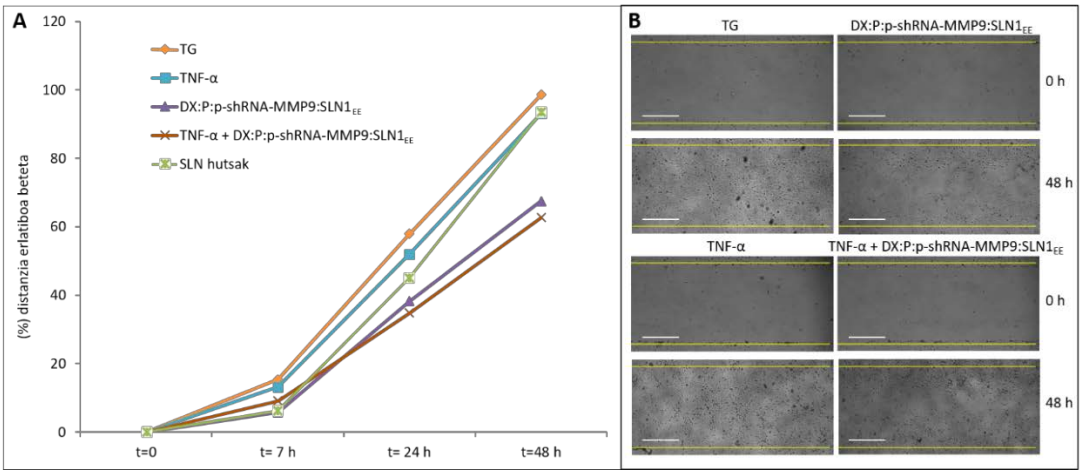

*10. irudia. DX:P:shRNA-p-MMP9:SLN1$_{EE}$ bektorearen efektua HCE-2 zelulen migrazioan. (A) Zauriaren ertzeko zelulen arteko distantziaren eboluzioa; zauriaren zabaleraren murrizketaren baldintza bakoitzeko 4 errepliken batezbesteko neurketak. (B) Fase-kontrastearen irudi adierazgarriak (4×). TG: Tratatu gabeko zelulak. TNF-α: tumor necrosis alfa faktorea. P: protamine. DX: dextranoa. SLN1$_{EE}$: DOTAP lipido kationikoa duen disolbatzailearen emultsifikazioa/lurrunketa bidez prestatutako SLN. Estatistika 48 ordura. * p<0.05 TG-rekiko, ** p<0.05 TNF-α-rekin tratatutako zelulekiko. Eskala-barra: 60 µm.*

MMP-9ak angiogenesian eta, zehazki, keratitis herpetikoari lotutako angiogenesian paper garrantzitsua betetzen du [125]. Kornearen abaskularitazioa faktore proangiogenikoen eta antiangiogenikoen arteko orekaren menpe dago [186]. Korneako zelula epitelialek faktore angiogenikoak askatzen dituzte estimulu bati erantzuteko, eta faktore horiek hodi perikornealetako zelula endotelial baskularren hartzaileei lotzen zaizkie [134]. Gainera, CNV korneako estroman gertatzen den arren, korneako epitelioan adierazitako faktoreek erregulatzen dute. DX:P:shRNA-p-MMP9:SLN1$_{EE}$ bektoreak hodi kapilarren eraketa partzialki ezabatzeko gai izan ziren HUVEC zeluletan hodi kapilarrak *in vitro* eratzeko entseguan (5. irudia). Neurketa morfometrikoek agerian utzi zuten segmentu nagusien luzera osoa, sare-kopurua, segmentuen luzera osoa eta luzera osoa txikiagotu egin zirela HUVEC zeluletan, bektoreekin tratatutako HCE-2 zezulekin sortutako hazkuntza-medioa gehitu zitzaienean . Eratutako hodi-kapilarren inhibizioa HCE-2 zelulek jariatutako MMP-9 murrizketaren neurrikoa izan zen. Gure bektorearen efektua TNF-α bidez estimulatutako zeluletan ere bermatu zen.

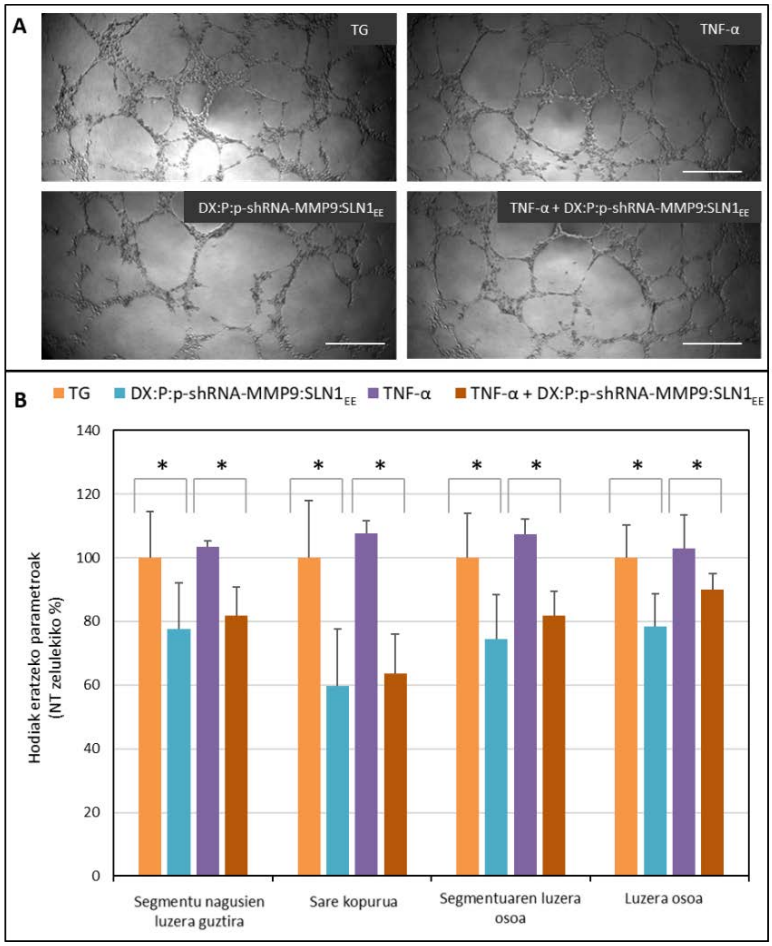

5. irudia. (A) Giza zilbor-zaineko zelula endotelialetan (HUVEC) hodiak eratzeko saiakuntzan lortutako irudi adierazgarriak eta (B) hodien eraketaren kuantifikazioa. TG: Tratatu gabeko zelulak. TNF-α: tumor necrosis alfa faktorea. P: protamine. DX: dextranoa. SLN1$_{EE}$: DOTAP lipido kationikoa duen disolbatzailearen emultsifikazioa/lurrunketa bidez prestatutako SLN. Datuak normalizatu egin ziren TG zelulen balioen arabera . p<0.05. Eskala-barra: 60 µm.*

4.2.2. IL-10 ekoizteko gehikuntza genikoa

Korneako zeluletan hanturaren aurkako bitartekarien *de novo* sintesia eragitea izan daiteke kornearen hantura tratatzeko beste estrategia bat, horretarako azido nukleikoen bitartez, beharreko proteinak ekoiztu behar direlarik, IL10, esaterako. Kasu honetan, RNAm edo DNAp azido nukleikoak zeramaten nanobektoreen bidezko gehikuntza genikoa ebaluatu zen. Kornea-transfekzioa ebaluatzeko helburuarekin, hiru SLN mota desberdin prestatu ziren, hiru metodo desberdinak erabiltzen: SLN_{EE}ak, urtze bero bidezko emulsifikazioaren bidez prestatutako SLNak (SLN_{HM}) edo koazerbazioa erabilita egindako SLNak (SLN_C). Bereziki, SLN_{EE}-ak eta SLN_{HM}-ak DOTAP lipido kationikoarekin prestatu ziren, eta SLN_C-ak, berriz, beste osagai kimikoekin. 7. taulak SLNen batezbesteko diametroa, PDI eta ζ-potentziala erakusten ditu. SLNak prestatzeko metodoak SLNen ezaugarri fisiko-kimikoetan eragina izan zuen, partikularen tamainari eta gainazaleko kargari dagokienez. Disolbatzailerik gabeko koazerbazio metodoarekin, partikula tamaina handiagoa (307.8 nm) eta ζ-potentzial txikiagoa (+21.1 mV) lortu zen. Partikulen tamaina 93.3 nm ingurukoa izan zen urtze bero bidezko emulsifikazio prozeduraren kasuan. Honek disolbatzaile organikoa erabiltzea saihesten du, baina tenperatura altuak erabiltzea eskatzen du. Disolbatzailearen emultsifikazioa/lurrunketa bidez prestatutako SLNen batezbesteko tamaina, aldiz, 198.7 nmkoaizan zen.

7. taula. Nanopartikula lipidiko solidoen (SLN) karakterizazio fisikoa.

SLN mota	Agente kationikoa		Tamaina (nm)	PDI	ζ-Potentziala (mV)
	DOTAP	DEAE-dextranoa			
$SLN1_{EE}$	X		198.7 ± 2.0	0.26 ± 0.01	+57.8 ± 1.7
$SLN1_{HM}$	X		93.3 ± 0.4	0.28 ± 0.01	+68.5 ± 0.7
SLN_C		X	307.8 ± 3.5	0.17 ± 0.01	+21.1 ± 0.8

$SLN1_{EE}$: DOTAP lipido kationikoa duen disolbatzailearen emultsifikazioa/lurrunketa bidez prestatutako SLN. $SLN1_{HM}$: DOTAP lipido kationikoa duen urtze bero bidezko emultsifikazioarekin prestatutako SLN. SLN_C: koazerbazio metodoarekin lortutako SLN. PDI: polidispertsitate indizea. Datuak batezbesteko ± desbiderapen estandar adierazten dira; n = 3.

SLNen karakterizazioaren ondoren, bektoreak GFP edo IL-10 kodetzen zuten RNAm edo DNAp-rekin prestatu ziren. GFP zelula-barneko proteina da, transfektatutako zelula kopurua eta transfektatutako zelulen fluoreszentzia-intentsitateakuantifikatzeka ahalbidetzen duena transfekzioaren eraginkortasuna ebaluatzeko. Bestalde, zelulek jariatzen duten IL-10 (proteina terapeutikoa) transfekzioaren eraginkortasuna ebaluatzeko erabiltzen da, IL.10en ekoizpena kuantifikatuz. Azido nukleikoarekin, protaminarekin eta polisakaridoarekin osatutako konplexua SLNei gehitu zitzaien azkeneko formulazioak lortzeko.

Kornea-transfekziorako, tamaina txikiko partikulek, 10 eta 1,000 nm bitartekoek hain zuzen ere, administrazio topikoarekin sortutako suminkortasuna murrizten dute. Gainera, propietate mukoitsasgarriak dituzte, atxikipen-denbora luzatzen laguntzen dute eta, ondorioz, farmakoaren bioerabilgarritasuna handitzen dute begi-ehunetan [98,187]. Atal honetan prestatutako bektoreek 300 nm-tik beherako batezbesteko tamaina zuten eta gainazaleko karga positiboa, zelula-sarrera errazten duena [99] eta korneako epitelioan atxikipen-denbora luzatzen duena, negatiboki kargatutako begi-gainazalarean ematen diren interakzio elektrostatikoei esker [188].

SLN_C-bektoreek azido nukleikoa kanpoko agenteen aurka babesteko eta askatzeko gaitasun ahula erakutsi zuten. RNAm-$SLN1_{EE}$ eta RNAm-$SLN1_{HM}$ bektoreen kasuan, berriz, desberdintasun nagusiak kondentsazio-mailan antzeman ziren. Hala ere, bi formulazioek RNAm modu eraginkorrean babestu eta askatu zuten. Doktorego-tesi honen lehen zati esperimentalean azaldu bezala, badirudi RNAm DNAp baino sentikorragoa dela formulazioarekin lotutako faktoreekiko.

Tenperaturak HCE-2 zelulak transfektatzeko eraginkortasunean duen eragina aztertu zen, bi tenperatuka ezberdinetan lortutako emaitzak konparatuz (37 °C eta 4 °C). Zeluletan sarrera egonkor mantendu zen bi tenperaturetan, eta horrek adierazten du energiaren mendeko sarrera-mekanismoak ez ezik, energiarekiko independenteak diren sarrera-mekanismoak ere gauzatzen direla. Aitzitik, GFPrekin transfektatutako zelulen ehunekoa (12. irudia) nabarmen jaitsi zen 4 °C-tan, eta fluoreszentziaren intentsitatea, transfektatutako zelulek sortutako proteina kopuruaren adierazle dena, ia egonkor mantendu zen. Beraz, tenperatura hotzean, zelula transfektatu gutxik proteina ugari sortzeko gai izan ziren. Emaitza horiek erakusten zutenez, energiaren mendeko mekanismoek HCE-2 zelulen transfekzioa bultzatzen dute, baina badirudi protein ekoizpena eraginkorragoa dela bektoreak energiaren mekanismo independenteen bidez sartzen direnean. RNAm-n eta DNAp-n oinarritutako bektoreen transfekzio-gaitasuna antzekoa izan zen zelula transfektatuei eta fluoreszentzia-intentsitateari dagokienez. Emaitza horiek adierazten dute korneako zelula epitelialetan transfekzio arrakastatsua lortzeko oztopoa nukleoan sartu aurretik dagoela; ondorioz, badirudi gure nanosistemen portaera intrazitoplasmatikoa transfekziorako oztopo mugatzailea dela.

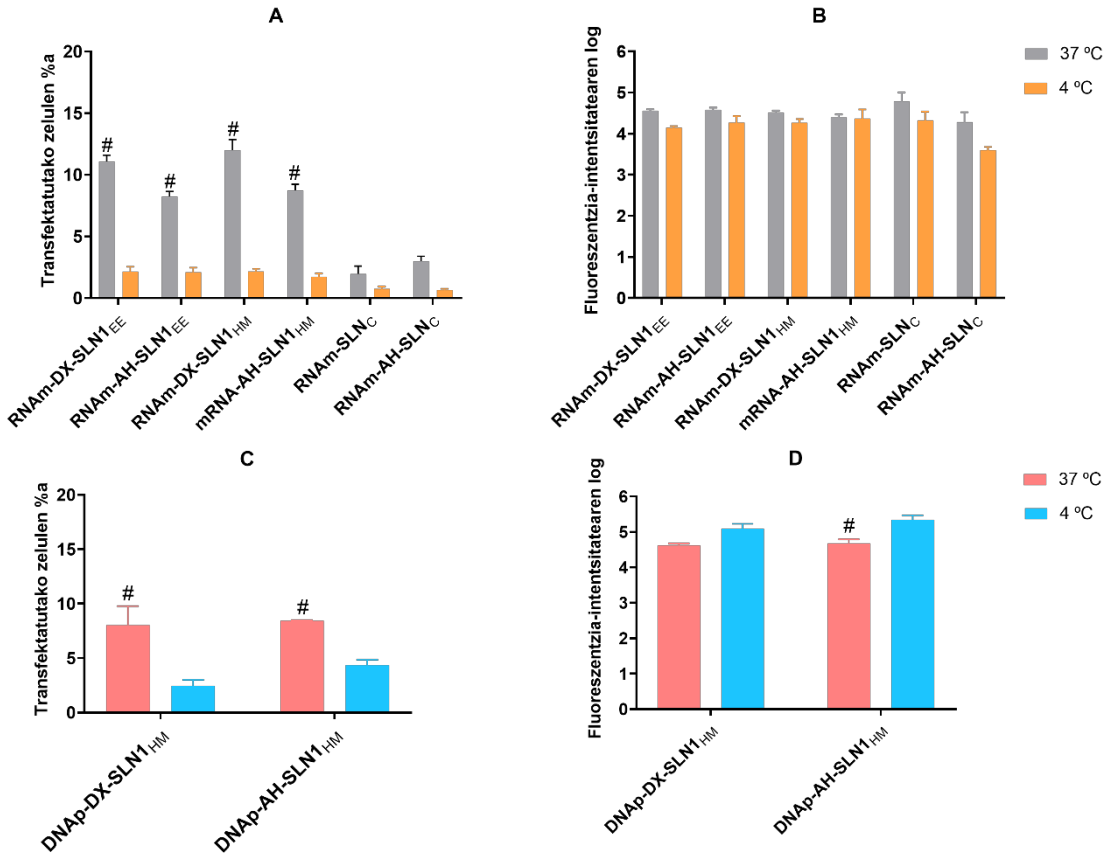

12. irudia. GFPrekin transfektatutako HCE-2 zelulen ehunekoaren eta fluoreszentzia-intentsitatearen fluxu-zitometria bidezko analisia, $SLN1_{EE}$, $SLN1_{HM}$ eta SLN_C bektoreekin 37 ° C eta 4 ° C-tan inkubatu ondoren. Transfekzio-ehunekoaren balioak zelula guztietatik GFP zelula fluoreszente positiboei dagozkie. Fluoreszentzia-intentsitatearen logaritmoak markatutako zelula bakoitzeko fluoreszentziaren batez besteko intentsitatea adierazten du. (A) RNAm bektoreekin tratatu eta 48 ordura transfektatutako HCE-2 zelulen ehunekoa. (B) RNAm bektoreekin tratatu eta 48 ordura transfektatutako HCE-2 zelulen fluoreszentzia-intentsitatearen logaritmoa. (C) DNAp bektoreekin tratatu eta 72 ordura transfektatutako HCE-2 zelulen ehunekoa. (D) DNAp bektoreekin tratatu eta 72 ordura transfektatutako HCE-2 zelulen fluoreszentzia-intentsitatearen logaritmoa. Datuak batezbesteko ± desbiderapen estandar adierazten dira; n = 3. # p<0.05 4 °C-ko bektore berarekiko. DX: dextranoa; AH: azido hialuronikoa; $SLN1_{EE}$: DOTAP lipido kationikoa duen disolbatzailearen emultsifikazioa/lurrunketa bidez prestatutako SLN. $SLN1_{HM}$: DOTAP lipido kationikoa duen urtze bero bidezko emultsifikazioarekin prestatutako SLN. SLN_C: koazerbazio metodoarekin prestatutako SLN.

Transfekzioa IL-10 hanturaren aurkako zitokina kodetzen zuten DNAp-dun edo RNAm-dun nanobektoreekin HCE-2 zeluletan ere ebaluatu zen (13. irudia). Hazkuntza-medioan jariatutako IL-10 eta zelula-barneko IL-10 kuantifikatu ziren. IL-10en ekoizpenari dagokionez, RNAm-$SLN1_{EE}$ bektoreak eraginkorrenak izan ziren. $SLN1_{EE}$ eta $SLN1_{HM}$ bektoreen kasuan, DX zuten bektoreak AH zutenak baino eraginkorragoak izan ziren. SLN_C bidez formulatutako RNAm bektoreek ez zuten ia IL-10 ekoiztu. $SLN1_{HM}$ eta RNAm edo DNAp bidez prestatutako bektoreekin tratatutako zelulek IL-10 kantitate antzekoak jariatu zituzten. Suposatzen da IL-10ren 0.8 ng/mL baino gehiagoko kontzentrazioek hanturaren aurkako efektua izango dutela [189]. Kasu honetan,

RNAm-SLN1$_{EE}$ formulazioarekin lortutako IL-10 kontzentrazioak balio hori gainditzen zuten; bereziki, formulazio eraginkorrenekin, RNAm-DX-SLN1$_{EE}$, IL-10 kontzentrazioak ia hiru aldiz handiagoak izan ziren.

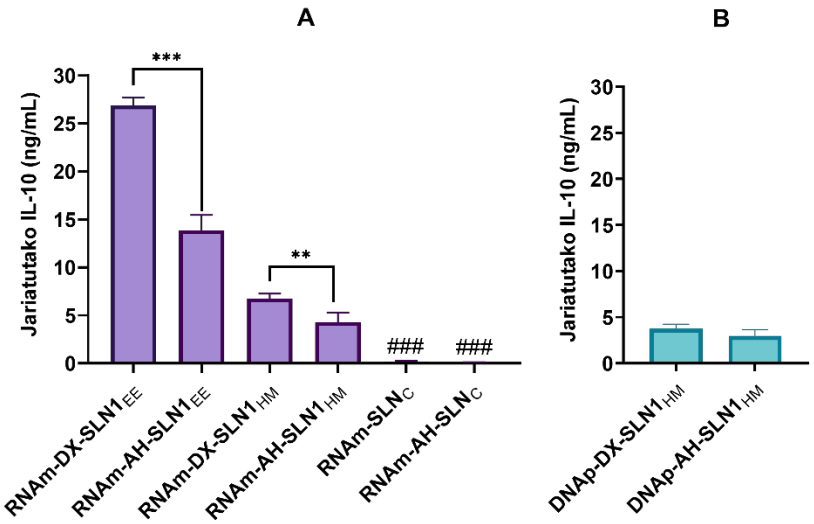

*13. irudia. HCE-2 zelulek jariatutako IL-10 mailak, IL-10 RNAm eta pUNO1-hIL10 plasmidoa daramaten SLNetan oinarritutako bektoreak administratu ondoren. (A) Jariatutako IL-10ren kontzentrazioa, RNAm-n oinarritutako bektoreak administratu eta 48 ordura. (B) Jariatutako IL-10ren kontzentrazioa, DNAp-n oinarritutako bektoreak administratu eta 72 ordura. ### p<0.001 RNAm-SLN1$_{EE}$ and RNAm-SLN$_C$ formulazioekiko. ** p<0.01 beste formulazioarekiko. *** p<0.001 beste formulazioarekiko. DX: dextranoa; AH: azido hialuronikoa; SLN1$_{EE}$: DOTAP lipido kationikoa duen disolbatzailearen emultsifikazioa/lurrunketa bidez prestatutako SLN; SLN1$_{HM}$: DOTAP lipido kationikoa duen urtze bero bidezko emultsifikazioarekin prestatutako SLN. SLN$_C$: koazerbazio metodoarekin prestatutako SLN.*

Kornearen hantura tratatzeko estrategia desberdinak *in vitro* ebaluatu ondoren, eta aurreko formulazioekin lortutako IL-10 kontzentrazio altuak kontuan hartuta, atal honetan azaldutako IL-10 ekoizteko gehikuntza genikoan oinarritutako estrategia hautatu zen *in vivo* ebaluatzeko.

4.3. DNAp edo RNAm duten SLNetan oinarritutako formulazioen *in vivo* ebaluazioa, saguen begi-azaleran instilazio topikoa egin ondoren

Nanoaskapen sistemen formulazioak berebiziko garrantzia du gene-terapian oinarritutako sendagaien garapenean, eta zehazki, begiko gene-terapian. Prestakin oftalmiko baten formulazio optimoak honako hauek bete behar ditu: bioerabilgarritasun egokia, iragazkortasun areagotua, degradazioaren aurkako egonkortasun hobetua, begiaren gainazalarekiko atxikipen luzea, eta kornearen eta itu-askapenaren arteko interakzio areagotua [190]. Izan ere, malkoen propietate pseudoplastikoak direla eta, agente lodigarriak gehitzea onuragarria izan liteke kornearen atxikipen-denbora eta begi-bioerabilgarritasuna areagotzearren [191].

In vivo entseguetarako, bektoreei PVA agente lodigarria gehitu zitzaien. PVA polimero hidrofiliko ez-ionikoa eta sintetikoa da [192] eta FDAk formulazio oftalmikoetan erabiltzea onartzen du [193]. PVA maiz erabili da ezaugarri mukomimetikoak dituelako, ura atxikitzeko ahalmen handia duelako, oxigenoarekiko iragazkortasuna duelako eta toxikotasun txikia duelako [194]. Propietate horiek gure nanosistemei atxikipen-denbora luzatzeko gaitasuna ematen diete, eta, ondorioz, begi-bioerabilgarritasuna hobetzen da, malkoen drainatzea murriztuz. Gainera, formulazio oftalmikoek malkoen pHa izan behar dute edo begietako erosotasun-tartean mantentzen den pH baten barruan egon behar dute, tolerantzia ona ziurtatzearren [195,196]. Begiko pHak 6.6 eta 7.8 artekoa izan behar du. Izan ere, begietako prestakin baten pHa 5.0-8.5 tartetik at badago malko-jarioa eragiten du eta begietako atxikipen-denbora murrizten da [197]. Gure formulazioek begi-tolerantziaren tartearen barruko pH balioak erakutsi zituzten, 7.1etik 7.5era bitartekoak.

Lehenik eta behin, PVA eta RNAm edo DNAp zeramaten formulazioek GFP adierazteko zuten gaitasuna ebaluatzeko *in vivo* entseguak egin ziren, saguen begietan instilazioz administratuz. GFP sintetizatu ostean zelula barruan geratzen da eta horrek transfektatutako korneako geruzak identifikatzeko aukera eman zuen. DNAp-dun formulazioen kasuan, $SLN1_{HM}$ bektoreak baino ez ziren aztertu, DNAp-$SLN1_{EE}$ eta DNAp-SLN_C bektoreak aldez aurretik argituratatutako lan batean ebaluatu baitziren [80].

Lan honetan ebaluatutako bektore guztiekin, GFP begien sekzio guztietan hauteman zen; hau da, formulazio guztiak korneako epitelioa transfektatzeko eta GFP ekoizteko gai izan ziren, 14. irudian ikus daitekeen bezala. GFPak sortzen zuen fluoreszentziaren intentsitatea nabarmenki handiagoa izan zen RNAm bektoreetan formulatuta zegoenean, biluzik administratu zenean baino. Emaitza hauek agerian usten dute SLNen beharra eraginkortasun handiagoa lortzeko.

SLNetan oinarritutako formulazioek zelula epitelialak soilik transfektatu ahal izan zituzten, baina ez ziren gai izan korneako barne-geruzak transfektatzeko, formulazioek partikula-tamaina ezberdina izanda ere. Izan ere, RNAm-DX-$SLN1_{EE}$ eta RNAm-DX-$SLN1_{HM}$ formulazioekin sortutako GFP epitelioaren gainazal osoan zehar etengabe aurkitu zen. RNAm-AH-$SLN1_{EE}$, RNAm-AH-$SLN1_{HM}$ eta RNAm-SLN_C bektoreen kasuan, GFPak eragindako fluoreszentzia segmentu etengabeetan ikusi zen. Aldiz, RNAm-AH-SLN_C-rekin transfektatutako korneetan fluoreszentzia modu etenean detektatu zen. DNAp-dun bektoreekin egindako kornea-transfekzioari dagokionez, GFP eremu zabalago batean hauteman zen, DNAp-AH-$SLN1_{HM}$ formulazioarekin DNAp-DX- $SLN1_{HM}$ formulazioarekin baino.

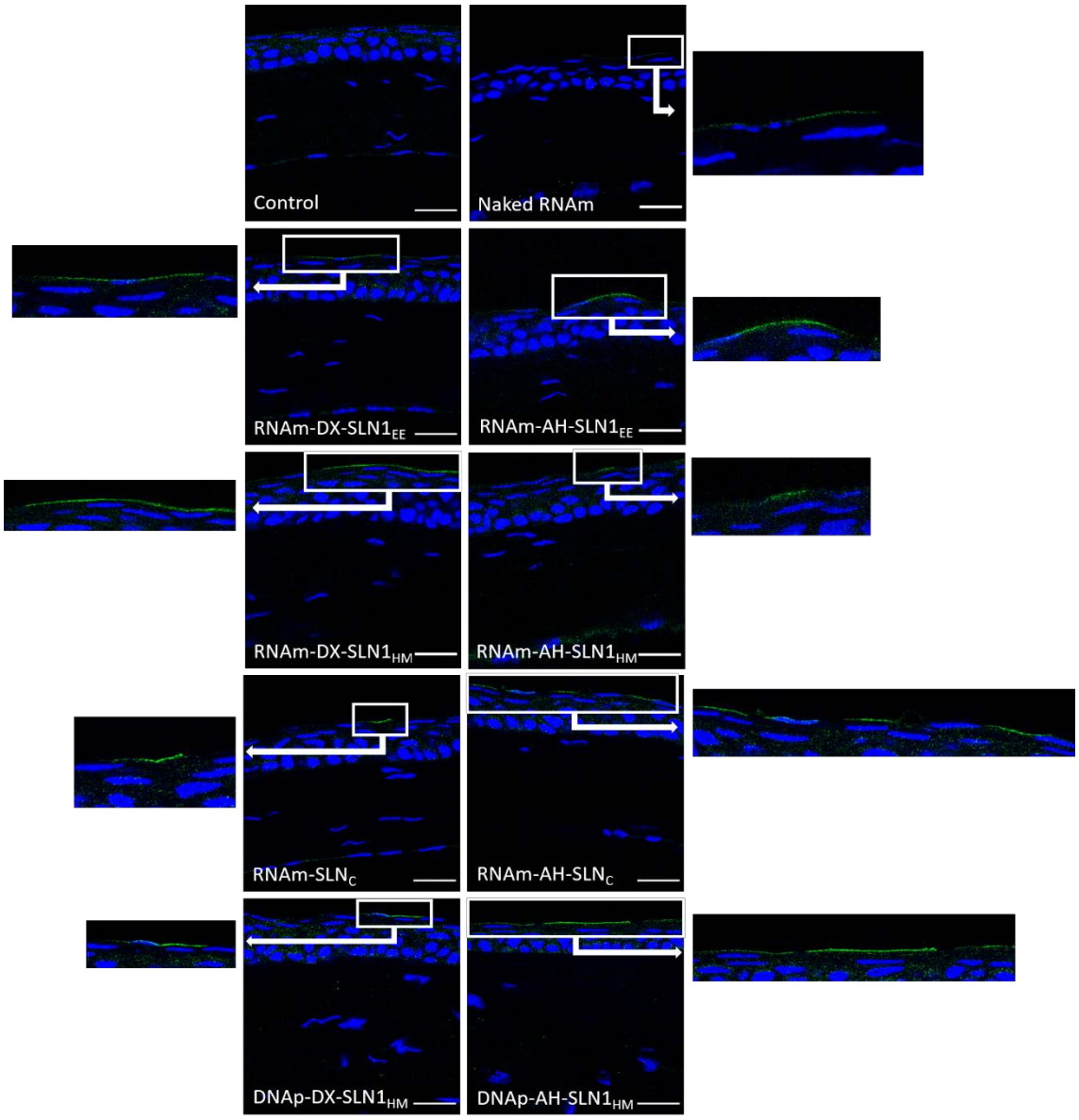

14. irudia. In vivo transfekzioa saguen kornean PVA agente lodigarria eta GFP kodetzen duten RNAm eta DNAp bektoreak administratu eta 48 ordutara (63 ×). Urdina: DAPIz tindaturiko nukleoak. Berdea: Alexa Fluor 488rekin markatutako antigorputz sekundarioarekin immunofluoreszentzia bidez detektatutako GFP. Eskala-barra: 20 µm. DX: dextranoa; AH: azido hialuronikoa SLN1$_{EE}$: DOTAP lipido kationikoa duen disolbatzailearen emultsifikazioa/lurrunketa bidez prestatutako SLN. SLN1$_{HM}$: DOTAP lipido kationikoa duen urtze bero bidezko emultsifikazioarekin prestatutako SLN. SLN$_C$: koazerbazio metodoarekin prestatutako SLN.

Kornearen egitura konplexua denez, azido nukleikodun askapen sistemak proteina terapeutikoaren adierazpena kornearen geruza epitelial estratifikatu eta berriztagarrian bereziki adierazteko diseinatzen dira, bertan zelula kopuru handi bat transfektatu baitaiteke. Beste aukera bat korneako geruza endotelialaren transfekzioa izan daiteke, zein eskuragarriagoa den. Izan ere, geruza horrek banatzen ez diren zelulen kopuru txikia du, eta adierazpen genetikoa denbora gehiagoz mantendu daiteke. Horretarako, DNA RNAm baino onuragarriagoa izan liteke, transgene-ekoizpen iraunkorragoa ematen baitu. Hala ere, RNAm-k hainbat abantaila ditu, hala

nola eraginkortasun handia, segurtasun-profila eta proteinak azkar ekoizteko moldakortasuna, eta horrek kornearen hantura tratatzeko aukera hobea bihur lezake. Gainera, kontuan hartuta korneako epitelioa 7 eta 14 egunez erabat berritzen dela [198], proteinaren epe laburreko adierazpena nahikoa izan liteke eraginkortasun egokia lotzeko.

GFP kodetzen zuten azido nukleikoekin saioak egin ostean, hurrengo entseguak hanturaren aurkako IL-10 kodifikatzen zuen RNAm-dun SLNekin egin ziren. Formulazioak begi-tantetan administratu ziren topikoki saguetan IL-10 ekoizteko zuten gaitasuna *in vivo* ebaluatzeko. IL-10 zelulek jariatzen duten proteina denez, korneako zelula epitelialetan sortu ostean kornean zehar zabaltzen da, geruza sakonagoetara iristen. Gainera, kornearen hantura kudeatzeko, IL-10 azkar adierazteak gaixotasunaren progresioari aurre egiten lagunduko luke. Testuinguru horretan, PVA zuten formulazioak administratu ziren hiru egunez, eta azken administraziotik 24 ordura IL-10ren presentzia kornean ebaluatu zen.

IL-10 modu etenean detektatu zen korneako epitelioan zehar aztertutako atal guztietan. Nanosistemekin tratatutako korneen fluoreszentziaren intentsitatea RNAm biluziarekin tratatutakoekin baino handiagoa izan zen. Saguetan RNAm-DX-SLN1$_{EE}$ administratzerakoan IL-10 kornearen epitelioaren geruza sakonenetan ere hauteman zen (15. irudia). Kontutan hartu behar da formulazio horrekin errendimendurik handiena lortu zela HCE-2 zelulekin egindako entseguan (13. irudia). RNAm-AH-SLN$_C$ bektoreak ere IL-10 ekoizteko gaitasun handia erakutsi zuen, *in vitro* oso eraginkortasun baxua izan bazuten ere.

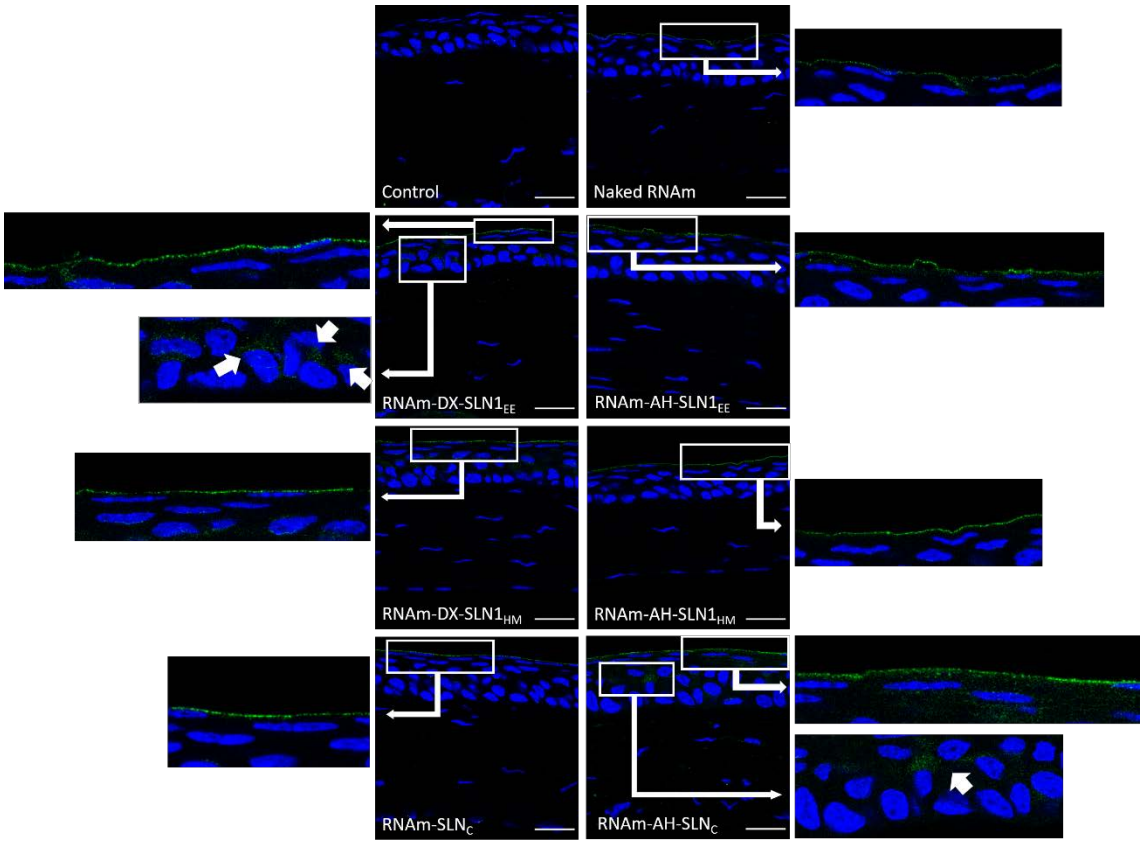

15. irudia. In vivo transfekzioa saguen kornean, PVA agente lodigarria eta IL-10 kodetzen duten RNAm bektoreak administratu eta 24 ordura (63 ×). Urdina: DAPIz tindaturiko nukleoak. Berdea: Alexa Fluor 488rekin markatutako antigorputz sekundarioarekin immunofluoreszentzia bidez detektatutako IL-10. Eskala-barra: 20 µm. DX: dextranoa; AH: azido hialuronikoa; $SLN1_{EE}$: DOTAP lipido kationikoa duen disolbatzailearen emultsifikazioa/lurrunketa bidez prestatutako SLN. $SLN1_{HM}$: DOTAP lipido kationikoa duen urtze bero bidezko emultsifikazioarekin prestatutako SLN. SLN_C: koazerbazio metodoarekin prestatutako SLN.

Azterlan honetako *in vitro* eta *in vivo* entseguen arteko korrelazio ezak [199–202], agerian uzten du azken horiek garapen farmazeutikoaren prozesuko faserik goiztiarrenetan egin behar direla, hautagaien formulazioak behar bezala hautatu eta optimizatzeko.

Gure nanosistemekin lortutako transfekzioaren eraginkortasuna eta aldakortasuna hobetzeko, doktorego-tesi honen azken atalean DNAp eta RNAm administratzeko nanobektore berriak diseinatu ziren, zeintzuk SLNez, protaminez eta polisakaridoez gain AuNPk ere osagai bezala zutenak.

4.4. Azido nukleikoen askapenerako nanopartikula ez-organikoak dituzten lipidoetan oinarritutako nanobektoreen ebaluazioa *in vitro* eta *in vivo*

Partikula ez-organikoen artean, metal nobleek, eta bereziki AuNPek, ezaugarri kimiko, fisiko eta optiko paregabeak dituzte. Ezaugarri horiek AuNPak aplikazio biomedikoetan erabiltzeko erakargarri egiten ditu, bereziki, farmakoak eta geneak emateko eta minbiziaren tratamendu

fototermikorako [203–205]. AuNPak bioinerteak eta biobateragarriak dira, zitotoxikotasun txikia dute eta *in vivo* oxidazioaren eta degradazioaren aurka egonkorrak dira; gainera, erraz funtzionalizatzen dira era askotako estekatzaileekin, honek haien tamainan eta propietateetan eragina duelarik [206]. Bestalde, AuNPek berezko propietate terapeutikoak dituzte, hala nola efektu antiangiogenikoak [207,208] eta antiinflamatorioak [209]. Gainera, nanopartikula inorganiko hauek material genetikoa modu sakonean kondentsatzeko ahalmena dute, eraginkortasun handiko askapena lortuz eta aldi berean degradazio entzimatikoa murriztuz [210,211]. Ezaugarri horiek direla eta, AuNPak osagai interesgarria dira RNAm-dun eta DNAdun bektore ez-biraletan sartzeko eta CNVri lotutako hantura tratatzeko [204].

GFP kodetzen zuen DNAp edo RNAm, protamina, polisakaridoa (DX edo AH), $SLN1_{EE}$ eta AuNPak zituzten urrezko nanopartikula lipidikoak optimizatu ziren, *in vitro* aztertu eta, ondoren, *in vivo* ebaluatu ziren saguen begietako administrazio topikoaren ondoren.

8. taulak AuNPek dituzten bektoreen tamaina, PDI eta gainazaleko karga erakusten ditu.

8. taula. Urrezko nanopartikula lipidikoen karakterizazio fisikoa.

Bekoterearen izena	Tamaina (nm)	PDI	ζ-Potentziala (mV)
RNAm-DX-$SLN1_{EE}$_Au	184.33 ± 2.22	0.29 ± 0.02	+39.78 ± 1.54
RNAm-AH-$SLN1_{EE}$_Au	212.80 ± 5.46	0.32 ± 0.04	+28.23 ± 0.61
DNAp-DX-$SLN1_{EE}$_Au	151.33 ± 1.70	0.28 ± 0.03	+43.75 ± 1.74
DNAp-AH-$SLN1_{EE}$_Au	208.97 ± 3.62	0.34 ± 0.01	+29.35 ± 0.39

DX: dextranoa; AH: azido hialuronikoa; Au: urrea; SLN1EE: DOTAP lipido kationikoa duen disolbatzailearen emultsifikazioa/lurrunketa bidez prestatutako SLN. Datuak batezbesteko ± desbiderapen estandar adierazten dira; n = 3.

Ezaugarri fisiko-kimikoek AuNPak SLNen tamaina eta PDI murrizteko gai izan zirela erakutsi zuten, batez ere RNAm-dun nanobektoreetan. Beste osagai bat gehiago zuten ere, urrezko nanopartikula lipidikoek 0.35etik beherako PDI erakutsi zuten. PDI zenbat eta txikiagoa izan, orduan eta homogeneoagoa da laginaren partikulen tamaina, farmakoak eta geneak administratzeko egokia izanik [212]. 16. irudiak RNAm-dun eta DNAp-dun urrezko nanopartikula lipidikoen TEM argazkiak erakusten ditu.

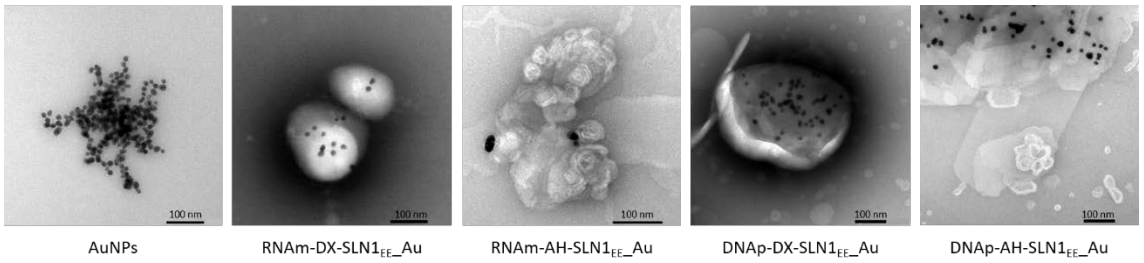

16. irudia. TEM bidez eskuratutako RNAm-dun eta DNAp-dun urrezko nanopartikula lipidikoen irudiak. DX: dextranoa; AH: azido hialuronikoa; Au: urrea; AuNPs: urrezko nanopartikulak; SLN1$_{EE}$: DOTAP lipido kationikoa duen disolbatzailearen emultsifikazioa/lurrunketa bidez prestatutako SLN.

Urrezko nanopartikula lipidikoak RNAm (17.A irudia) eta DNAp (17.B irudia) lotzeko, babesteko eta askatzeko duten gaitasuna ere ebaluatu zen agarosa-gel elektroforesiren bidez.

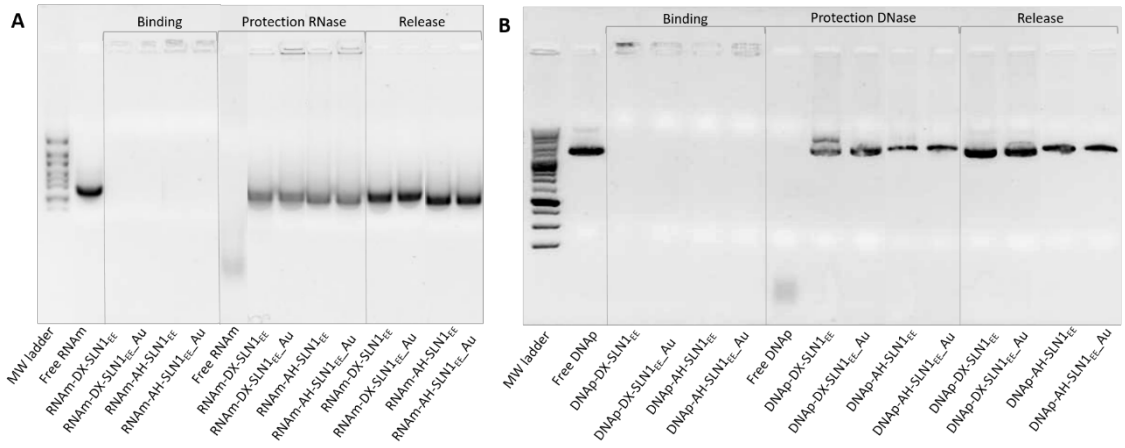

17. irudia. Urrezko nanopartikula lipidikoek lotzeko, babesteko eta askatzeko duten gaitasuna. A: RNAm-urrezko nanobektoreak. B: DNAp-urrezko nanobektoreak. DX: dextranoa; AH: azido hialuronikoa; Au: urrea; SLN1$_{EE}$: DOTAP lipido kationikoa duen disolbatzailearen emultsifikazioa/lurrunketa bidez prestatutako SLN.

Lotzeko gaitasunari dagokionez, agarosa geletan lortutako emaitzek demostratzen dute azido nukleikoek ezin izan zutela gelaren bidez migratu eta, beraz, bektorearekin erabat lotuta zeudela. Izan ere, bi agarosa-geletan dagozkien errailetan bandarik ez zen agertu eta RNAm eta DNAp karga-putzuetan zeuden. Azido nukleikoen babesaren kasuan, urrezko nanopartikula lipidikoak RNAm eta DNAp babesteko gai izan ziren RNasa I eta DNasa I entzimekin tratatu zirenean; hurrenez hurren. RNAm eta DNAp biluziak, berriz, erabat degradatu ziren. Hala ere, AuNPak formulazioan gehitu zirenean DNAp-DX-SLN1$_{EE}$ formulazioan bi bandetik bat desagertu izanak azido nukleikoaren osaera aldatu egin zela adierazten du. AuNPek azido nukleikoen kondentsazioa areagotzeko duten gaitasunarekin erlazionatuta egon liteke, eta, beraz, azido nukleikoa degradaziotik babesteko gaitasunarekin, horrek egonkortasuna ematen baitie sistemei zelula barnean. Azkenik, SDS bidezko tratamenduaren ondoren, RNAm-k eta DNAp-k

karga-putzuetatik migratu ahal izan zuten, hau da, azido nukleikoek urrezko nanopartikula lipidikoetatik askatzeko gaitasuna izan zuten.

Urrezko nanopartikula lipidikoen transfekzio-eraginkortasuna ebaluatzeko entseguak zelula-lerro desberdinetan burutu ziren: ARPE-19 (18.A irudia), HEK-293 (18.B irudia) eta HCE-2 zeluletan, hurrenez hurren. AuNPak gehitzeak zelula transfektatuen ehunekoa eta fluoreszentziaren intentsitatea (proteinen ekoizpenaren adierazle) handitu zituen zelula-lerro guztietan, oro har. RNAm-dun formulazioen kasuan, ARPE-19 zeluletan AuNPak gehitzeak, transfektatutako zelulen ehunekoa %58tik %86ra igo zen. HEK-293 zeluletan, gehikuntza are handiagoa izan zen RNAm-DX-SLN1$_{EE}$ bektorean. Izan ere, transfekzioa %4tik %48ra igo zen. RNAm-AH-SLN1$_{EE}$ bektorearen kasuan, zelula transfektatuen ehunekoa AuNPekin mantendu bazen ere, fluoreszentzia-intentsitatea handitu egin zen. HCE-2 zelulen kasuan, RNAm-urrezko nanopartikula lipidikoen transfekzioaren eraginkortasuna AuNP gabeko bektoreetan lortutakoaren antzekoa izan zen. Izan ere, RNAm formulazioetako zelula transfektatuen ehunekoa %12 artekoa izan zen AuNPrik gabe eta % 18koa AuNPekin. Hala ere, fluoreszentziaren intentsitatea handitu zen. Zelulen bideragarritasuna %98 ingurukoa izan zen formulazio guztiekin.

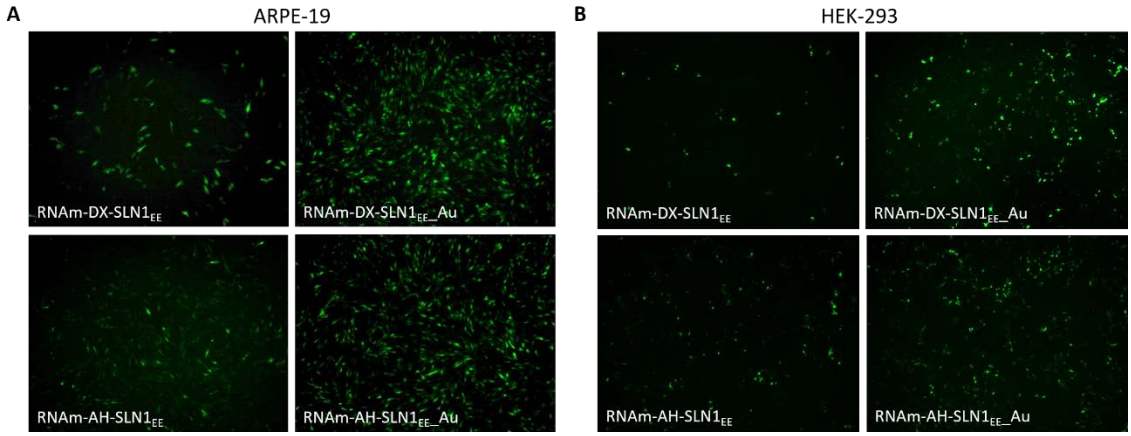

18. irudia. RNAm-dun urrezko nanopartikula lipidikoen transfekzioa-eraginkortasuna (A) ARPE-19 eta (B) HEK-293 zeluletan. DX: dextranoa; AH: azido hialuronikoa; Au: urrea; SLN1$_{EE}$: DOTAP lipido kationikoa duen disolbatzailearen emultsifikazioa/lurrunketa bidez prestatutako SLN.

Azkenik*, in vivo* ebaluatzeko, GFP kodetzen zuen RNAm-dun urrezko nanopartikula lipidikoak saguei administratu zitzaizkien begi-tanta instilazio moduan. 19. irudiak erakusten du nanosistema guztiak gai izan zirela kornean GFP sortzeko. Gainera, fluoreszentziaren intentsitatea AuNPak zituzten nanosistemetan partikula inorganikorik ez zituzten bektoreetan baino biziagoa izan zen geruza epitelial eta endotelialetan, bereziki RNAm-AH-SLN1$_{EE}$_Au bektorearekin. Transfekzio emaitza horiek, efektu antiangiogenikoen [207,208] eta

antiinflamatorioen [209] berezko ezaugarri terapeutikoekin batera, urrezko nanopartikula lipidikoak kornearen hanturarako sendagai potentzial bihurtzen dituzte, azterketa gehigarriak beharrezkoak diren arren.

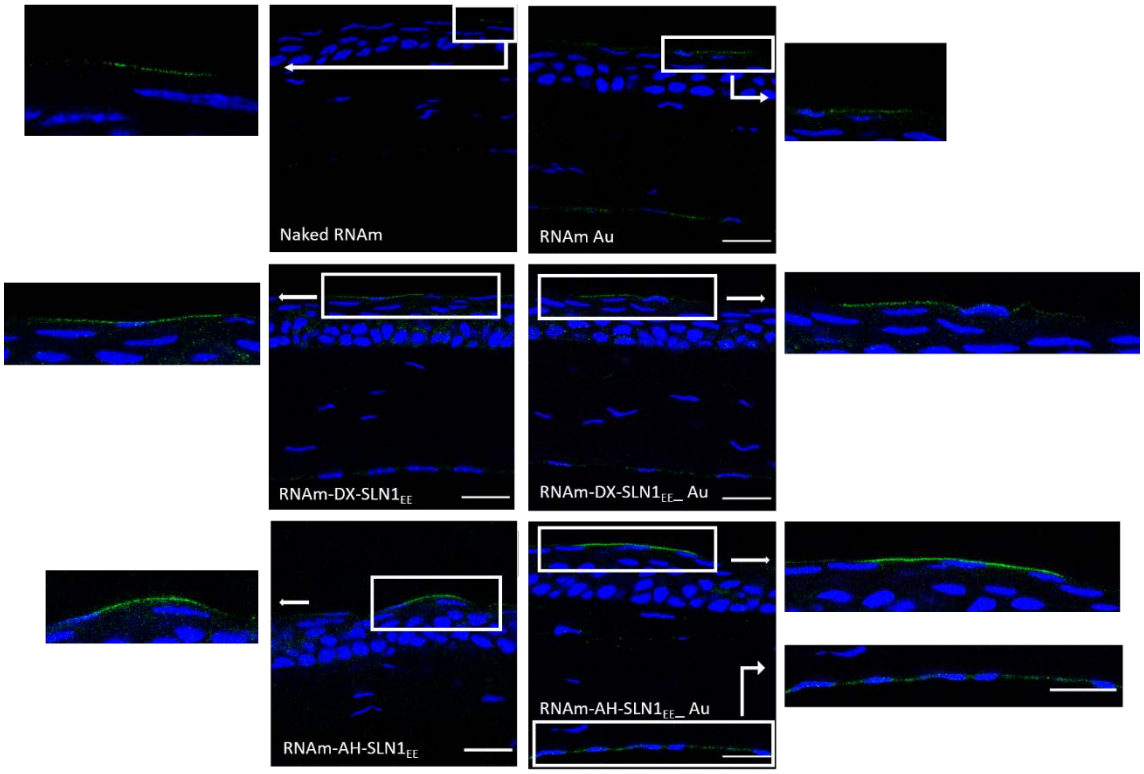

19. irudia. In vivo kornea-transfekzioa saguetan, PVA agente lodigarria eta GFP kodetzen eta AuNPak dituzten RNAm eta DNAp bektoreak administratu eta 48 ordura (63 ×). Urdina: DAPIz tindaturiko nukleoak. Berdea: Alexa Fluor 488rekin markatutako antigorputz sekundarioarekin immunofluoreszentzia bidez detektatutako. Eskala-barra: 20 µm. DX: dextranoa; AH: azido hialuronikoa; Au: urrea; SLN1$_{EE}$: DOTAP lipido kationikoa duen disolbatzailearen emultsifikazioa/lurrunketa bidez prestatutako SLN.

Laburbilduz, doktorego-tesi honetan SLNetan oinarritutako DNAp eta RNAm administratzeko sistemak diseinatu dira, gene-terapiaren bidez kornea-hantura tratatzeko. Lehenik eta behin, SLNen konposizioa, SLNak prestatzeko teknika eta estekatzaile desberdinen gehiketa optimizatu zen, *in vitro* eraginkortasun handia eta epe luzerako egonkortasuna duten azido nukleikoetan oinarritutako prestakin kationikoak lortzeko. MMP-9 faktore proangiogenikoaren aurka garatutako shRNA-dun prestakinak RNAi teknologiak CNVari lotutako hantura gene-isiltzearen bitartez tratatzeko duen potentziala erakutsi zuen *in vitro*. Beste alde batetik, tesi honek, saguen begietan,-tanten bidez administratutako RNAm-dun eta DNAp-dun formulazio topikoak kornean IL-10 hanturaren aurkako zitokina ekoizteko gai direla erakusten du. Hori guztia kontuan hartuta, birusak erabiltzen ez dituzten gehikuntza genikoan oinarritutako terapiak kornea-hanturaren aurkako tratamenduari klinikan egin diezaiokeen ekarpena nabarmentzen du. Azkenik, AuNPen eta SLNetan oinarritutako nanobektoreen arteko konbinazioak abantaila handia erakutsi du

propietate fisikoei eta *in vivo* transfekzioaren eraginkortasunari dagokienez, urrezko nanopartikula lipidikoak azido nukleikoak administratzeko duten potentzial berritzailea agerian utziz. Emaitza hauen berritasunak patente-eskaera bat ekarri du, “Golden lipid nanoparticles for gene therapy” (WO 2021/130215 A1 nazioarteko argitalpen-zenbakia) izenekoa.

2. ATALA: ONDORIOAK

1. IVT RNAm-ren funtzionalitatea eta eraginkortasuna hobetzeko erabilitako estrategien berrikusketak agerian utzi du RNAm sintetikoak interes handia pizten duela molekula terapeutiko gisa. RNAm-ren hedapena sustatu duen ezaugarri nagusia azido nukleikoaren adierazpen kontrolatua da, mutagenesia eta alterazio genomiko iraunkorren arriskurik gabe. Beste abantaila batzuk ekoizpen ekonomikoa, fabrikazio eskalagarria eta aplikazioekiko moldakortasuna dira. Hornikuntzarekin eta egonkortasunarekin loturiko hainbat zailtasun teknologiko oraindik gainditzeke daude, baina azken urteetan aurrepauso handiak eman dira.

2. Diseinatutako azido nukleikodun sendagaien ezaugarri fisiko-kimikoak honako faktore hauen menpe daude: gehitutako estekatzailea, SLNen prestakuntzan erabilitako lipido mota (kationikoa edo ionizagarria), eta SLNen prestaketa metodoa (disolbatzailearen emultsifikazioa/lurrunketa, urtze bero bidezko emulsifikazioa edo koazerbazioa). Bektoreak SLNen, RNAm-ren edo DNAp-ren eta estekatzaile desberdinen (protamina, dextranoa eta azido hialuronikoa) arteko elkarrekintza elektrostatikoen ondorioz sortu ziren; formulazioek nanometroko partikula tamaina (90 eta 350 nm artekoak) eta gainazaleko karga positiboa zuten (+18 eta +50 mV artekoak). Nanobektoreek azido nukleikoa behar bezala babestu eta askatu zuten, eta ARPE-19, HEK-293 eta HCE-2 zeluletan eraginkortasunez internalizatu ziren. Formulazioaren ezaugarriek azido nukleikoen askapenean, transfekzio-eraginkortasunean eta nanobektoreen epe luzeko egonkortasunean eragin nabarmena izan zuten, eta RNAm izan zen formulazio-aldaketekiko sentikorrena.

3. Diseinatutako azido nukleikodun sendagaien *in vitro* eraginkortasuna zelula barneko portaeraren araberakoa da. Proteinen ekoizpena energiarekiko mendekoak edo independenteak diren sarrera-mekanismoek baldintzatzen dute. Sarrera mekanismo horiek administratutako azido nukleikoaren, nanobektoreen ezaugarri fisiko-kimikoen eta zelula-lerroaren araberakoak dira. Proteinen sintesia azkarragoa eta adierazpenaren iraupena laburragoa da RNAm-rekin DNAp-rekin baino. Azido nukleikoaren ezaugarrietara eta helburu terapeutikora berariaz egokitutako sendagaiak diseinatzeko, azido nukleikoak askatzeko sistemen portaera intrazelularraren ezagutza sakona funtsezkoa da.

4. Epe-luzeko egonkortasuna ebaluatzeko burututako entseguek erakutsi zuten DNAp-dun formulazioek transfekzio-eraginkortasuna gutxienez zazpi hilabetez mantendu zutela 4 °C-tan biltegiratu ostean, nahiz eta, bigarren hilabetetik aurrera aldaketa fisiko-kimikoak ikusi ziren. Tamaina eta zeta potentziala kontuan izanik RNAm bektoreak egonkorragoak dira,

hala ere, haiekin transfekzio-eraginkortasuna lehen hilabetetik aurrera murriztu egiten da, nahiz eta murrizketa horiformulazioaren arabera ezberdina izan. DOTAP lipido kationikoa baino ez zuten RNAm sendagaiak eraginkorrenak izan ziren, eta dextranoa edo azido hialuronikoa sartzeak egonkortasuna hobetu zuen. Epe-luzerako eraginkortasuna eta egonkortasuna kontuan hartuta, lipido kationiko bezala DOTAP baino ez duten bektoreak, DOTAP eta DODAP lipido ionizagarria dutenak baino etorkizun handiagoko formulazioak dira azido nukleikoak administratzeko.

5. MMP-9 faktore proangiogenikoaren aurkako shRNA duten sendagaiak gene-isiltzearen bitartez prestatu ziren CNV saihesteko. SLN, protamina eta dextranorekin prestatutako formulazioak HCE-2 zeluletan MMP-9ren adierazpena murrizteko gai izan ziren. Horrela, HCE-2 zelulen migrazioa gutxitu zen zauriak sendatzeko *in vitro* saiakuntzan, eta hodi kapilarren eraketa txikiagotu zen *in vitro* HUVEC zeluletan hodiak eratzeko saiakuntzan. Emaitza hauek agerian jartzen dute SLNetan oinarritutako azido nukleikodun sistemek duten potentziala RNAi teknologiaren bidez CNVari lotutako hantura tratatzeko.

6. GFP kodetzen zuten RNAm eta DNAp sendagaien tanten bidezko instilazio topikoak saguen korneako epitelioaren kanpo-geruzaren transfekzioa eragin zuen; formulazio horietako batzuek aldez aurretik *in vitro* HCE-2 zeluletan transfekzio oso balio baxuak lortu bazituzten ere. *In vitro* eta *in vivo* emaitzen arteko korrelazio ezak azido nukleikoak administratzeko sistemen garapen farmazeutikoaren lehen faseetan *in vivo* azterketak egiteko beharra erakusten du, eta formulazio hautagaiak egoki hautatu eta optimizatu behar dira.

7. IL-10 proteina terapeutikoa kodetzen zuten RNAm-dun nanobektoreek, hanturaren aurkako zitokina horren sintesia eragin zuten saguen korneako epitelioan. Entsegu horretan begi tantak instilazio topiko bidez hiru egunez administratu ziren. Jariatutako IL-10 zitokina epitelioaren geruza sakonetan ere antzeman zen. Lortutako emaitzek agerian uzten dute gehikuntza geniko ez-biralak kornearen hantura tratatzeko etorkizunean balio dezakela.

8. SLNetan oinarritutako RNAm-dun eta DNAp-dun nanobektoreetan urrezko nanopartikulak gehitzeak RNAm nanobektoreen tamaina eta polidispertsioa murriztu zuen, eta DNAp-dun formulazioek beren ezaugarri fisiko-kimikoak mantendu zituzten. Saguei administratutako GFP kodetzen zuen RNAm zeramaten urrezko nanopartikula lipidiko berriak urrezko nanopartikularik gabeko formulazioak baino eraginkortasun handiagoa erakutsi zuten kornea transfektatzeko (fluoreszentziaren intentsitatean oinarrituta). Beraz, urrezko

nanopartikulen eta SLNen arteko konbinazioak azido nukleikoak administratzeko sistemen propietate fisikoak eta transfekzio-eraginkortasuna hobetzen ditu.


Universidad del País Vasco
Euskal Herriko Unibertsitatea